ERDC/CHL TR-11-1

Coastal and Hydraulics Laboratory

US Army Corps
of Engineers®
Engineer Research and
Development Center

ERDC
INNOVATIVE SOLUTIONS
for a safer, better world

FEMA Region III Storm Surge Study

Coastal Storm Surge Analysis: Modeling System Validation

Report 4: Intermediate Submission No. 2.0

Jeffrey Hanson, Heidi Wadman, Brian Blanton,
and Hugh Roberts

July 2013

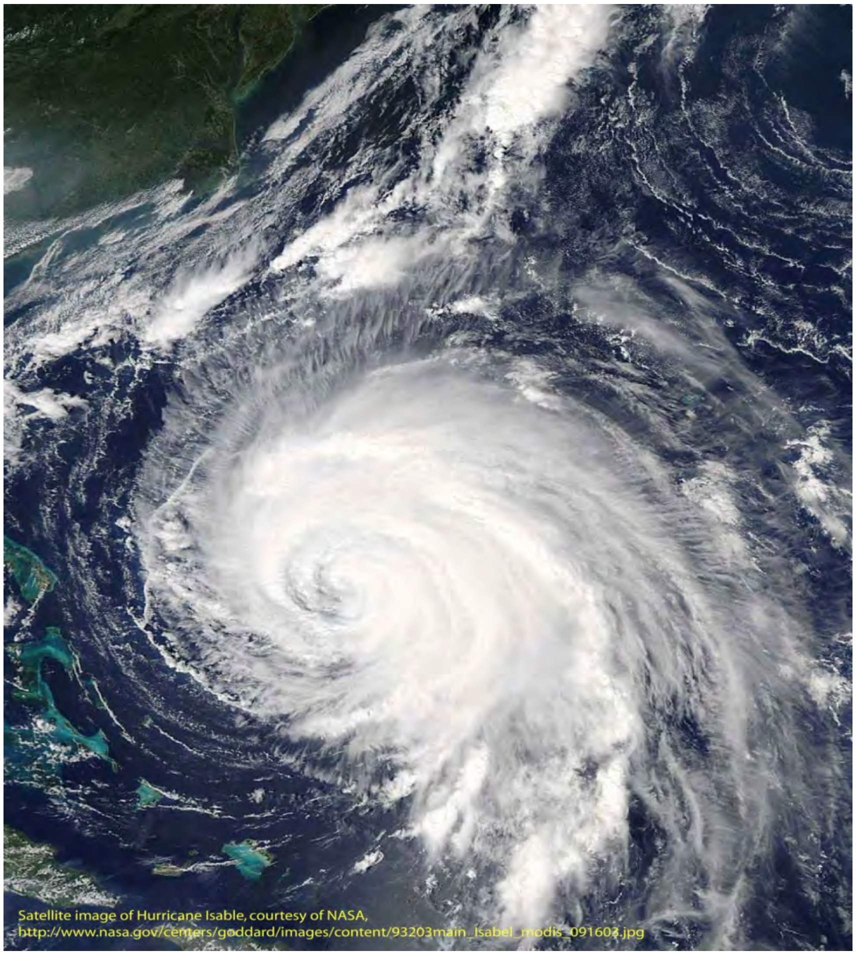

Satellite image of Hurricane Isable, courtesy of NASA,
http://www.nasa.gov/centers/goddard/images/content/93203main_isabel_modis_091603.jpg

Approved for public release; distribution is unlimited.

The US Army Engineer Research and Development Center (ERDC) solves the nation’s toughest engineering and environmental challenges. ERDC develops innovative solutions in civil and military engineering, geospatial sciences, water resources, and environmental sciences for the Army, the Department of Defense, civilian agencies, and our nation’s public good. Find out more at www.erdc.usace.army.mil.

To search for other technical reports published by ERDC, visit the ERDC online library at http://acwc.sdp.sirsi.net/client/default.

ERDC/CHL TR-11-1
July 2013

Coastal Storm Surge Analysis: Modeling System Validation

Report 4: Intermediate Submission No. 2.0

Jeffrey L. Hanson and Heidi M. Wadman

Field Research Facility
US Army Engineer Research and Development Center
1261 Duck Road
Kitty Hawk, NC 27949

Brian Blanton

Renaissance Computing Institute
100 Europa Drive, Suite 540
Chapel Hill, NC 27517

Hugh Roberts

ARCADIS
4999Pearl East Circle, Suite 200
Boulder, CO 80301

Report 4 of a series

Approved for public release; distribution is unlimited.

Prepared for Federal Emergency Management Agency
615 Chestnut Street
One Independence Mall, Sixth Floor
Philadelphia, PA 19106-4404

Under US Army Corps of Engineers Work Unit J64C87

Abstract

The Federal Emergency Management Agency, Region III office, has initiated a study to update the coastal storm surge elevations within the states of Virginia, Maryland, and Delaware, and the District of Columbia including the Atlantic Ocean, Chesapeake Bay including its tributaries, and the Delaware Bay. This effort is one of the most extensive coastal storm surge analyses to date, encompassing coastal floodplains in three states and including the largest estuary in the world. The study will replace outdated coastal storm surge stillwater elevations for all flood insurance studies in the area, and serve as the basis for new coastal hazard analysis and ultimately updated Flood Insurance Rate Maps (FIRMs).

The end-to-end storm surge modeling system includes the Advanced Circulation Model for Oceanic, Coastal, and Estuarine Waters (ADCIRC), used to simulate two-dimensional hydrodynamics. ADCIRC was dynamically coupled to the unstructured numerical wave model Simulating WAves Nearshore (unSWAN) to calculate the contribution of waves to total storm surge. The modeling system validation included a comprehensive tidal calibration followed by an assessment using carefully reconstructed wind and pressure fields from three major flood events for the Region III domain: Hurricane Isabel, Hurricane Ernesto, and Extratropical Storm Ida. Model skill was accessed by quantitative comparison of model output to wind, wave, water level, and observation of high-water marks.

Prior reports covered Submittal 1 requirements by providing details on the bathymetric/topographic digital environmental model (Report 1.1), describing the computational system (Report 1.2), and documenting the selection process for storms used in the study (Report 1.3). This report (2.0) completes the required Submittal 2 documentation by providing details of the modeling system calibration and performance.

DISCLAIMER: The contents of this report are not to be used for advertising, publication, or promotional purposes. Citation of trade names does not constitute an official endorsement or approval of the use of such commercial products. All product names and trademarks cited are the property of their respective owners. The findings of this report are not to be construed as an official Department of the Army position unless so designated by other authorized documents.

DESTROY THIS REPORT WHEN NO LONGER NEEDED. DO NOT RETURN IT TO THE ORIGINATOR.

Contents

Abstract ii

Figures and Tables v

Preface ix

Unit Conversion Factors x

1 Overview 1

2 Mesh Updates 4

3 Tidal Calibrations 6

3.1 Tidal observations in the region 7
3.2 Model and run setup 7
3.3 Characteristics of the modeled tides in the region 10

4 Validation Storm Descriptions 22

5 Modeling System Validation Approach 26

5.1 Error metrics 26
5.1.1 Temporal correlation (TC) analysis 27
5.1.2 Peak event (PE) analysis 27
5.1.3 High-water mark analysis 28
5.2 Performance scores 28

6 Wind Field Validation 29

6.1 Wind validation approach 29
6.2 Wind validation data 30
6.3 Wind validation results 31
6.3.1 Hurricane Isabel (2003) 31
6.3.2 Ernesto (2006) 33
6.3.3 Extra-tropical storm Nor'Ida (2009) 41
6.3.4 Wind peak event analysis 46

7 Wave Validation 48

7.1 Wave validation approach 48
7.2 Wave validation data 49
7.3 Wave validation results 49
7.3.1 Hurricane Isabel (2003) 50
7.3.2 Ernesto (2006) 56
7.3.3 Nor'Ida (2009) 59
7.3.4 Peak wave event summary 63

8 Storm Surge Validation 67

8.1 Removal of tidal forcing 67

8.2 Water level validation error metrics 69

8.3 Water level error assessment 71

8.4 Storm surge validation 72

8.5 Hurricane Isabel, September 2003 76

8.5.1 Isabel model output versus observation: Detided TidesSurgeWaves 77

8.5.2 High-water mark validation – Hurricane Isabel data 80

8.6 Hurricane Ernesto, August-September 2006 82

8.7 Ernesto model output versus observation – Detided TidesSurgeWaves 83

8.8 Extra-tropical Storm Ida (Nor’Ida), November 2009 87

8.8.1 Nor'Ida model output versus observation – Detided TidesSurgeWaves 89

8.8.2 USGS storm response data, Nor’Ida 94

8.9 Peak water level validation summary 97

References 100

Appendix A: Detided TidesSugeWaves Water Level Data, Hurricane Isabel 102

Appendix B: Detided TidesSugeWaves Water Level Data, Hurricane Ernesto 137

Appendix C: Detided TidesSugeWaves Water Level Data, Extra-tropical Storm Ida 175

Appendix D: USGS Real-Time Storm Surge Data, Extra-tropical Storm Ida 213

Appendix E: TidesSugeWaves Water Level Data 225

Report Documentation Page

Figures and Tables

Figures

Figure 1. ADCIRC finite element grid for the Region III project.......... 6
Figure 2. Spatial distribution of total water level variance explained by tides.......... 9
Figure 3. M_2 elevation [m] and phase [degrees UTC] from equilibrium tidal simulation. 10
Figure 4. K_1 elevation [m] and phase [degrees UTC] from equilibrium tidal simulation. 11
Figure 5. Amplitude of M_2 and K_1 tides.......... 14
Figure 6. Scatter plots of the M_2 and K_1 modeled and observed tidal amplitude.......... 14
Figure 7. Histogram of errors in the M_2 and K_1 tidal amplitudes.......... 15
Figure 8. Time series plots for October 2006 of reconstructed tidal water levels at NOAA NOS Delaware stations, as well as the Cape May Ferry Terminal station.......... 16
Figure 9. Time series plots for October 2006 of reconstructed tidal water levels at NOAA NOS Pennsylvania and Maryland stations.......... 17
Figure 10. Time series plots for October 2006 of reconstructed tidal water levels at NOAA NOS Maryland stations.......... 18
Figure 11. Time series plots for October 2006 of reconstructed tidal water levels at NOAA NOS District of Columbia and Virginia stations. 19
Figure 12.Time series plots for October 2006 of reconstructed tidal water levels at NOAA NOS Virginia stations, as well as the Duck Pier, NC, station. 20
Figure 13. Storm tracks for Hurricanes Isabel (2003) and Ernesto (2006).......... 23
Figure 14. Storm tracks for Hurricane Ida and Nor'Ida (2009). 25
Figure 15. Hurricane Isabel maximum wind speeds. 32
Figure 16. Hurricane Isabel wind validation stations.......... 33
Figure 17. Comparisons of Hurricane Isabel wind speeds at each validation station.......... 34
Figure 18. Comparisons of Hurricane Isabel wind directions at each validation station.......... 35
Figure 19. Hurricane Isabel wind speed scatter plots. 36
Figure 20. Hurricane Ernesto maximum wind speeds. 37
Figure 21. Hurricane Ernesto wind validation stations. 37
Figure 22. Comparisons of Hurricane Ernesto wind speeds at each validation station. 38
Figure 23. Comparisons of Hurricane Ernesto wind directions at each validation station.......... 39
Figure 24. Hurricane Ernesto wind speed scatter plots. 40
Figure 25. Extratropical Storm Nor'Ida maximum wind speeds.......... 41
Figure 26. Extratropical Storm Nor'Ida wind validation stations. 42
Figure 27. Comparisons of Extratropical Storm Nor'Ida wind speeds at each validation station.......... 43
Figure 28. Comparisons of Extratropical Storm Nor'Ida wind directions at each validation station.......... 44
Figure 29. Extratropical Storm Nor'Ida wind speed scatter plots.......... 45
Figure 30. Wind peak event analysis results for (a) wind speed, and (b) wind direction.......... 47
Figure 31. Wave validation stations used in the Region III study.......... 51

Figure 32. Hurricane Isabel SWAN output fields. 52

Figure 33. Hurricane Isabel bulk wave height and period time series from Station 44056 53

Figure 34. Hurricane Isabel bulk wave height, period, and direction time series from Taylors Island Station. 54

Figure 35. Hurricane Isabel bulk wave height and period time series from Station 44009 55

Figure 36. Scatter plot comparison of Hurricane Isabel observed and hindcast wave heights. 55

Figure 37. Hurricane Ernesto SWAN output fields. 57

Figure 38. Hurricane Ernesto bulk wave height and period time series from Station 44014. 58

Figure 39. Hurricane Ernesto bulk wave height and period time series from Station 44009. 58

Figure 40. Scatter plot comparison of Hurricane Ernesto observed and hindcast wave heights. 59

Figure 41. Extratropical Storm Nor'Ida SWAN output fields. 60

Figure 42. Extratropical Storm Nor'Ida bulk wave height and period time series from Station 44014. 61

Figure 43. Extratropical Storm Nor'Ida bulk wave height and period time series from Station 44009. 62

Figure 44. Extratropical Storm Nor'Ida bulk wave height and period time series from the Norfolk City Station 63

Figure 45. Sample directional wave spectra from the Norfolk City wave gage during Extratropical Storm Nor'Ida. 64

Figure 46. Scatter plot comparison of Extratropical Storm Nor'Ida observed and hindcast wave heights. 65

Figure 47. Results of peak event analysis. 66

Figure 48. Time series of water level amplitudes for NOAA Station 8638610, Sewells Point, VA, for Hurricane Ernesto. 68

Figure 49. Example of residual tide signals in both modeled and observed detided water levels, NOAA Station 8536110, for Nor'Ida. 70

Figure 50. Location of NOS stations meeting preliminary criteria. 73

Figure 51. Examples of NOS stations not adequately resolved by the ADCIRC mesh 74

Figure 52. Location of NOS Stations used for storm surge validation, Region III. 75

Figure 53. Location of USGS rapid response storm surge gauges deployed for Nor'Ida. 76

Figure 54. Maximum water elevation as modeled during Hurricane Isabel by SWAN+ADCIRC. 77

Figure 55. Examples of successful SWAN+ADCIRC water level versus observations, Isabel, Stations 8551762 and 8638610. 79

Figure 56. Low-scoring SWAN+ADCIRC water level versus observations, Isabel, NOS 8536110. Water level. 79

Figure 57. Peak event analysis, SWAN+ADCIRC versus NOAA high water level, Hurricane Isabel. 80

Figure 58. Map of modeled HWM data versus observed HWM data, Hurricane Isabel. 82

Figure 59. High-water mark (HWM) data scatter plot for Hurricane Isabel. 83

Figure 60. Maximum water elevation as modeled during Hurricane Ernesto by SWAN+ADCIRC. Dashed black line indicates the storm's track across Region III. 84

Figure 61. Examples of successful SWAN+ADCIRC water level versus observations, Ernesto, Stations 8536110 and 8637689. 86

Figure 62. Station 8573364, Ernesto Water levels. 87

Figure 63. Peak event analysis, SWAN+ADCIRC versus NOAA high water level, Hurricane Ernesto. 87
Figure 64. Maximum water elevation as modeled during Nor'Ida by SWAN+ADCIRC. 88
Figure 65. Examples of successful SWAN+ADCIRC water level versus observations, Nor'Ida, Stations 8536110 and 8632200. 91
Figure 66. Unsuccessful SWAN+ADCIRC water level versus observations, Nor'Ida, Stations 8548989, 8571892, and 8573364. 92
Figure 67. Water level time series for NOS 8551910, Nor'Ida. 93
Figure 68. Peak event analysis, SWAN+ADCIRC versus NOAA high water level, Nor'Ida. 93
Figure 69. Extremes analysis station examples, Nor'easter Nor'Ida 94
Figure 70. Examples of successful SWAN+ADCIRC water level versus observations, Nor'Ida Stations 1136780 and 1136784. 95
Figure 71. Peak event analysis for SWAN+ADCIRC versus USGS rapid response stations, Nor'Ida. 97
Figure 72. Final water level peak event analysis results for Region III. 99
Figure A1. NOAA water level station locations for Detided TidesWindsWaves, Isabel. 102
Figure A2. High-water level extremes analysis, Detided TidesWindsWaves, Isabel. 103
Figure B1. NOAA water level station locations for Detided TidesWindsWaves, Ernesto. 137
Figure B2. High-water level extremes analysis, Detided TidesWindsWaves, Ernesto. 138
Figure C1. NOAA water level station locations for Detided TidesWindsWaves, Nor'Ida. 175
Figure C2. High-water level extremes analysis, Detided TidesWindsWaves, Nor'Ida. 176
Figure D1. USGS real-time water level station locations for TidesWindsWaves, Nor'Ida. 213
Figure D2. High-water level extremes analysis, TidesWindsWaves, Nor'Ida. 214
Figure E1. NOAA water level station locations for TidesWindsWaves, Isabel. 226
Figure E2. NOAA water level station locations for TidesWindsWaves, Ernesto. 236
Figure E3. NOAA water level station locations for TidesWindsWaves, Nor'Ida. 244

Tables

Table 1. Study team. 2
Table 2. Contents of the Submittal 1 reports. 3
Table 3. Tidal constituents used for open boundary and tidal potential forcing. 7
Table 4. Location of NOAA NOS stations used in tidal analysis. 8
Table 5. Observed tides at four representative stations. 9
Table 6. Modeled and observed M_2 amplitude (m) and phase (deg UTC) at the NOS station locations. 12
Table 7. Modeled and observed K_1 amplitude (m) and phase (deg UTC) at the NOS station locations. 13
Table 8. Tidal time series comparison statistics. 21
Table 9. IMEDS evaluation parameters. 27
Table 10. Validation events and available wave observations. 30
Table 11. Wind validation station details. 30
Table 12. Hindcast winds performance summary. 31

Table 13. Hurricane Isabel wind statistics. 36
Table 14. Hurricane Ernesto wind statistics. 41
Table 15. Extratropical Storm Nor'Ida wind statistics. 46
Table 16. Validation events and available wave observations. 50
Table 17. Wave validation station details. 50
Table 18. SWAN overall performance summary. 50
Table 19. Hurricane Isabel wave hindcast performance statistics. 56
Table 20. Hurricane Ernesto Wave Hindcast Performance Statistics 59
Table 21. Extratropical Storm Nor'Ida wave hindcast performance statistics. 65
Table 22. Statistics for NOAA water level gauge comparisons, Hurricane Isabel. 78
Table 23. Statistics for NOAA water level gauge comparisons, Hurricane Ernesto. 85
Table 24. Statistics for NOAA water level gauge comparisons, Nor'Ida. 90
Table 25. Statistics for USGS rapid response storm surge gauge comparisons, Nor'Ida. 96
Table 26. Percent differences (upper table in m; lower table in ft) between SWAN+ADCIRC and observed peak storm surge. 98

Preface

This study was conducted for the Federal Emergency Management Agency (FEMA) under Project HSFE03-06-X-0023, NFIP Coastal Storm Surge Model for Region III and Project HSFE03-09-X-1108, Phase II Coastal Storm Surge Model for FEMA Region III. The FEMA technical monitor was Robin Danforth.

The work was performed by the Coastal Processes Branch of the Flood and Storm Protection Division, U.S. Army Engineer Research and Development Center – Coastal and Hydraulics Laboratory (CHL). At the time of publication, Dr. Ty V. Wamsley was Chief, Coastal Processes Branch; Bruce Ebersole was Chief, Flood and Storm Protection Division; and Dr. Jeffrey L. Hanson was the Project Manager. The Deputy Director of CHL was Jose E. Sanchez and the Director was Dr. William D. Martin.

COL Kevin J. Wilson was the ERDC Commander, and Dr. Jeffery P. Holland was the Director.

Unit Conversion Factors

Multiply	By	To Obtain
degrees (angle)	0.01745329	radians
fathoms	1.8288	meters
feet	0.3048	meters
inches	0.0254	meters
knots	0.5144444	meters per second
miles (nautical)	1,852	meters
miles (U.S. statute)	1,609.347	meters
square miles	2.589998 E+06	square meters
square yards	0.8361274	square meters
yards	0.9144	meters

1 Overview

The Federal Emergency Management Agency (FEMA) is responsible for preparing Flood Insurance Rate Maps (FIRMs) that delineate flood hazard zones in coastal areas of the United States. Under Task Order HSFE03-06-X-0023, the US Army Corps of Engineers (USACE) and project partners are assisting FEMA in the development and application of a state-of-the-art storm surge risk assessment capability for the FEMA Region III domain. This domain includes the Delaware Bay, Chesapeake Bay, District of Columbia, Delaware-Maryland-Virginia Eastern Shore, Virginia Beach, and all tidal tributaries and waterways connected to these systems. The goal is to develop and apply a complete end-to-end modeling system, with all required forcing inputs, for updating the floodplain levels for coastal and inland watershed communities. Key components of this work include the following:

- Develop a high-resolution Digital Elevation Model (DEM) for Region III, and convert this to an unstructured modeling grid, with up to 50-m horizontal resolution, for use with the production system
- Define the Region III storm hazard in terms of historical extratropical storms and synthetic hurricane parameters
- Prepare an end-to-end modeling system for assessment of Region III coastal storm surge and wave hazards
- Perform a comprehensive tidal calibration and verify model accuracy on a variety of reconstructed tropical and extratropical storm events
- Apply the modeling system to compute the 10-, 50-, 100-, and 500-year floodplain levels
- Develop a database with GIS tools to facilitate archiving, distribution, and analysis of the various storm surge data products

Under the direction of the FEMA Region III Program Manager, Robin Danforth, USACE assembled a multi-organization partnership to meet the Region III objectives. Work on this project has made extensive use of the capabilities and technology developed for the North Carolina Floodplain Mapping Program (NCFMP). The availability of the NCFMP storm surge modeling system (Blanton et al. 2008) has resulted in a significant cost savings for FEMA Region III. Experts in the fields of coastal storm surge, wind-driven waves, Geospatial Information Systems (GIS), and high-performance computational systems have worked together in this effort. The project partners and their primary roles are listed in Table 1.

Table 1. Study team.

Organization	Contacts	Primary Role(s)
US Army Corps of Engineers Field Research Facility (USACE-FRF)	Jeff Hanson Mike Forte Heidi Wadman	Project Manager DEM Construction Model Validations
Applied Research Associates/IntraRisk (ARA)	Peter Vickery	Simulated Hurricanes
ARCADIS	Hugh Roberts John Atkinson Shan Zou	Modeling Mesh Modeling Mesh Modeling Mesh
Elizabeth City State University	Jinchun Yuan	Web/GIS
Oceanweather	Vince Cardone Andrew Cox	Wind Field Reconstructions
Renaissance Computing Institute (RENCI)	Brian Blanton Lisa Stillwell Kevin Gamiel	Modeling System DEM Construction Database/Web/GIS
University of North Carolina- Chapel Hill (UNC-CH)	Rick Luettich	Technical Oversight
US Army Corps of Engineers District Offices (NAP, NAO, NAB)	Jason Miller Paul Moye Jared Scott	Bathy/Topo Data Inventory

In addition to the study team, a Technical Oversight Group provided guidance and input to all project phases. This group included members from the following organizations:

- Chesapeake Bay Research Consortium
- Delaware Flood Mitigation Program
- Federal Emergency Management Agency
- Dewberry, Inc.
- North Carolina Floodplain Mapping Program
- USACE Engineer Research and Development Center

A series of three prior reports (Forte et al. 2011; Blanton et al. 2011; Vickery et al., in preparation) covered preliminary documentation (Submittal 1) requirements by providing details on the following: (1) construction of the bathymetric/topographic digital environmental model, (2) preparation of the modeling system including development of the ADCIRC mesh, and (3) the process for selecting the storms used in this study. The contents of each Submittal 1 report are listed in Table 2.

Table 2. Contents of the Submittal 1 reports.

Report	Title	Contents
1.1	FEMA Region III Coastal Storm Surge Analysis: System Digital Elevation Model (DEM)	Project Overview Study Area DEM Development
1.2	FEMA Region III Coastal Storm Surge Analysis: Computational System	Modeling System Mesh Development
1.3	FEMA Region III Coastal Storm Surge Analysis: Storm Forcing	Hurricane Parameters Extratropical Storms

This report (Submittal 2) completes the required Submittal 2 documentation by providing details of the modeling system calibration and performance. Guidelines for study conduct and documentation appear in FEMA (2007).

The following sections detail the calibration and validation of a state-of-the-art computational storm surge system for the FEMA Region III, and provide the following information:

- Descriptions of improvements made to the modeling mesh since Submittal 1.2
- A review of the tidal validation results
- A description of the three validation storms
- Quantitative assessments of modeling system performance in hindcasting winds, waves, and water levels in the Region III domain

2 Mesh Updates

Several improvements have been made to the SWAN+ADCIRC modeling mesh since the original development described in Submittal 1.2 (Blanton et al. 2011). Specifically, mesh edits have been completed in specific areas throughout the domain to address the following (Roberts 2011):

- Comments by the FEMA review team (RAMPP), including concerns about model resolution and depths near the coastline
- Comments by external reviewers
- Areas of concern discovered during the tidal and storm validation process, which include model inaccuracies and model instabilities
- Adjustment to the boundary conditions to incorporate flow rates into the system from the Delaware, Potomac, and Susquehanna Rivers

Most of the coastal resolution issues were resolved by editing the DEM (Forte et al. 2011) and re-interpolating the DEM onto the mesh. In specific cases where the DEM was not edited to resolve issues, improvements were made by either re-triangulating the mesh or editing the elevations assigned in the mesh. Re-triangulation was done to better conform to features or add resolution where necessary. Mesh elevations were adjusted using available sources such as nautical charts and satellite imagery. In a few cases where no data were available, experienced engineering judgment was applied.

The primary edits completed in response to external review were in the Lewes, Delaware area. During validation, a reviewer noted that surge was not adequately entering the Cape Henlopen State Park area. After examining the mesh, it was determined that the channel that crosses Lewes and connects the state park with Delaware Bay was not adequately resolved. Resolution was thus increased in this area to properly reflect the conveyances in the area.

Aside from the edits in Lewes, three additional edits were completed in response to validation results. First, bathymetric values on the Atlantic side of the Delmarva Peninsula were adjusted in the mesh using nautical charts and a tidal mesh provided by NOAA. Secondly, the area adjacent to the Chesapeake Bay Bridge Tunnel was better resolved to capture features such as the Thimble Islands. Lastly, any areas in which the model went unstable were adjusted by strategically increasing resolution to stabilize the mesh. The most notable edit of this type was in a narrow channel northeast of Washington DC.

The last major mesh edits incorporated river flux boundary conditions for the Delaware, Potomac, and Susquehanna Rivers. At these locations, the model boundary was adjusted to strategically locate the boundary at an area with adequate channel depth and width. Resolution was increased at all three locations to better capture incoming flows.

3 Tidal Calibrations

The first step in validating the modeling system is to evaluate the performance of modeling the tides. In many East Coast areas, tides are the largest source of water level variability. Accurate simulation of tides reflects the accuracy of the model grid's bathymetry, the accuracy of the tidal boundary conditions, and the appropriate selection of frictional parameters in the model.

The Region III area is represented by a high-resolution finite element mesh, which itself is embedded in a coarser background mesh of the western North Atlantic ocean, west of 60 deg W (Figure 1). This simplifies boundary condition application substantially, since the only open boundary is at 60 deg W. Boundary conditions for the tidal elevations are extracted from the most recent regional Atlantic Ocean Inverse Solution of the TOPEX (Egbert and Erofeeva 2002). The constituents used are M_2, N_2, S_2, K_2, K_1, O_1, P_1, and Q_1. The same constituents are used for tidal potential forcing. The constituent characteristics are given in Table 3, and the boundary conditions are reported in the ADCIRC fort.15 file for the tidal simulation.

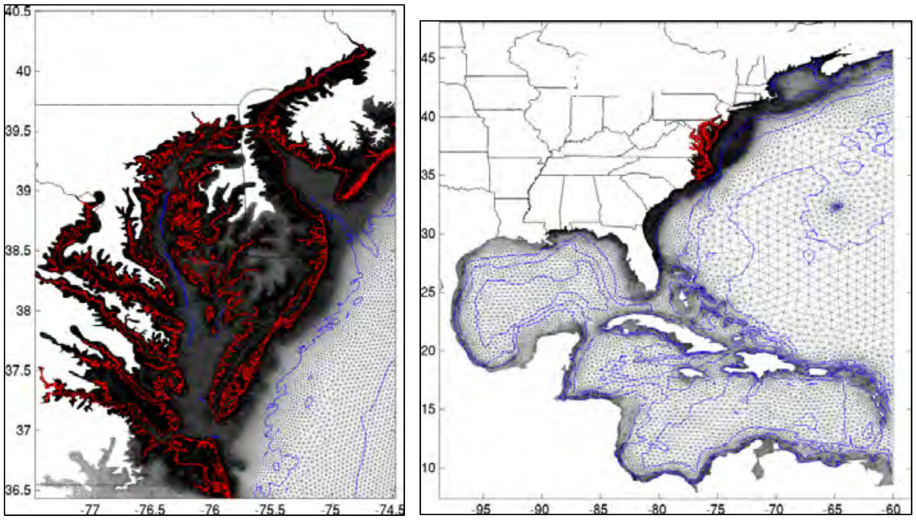

Figure 1. ADCIRC finite element grid for the Region III project. Left) the high-resolution part of the grid in the region. There are about 1.8 million nodes in the region. The red line indicates mean sea level, with the 25- and 100-m isobaths shown with blue lines. Right) the entire grid, showing the coarse resolution outside the area of interest. The red line indicates mean sea level in the region, with the 100-, 1000-, 3000-, and 5000-m isobaths shown with blue lines.

Table 3. Tidal constituents used for open boundary and tidal potential forcing.

Const.	Per [hr]	Freq [rad/sec]	Tidal Pot. Amp [m]	Earth Elast. Fac.	Description
M_2	12.42	0.5058	0.242334	0.693	Principal lunar semidiurnal diurnal
N_2	12.66	0.4964	0.046398	0.693	Larger lunar elliptic semidiurnal
S_2	12.00	0.5236	0.112841	0.693	Principal solar semidiurnal
K_2	11.97	0.5250	0.030704	0.693	Lunisolar semidiurnal
K_1	23.93	0.2625	0.141565	0.736	Lunisolar diurnal
O_1	25.82	0.2434	0.100514	0.695	Principal lunar diurnal
P_1	24.07	0.2611	0.046843	0.706	Principal solar diurnal
Q_1	26.87	0.2339	0.019256	0.695	Larger lunar elliptic diurnal

3.1 Tidal observations in the region

There are many NOAA NOS stations in the region that provide tidal harmonic constants (Table 4). Station locations range from open coast to riverine. Examination of the tidal harmonics at these stations shows that the largest constituent is M_2 (main semi-diurnal), followed by lesser constituents. Table 5 reports the 10 largest tidal constituents at 4 representative stations in the region. The constituent amplitudes at each station are sorted in descending order. Note that semi-diurnal M_2 is always the largest tide, and the next largest tide at each station is either the semidiurnal N_2 or the long period steric anomaly (SA).

Harmonic analysis of the observed water level at each station was performed for the years 2002-2004. The resulting tidal variance was then compared to the total water level variance. Figure 2 shows the percent of the total variance explained by the tidal analysis. Overall, tidal variability explains 45-95% of the total water level variance, with a strong dependence on the location of the tide gauge. Open coast and Delaware Bay locations are dominated by tides, whereas less variance can be explained by tides in the more sheltered stations in Chesapeake Bay.

3.2 Model and run setup

For the tidal validation simulation, ADCIRC version 49.28 was used, in two-dimensional, depth-integrated mode. All nonlinearities are included (finite amplitude, advection, time derivative terms, and bottom friction). The time weighting factors for the Generalized Wave Continuity Equation (GWCE)

Table 4. Location of NOAA NOS stations used in tidal analysis.

Station ID	Long.	Lat.	Station Description
8536110	-74.9600	38.9683	Cape May Ferry Terminal, NJ
8537121	-75.3750	39.3005	Ship John Shoal, DE
8551762	-75.5838	39.5817	Delaware City, DE
8551910	-75.5733	39.5583	Reedy Point, DE
8555889	-75.1133	38.9837	Brandywine Shoal Light, DE
8557380	-75.1170	38.7817	Lewes, DE
8540433	-75.4010	39.8117	Marcus Hook, PA
8545240	-75.1417	39.9333	Philadelphia, PA
8548989	-74.7517	40.1337	Newbold, PA
8570283	-75.0917	38.3283	Ocean City Inlet, MD
8571892	-76.0683	38.5733	Cambridge, MD
8573364	-76.2450	39.2133	Tolchester Beach, MD
8573927	-75.8010	39.5177	Chesapeake City, MD
8574680	-76.5783	39.2667	Baltimore, MD
8575512	-76.4800	38.9833	Annapolis, MD
8577330	-76.4517	38.3167	Solomons Island, MD
8571421	-76.0380	38.2200	Bishops Head, MD
8571559	-76.0050	38.3000	McCreadys Creek, MD
8594900	-77.0172	38.8733	Washington, DC
8632200	-75.9838	37.1650	Kiptopeake, VA
8635750	-76.4633	37.9950	Lewisetta, VA
8636580	-76.2900	37.6150	Windmill Point, VA
8638610	-76.3300	36.9467	Sewells Point, VA
8638863	-76.1133	36.9667	Chesapeake Bay Bridge Tunnel, VA
8639348	-76.3017	36.7783	Money Point, VA
8637624	-76.5000	37.2466	Gloucester Point, VA
8632837	-76.0150	37.5380	Rappahannock Light, VA
8637689	-76.4780	37.2270	Yorktown USGS Training Center, VA
8651370	-75.7466	36.1833	Duck Pier, NC

Table 5. Observed tides at four representative stations (Duck Pier, NC, is included for reference). For each station, the 10 largest amplitude tidal constituents are reported, as well as the cumulative percentage of the total tidal water level.

Tidal Constituent	8555889			8545240			8575512			8651370		
	Brandywine Light Shoals, DE			Philadelphia, PA			Annapolis, MD			Duck Pier, NC		
	Const	Amp (m)	% Tide	Const	Amp (m)	% Tide	Const	Amp (m)	% Tide	Const	Amp (m)	% Tide
1	M_2	0.72	43	M_2	0.84	39	M_2	0.14	27	M_2	0.49	44
2	N_2	0.16	53	SA	0.15	46	SA	0.10	46	N_2	0.11	54
3	S_2	0.12	60	N_2	0.15	53	K_1	0.06	58	S_2	0.09	62
4	K_1	0.10	66	K_1	0.10	57	O_1	0.05	67	K_1	0.09	70
5	SA	0.10	72	S_2	0.09	62	SSA	0.04	75	O_1	0.06	76
6	O_1	0.08	77	L_2	0.09	66	N_2	0.03	81	SA	0.06	81
7	SSA	0.07	81	SSA	0.09	70	S_2	0.02	85	SSA	0.04	85
8	MSF	0.04	83	M_4	0.08	74	S_1	0.02	88	P_1	0.03	87
9	L_2	0.04	86	O_1	0.08	77	P_1	0.02	92	NU_2	0.02	89
10	K_2	0.04	88	M_6	0.05	80	L_2	0.01	94	K_2	0.02	91

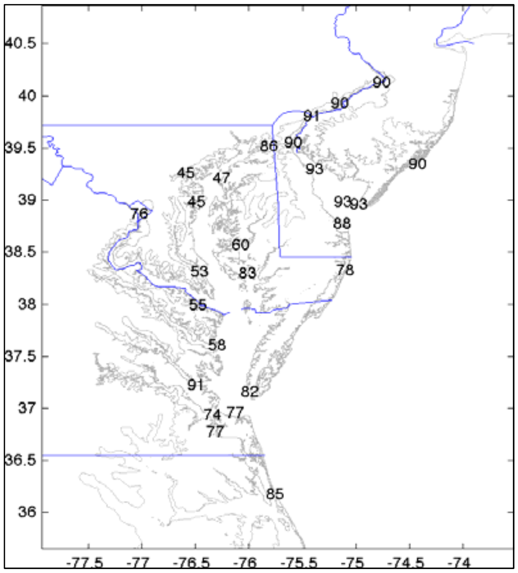

Figure 2. Spatial distribution of total water level variance explained by tides. Harmonic analysis was performed on observed water levels over the period 01 Jan 2001 through 31 Dec 2004, and the variance of the tidal content and total water levels was evaluated.

are (0.00, 1.00, and 0.00). The exact ADCIRC input parameter file (fort.15) is included in the project data files. The equilibrium tides were simulated for a period of 77 days, with a ramp-up time of 10 days. The harmonic analysis was performed on the global solution over the period of 10-77 days.

3.3 Characteristics of the modeled tides in the region

As is typical of tides on the US East Coast, the tides in Region III are largely semi-diurnal, dominated by the primary lunar tide M_2. Semi-diurnal tides are amplified across the continental shelf. The largest diurnal tide is usually K_1 or O1. Smaller contributions to the total tide are made by the other semi-diurnal and diurnal tides, as well as the nonlinear, shallow-water tides.

The M_2 tide is shown in Figure 3. It is generally the largest tidal component, with an amplitude of about 0.35 m at the continental shelf break, with an increasing amplitude across the shelf to about 0.50-0.60 m near the coastline. M_2 is substantially amplified in Delaware Bay to about 0.75 m along the northern shore, and then to about 0.85 m up the Delaware River. M_2 is substantially damped as it propagates through the Chesapeake Bay entrance, decreasing to about 0.20-0.25 m throughout the bay. The K_1 (Figure 4) tide is comparatively flat across the continental shelf at about 0.09 m, and is damped to about 0.03-0.06 m as it propagates into and up Chesapeake Bay. It is relatively undamped in Delaware Bay. Note that M_2 is about an order of magnitude larger than K_1.

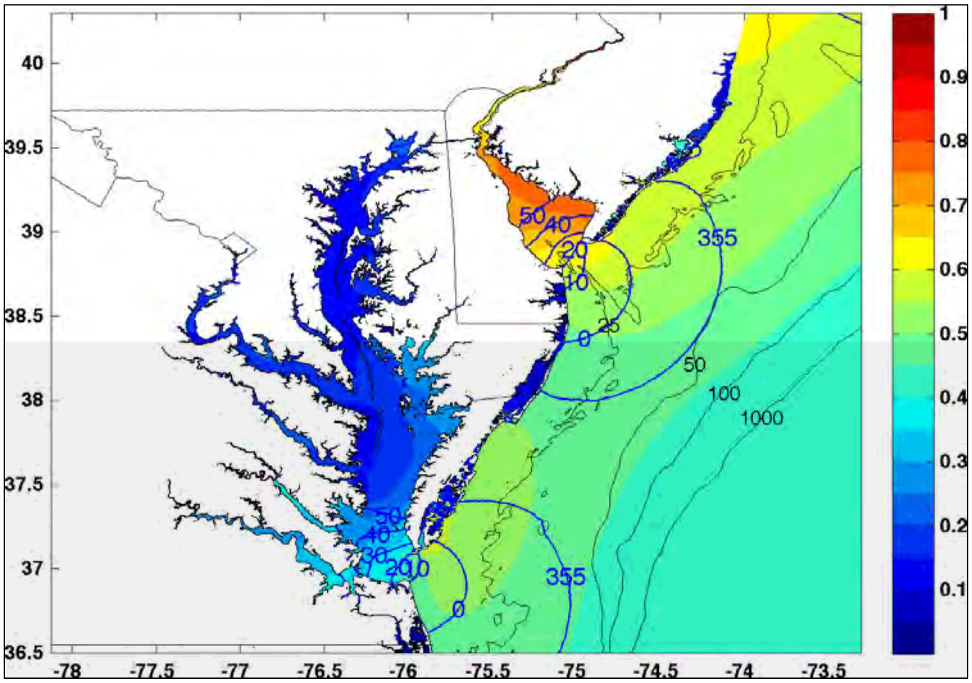

Figure 3. M_2 elevation [m] and phase [degrees UTC] from equilibrium tidal simulation. Phase is shown with the blue contour lines; only contours in the vicinity of the bay entrances are shown for clarity. Contours of bathymetry [m MSL] are shown with the black lines.

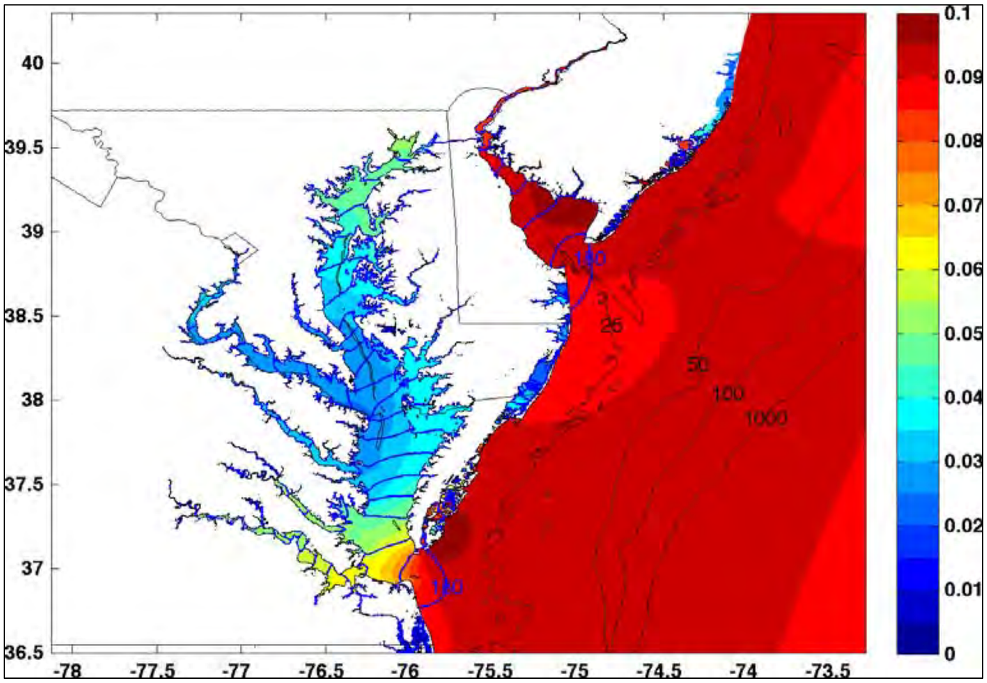

Figure 4. K_1 elevation [m] and phase [degrees UTC] from equilibrium tidal simulation. Phase is shown with the blue contour lines at 10-degree increments starting at 180 degrees. Contours of bathymetry [m MSL] are shown with the black lines.

Tables 6 and 7 report the modeled and observed M_2 and K_1 tidal amplitudes and phases at the NOS stations. M_2 and K_1 are the main semi-diurnal and diurnal tidal constituents in the region. The amplitudes and phases generally agree well, with root-mean-square errors (RMSE) of 0.03 m/7 deg and 0.01 m/8 deg for M_2 and K_1, respectively. While there are a few locations where the K_1 phase difference is relatively high, this constituent is relatively small. Figure 5 shows the same amplitudes as Figures 3 and 4, but with the M_2 and K_1 amplitude error included as colored dots.

Figure 6 shows the M_2 and K_1 tidal amplitudes and phases as scatter plots. The M_2 amplitudes are well represented by the ADCIRC tidal simulation, and the phases show a slight low bias at the Maryland stations. Overall, the distribution of the amplitude errors (Figure 7) is unbiased with means and standard deviations of about 0.0 and 0.03 m for M_2, and 0.0 and 0.01 m for K_1.

For the tidal comparison, time series of predicted and simulated water levels have been reconstructed from NOAA-reported and ADCIRC-modeled amplitudes and phases for the month of October 2006. Among the 37 NOS constituents, 14 tidal constituents were identified as being in common. Those 14 constituents were harmonically analyzed by ADCIRC: $2SM_2$, K_1,

Table 6. Modeled and observed M_2 amplitude (m) and phase (deg UTC) at the NOS station locations.

Station ID	M_2 Amp ADC	M_2 Pha ADC	M_2 Amp NOS	M_2 Pha NOS	Station Description
8531680	0.72	357	0.69	6	Sandy Hook, NJ
8534720	0.56	354	0.59	355	Atlantic City, NJ
8536110	0.74	22	0.71	29	Cape May Ferry Terminal, NJ
8537121	0.86	62	0.83	72	Ship John Shoal, DE
8551762	0.76	101	0.74	114	Delaware City, DE
8551910	0.76	97	0.77	109	Reedy Point, DE
8555889	0.75	30	0.72	37	Brandywine Shoal Light, DE
8557380	0.63	26	0.62	31	Lewes, DE
8540433	0.73	140	0.78	146	Marcus Hook, PA
8545240	0.87	175	0.84	186	Philadelphia, PA
8548989	1.17	197	1.07	220	Newbold, PA
8570283	0.37	4	0.32	8	Ocean City Inlet, MD
8571892	0.22	236	0.24	263	Cambridge, MD
8573364	0.19	329	0.17	347	Tolchester Beach, MD
8573927	0.44	87	0.43	94	Chesapeake City, MD
8574680	0.18	324	0.16	337	Baltimore, MD
8575512	0.14	284	0.14	292	Annapolis, MD
8577330	0.17	184	0.17	199	Solomons Island, MD
8571421	0.27	169	0.27	182	Bishops Head, MD
8571559	0.34	176	0.31	192	McCreadys Creek, MD
8594900	0.33	28	0.41	20	Washington, DC
8632200	0.38	30	0.39	33	Kiptopeke, VA
8635750	0.18	168	0.18	176	Lewisetta, VA
8636580	0.17	100	0.17	103	Windmill Point, VA
8638610	0.36	45	0.37	47	Sewells Point, VA
8638863	0.39	21	0.38	21	Chesapeake Bay Bridge Tunnel, VA
8639348	0.39	51	0.42	54	Money Point, VA
8637624	0.34	51	0.36	54	Gloucester Pt., VA
8632837	0.22	83	0.24	87	Rappahannock Light, VA
8637689	0.33	51	0.34	52	Yorktown USGS Training Center, VA
8651370	0.47	358	0.49	358	Duck Pier, NC
RMSE	0.03	7			

Table 7. Modeled and observed K_1 amplitude (m) and phase (deg UTC) at the NOS station locations.

Station ID	K_1 Amp ADC	K_1 Pha ADC	K_1 Amp NOS	K_1 Pha NOS	Station Description
8531680	0.10	176	0.10	176	Sandy Hook, NJ
8534720	0.09	177	0.11	183	Atlantic City, NJ
8536110	0.09	185	0.10	200	Cape May Ferry Terminal, NJ
8537121	0.10	208	0.10	221	Ship John Shoal, DE
8551762	0.09	234	0.10	247	Delaware City, DE
8551910	0.08	232	0.09	244	Reedy Point, DE
8555889	0.09	189	0.10	203	Brandywine Shoal Light, DE
8557380	0.09	188	0.10	202	Lewes, DE
8540433	0.09	254	0.10	262	Marcus Hook, PA
8545240	0.10	269	0.10	284	Philadelphia, PA
8548989	0.10	279	0.11	299	Newbold, PA
8570283	0.06	183	0.06	208	Ocean City Inlet, MD
8571892	0.05	330	0.05	340	Cambridge, MD
8573364	0.06	359	0.07	3	Tolchester Beach, MD
8573927	0.03	299	0.03	344	Chesapeake City, MD
8574680	0.06	1	0.07	8	Baltimore, MD
8575512	0.05	349	0.06	357	Annapolis, MD
8577330	0.03	308	0.03	316	Solomons Island, MD
8571421	0.04	274	0.04	283	Bishops Head, MD
8571559	0.04	275	0.04	282	McCreadys Creek, MD
8594900	0.04	23	0.05	357	Washington, DC
8632200	0.07	197	0.06	193	Kiptopeke, VA
8635750	0.03	282	0.02	276	Lewisetta, VA
8636580	0.03	235	0.03	227	Windmill Point, VA
8638610	0.07	206	0.05	201	Sewells Point, VA
8638863	0.07	191	0.06	185	Chesapeake Bay Bridge Tunnel, VA
8639348	0.07	210	0.05	201	Money Point, VA
8637624	0.06	208	0.05	198	Gloucester Pt., VA
8632837	0.04	226	0.04	222	Rappahannock Light, VA
8637689	0.06	208	0.04	189	Yorktown USGS Training Center, VA
8651370	0.09	177	0.09	173	Duck Pier, NC
RMSE	0.01	8			

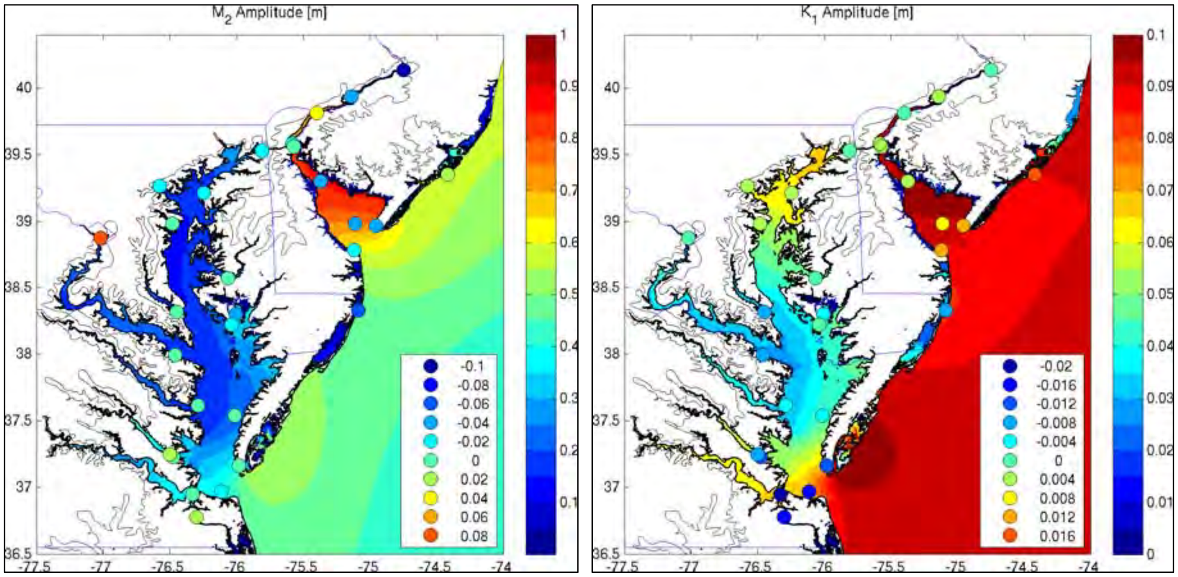
M2 Amplitude [m]
K1 Amplitude [m]
40
39.5
39
38.5
38
37.5
37
36.5
-77.5
-77
-76.5
-76
-75.5
-75
-74.5
-74
-0.1
-0.08
-0.06
-0.04
-0.02
0
0.02
0.04
0.06
0.08
-0.02
-0.016
-0.012
-0.008
-0.004
0
0.004
0.008
0.012
0.016
1
0.9
0.8
0.7
0.6
0.5
0.4
0.3
0.2
0.1
0.1
0.09
0.08
0.07
0.06
0.05
0.04
0.03
0.02
0.01
0

Figure 5. Amplitude of M_2 and K_1 tides. The error (observed – modeled) between the observed and modeled amplitudes is shown with the colored dots. Note that the range of values represented by the color map differs between the two panels.

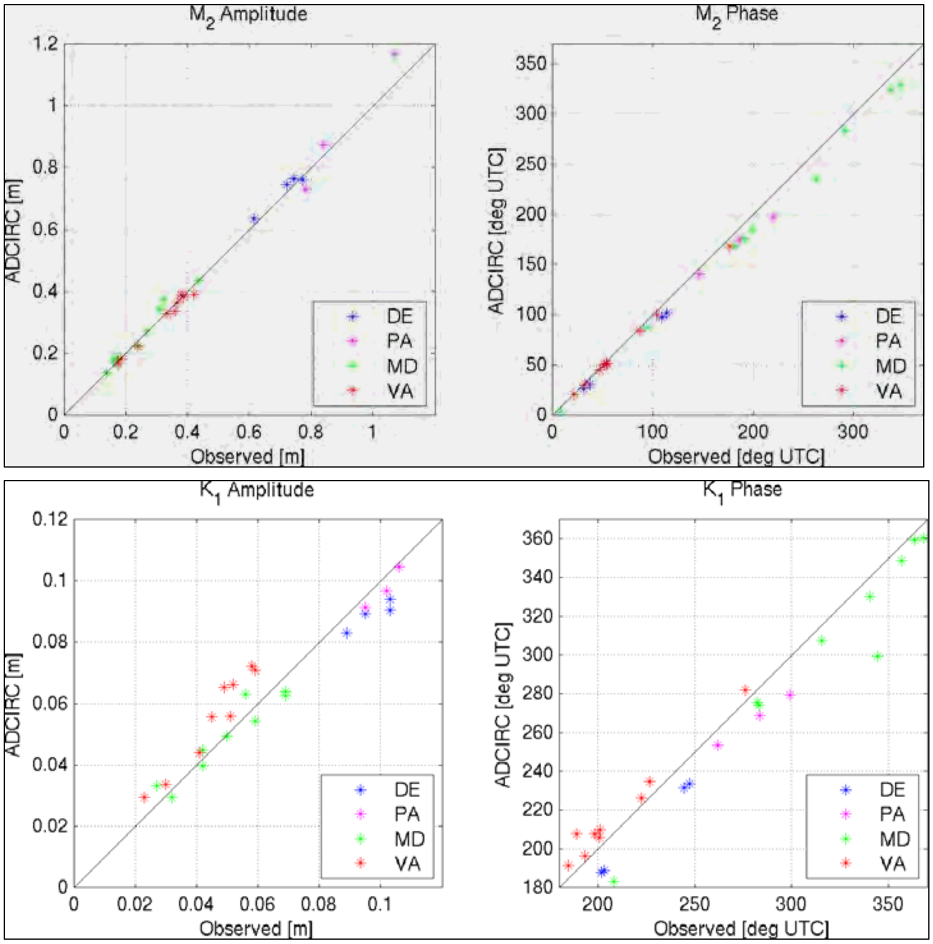

Figure 6. Scatter plots of the M_2 and K_1 modeled and observed tidal amplitude.

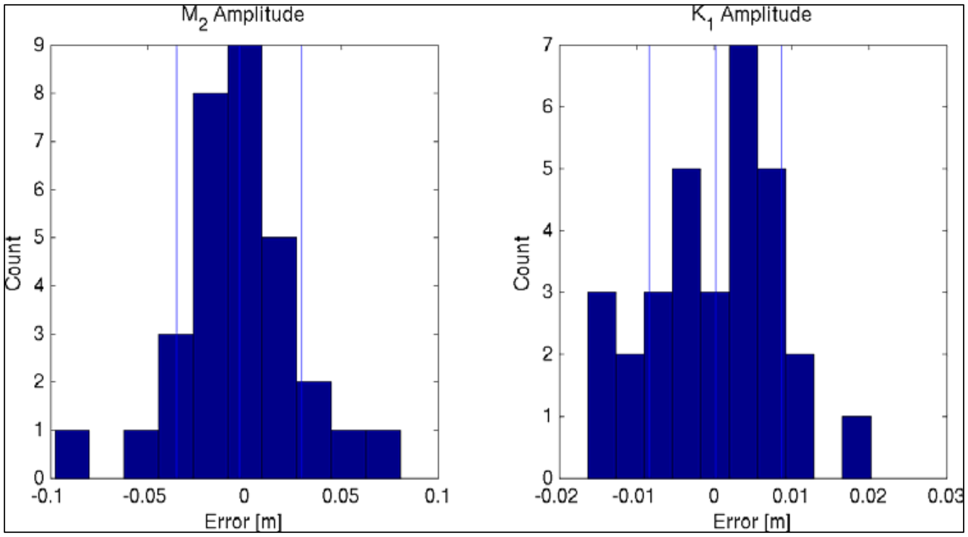

Figure 7. Histogram of errors in the M_2 and K_1 tidal amplitudes. The thin blue lines are the mean and one standard deviation values.

K_2, M_2, M_4, M_6, M_8, MN_4, MS_4, N_2, O_1, P_1, Q_1, and S_2. These 14 tidal constituents account for 94-95% of the tidal variance in the NOS-predicted water levels at the station locations. The temporal resolution of the 31-day time series is 6.0 min, set to match the NOAA-reported raw time series of water level observations. Nodal factors and equilibrium arguments are included to adjust the amplitude and phase of both NOAA-predicted and ADCIRC-modeled tides to the date-specific starting time of the analysis.

Time series reconstructions are shown in Figures 8-12. Results for the phase-shifted and unadjusted tidal comparisons are shown in Table 8. Generally, the root-mean-square error (RMSE) is small, from 0.01-0.17 m, except at Newbold, PA (RMSE of 0.34). Correlation coefficients are between 0.90 and 1.00. In general, the modeled tides are slightly early, and a 6- to 54-min phase shift in the modeled time series lowers the RMSE to 0.01-0.07 m and to 0.10 m at Newbold, PA. The phase-shifted time series brings the correlation coefficients up to 0.99 to 1.00.

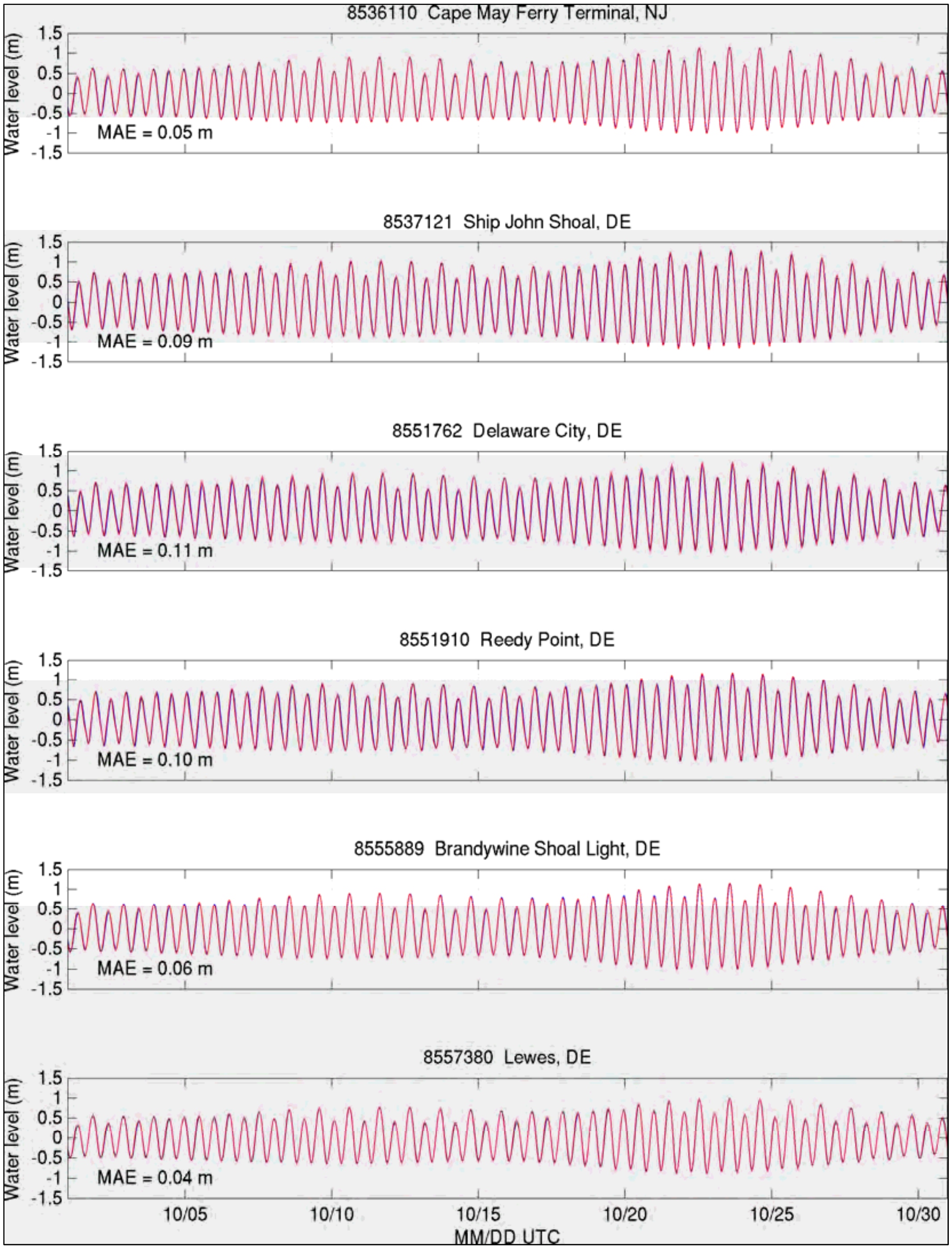

Figure 8. Time series plots for October 2006 of reconstructed tidal water levels at NOAA NOS Delaware stations, as well as the Cape May Ferry Terminal station. The time series are reconstructed from the tidal harmonic constituents in common between the NOAA NOS published harmonics and the ADCIRC harmonic analysis. MAE is the mean absolute error of the difference between the modeled and observed time series.

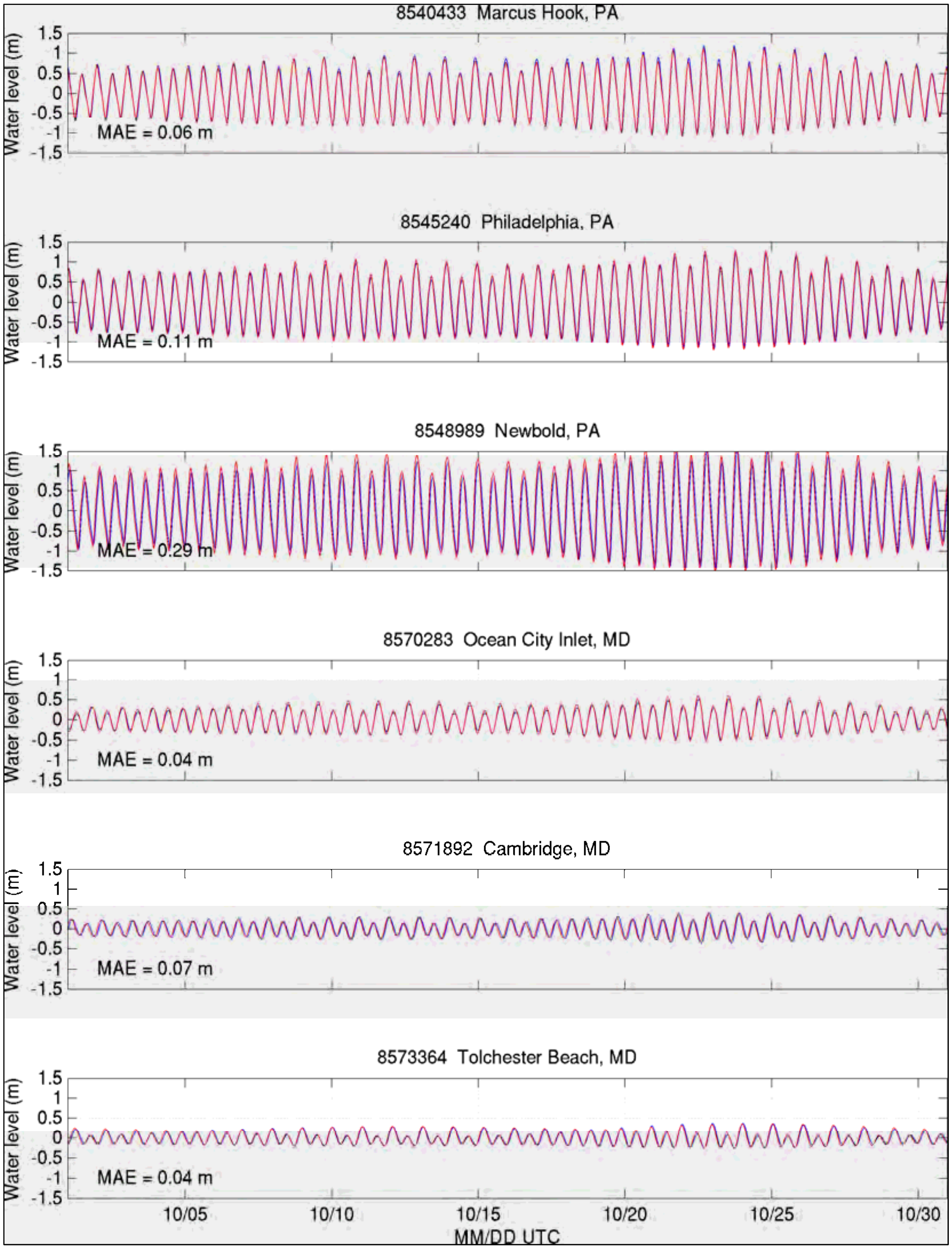

Figure 9. Time series plots for October 2006 of reconstructed tidal water levels at NOAA NOS Pennsylvania and Maryland stations. The time series are reconstructed from the tidal harmonic constituents in common between the NOAA NOS published harmonics and the ADCIRC harmonic analysis. MAE is the mean absolute error of the difference between the modeled and observed time series.

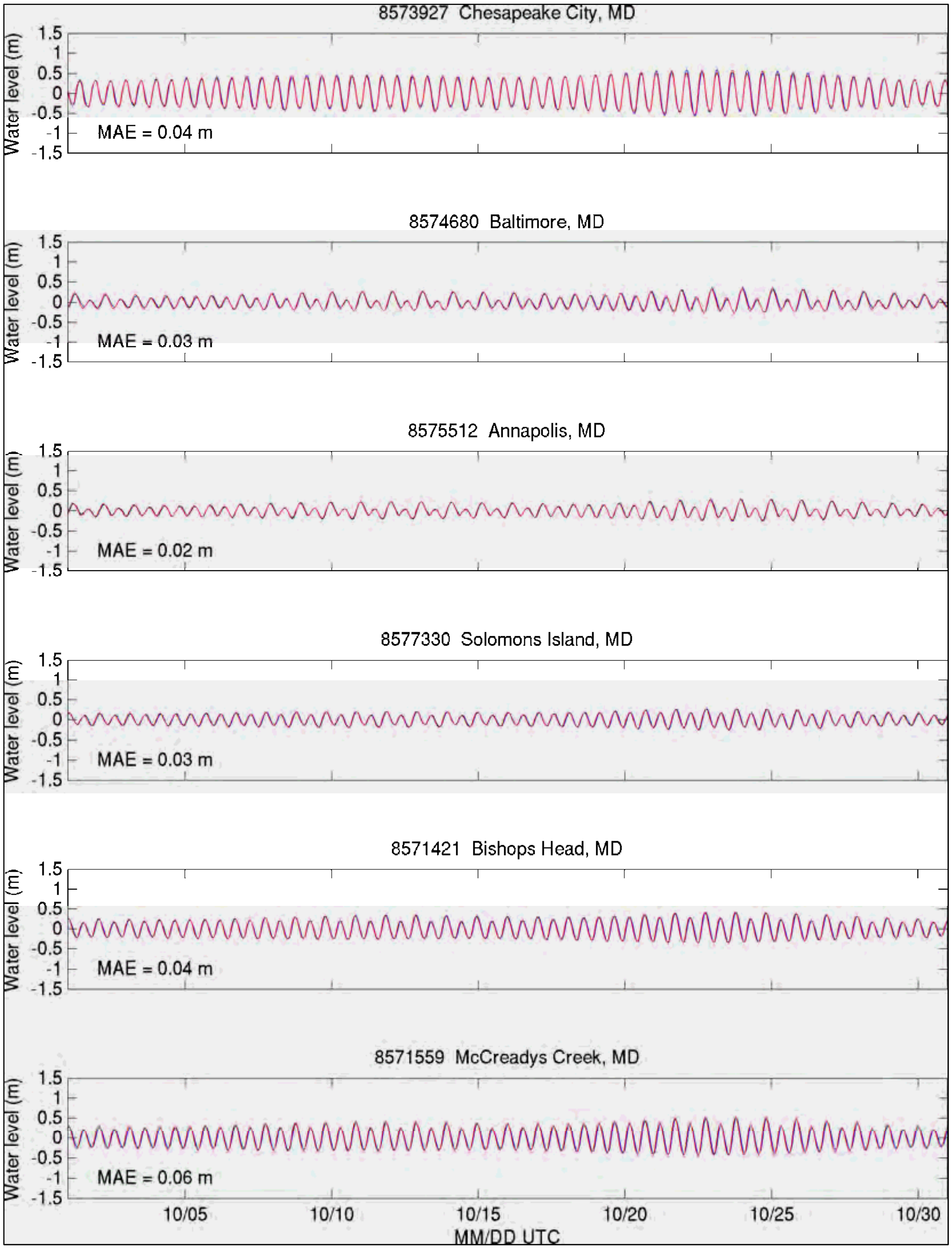

Figure 10. Time series plots for October 2006 of reconstructed tidal water levels at NOAA NOS Maryland stations. The time series are reconstructed from the tidal harmonic constituents in common between the NOAA NOS published harmonics and the ADCIRC harmonic analysis. MAE is the mean absolute error of the difference between the modeled and observed time series.

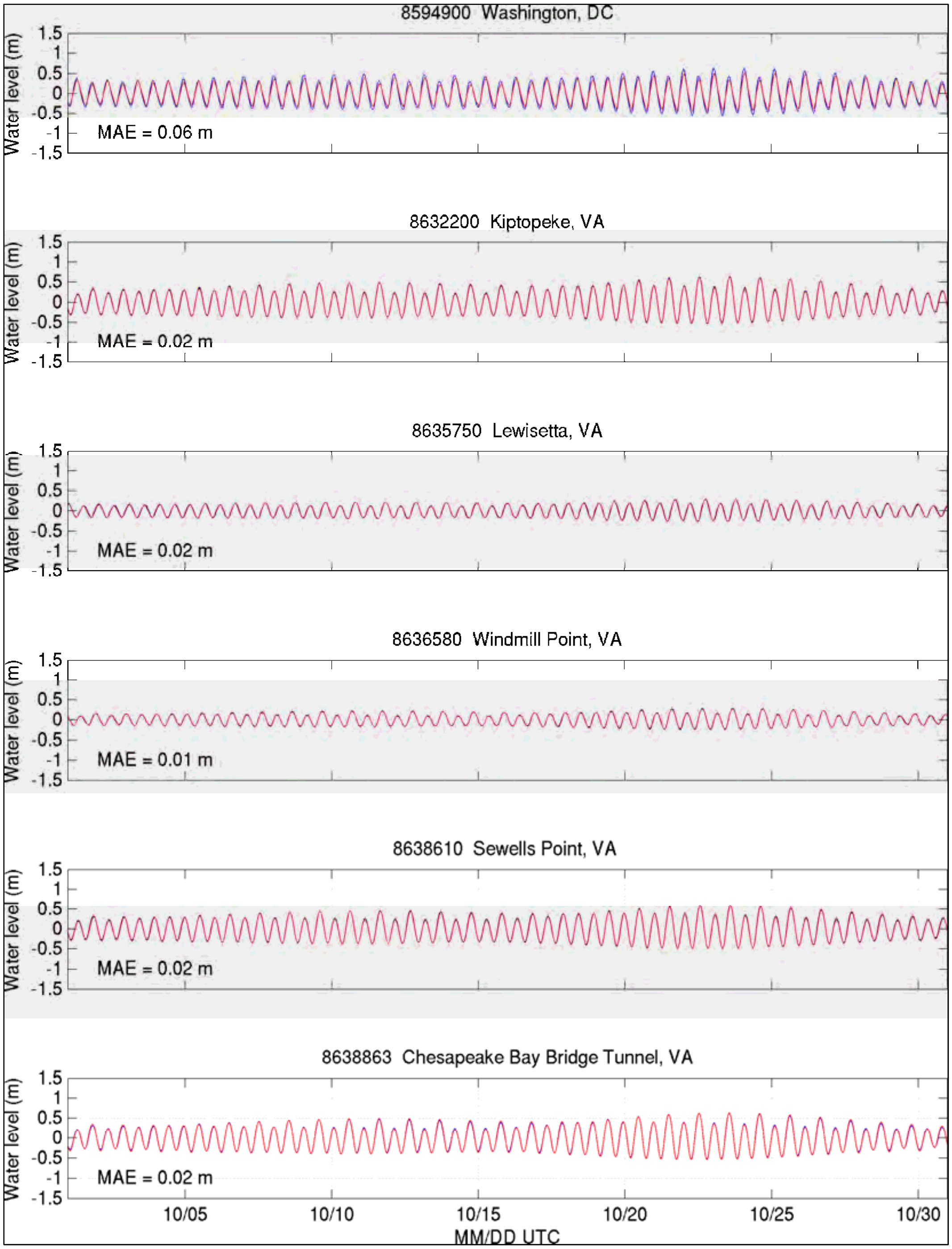

Figure 11. Time series plots for October 2006 of reconstructed tidal water levels at NOAA NOS District of Columbia and Virginia stations. The time series are reconstructed from the tidal harmonic constituents in common between the NOAA NOS published harmonics and the ADCIRC harmonic analysis. MAE is the mean absolute error of the difference between the modeled and observed time series.

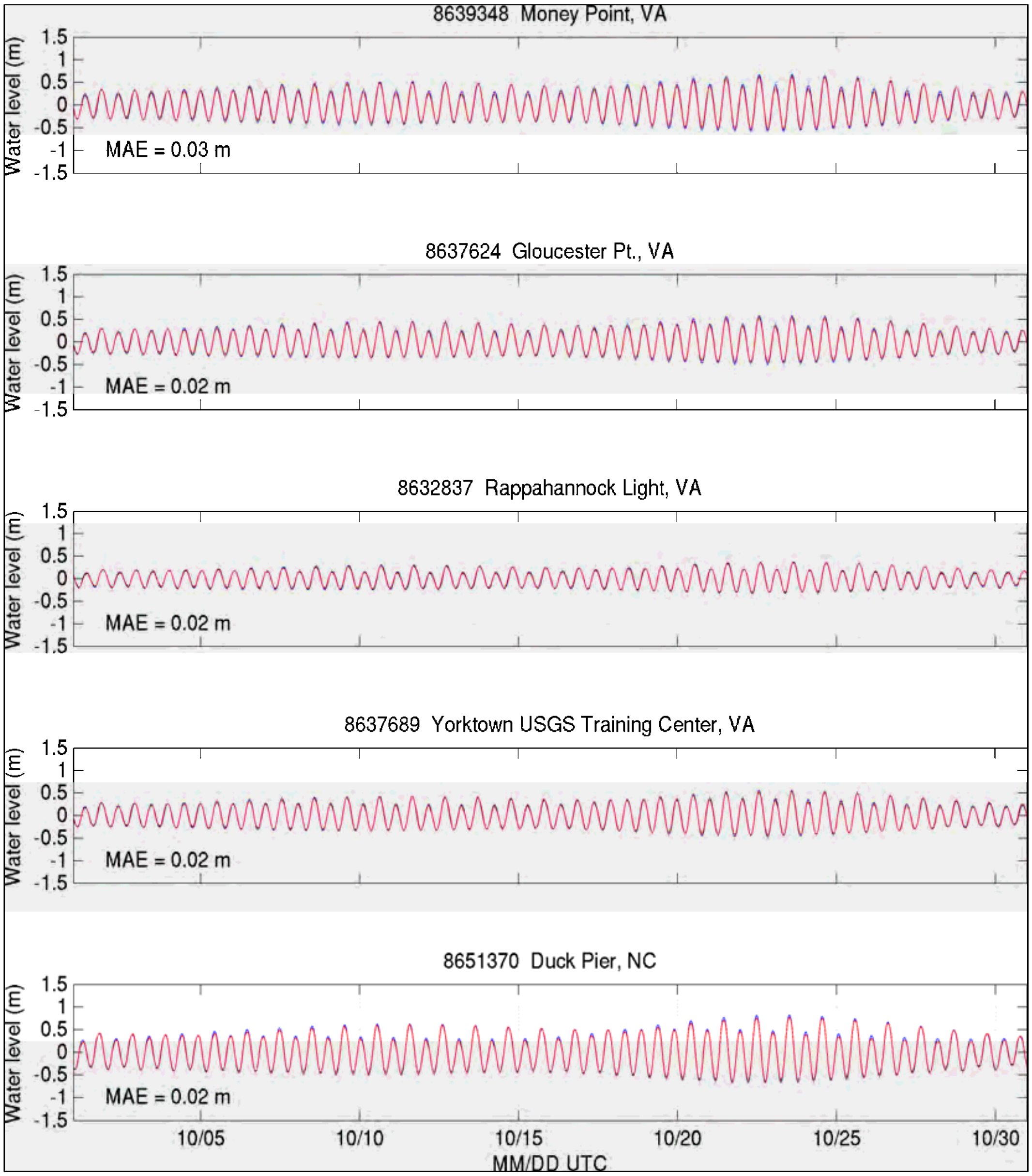

Figure 12.Time series plots for October 2006 of reconstructed tidal water levels at NOAA NOS Virginia stations, as well as the Duck Pier, NC, station. The time series are reconstructed from the tidal harmonic constituents in common between the NOAA NOS published harmonics and the ADCIRC harmonic analysis. MAE is the mean absolute error of the difference between the modeled and observed time series.

Table 8. Tidal time series comparison statistics.[1]

Station ID	RMSE	MAE	PHASE SHIFT	CORCF	RMSE Adj	MAE Adj	CORCF Adj	% VAR	Station Name
8536110	0.06	0.05	-12	0.99	0.03	0.03	1.00	93	Cape May Ferry Term, NJ
8537121	0.10	0.09	-18	0.98	0.03	0.03	1.00	93	Ship John Shoal, DE
8551762	0.12	0.11	-24	0.97	0.04	0.03	1.00	90	Delaware City, DE
8551910	0.11	0.10	-24	0.98	0.03	0.03	1.00	90	Reedy Point, DE
8555889	0.06	0.05	-12	0.99	0.03	0.02	1.00	93	Brandywine Shoal Lgt, DE
8557380	0.05	0.04	-12	0.99	0.03	0.02	1.00	88	Lewes, DE
8540433	0.08	0.06	-12	0.99	0.04	0.04	1.00	91	Marcus Hook, PA
8545240	0.14	0.13	-24	0.97	0.05	0.04	1.00	90	Philadelphia, PA
8548989	0.34	0.31	-48	0.92	0.10	0.08	1.00	91	Newbold, PA
8570283	0.03	0.02	-6	0.99	0.02	0.02	1.00	78	Ocean City Inlet, MD
8571892	0.08	0.07	-54	0.90	0.02	0.02	1.00	61	Cambridge, MD
8573364	0.05	0.04	-36	0.95	0.02	0.02	0.99	47	Tolchester Beach, MD
8573927	0.05	0.04	-12	0.99	0.04	0.03	0.99	86	Chesapeake City, MD
8574680	0.04	0.03	-30	0.96	0.02	0.02	0.99	45	Baltimore, MD
8575512	0.02	0.02	-18	0.98	0.02	0.01	0.99	45	Annapolis, MD
8577330	0.03	0.03	-30	0.97	0.01	0.01	1.00	53	Solomons Island, MD
8571421	0.05	0.04	-30	0.97	0.01	0.01	1.00	-	Bishops Head, MD
8571559	0.07	0.06	-36	0.96	0.03	0.02	1.00	83	McCreadys Creek, MD
8594900	0.08	0.07	24	0.98	0.07	0.06	0.99	76	Washington, DC
8632200	0.02	0.01	-6	1.00	0.02	0.01	1.00	82	Kiptopeke, VA
8635750	0.02	0.02	-18	0.99	0.01	0.01	1.00	56	Lewisetta, VA
8636580	0.01	0.01	-6	1.00	0.01	0.01	1.00	59	Windmill Point, VA
8638610	0.02	0.02	-6	1.00	0.02	0.02	1.00	74	Sewells Point, VA
8638863	0.02	0.02	0	1.00	0.02	0.02	1.00	77	Ches Bay Bridge Tun, VA
8639348	0.03	0.03	-6	1.00	0.03	0.02	1.00	78	Money Point, VA
8637624	0.02	0.02	-6	1.00	0.02	0.02	1.00	85	Gloucester Pt., VA
8631044	0.17	0.15	-48	0.91	0.05	0.04	0.99	-	Wachapreague, VA
8632837	0.02	0.02	-6	1.00	0.02	0.01	1.00	-	Rappahannock Light, VA
8637689	0.02	0.02	0	1.00	0.02	0.02	1.00	91	Yorktown USGS Training, VA
8651370	0.02	0.02	0	1.00	0.02	0.02	1.00	85	Duck Pier, NC

[1] RMSE is the root-mean-square-error, MAE is the mean absolute error, Phase Shift is the shift in minutes needed to maximize the correlation, CORCF is the correlation coefficient, and CORCF Adj ,RMSE Adj, and MAE Adj are the CORCF, RMSE and MAE after the phase shift is applied. The % VAR column indicates the percentage of the total water level variance that is accounted for by the tidal analysis, over the period 2002-2004. Observed water levels for Bishops Head, MD, and Rappahannock Light, VA, are not available for the analysis period.

4 Validation Storm Descriptions

To validate the modeling system, data from three significant historical storms were selected to represent a range of impacts to the Region III domain. Storms were chosen based on overall impact as well as number and quality of available data sets for model validation. Two tropical storms and one extra-tropical storm were selected for validation.

The validation tropical storm tracks are shown in Figure 13. Both Hurricanes Isabel (September 2003) and Ernesto (August-September 2006) brought significant levels of flooding to the Region III coastal domain. Both hurricanes made landfall along the coast of North Carolina and tracked northward, into Region III. Hurricane Isabel maintained hurricane strength throughout much of Region III. Hurricane Ernesto quickly evolved into an extratropical system as it transited Region III, providing an opportunity to model an evolving storm system.

Hurricane Isabel was the most destructive tropical system of the 2003 season. Isabel intensified after initial formation into a Category V storm while over the Atlantic; however, increased vertical wind shear as the storm neared the Mid-Atlantic coast caused it to gradually weaken to a Category II. Isabel made landfall on 18 September 2003, south of Cape Hatteras, NC as a Category II storm with sustained winds of 47 m/sec. The storm weakened as it transited North Carolina, and lost its tropical characteristics while centered over Pennsylvania. It was eventually absorbed into a larger, baroclinic system on 20 September 2003.

Hurricane Ernesto was the costliest tropical system of the 2006 season. Ernesto was only a weak tropical storm when it first made landfall in southwest Miami-Dade County, FL on 30 August 2006. The storm moved northward along the center of the Florida peninsula and re-emerged over the Atlantic Ocean near Cape Canaveral, FL on 31 August 2006. Ernesto then re-intensified over the warm waters of the mid-Atlantic and combined with a high-pressure system centered over southeastern Canada. The storm then made a second landfall at the threshold of a tropical storm and a Category I hurricane near Oak Island, NC on 1 September 2006. As it entered Region III, it was producing gale-force winds near the coasts of Virginia, Maryland, Delaware, and New Jersey. Ernesto began to weaken when it was centered over Washington DC and was fully absorbed into a large, extratropical pressure system on 4 September 2006.

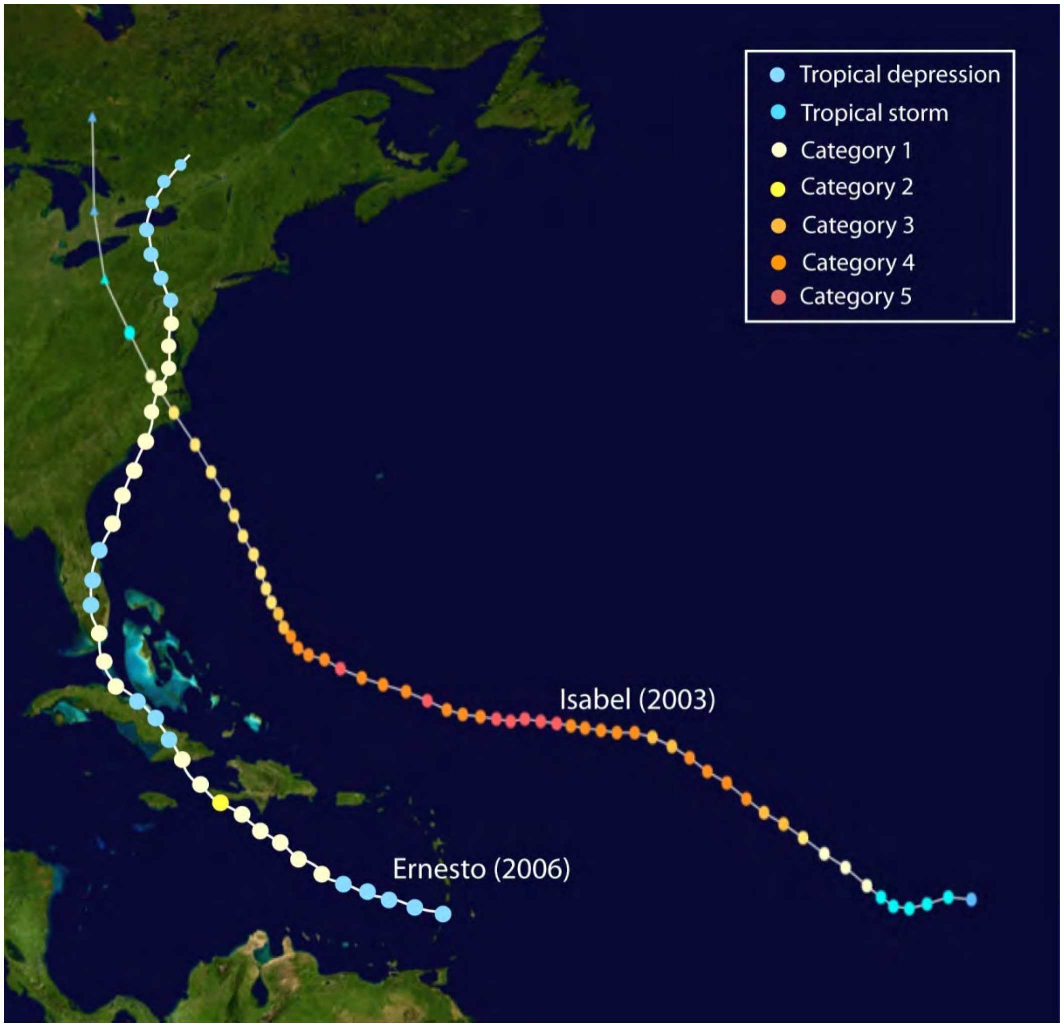
Tropical depression
Tropical storm
Category 1
Category 2
Category 3
Category 4
Category 5
Isabel (2003)
Ernesto (2006)

Figure 13. Storm tracks for Hurricanes Isabel (2003) and Ernesto (2006).

East Coast extratropical storms, typically referred to as nor'easters, have historically caused extensive coastal flooding in Region III due to strong winds, intense currents, and high energy waves. These characteristics, coupled with the long average duration of a nor'easter, result in significant levels of coastal storm surge, especially when these storms coincide with high tides. Accordingly, nor'easters need to be taken into account as part of a storm surge frequency analysis.

Very good observational data are available for one of the strongest nor'easters in recent memory – Nor'Ida, or the Veteran's Day Storm, which impacted Region III in November of 2009. The track for Nor'Ida is shown in Figure 14. Nor'Ida originated from the remnants of Hurricane Ida and a low pressure system in South Carolina. Hurricane Ida was a late season tropical cyclone that made initial landfall in Nicaragua as a Category I hurricane on 4 November 2009. The storm weakened after encountering strong shear and cooler waters in the Gulf of Mexico, and made a second landfall along the Alabama coast as a strong extratropical storm on 9 November 2009. Ida continued to weaken as it moved north and east, eventually dissipating over the Florida Panhandle on 11 November 2009. However, as the remnants of Ida continued to move northeast, they combined with a strong low-pressure system in South Carolina. This system moved off of the coast of North Carolina and quickly strengthened into an extremely powerful nor'easter on 12 November 2009, with sustained winds of 29 m/sec. By the time Nor'Ida weakened and moved northeast over Atlantic Canada on 17 November 2009, most of Region III had experienced major damage due to heavy winds and extensive rainfall.

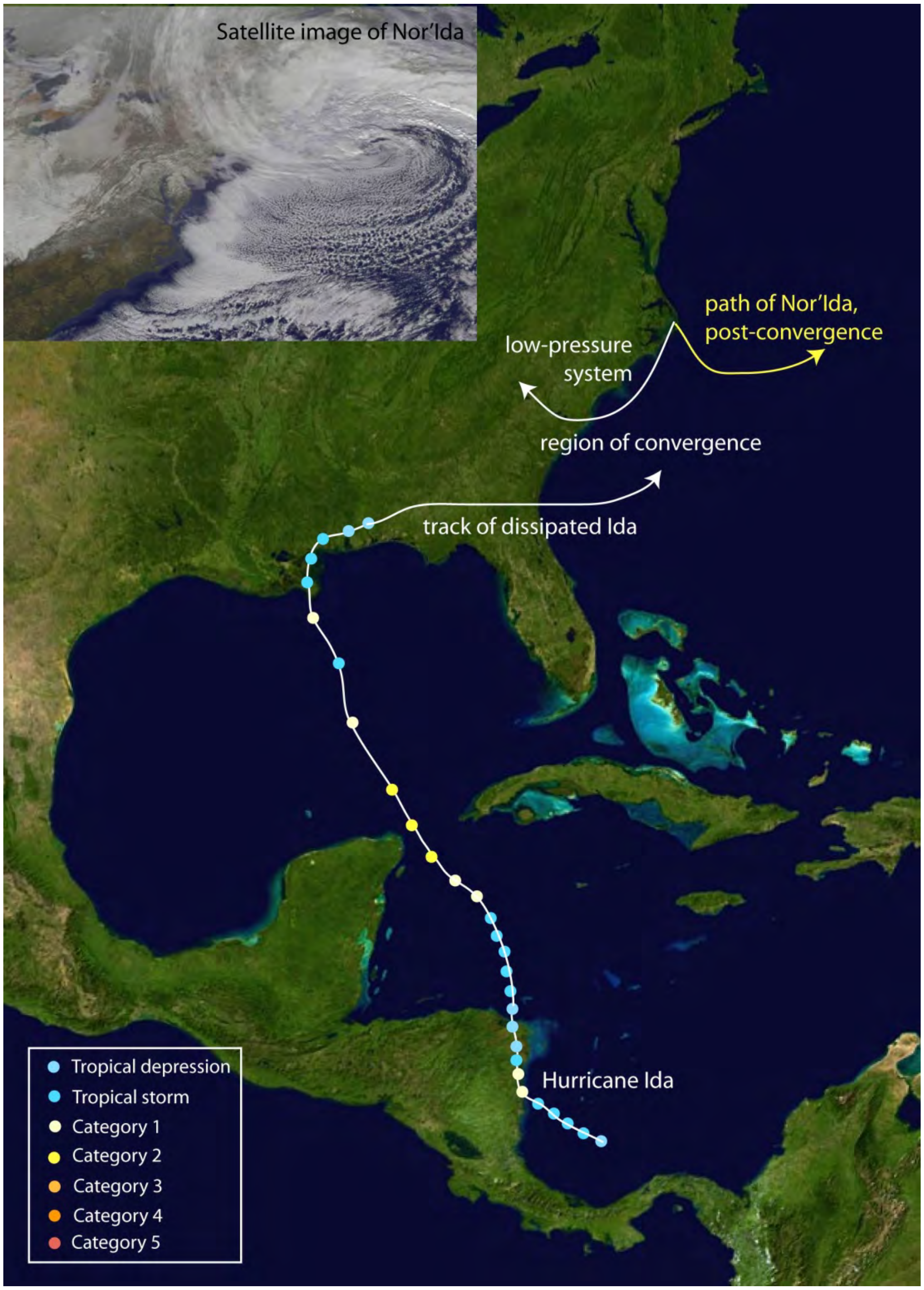
Satellite image of Nor'Ida
path of Nor'Ida,
post-convergence
low-pressure
system
region of convergence
track of dissipated Ida
Hurricane Ida
● Tropical depression
● Tropical storm
● Category 1
● Category 2
● Category 3
● Category 4
● Category 5

Figure 14. Storm tracks for Hurricane Ida and Nor'Ida (2009). See text for path discussion. A satellite image of the storm is provided as an inset.

5 Modeling System Validation Approach

Performance of the Region III modeling system in hindcasting the three historical storms (Isabel, Ernesto, and Ida) was validated and quantified using data from National Data Buoy Center (NDBC) and National Ocean Service (NOS) observation stations, as well as other various available data sets. The full set of available observations is described fully in the next chapter. Model output was compared to observed quantities using the US Army Corps of Engineers (USACE) Interactive Model Evaluation and Diagnostics System (IMEDS). A significant challenge in evaluating large temporal- or spatial-scale simulations is the need to statistically reduce millions of model estimates to a meaningful measure of prediction skill, while retaining sufficient levels of detail to identify model strengths and deficiencies. IMEDS provides this capability through a robust quantitative assessment of model errors; IMEDS also provides a diagnostic evaluation of model strengths and weaknesses.

IMEDS requires an observation data set as ground truth, and a model or test data set to evaluate. The data are composed of time series output at specific geographic stations (i.e., NDBC buoys). The observation data are decomposed into a series of components, such as wind-sea, young swell, and mature swell for wave spectrum data. These are further broken down into specific data attributes, such as the height, period, and direction of each wave component. More information on this particular technique can be found in Hanson et al. (2009). A variety of error metrics (such as root-mean-square error, bias, scatter index) are calculated for the model predictions at each station, and performance (skill) scores are then calculated from the errors. The performance scores are then folded through space and time, giving the user an assessment of the total model performance. As a diagnostic tool, the user can then explore model errors and performance as a function of many variables (station, time, components, etc).

IMEDS is fully functional with wind, wave, and water level data, and was developed to comply with Published NOAA standards (Hess et. al. 2003, Zhang et.al. 2006).

5.1 Error metrics

IMEDS applies standardized error metrics depending on the type of the input data. Table 9 lists the various data types that IMEDS evaluates.

Table 9. IMEDS evaluation parameters.

Data Type	Components	Attributes
Winds	n/a	Wind Speed Wind Direction
Waves	Bulk Windsea Primary Swell Secondary Swell	Height Period Direction
Storm Surge	n/a	Water Levels High Water Marks

For each data type, the following statistical analyses were used in the Region III validation. The mathematical expressions used to perform these analyses appear in Hanson et al. (2009).

5.1.1 Temporal correlation (TC) analysis

The TC analysis is a direct comparison of time-paired data attributes. The TC analysis indicates how well the hindcast quantities match the observed quantities in absolute time. The following metrics are used to quantify the TC errors.

For non-directional data (speed, time, height, period, and water level), the error metrics are

- RMS error,
- bias, and
- scatter index.

For directional data the error metrics are:

- circular correlation, and
- angular bias.

5.1.2 Peak event (PE) analysis

The PE analysis extends the IMEDS capability by isolating and computing statistics on event peak data. The data types supported by this analysis are

- wind speed,
- wave height, and
- water level.

A peaks-over- threshold (POT) method, using a standard-deviation threshold, is used to identify and match modeled and observed peaks. For waves, only the bulk (full-spectrum) statistics are used for this analysis. The attributes extracted from each peak event form data pairs that are then used to compute the standard non-directional error metrics (see list above).

5.1.3 High-water mark analysis

High-water mark (HWM) data are statistically compared to peak water level output at the location of each water mark. The standard non-directional error metrics (see list above) are then computed for the population of HWM data.

5.2 Performance scores

The above-described analyses result in a set of error metrics that quantify the hindcast skill in reproducing the physical attributes at each observation station. For a one-year wave study with six stations, this can result in a database of 3,500 independent measures of model skill for each hindcast run. A performance scoring method was developed to reduce the error metric database into a small set of performance indicators for overall skill assessment. Performance scores are computed by normalizing the error metrics to mean quantities and averaging them across metrics, months, and stations with contributions weighted by sample size. The resulting non-dimensional performance scores range from zero (uncorrelated) to one (perfect correlation) and provide a measure of error levels relative to mean observed quantities. For example, a wind speed performance score of 0.8 implies that error levels are within approximately (1-0.8)*100 = 20% of the mean wind speed for the time period under investigation.

6 Wind Field Validation

Once tidal influences are accounted for, winds are the primary driving mechanisms for wave growth and coastal storm surge. Although reasonably accurate wind fields are required to successfully model these processes, they are very difficult to produce. Fast-moving storms, strong spatial gradients, and an absolute scarcity of available data challenge the meteorologist in developing high-resolution evolving wind fields with sufficient accuracy to perform a detailed coastal storm surge study.

As described in Chapter 4, three major storm events were selected to fully test the Region III modeling system: Hurricane Isabel, Hurricane Ernesto, and Extratropical Storm Nor'Ida. To minimize the potential sources of error, the best possible wind field reconstructions were required to force the modeling system for the validation study. As described in Submittal 1.3 Appendix A, an Interactive Objective Kinematic Analysis (IOKA) system (Cox et al. 1995) was applied by Oceanweather, Inc. to prepare high-resolution hindcasts of the selected storms.

The reconstructed winds that were used to validate the modeling system wave and storm surge outputs are assessed here for quality. Both wind speed and direction time series are evaluated at specific locations using available data from operational wind observation stations. It is important to note that observed winds have their own associated errors (Taylor et al. 2003). Hence, the comparisons included here do not provide an absolute measure of hindcast wind error. However, the results do quantify the wind field variability introduced into the validation process.

6.1 Wind validation approach

Region III wind validation was performed using the USACE Interactive Model Evaluation and Diagnostic System (IMEDS) described in Chapter 5. Using meteorological station observations as ground truth, temporal correlation (TC) and peak event (PE) statistical analyses were used to quantify hindcast skill in reproducing measured wind speed and direction attributes. All observed winds were scaled to a 10-m neutral stability reference height above the ocean (Large and Pond 1981). Wind speed error metrics include the RMS error, bias, and scatter index. Wind direction metrics include the angular bias and circular correlation. A performance analysis synthesizes the TC error results into a convenient overall set of model performance (skill) scores. Performance scores are normalized to mean quantities and range from 0.00 to 1.00, with 1.00 representing perfect agreement between model output and observations.

For each storm event, wind outputs from the ADCIRC model runs were saved at the location of each observation station. Over water, these winds are equivalent to the input Oceanweather winds, with the exception of a 1.09 multiplier to follow the Oceanweather-recommended approach for transforming reanalysis winds to 10-min averages. The IMEDS analysis was then performed separately on the results from each model run using all available observations as ground truth.

6.2 Wind validation data

The Region III wind validation data were obtained from the National Data Buoy Center (NDBC; http://www.ndbc.noaa.gov/), the Chesapeake Bay Observing System (CBOS), and the US Army Corps of Engineers Field Research Facility (FRF; http://www.frf.usace.army.mil/). The observation sets used for each storm are listed in Table 10. These stations comprise a mix of floating buoys and fixed weather stations. Instrument and deployment details for each station appear in Table 11. Wind speed and direction data were available from all stations. Note that stations DUCN7 and FRF 44056 are both located on the FRF pier; however, they are physically mounted on different observation towers.

Table 10. Validation events and available wave observations.

Storm	Date	Wind Observation Stations
Isabel	SEP 2003	NDBC 44009, 44014, TPLM2, FRF 44056
Ernesto	SEP 2006	NDBC 44009, 44014, TPLM2, DUCN7, CBOS MB
Ida	NOV 2009	NDBC 44009, 44014, TPLM2, CBOS MB, FRF 44056

Table 11. Wind validation station details.

Station	Type	Anemometer Height (m)	North Latitude	West Longitude
NDBC 44009 Delaware Bay	3-m Discus buoy; ARES payload	5.0	38.464	74.702
NDBC 44014 Virginia Beach	3-m Discus buoy; ARES payload	5.0	36.611	74.836
NDBC TPLM2 Thomas Point, MD	C-MAN Station; MARS payload	18	38.898	76.437

Station	Type	Anemometer Height (m)	North Latitude	West Longitude
NDBC DUCN7 Duck Pier, NC	C-MAN Station; ARES payload	20.4	36.184	75.745
FRF 44056	FRF Weather Station	17.4	36.2	75.714
CBOS Mid-Bay (MB)	Data Buoy	3.5	38.4729	76.379

6.3 Wind validation results

Analysis of the three validation wind sets from Oceanweather has resulted in a comprehensive set of error metrics and performance scores that quantify the differences between the model forcing winds and those from the observation stations. Table 12 is an overall summary of the hindcast skill in replicating the observed wind conditions in each storm event, as reflected by summary skill scores. The performance scores for wind speed and direction are obtained by averaging the scores across all available observation stations using sample size weighting functions. All of the scores are 0.86 or greater, suggesting that mean errors are within 14% of the mean observed quantities. Details from the station results during each event are described in the following three sections. A final section summarizes wind peak analyses from all three events.

Table 12. Hindcast winds performance summary.

Event	Wind Speed	Wind Direction
Isabel	0.93	0.98
Ernesto	0.86	0.94
Nor'Ida	0.88	0.95

6.3.1 Hurricane Isabel (2003)

Hurricane Isabel made landfall near Drum Inlet, NC, midway between Cape Lookout and Ocracoke Inlet, as a Category II storm (Figure 13). The highest observed wind on land as reported by NOAA was sustained at 35.5 m/sec with a gust to 44 m/sec at an instrumented tower near Cape Hatteras, NC, just after landfall. Tropical storm conditions with sustained winds of 21-31 m/sec were reported throughout the Chesapeake Bay Region, with the highest winds in the southern part of the bay.

The Oceanweather wind fields captured the observed wind magnitudes and variability throughout the region. Figure 15 is a map of the peak wind speeds extracted from the Hurricane Isabel storm surge simulation. Note that peak winds ranged from 28-30 m/sec in the lower Chesapeake Bay to 16-18 m/sec in the Delaware Bay region.

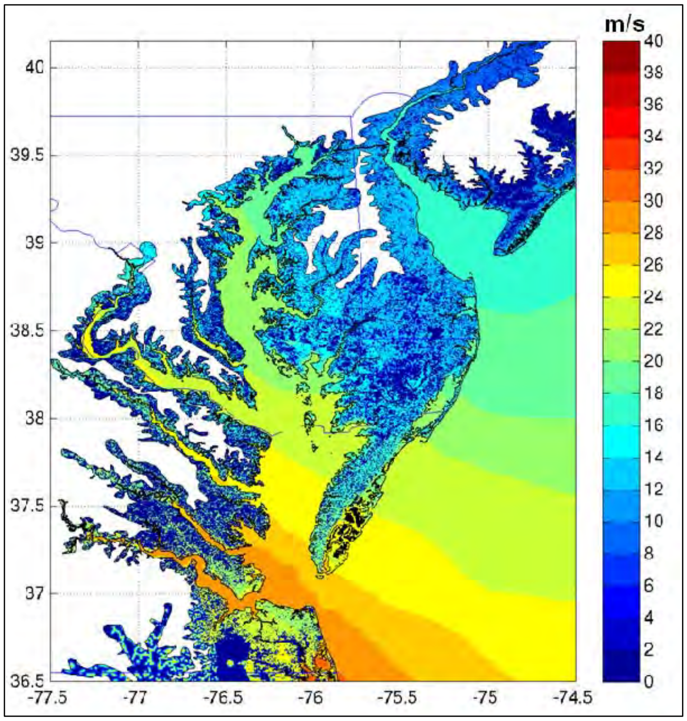

Figure 15. Hurricane Isabel maximum wind speeds.

Four observation stations were used to validate the Oceanweather Hurricane Isabel wind fields. As depicted in the station location map of Figure 16, the validation stations represent a range of environments including the upper Chesapeake Bay, coastal North Carolina, and the open ocean. Time series comparisons of observed and hindcast wind speeds and directions during Isabel appear in Figures 17 and 18, respectively. These results show excellent agreement between the observed and hindcast wind fields.

Results of the temporal correlation analysis quantify the agreement between the observed and hindcast winds. Wind speed scatter plots, depicted in Figure 19, indicate good agreement with very little scatter in the coastal and open ocean stations. The Chesapeake Bay station TPLM2 exhibits somewhat higher scatter; this is expected due to complex interactions known to occur between marine winds and coastal landforms (Thompson and Leenknecht 1994). Resulting Isabel error metrics and performance scores

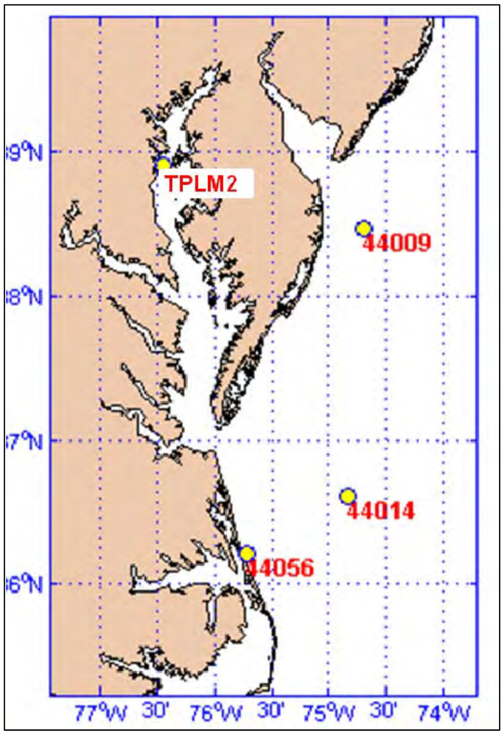

Figure 16. Hurricane Isabel wind validation stations.

(Perf) for both wind speed and direction at each station appear in Table 13. At each of these stations, the wind speed bias is less than 1.0-m/sec, wind direction (angular) bias is less than 10 degrees, and performance scores are 0.92 or greater.

6.3.2 Ernesto (2006)

Ernesto was at the threshold between a tropical storm and a Category I hurricane, with maximum sustained winds estimated at approximately 31 m/sec when it made landfall near Oak Island, NC. As the storm moved into Region III, it evolved into a powerful extratropical system as it interacted with a pre-existing frontal zone that extended eastward from Virginia. As an extratropical cyclone, Ernesto briefly strengthened, with a maximum wind gust of 39 m/sec at the Virginia Institute of Marine Science, Gloucester Point, VA. Maximum sustained winds of 21 m/sec were reported at several locations along the Virginia, Maryland, and Delaware coastlines (Knabb and Mainelli 2006). Even as Ernesto began to weaken near Washington, DC, it interacted with a strong ridge over the western Atlantic, and the resulting pressure gradient was sufficient to produce gusts of up to 20 m/sec.

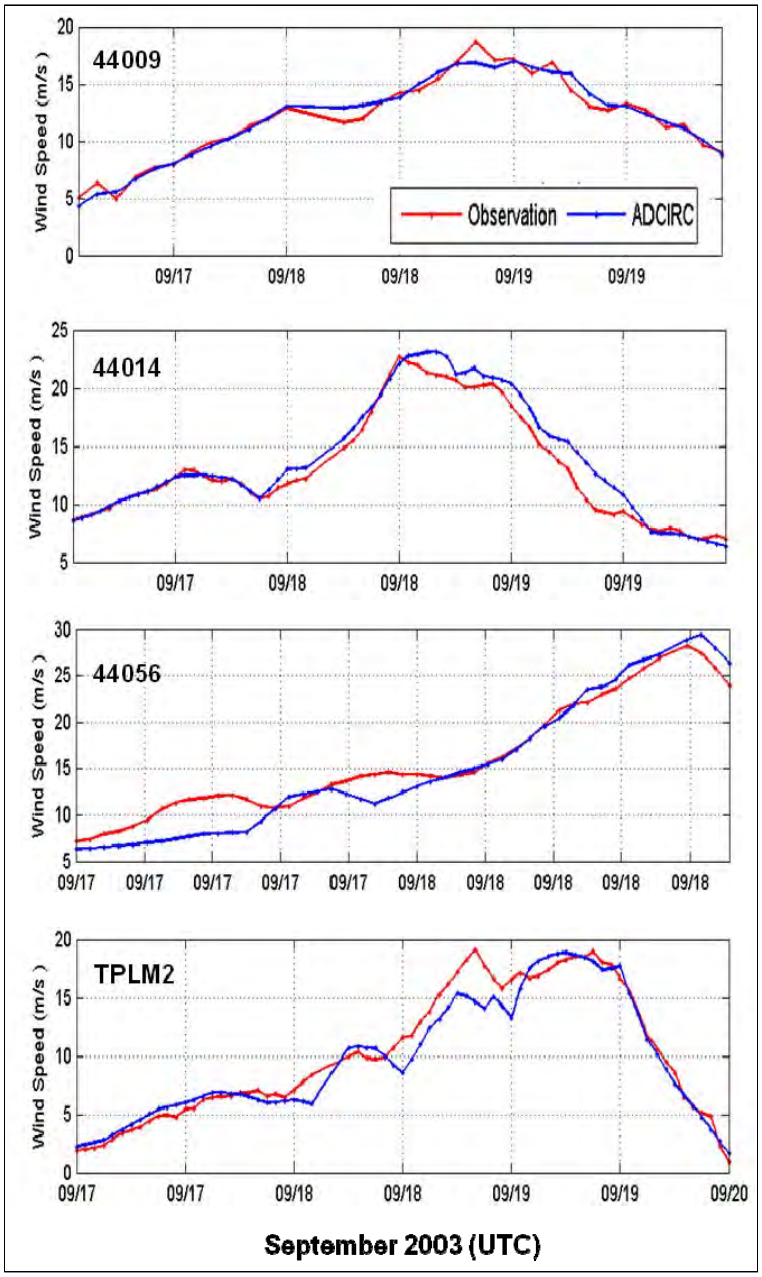

Figure 17. Comparisons of Hurricane Isabel wind speeds at each validation station.

These observed trends are well captured by the Oceanweather wind fields used to force the Ernesto hindcast. Peak winds, extracted from the Ernesto hindcast, are depicted in Figure 20. In agreement with the observations, maximum winds of 20-24 m/sec occurred throughout the entire Region III coastal domain.

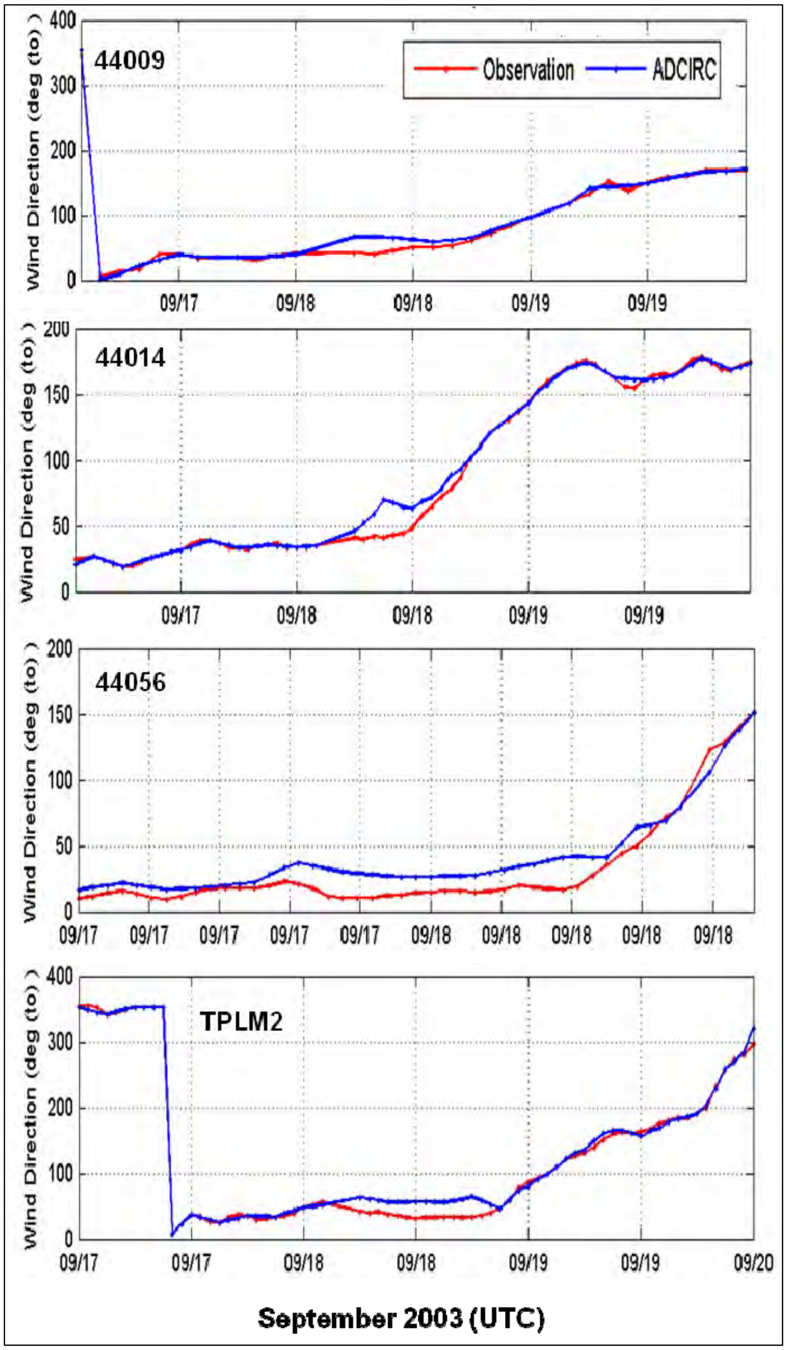

Figure 18. Comparisons of Hurricane Isabel wind directions at each validation station.

Five observation stations were used to validate the Oceanweather Hurricane Ernesto wind fields. As depicted in the station location map of Figure 21, the validation stations include two stations within the Chesapeake Bay, a coastal North Carolina station, and two stations in the open ocean.

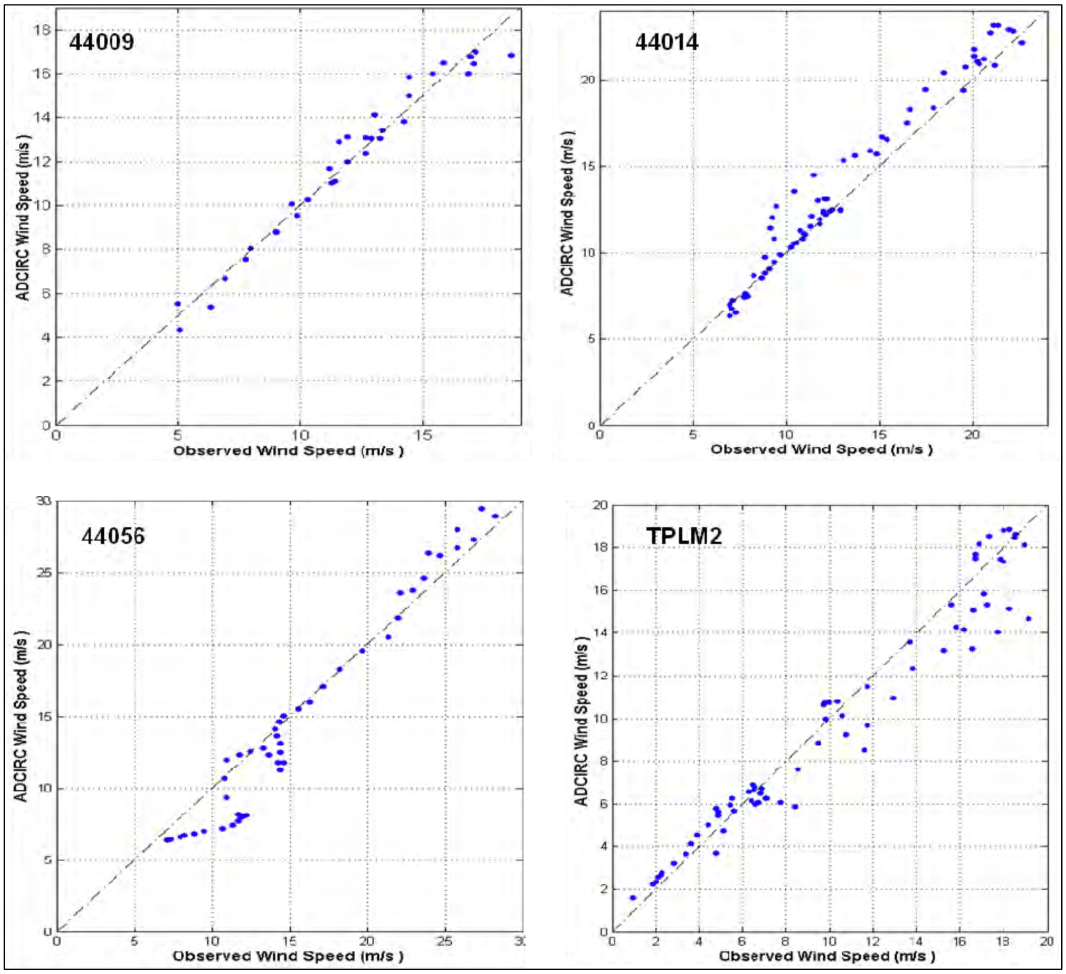

Figure 19. Hurricane Isabel wind speed scatter plots.

Table 13. Hurricane Isabel wind statistics.

Station	Wind Speed				Wind Direction		
	Bias (m/sec)	RMS Error (m/sec)	Scatter Index	Perf	Ang. Bias (Deg)	Circular Corr.	Perf
44009	0.02	0.67	0.06	0.97	3.17	0.99	0.99
44014	0.69	1.19	0.07	0.93	2.29	0.99	0.99
44056	-0.82	1.97	0.11	0.92	9.51	0.97	0.96
TPML2	-0.42	1.33	0.12	0.92	5.1	0.99	0.98

Time series comparisons of observed and hindcast wind speeds and directions during Ernesto appear in Figures 22 and 23, respectively. Three of these stations show excellent agreement (44009, CBOS-MB, TPLM2). Stations 44014 and DUCN7 depict Oceanweather wind speeds that are elevated above the observed quantities.

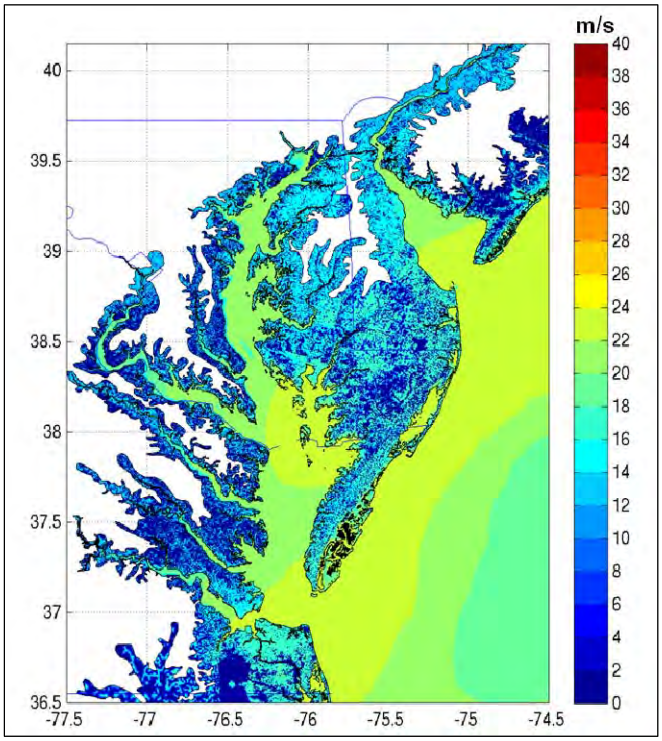
m/s
40
38
36
34
32
30
28
26
24
22
20
18
16
14
12
10
8
6
4
2
0
40
39.5
39
38.5
38
37.5
37
36.5
-77.5
-77
-76.5
-76
-75.5
-75
-74.5

Figure 20. Hurricane Ernesto maximum wind speeds.

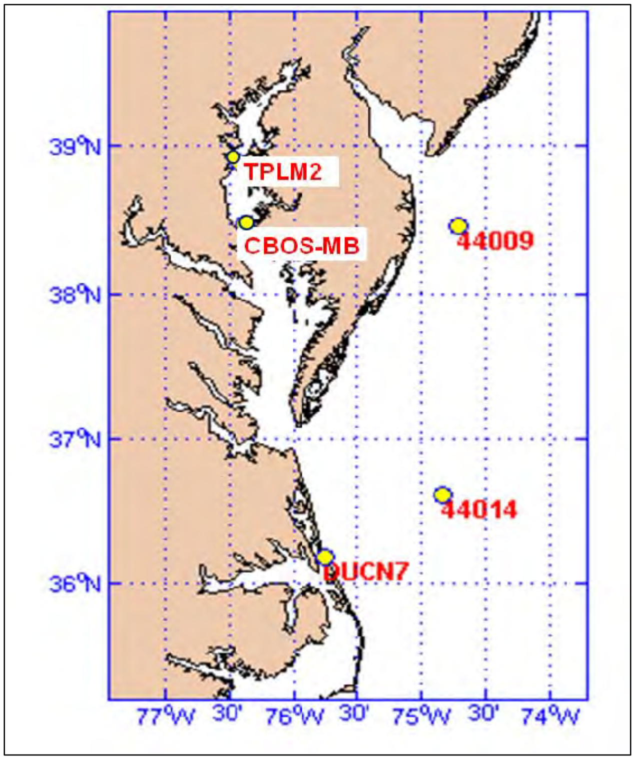
39°N
38°N
37°N
36°N
77°W
30'
76°W
30'
75°W
30'
74°W
TPLM2
CBOS-MB
44009
44014
DUCN7

Figure 21. Hurricane Ernesto wind validation stations.

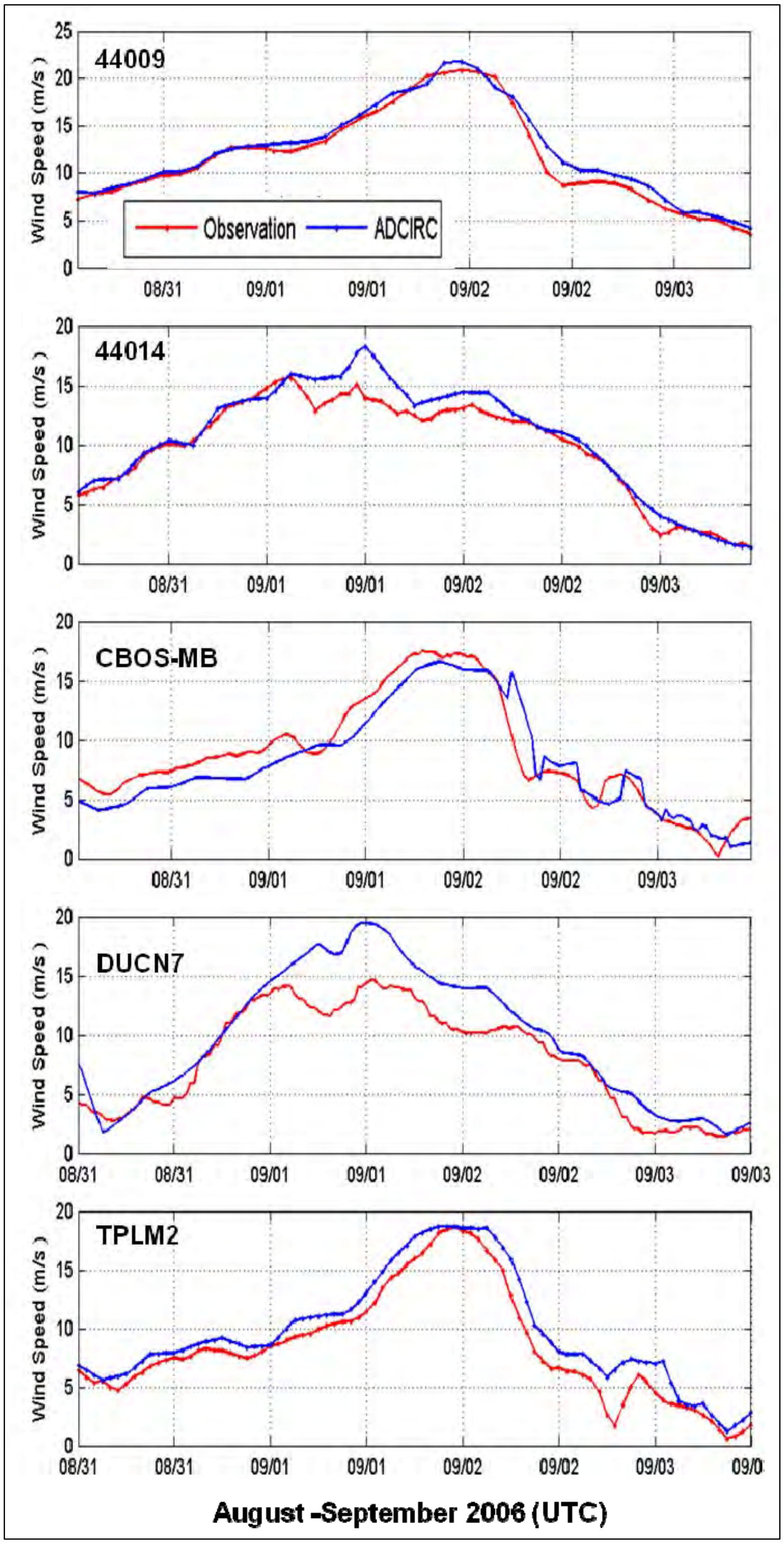

Figure 22. Comparisons of Hurricane Ernesto wind speeds at each validation station.

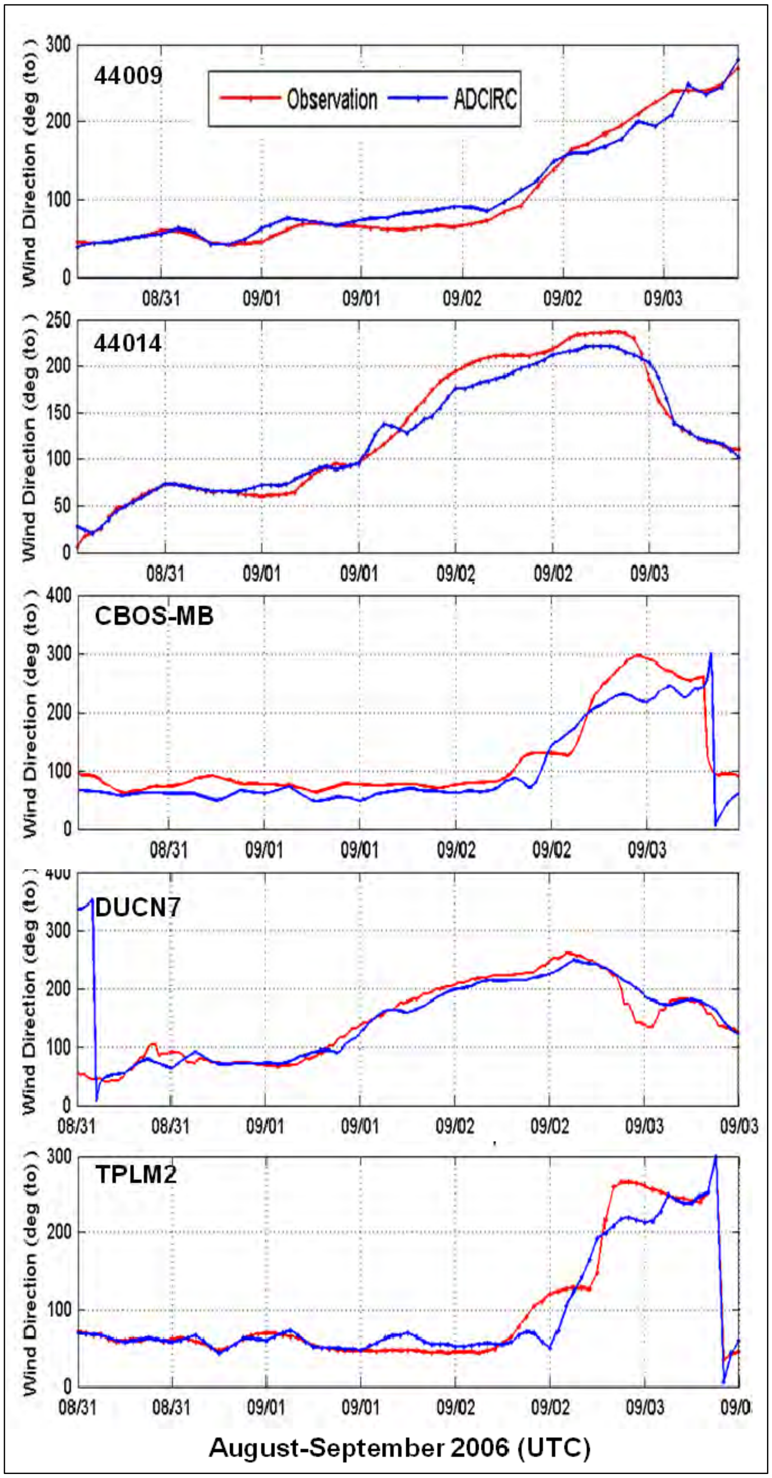

Figure 23. Comparisons of Hurricane Ernesto wind directions at each validation station.

Results of the temporal correlation analysis provide additional detail on the Ernesto wind field variability. Wind speed scatter plots from each of the five stations appear in Figure 24. At station 44014, the peak winds are overestimated by 4.0 m/sec and at DUCN7, by 5.5 m/sec. Wind speed and direction error statistics appear in Table 14. The bias at Duck results in a low performance score of 0.76. It should be noted that wind directions at the time of peak winds were excellent at all stations. Wind direction offsets well after the storm peak, resulting in overall higher wind direction errors at CBOS-MB.

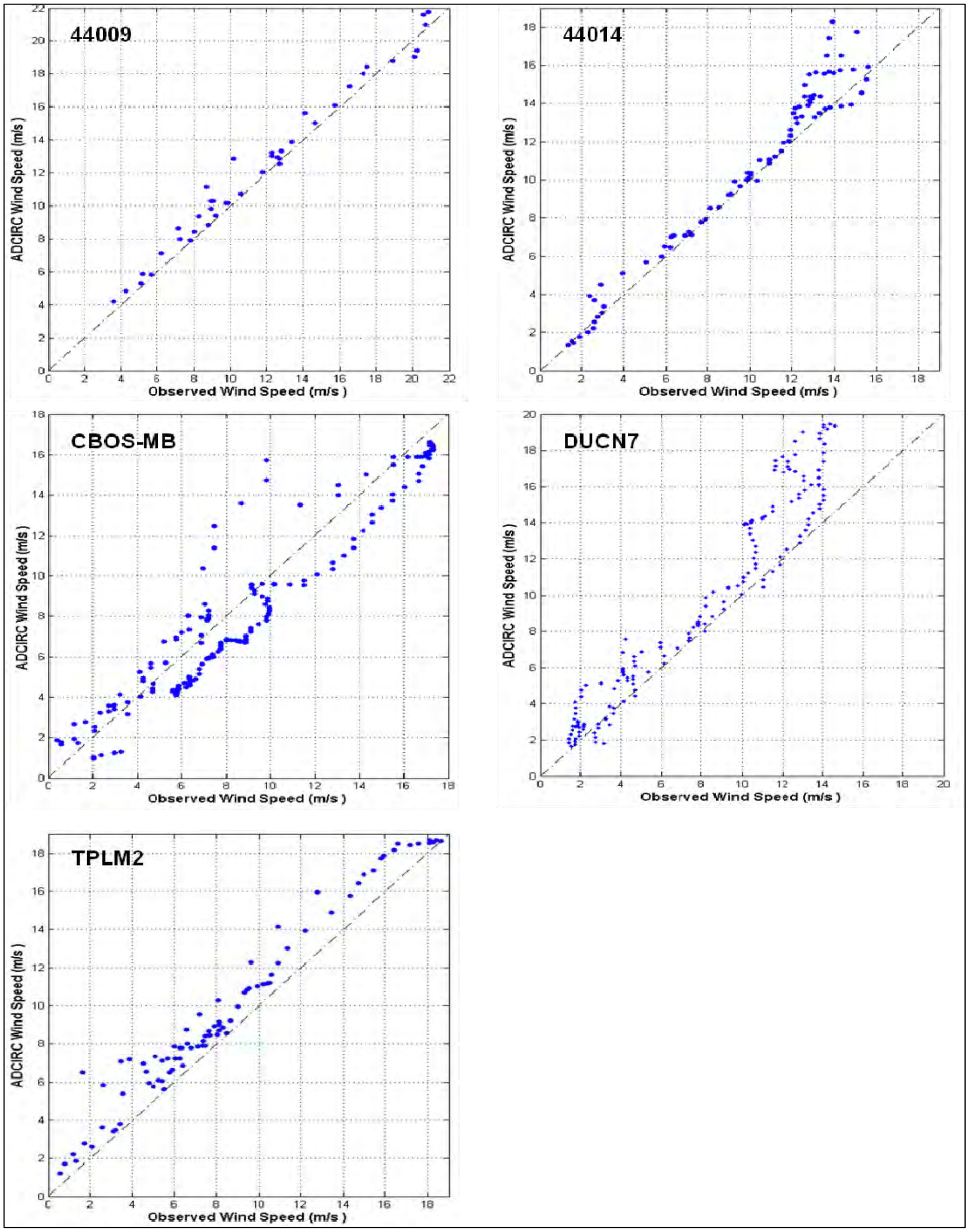

Figure 24. Hurricane Ernesto wind speed scatter plots.

Table 14. Hurricane Ernesto wind statistics.

	Wind Speed				Wind Direction		
Station	Bias (m/sec)	RMS Error (m/sec)	Scatter Index	Perf	Ang. Bias (Deg)	Circular Corr.	Perf
44009	0.61	0.91	0.06	0.94	3.14	0.98	0.98
44014	0.75	1.23	0.10	0.91	-3.47	0.98	0.98
CBOSMB	-0.61	1.68	0.18	0.88	-20.29	0.91	0.90
DUCN7	1.79	2.49	0.22	0.76	-3.3	0.94	0.96
TPLM2	1.28	1.55	0.10	0.85	-3.02	0.89	0.94

6.3.3 Extra-tropical storm Nor'Ida (2009)

Nor'Ida was a powerful mid-Atlantic nor'easter that developed from the remnants of Hurricane Ida (2009). The extra-tropical system moved offshore and continued to intensify over the Atlantic for several days. By November 12, the system attained offshore winds of 33 m/sec. In combination with a large area of high pressure, a long stretch of easterly, onshore winds of 20-24 m/sec impacted areas from Virginia to southern New England. Eventual gradual weakening brought heavy rains across much of the Chesapeake Bay area. The observed wind trends are reflected in the Oceanweather wind fields used to force the Nor'Ida hindcast. Peak winds are depicted in Figure 25. Like Ernesto, the Nor'Ida peak wind forcing was fairly uniform across the coastal domain and similar in magnitude.

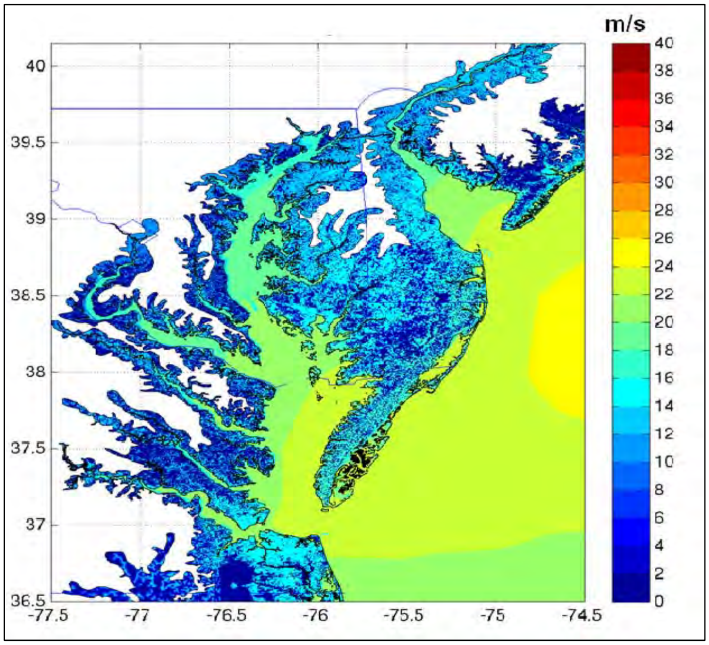

Figure 25. Extratropical Storm Nor'Ida maximum wind speeds.

The same five observation locations used to evaluate Hurricane Ernesto winds were used to authenticate the Oceanweather Extratropical Storm Nor'Ida wind fields. These stations are depicted in the station location map (Figure 26). Note that the DUCN7 designator from Ernesto is replaced with 44056 to reflect that the Nor'Ida winds were taken from the FRF wind tower as opposed to the NOAA C-Man station located onsite.

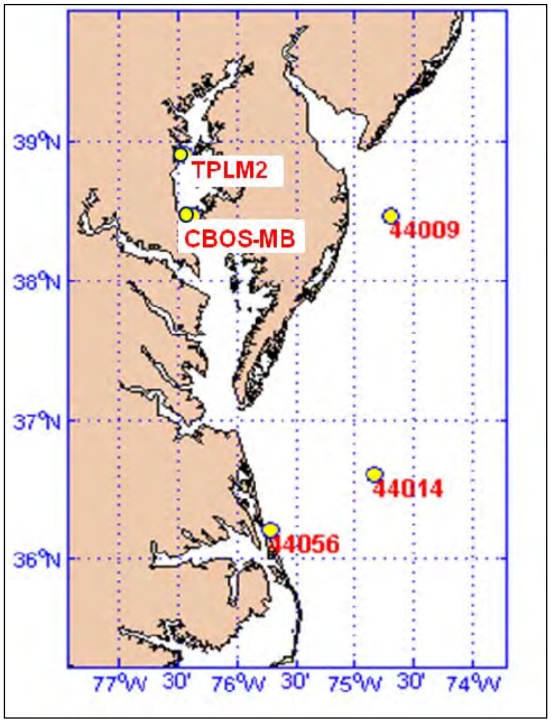

Figure 26. Extratropical Storm Nor'Ida wind validation stations.

Time series comparisons of observed and hindcast wind speeds and directions during Nor'Ida appear in Figures 27 and 28, respectively. It is noteworthy in Figure 27 that the wind speed event duration at each station is on an order of two days, which is twice the duration of both Isabel and Ernesto (Figures 17 and 22, respectively). Long-duration events are typical of mid-Atlantic nor'easters.

As with Ernesto, three of the validation stations show excellent observed and modeled wind speed agreement (44009, CBOS-MB, TPLM2). Stations 44014 and 44056 have comparable peak wind speed magnitudes but depict more variability in the observed winds than exist in the Oceanweather winds. Oceanweather wind directions during the peak of the wind events are excellent at three stations (44009, 44014, CBOS-MB) and show only minor offsets at 44056 and TPLM2.

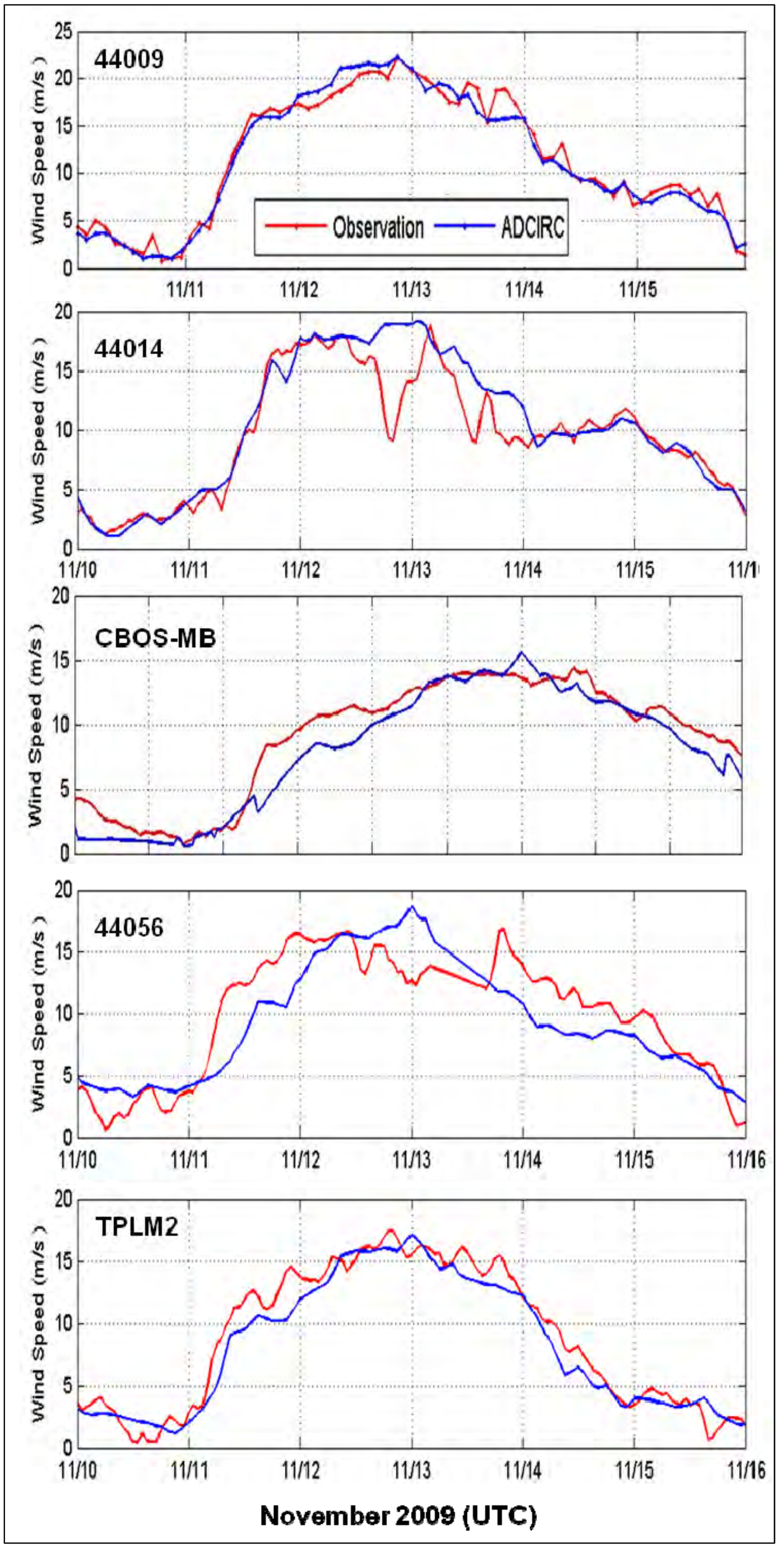

Figure 27. Comparisons of Extratropical Storm Nor'Ida wind speeds at each validation station.

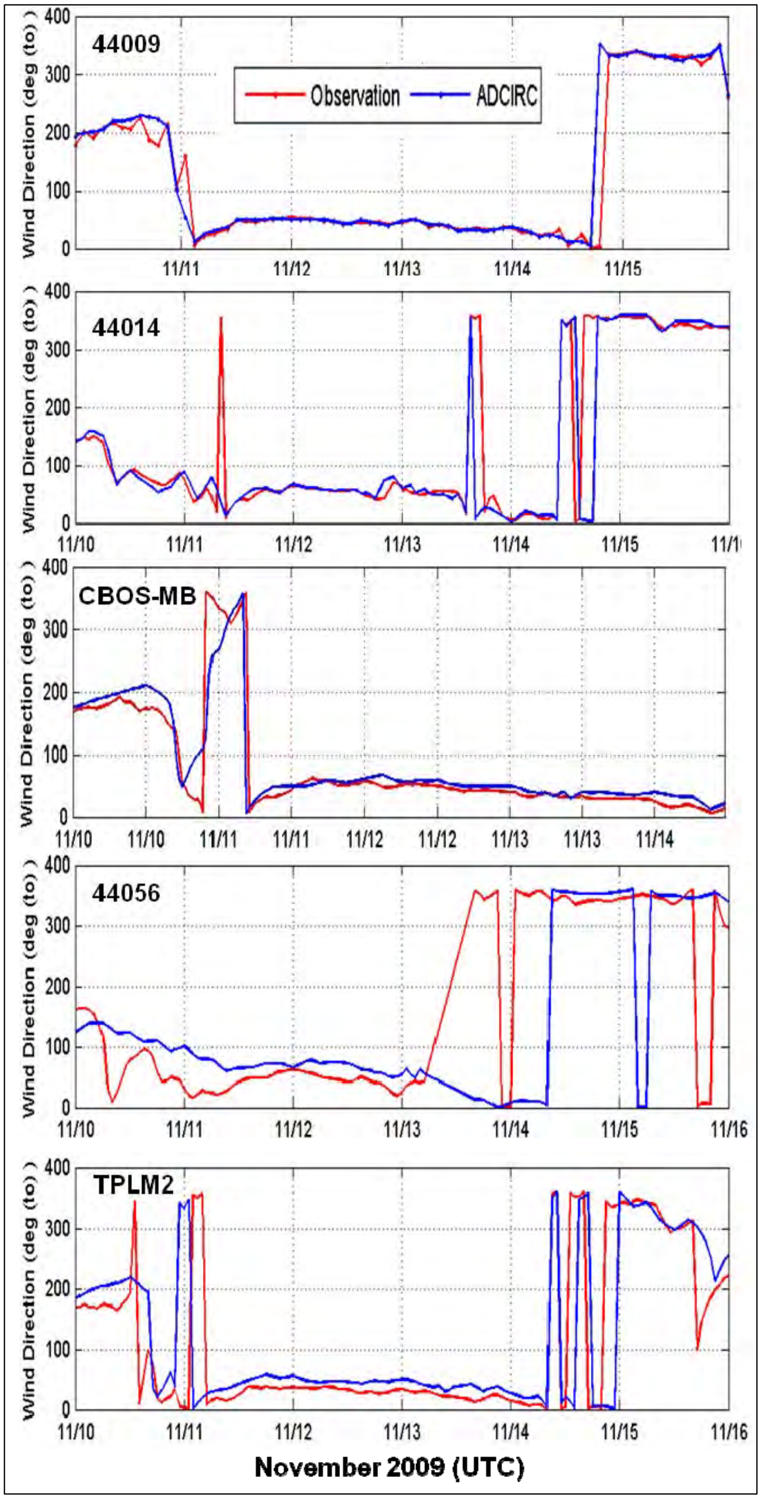

Figure 28. Comparisons of Extratropical Storm Nor'Ida wind directions at each validation station.

Results of the Nor'Ida wind field temporal correlation analyses appear in Figure 29 and Table 15. Wind speed scatter plots from each of the five stations (Figure 29) show the increased variability that occurs at 44014 and 44056. Wind speed and direction error statistics (Table 14) show a slight improvement over those from Ernesto (Table 13).

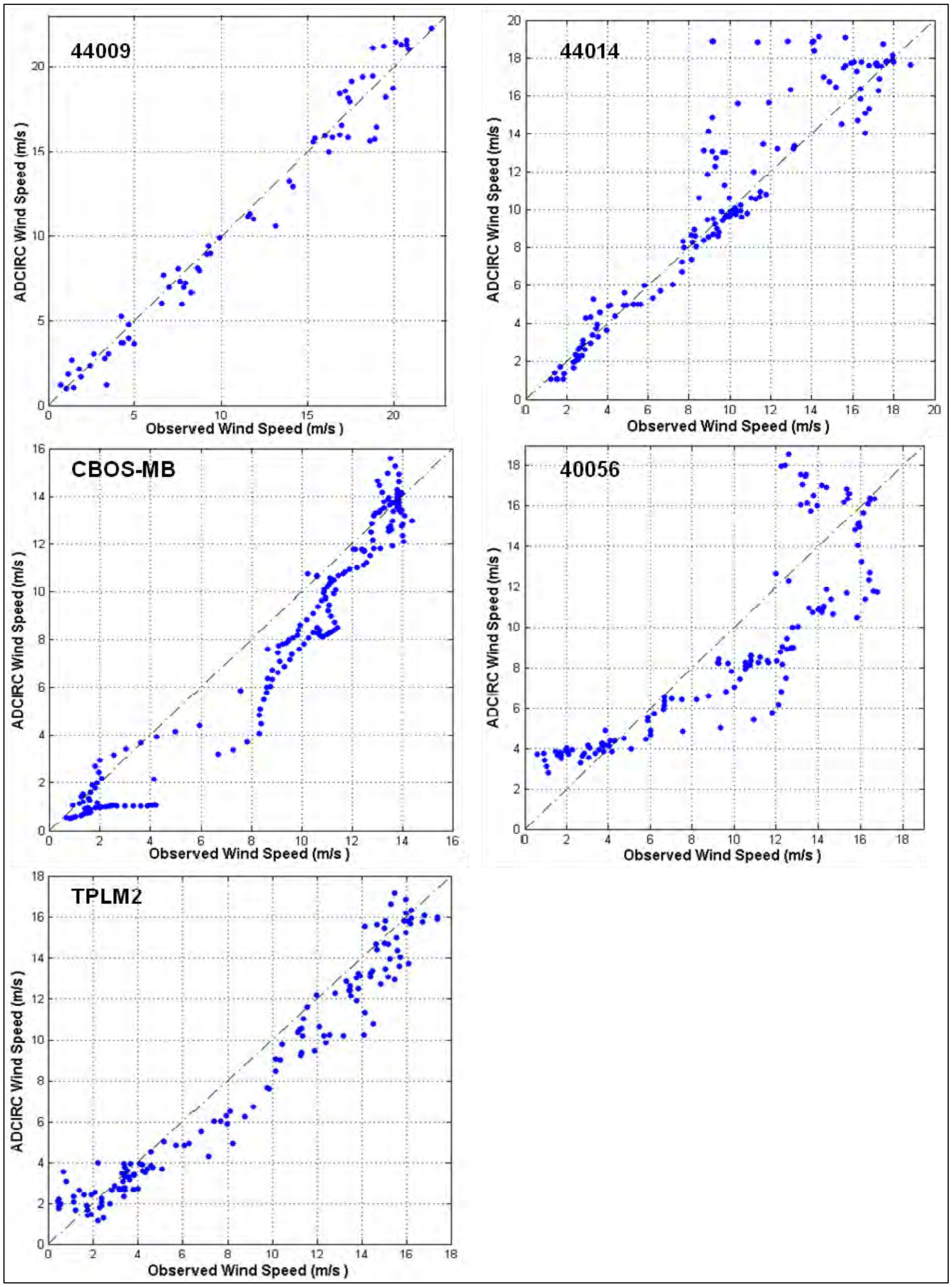

Figure 29. Extratropical Storm Nor'Ida wind speed scatter plots.

Table 15. Extratropical Storm Nor'Ida wind statistics.

Station	Wind Speed				Wind Direction		
	Bias (m/sec)	RMS Error (m/sec)	Scatter Index	Perf	Ang. Bias (Deg)	Circular Corr.	Perf
44009	-0.22	1.14	0.10	0.95	1.24	0.98	0.99
44014	0.75	2.15	0.21	0.87	2.48	0.99	0.99
CBOSMB	-1.03	1.58	0.14	0.87	9.33	0.93	0.94
44056	-0.79	2.73	0.27	0.84	20.3	0.93	0.91
TPLM2	-0.68	1.36	0.13	0.90	14.49	0.94	0.93

6.3.4 Wind peak event analysis

A synopsis of the Oceanweather wind field accuracy is provided by an overall peak event analysis. To perform this analysis, peak wind speeds at each observation station were obtained using a peak-over-threshold analysis. Winds were smoothed over a 3.0-hr window, and a threshold of 1.0 standard deviation above the station means was applied. Wind speed peaks rising above this threshold were isolated for analysis. Corresponding Oceanweather wind speed peaks, occurring within +/- 3.0 hr of the observed peaks, were also extracted. Finally, the observed and hindcast wind directions at the time of the isolated peaks were also extracted.

Results of the wind peak event analysis, depicted in Figure 30, quantify the overall accuracy in the validation storm-driving winds during the most critical peak conditions for storm surge. Peak wind speed bias is small (<1.5 m/sec) and an RMS error of 2.37 m/sec is driven by scatter at the lowest wind speeds. Overall performance is reasonable at 0.89, indicating that the peak errors are within 11% of the mean quantities. Wind directions are also reasonable with less than 6 deg angular bias and an overall performance of 0.96. These results suggest that the Oceanweather wind fields are adequate for performing a full validation of the Region III storm surge modeling system.

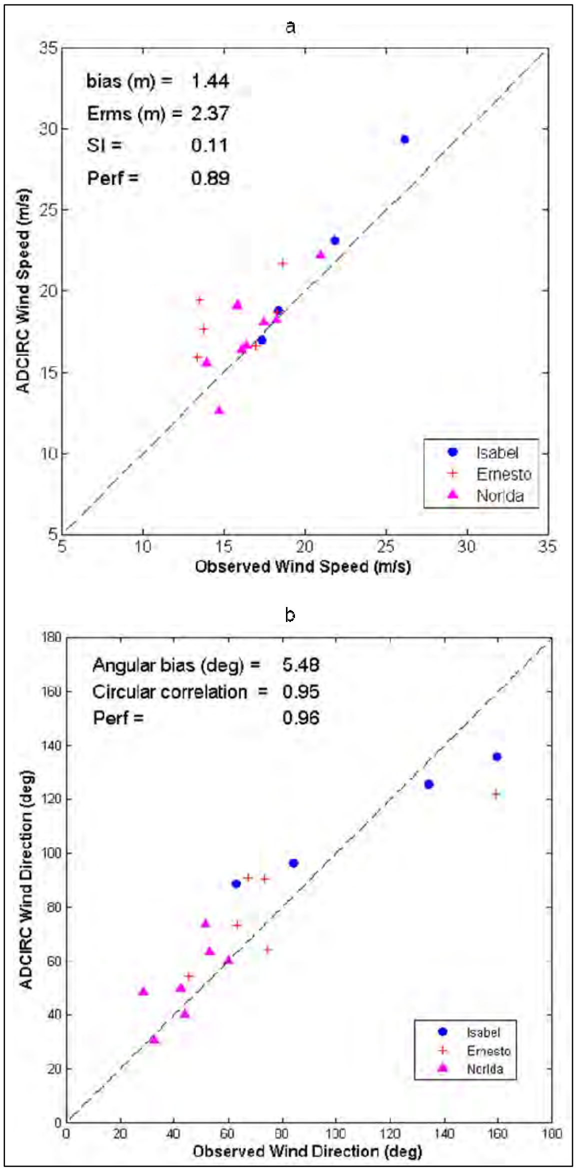

Figure 30. Wind peak event analysis results for (a) wind speed, and (b) wind direction.

7 Wave Validation

A state-of-the-art numerical wave modeling application has been configured and applied to support the FEMA Region III study. The U.S. Army Corps of Engineers (USACE) has worked with the Renaissance Computing Institute (RENCI) to implement the unstructured SWAN numerical wave model for basin-scale and regional wave forcing. The wave modeling grid resolution is identical to that used for ADCIRC, with a minimum spacing between nodes of approximately 50 m in coastal regions. The SWAN output includes directional wave spectra at selected validation points as well as spatial fields of wave height, wave period, wave direction, and radiation stress gradient. The cross-shore gradient in wave radiation stress, physically caused by a change in wave momentum in shallow water (associated with a decrease in wave height due to breaking), can be an important component to storm surge, as it leads to an increase in the stillwater level near the coast. Details of the implementation of SWAN are given in Submittal 1.2 (Blanton et. al. 2011).

This report documents the performance of this wave modeling system based on the evaluation of two historical hurricane events and a historical extra-tropical storm event. For each event, model performance was quantified using ground-truth measurements of various wave field properties. The results provide guidance on the suitability of the implemented modeling approach for moving forward with the production phase of the FEMA Region III study.

7.1 Wave validation approach

Region III wave validation was performed using the USACE Interactive Model Evaluation and Diagnostic System (IMEDS) described in Chapter 5. Using buoy observations as ground truth, temporal correlation (TC) and peak event (PE) statistical analyses are used to quantify model skill in reproducing measured wave height, period, and direction attributes. Wave height and period error metrics include the RMS error, bias, and scatter index. Wave direction metrics include the angular bias and circular correlation. A performance analysis synthesizes the TC error results into a convenient overall set of model performance scores. Performance scores are normalized to mean quantities and range from 0.00 to 1.00, with 1.00 representing perfect agreement between model output and observations.

For each storm event, outputs from the SWAN model runs were saved at the location of each observation station. The IMEDS analysis was then performed separately on the results from each model run using all available observations as ground truth.

7.2 Wave validation data

A significant effort was made to obtain and use all available sources of wave data (bulk and spectral) in the Region III wave validation analysis. However, reliable wave data are generally scarce during the validation events, as intense storms often disable measurement stations. Region III wave validation data were obtained from the National Data Buoy Center (NDBC; http://www.ndbc.noaa.gov/), US Army Corps of Engineers Field Research Facility (FRF; http://www.frf.usace.army.mil/) City of Norfolk, VA (Moffatt and Nichol, Engineers 2010), and the National Ocean Service (NOS)[1]. The available observation stations for each storm are listed in Table 16. NDBC stations 44009, 44014, and FRF 44056 were floating buoys; the Norfolk and NOS stations were bottom-mounted acoustic profilers. Instrument and deployment details for each station appear in Table 17. Wave spectral data are used from all stations with the exception of the NOS and Norfolk stations, from which only bulk statistics are available.

7.3 Wave validation results

Validation of the Region III wave modeling system has resulted in a comprehensive set of error metrics and performance scores that identify hindcast strengths and weaknesses. Table 18 is an overall summary of model skill in replicating the observed wave conditions in each storm event. The performance scores for SWAN wave height, period, and direction are obtained by averaging the scores across all available observation stations using sample size weighting functions. All of the scores are 0.85 or greater, suggesting that mean errors are within 15% of the mean observed quantities. Details from the station results during each event are described in the following three sections. A final section summarizes wave peak analyses from all three events.

---

[1] Taylors Island ADCP Data provided by H.H. Shih, NOAA/National Ocean Service, Center for Operational Oceanographic Products and Services, Silver Spring, MD.

Table 16. Validation events and available wave observations.

Storm	Date	Wave Observation Stations
Isabel	SEP 2003	NDBC 44009, FRF 44056, NOS Taylors
Ernesto	SEP 2006	NDBC 44009, 44014
Ida	NOV 2009	NDBC 44009, 44014, Norfolk AWAC

Table 17. Wave validation station details.

Station	Type	Depth (m)	North Latitude	West Longitude
NDBC 44009 Delaware Bay	3-m Discus; ARES payload	28.0	38.464	74.702
NDBC 44014 Virginia Beach	3-m Discus; ARES payload	47.5	36.611	74.836
FRF 44056	Datawell Waverider Buoy	17.4	36.200	75.714
NOS Taylors Island	RDI Sentinel ADCP 1200 KHz	7.5	38.486	76.365
City of Norfolk	NORTEK AWAC-AST	6.4	36.961	76.224

Table 18. SWAN overall performance summary.

Event	Wave Height	Peak Period	Mean Direction
Isabel	0.85	0.86	0.95
Ernesto	0.87	0.91	0.99
Nor'Ida	0.90	0.93	0.96

7.3.1 Hurricane Isabel (2003)

Hurricane Isabel exhibited the highest coastal wave heights of all three events. SWAN output fields at the time of maximum wave height during Isabel appear in Figure 32. Wave heights reached 8-10 m offshore and 2.0-3.0 m in the lower Chesapeake Bay. The wave height plot shows the propagation of wave energy from the Atlantic basin into the Delaware and Chesapeake Bays. The wave radiation stress, which drives the contribution of waves to storm surge, is clearly most important along the coast with a maximum near the southern border (Virginia Beach). The effect of waves on overall water levels is shown in the wave setup plot. Wave setup values of 0.2-0.4 m were observed along the Virginia coast north of the Chesapeake Bay entrance. It is striking that, even within the lower Chesapeake Bay, the wave influence on storm surge is on an order of 0.1-0.2 m. Validation results from the three Isabel wave observation stations (Table 16) appear below.

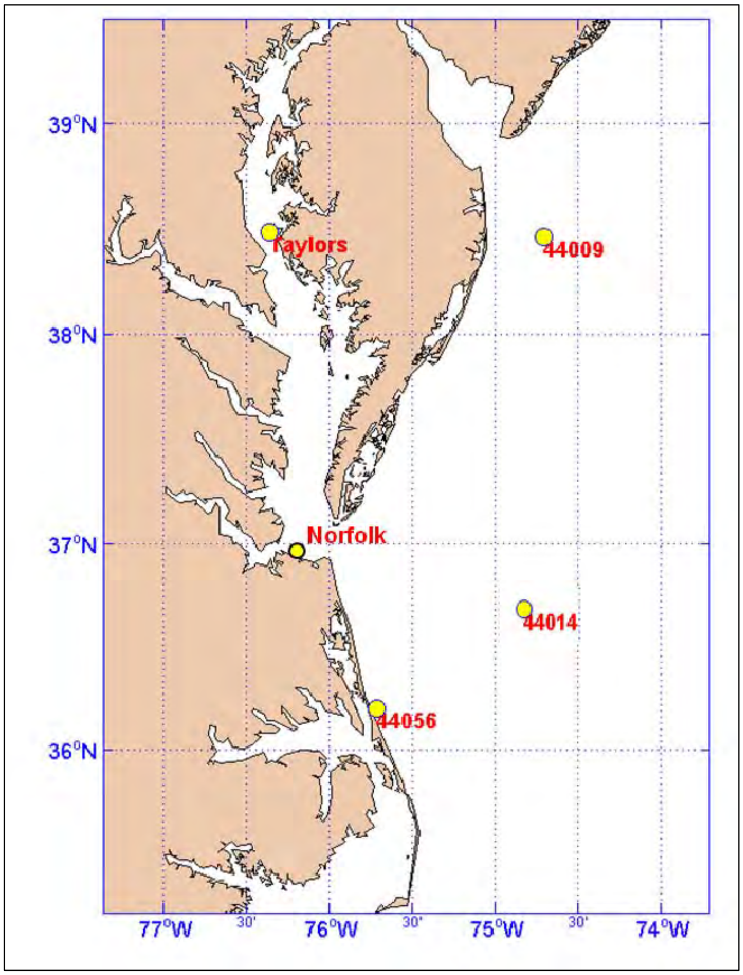

Figure 31. Wave validation stations used in the Region III study.

7.3.1.1 Hurricane Isabel at Station 44056

FRF station 44056 is located just outside the Region III domain off the coast of North Carolina (Figure 31). It is an important validation station for this study as it is in relatively shallow water (17-m depth) in an open coast environment. Observed and SWAN wave height, period, and direction time series at this station during Hurricane Isabel are compared in Figure 33. The peak attributes are captured quite nicely at this station. Observed wave periods are higher than SWAN preceding the storm. This is a result of precursor swells that were generated outside of the modeling domain.

7.3.1.2 Hurricane Isabel at Taylor Island Station (NOS ADCP)

The NOS ADCP at Taylor Island is a unique wave measurement from Hurricane Isabel in the mid section of Chesapeake Bay (Figure 31). A comparison of observed and SWAN wave height, period, and direction time

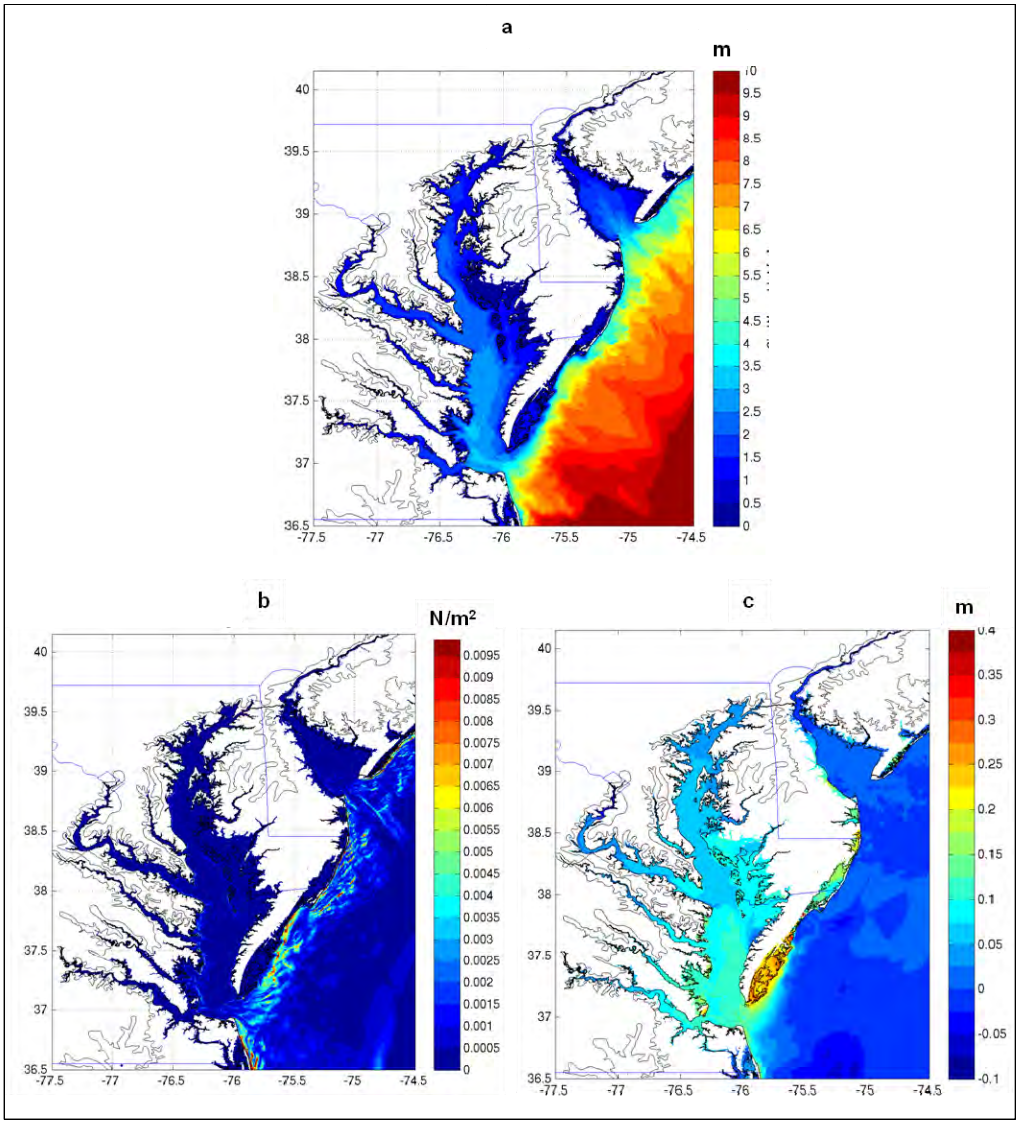
a
m
10
9.5
9
8.5
8
7.5
7
6.5
6
5.5
5
4.5
4
3.5
3
2.5
2
1.5
1
0.5
0
40
39.5
39
38.5
38
37.5
37
36.5
-77.5
-77
-76.5
-76
-75.5
-75
-74.5
b
N/m²
0.0095
0.009
0.0085
0.008
0.0075
0.007
0.0065
0.006
0.0055
0.005
0.0045
0.004
0.0035
0.003
0.0025
0.002
0.0015
0.001
0.0005
0
c
m
0.4
0.35
0.3
0.25
0.2
0.15
0.1
0.05
0
-0.05
-0.1

Figure 32. Hurricane Isabel SWAN output fields: a. maximum significant wave height, b. maximum radiation stress gradient magnitude, and c. wave setup (difference between the TidesSurgeWaves and TidesSurge solutions).

series from this station during Hurricane Isabel appear in Figure 34. Although the general trend of this event is captured well, SWAN underestimated the observed peak wave height by approximately 0.4 m. Wave period and direction during the main event (19 September) are represented reasonably well by SWAN.

7.3.1.3 Hurricane Isabel at Station 44009

Non-directional NDBC station 44009 is located in the open ocean off the coast of Delaware (Figure 31), at a significant distance from the storm track (Figure 13). Observed and SWAN wave height and period time series from

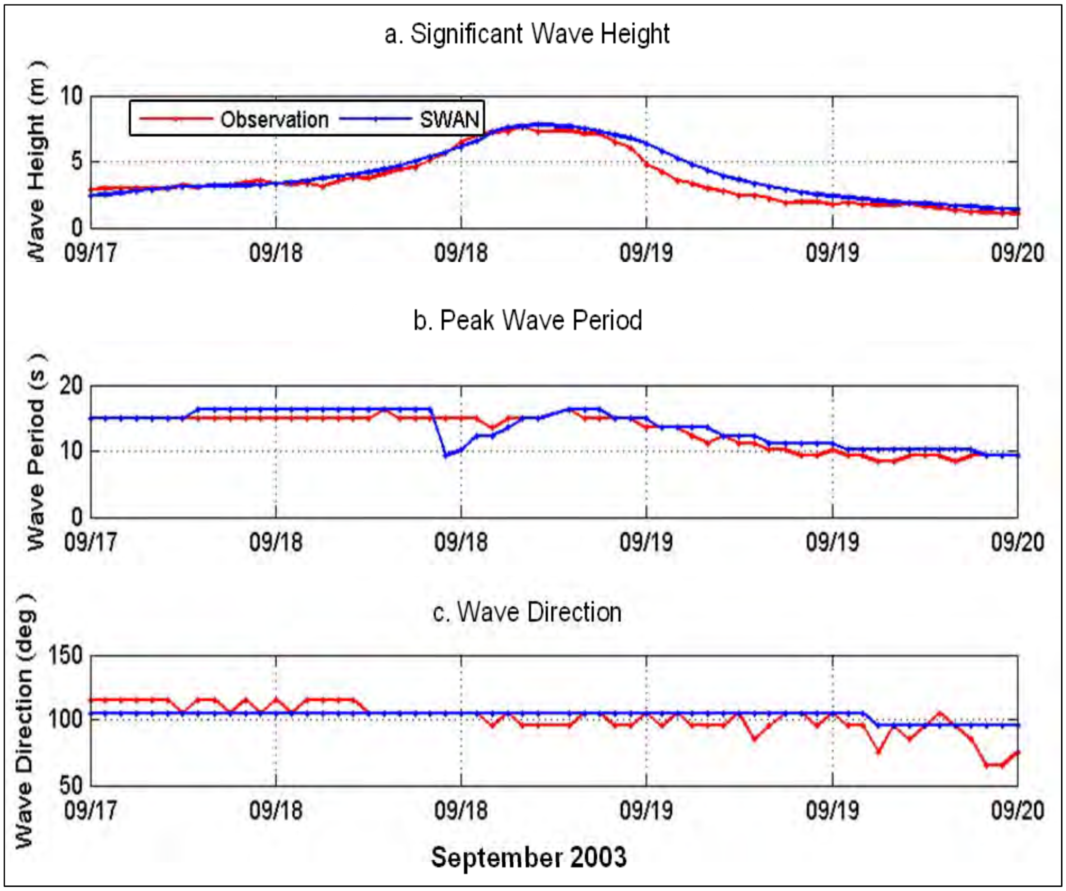

Figure 33. Hurricane Isabel bulk wave height and period time series from Station 44056: a. significant wave height, b. peak wave period, and c. wave direction.

this station during Hurricane Isabel are compared in Figure 35. The wave heights at this station show good agreement, with excellent agreement at the storm peak. SWAN peak wave periods at this station do not agree well with observations, with wave periods leading up to the event significantly overestimated.

An examination of the wave spectrum details from this station indicates that a bi-modal wave field existed with wind, sea, and swell components at peak periods of 5-10 sec and 15-16 sec, respectively. As these two peaks are close in total energy, the wave period disparity between 44009 and SWAN is a result of the swell being somewhat more energetic in SWAN than was actually observed. This also explains why the SWAN significant wave heights are higher over most of the record. This is perhaps understandable, given this station's significant distance away from the storm center.

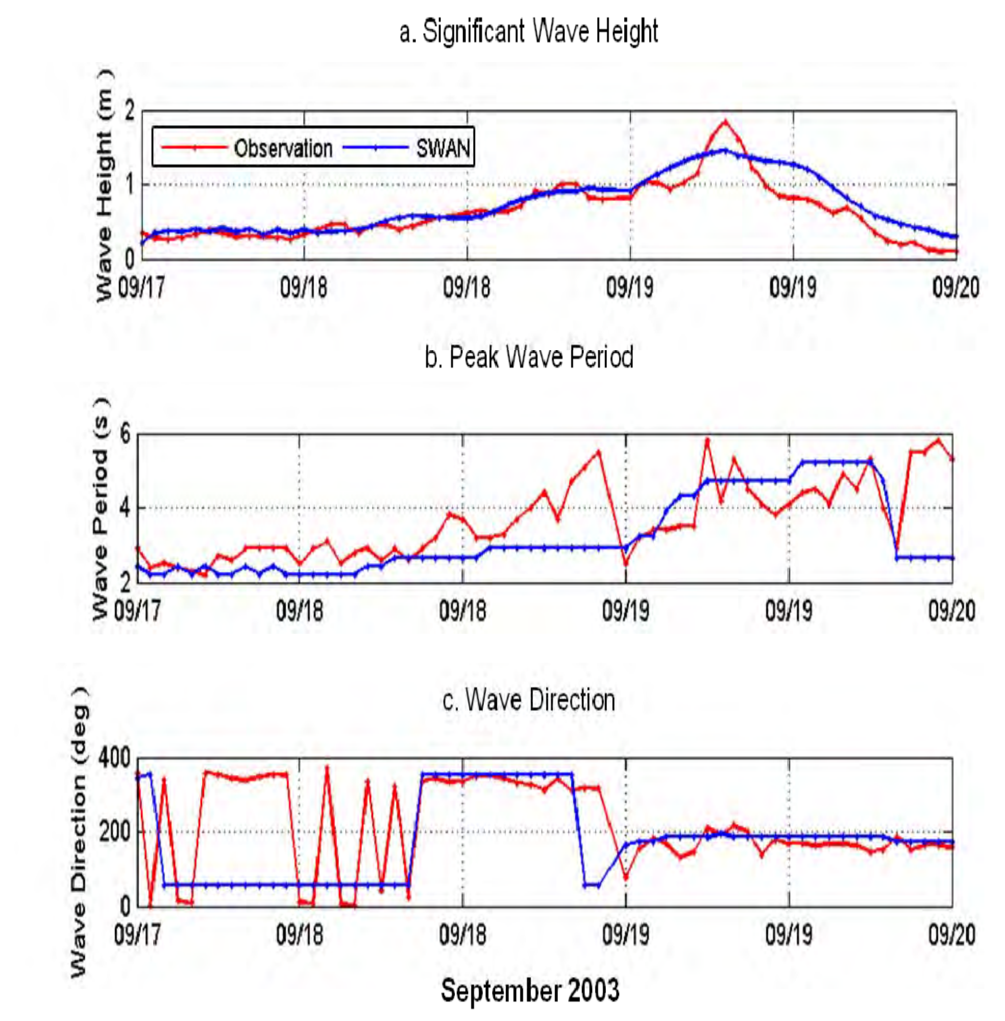

Figure 34. Hurricane Isabel bulk wave height, period, and direction time series from Taylors Island Station: a. significant wave height, b. peak wave period, and c. wave direction.

7.3.1.4 Hurricane Isabel wave hindcast summary

Results from the Hurricane Isabel temporal correlation analysis quantify SWAN hindcast performance during this event. Scatter plots of observed versus hindcast wave heights appear in Figure 36. Wave height, period, and direction error metrics and performance (skill) scores from each station appear in Table 19. Error metrics are provided for both wave period and direction. However, the primary emphasis should be placed on wave height because tropical and extra-tropical storm wavefields are often composed of mixed combinations of wind, sea, and swell. The peak wave period parameter only represents one of these systems, and the mean wave direction parameter is an average of the two. As a result, the bulk statistical period and direction quantities typically have increased scatter when compared to model output.

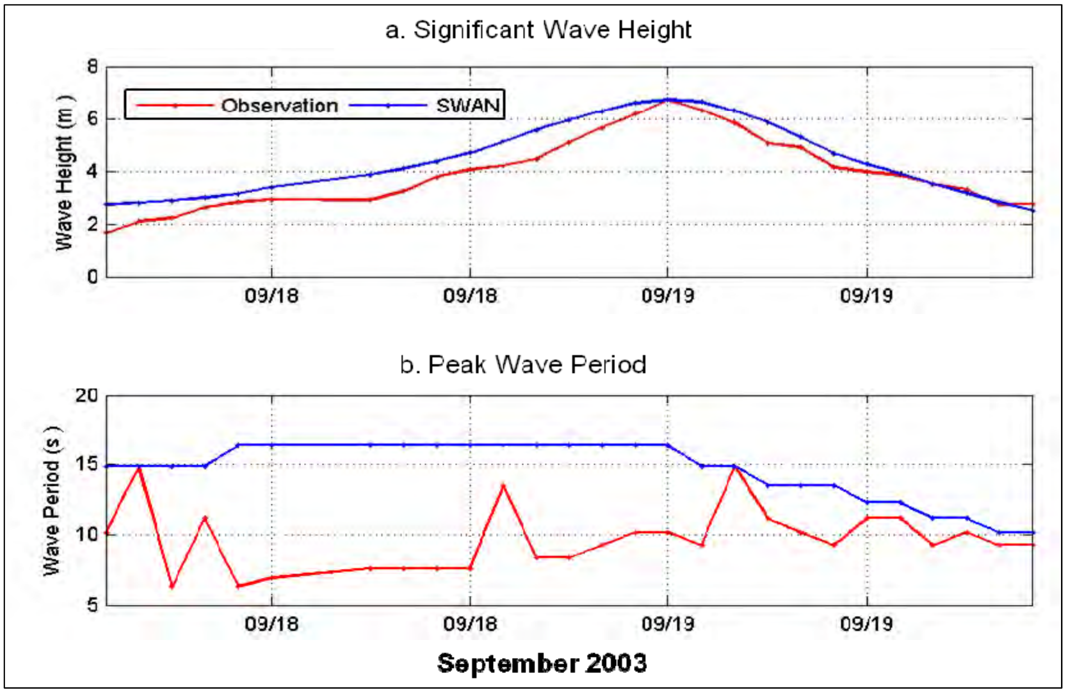

Figure 35. Hurricane Isabel bulk wave height and period time series from Station 44009: a. significant wave height, and b. peak wave period.

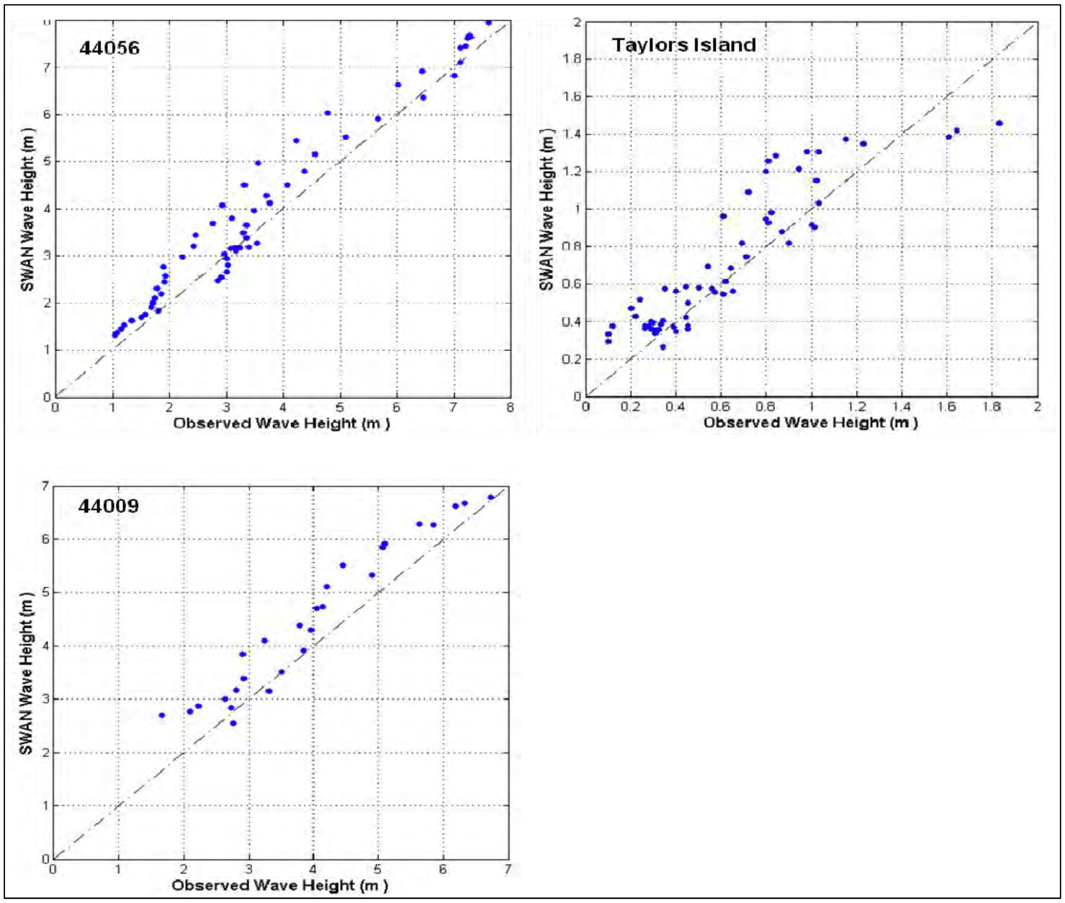

Figure 36. Scatter plot comparison of Hurricane Isabel observed and hindcast wave heights.

Table 19. Hurricane Isabel wave hindcast performance statistics.

Station	Wave Height				Wave Period				Wave Direction		
	Bias (m)	RMS Error (m)	Scatter Index	Perf	Bias (s)	RMS Error (s)	Scatter Index	Perf	Ang. Bias (Deg)	Circular Corr.	Perf
44056	0.34	0.54	0.12	0.89	0.73	1.13	0.07	0.93	3.46	0.36	0.67
44009	0.49	0.6	0.09	0.87	4.93	5.83	0.33	0.46	---	---	---
Taylors	0.09	0.19	0.26	0.81	-0.50	1.01	0.24	0.80	34.04	0.89	0.85

The statistical analysis results (Figure 36 and Table 19) show that SWAN did a reasonable job of estimating wave conditions at the validation stations. Station 44056 exhibits a small positive wave height bias (0.34 m) resulting from SWAN wave heights after the event not dropping off as quickly as those observed at the station (Figure 33). Although the hindcast underestimated peak wave conditions at Taylors Island by approximately 0.2 m, the overall bias is quite low at 0.09 m. Station 44009 exhibits a 0.49-m height bias in the SWAN results; however, wave heights at the event peak show perfect agreement with the observations.

7.3.2 Ernesto (2006)

Hurricane Ernesto exhibited the lowest wave heights of the three validation storms. SWAN output fields at the time of maximum wave height during Ernesto appear in Figure 37. Wave heights reached 5.0-6.0 m offshore of Delaware Bay and 3.0-4.0 m in the mouths of both Delaware and Chesapeake Bays. The wave height plot shows some transfer of wave energy from the Atlantic basin into the bays. The Ernesto wave-induced force is concentrated along the coasts but with much narrower bands than were exhibited by Isabel (Figure 32). As a result, the wave-induced setup is below 0.1 m throughout most of the domain, with the exception of some coastal areas and the southern Delaware Bay shoreline, where a setup of 0.1-0.2 m is exhibited. Wave observation data were only available for two offshore stations during Hurricane Ernesto (Table 16). Validation results from these stations appear below.

7.3.2.1 Hurricane Ernesto at Station 44014

NDBC station 44014 is located well offshore of the entrance to Chesapeake Bay (Figure 31). Observed and modeled wave height, period, and direction time series at 44014 during Hurricane Ernesto are compared in Figure 38. The SWAN results show excellent agreement with the observations.

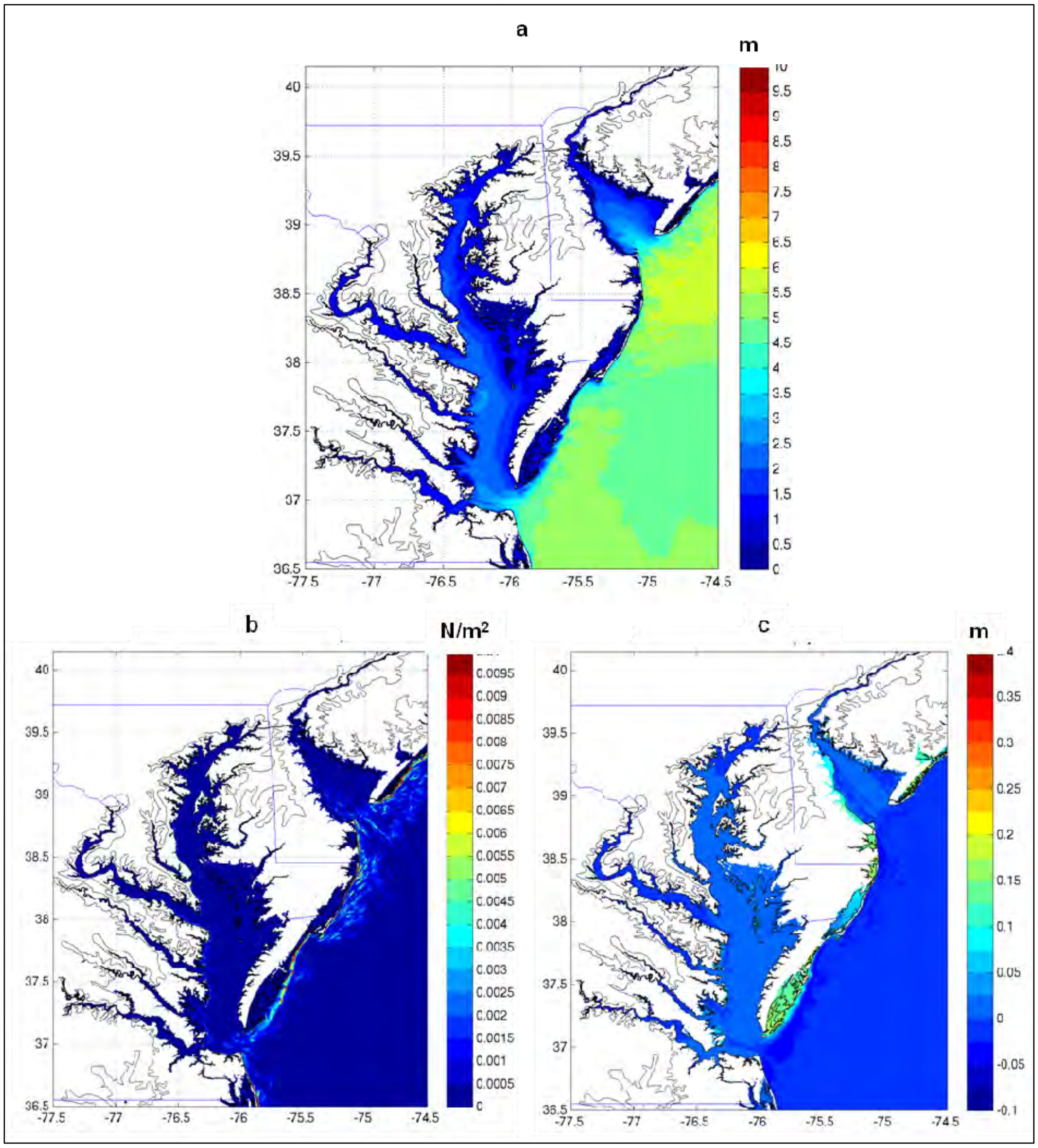
a
m
10
9.5
9
8.5
8
7.5
7
6.5
6
5.5
5
4.5
4
3.5
3
2.5
2
1.5
1
0.5
0
40
39.5
39
38.5
38
37.5
37
36.5
-77.5
-77
-76.5
-76
-75.5
-75
-74.5
b
N/m2
0.0095
0.009
0.0085
0.008
0.0075
0.007
0.0065
0.006
0.0055
0.005
0.0045
0.004
0.0035
0.003
0.0025
0.002
0.0015
0.001
0.0005
0
c
m
0.4
0.35
0.3
0.25
0.2
0.15
0.1
0.05
0
-0.05
-0.1

Figure 37. Hurricane Ernesto SWAN output fields: a. Maximum significant wave height, b. maximum radiation stress gradient magnitude, and, c. wave setup (difference between the TidesSurgeWaves and TidesSurge solutions).

7.3.2.2 Hurricane Ernesto at Station 44009

Non-directional NDBC station 44009, also used for the Isabel validation, is located in the open ocean off the coast of Delaware (Figure 31), at a significant distance from the storm tracks (Figure 13). A comparison of observed and SWAN wave height and period time series from this station during Hurricane Ernesto appear in Figure 39. The growth of Ernesto is captured quite well by SWAN; however, the wave peak is underestimated by approximately 1.0 m.

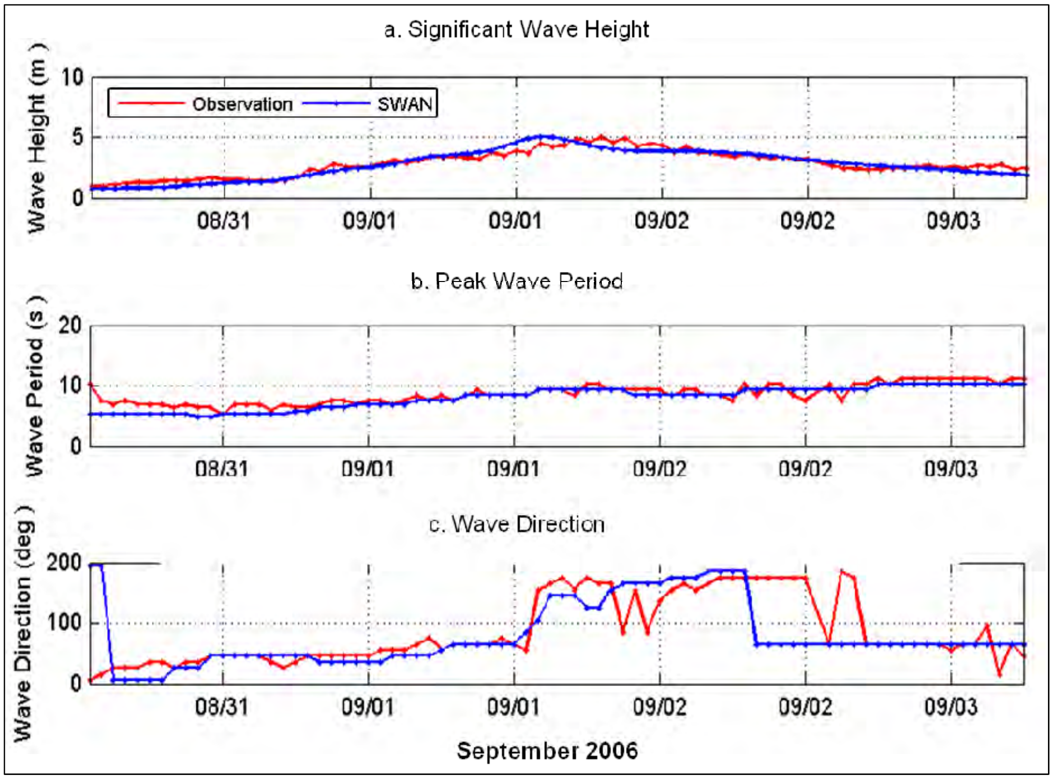

Figure 38. Hurricane Ernesto bulk wave height and period time series from Station 44014: a. significant wave height, b. peak wave period, and, c. wave direction.

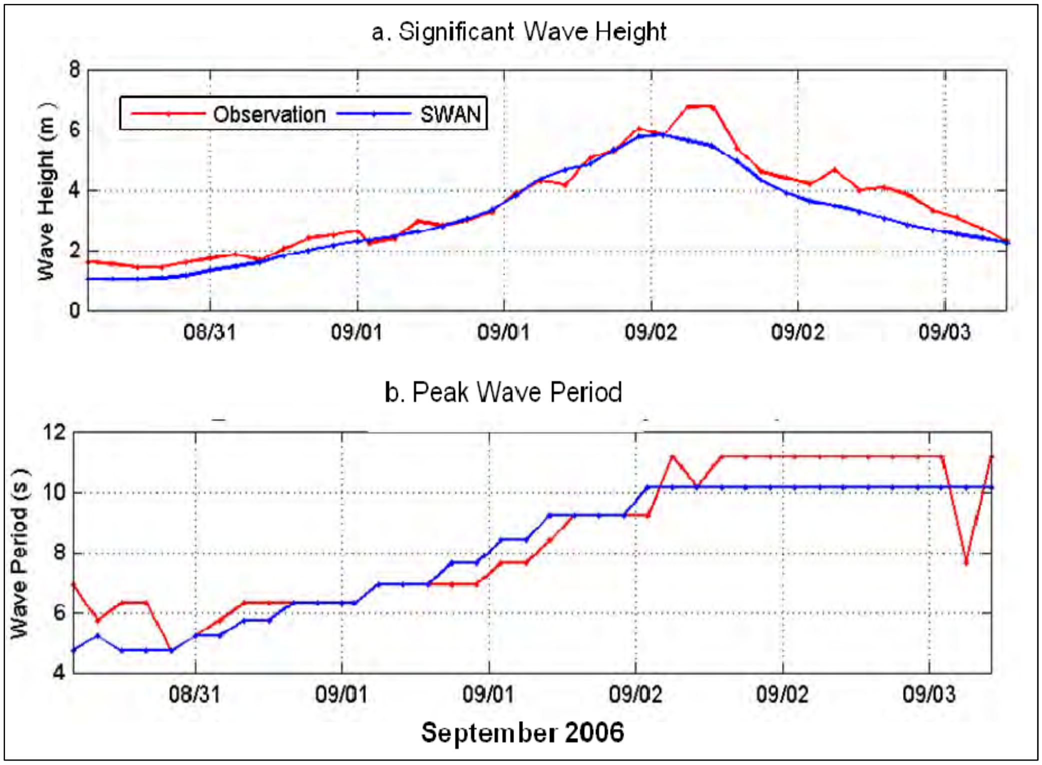

Figure 39. Hurricane Ernesto bulk wave height and period time series from Station 44009: a. significant wave height, and b. peak wave period.

7.3.2.3 Hurricane Ernesto wave hindcast summary

Results from the Hurricane Ernesto temporal correlation analysis confirm that SWAN performed well in hindcasting this event. Scatter plots of observed versus hindcast wave heights appear in Figure 40. Wave height, period, and direction error metrics and performance (skill) scores from each station appear in Table 20. The wave height peak was underestimated by about 1.0 m at 44009. As with the Isabel validation at 44009, it is argued that wave height errors are expected to increase with distance away from the storm track. This is a result of the wind field reconstructions being focused on the primary storm event. In general, the Ernesto wave hindcast exhibits relatively low errors and high performance.

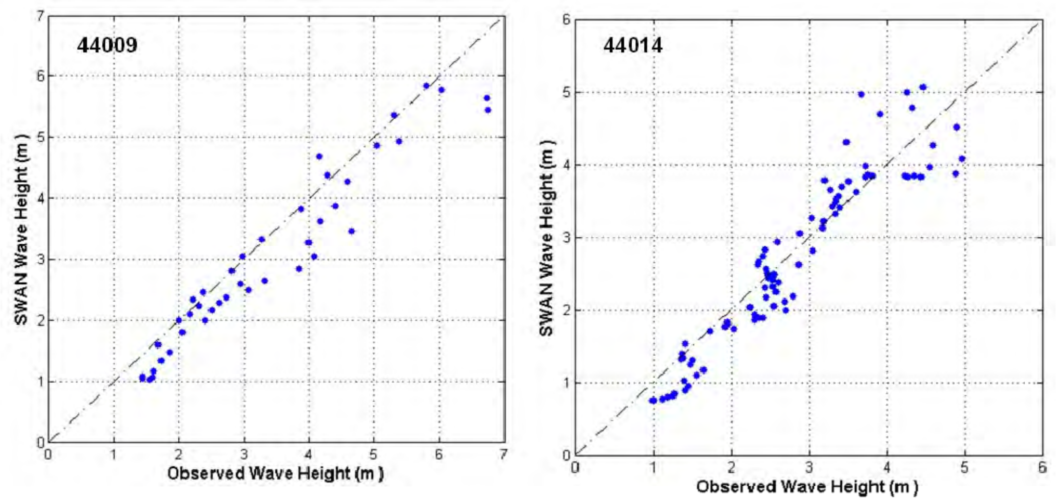

Figure 40. Scatter plot comparison of Hurricane Ernesto observed and hindcast wave heights.

Table 20. Hurricane Ernesto Wave Hindcast Performance Statistics

	Wave Height				Wave Period				Wave Direction		
Station	Bias (m)	RMS Error (m)	Scatter Index	Perf	Bias (s)	RMS Error (s)	Scatter Index	Perf	Ang. Bias (Deg)	Circular Corr.	Perf
44014	-0.09	0.41	0.15	0.92	-0.72	1.17	0.11	0.89	-7.88	0.7	0.83
44009	-0.34	0.52	0.12	0.88	-0.34	0.94	0.10	0.93	---	---	---

7.3.3 Nor'Ida (2009)

Extra-tropical Storm Nor'Ida had a significant impact on the Region III domain, with peak wave heights almost approaching those from Isabel. SWAN output fields at the time of maximum wave height during Nor'Ida appear in Figure 41. Wave heights reached 7.0-9.0 m offshore and

3.0-4.0 m in the mouths of both Delaware and Chesapeake Bays. The Nor'Ida wave radiation stress is concentrated along the coasts, but with much narrower bands than those exhibited by Isabel (Figure 32). The resulting wave setup heights range from 0.2-0.3 m along the open coasts to < 0.15 m in the bays. Wave observation data were only available for three stations during Nor'Ida (Table 16). Validation results from these stations appear below.

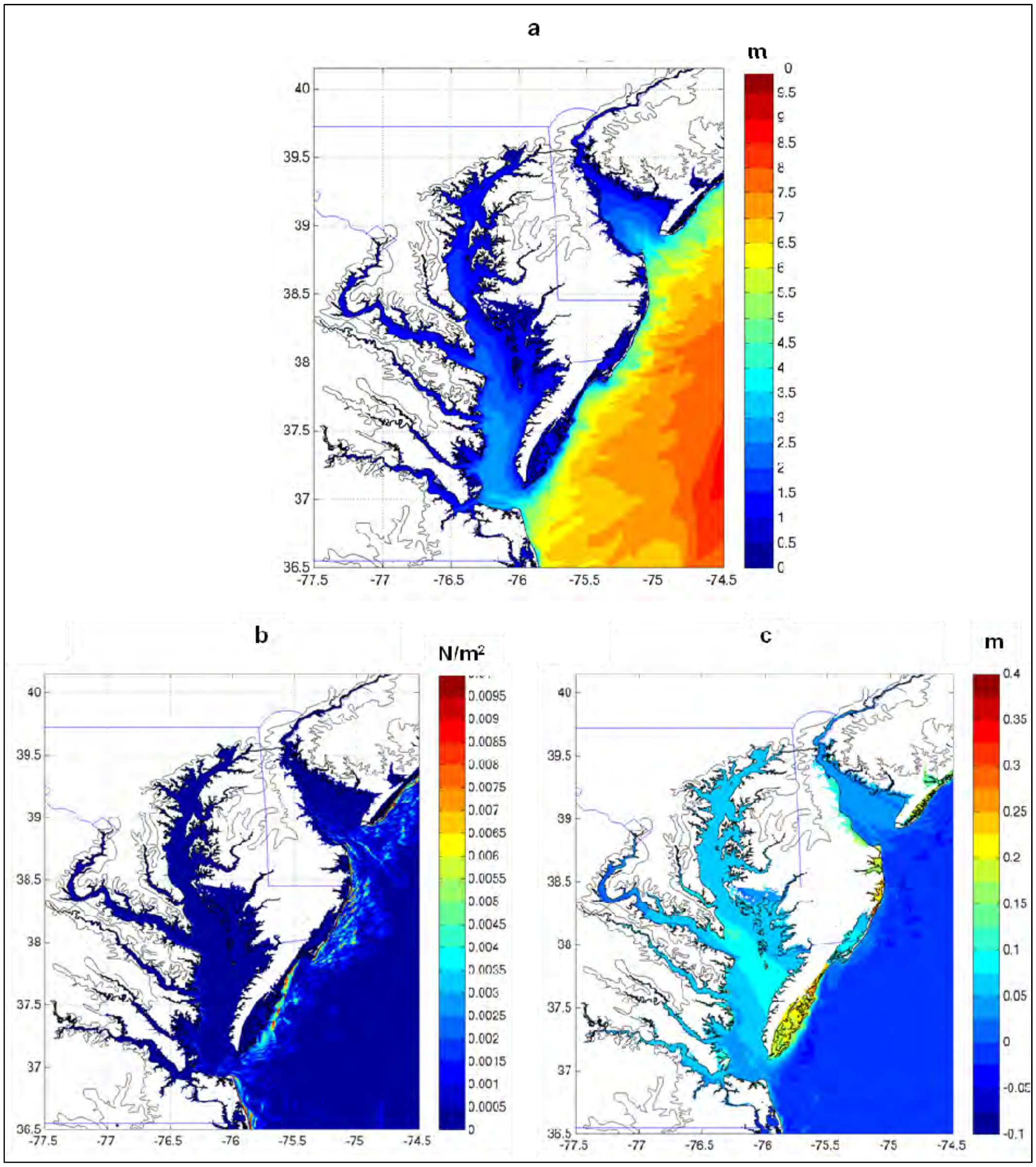
a
m
0
9.5
9
8.5
8
7.5
7
6.5
6
5.5
5
4.5
4
3.5
3
2.5
2
1.5
1
0.5
0
40
39.5
39
38.5
38
37.5
37
36.5
-77.5
-77
-76.5
-76
-75.5
-75
-74.5
b
N/m²
0.0095
0.009
0.0085
0.008
0.0075
0.007
0.0065
0.006
0.0055
0.005
0.0045
0.004
0.0035
0.003
0.0025
0.002
0.0015
0.001
0.0005
0
c
m
0.4
0.35
0.3
0.25
0.2
0.15
0.1
0.05
0
-0.05
-0.1

Figure 41. Extratropical Storm Nor'Ida SWAN output fields: a. maximum significant wave height, b. maximum radiation stress gradient magnitude. and, c. wave setup (difference between the TidesSurgeWaves and TidesSurge solutions).

7.3.3.1 Extratropical Storm Nor'Ida at Station 44014

Figure 42 compares observed and modeled wave height, period, and direction time series at 44014 (Figure 31) during Extratropical Storm Nor'Ida. The SWAN results show excellent agreement with the observations.

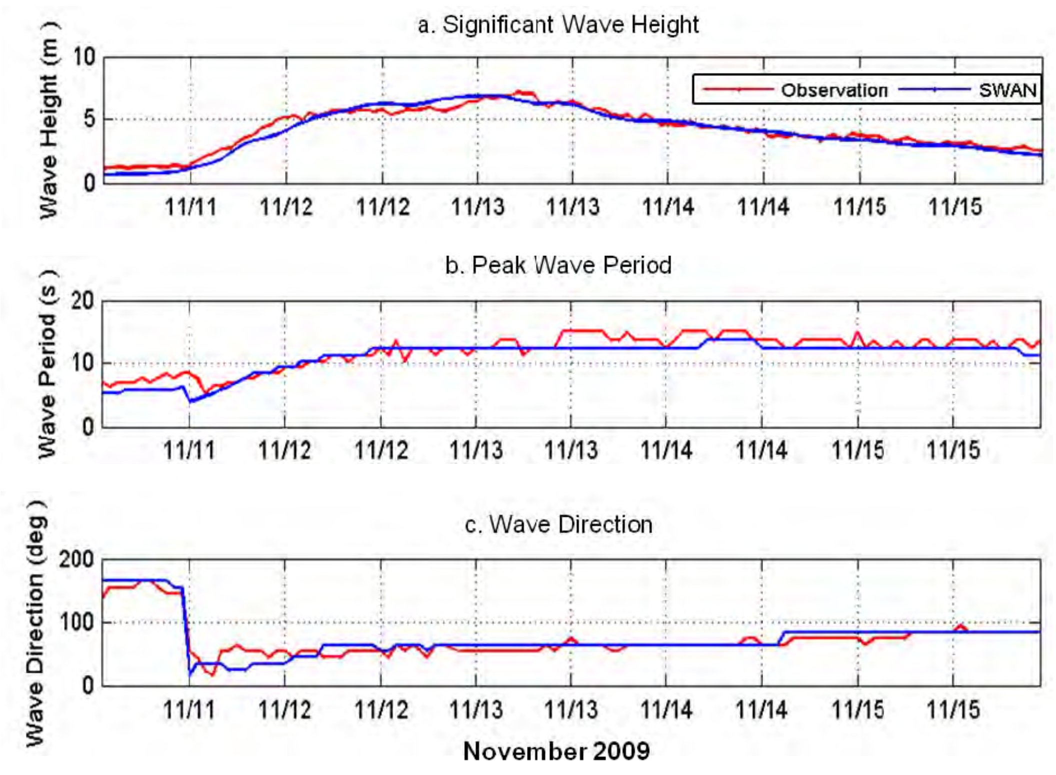

Figure 42. Extratropical Storm Nor'Ida bulk wave height and period time series from Station 44014: a. significant wave height, b. peak wave period, and, c. mean wave direction.

7.3.3.2 Extratropical Storm Nor'Ida at Station 44009

Figure 43 compares observed and modeled wave height and period time series at 44009 (Figure 31) during Extratropical Storm Nor'Ida. As with station 44014, the SWAN results show excellent agreement with the observations. It should be noted that the Nor'Ida offshore significant wave heights were greater than 5.0 m for approximately 48 hr at each of these stations (each x-axis tick represents 12 hr in Figures 42 and 43). This makes a striking comparison with Hurricane Isabel, the recent storm of record for the region, during which offshore significant wave heights were greater than 5,0 m for only 12 hr (Figure 35).

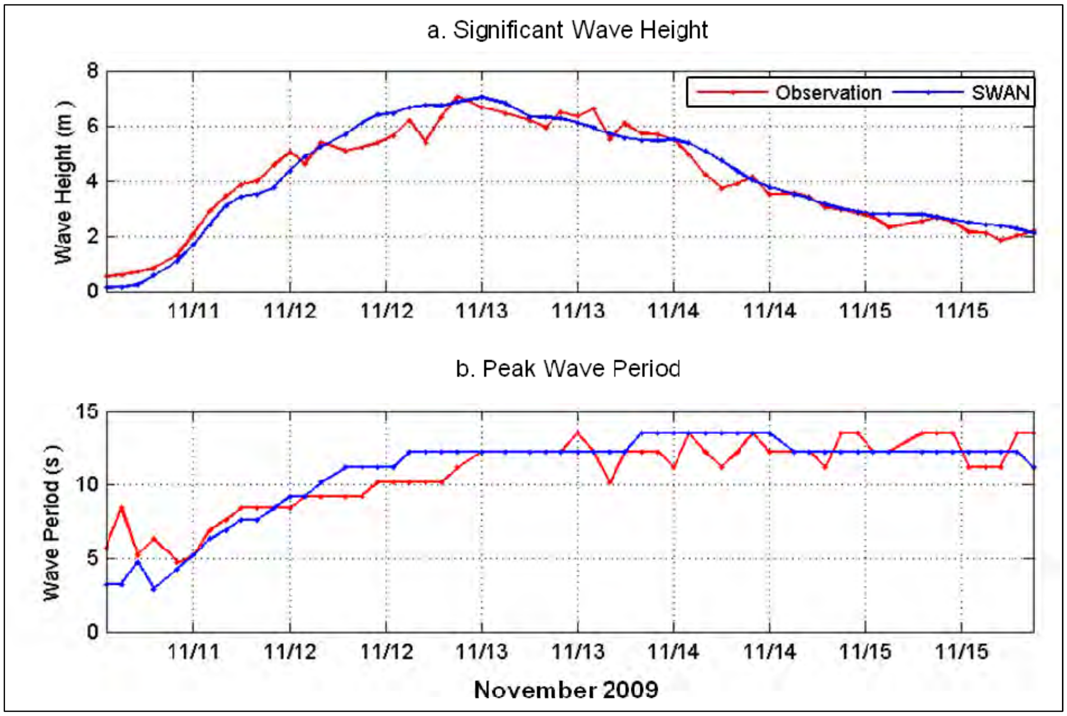

Figure 43. Extratropical Storm Nor'Ida bulk wave height and period time series from Station 44009: a. significant wave height, and b. peak wave period.

7.3.3.3 Extratropical Storm Nor'Ida at Norfolk station

The Norfolk AWAC station was located in the lower Chesapeake Bay (Figure 31). Figure 44 compares observed and modeled wave height, period, and direction time series at Norfolk during Extratropical Storm Nor'Ida. SWAN exhibited mixed results at this station. Wave height is underestimated during the growth of the event and overestimated at the storm peak. This station exhibited a complex wave environment, as it was influenced by both wind sea from the northeast and swell from the east (through the mouth of the bay). This is demonstrated by the sample Norfolk station directional wave spectra (during Nor'Ida) appearing in Figure 45. A clear bimodal wave field can be seen with wave field components arriving from both the east (swell) and northeast (sea). Further evidence of this directional bimodality is reflected in the Norfolk station wave direction comparison (Figure 44), as SWAN wave directions flip back and forth between the two dominant directions.

7.3.3.4 Extratropical Storm Nor'Ida wave hindcast summary

Results from the Extratropical Storm Nor'Ida temporal correlation analysis confirm that SWAN also performed very well in hindcasting this event at the offshore stations, and had exhibited fair results at the Norfolk station. Scatter plots of observed versus hindcast wave heights appear in Figure 46. Table 21 lists wave height, period, and direction error metrics and performance (skill) scores from each station. The two offshore stations both had very low errors and high performance scores. Although the Norfolk station wave height results have a low bias (0.04), they exhibit a higher than normal scatter (SI = 0.28). However, given the complex environment of the lower Chesapeake, including a bi-modal wave field to account for (Figure 45) and uncertainties in the local wind field (Figure 29), it is argued that this is an acceptable wave hindcast of this event.

7.3.4 Peak wave event summary

Of significant importance is the ability of the hindcast to match the wave attributes at the peak of the event. Typically, the event peak is the time period when the waves may contribute most to overall storm surge. A wave

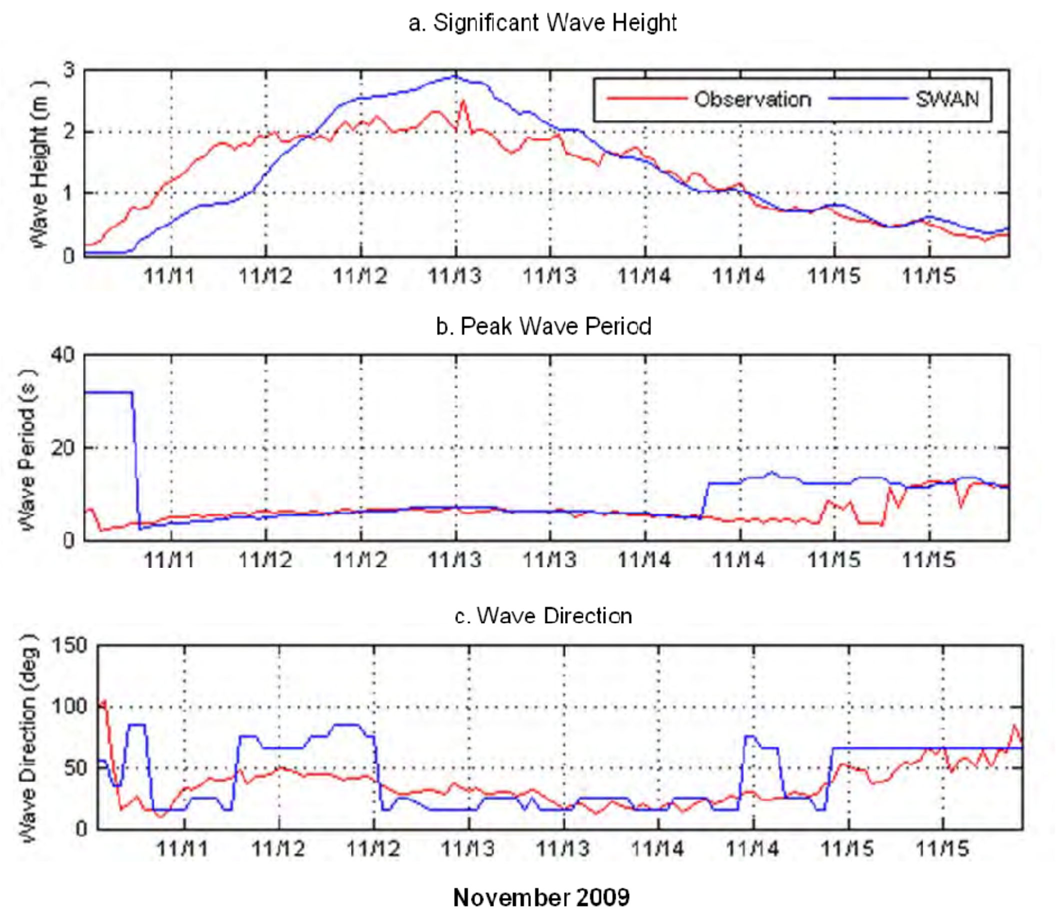

Figure 44. Extratropical Storm Nor'Ida bulk wave height and period time series from the Norfolk City Station: a. significant wave height, b. peak wave period, and c. mean wave direction.

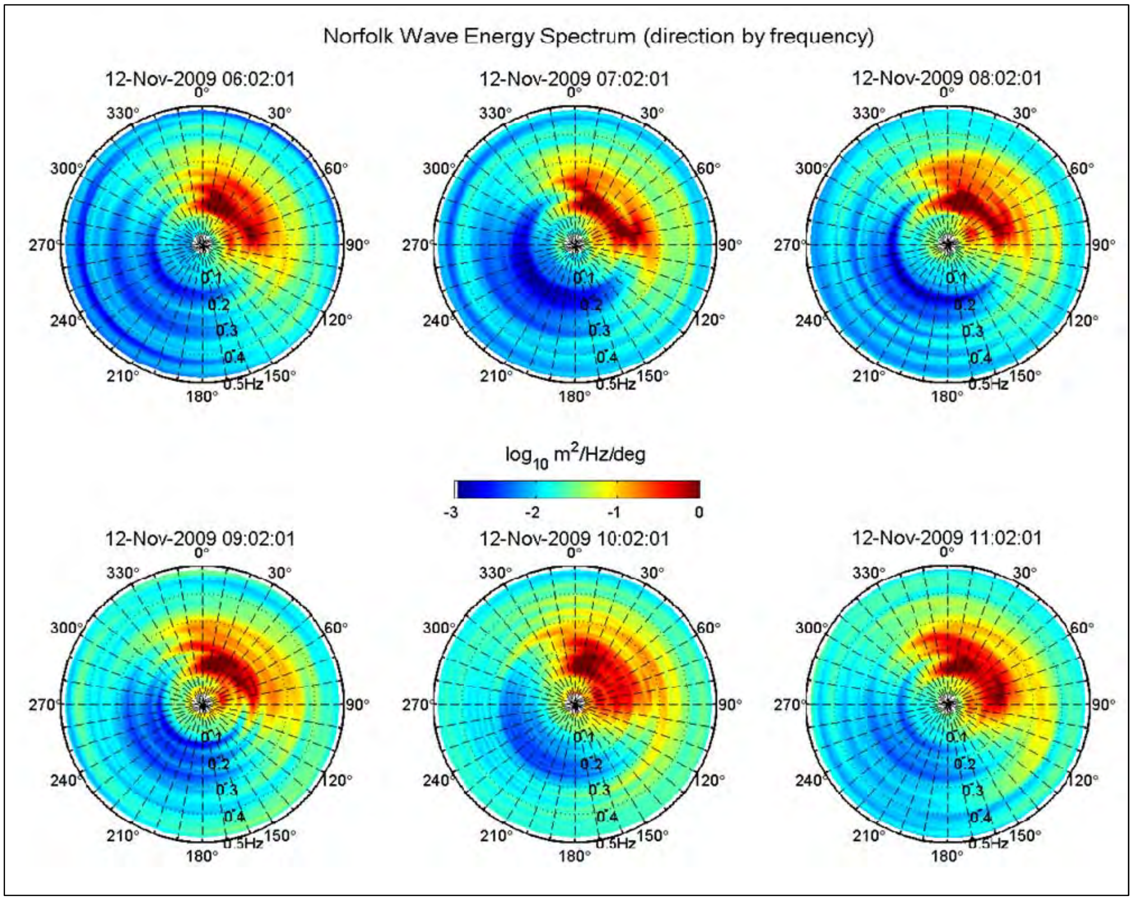

Figure 45. Sample directional wave spectra from the Norfolk City wave gage during Extra-tropical Storm Nor'Ida (12 November 2009, 0602-1102 UTC).[1] Wave direction convention is degrees from north.

peak event (PE) analysis was performed to quantify model performance at these times. Peaks were identified in the observed wave height record using a threshold-crossing approach (Chapter 5). In addition to comparing observed and modeled significant wave heights at these times, the corresponding peak periods and mean directions (extracted at the time of peak wave heights) are compared as well.

The peak wave event analysis synthesizes the data from all three validation storms. Results of the peak event analysis are shown in Figure 47. Included are scatter plots, error metrics, and performance scores for peak significant wave height (a), corresponding peak wave periods (b), and corresponding mean wave directions (c). There are too few wave observation stations to claim that the peak event analysis is a robust wave validation for Region III. Nevertheless, the results are encouraging. The peak event performance scores are 0.95, 0.88, and 0.94 for height, period, and direction, respectively. The wave height scatter plot is especially encouraging with a scatter index of only 0.08. As mentioned previously, multiple wave systems (sea and swell) during tropical and extra-tropical events make wave period and direction comparisons difficult to interpret. In general, however, the results suggest that the wave modeling system adequately captures the peak wave event characteristics.

---

[1] Figure 45 provided by Moffatt & Nichol.

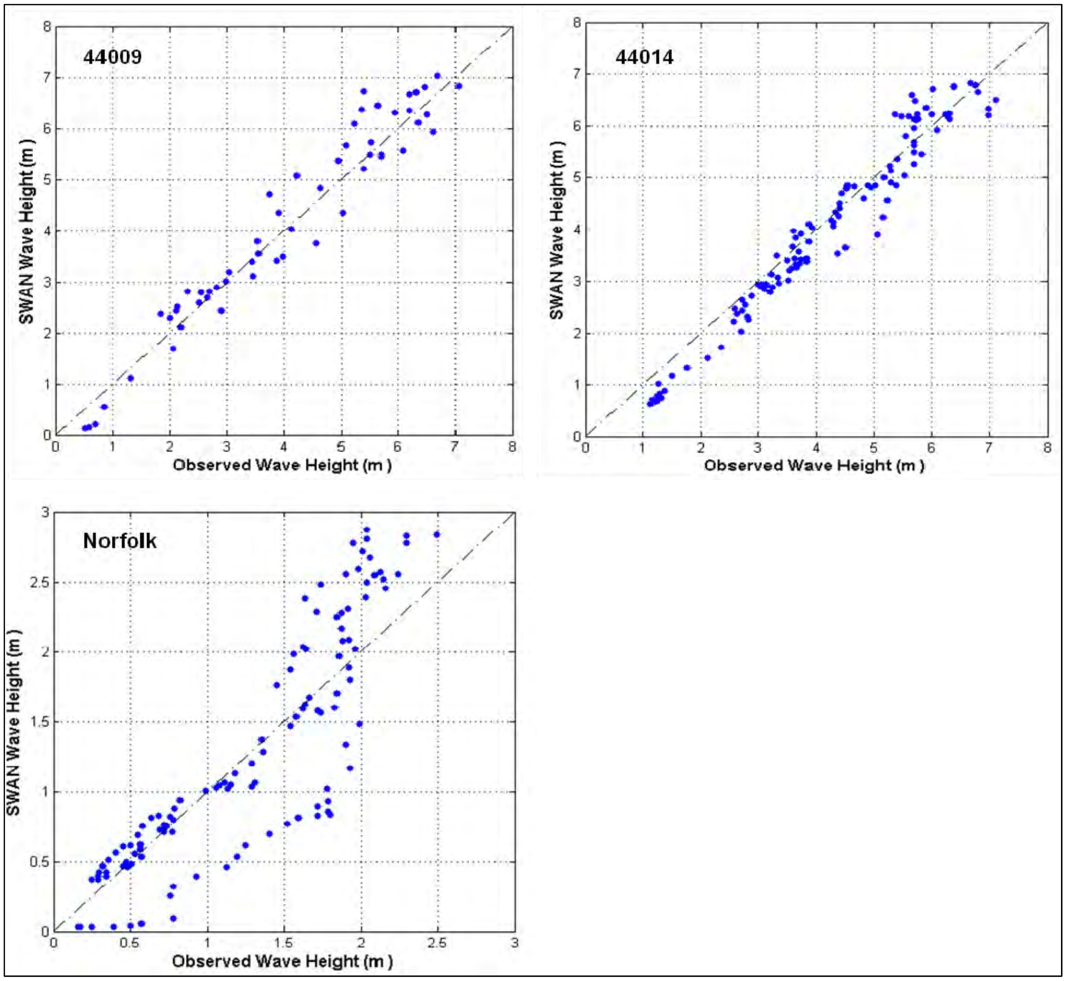

Figure 46. Scatter plot comparison of Extratropical Storm Nor'Ida observed and hindcast wave heights.

Table 21. Extratropical Storm Nor'Ida wave hindcast performance statistics.

	Wave Height				Wave Period				Wave Direction		
Station	Bias (m)	RMS Error (m)	Scatter Index	Perf	Bias (s)	RMS Error (s)	Scatter Index	Perf	Ang. Bias (Deg)	Circular Corr.	Perf
44014	-0.14	0.41	0.09	0.94	-0.75	1.35	0.10	0.91	1.36	0.93	0.96
44009	0.08	0.47	0.12	0.94	0.13	1.46	0.14	0.93	---	---	---
Norfolk	0.04	0.45	0.28	0.85	1.62	3.93	0.66	0.50	6.12	0.64	0.80

a. Wave Height

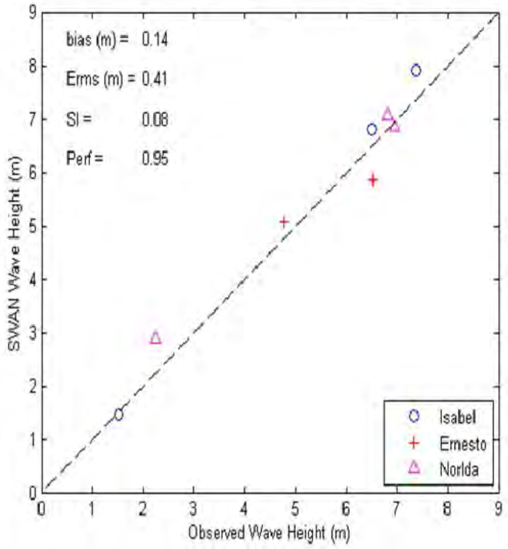

b. Peak Period

c. Mean Wave Direction

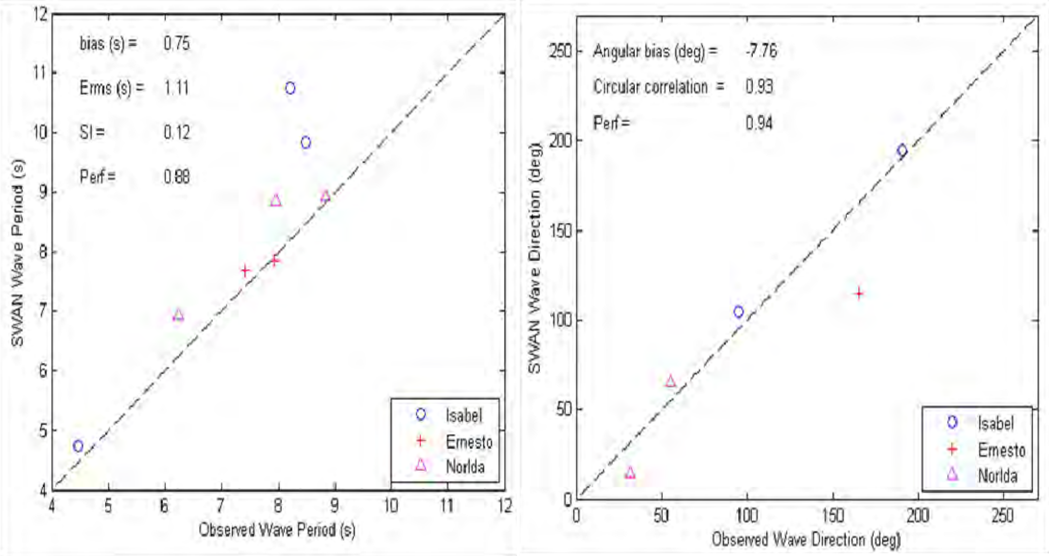

Figure 47. Results of peak event analysis: a. peak significant wave height, b. corresponding peak periods, and c. corresponding mean wave direction.

8 Storm Surge Validation

Region III's storm surge modeling system, SWAN+ADCIRC, is comprised of two coupled, numerical models: ADCIRC (tide, wind-driven water level, circulation, and storm surge model) and unSWAN (unstructured SWAN wave model). SWAN+ADCIRC's accuracy in modeling storm surge is evaluated in two different ways: (1) high-water marks, and (2) water levels. High-water marks are determined by extracting the maximum water level during the storm event at a given location. Water levels are generated by SWAN+ADCIRC at a given location over the course of the storm. Given the influence of local tides, however, the storm water levels actually observed at any one location may be significantly different (i.e. higher or lower) than the pure storm surge component of the mean water level (e.g. Figure 48). It is desirable to fully quantify the model's ability to reproduce the pure storm surge component, without the complicating influence of local tides. To assess SWAN+ADCIRC's ability to correctly reconstruct the pure storm surge component of the water level associated with a given storm, SWAN+ADCIRC was forced with atmospheric pressure gradients, and wind stress, tides, and wave radiation stress gradients. The resulting modeled water levels were subsequently detided and compared to detided observational data. SWAN+ADCIRC results are referred to as "PADCSWAN" in all figures in Chapter 8.

8.1 Removal of tidal forcing

Tides and tidal currents are driven by the interaction of the earth's rotation and the gravitational forces of the sun and moon acting on the earth's oceans. The solar and lunar orbits, together with the rotation of the earth, result in the cyclical rise and fall of the ocean levels on a semi-diurnal and diurnal basis. Variations in the relative positions of the earth, sun, and moon result in additional fluctuations in the strength of tidal forcing. While tides can be predicted into the future at any one point on the earth due to the predictability of this astronomical forcing, the total water level at any location is also affected by local bathymetry as well as highly variable meteorological influences.

As a result, the pure storm surge component of the observed water levels for any given storm is frequently obscured in data that also include the influence of tides. Given the need to assess SWAN+ADCIRC's ability to

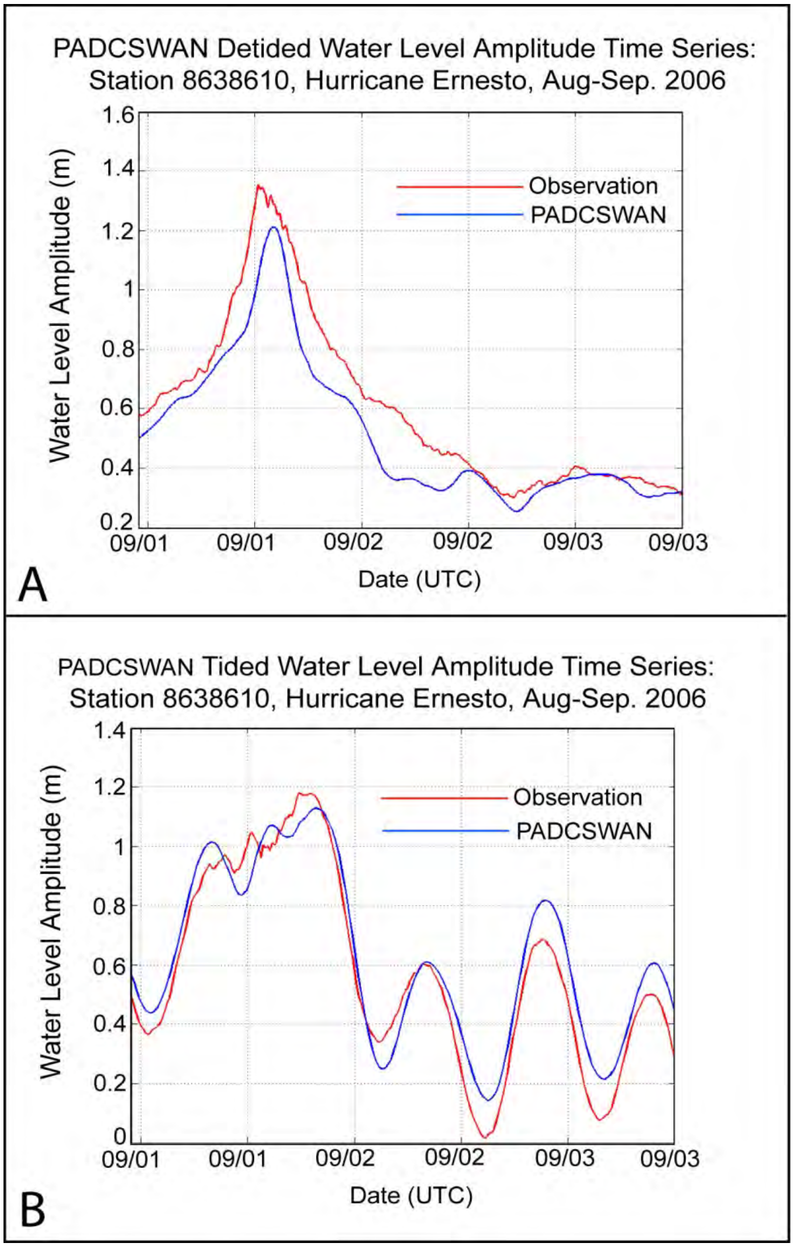

Figure 48. Time series of water level amplitudes for NOAA Station 8638610, Sewells Point, VA, for Hurricane Ernesto:a) without tides, and b) with tides.

reproduce the actual storm surge accurately, this report primarily highlights the detided results. To do this, the modeled water level data described above were subsequently detided. This was done initially by forcing SWAN+ADCIRC with the forcing described above, and these results are hereafter referred to, in the figures, tables, and text, as “TidesSurgeWaves.” The next step involved running a separate “TidesOnly” simulation for each storm so that the tides could be directly subtracted from the TidesSurgeWaves water levels. The TidesOnly simulation is driven by eight major tidal constituents on the open boundary and by the tidal potential. The result is eight “linear” tides as well as associated compound and harmonic tides. For most water level stations, subtracting the above tidal solution from the TidesSurgeWaves modeled water levels removes the majority of the tidal component, resulting in detided water levels, referred to hereafter as “Detided TidesSurgeWaves” (Figure 48). The process does leave behind any nonlinear interactions between the surge and tides, resulting in occasional, visible residual tidal effects in the detided water levels.

The Detided TidesSurgeWaves water level data are then validated using detided NOS observations. Observational data are detided by taking the observed NOS water level data and subtracting the NOS predicted tides over the same time period. NOS tidal predictions are usually based on a least squares harmonic analysis of 37 tidal constituents (National Ocean Service 2000). While this provides a potentially more robust tidal analysis than that performed for the SWAN+ADCIRC data, some nonlinear interactions between the surge and tides remain in the observed data as well (Figure 49). For both the modeled and observed detided data, however, the best possible tidal predictions have been calculated and the remaining nonlinear interactions are small. It should be noted that the observed tidal constituents, and their associated compound and harmonic tides, when removed from the observed data, do differ slightly from the internally generated SWAN+ADCIRC tides. This is an additional source of error at some locations, resulting in scatter indices of ≥0.25 at the affected stations. Given the need to assess the actual storm surge itself, only the Detided TidesSurgeWaves results are analyzed over the course of all three storms in this report. For reference, plots of water levels with tides (TidesSurgeWaves) at each station are provided in Appendix E.

The spatial character of these detided, modeled water levels, as well as the model skill in reproducing detided, observed water levels from available NOAA tide gauges, are described here. Details regarding the validation data sets, as well as comparisons between SWAN+ADCIRC output and validation data, are discussed in detail for each storm.

8.2 Water level validation error metrics

The ability of SWAN+ADCIRC to model storm surge correctly is measured through the validation of the model data with observed data. Model validation was conducted using IMEDS, previously described in Chapter 5

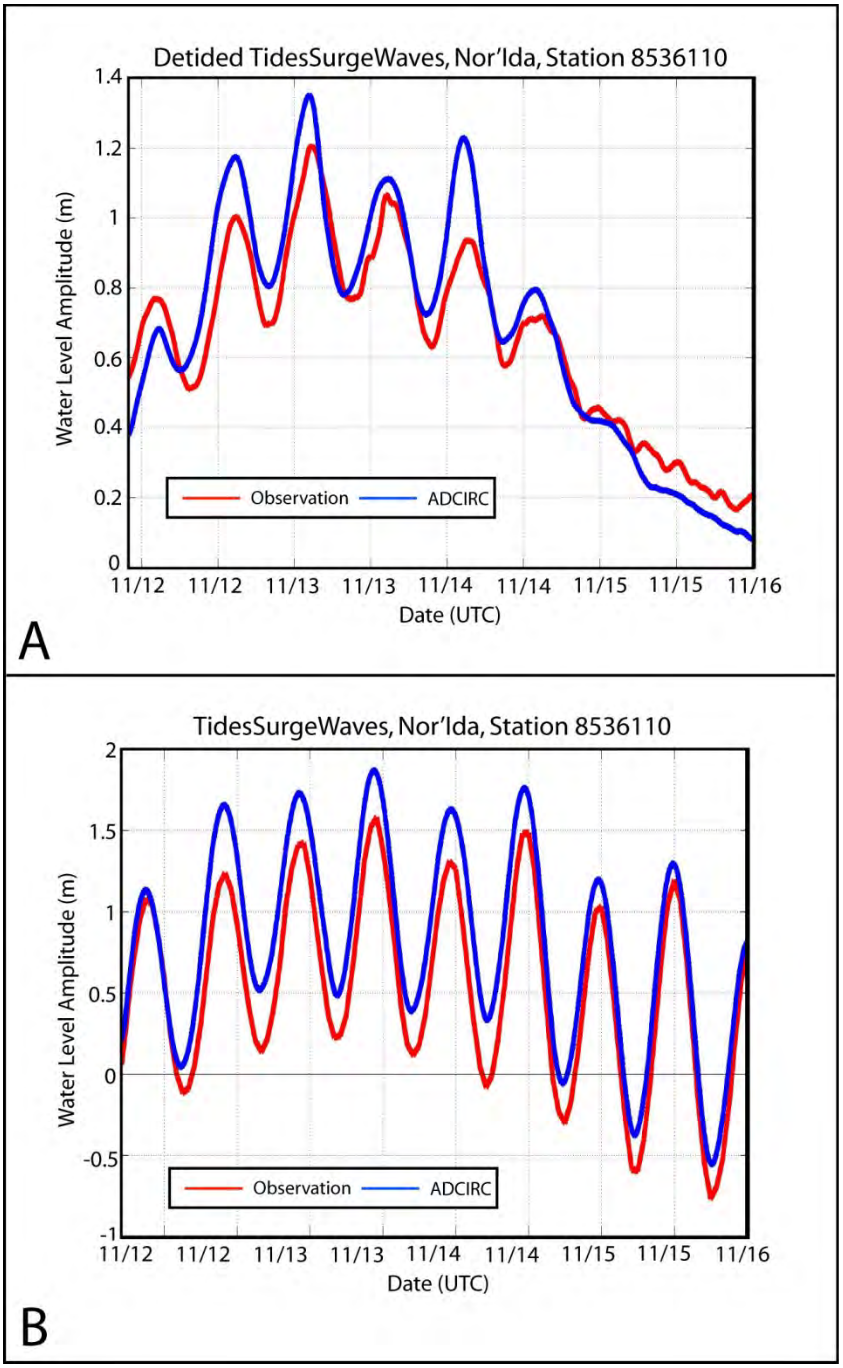

Figure 49. Example of residual tide signals in both modeled and observed detided water levels, NOAA Station 8536110, for Nor'Ida: a) without tides, and b) with tides.

of this report. Error metrics specific to water level validation at each validation station are reported in tables for the duration of every storm. Details regarding the calculation of these metrics are explained in Hanson et al. (2009), but can be summarized as follows:

- BIAS: a measurement of the mean non-random differences between SWAN+ADCIRC water level predictions versus the observations;
- RMS error: an indicator of model accuracy that quantifies the differences between the SWAN+ADCIRC predicted water levels and the actual observed water levels (note that bias is removed before this value is calculated);
- SI: scatter index, a normalized measure of error defined by dividing the standard deviation of the model errors in water levels by the average observed water level (note that bias is removed before this value is calculated); and
- PERF: an overall, non-dimensional performance score computed by normalizing the above error metrics with mean observation quantities, where a skill score = 1.0 indicates perfect correlation between the modeled and observed water level time series data.

Finally, a peak event analysis is performed for each storm, providing a quantitative measurement of model skill reproducing the observed maximum water levels.

8.3 Water level error assessment

Determining whether or not SWAN+ADCIRC successfully reproduced the observed water levels during the peak of the modeled storms requires an assessment of the potential sources of error in both the model results and observed data. While not an exhaustive exploration of all the potential errors, possible sources of error specific to water level modeling and validation include:

- Errors in the forcing winds;
- Vertical error in the modeling mesh, which is due to errors associated with bathymetric and topographic surveying as well as errors associated with gridding multiple data sets into a single DEM;
- Error in the water level observational measurements used to validate the modeled results; and
- Error inherent in the tidal calibration and associated detiding process that does not account for the influence of storms on tidal phasing.

Of these sources of error, wind is likely the most significant source of error in storm surge predictions. Furthermore, SWAN+ADCIRC does not account for increased river discharge related to heavy rainfall in its water level reconstructions. These additional errors are addressed in the appropriate sections of this report.

The above errors, however, cannot be directly translated to the associated water level measurements. This is because the total potential error in modeled storm surge is a function of how all of these various errors propagate through the shallow water continuity equations, compiled in Generalized Wave Continuity Equation (GWCE) form, used by ADCIRC to generate predicted water levels. A full analysis of this potential error propagation in SWAN+ADCIRC is beyond the scale of this report. Instead, a quantitative assessment of the error in the modeled storm surge was obtained from the differences between modeled and observed peak water levels for every station and every storm.

8.4 Storm surge validation

All data analysis is performed in NAVD88 and the SWAN+ADCIRC water levels are converted from MSL to NAVD88. Two different data sets were used to validate water levels as modeled by SWAN+ADCIRC: (1) detided observations from NOAA tide gauges; and (2) observations from USGS storm surge sensors. For each storm, 6.0-min water level observations from NOAA tide gauges in Region III, as published on the NOS Tides Online website (URL: http://tidesonline.nos.noaa.gov/), were collected for comparison to the SWAN+ADCIRC time series output. SWAN+ADCIRC water levels were output at each gauge station every 6.0 min for validation. Detiding of the observed and modeled data was performed as described previously in this chapter.

To be included as observational data in the Region III Storm Surge Validation Study, a NOAA tide gauge needed to conform to the following criteria:

- Either be recorded in NAVD88 or have the applicable conversion information published; and
- Have both predicted and observed tidal data available to generate the necessary observed detided water level data.

These preliminary criteria were initially met by 26 NOS stations (Figure 50). However, eight of these stations, identified by blue circles and text in Figure 50, were located in topographically complex and/or inland regions, such as on the edge of a pier, within a partiallysheltered bay, or far up an inland creek (see Figure 51 for examples of NOS 8557380, 8571559, and 8636580). In these locations, the resolution of the bathymetric mesh was insufficient to allow SWAN+ADCIRC to wet the grid cell containing the observed station during some or all of the event duration. In addition, flooding in the far inland sites may have been driven primarily from increased river discharge due to storm-related heavy rainfall. SWAN+ADCIRC does not account for these rainfall-induced increases in local water level in its storm surge reconstruction. Accordingly, these eight stations were not included in the statistical analysis. The remaining 18 stations were spatially distributed in such a way as to adequately demonstrate model performance throughout Region III (Figure 52).

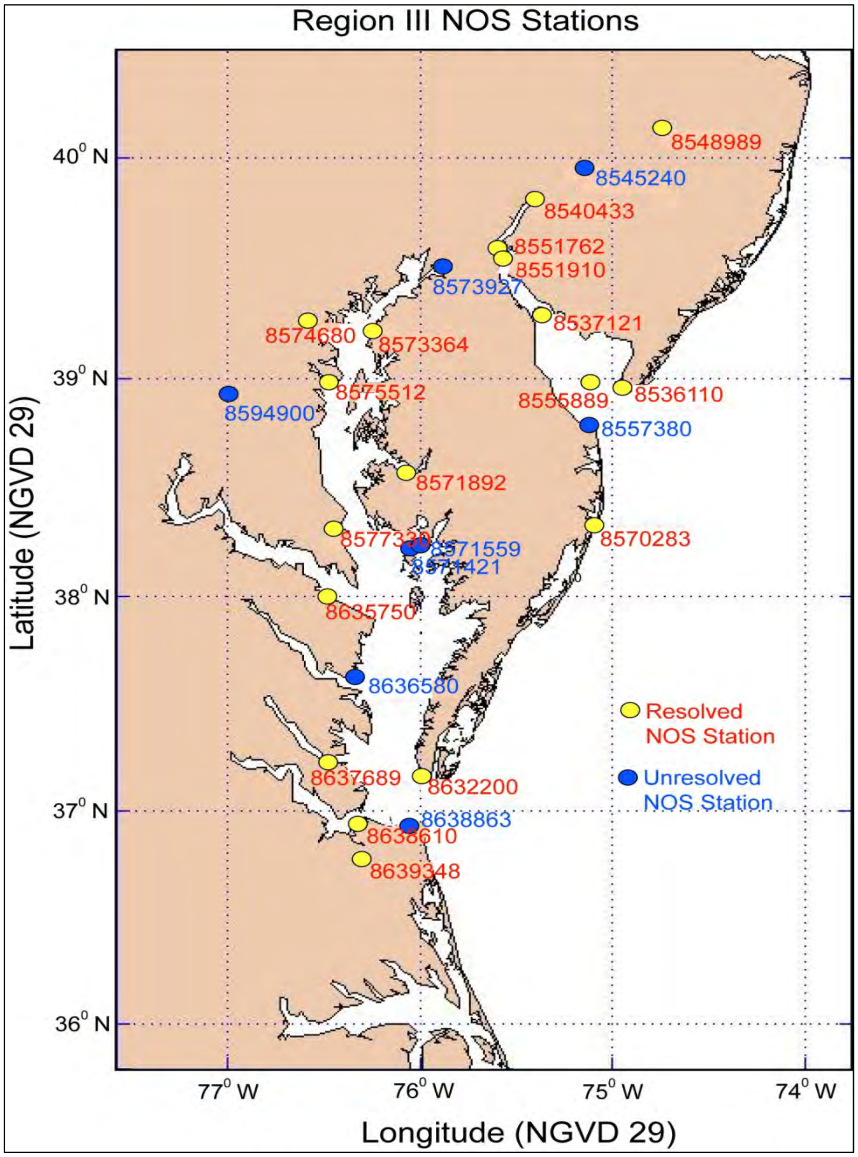
Region III NOS Stations
8548989
8545240
8540433
8551762
8551910
8573927
8537121
8574680
8573364
8575512
8594900
8555889
8536110
8557380
8571892
8577330
8571559
8571421
8570283
8635750
8636580
Resolved NOS Station
Unresolved NOS Station
8637689
8632200
8638863
8638610
8639348
40° N
39° N
38° N
37° N
36° N
Latitude (NGVD 29)
77° W
76° W
75° W
74° W
Longitude (NGVD 29)

Figure 50. Location of NOS stations meeting preliminary criteria described in Section 8.4.

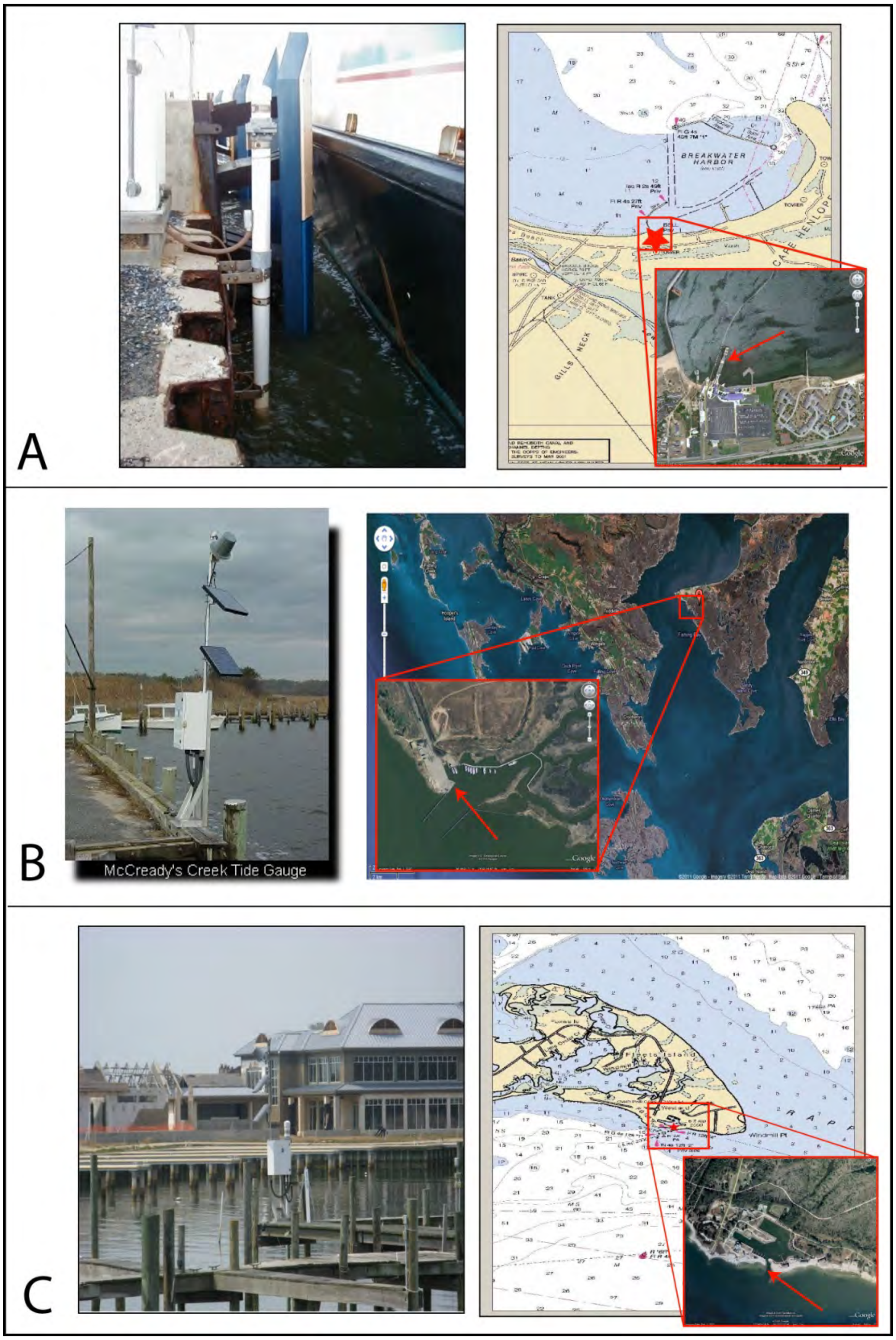
BREAKWATER HARBOR
CAPE HENLOPEN
GILLS NECK
A
McCready's Creek Tide Gauge
B
Fleets Island
Windmill Pt
C

Figure 51. Examples of NOS stations not adequately resolved by the ADCIRC mesh: a) NOS 8557380, Lewes, DE; b) NOS 8571559, McCready's Creek, MD; and c) NOS 8636580, Windmill Point, VA.

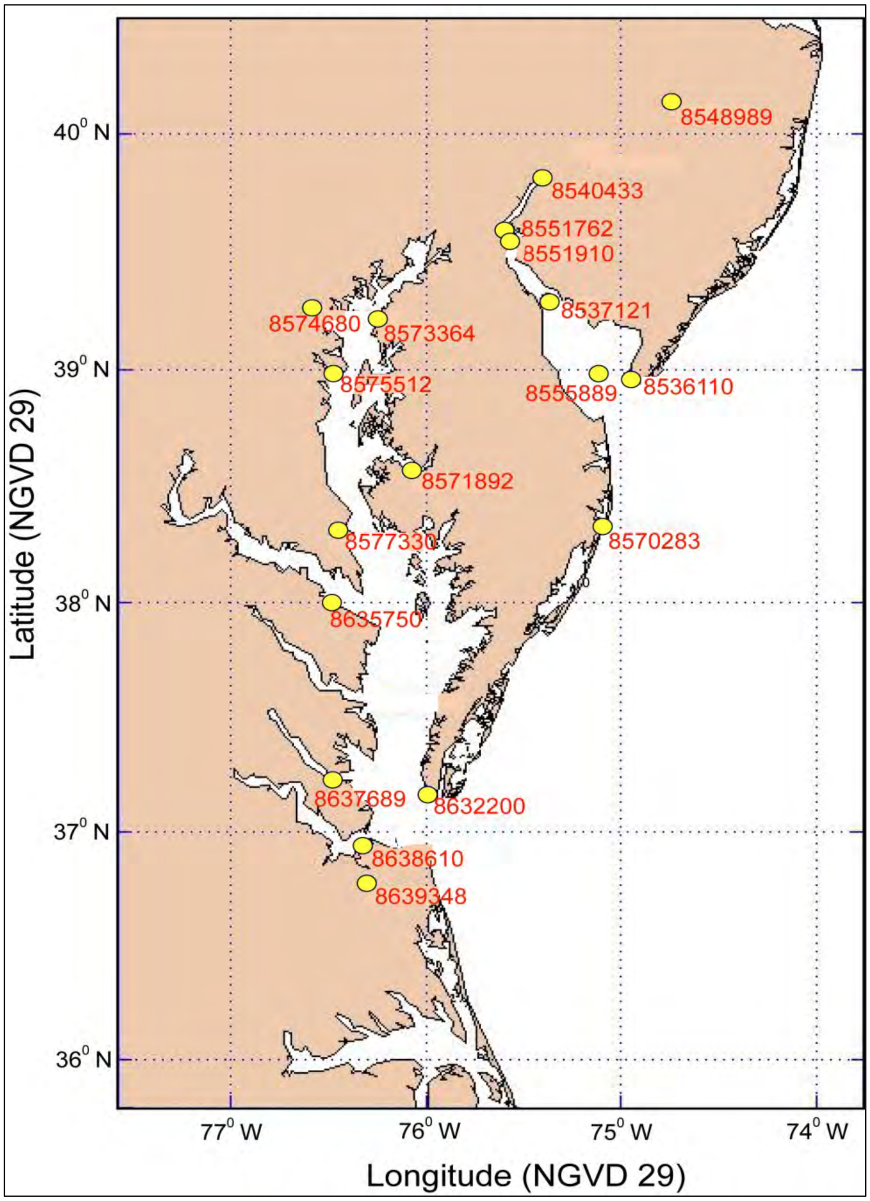
8548989
8540433
8551762
8551910
8537121
8574680
8573364
8575512
8555889
8536110
8571892
8577330
8570283
8635750
8637689
8632200
8638610
8639348
40° N
39° N
38° N
37° N
36° N
77° W
76° W
75° W
74° W
Latitude (NGVD 29)
Longitude (NGVD 29)

Figure 52. Location of NOS Stations used for storm surge validation, Region III.

To augment the fixed location storm-surge gauge locations, the USGS has recently begun deploying storm surge sensors in the projected hurricane paths on land, including along coastal rivers, barrier islands, low-lying areas, and wetlands (Figure 53). Data collected by these “rapid response” storm surge gauges include barometric pressure as well as time series of water level (via non-vented pressure transducers) if and when the gauges are flooded. These data provide a valuable opportunity not only to validate storm surge peaks at these locations (high-water marks), but also to assess SWAN+ADCIRC’s ability to successfully flood, and generate water level data, for a topographically high point on land. Due to the very short timeframe over which the instruments are deployed (e.g. days), it is not possible to detide the observed water levels and thus the observed data are validated using the fully tided TidesSurgeWaves modeled water levels at these eight locations. These data are available only for Nor'Ida.

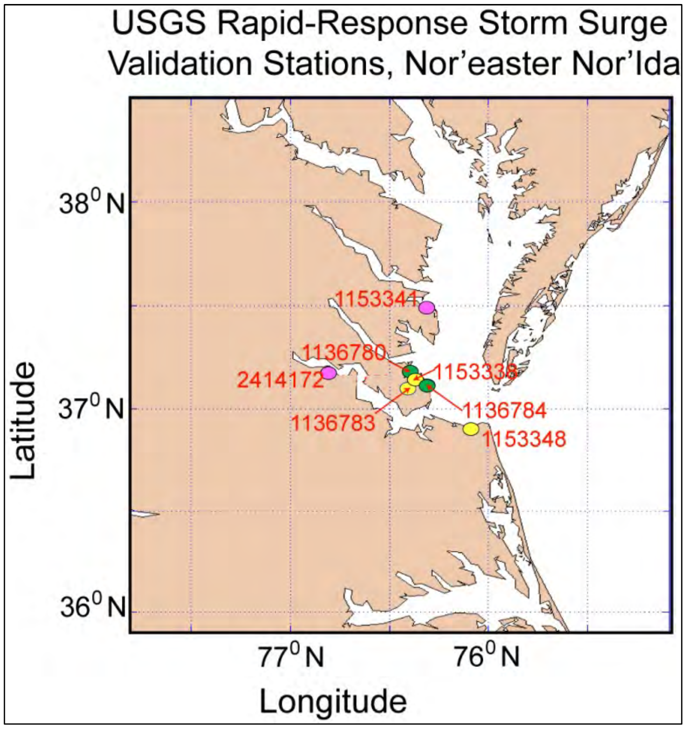
USGS Rapid-Response Storm Surge
Validation Stations, Nor'easter Nor'Ida
38⁰N
37⁰N
36⁰N
Latitude
77⁰N
76⁰N
Longitude
1153344
1136780
2414172
1153338
1136784
1136783
1153348

Figure 53. Location of USGS rapid response storm surge gauges deployed for Nor'Ida.

8.5 Hurricane Isabel, September 2003

Hurricane Isabel made landfall near Drum Inlet, NC, midway between Cape Lookout and Ocracoke Inlet, as a Category II storm (Figure 13). Isabel produced storm surges of 1.8-2.4 m above normal tide levels near the point of landfall on the North Carolina coast. In Region III, storm surge values ranged from 1.2-1.8 m along the Virginia coast, with the highest surges (1.3-1.8 m) over the southern portion of the Chesapeake Bay near Hampton Roads, VA. The coastlines along Maryland, Delaware, and New Jersey experienced average storm surges of 0.6-1.3 m, with higher surges more inland, in the upper reaches of the Chesapeake Bay (e.g. 1.8-2.4 m above normal near Annapolis, MD) and in the Delaware Bay and River near Philadelphia, PA (0.9-1.3 m at the Delaware Bay mouth, 1.7-1.9 m near the Delaware River head; http://www.nhc.noaa. gov/2003isabel.shtml#FIG1). Overall, the highest storm surges were observed spatially adjacent to where Hurricane Isabel made landfall and subsequently tracked along the coastline while transiting Region III (Figures 13 and 54). The maximum modeled water level elevations, as forced by tides, winds and waves, as well as the storm's track, are shown in Figure 54.

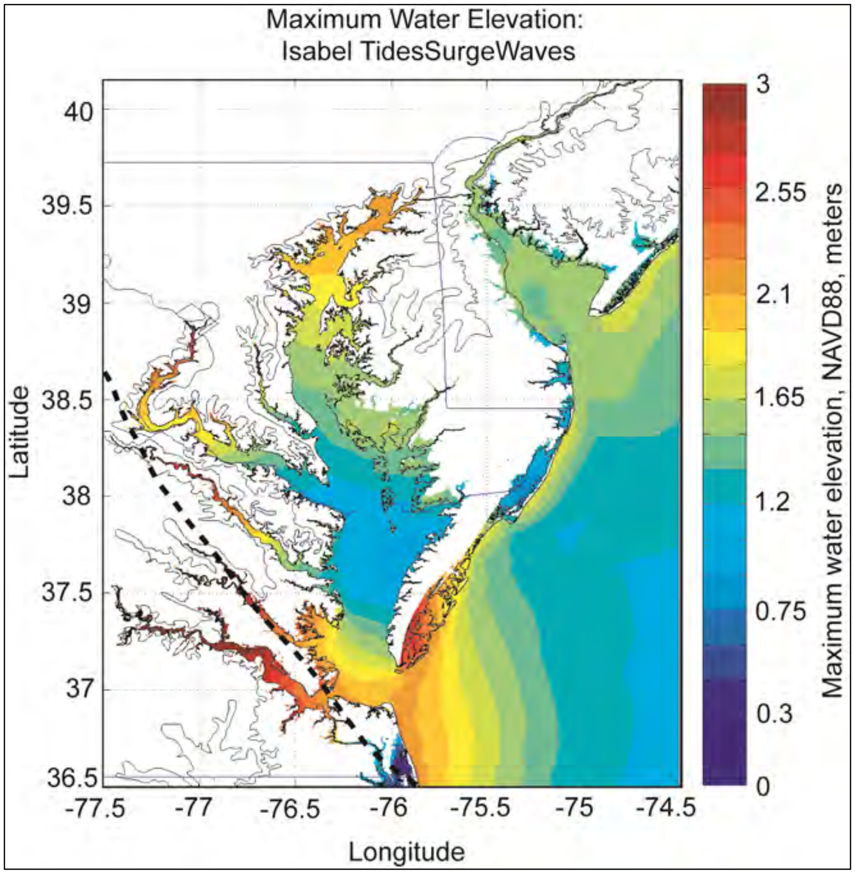
Maximum Water Elevation:
Isabel TidesSurgeWaves
40
39.5
39
38.5
38
37.5
37
36.5
Latitude
-77.5
-77
-76.5
-76
-75.5
-75
-74.5
Longitude
3
2.55
2.1
1.65
1.2
0.75
0.3
0
Maximum water elevation, NAVD88, meters

Figure 54. Maximum water elevation as modeled during Hurricane Isabel by SWAN+ADCIRC. Dashed black line indicates the storm's track across Region III.

8.5.1 Isabel model output versus observation: Detided TidesSurgeWaves

Modeled and detided SWAN+ADCIRC water levels were compared with observational data at 17 validation stations in Region III (Table 22). Statistics for NOAA water level gauge comparisons were computed over 18-20 September 2003. SWAN+ADCIRC successfully reproduced the observed water levels at all but one of the validation stations with an average difference between modeled and observed water levels of approximately 0.06 m (Table 22, Appendix A). SWAN+ADCIRC modeled water levels were highest in the southern portion of the Chesapeake Bay, inside the James River Estuary, and along the southeastern edge of Virginia's Eastern Shore. The modeled storm surge, as shown by the detided water level elevations, exceeded 1.6 m in many locations (Figure 54). Overall, the model reconstructed the detided water levels very well (skill scores ≥ 0.77; average skill score = 0.86) at 16 of the 17 stations (Table 22, Figure 55; Appendix A). Two examples of the successful observed and modeled water levels, as noted by green rows in Table 22, are shown in Figure 55. Observed water level data were not available for station 8637689 during Hurricane Isabel. Accordingly, validation results are not available for that station.

Only one station earned a skill score of less than 0.77: NOS 8536110, near Cape May, NJ. At this location, SWAN+ADCIRC initially overestimated the water level during the rising portion of the storm, up to ~0.25 m, and carried this higher water level throughout the storm (Figure 56). This water level overestimation is clearly shown by a plot of the residuals throughout the storm (Figure 56). Despite this error, SWAN+ADCIRC still reproduced the storm surge throughout the evaluation period with an overall RMS ERROR of only 0.14 m (< 0.5 ft).

Table 22. Statistics for NOAA water level gauge comparisons, Hurricane Isabel.

Hurricane Isabel detided water level validation				
SWAN+ADCIRC versus observations				
Station	Bias (m)	RMS (m)	SI	Perf
8536110	0.13	0.16	0.25	0.68
8537121	0.03	0.12	0.18	0.9
8540433	-0.03	0.16	0.22	0.89
8548989	-0.01	0.26	0.42	0.83
8551762	-0.01	0.15	0.21	0.91
8551910	0.08	0.18	0.27	0.83
8555889	0.06	0.1	0.16	0.86
8570283	0.12	0.13	0.12	0.77
8571892	0.02	0.12	0.22	0.91
8573364	0.13	0.21	0.25	0.83
8574680	0.06	0.15	0.18	0.9
8575512	0.06	0.14	0.18	0.9
8577330	0.02	0.07	0.21	0.89
8632200	0.13	0.15	0.16	0.77
8635750	0.05	0.14	0.19	0.87
8637689		no observational data		
8638610	0.06	0.1	0.11	0.9
8639348	0.03	0.11	0.15	0.92
Average	0.06	0.14	0.20	0.86

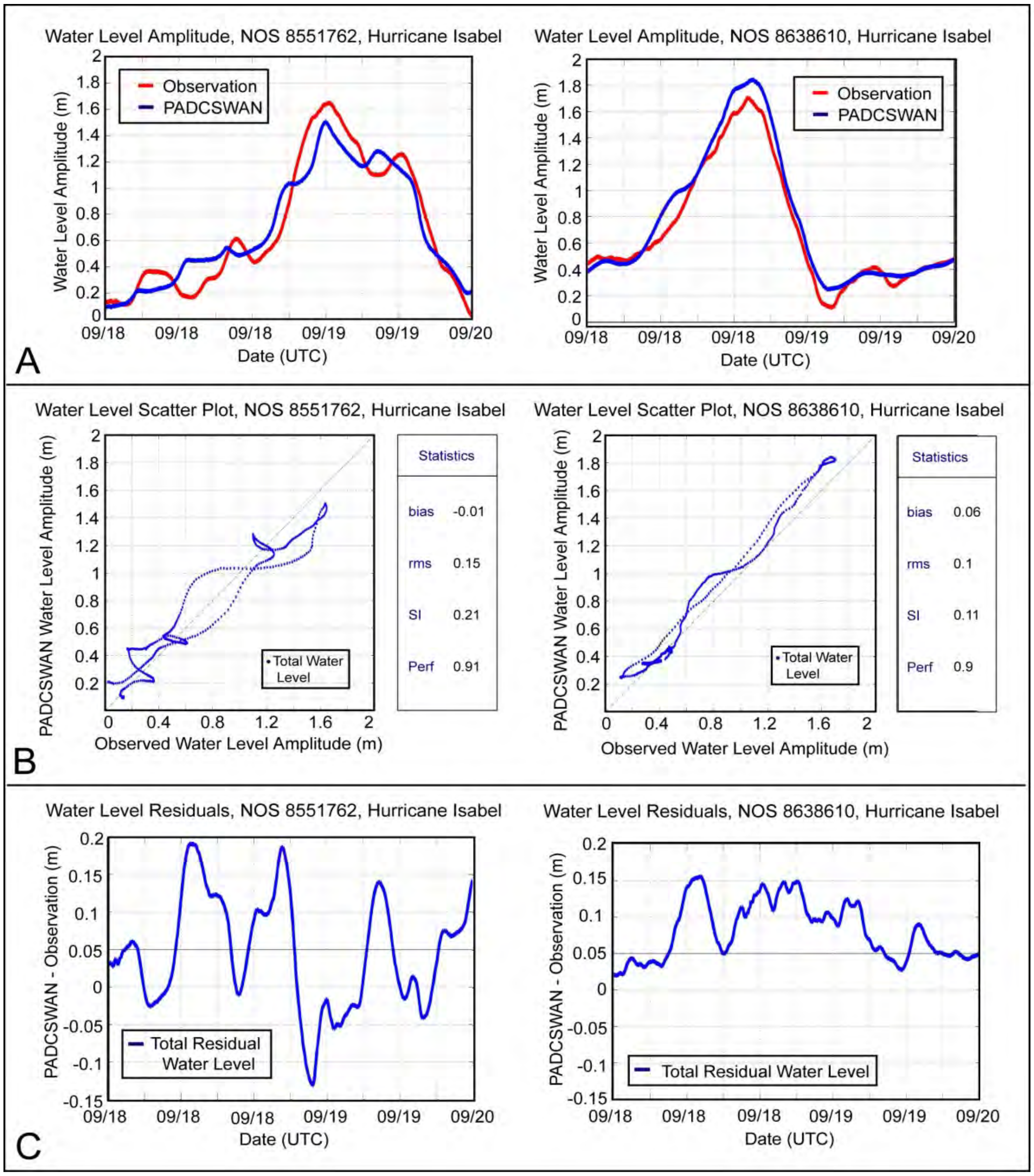

Figure 55. Examples of successful SWAN+ADCIRC water level versus observations, Isabel, Stations 8551762 and 8638610. Water level: A) time series, B) scatter plots, and C) residuals.

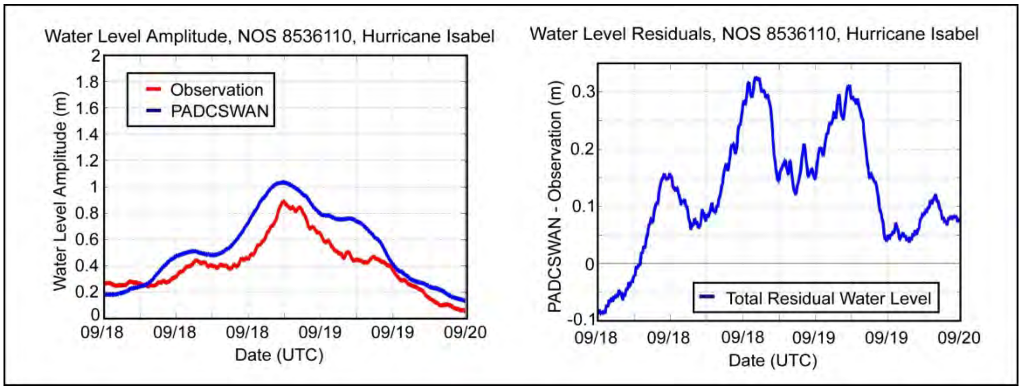

Figure 56. Low-scoring SWAN+ADCIRC water level versus observations, Isabel, NOS 8536110. Water level: A) time series, and B) residuals.

The peak event extremes analysis of the high peaks in the modeled versus observed water level time series data provides the most robust metric for quantifyingADCIRC's ability to successfully reproduce the observed storm surge. In a perfect analysis, the high extreme model and observed data points would be equal, generating a model skill score of 1.0. Peaks were identified using a threshold of 0.5 standard deviations above the mean over a search period of 3.0 hr. In the case of Hurricane Isabel, the peak event analysis yielded a performance score of 0.96, with negligible bias and RMS error of only 0.11 m (Figure 57). These data further support the conclusion that SWAN+ADCIRC successfully reproduced the maximum, pure storm surge for Hurricane Isabel.

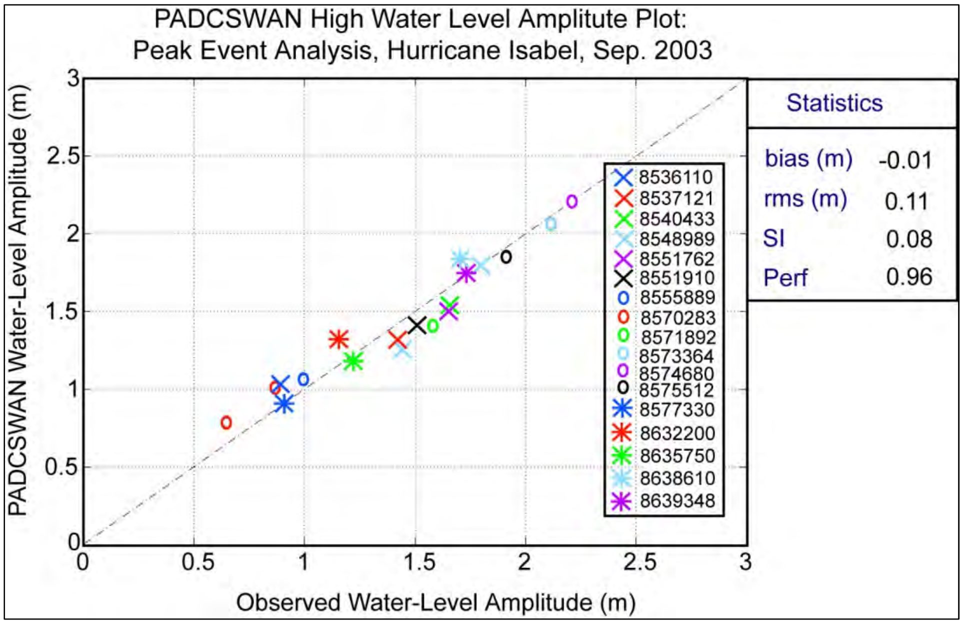

Figure 57. Peak event analysis, SWAN+ADCIRC versus NOAA high water level, Hurricane Isabel.

8.5.2 High-water mark validation – Hurricane Isabel data

Post-Isabel high-water mark data (HWM) observations were collected by a variety of agents, including:

- The Hazard Mitigation Technical Assistance Program, URS Group, Maryland; and
- The US Army Corps of Engineers (USACE), Norfolk District.

Given the lack of a common reporting strategy across data sets, each data set was screened independently for data quality.

Several potential sources of error are associated with these HWM data. Many of the points are collected in topographically complex regions, such as within inland tributaries and/or within small, nearly-enclosed bays. Such locations might be too small to be fully resolved in the modeling mesh and, thus, flooding by SWAN+ADCIRC might be impossible. Other complicating factors include potential human error, both in identifying and interpreting the high-water marks (which are not always clear) and in properly surveying in the mark locations. Finally, rainfall, and associated increases in river discharge, are not accounted for by SWAN+ADCIRC. It is very likely that creeks and rivers, swollen by heavy Isabel-generated rainfall, exceeded their banks, resulting in inland flooding and the associated inland high-water marks. This process is not part of SWAN+ADCIRC's storm surge solution.

To eliminate as many of the above errors as possible, an initial screening was conducted and suspicious HWM data were eliminated. The URS Group HWM data included quality designations for every point of Excellent, Good, Fair, and Poor. Only data rated as Excellent or Good were initially considered for the validation data set. Of those data, each individual point was checked and those with questionable descriptions and/or documentation were removed. If apparent in the descriptions of each individual point, data were further screened and separated according to type (e.g. surge, wave runup, wave height, etc.). Points classified as "wave runup" or "wave height" were removed from the validation dataset to minimize contamination by un-modeled effects such as water level excursions associated with individual wave heights, wave runup, and wave splash up. While the USACE HWM data do not include quality designations, they do contain descriptions and documentation for each point. Accordingly, each individual point was checked and those with questionable descriptions and/or documentation were removed.

Modeled HWM data were obtained using the SWAN+ADCIRC maximum elevation file, which is updated every model time-step to provide the highest water levels computed throughout the simulation. The SWAN+ADCIRC maximum water levels are converted from MSL to NAVD88 (using the translation grid described in Submittal 1). Observed HWM data were compared to the SWAN+ADCIRC maximum elevation data, as they most closely represent the actual conditions experienced for any one location. Figure 58 is a map comparing the SWAN+ADCIRC HWM elevations to observed levels. The colored background indicates the actual maximum

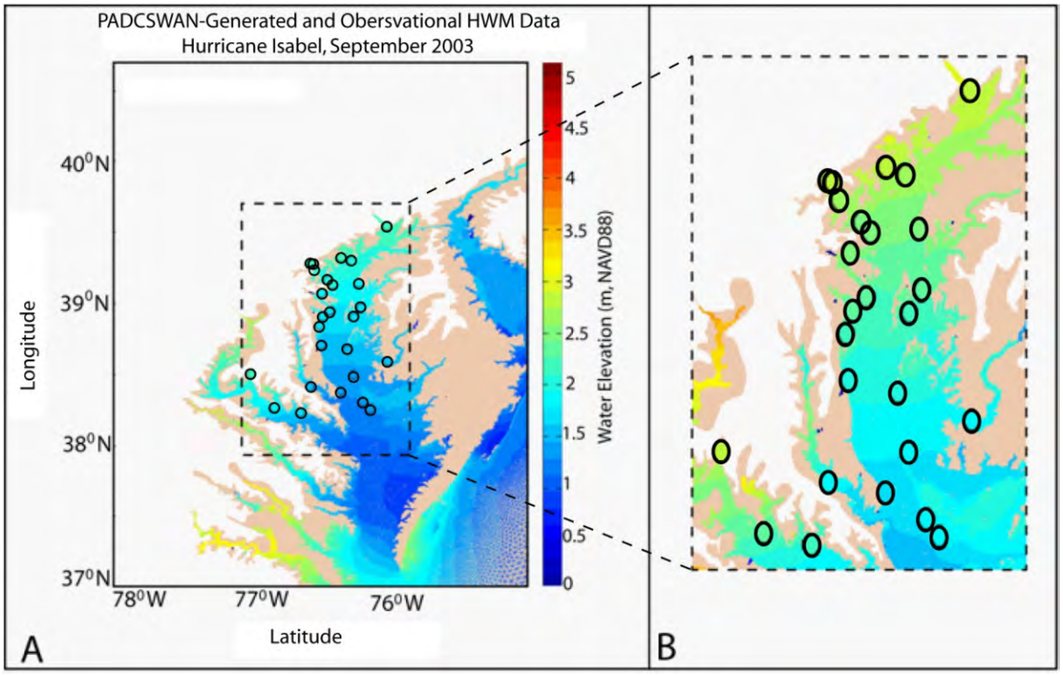
PADCSWAN-Generated and Obersvational HWM Data
Hurricane Isabel, September 2003
40°N
39°N
38°N
37°N
78°W
77°W
76°W
Longitude
Latitude
Water Elevation (m, NAVD88)
5
4.5
4
3.5
3
2.5
2
1.5
1
0.5
0
A
B

Figure 58. Map of modeled HWM data versus observed HWM data, Hurricane Isabel. Dashed box in (A) indicates the outline of the inset shown in (B).

water elevation, as modeled by SWAN+ADCIRC TidesSurgeWaves. The elevation of each observed HWM data point is plotted as a colored circle using the same color scale. The accuracy of the SWAN+ADCIRC representations of HWM elevations is reasonable, as indicated by the similar colors between any single HWM elevation and the maximum water level elevation at the same location (Figure 58). A scatter plot of these results appears in Figure 59. The SWAN+ADCIRC HWMs have an overall performance score of 0.9, and relatively small errors (bias, RMS error, and scatter index of -0.12, 0.26, and 0.12, respectively). These results support the conclusion that SWAN+ADCIRC adequately reconstructed observed maximum water levels in Region III.

8.6 Hurricane Ernesto, August-September 2006

Hurricane Ernesto was at the threshold between a tropical storm and a Category I hurricane, with maximum sustained winds of 31 m/sec, when it made landfall near Oak Island, NC (Figure 13). As the storm moved into Region III, it interacted with a pre-existing frontal zone, which extended eastward from Virginia and evolved into a powerful extra-tropical system. The storm produced surges of ~0.9 m along the North Carolina coastline (e.g. 0.88 m at Wrightsville Beach NOS; Knabb and Mainelli 2006). Even as the storm evolved into an extra-tropical system, it continued to produce gale-strength winds (surface measurements of sustained 21 m/sec winds near the coast) while it transited much of Region III. Accordingly, storm surges in Region III ranged from ~0.5-1.9 m, (1.9 m near Virginia Beach, 0.5 m at Tolchester Beach NOS, 0.7 m at Cape May NOS, and 1.1 m at Lewes NOS). Additional storm tides of up to 2.0 m were reported along some of the western shores of Chesapeake Bay and the adjacent rivers (Knabb and Mainelli 2006).

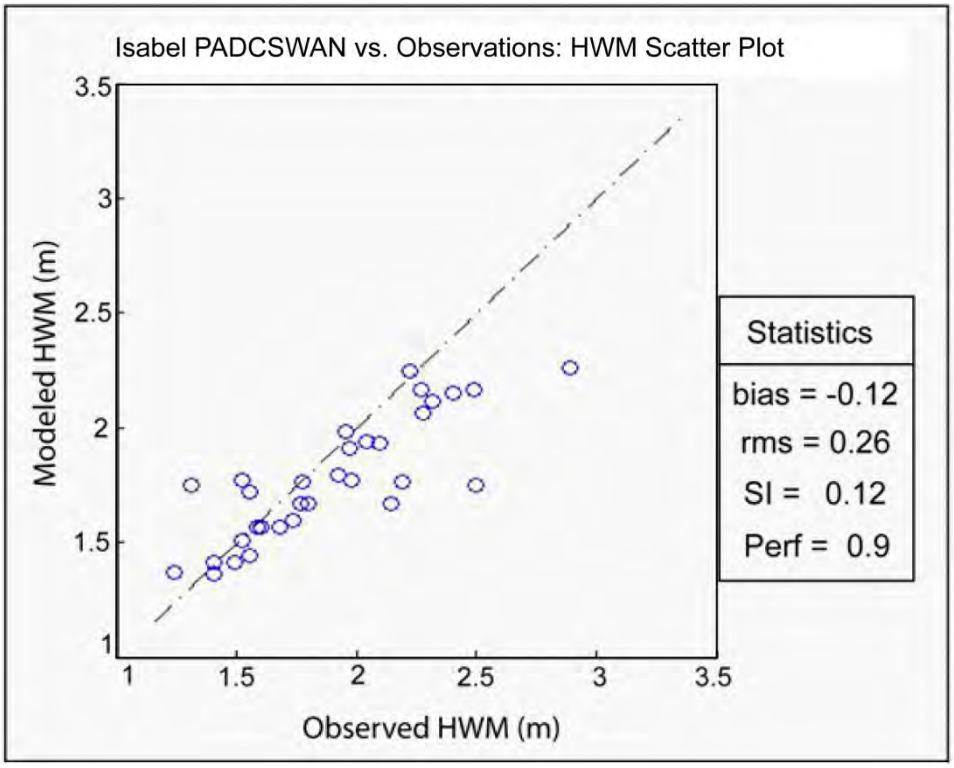

Figure 59. High-water mark (HWM) data scatter plot for Hurricane Isabel.

8.7 Ernesto model output versus observation – Detided TidesSurgeWaves

The maximum modeled water level elevations, as forced by tides, winds and waves, are shown in Figure 60. The highest water level elevations associated with Hurricane Ernesto were primarily seen along the outer coastline, primarily due to the large fetch along the Atlantic Ocean. Water levels were also elevated in the James and York River tributaries as Ernesto transited Region III (dashed black line, Figure 60), and in the Delaware Bay. Overall, the highest modeled storm surge was seen along the southern edge of Delaware Bay, the seaward edge of the Virginia Eastern Shore, and the western extent of the Chesapeake Bay tributaries. These trends compared favorably to observed water level elevations (Appendix B).

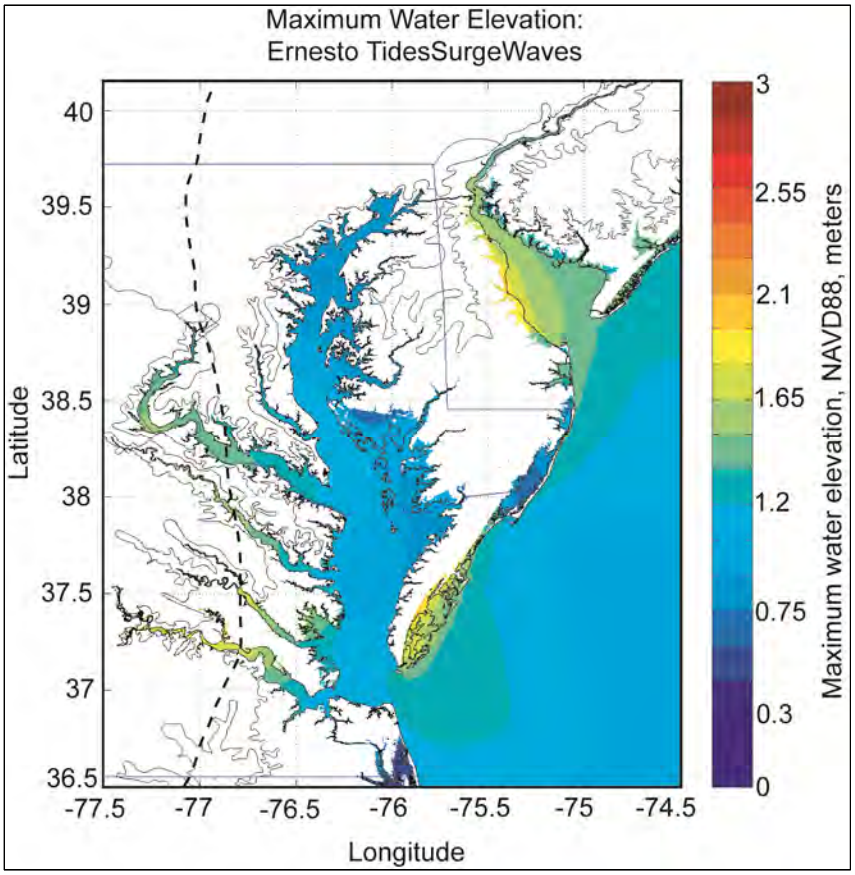
Maximum Water Elevation:
Ernesto TidesSurgeWaves
40
39.5
39
38.5
38
37.5
37
36.5
Latitude
-77.5
-77
-76.5
-76
-75.5
-75
-74.5
Longitude
3
2.55
2.1
1.65
1.2
0.75
0.3
0
Maximum water elevation, NAVD88, meters

Figure 60. Maximum water elevation as modeled during Hurricane Ernesto by SWAN+ADCIRC. Dashed black line indicates the storm's track across Region III.

SWAN+ADCIRC reproduced the observed water levels for the duration of the storm with skill scores ≥0.7 at 17 of the 18 validation stations (average score of 0.82; Table 23). Fourteen stations generated skill scores ≥ 0.8. Statistics for all of the stations, including bias, RMS error, scatter index, and overall station performance scores, are reported in Table 23. In general, the bias measurements were very low (average of 0.01 m), and all of the stations demonstrated an average RMS error of only 0.15 m (Table 23, Figure 61, Appendix B). Two examples of the 18 successful water level stations, noted by green shaded rows in Table 23, are shown in Figure 61.

Only one of the validation stations received a performance score of < 70% , (NOS 8573364; Tolchester Beach, MD). Water level time series and residual data are presented in Figure 62. Despite the low overall performance score (0.6; Table 23), the difference between the modeled and observed water levels at the peak of the storm was less than 0.13 m. Overall, the low bias and RMS error scores, coupled with high scatter index values (0.06 m, 0.19 m, and 0.65, respectively; Table 23), suggest that the majority of the error between the modeled and observed water levels is due to overlooking relatively low-amplitude, high-frequency variability in the system. The most likely causes are inconsistencies in the tidal solutions between the two data sets, as explored previously in Section 8.1, or local wind variability, particularly in the complex, estuarine areas.

The peak event analysis of the extremes in the modeled versus observed water level time series data provides the most robust metric for quantifying ADCIRC's ability to successfully reproduce the observed storm surge. As in the case of Hurricane Isabel, the peak events for Hurricane Ernesto were selected using a threshold of 0.5 standard deviations above the mean over a search period of 3.0 hr. In the case of Ernesto, the peak event analysis

Table 23. Statistics for NOAA water level gauge comparisons, Hurricane Ernesto.

Hurricane Ernesto detided water level validation				
SWAN+ADCIRC versus observations				
Station	BIAS (m)	RMS (m)	SI	PERF
8536110	0.02	0.09	0.18	0.9
8537121	0.06	0.21	0.34	0.8
8540433	-0.01	0.21	0.35	0.83
8548989	-0.01	0.09	0.16	0.91
8551762	0.04	0.21	0.32	0.82
8551910	0.11	0.25	0.42	0.7
8555889	-0.01	0.09	0.16	0.91
8570283	0.04	0.07	0.11	0.9
8571892	0	0.16	0.43	0.79
8573364	0.06	0.19	0.65	0.6
8574680	0.06	0.18	0.43	0.71
8575512	0.03	0.15	0.34	0.8
8577330	0.04	0.14	0.26	0.83
8632200	-0.03	0.09	0.16	0.89
8635750	-0.03	0.16	0.24	0.87
8637689	-0.05	0.1	0.13	0.89
8638610	-0.08	0.11	0.12	0.86
8639348	-0.08	0.13	0.19	0.83
Average	0.04	0.15	0.28	0.82

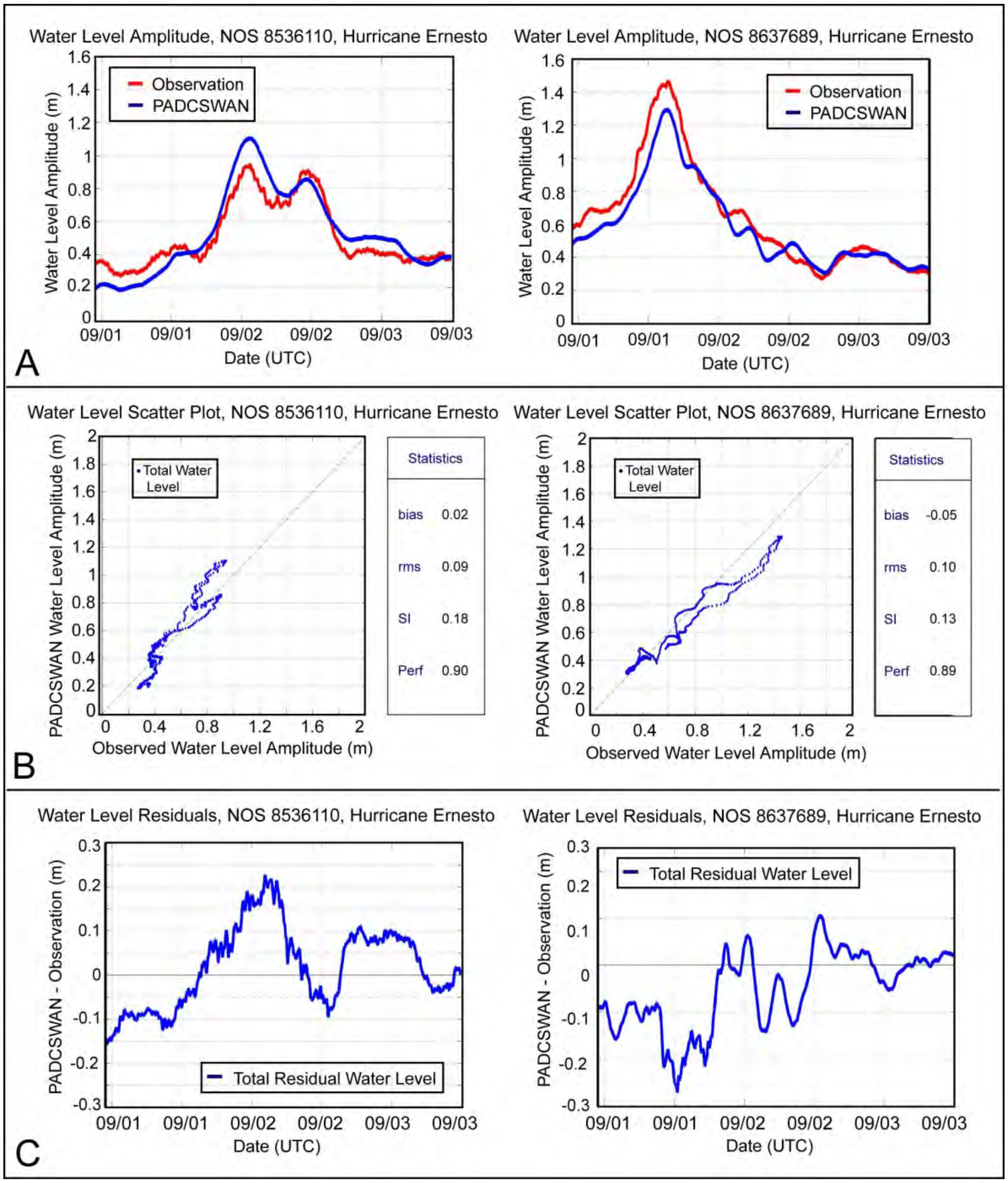

Figure 61. Examples of successful SWAN+ADCIRC water level versus observations, Ernesto, Stations 8536110 and 8637689. Water level: A) time series, B) scatter plots, and C) residuals.

yielded a performance score of 0.88, with negligible bias and an RMS error of only 0.23 m (Figure 63). Although the Ernesto water level errors are greater than those from Isabel (Table 22), it is likely that these errors are a result of increased uncertainty in Ernesto's driving wind fields (Table 12). In spite of this uncertainty, the previously stated low errors and high skill scores indicate that SWAN+ADCIRC was able to successfully reproduce the storm surge for Hurricane Ernesto in Region III.

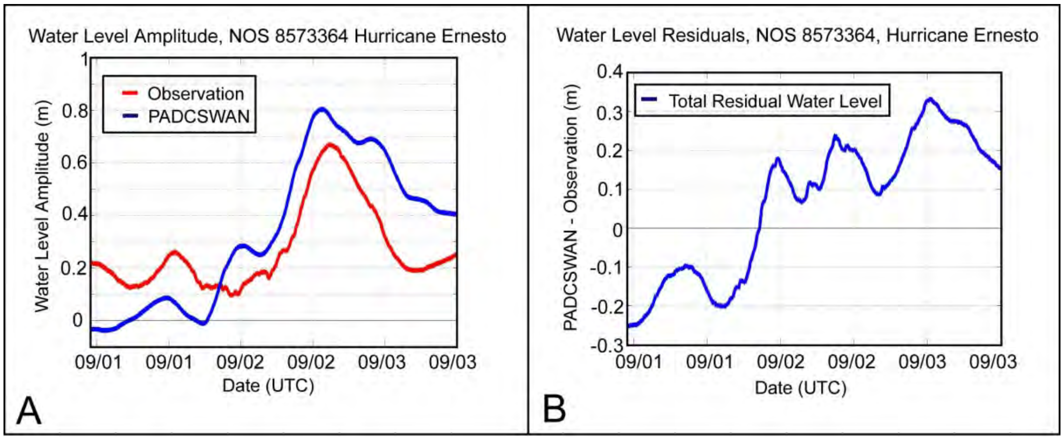

Figure 62. Station 8573364, Ernesto Water levels: A) time series, and B) residuals.

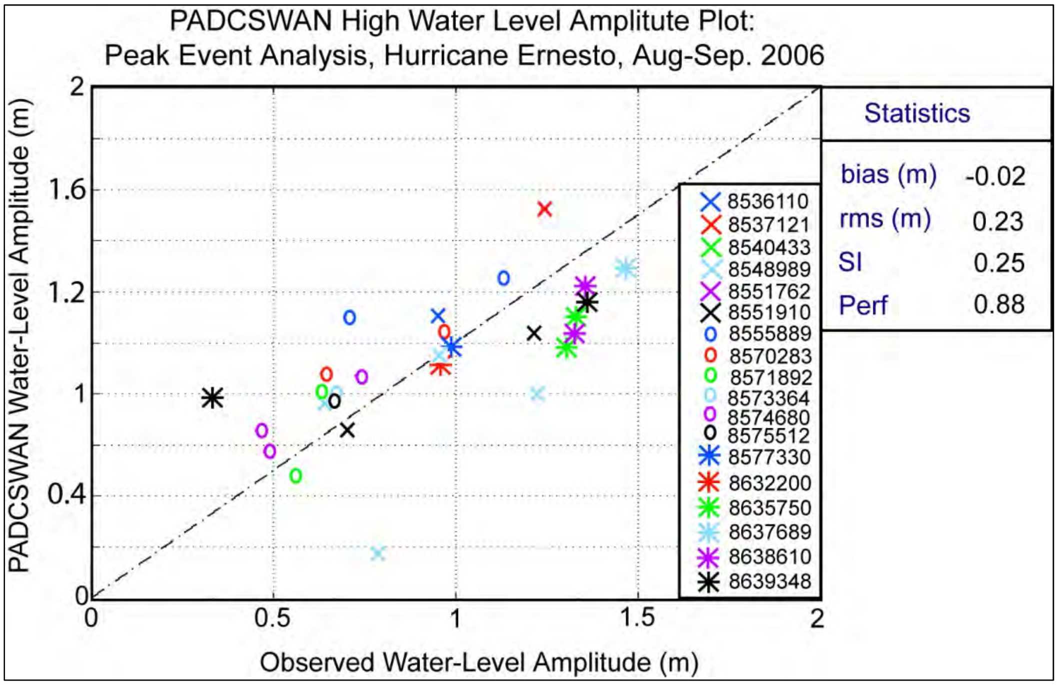

Figure 63. Peak event analysis, SWAN+ADCIRC versus NOAA high water level, Hurricane Ernesto.

8.8 Extra-tropical Storm Ida (Nor'Ida), November 2009

Weakened by strong wind shear and cool waters in the Gulf of Mexico, Hurricane Ida ultimately made landfall along the Alabama coast on 9 November 2009 as a strong extra-tropical storm (Figure 14). As Ida dissipated over the mid-Atlantic, remnant mid-level circulation combined with a strong, low-pressure system in South Carolina. The new low subsequently moved offshore of North Carolina and rapidly intensified into a powerful nor'easter on 12 November, with sustained winds of 29 m/sec. Storm surges from what had become nor'easter Ida (Nor'Ida) were almost comparable to those produced by Hurricane Isabel (2003). Storm surges from 0.6–3.2 m were reported all along Region III, including 1.4 m at Lewisetta and 1.1 m at Lewes. The Sewells Point NOAA gauge storm surge peaked at 2.4 m above MLLW, the fifth highest water level for this station on record since 1930.

Numerous colloquial reports suggest that the combination of the storm surge plus several days of heavy rainfall from Nor'Ida resulted in overall flooding nearly equal to, and occasionally greater than, that caused by Hurricane Isabel in coastal regions of Virginia, particularly in the Hampton Roads area. These colloquial reports are partly supported by maximum water elevation maps, as modeled by SWAN+ADCIRC. As previously stated, rainfall-induced flooding is not incorporated into the SWAN+ADCIRC results. Maximum modeled storm surge elevations are, however, very close to Isabel levels in the Hampton Roads region (Figure 64).

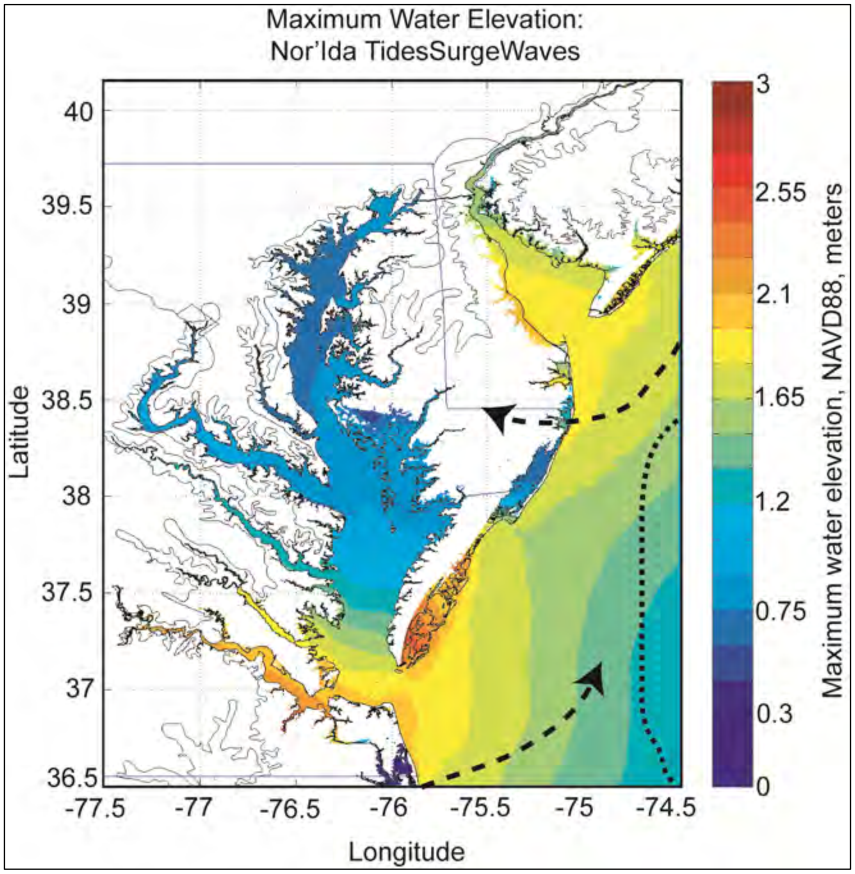
Maximum Water Elevation:
Nor'Ida TidesSurgeWaves
40
39.5
39
38.5
38
37.5
37
36.5
Latitude
-77.5
-77
-76.5
-76
-75.5
-75
-74.5
Longitude
3
2.55
2.1
1.65
1.2
0.75
0.3
0
Maximum water elevation, NAVD88, meters

Figure 64. Maximum water elevation as modeled during Nor'Ida by SWAN+ADCIRC. See text for explanation of dashed arrows and lines.

8.8.1 Nor'Ida model output versus observation – Detided TidesSurgeWaves

After transiting offshore east of the Carolinas (lower dashed arrow, Figure 64), Nor'Ida persisted offshore of Region III for several days, generally staying within the dotted region outlined in Figure 64. The nearly stationary system set up strong alongshore and onshore winds (upper dashed arrow, Figure 64). These winds, coupled with the storm's extensive rainfall (i.e. >0.18 m in Virginia), were largely responsible for the extremely high storm surge that impacted large portions of Region III. The highest modeled storm surges, as shown by the maximum water level elevations in Figure 64, were seen along the seaward edge of Virginia's eastern shore and in the lower Chesapeake Bay, including within the York and James Rivers. Storm surges of ~1.5–2.0 m were also modeled in Delaware Bay and the lower reaches of the Delaware River. These trends compared favorably to observed water level elevations (Appendix C).

SWAN+ADCIRC was able to reproduce the observed water levels successfully for the duration of the storm with skill scores ≥0.7 at 15 of the 18 validation stations (average skill score of 0.82; Table 24). Thirteen of the successful stations generated skill scores ≥ 0.82. Statistics for all of the stations, including bias, RMS error, scatter index, and overall station performance scores, are reported in Table 24. At the 15 successful stations, the bias measurements were very low (average of -0.04 m) and the average difference between modeled and observed detided water levels was low (~0.13 m; Table 24, Figure 65, Appendix C). Two examples of the 15 successful water level stations, noted by green shaded rows in Table 24, are shown in Figure 65. Finally, it is worth noting that significant residual tidal data are apparent in both the modeled and observed water levels for all of the stations.

Of the 18 validation stations, 3 received performance scores of ≤ 70%. Water level time series and residual data for all three of these stations are presented in Figure 66. For NOS 8548989, near Newbold, DE (station skill score = 0.69; Table 24), differences of up to 0.42 m are seen between the observed and modeled water levels. The slight temporal offset between the observed and modeled peaks and the consistently high/low alternating nature of the residuals indicate a possible tidal component influencing this error. It is worth noting, however, that even with these errors, the difference between the modeled and observed water levels at the peak of the storm was only -0.07 m (Figure 66).

Table 24. Statistics for NOAA water level gauge comparisons, Nor'Ida.

Extratropical Storm Nor'Ida Detided water level validation				
SWAN+ADCIRC versus observations			SI	PERF
Station	BIAS (m)	RMS (m)		
8536110	0.03	0.11	0.16	0.9
8537121	0.04	0.13	0.21	0.87
8540433	-0.01	0.12	0.26	0.87
8548989	0.01	0.22	0.65	0.69
8551762	0.04	0.14	0.26	0.83
8551910	0.05	0.14	0.26	0.82
8555889	0.03	0.11	0.16	0.9
8570283	0.1	0.14	0.14	0.83
8571892	-0.12	0.17	0.31	0.66
8573364	-0.08	0.13	0.36	0.67
8574680	-0.07	0.1	0.2	0.76
8575512	-0.07	0.09	0.16	0.79
8577330	-0.09	0.1	0.1	0.83
8632200	-0.07	0.1	0.1	0.9
8635750	-0.08	0.1	0.1	0.86
8637689	-0.07	0.13	0.13	0.89
8638610	-0.12	0.17	0.12	0.87
8639348	-0.18	0.22	0.12	0.83
Average	0.07	0.13	0.21	0.82

For NOS 8571892, near Cambridge, MD (station score = 0.66, Table 24), the largest differences between the detided modeled and observed data are for the time period between 1200 UTC on 12 November and 0000 UTC on 14 November (Figure 66). The peak of the storm reached Cambridge during the day on 14 November, and the peak storm surge itself is well-replicated by the modeled water levels (within -0.06 m; Figure 66). The situation is similar for NOS 8573364, near Tolchester Beach, MD (station score = 0.67; Table 24). Again, the highest differences between the modeled and observed stations are seen during the time period leading up to the peak storm surge, which is modeled to within ≤ -0.03 m at the peak of the surge at NOS 8573364 (Figure 66). Plots of the residuals for both NOS 8571892 and 8573364 show the total residual decreasing during the course of the storm, and thus support this conclusion (Figure 66).

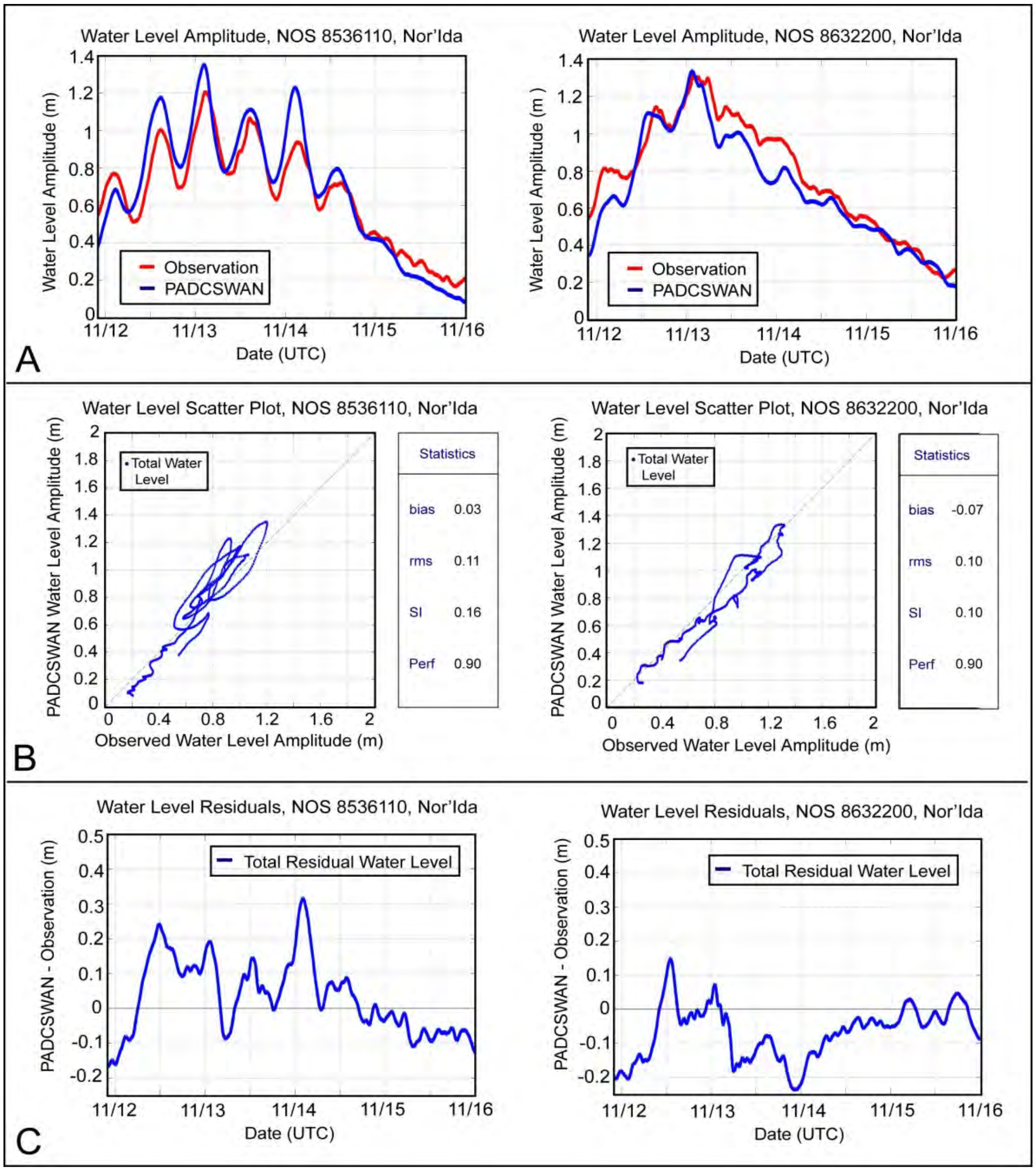

Figure 65. Examples of successful SWAN+ADCIRC water level versus observations, Nor'Ida, Stations 8536110 and 8632200. Water level: A) time series, B) scatter plots,and C) residuals.

Of the 18 validation stations, 1 was only partially wet by SWAN+ ADCIRC: NOS 8551910, near Reedy Point, DE (Figure 67). Despite this, the station had an overall performance score of 0.82 and very low bias and RMS errors (0.05 and 0.14, respectively; Table 24). The dropping out of the SWAN+ADCIRC water level signal at this station is caused by the grid cells going dry during the hindcast, as explained in Section 8.4. Of the three storms hindcast, the tidal component of Nor'Ida was the most difficult to remove from both the observed and the modeled data (see Figure 49 for an example of tided and detided water level data). Despite this tidal complication, overall the model reconstructed the detided observed peak storm surge within 0.19 m at this station.

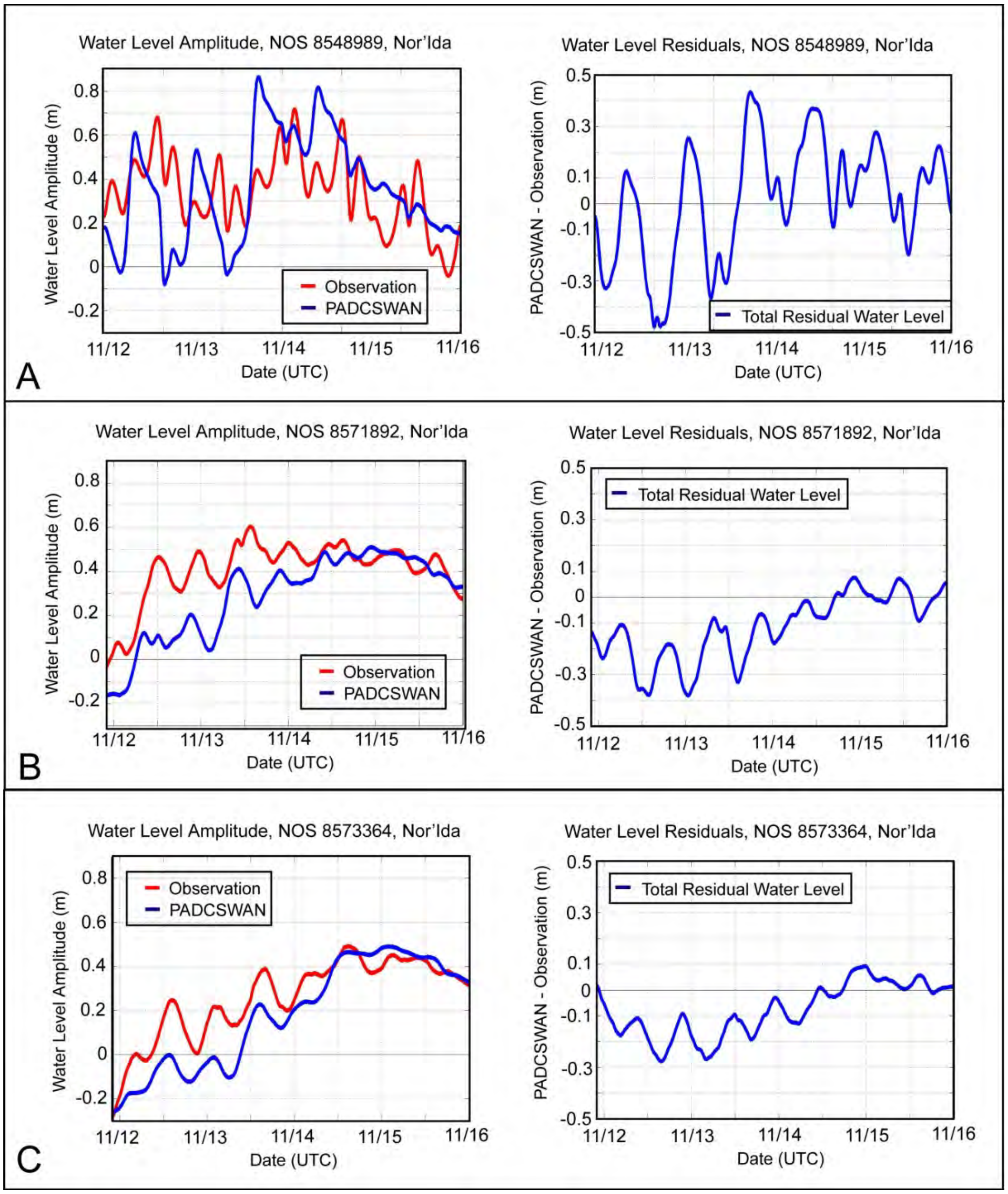

Figure 66. Unsuccessful SWAN+ADCIRC water level versus observations, Nor'Ida, Stations 8548989, 8571892, and 8573364. Water level: A) time series, and B) residuals.

As was the case with Hurricanes Isabel and Ernesto, the peak event analysis of the modeled versus observed Nor'Ida water level time series data provides the most robust metric for quantifying ADCIRC's ability to successfully reproduce the observed storm surge. As in the case of Hurricanes Isabel and Ernesto, the event peaks were identified using a threshold of 0.5 standard deviations above the mean over a search period of 3.0 hr. Due to the extremely strong relict tidal signal in the detided Nor'Ida water levels, both the observed and modeled data were further smoothed over a 1.0-hr time window in an effort to minimize the tidal noise in the data. The peak event analysis yielded a performance score of 0.90 with a bias of 0.0 m (Figure 68), indicating that SWAN+ADCIRC reproduced the maximum, pure storm surge successfully for Nor'Ida in Region III.

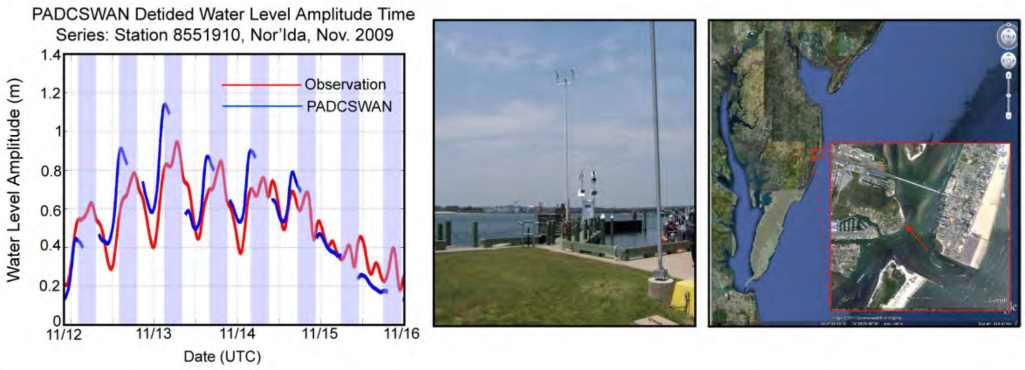

Figure 67. Water level time series for NOS 8551910, Nor'Ida. Periods of low tide are indicated by lavender shading.

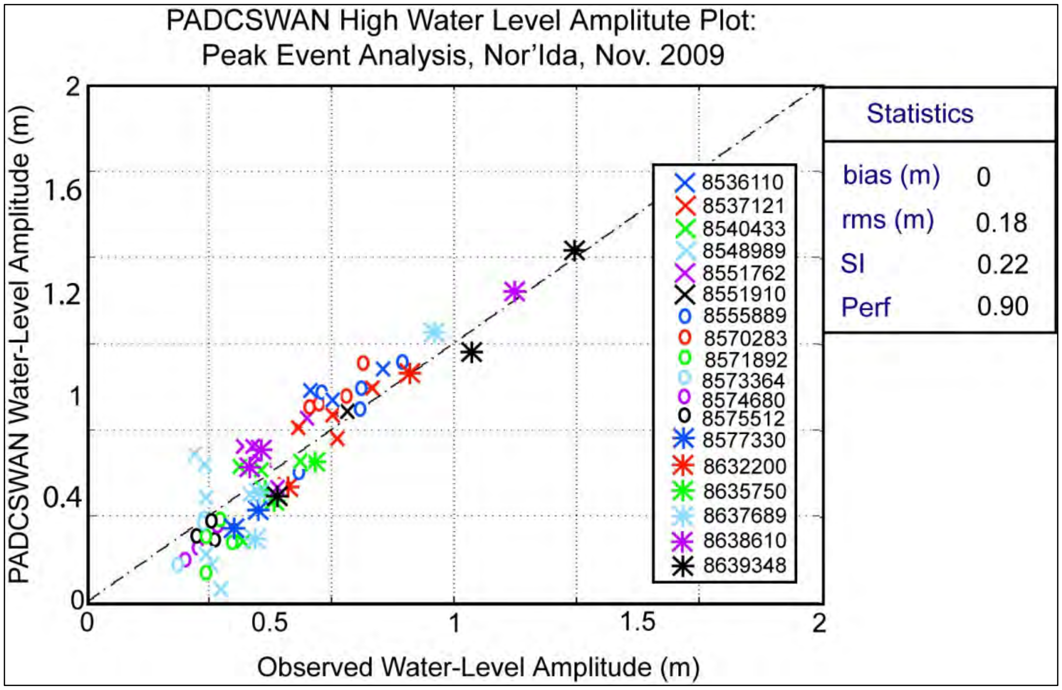

Figure 68. Peak event analysis, SWAN+ADCIRC versus NOAA high water level, Nor'Ida.

Unfortunately, it was not possible to fully smooth out the tidal noise in either the observed or model data for any station. Complicating this is the fact that for several of the validation stations, the storm surge was very small in amplitude compared to the amplitude of the relict tide. Due to the high tidal variability, some stations exhibited multiple peak events

(Figure 69). This observation is supported by the high scatter index associated with the peak analysis (0.22; Figure 68). However, the peak event analysis score of 0.90 for Nor'Ida indicates that these problems had little impact on SWAN+ADCIRC's ability to properly reproduce Nor'Ida's storm surge.

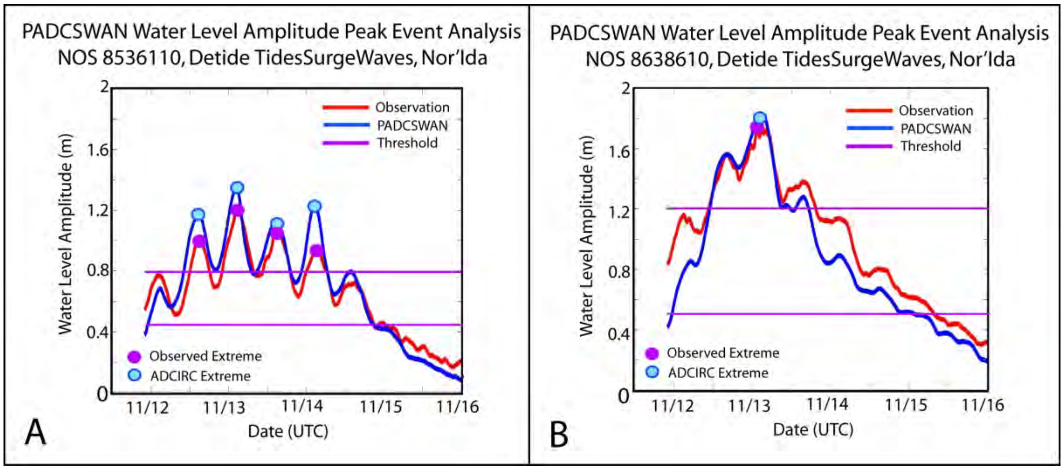

Figure 69. Extremes analysis station examples, Nor'easter Nor'Ida: A) multiple peaks: 8536110, and B) single peak: 8638610. Note plots show both high and low extremes.

8.8.2 USGS storm response data, Nor'Ida

Until recently, quantitative, real-time measurements of storm surge were available only from fixed stations, such as NOS tide gauges. To augment existing data, the USGS instituted a new program in 2006 whereby sensors are deployed on land in the immediate days prior to a hurricane event. Gauges are placed in the projected path of hurricanes and retrieved in the days directly after landfall. In addition to barometric pressure, the gauges also record a time series of water level if and when they are flooded. These rapid-response data were obtained from the USGS and used to evaluate SWAN+ADCIRC's ability to flood a region that is normally dry. Unfortunately, these data are only available for Nor'Ida and are limited to the Hampton Roads region of Virginia (Figure 53). Given the short duration of the observed measurements, the tidal component could not reliably be removed from the time series data. Accordingly, the TidesSurgeWaves SWAN+ADCIRC run was compared with tided observation data.

SWAN+ADCIRC was able to replicate the storm surge water levels successfully at five of the seven USGS Rapid Response stations (Figure 70, Appendix D, Table 25). It should be noted that these stations were all located in the greater Hampton Roads region of Virginia, a topographically complex region of tidal creeks, inlets, and bays. The fact that SWAN+ADCIRC was able to replicate flooding of dry land in this complicated region successfully, with a high level of accuracy (overall performance average of 0.90; Table 25), demonstrates the model's strong ability to flood inland topographic regions accurately, as well as replicating storm surge at coastal stations.

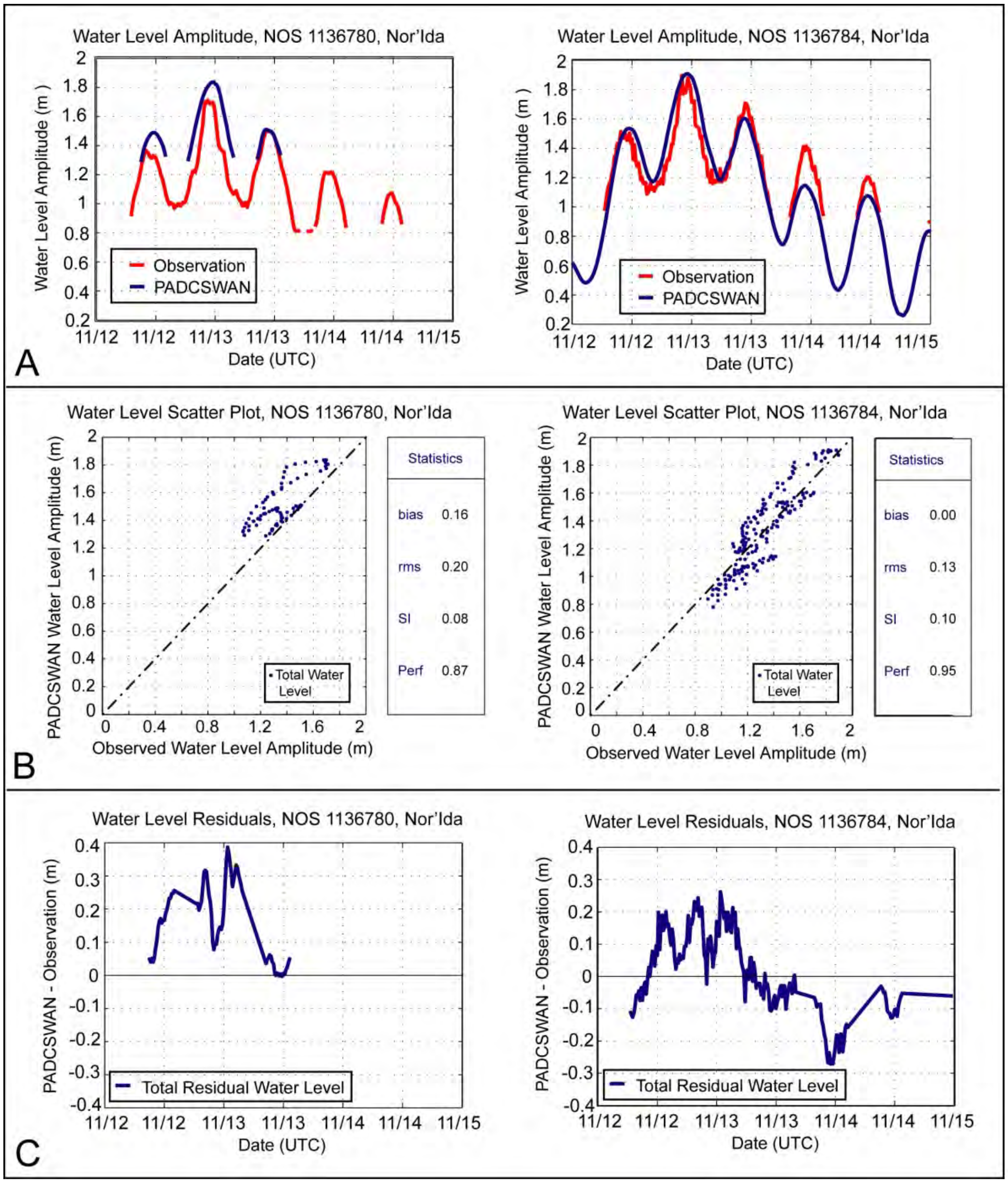

Figure 70. Examples of successful SWAN+ADCIRC water level versus observations, Nor'Ida Stations 1136780 and 1136784. Water level: A) time series, B) scatter plots, and C) residuals.

Table 25. Statistics for USGS rapid response storm surge gauge comparisons, Nor'Ida.

Nor'Ida USGS Rapid Response Water Level Validation					
SWAN+ADCIRC versus observations					
Station	BIAS (m)	RMS (m)	SI	PERF	Sensor Height (m)
1136780	0.16	0.20	0.08	0.87	2.58
1136783	0.21	0.23	0.05	0.87	2.34
1136784	0.10	0.12	0.09	0.95	2.55
1153338	0.17	0.10	0.08	0.88	2.36
1153341		-----			2.25
1153348	0.01	0.10	0.07	0.96	3.66
2414172		-----			1.51
Average	0.11	0.17	0.07	0.91	2.46

Statistics for all of the stations, including bias, RMS error, scatter index, and overall station performance scores, are reported in Table 25. Two examples of the successful five stations, as noted by green circles in Figure 53 and green shaded rows in Table 25, are plotted in Figure 70. SWAN+ADCIRC was unable to wet two of the rapid response stations, as noted by the pink circles in Figure 53 and pink shaded rows in Table 25. At all five successful stations, the bias measurements averaged 0.01 m and all of the stations demonstrated an average difference in modeled versus observed water elevations of ± 0.07 m (Figure 70; Appendix D). It should be noted that although the observational water levels at every rapid-response station go dry at times during the storm (due to lower tides no longer flooding the region), the SWAN+ADCIRC modeled water level data at stations 1136784 and 1153348 stay wet the entire time. This is likely due to a combination of factors, including slightly different tidal responses in the observed versus modeled data as well as the local accuracy of the modeling mesh. In addition, the sensors themselves are not at ground level (Table 25). Accordingly, the individual sensors may go dry even though the region around them stays flooded. This does not appear to have adversely affected SWAN+ADCIRC's ability to model the peak storm surge at both of these stations (individual station skill scores of 0.95 and 0.88, respectively; Table 25).

A peak event analysis of the USGS water levels indicates an overall performance score for SWAN+ADCIRC of 0.96 (Figure 71). It should be noted that, due to the uniqueness of the USGS rapid-response storm data, different parameters were applied to the peak event analysis than were applied to the longer-term, detided, NOAA-based analyses conducted for

Isabel, Ernesto, and Nor'Ida. The USGS rapid-response model and observed data were initially smoothed over 1.0 hr. The peaks were selected using a threshold of 0.75 standard deviations above the mean over a search period of 2.0 hr. Given that these data were not detided, multiple "high" peaks are associated with each station (Figure 71). However, the high extremes analysis score for these data (0.96; Table 25), and the low bias, RMS error, and scatter index for the extremes analysis (0.00, 0.11, and 0.08, respectively; Figure 71) support the conclusion that SWAN+ADCIRC successfully reproduced the maximum, pure storm surge on the short-term, land-based, USGS Rapid Response gauges during Nor'Ida in Region III.

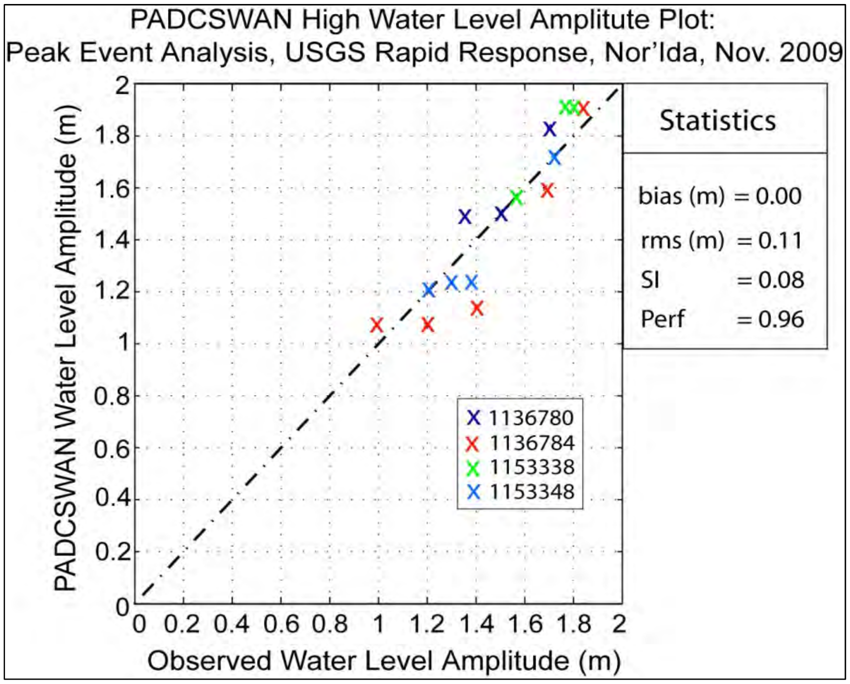

Figure 71. Peak event analysis for SWAN+ADCIRC versus USGS rapid response stations, Nor'Ida.

8.9 Peak water level validation summary

Overall, ADCIRC was able to resolve storm surge with a great deal of accuracy for Hurricanes Isabel and Ernesto, as well as Nor'easter Ida (peak event analysis scores of 0.93, 0.89, and 0.90, respectively). Specifically, the differences between the modeled and observed peak storm surge, at every station and for every storm, were less than 0.5 m (< 1.5 ft; Table 26). In fact, the majority of the stations showed differences between modeled and observed storm surge peaks of less than 0.25 m (94%, 72%, and 89% for Isabel, Ernesto, and Nor'Ida, respectively). The largest error was for station 8548989 during Hurricane Ernesto (-0.42 m; Table 26).

Table 26. Percent differences (upper table in m; lower table in ft) between SWAN+ADCIRC and observed peak storm surge.

Storm	< 0.1 m	< 0.25 m	< 0.5 m	max error (m)	min error (m)
Isabel	47	94	100	0.29	0
Ernesto	17	72	100	-0.42	0
Nor'Ida	44	89	100	0.26	0.02

Storm	< 0.25 ft	< 0.5 ft	< 0.75 ft	< 1 ft	< 1.5 ft	max error (ft)	min error (ft)
Isabel	41	82	94	100	100	0.96	0
Ernesto	17	44	78	89	100	-1.39	0
Nor'Ida	39	78	78	100	100	0.86	0.07

A final peak event analysis, combining all three storms, was performed to assess the total skill of SWAN+ADCIRC in replicating the peak storm surge in the Region III domain. This was done by selecting only the single maximum storm surge observed at each station during each storm. The corresponding modeled water levels associated with the observed peaks in storm surge were then extracted from the data. The results of this analysis are depicted in the scatter plot of Figure 72. Overall, the Region III SWAN+ ADCIRC modeling system did an impressive job at reproducing the peak storm surge during the three validation events (skill score = 0.93; Figure 72). The exceptional performance, combined with low bias and RMS errors, strongly supports the conclusion that the Region III SWAN+ ADCIRC modeling system is adequate for performing the coastal storm surge simulations required by FEMA.

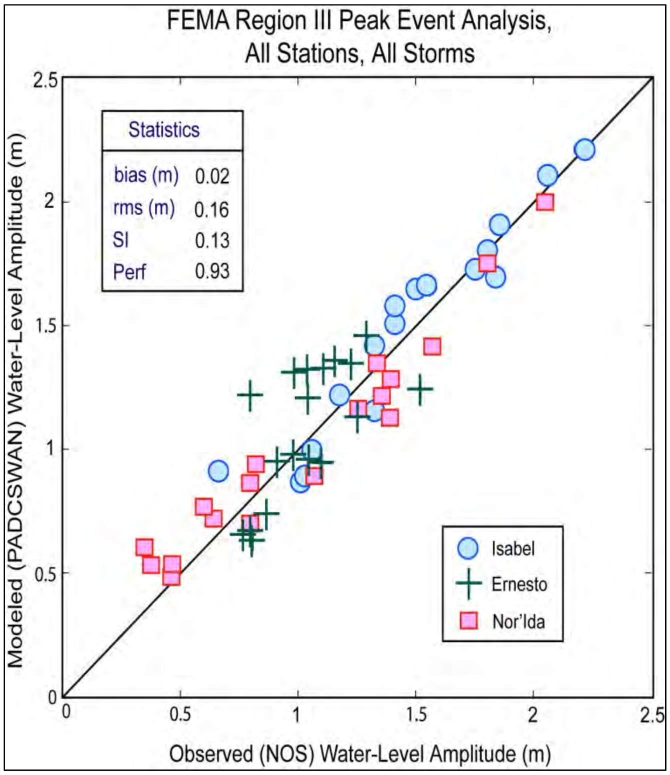

Figure 72. Final water level peak event analysis results for Region III.

References

Blanton, B. S., K. Madry, K. Galluppi, K. Gamiel, H. Lander, M. Reed, L. Stillwell, M. Blanchard-Montgomery, R. Luettich, C. Mattocks, C. Fulcher, P. Vickery, J. Hanson, E. Devaliere, and J. McCormick. 2008. *Coastal Flood Analysis System*. Report to the State of North Carolina Floodplain Mapping Project. Chapel Hill, NC: Renaissance Computing Institute.

Blanton, B., L. Stillwell, H. Roberts, J. Atkinson, S. Zou, M. Forte, J. Hanson, and R. Luettich. 2011. *Coastal Storm Surge Analysis: Computational System, Submittal 1.2 to FEMA*. ERDC/CHL TR 11-1. Vicksburg, MS: US Army Engineer Research and Development Center.

Cox, A. T., J. A. Greenwood, V. J. Cardone, and V. R. Swail. 1995. An interactive objective kinematic analysis system. In *Proceedings of the 4th International Workshop on Wave Hindcasting and Forecasting*, Banff, Alberta.

Egbert, G. D., and S. Y. Erofeeva. 2002. Efficient inverse modeling of barotropic ocean tides. *Journal of Atmospheric and Oceanic Technology* 19(2):183–204.

Federal Emergency Management Agency (FEMA). 2007. *Atlantic and Gulf of Mexico Coastal Guidelines Update*. Final Draft, Federal Emergency Management Office Report. Washington, DC.

Forte, M. F., J. L. Hanson, L. Stillwell, M. Blanchard-Montgomery, B. Blanton, R. Leuttich, H. Roberts, J. Atkinson, and J. Miller. 2011. *Coastal Storm Surge Analysis System: Digital Elevation Model, Submittal 1.1 to FEMA*. Technical Report ERDC/CHL-TR-11-1. Vicksburg, MS: US Army Engineer Research and Development Center.

Hanson, J. L., B. Tracy, H. Tolman, and R. Scott. 2009. Pacific hindcast performance of three numerical wave models. *Journal of Atmospheric and Oceanic Technology* 26: 1614-33.

Hess, K. W., T. F. Gross, R. A. Schmalz, J. G. W. Kelley, F. Aikmann III, and E. Wei. 2003. *NOS Standards for evaluating operational nowcast and forecast hydrodynamic model systems*. NOAA Technical Report NOS CS 17. Silver Spring, MD: National Ocean Service.

Knabb, R. D., and M. Mainelli. 2006. *Tropical Cyclone Report: Hurricane Ernesto (AL062006)*. U.S. National Hurricane Center online report. [Available online at: http://www.nhc.noaa.gov/pdf/TCR-AL062006_Ernesto.pdf].

Large, W., and S. Pond. 1981. Open Ocean momentum flux measurements in moderate to strong winds. *Journal of Physical Oceanography* 11: 324-36.

Moffatt and Nichol, Engineers. 2010. *Norfolk wave climate monitoring*. Interim Report #12. City of Norfolk, VA.

National Ocean Service (NOS). 2000. *Tidal datums and their applications.* NOAA Technical Report NOS COOPS 1. Silver Spring, MD: Center for Operational Oceanographic Products and Services.

Roberts, H. 2011. ADCIRC Mesh Updates. Personal correspondence.

Taylor, P. K., E. C. Kent, M. J. Yelland, and B. I. Moat. 2003. The accuracy of marine surface winds from ships and buoys. In *Advances in the Applications of Marine Climatology: The Dynamic Part of the WMO Guide to the Applications of Marine Meteorology*. WMO/TD-No. 1081 2003, JCOMM Technical Report 13: 27-40.

Thompson, E. F., and D. A. Leenknecht. 1994. Wind estimation for coastal modeling applications. *Journal of Coastal Research* 10(3): 628-636.

Vickery, P., D. Wadhera, A. Cox, V. Cardone, J. Hanson, and B. Blanton. *Coastal storm surge analysis: Storm forcing, Submittal 1.3 to FEMA.* In preparation. Vicksburg, MS: US Army Engineer Research and Development Center.

Zhang, A. K., W. Hess, E. Wei, and E. Myers. 2006. *Implementation of model skill assessment software for water level and current in tidal regions.* NOAA Technical Report NOS CS 24. Silver Spring, MD: National Ocean Service.

Appendix A: Detided TidesSugeWaves Water Level Data, Hurricane Isabel

Data plots in this section refer to the PADCSWAN Detided TidesWindsWaves water level analysis for Hurricane Isabel, September 2003.

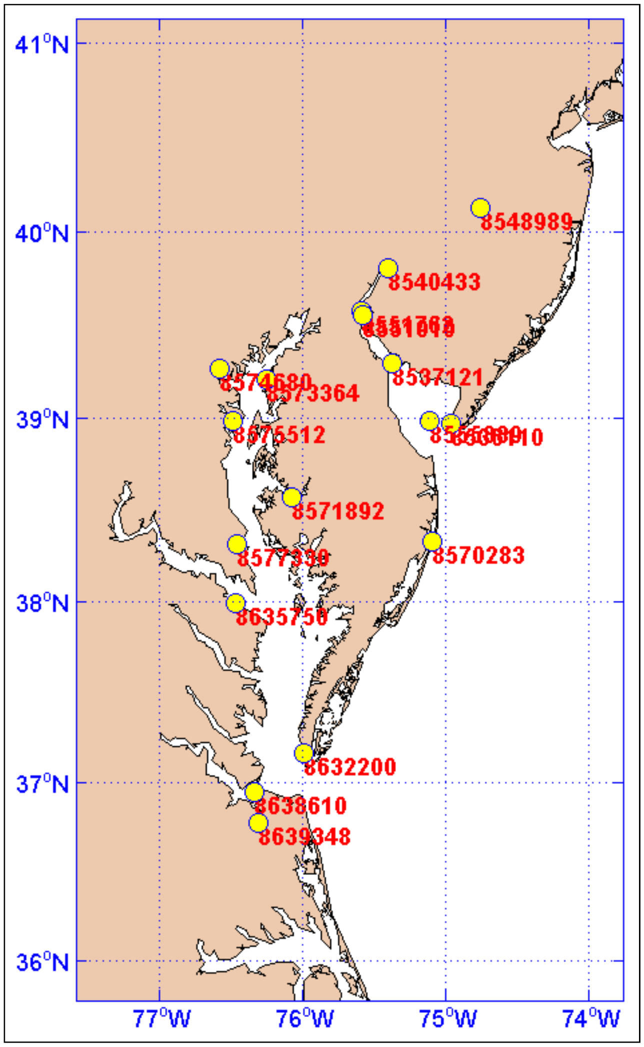
41°N
40°N
39°N
38°N
37°N
36°N
77°W
76°W
75°W
74°W
8548989
8540433
8537121
8574680
8573364
8575512
8571892
8577330
8570283
8635750
8632200
8638610
8639348

Figure A1. NOAA water level station locations for Detided TidesWindsWaves, Isabel.

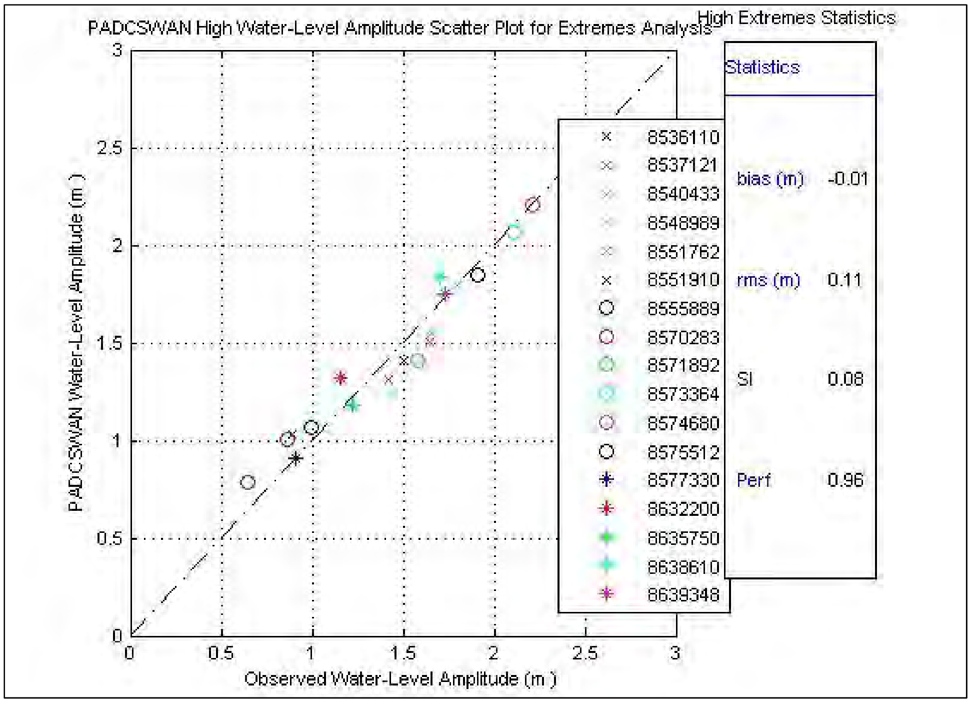

Figure A2. High-water level extremes analysis, Detided TidesWindsWaves, Isabel.

Station 8536110

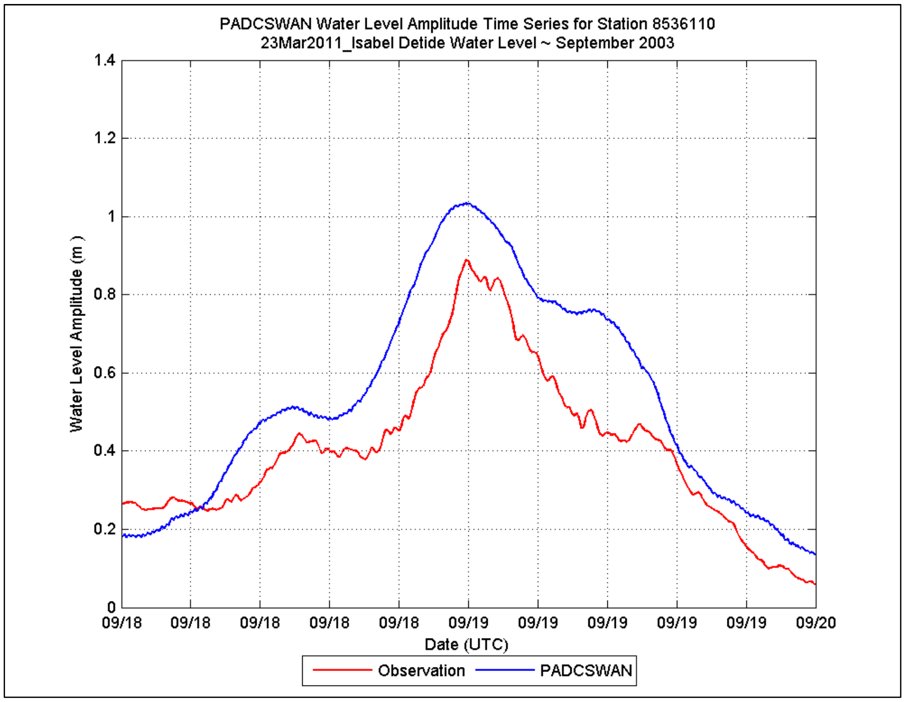

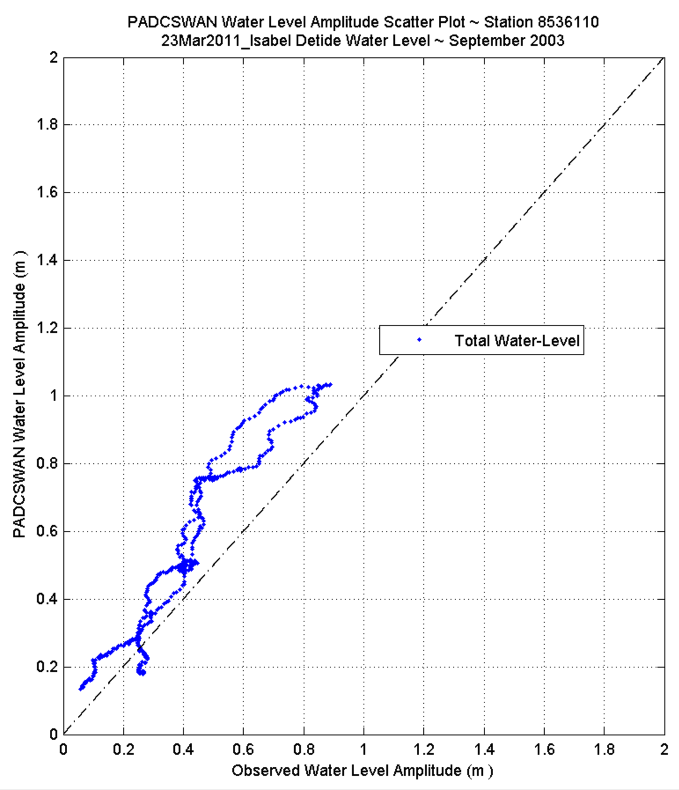

Water Level Amplitude Summary Table
For Station 8536110

Statistics	totwl
bias	0.13
rms	0.16
SI	0.25
Perf	0.68

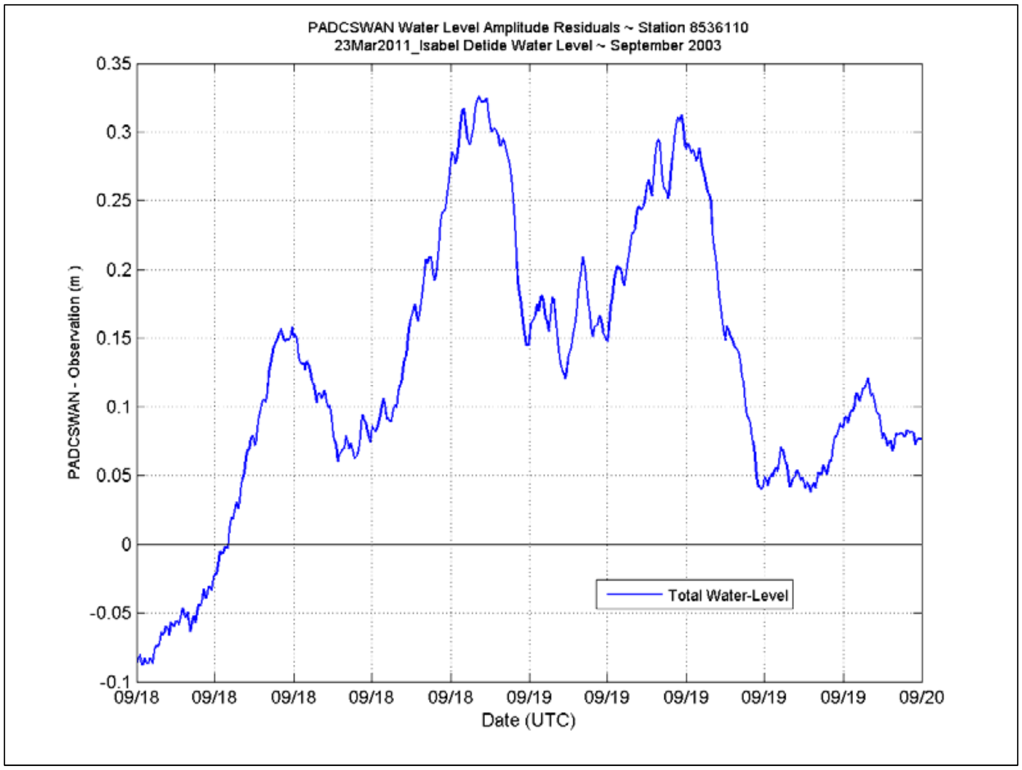
PADCSWAN Water Level Amplitude Residuals ~ Station 8536110
23Mar2011_Isabel Detide Water Level ~ September 2003
PADCSWAN - Observation (m)
0.35
0.3
0.25
0.2
0.15
0.1
0.05
0
-0.05
-0.1
09/18
09/18
09/18
09/18
09/18
09/19
09/19
09/19
09/19
09/19
09/20
Date (UTC)
Total Water-Level

Station 8537121

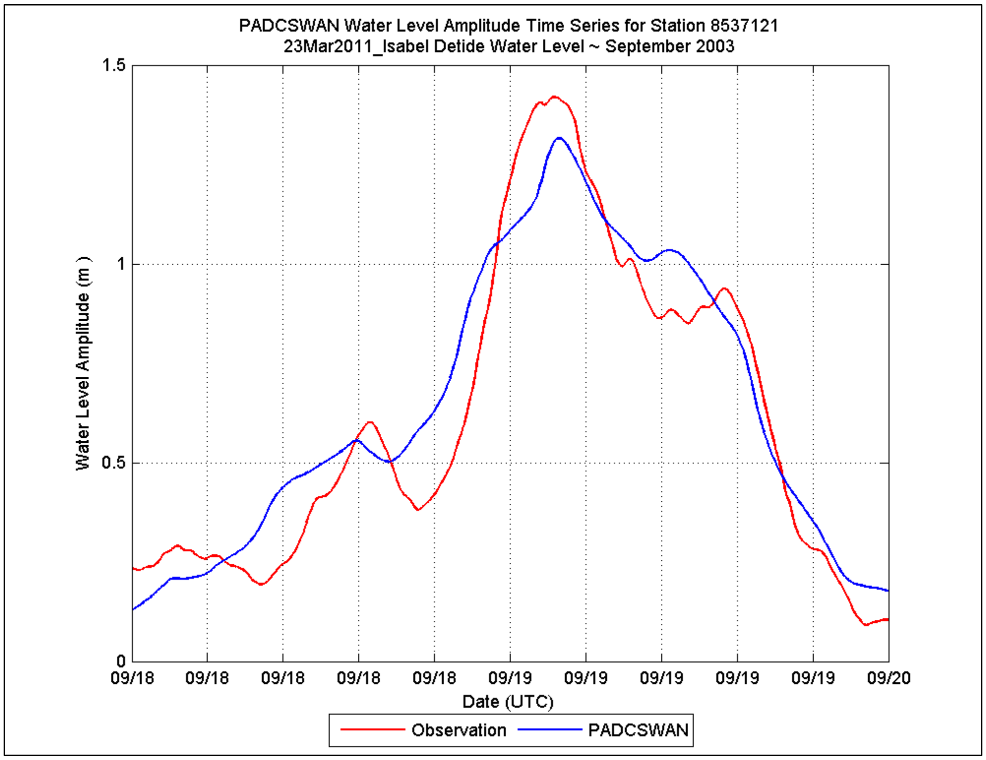

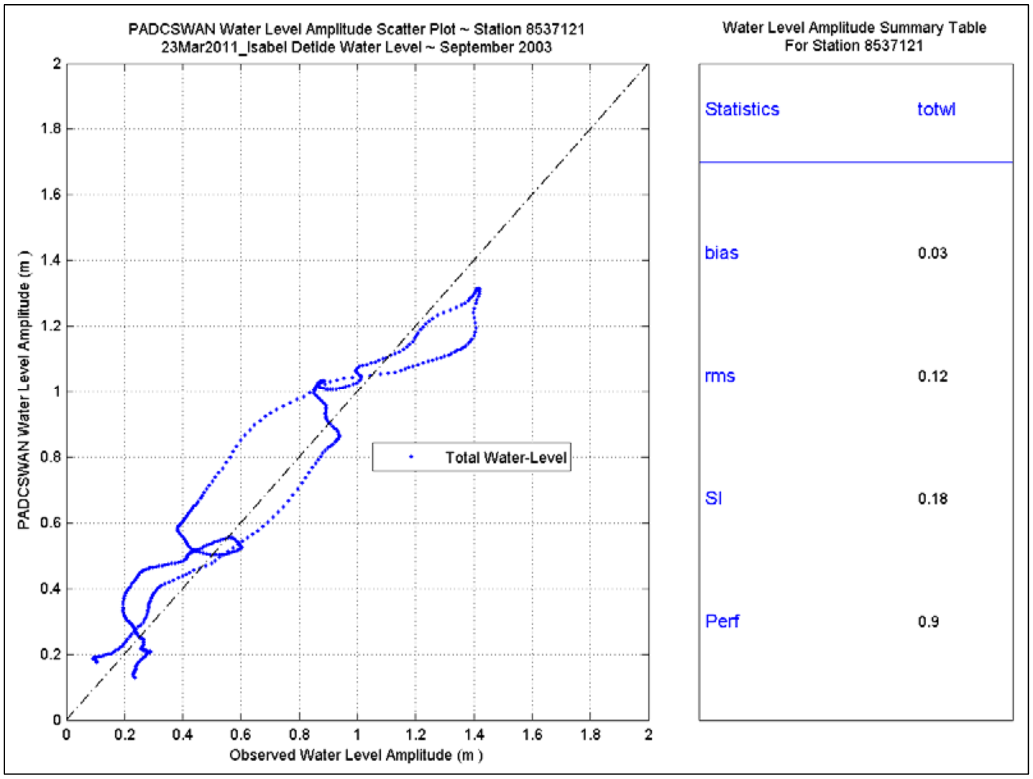

Water Level Amplitude Summary Table
For Station 8537121

Statistics	totwl
bias	0.03
rms	0.12
SI	0.18
Perf	0.9

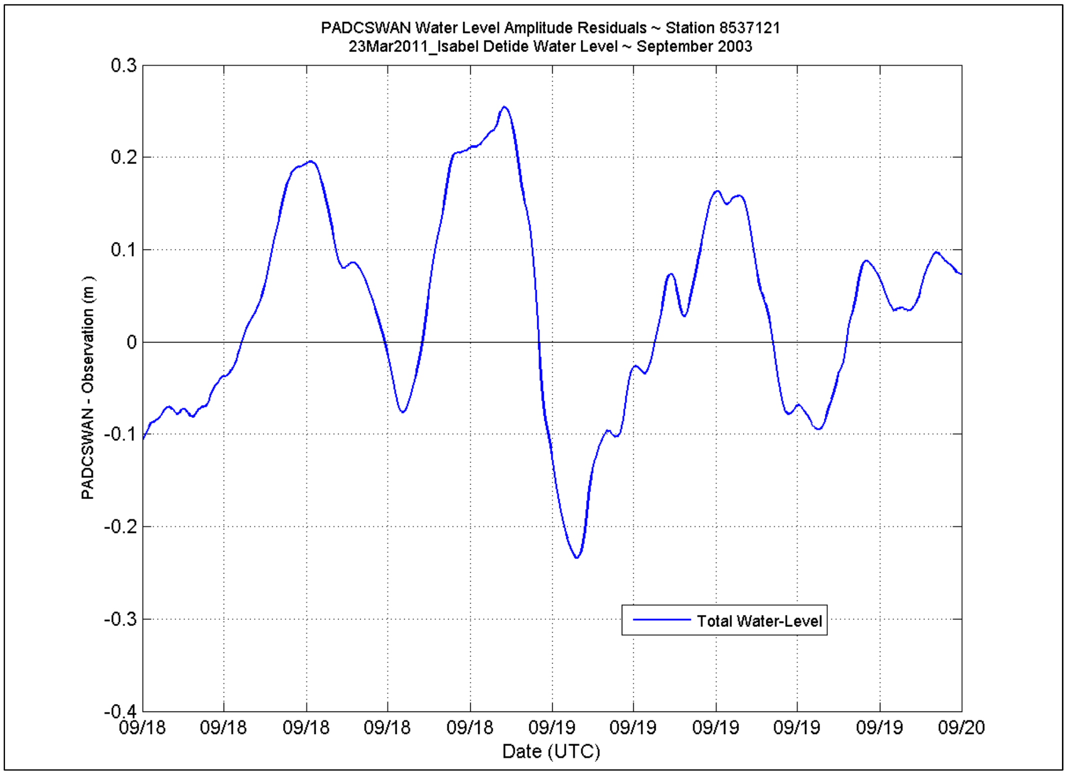
PADCSWAN Water Level Amplitude Residuals ~ Station 8537121
23Mar2011_Isabel Detide Water Level ~ September 2003
0.3
0.2
0.1
0
-0.1
-0.2
-0.3
-0.4
PADCSWAN - Observation (m)
09/18
09/18
09/18
09/18
09/18
09/19
09/19
09/19
09/19
09/19
09/20
Date (UTC)
Total Water-Level

Station 8540433

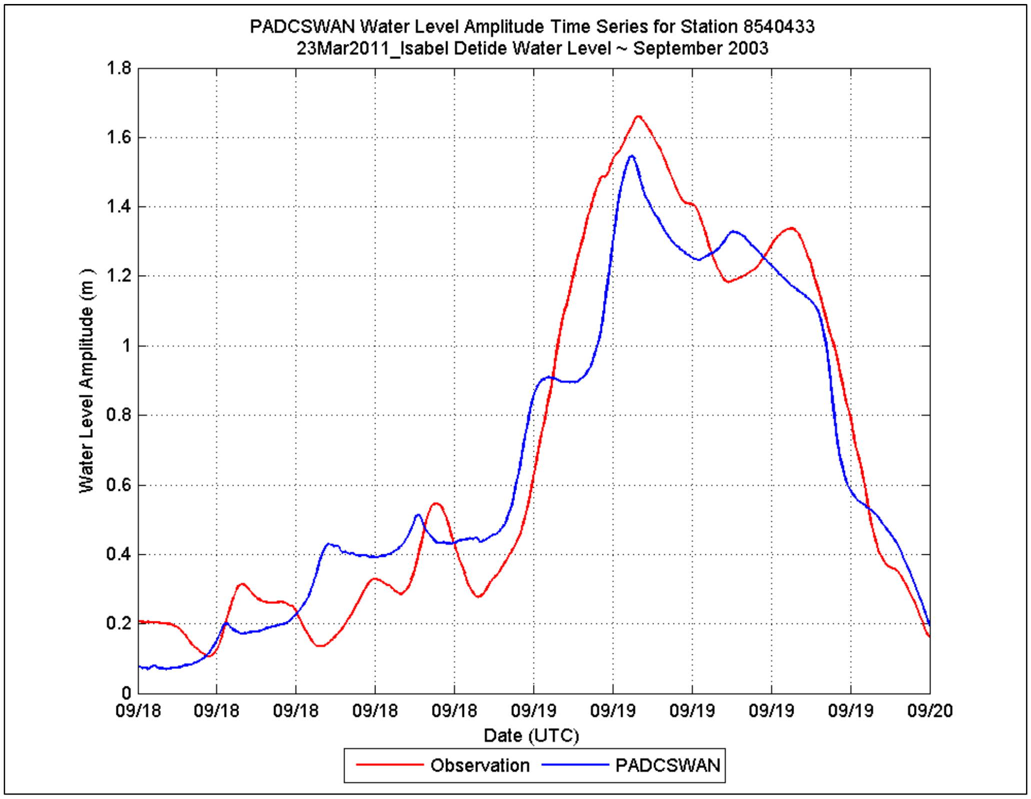

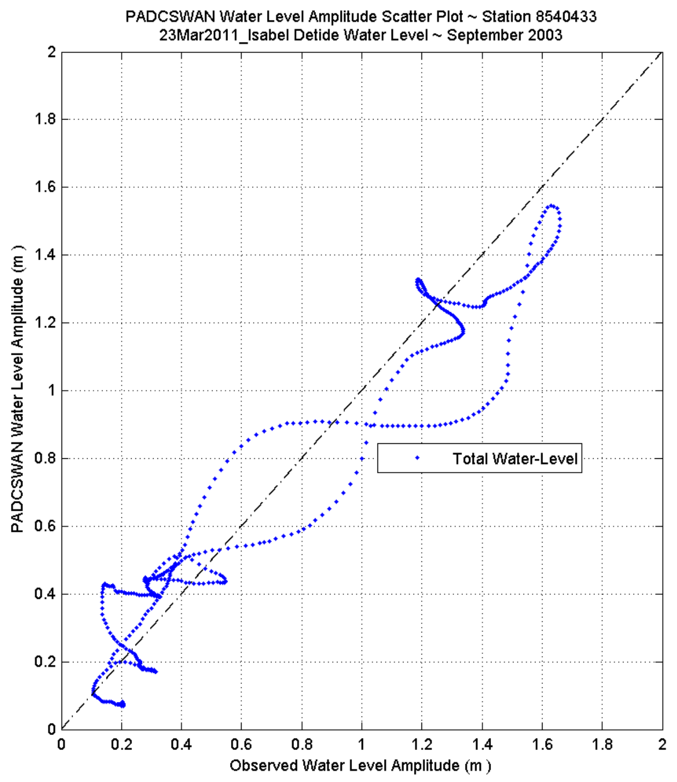

Water Level Amplitude Summary Table
For Station 8540433

Statistics	totwl
bias	-0.03
rms	0.16
SI	0.22
Perf	0.89

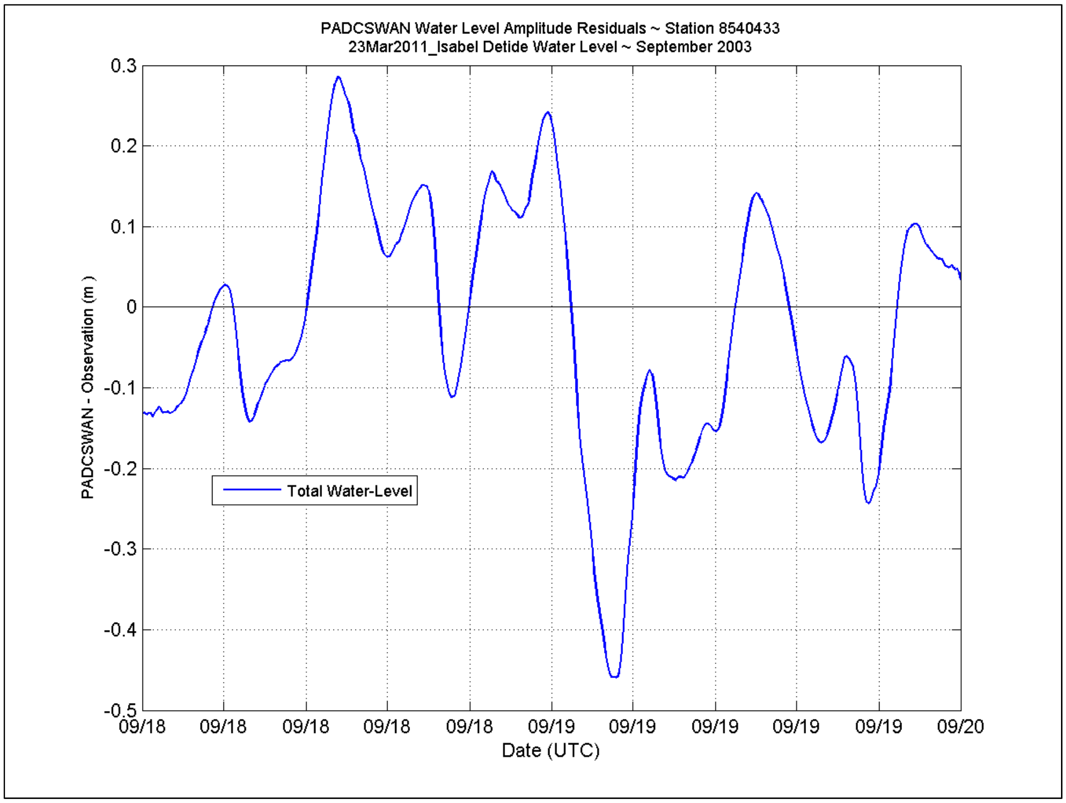
PADCSWAN Water Level Amplitude Residuals ~ Station 8540433
23Mar2011_Isabel Detide Water Level ~ September 2003
PADCSWAN - Observation (m)
0.3
0.2
0.1
0
-0.1
-0.2
-0.3
-0.4
-0.5
Total Water-Level
09/18
09/18
09/18
09/18
09/18
09/19
09/19
09/19
09/19
09/19
09/20
Date (UTC)

Station 8548989

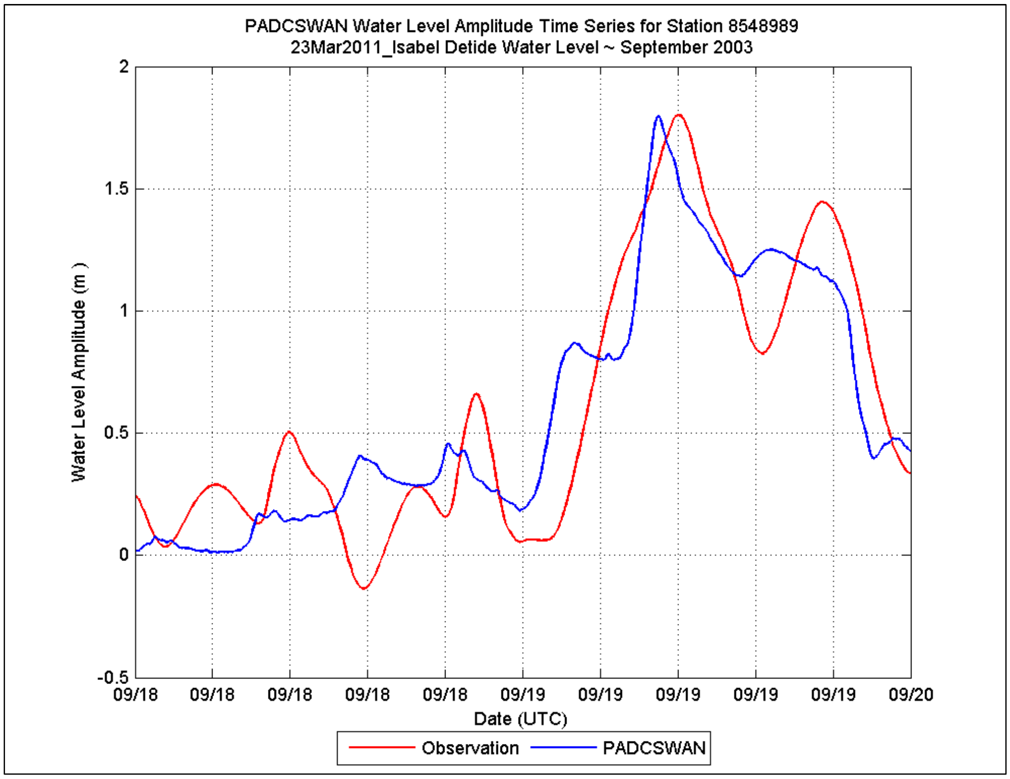

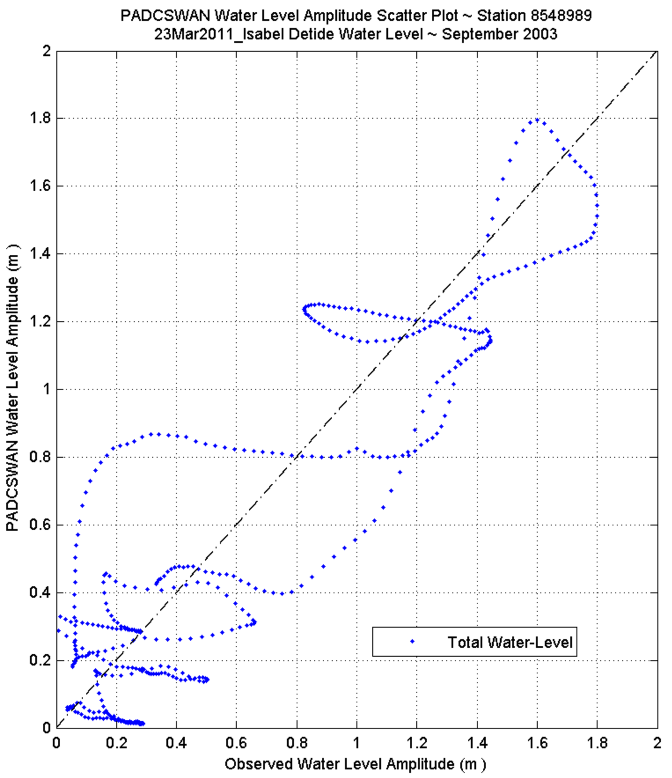

Water Level Amplitude Summary Table
For Station 8548989

Statistics	totwl
bias	-0.01
rms	0.26
SI	0.42
Perf	0.83

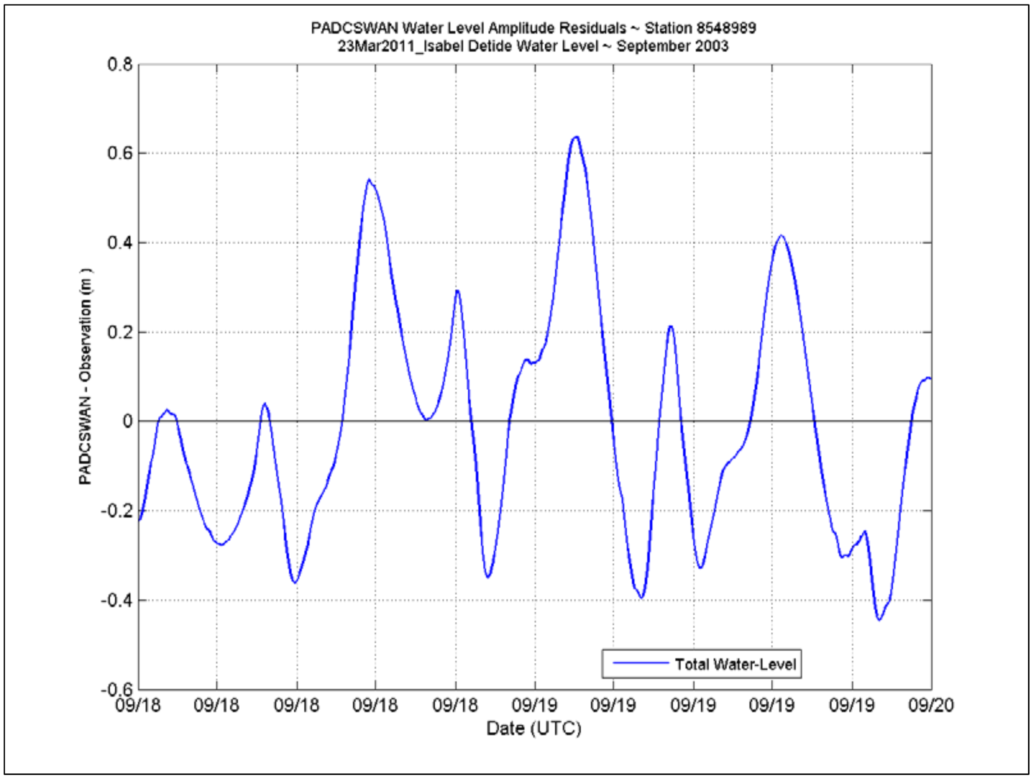
PADCSWAN Water Level Amplitude Residuals ~ Station 8548989
23Mar2011_Isabel Detide Water Level ~ September 2003
PADCSWAN - Observation (m)
0.8
0.6
0.4
0.2
0
-0.2
-0.4
-0.6
09/18
09/18
09/18
09/18
09/18
09/19
09/19
09/19
09/19
09/19
09/20
Date (UTC)
Total Water-Level

Station 8551762

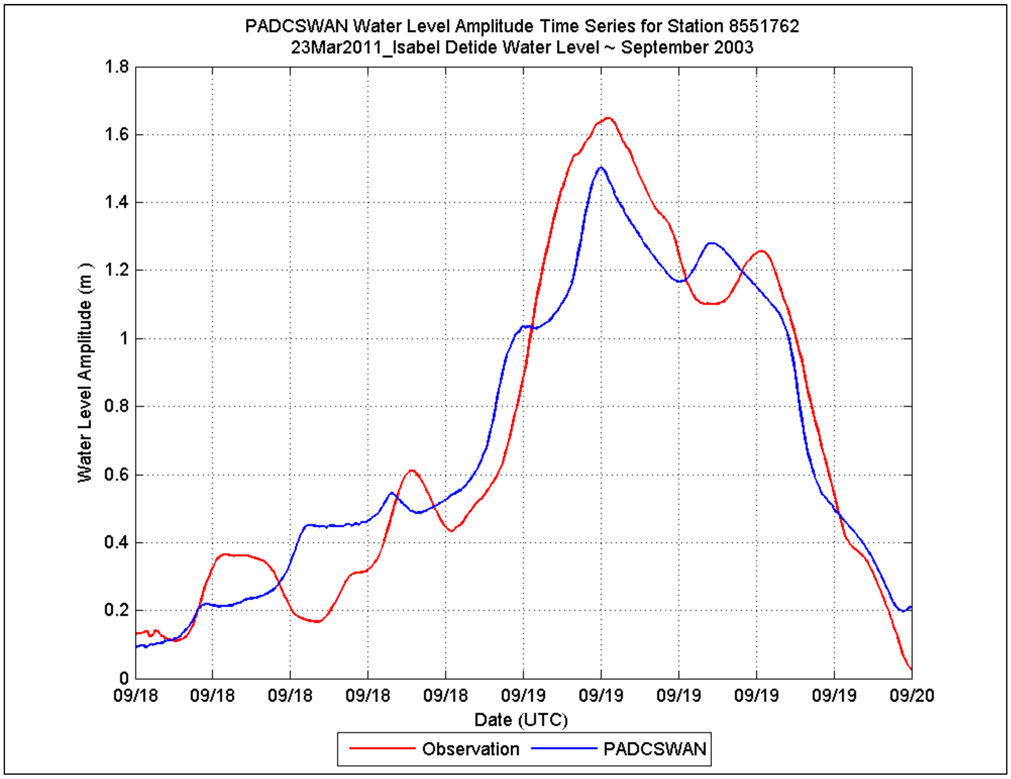

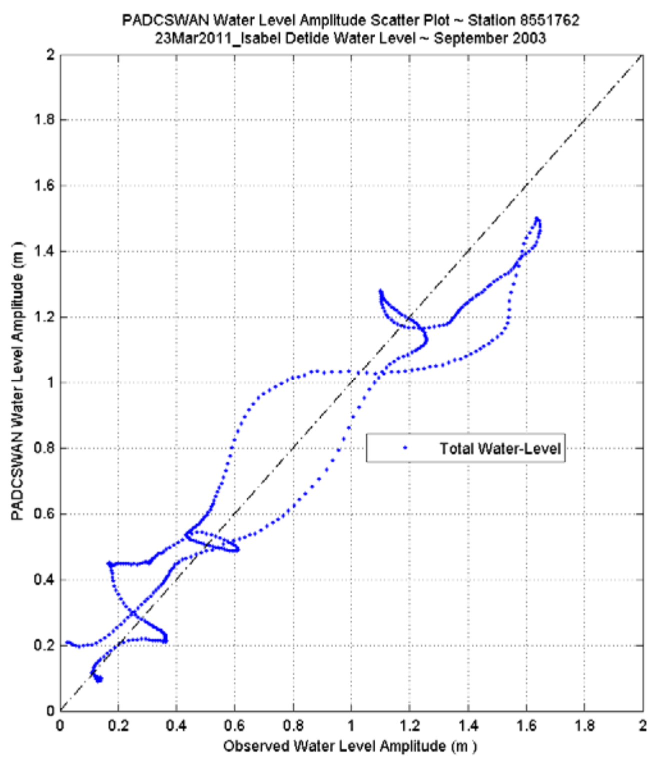

Water Level Amplitude Summary Table
For Station 8551762

Statistics	totwl
bias	-0.01
rms	0.15
SI	0.21
Perf	0.91

Station 8551910

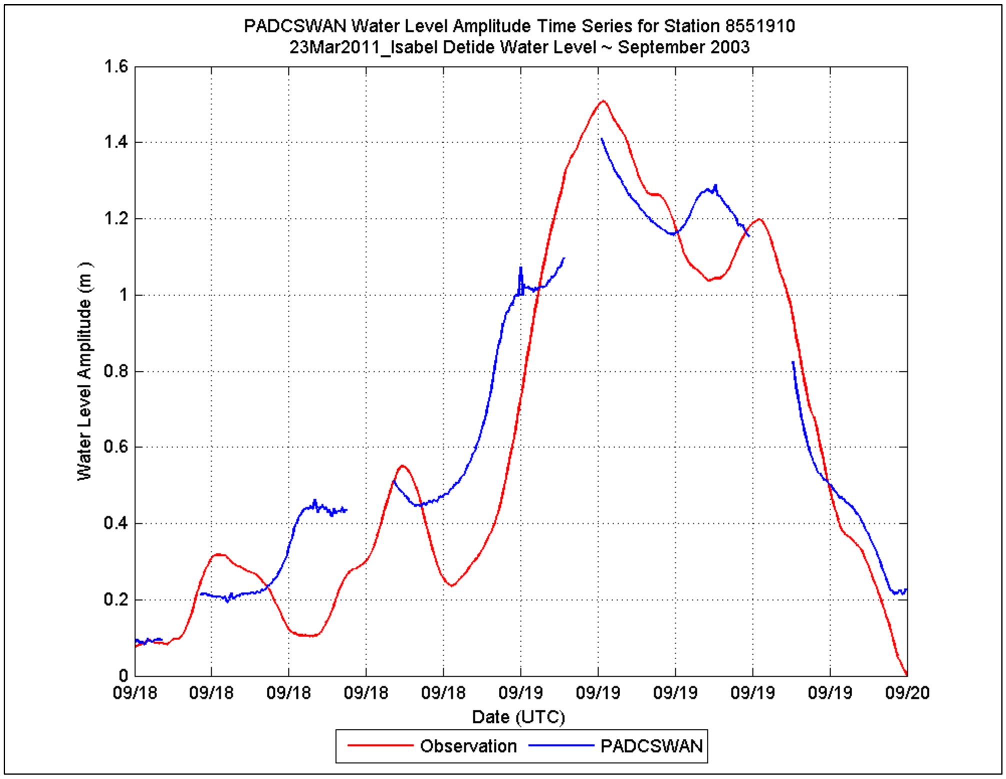

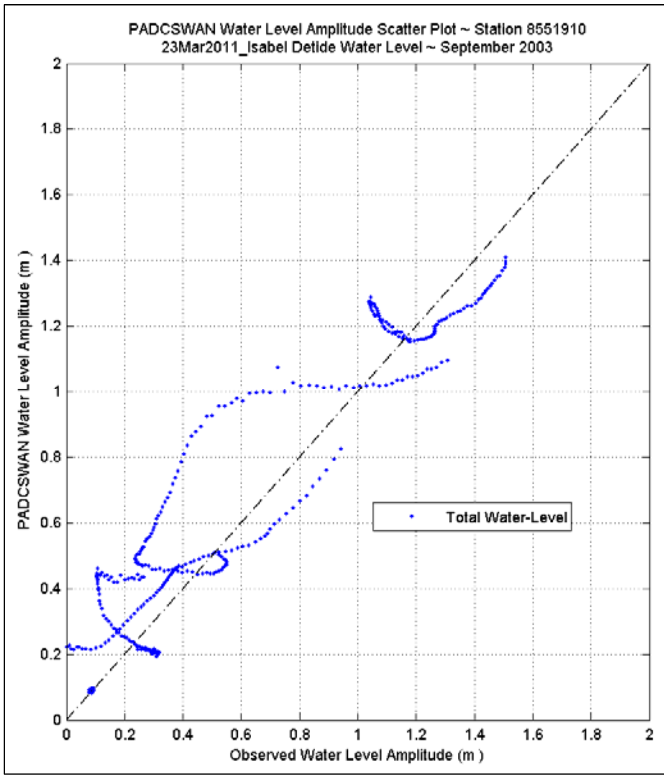

Water Level Amplitude Summary Table
For Station 8551910

Statistics	totwl
bias	0.08
rms	0.18
SI	0.27
Perf	0.83

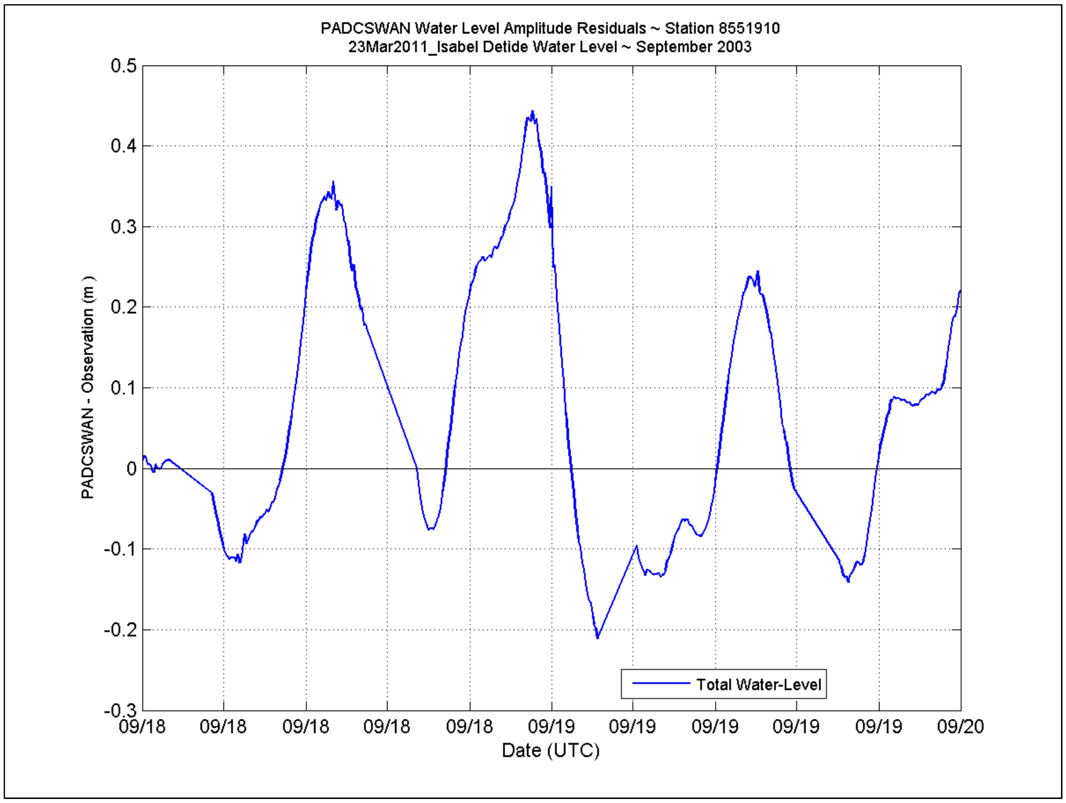
PADCSWAN Water Level Amplitude Residuals ~ Station 8551910
23Mar2011_Isabel Detide Water Level ~ September 2003
PADCSWAN - Observation (m)
0.5
0.4
0.3
0.2
0.1
0
-0.1
-0.2
-0.3
09/18
09/18
09/18
09/18
09/18
09/19
09/19
09/19
09/19
09/19
09/20
Date (UTC)
Total Water-Level

Station 8555889

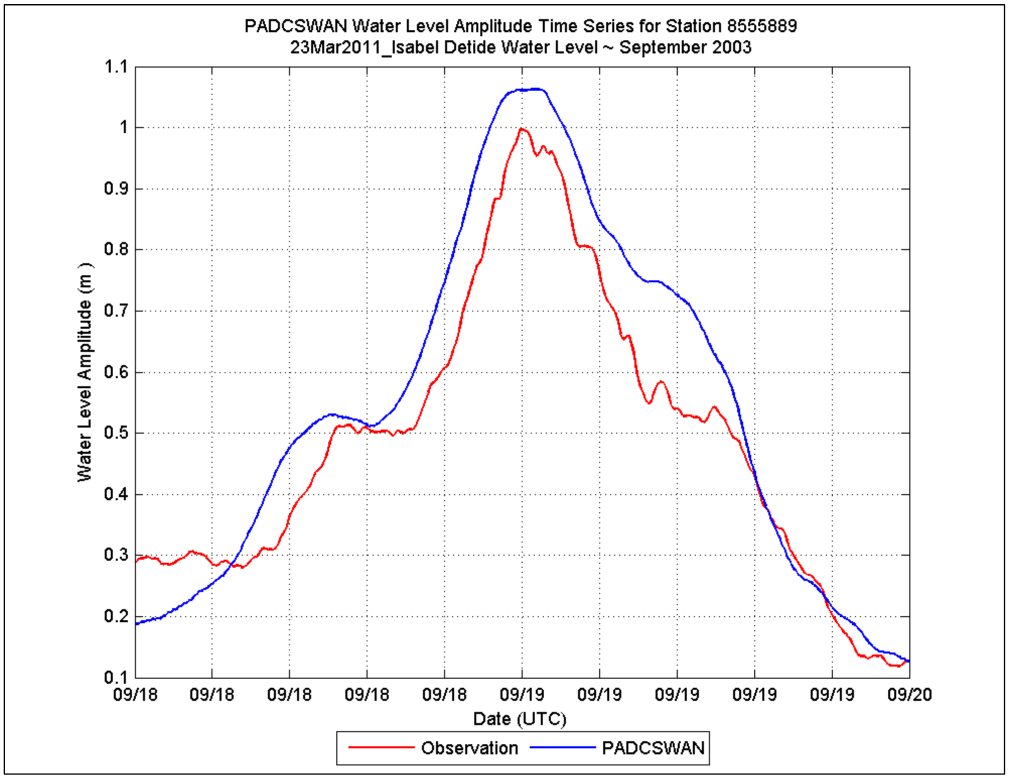

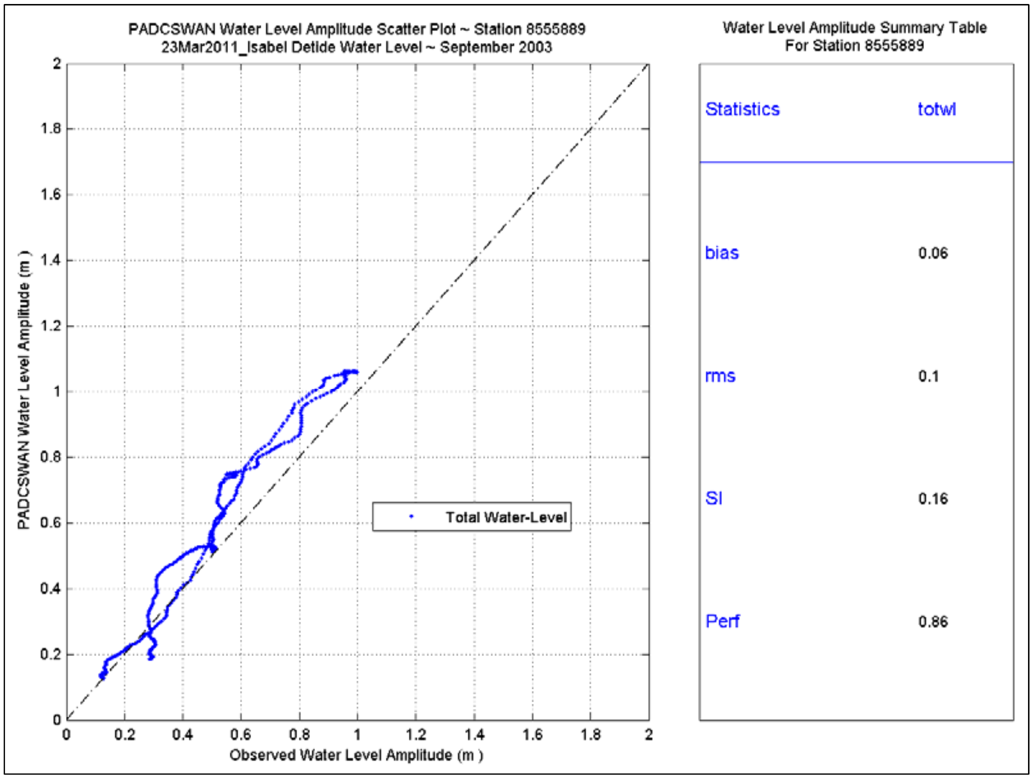

Water Level Amplitude Summary Table
For Station 8555889

Statistics	totwl
bias	0.06
rms	0.1
SI	0.16
Perf	0.86

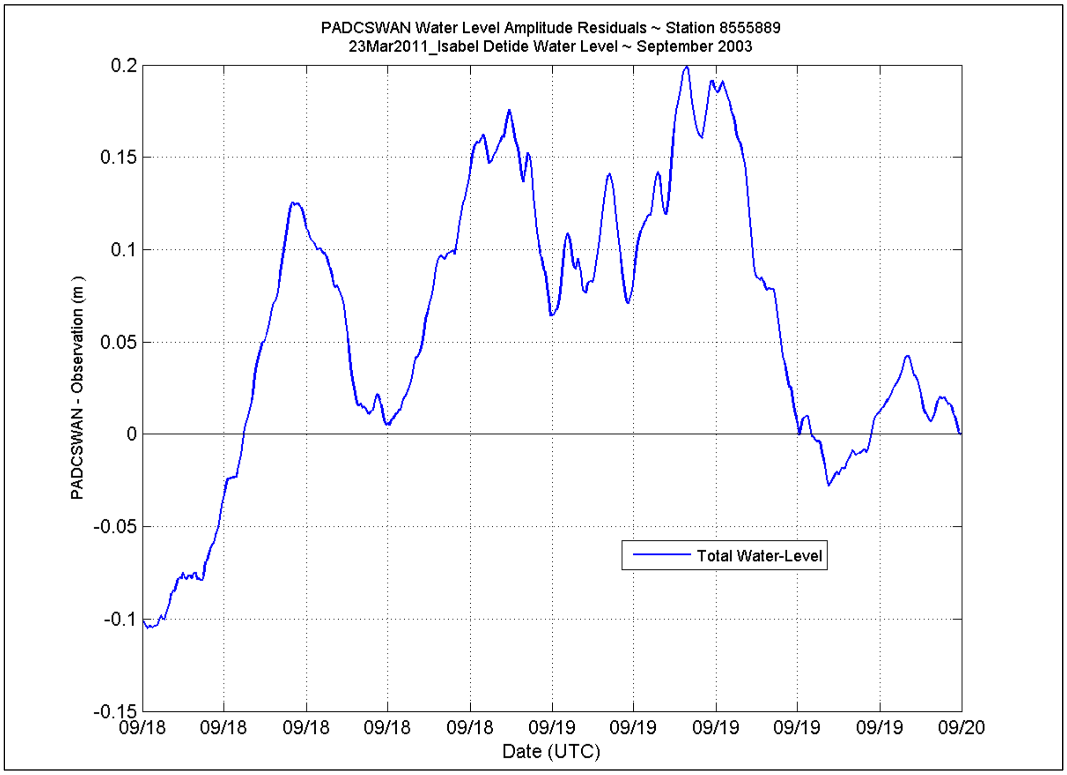
PADCSWAN Water Level Amplitude Residuals ~ Station 8555889
23Mar2011_Isabel Detide Water Level ~ September 2003
PADCSWAN - Observation (m)
0.2
0.15
0.1
0.05
0
-0.05
-0.1
-0.15
09/18
09/18
09/18
09/18
09/18
09/19
09/19
09/19
09/19
09/19
09/20
Date (UTC)
Total Water-Level

Station 8570283

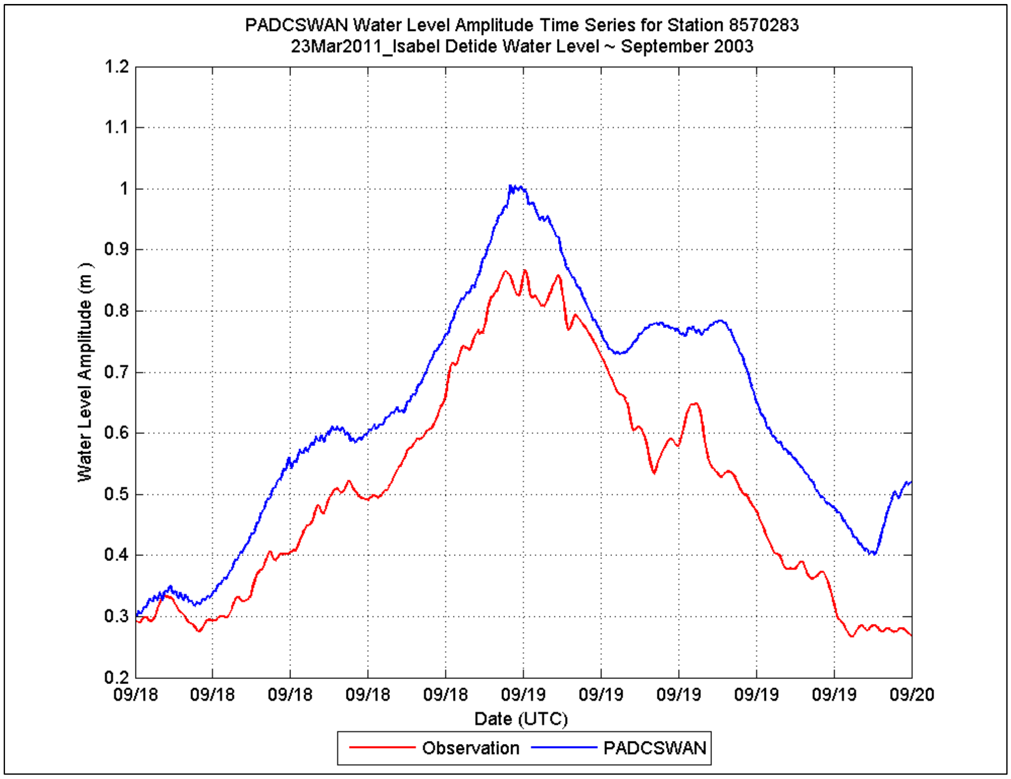

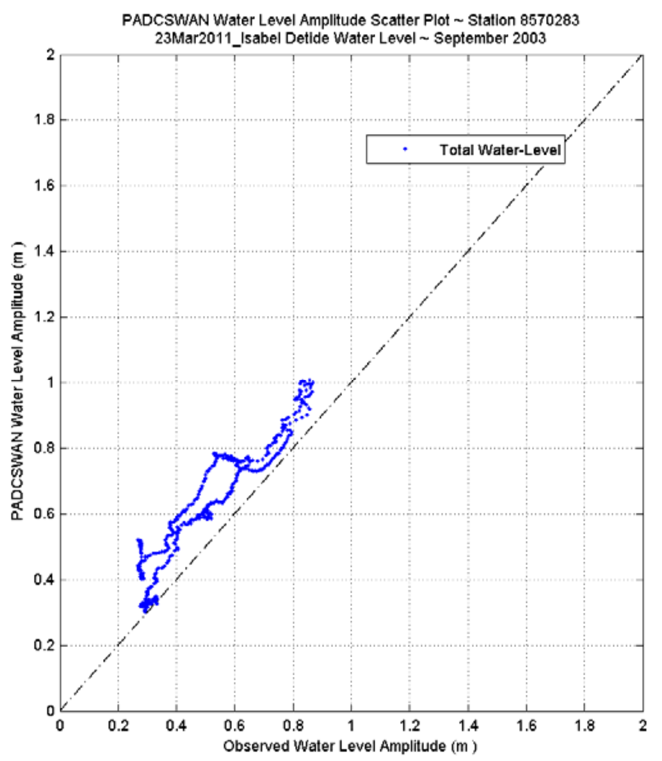

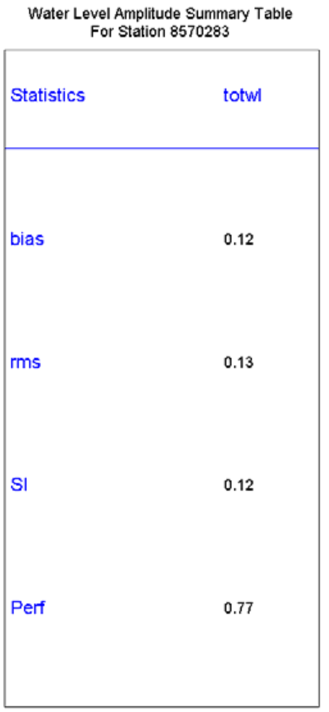
Water Level Amplitude Summary Table
For Station 8570283

Statistics	totwl
bias	0.12
rms	0.13
SI	0.12
Perf	0.77

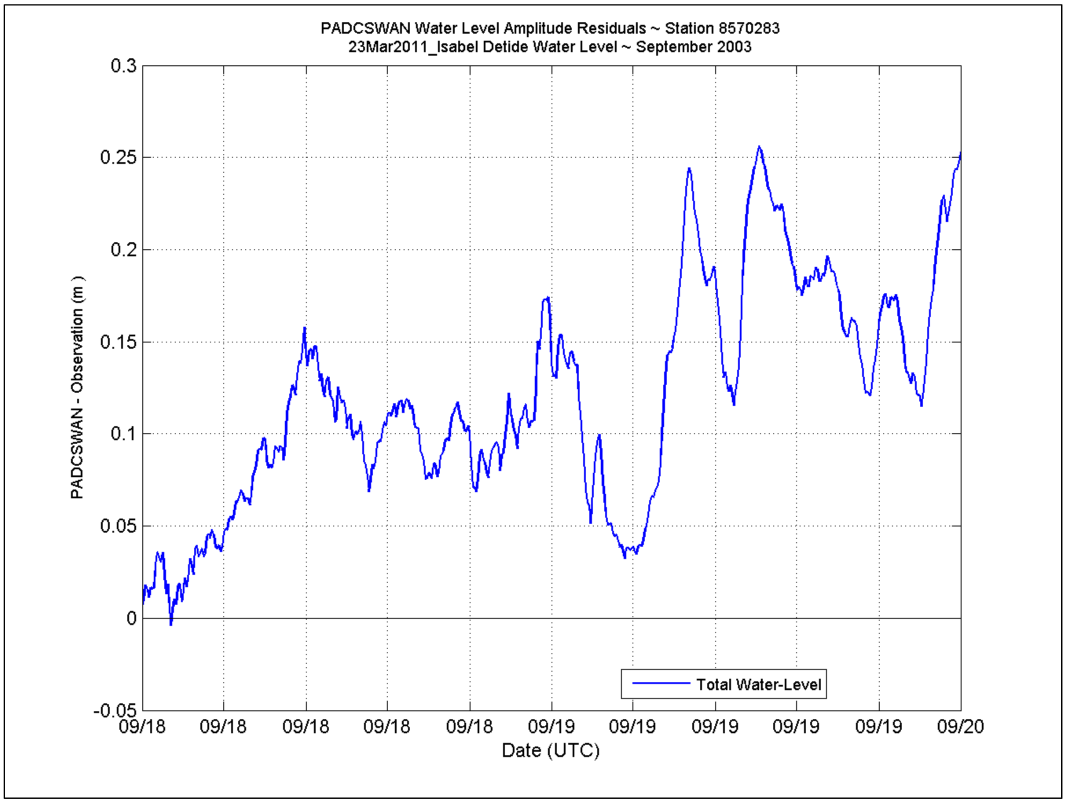
PADCSWAN Water Level Amplitude Residuals ~ Station 8570283
23Mar2011_Isabel Detide Water Level ~ September 2003
PADCSWAN - Observation (m)
0.3
0.25
0.2
0.15
0.1
0.05
0
-0.05
09/18
09/18
09/18
09/18
09/18
09/19
09/19
09/19
09/19
09/19
09/20
Date (UTC)
Total Water-Level

Station 8571892

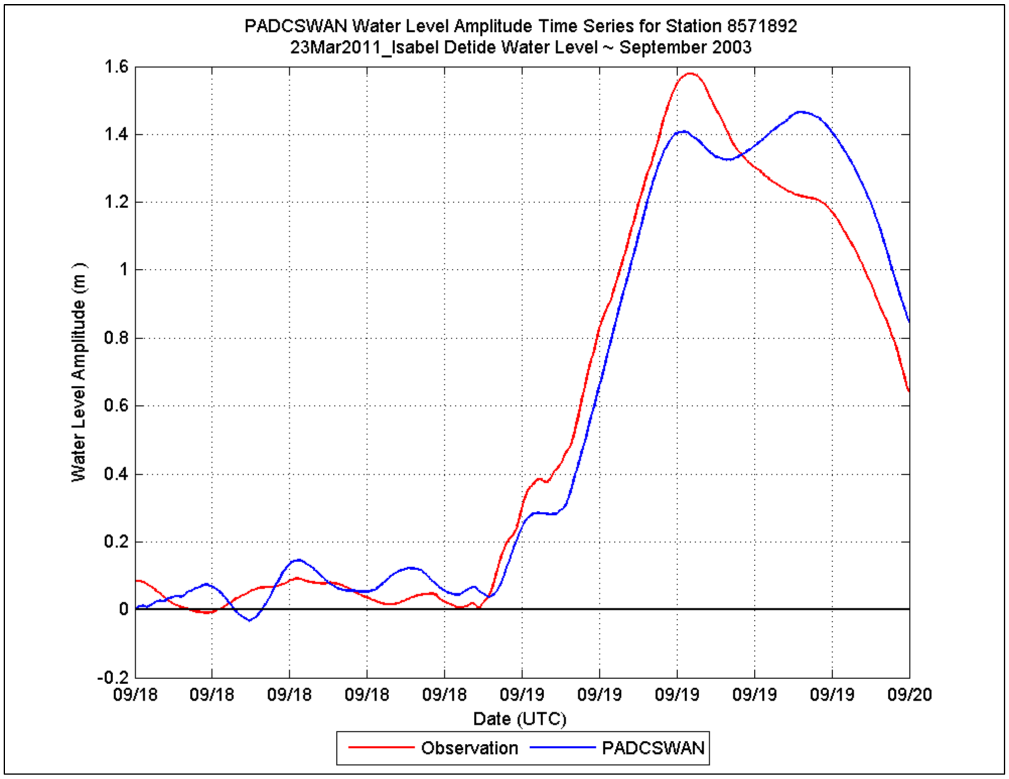

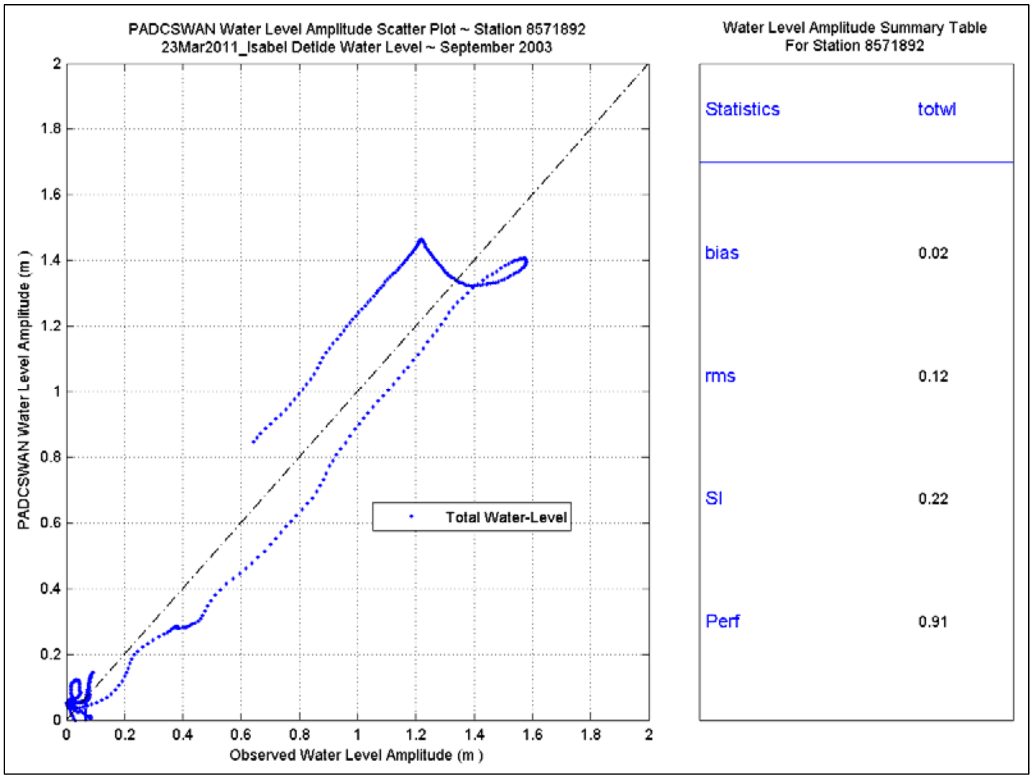

Statistics	totwl
bias	0.02
rms	0.12
SI	0.22
Perf	0.91

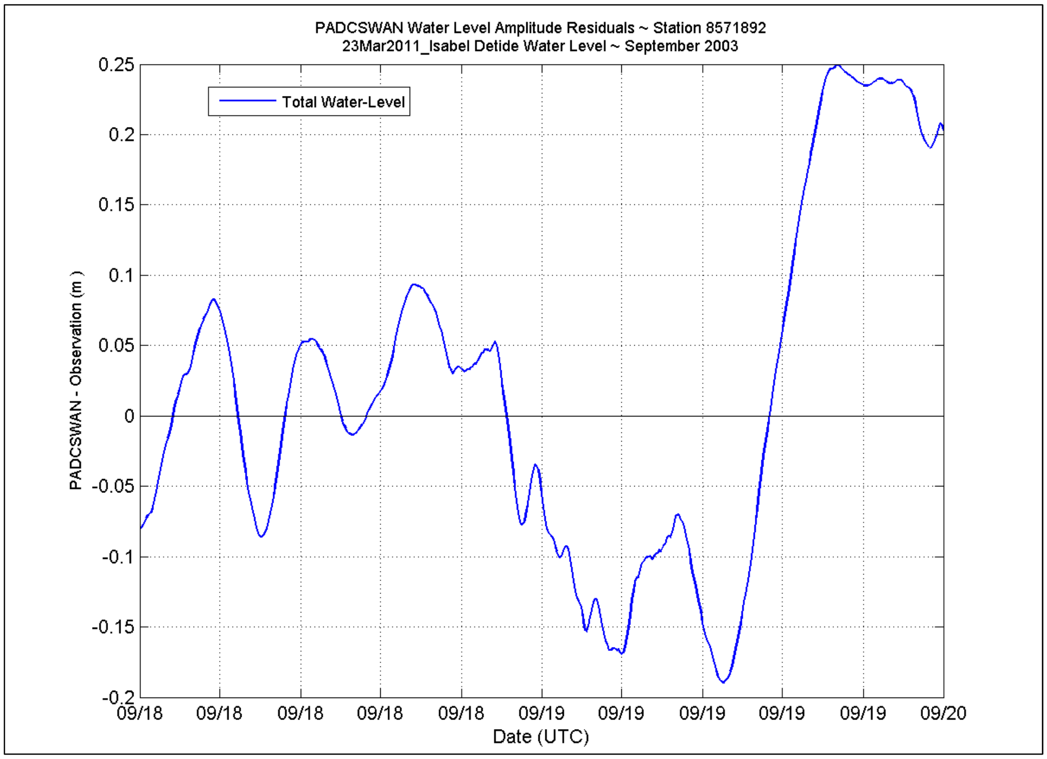
PADCSWAN Water Level Amplitude Residuals ~ Station 8571892
23Mar2011_Isabel Detide Water Level ~ September 2003
Total Water-Level
PADCSWAN - Observation (m)
0.25
0.2
0.15
0.1
0.05
0
-0.05
-0.1
-0.15
-0.2
09/18
09/18
09/18
09/18
09/18
09/19
09/19
09/19
09/19
09/19
09/20
Date (UTC)

Station 8573364

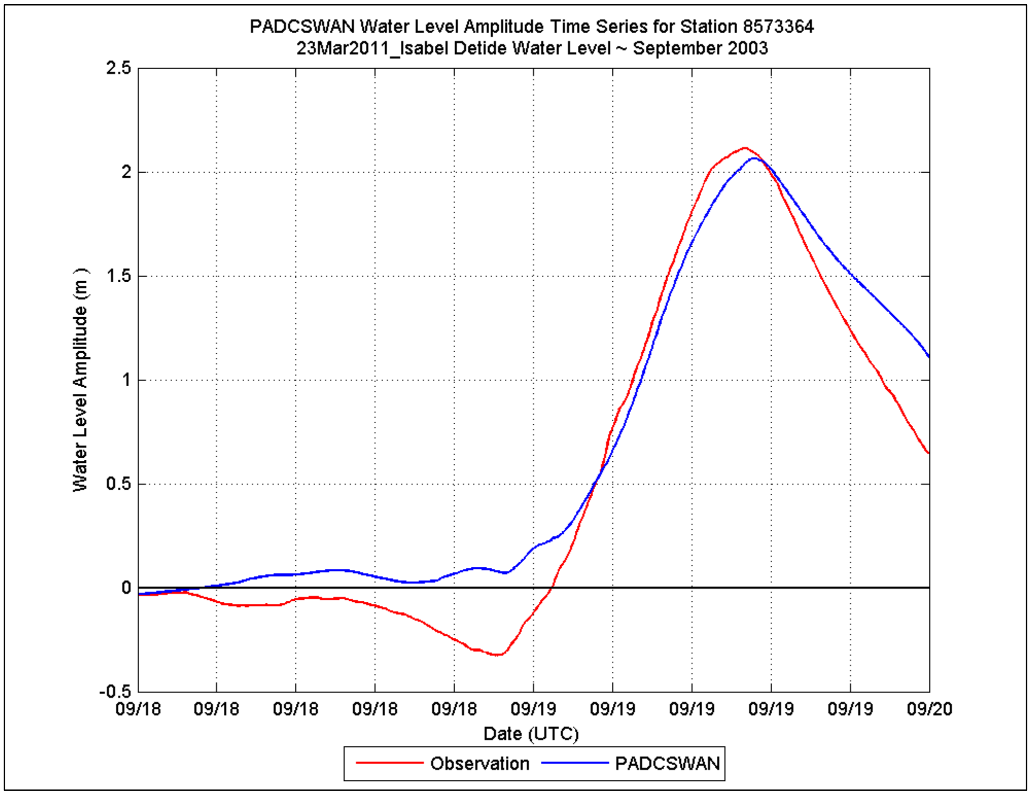

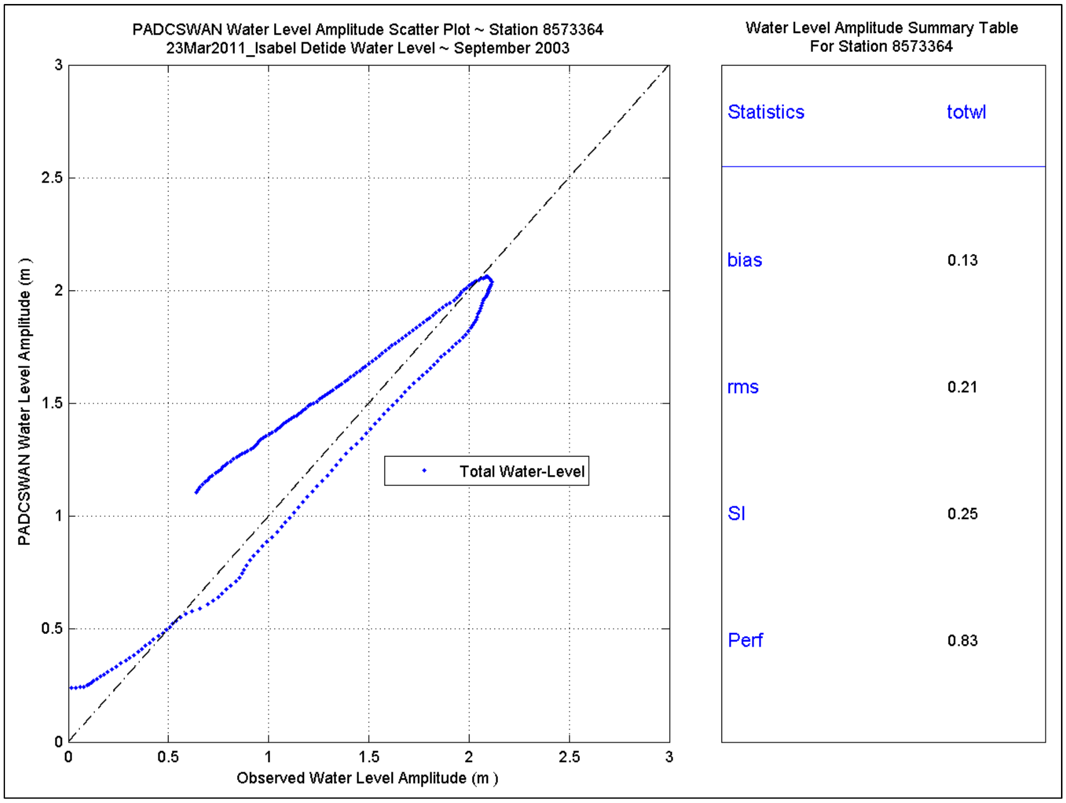

Water Level Amplitude Summary Table
For Station 8573364

Statistics	totwl
bias	0.13
rms	0.21
SI	0.25
Perf	0.83

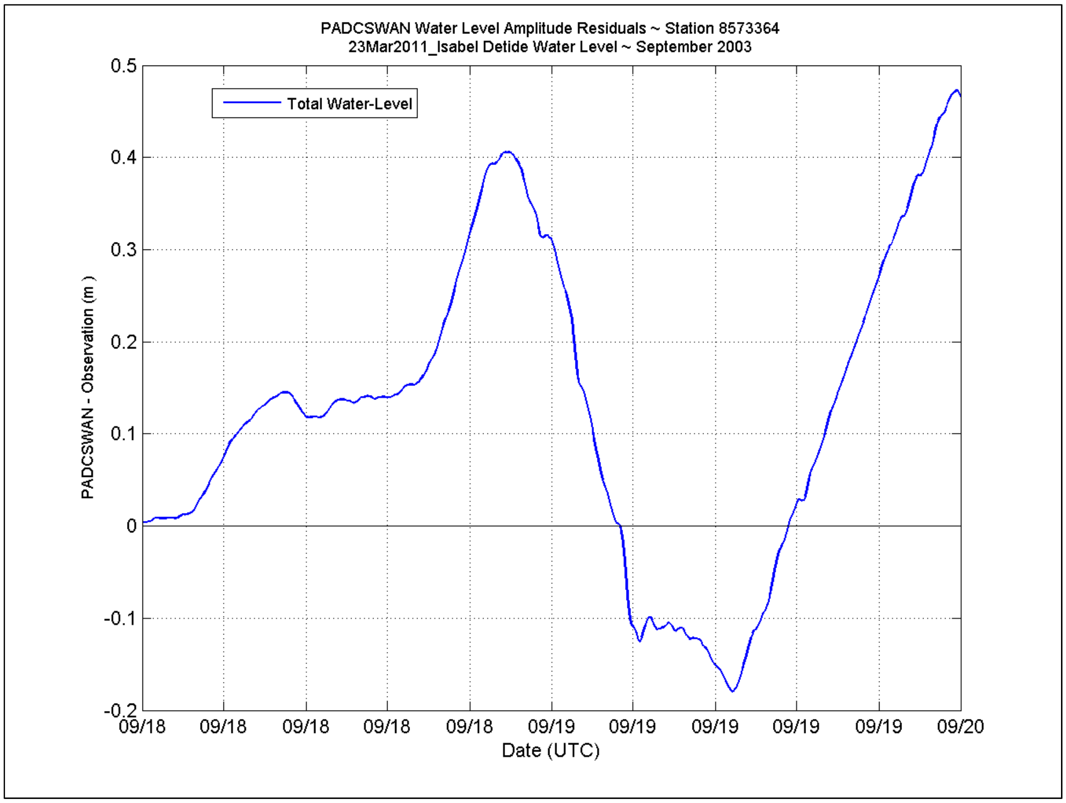
PADCSWAN Water Level Amplitude Residuals ~ Station 8573364
23Mar2011_Isabel Detide Water Level ~ September 2003
Total Water-Level
PADCSWAN - Observation (m)
0.5
0.4
0.3
0.2
0.1
0
-0.1
-0.2
09/18
09/18
09/18
09/18
09/18
09/19
09/19
09/19
09/19
09/19
09/20
Date (UTC)

Station 8574680

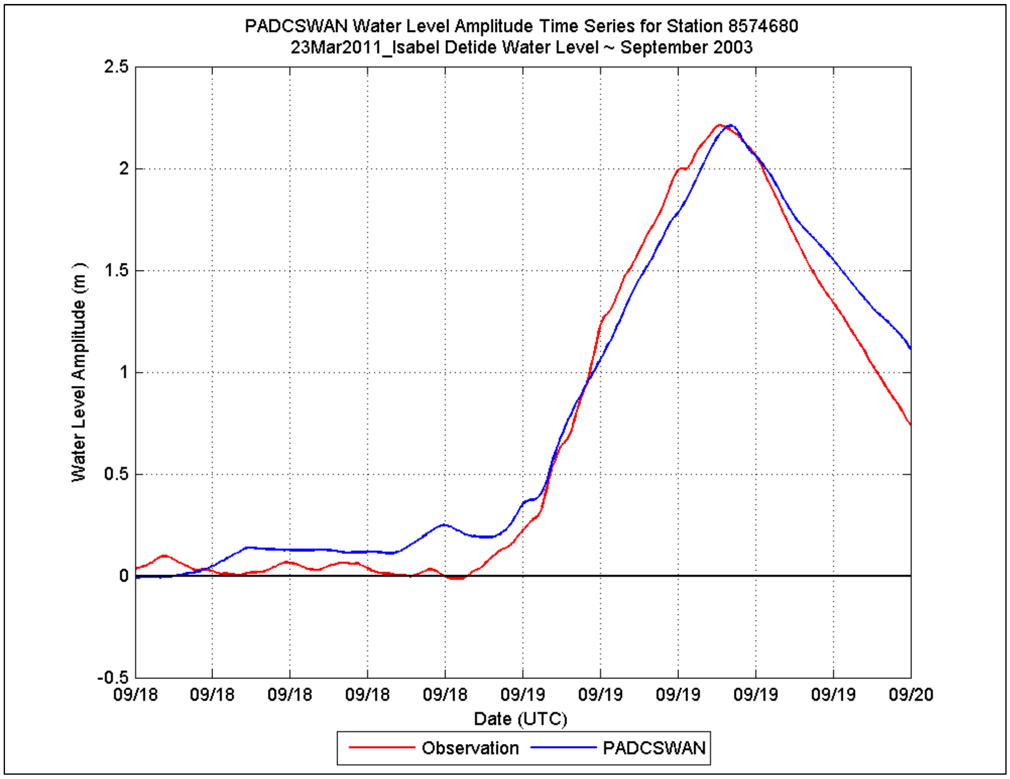

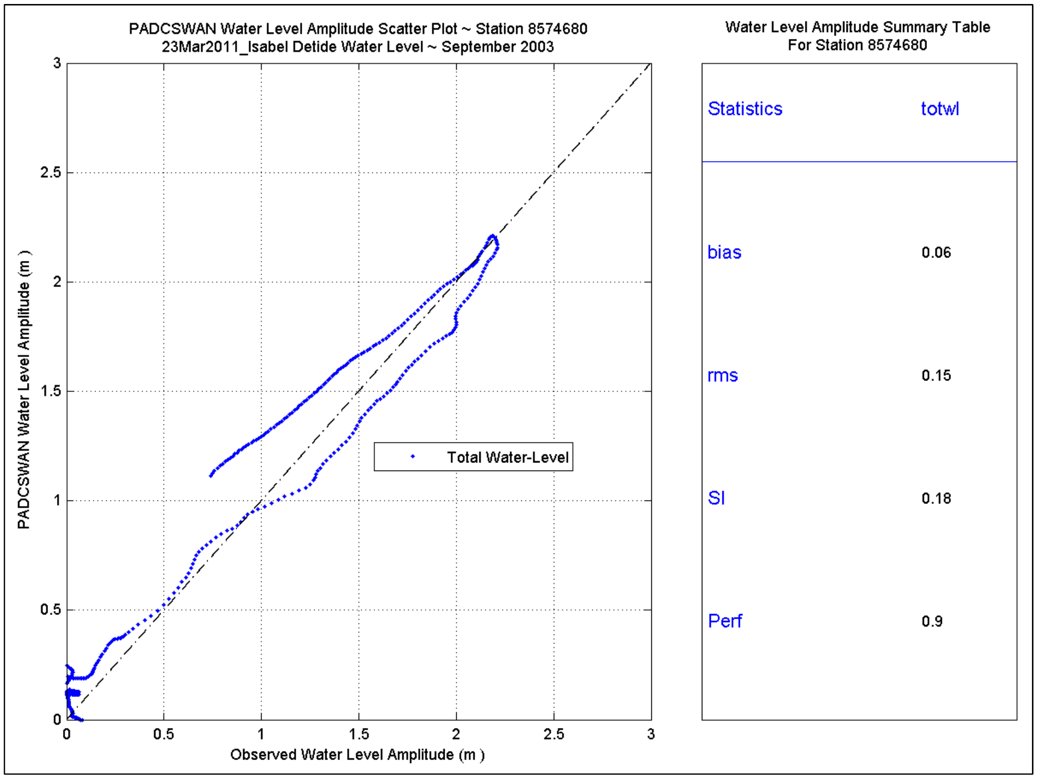

Statistics	totwl
bias	0.06
rms	0.15
SI	0.18
Perf	0.9

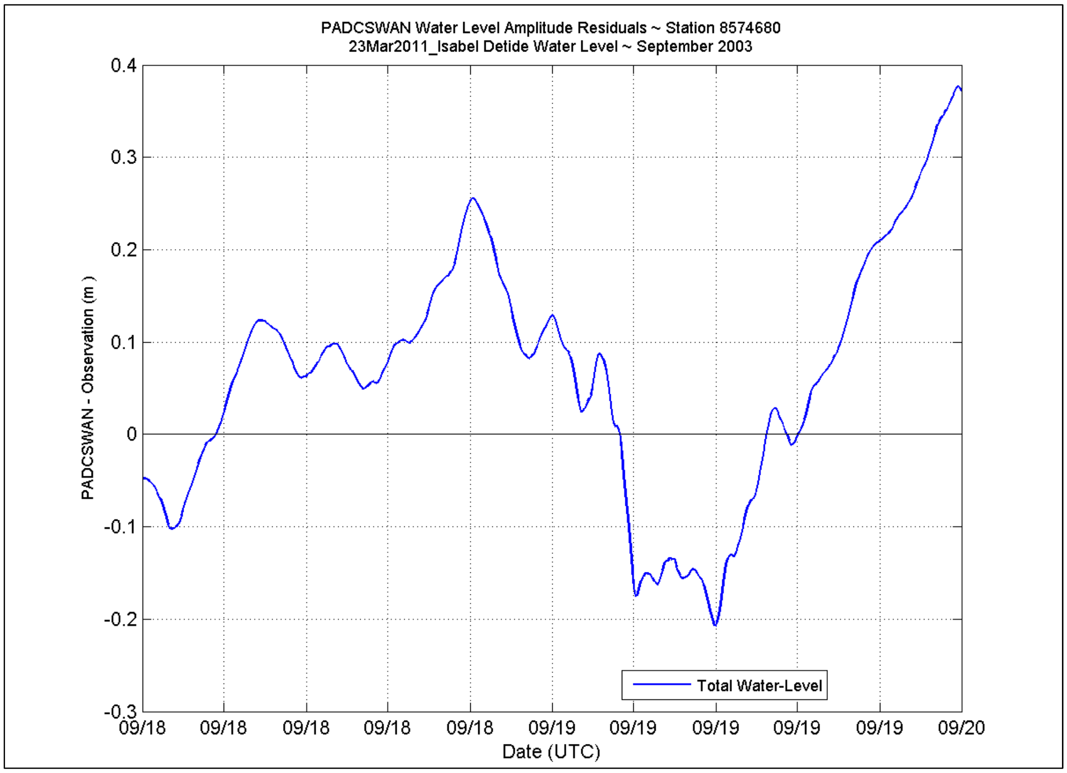
PADCSWAN Water Level Amplitude Residuals ~ Station 8574680
23Mar2011_Isabel Detide Water Level ~ September 2003
PADCSWAN - Observation (m)
0.4
0.3
0.2
0.1
0
-0.1
-0.2
-0.3
09/18
09/18
09/18
09/18
09/18
09/19
09/19
09/19
09/19
09/19
09/20
Date (UTC)
Total Water-Level

Station 8575512

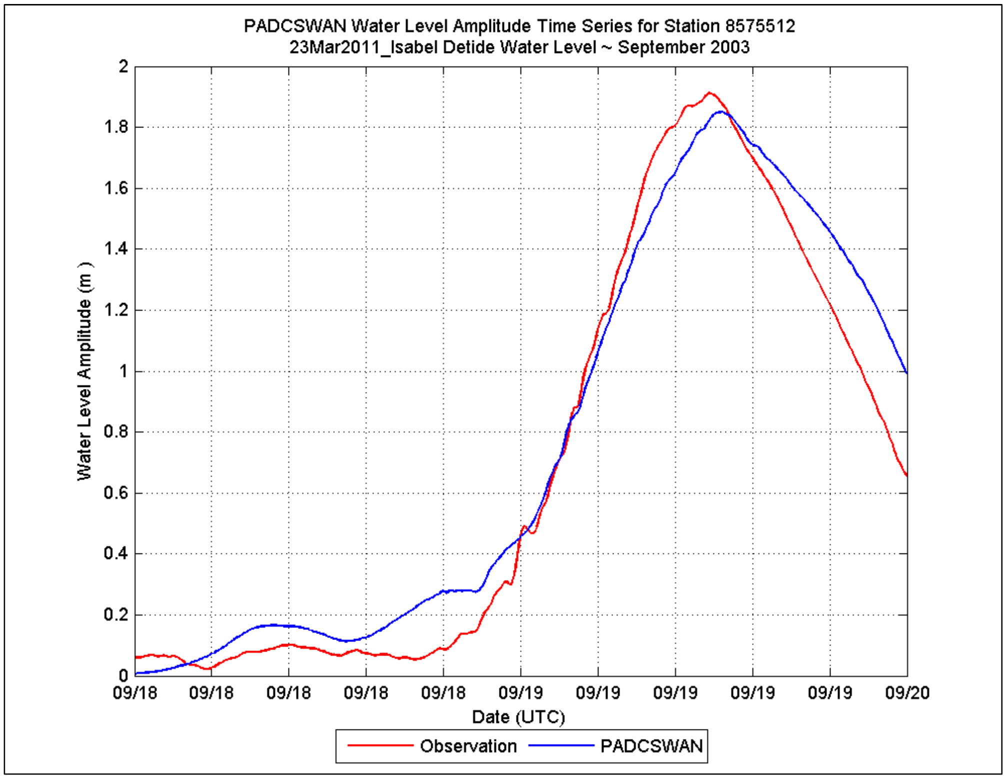

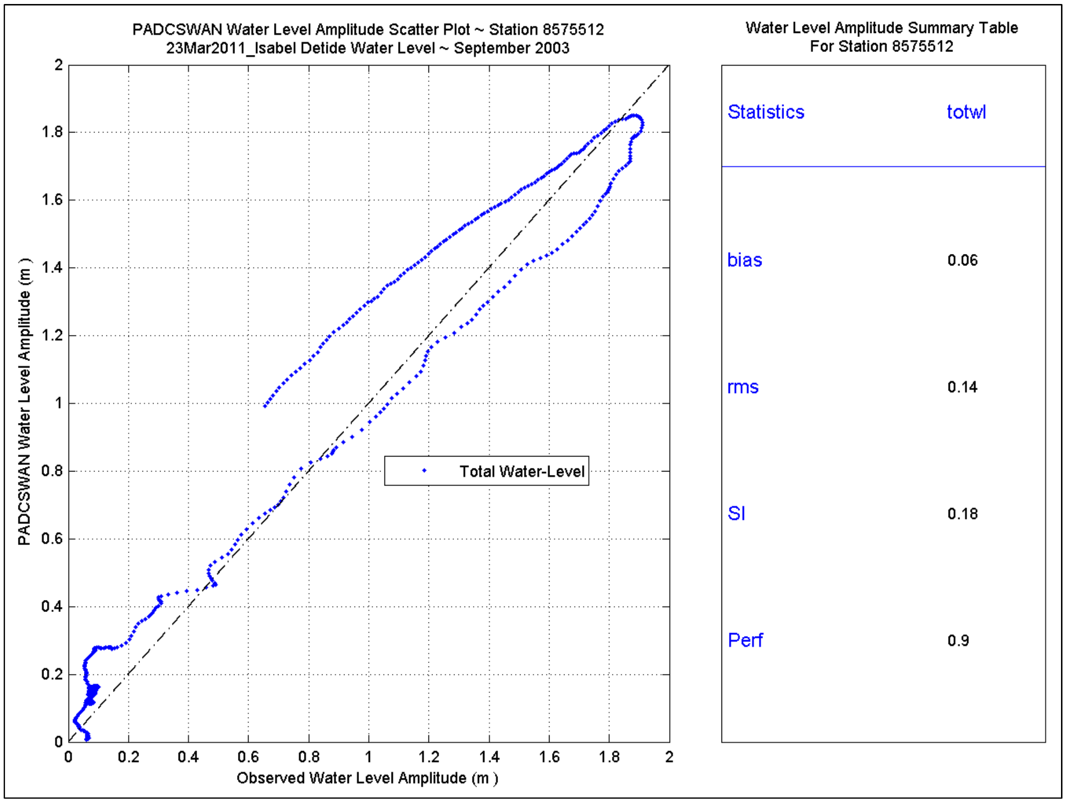

Statistics	totwl
bias	0.06
rms	0.14
SI	0.18
Perf	0.9

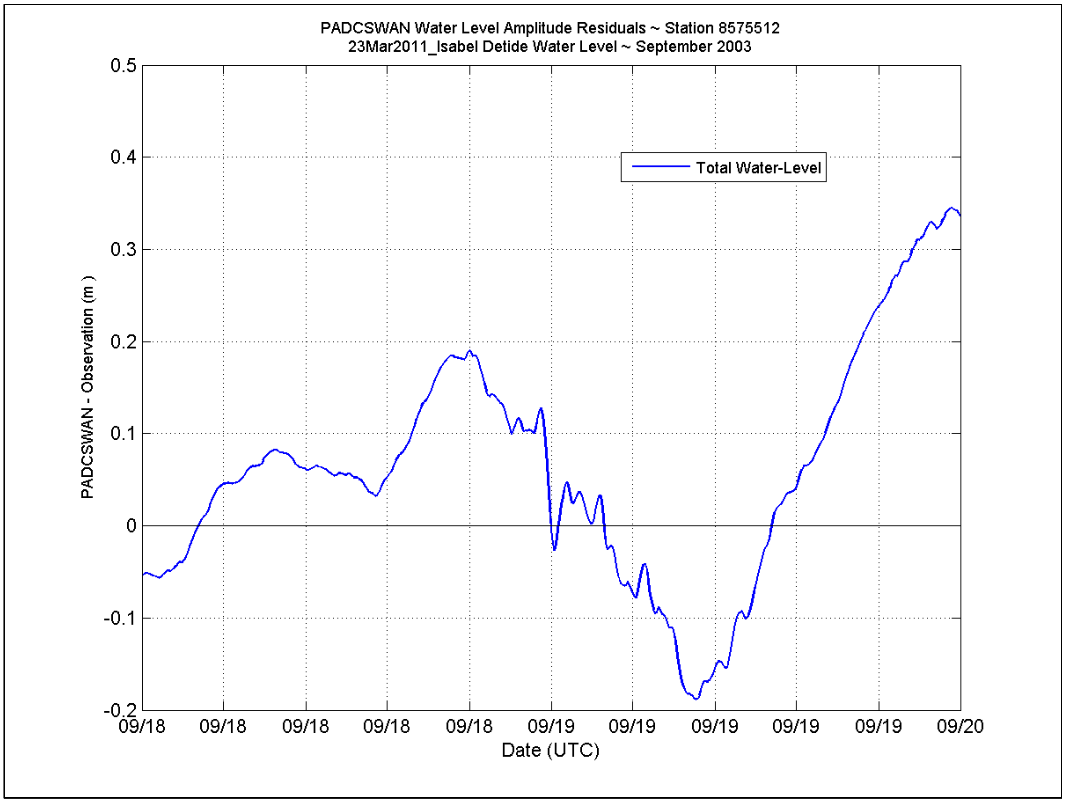
PADCSWAN Water Level Amplitude Residuals ~ Station 8575512
23Mar2011_Isabel Detide Water Level ~ September 2003
Total Water-Level
PADCSWAN - Observation (m)
0.5
0.4
0.3
0.2
0.1
0
-0.1
-0.2
09/18
09/18
09/18
09/18
09/18
09/19
09/19
09/19
09/19
09/19
09/20
Date (UTC)

Station 8577330

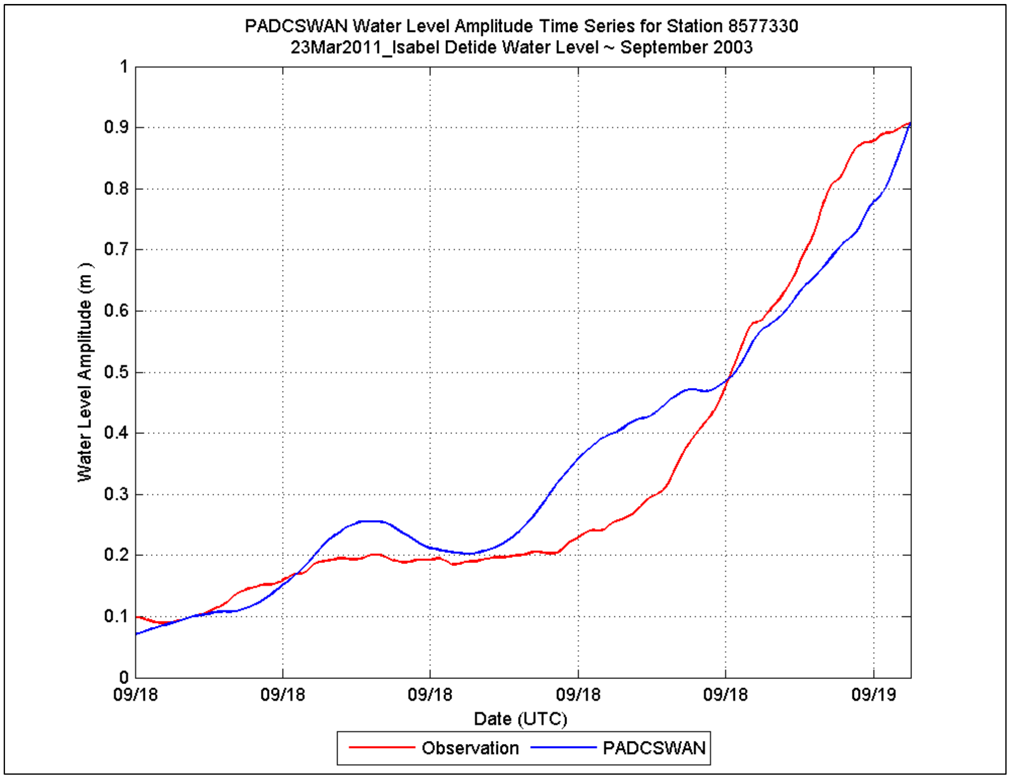

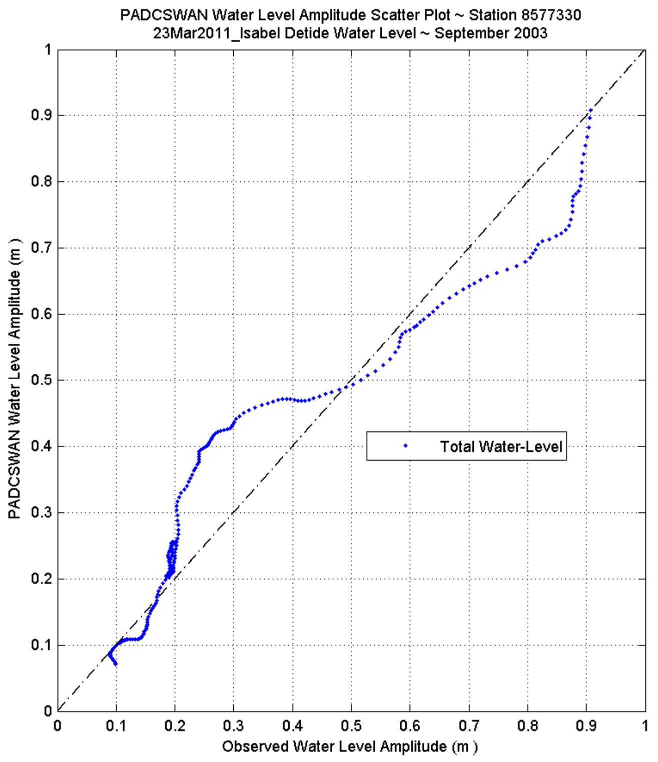

Water Level Amplitude Summary Table
For Station 8577330

Statistics	totwl
bias	0.02
rms	0.07
SI	0.21
Perf	0.89

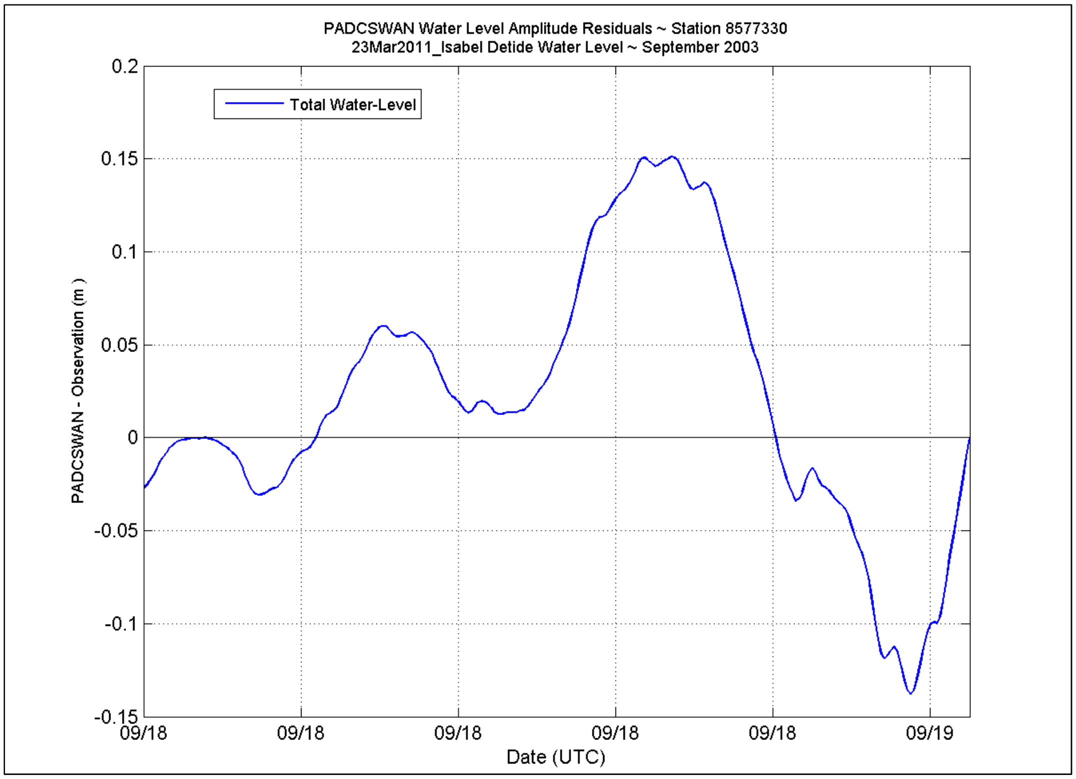
PADCSWAN Water Level Amplitude Residuals ~ Station 8577330
23Mar2011_Isabel Detide Water Level ~ September 2003
Total Water-Level
PADCSWAN - Observation (m)
0.2
0.15
0.1
0.05
0
-0.05
-0.1
-0.15
09/18
09/18
09/18
09/18
09/18
09/19
Date (UTC)

Station 8632200

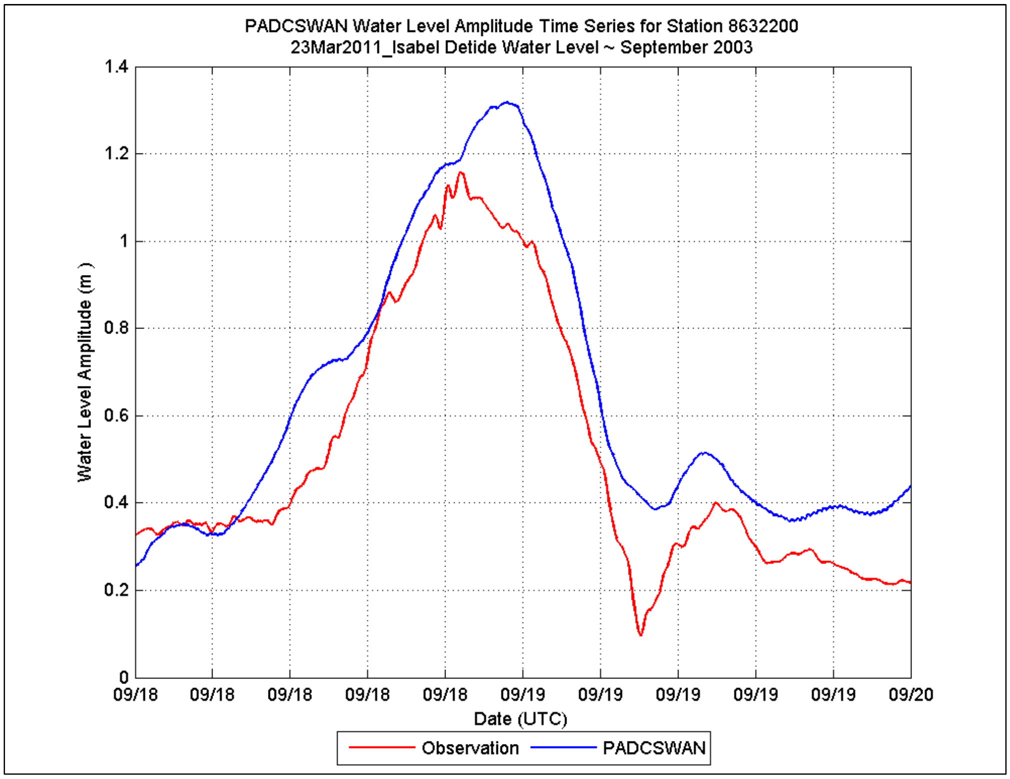

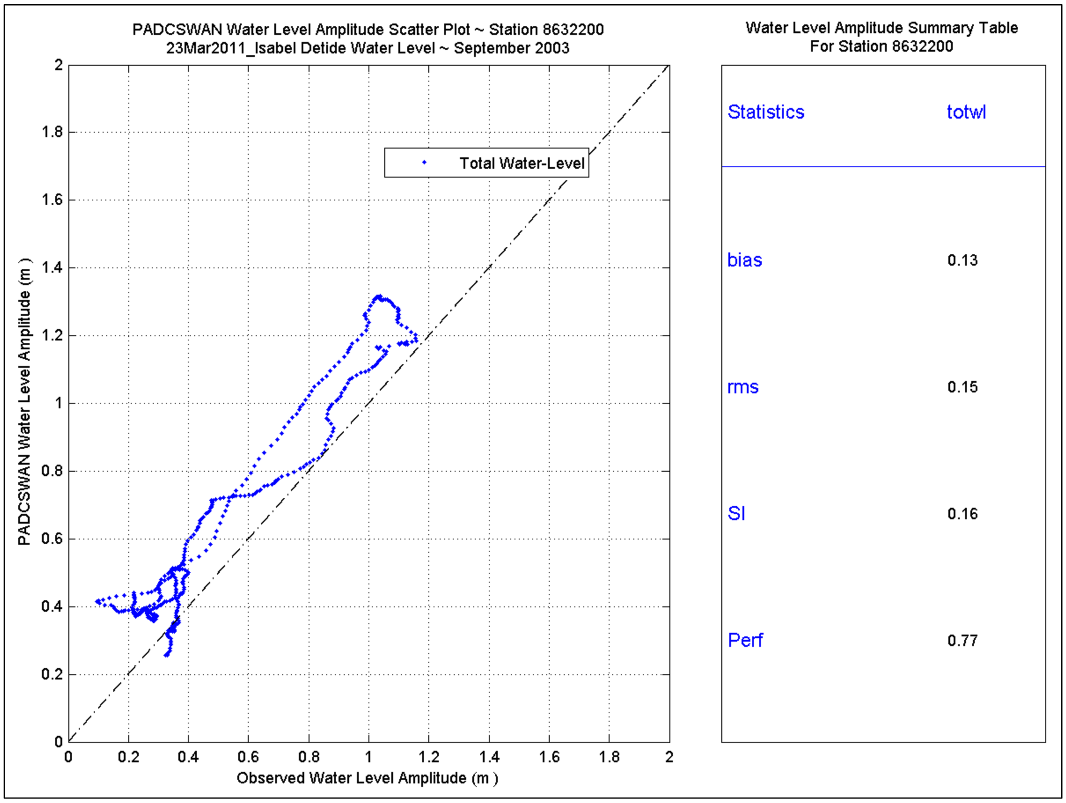

Water Level Amplitude Summary Table
For Station 8632200

Statistics	totwl
bias	0.13
rms	0.15
SI	0.16
Perf	0.77

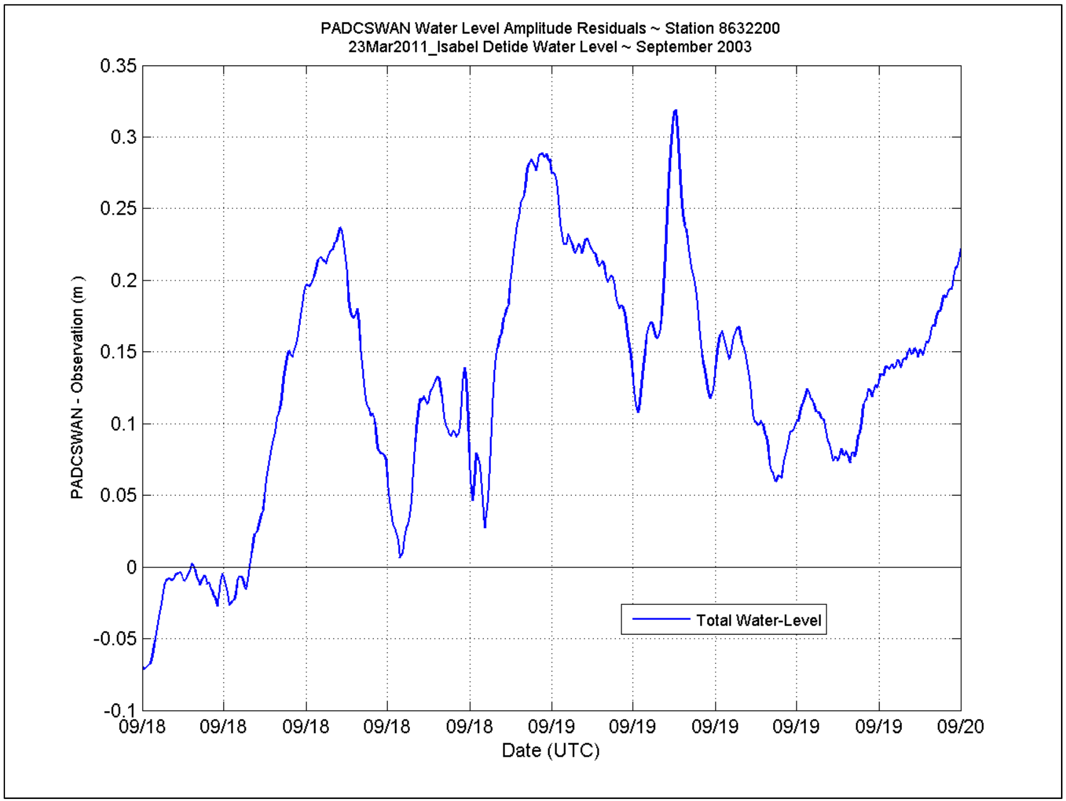
PADCSWAN Water Level Amplitude Residuals ~ Station 8632200
23Mar2011_Isabel Detide Water Level ~ September 2003
PADCSWAN - Observation (m)
0.35
0.3
0.25
0.2
0.15
0.1
0.05
0
-0.05
-0.1
09/18
09/18
09/18
09/18
09/18
09/19
09/19
09/19
09/19
09/19
09/20
Date (UTC)
Total Water-Level

Station 8635750

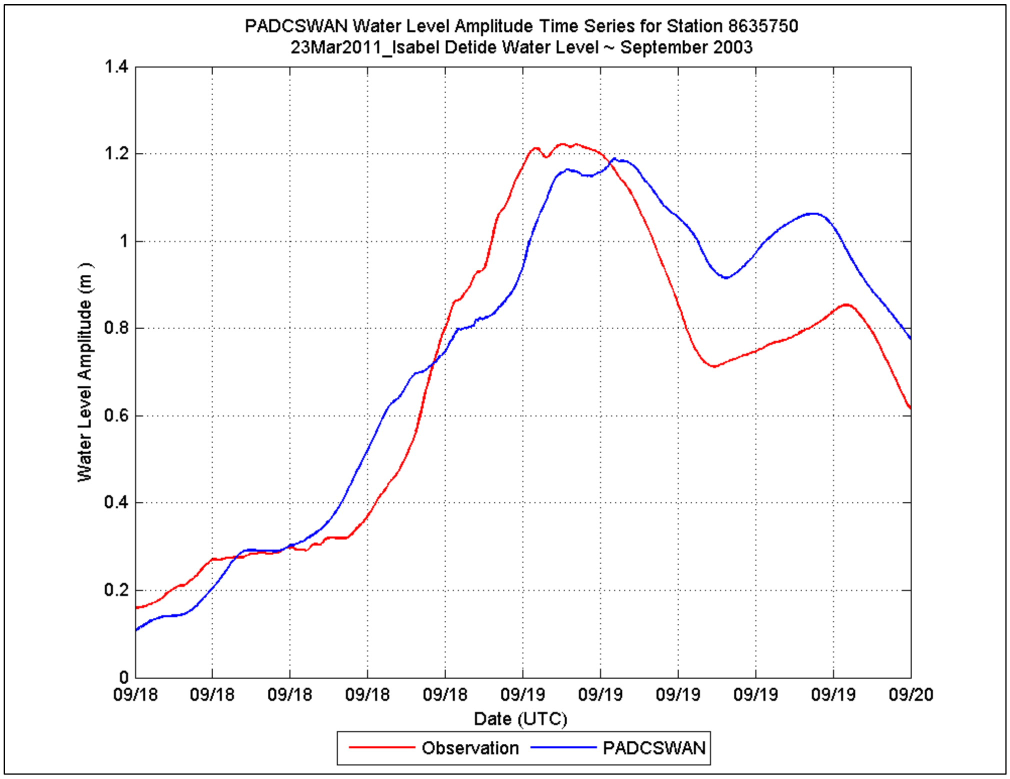

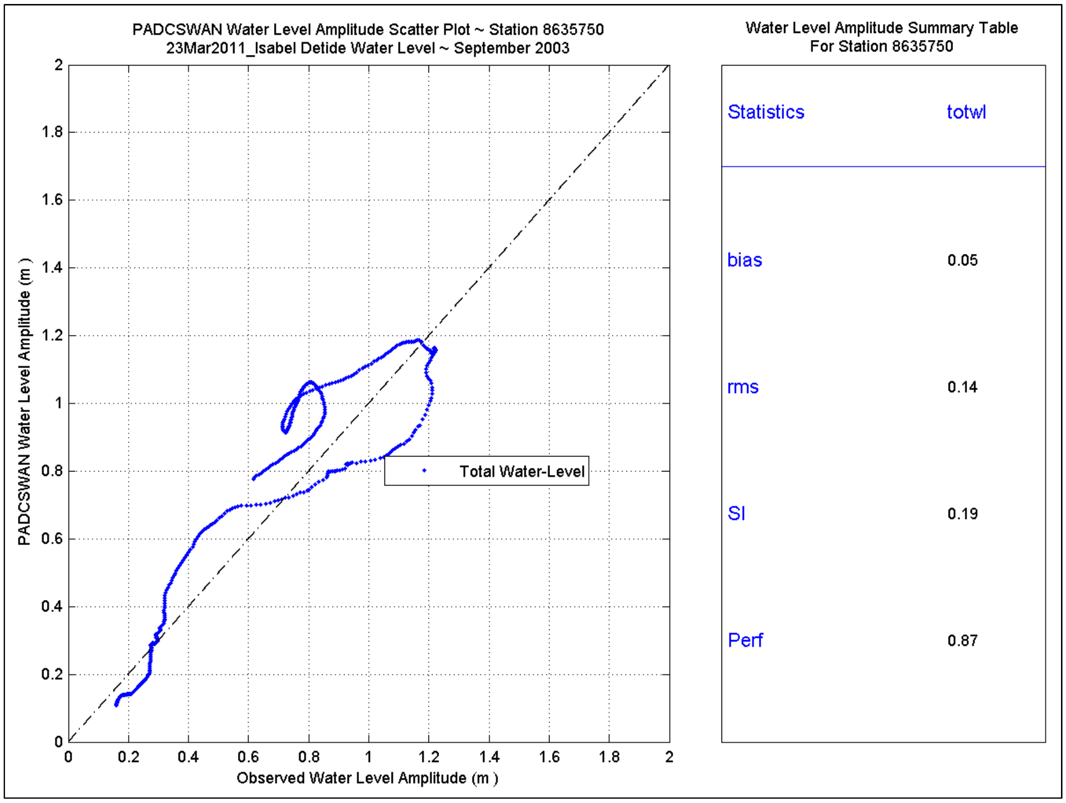

Water Level Amplitude Summary Table
For Station 8635750

Statistics	totwl
bias	0.05
rms	0.14
SI	0.19
Perf	0.87

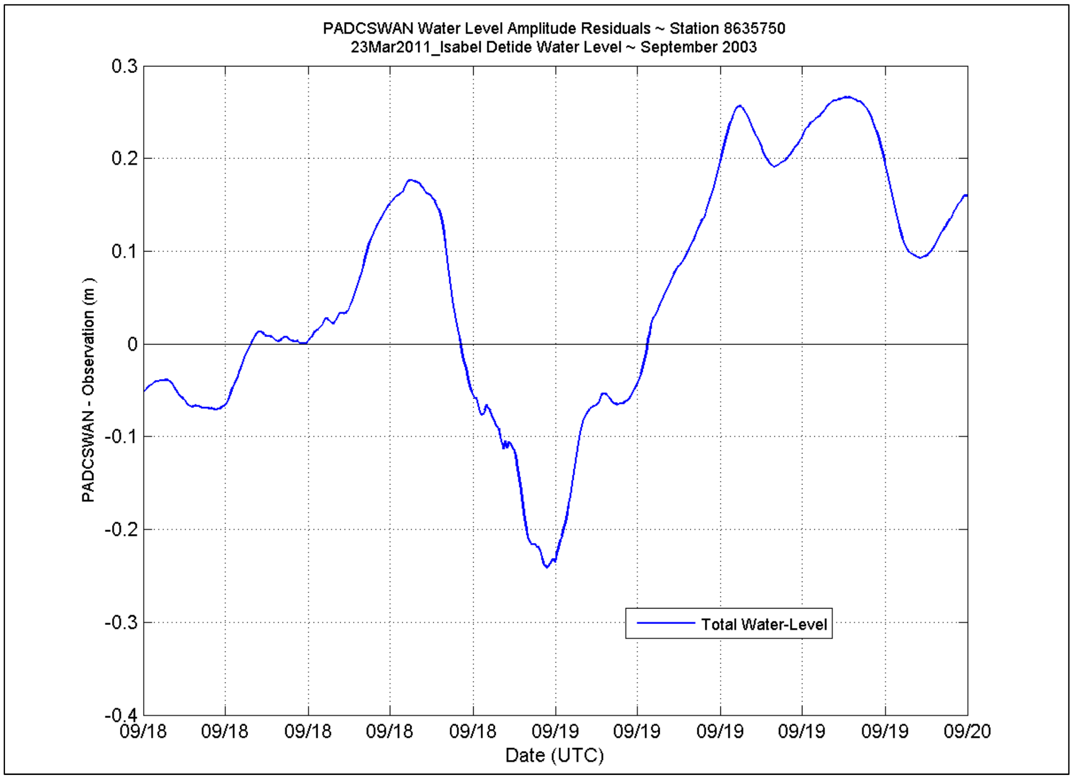
PADCSWAN Water Level Amplitude Residuals ~ Station 8635750
23Mar2011_Isabel Detide Water Level ~ September 2003
PADCSWAN - Observation (m)
0.3
0.2
0.1
0
-0.1
-0.2
-0.3
-0.4
09/18
09/18
09/18
09/18
09/18
09/19
09/19
09/19
09/19
09/19
09/20
Date (UTC)
Total Water-Level

Station 8638610

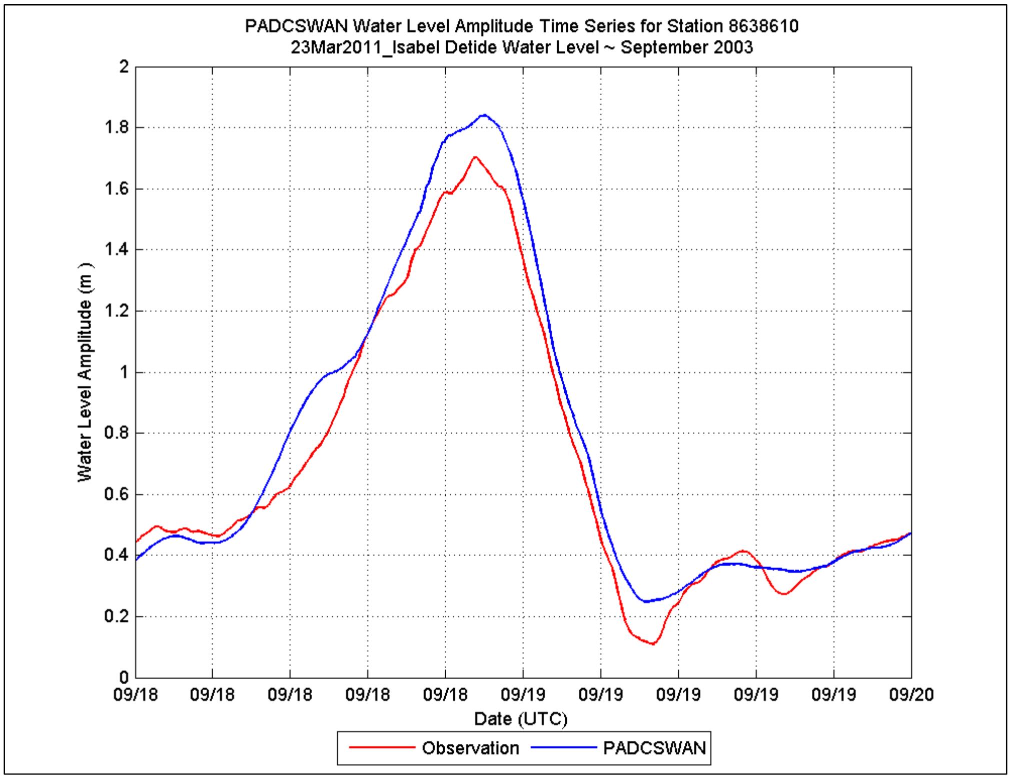

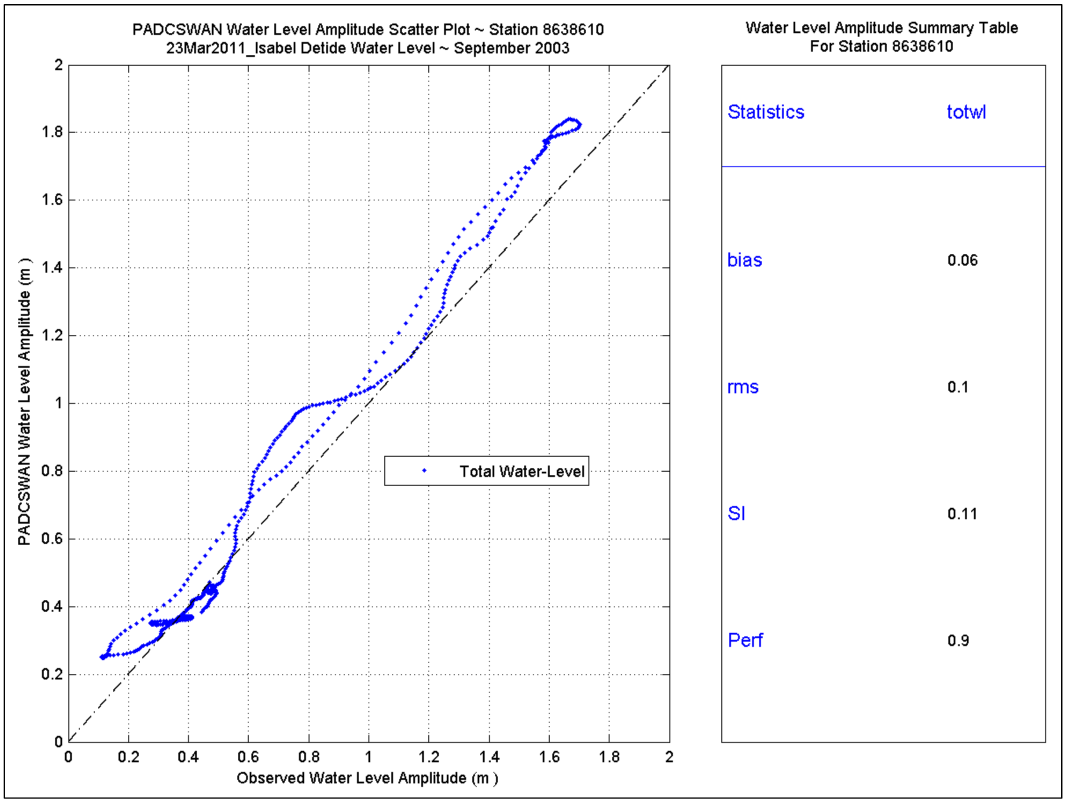

Water Level Amplitude Summary Table
For Station 8638610

Statistics	totwl
bias	0.06
rms	0.1
SI	0.11
Perf	0.9

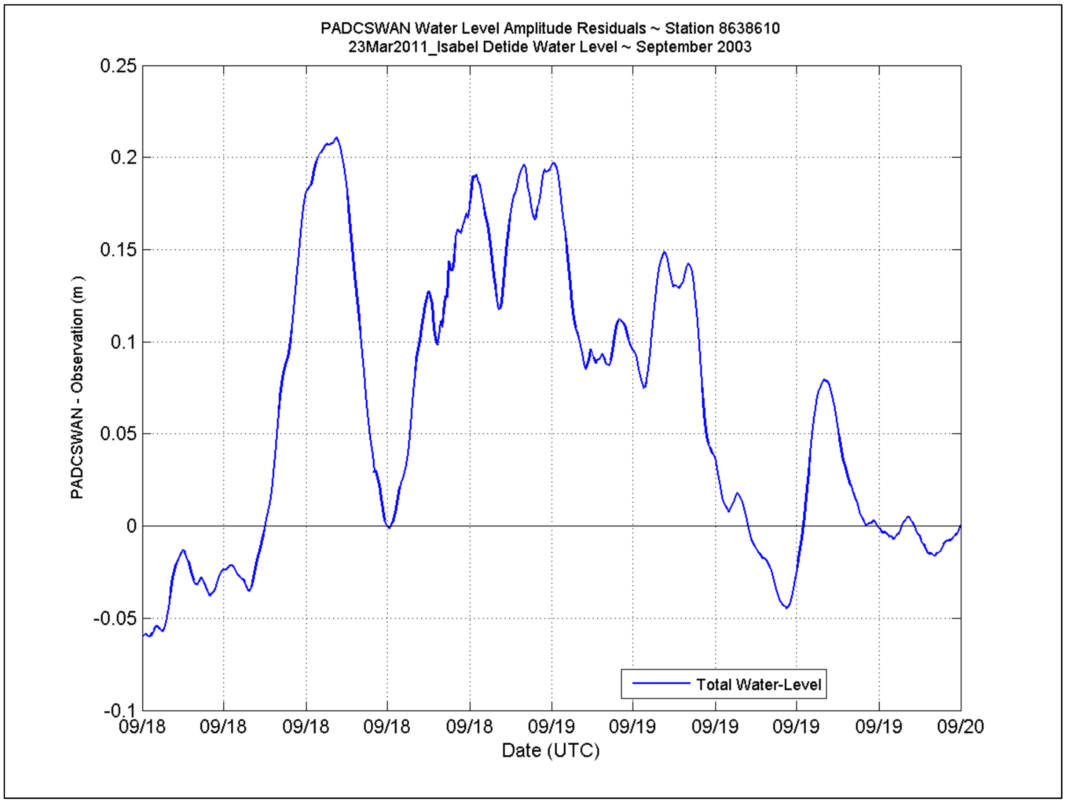
PADCSWAN Water Level Amplitude Residuals ~ Station 8638610
23Mar2011_Isabel Detide Water Level ~ September 2003
PADCSWAN - Observation (m)
0.25
0.2
0.15
0.1
0.05
0
-0.05
-0.1
09/18
09/18
09/18
09/18
09/18
09/19
09/19
09/19
09/19
09/19
09/20
Date (UTC)
Total Water-Level

Station 8639348

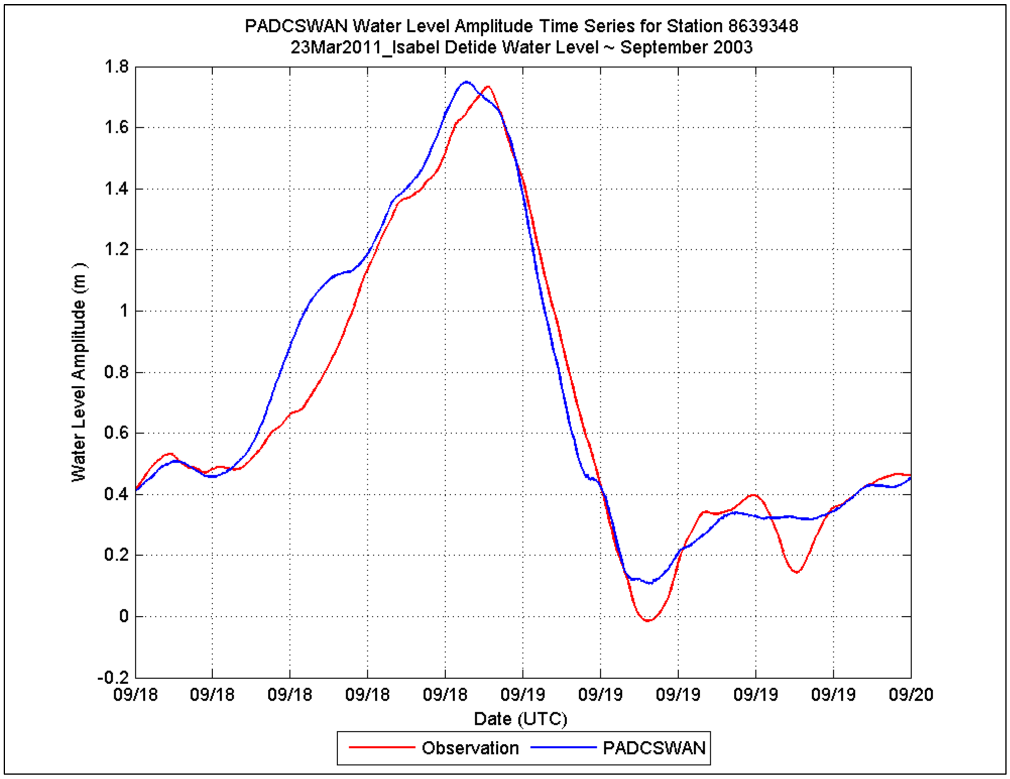

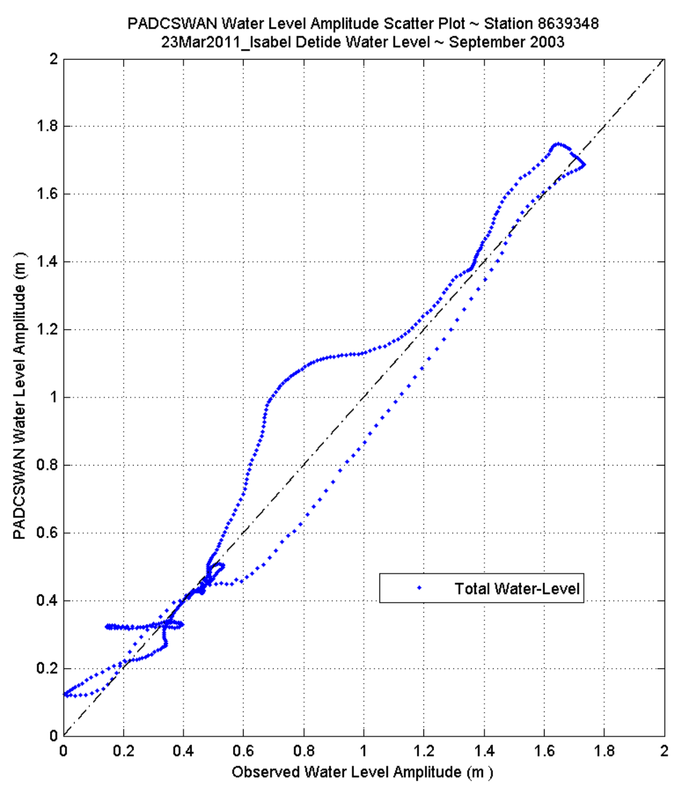

Water Level Amplitude Summary Table
For Station 8639348

Statistics	totwl
bias	0.03
rms	0.11
SI	0.15
Perf	0.92

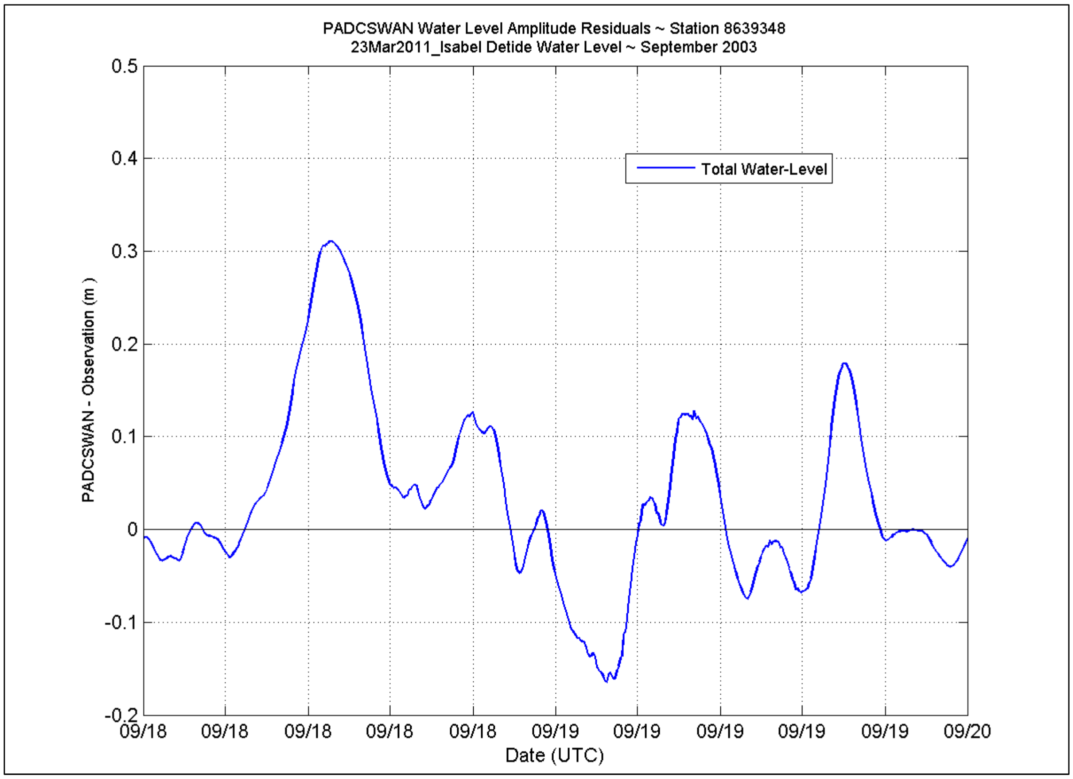
PADCSWAN Water Level Amplitude Residuals ~ Station 8639348
23Mar2011_Isabel Detide Water Level ~ September 2003
Total Water-Level
PADCSWAN - Observation (m)
0.5
0.4
0.3
0.2
0.1
0
-0.1
-0.2
09/18
09/18
09/18
09/18
09/18
09/19
09/19
09/19
09/19
09/19
09/20
Date (UTC)

Appendix B: Detided TidesSugeWaves Water Level Data, Hurricane Ernesto

Data plots in this section refer to the PADCSWAN Detided TidesWindsWaves water level for Hurricane Ernesto, August-September 2006.

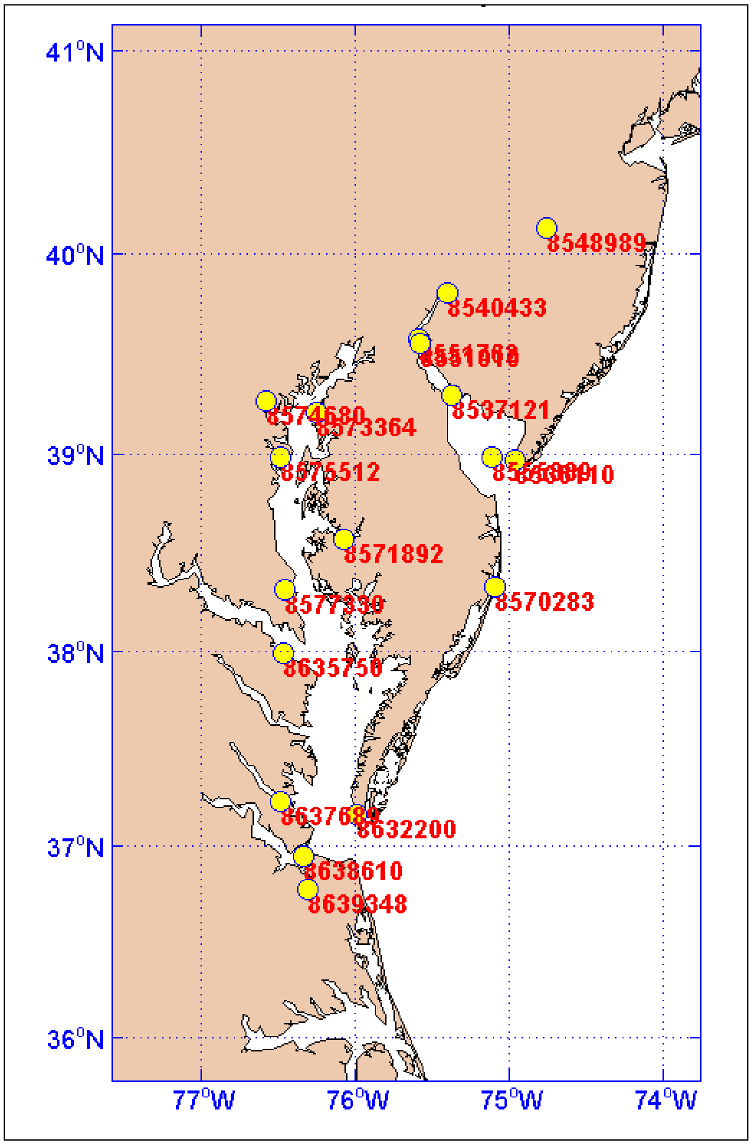
41°N
40°N
39°N
38°N
37°N
36°N
77°W
76°W
75°W
74°W
8548989
8540433
8537121
8574680
8573364
8575512
8571892
8570283
8577330
8635750
8637689
8632200
8638610
8639348

Figure B1. NOAA water level station locations for Detided TidesWindsWaves, Ernesto.

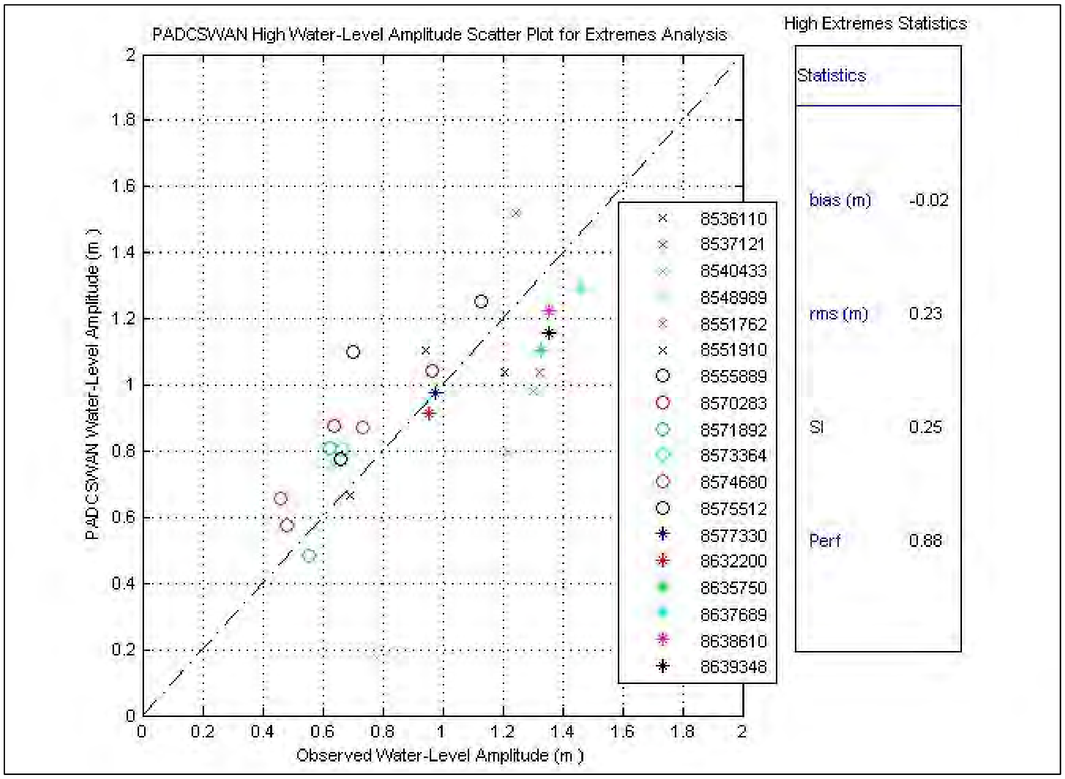

Figure B2. High-water level extremes analysis, Detided TidesWindsWaves, Ernesto.

Station 8536110

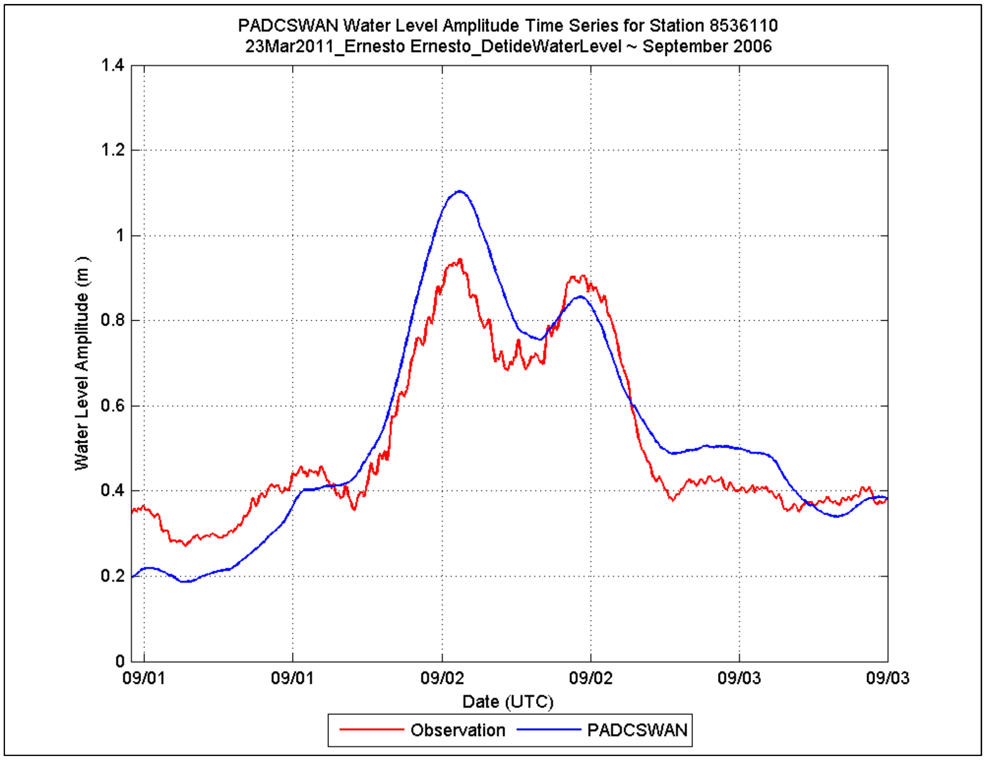

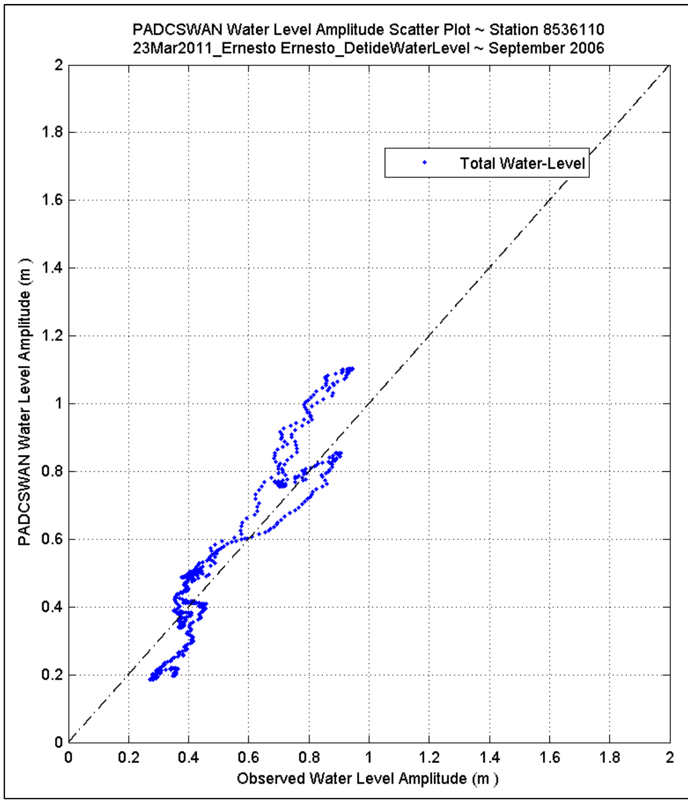

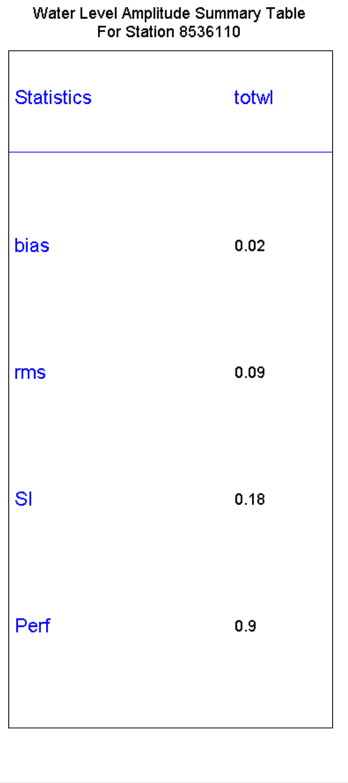
Water Level Amplitude Summary Table
For Station 8536110

Statistics	totwl
bias	0.02
rms	0.09
SI	0.18
Perf	0.9

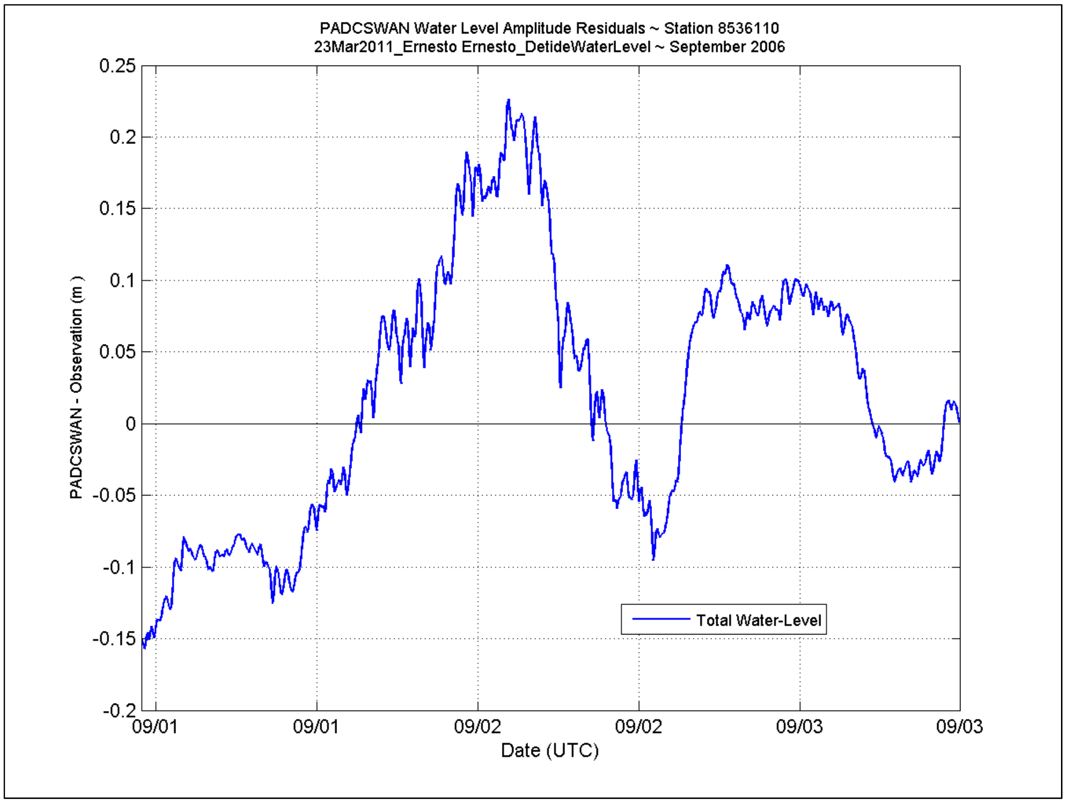
PADCSWAN Water Level Amplitude Residuals ~ Station 8536110
23Mar2011_Ernesto Ernesto_DetideWaterLevel ~ September 2006
PADCSWAN - Observation (m)
0.25
0.2
0.15
0.1
0.05
0
-0.05
-0.1
-0.15
-0.2
09/01
09/01
09/02
09/02
09/03
09/03
Date (UTC)
Total Water-Level

Station 8537121

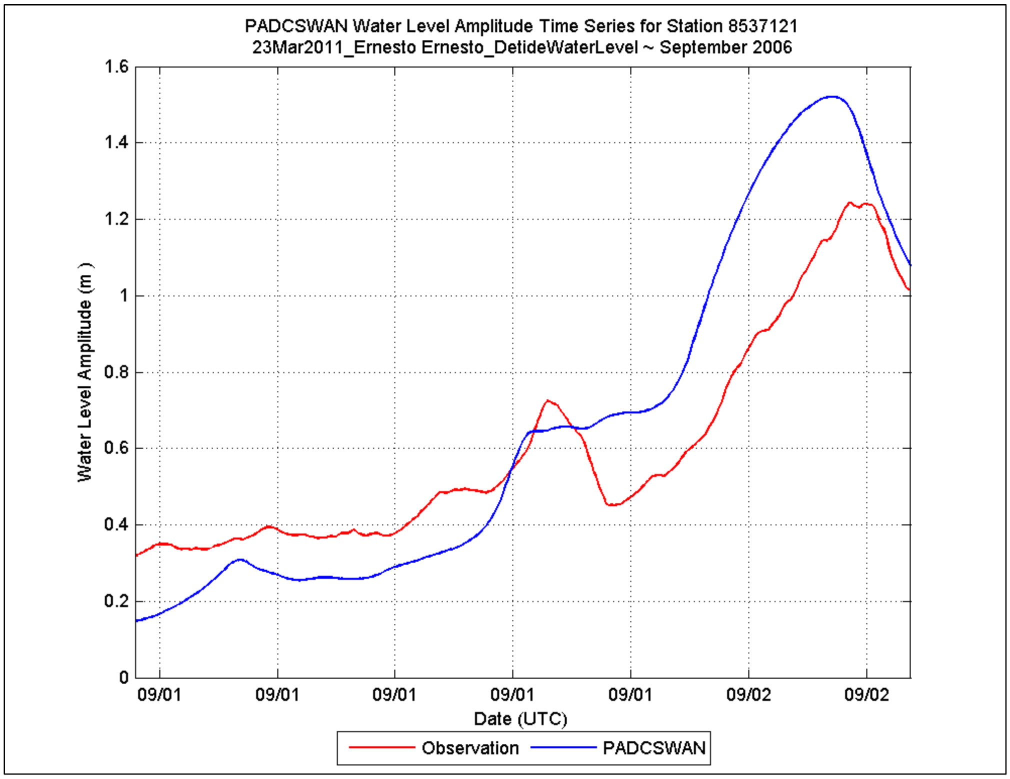

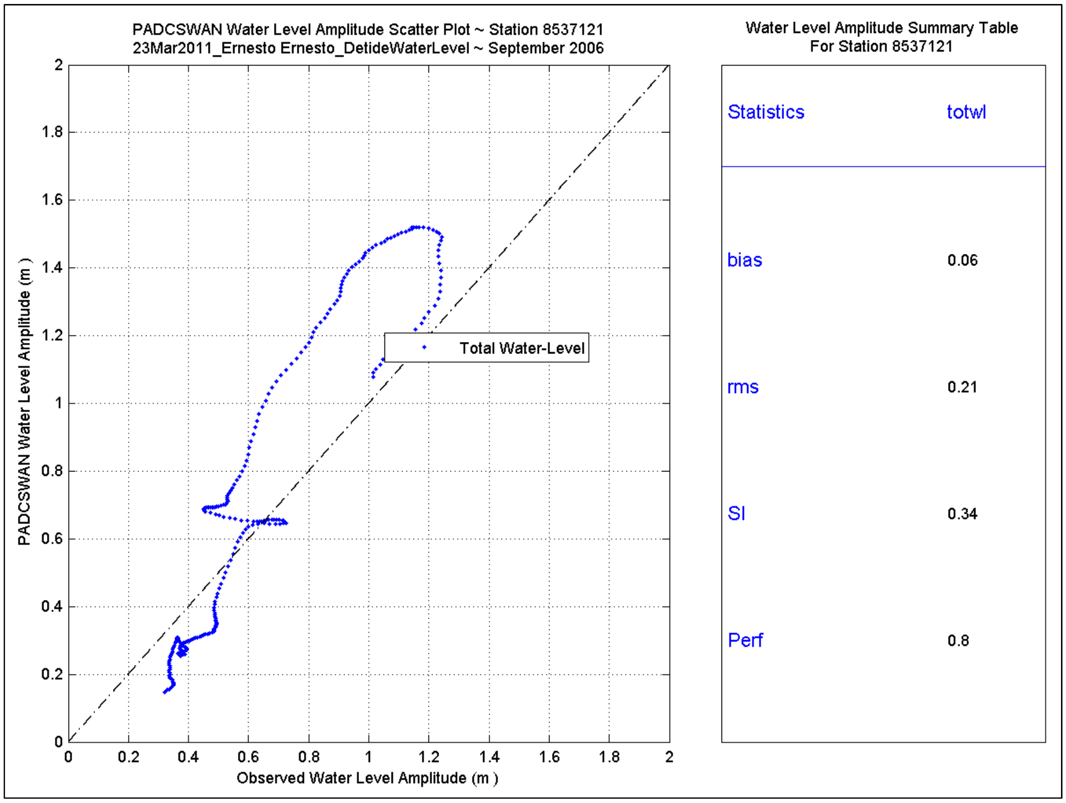

Water Level Amplitude Summary Table
For Station 8537121

Statistics	totwl
bias	0.06
rms	0.21
SI	0.34
Perf	0.8

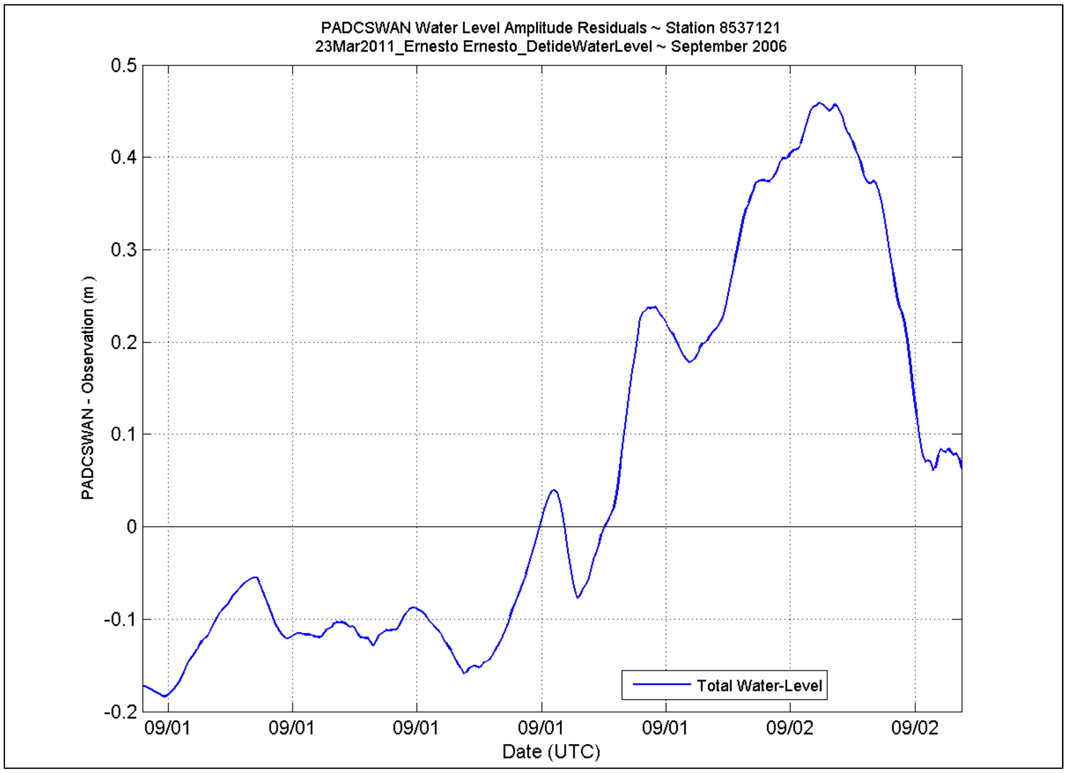
PADCSWAN Water Level Amplitude Residuals ~ Station 8537121
23Mar2011_Ernesto Ernesto_DetideWaterLevel ~ September 2006
PADCSWAN - Observation (m)
0.5
0.4
0.3
0.2
0.1
0
-0.1
-0.2
09/01
09/01
09/01
09/01
09/01
09/02
09/02
Date (UTC)
Total Water-Level

Station 8540433

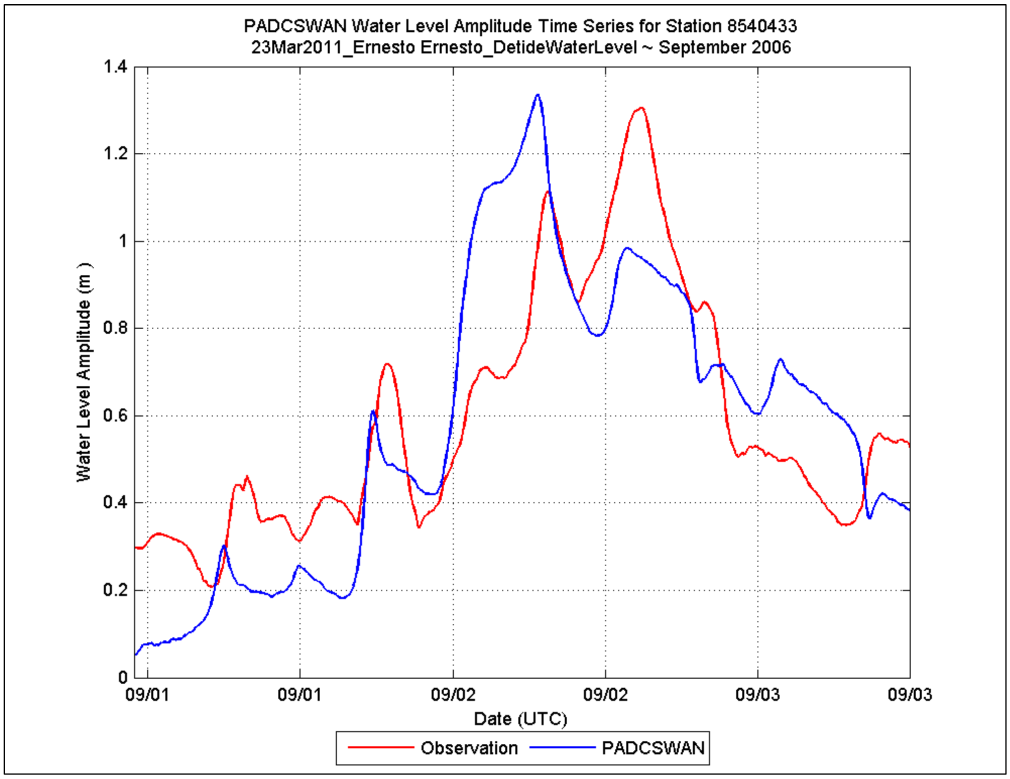

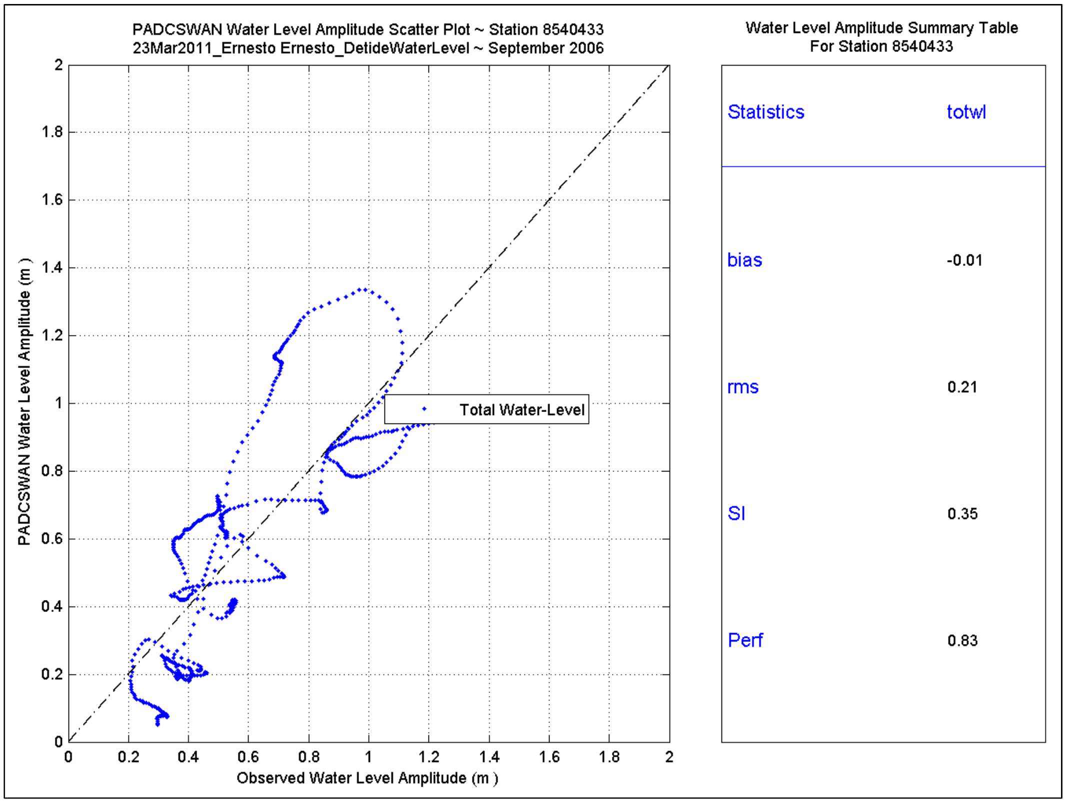

Water Level Amplitude Summary Table
For Station 8540433

Statistics	totwl
bias	-0.01
rms	0.21
SI	0.35
Perf	0.83

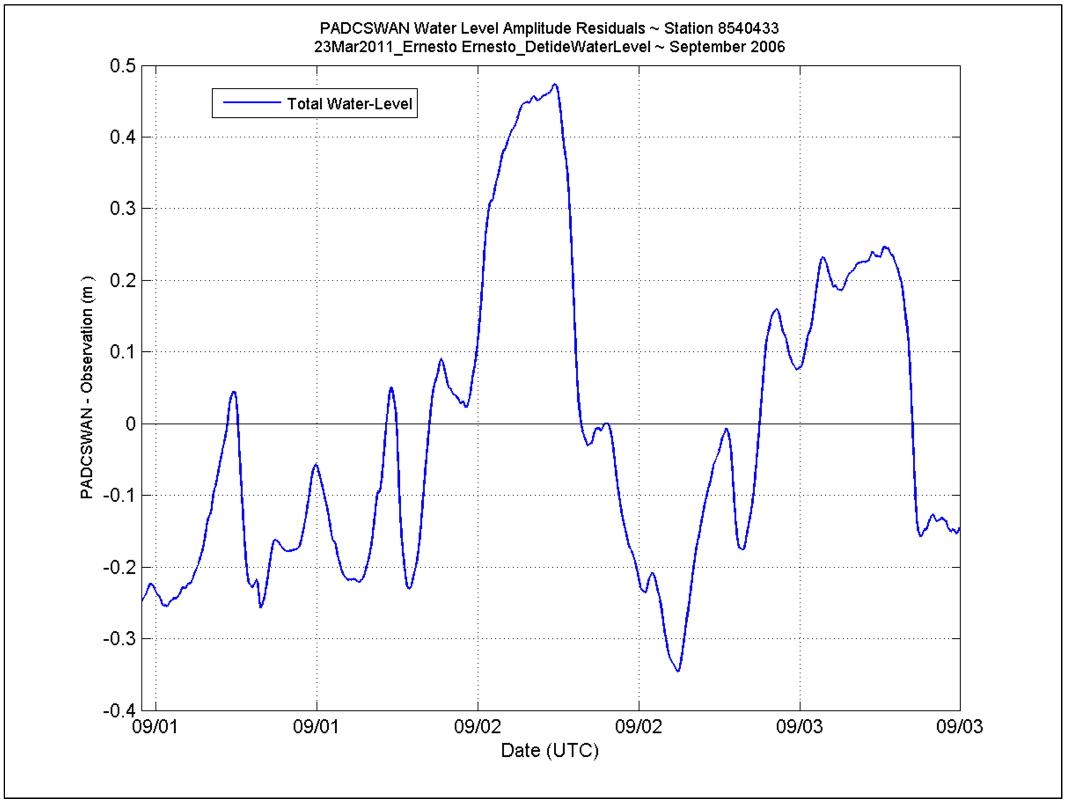
PADCSWAN Water Level Amplitude Residuals ~ Station 8540433
23Mar2011_Ernesto Ernesto_DetideWaterLevel ~ September 2006
Total Water-Level
PADCSWAN - Observation (m)
0.5
0.4
0.3
0.2
0.1
0
-0.1
-0.2
-0.3
-0.4
09/01
09/01
09/02
09/02
09/03
09/03
Date (UTC)

Station 8548989

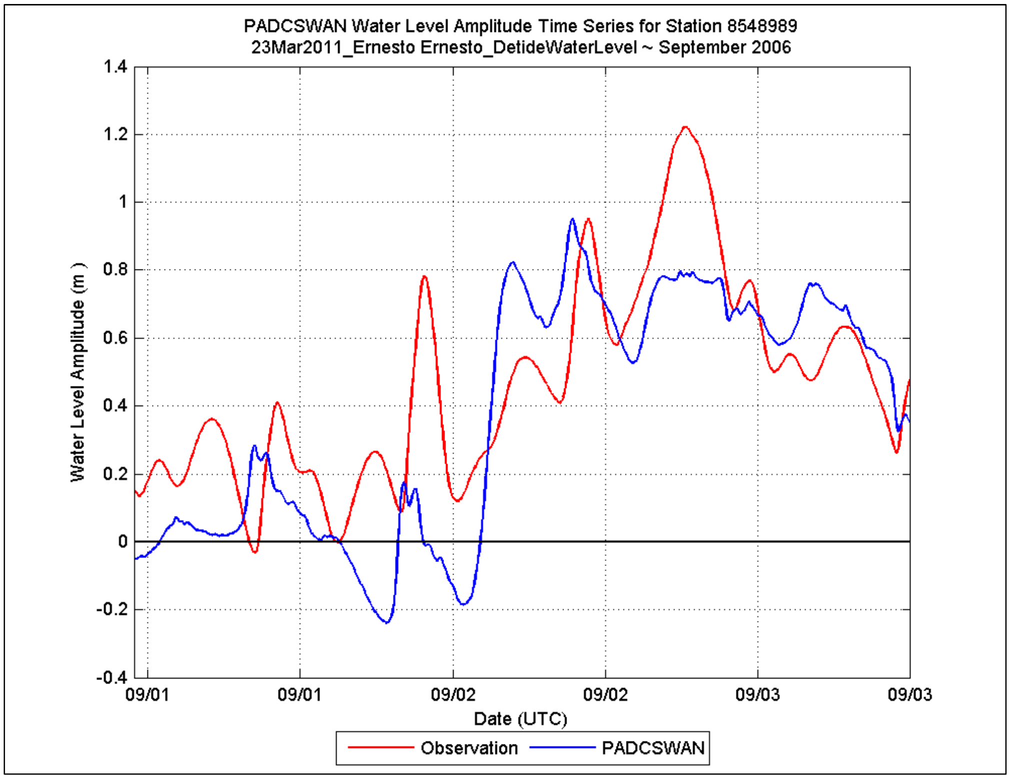

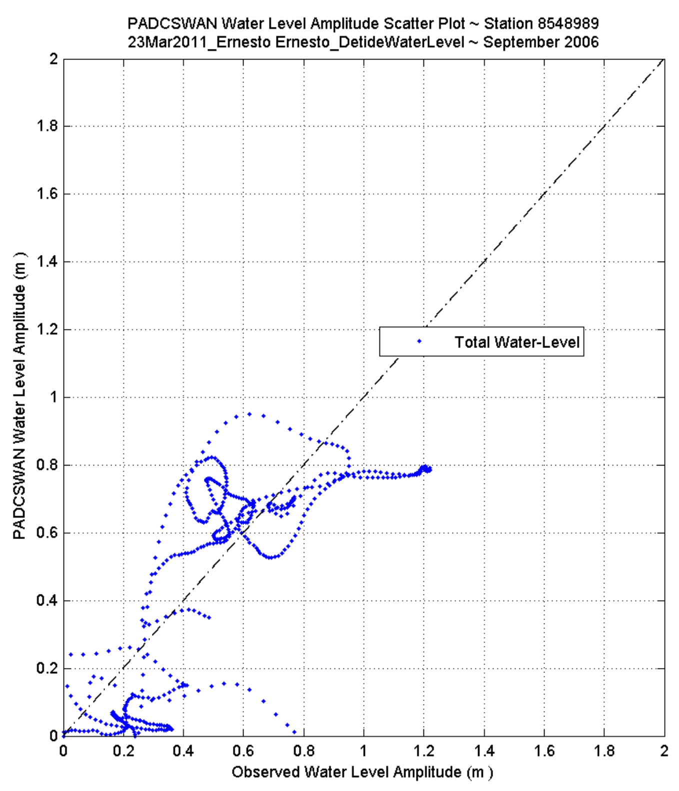

Water Level Amplitude Summary Table
For Station 8548989

Statistics	totwl
bias	-0.09
rms	0.25
SI	0.5
Perf	0.69

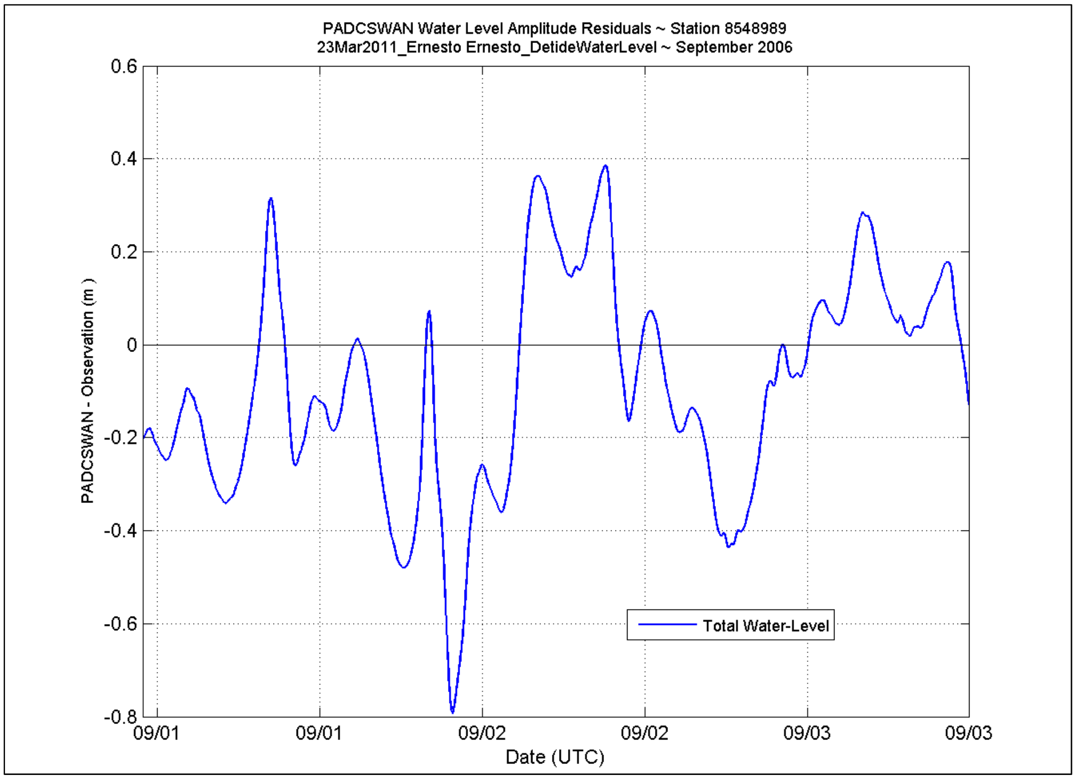
PADCSWAN Water Level Amplitude Residuals ~ Station 8548989
23Mar2011_Ernesto Ernesto_DetideWaterLevel ~ September 2006
PADCSWAN - Observation (m)
0.6
0.4
0.2
0
-0.2
-0.4
-0.6
-0.8
09/01
09/01
09/02
09/02
09/03
09/03
Date (UTC)
Total Water-Level

Station 8551762

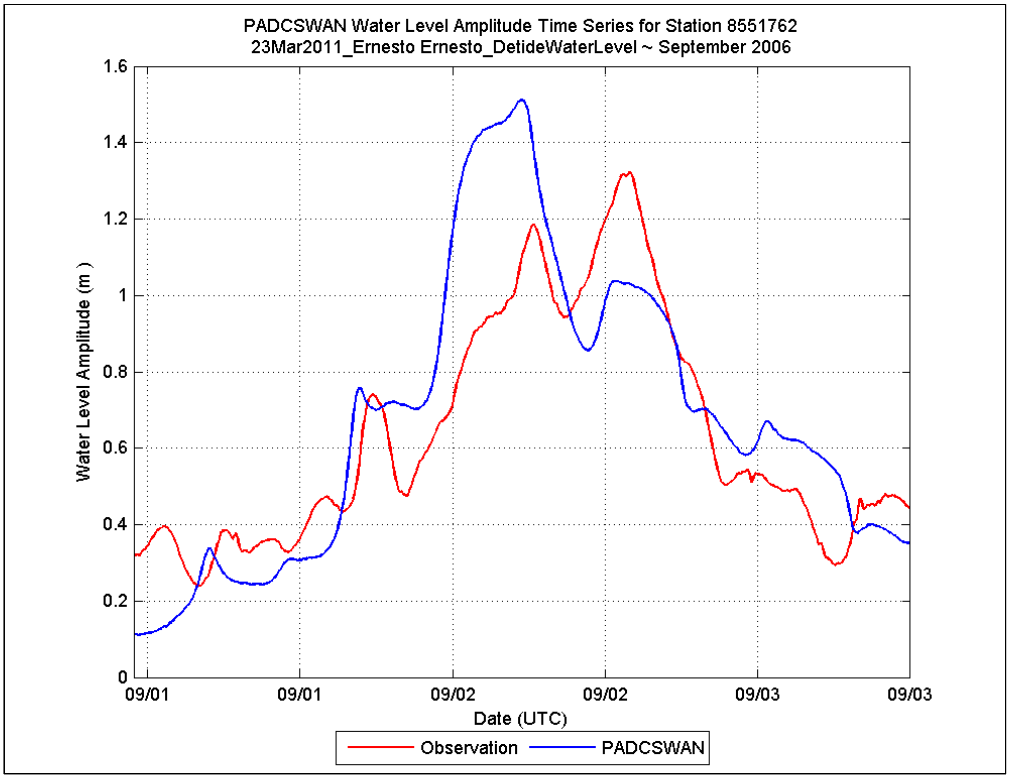
PADCSWAN Water Level Amplitude Time Series for Station 8551762
23Mar2011_Ernesto Ernesto_DetideWaterLevel ~ September 2006

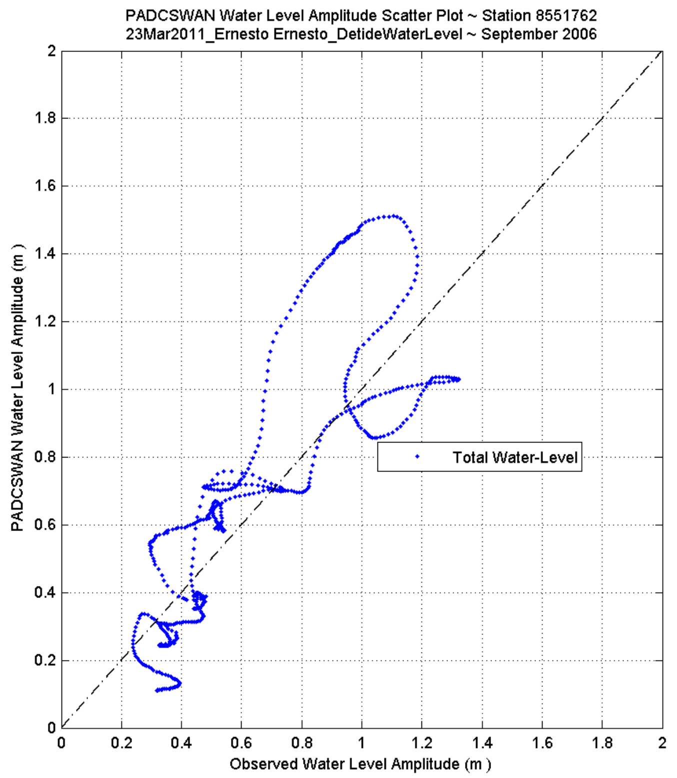
PADCSWAN Water Level Amplitude Scatter Plot ~ Station 8551762
23Mar2011_Ernesto Ernesto_DetideWaterLevel ~ September 2006

Water Level Amplitude Summary Table
For Station 8551762

Statistics	totwl
bias	0.04
rms	0.21
SI	0.32
Perf	0.82

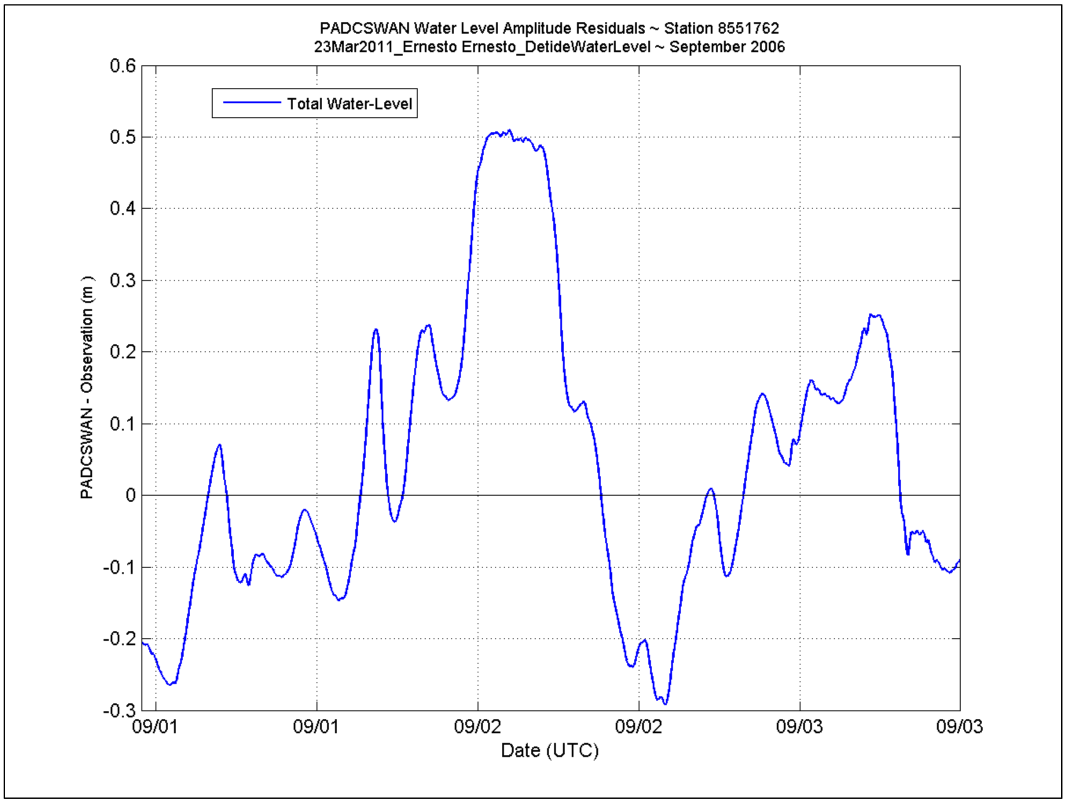
PADCSWAN Water Level Amplitude Residuals ~ Station 8551762
23Mar2011_Ernesto Ernesto_DetideWaterLevel ~ September 2006
Total Water-Level
PADCSWAN - Observation (m)
0.6
0.5
0.4
0.3
0.2
0.1
0
-0.1
-0.2
-0.3
09/01
09/01
09/02
09/02
09/03
09/03
Date (UTC)

Station 8551910

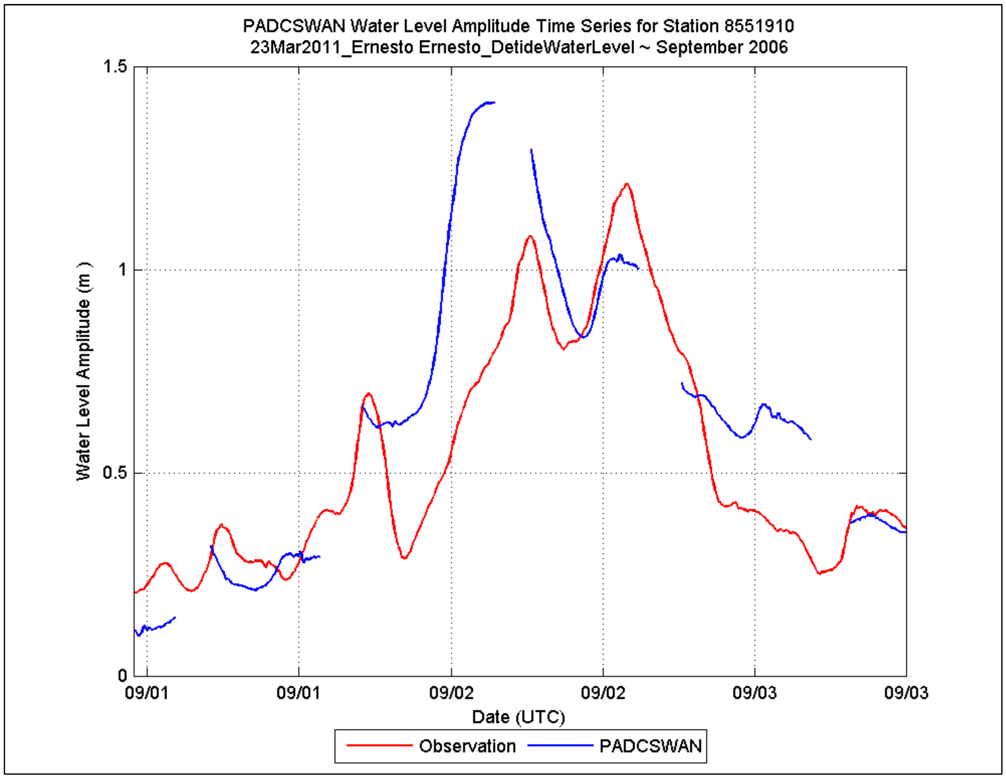

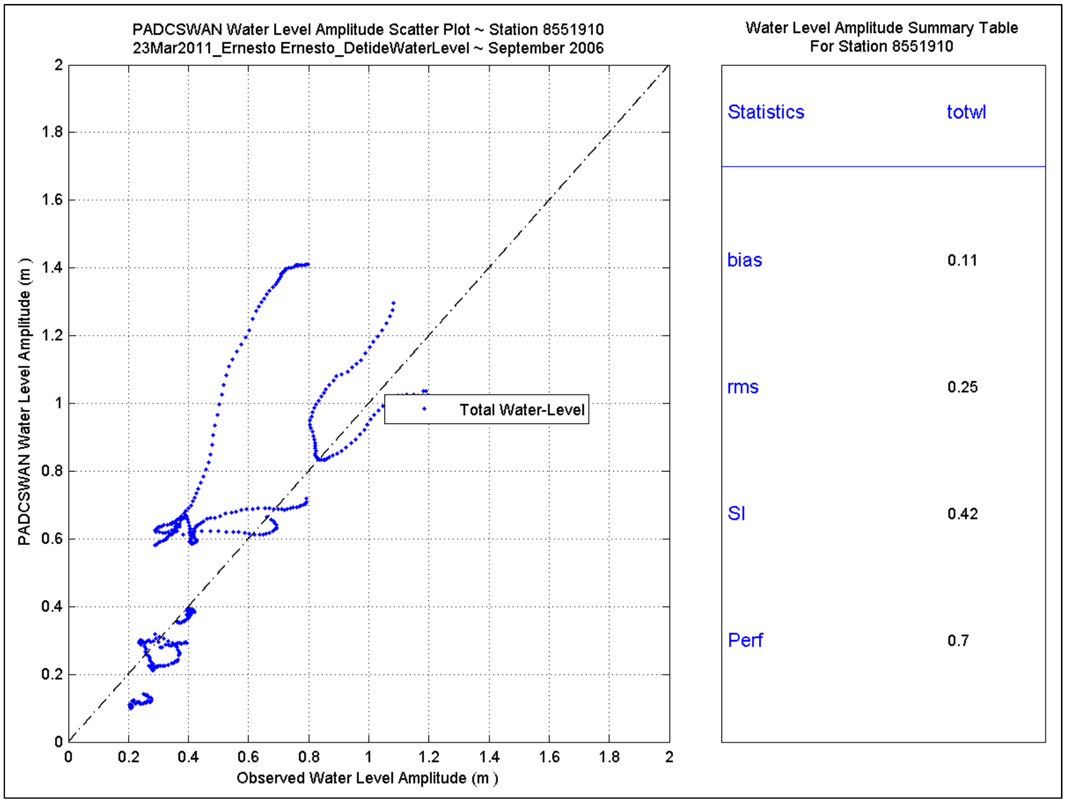

Water Level Amplitude Summary Table
For Station 8551910

Statistics	totwl
bias	0.11
rms	0.25
SI	0.42
Perf	0.7

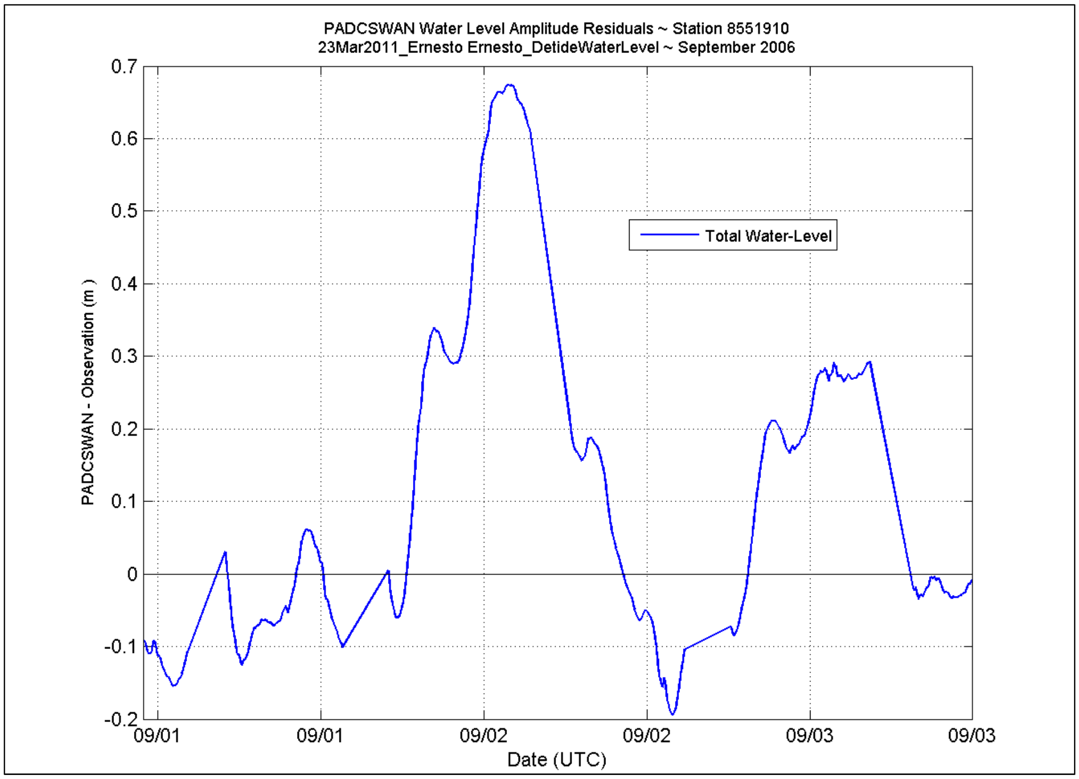
PADCSWAN Water Level Amplitude Residuals ~ Station 8551910
23Mar2011_Ernesto Ernesto_DetideWaterLevel ~ September 2006
Total Water-Level
PADCSWAN - Observation (m)
0.7
0.6
0.5
0.4
0.3
0.2
0.1
0
-0.1
-0.2
09/01
09/01
09/02
09/02
09/03
09/03
Date (UTC)

Station 8555889

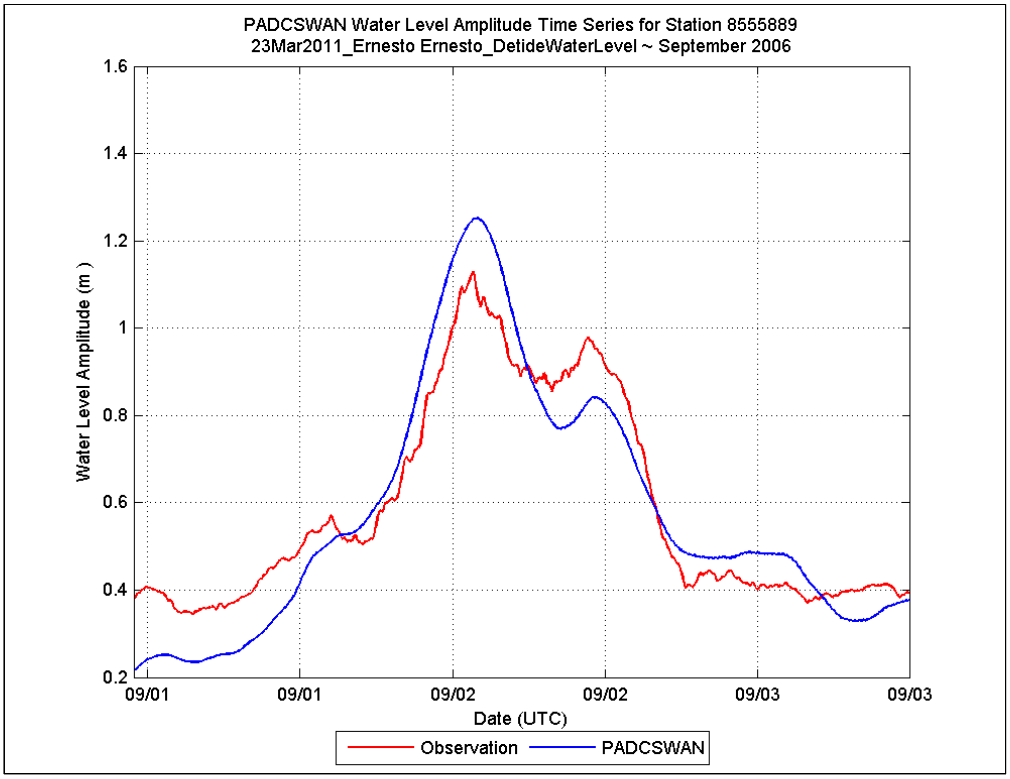

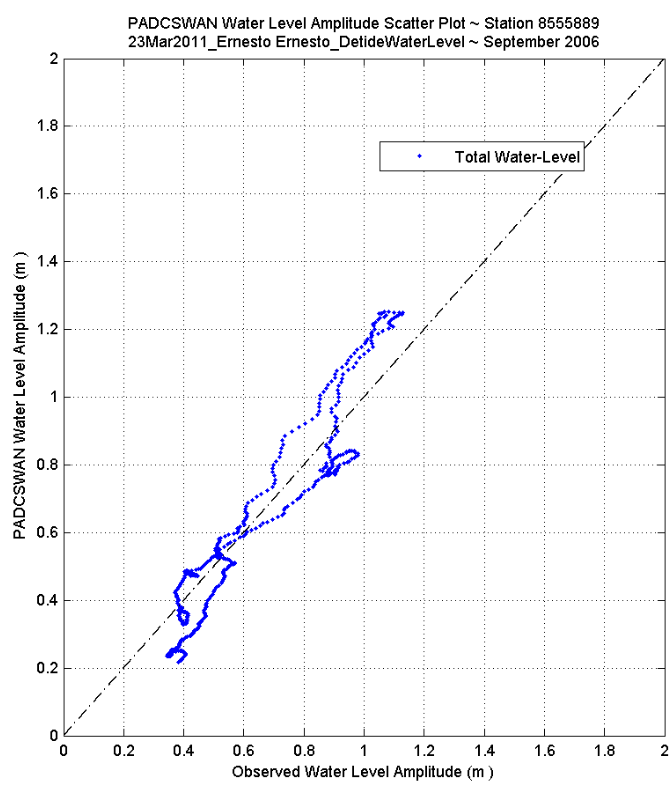

Water Level Amplitude Summary Table
For Station 8555889

Statistics	totwl
bias	-0.01
rms	0.09
SI	0.16
Perf	0.91

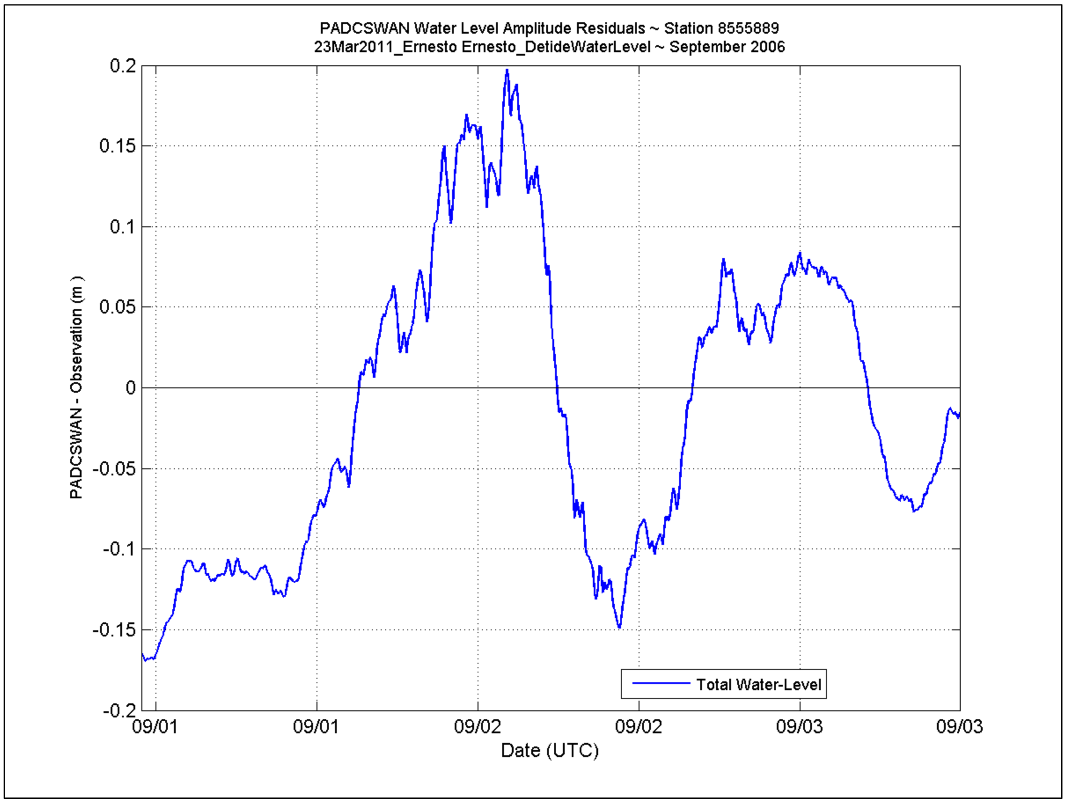
PADCSWAN Water Level Amplitude Residuals ~ Station 8555889
23Mar2011_Ernesto Ernesto_DetideWaterLevel ~ September 2006
PADCSWAN - Observation (m)
0.2
0.15
0.1
0.05
0
-0.05
-0.1
-0.15
-0.2
09/01
09/01
09/02
09/02
09/03
09/03
Date (UTC)
Total Water-Level

Station 8570283

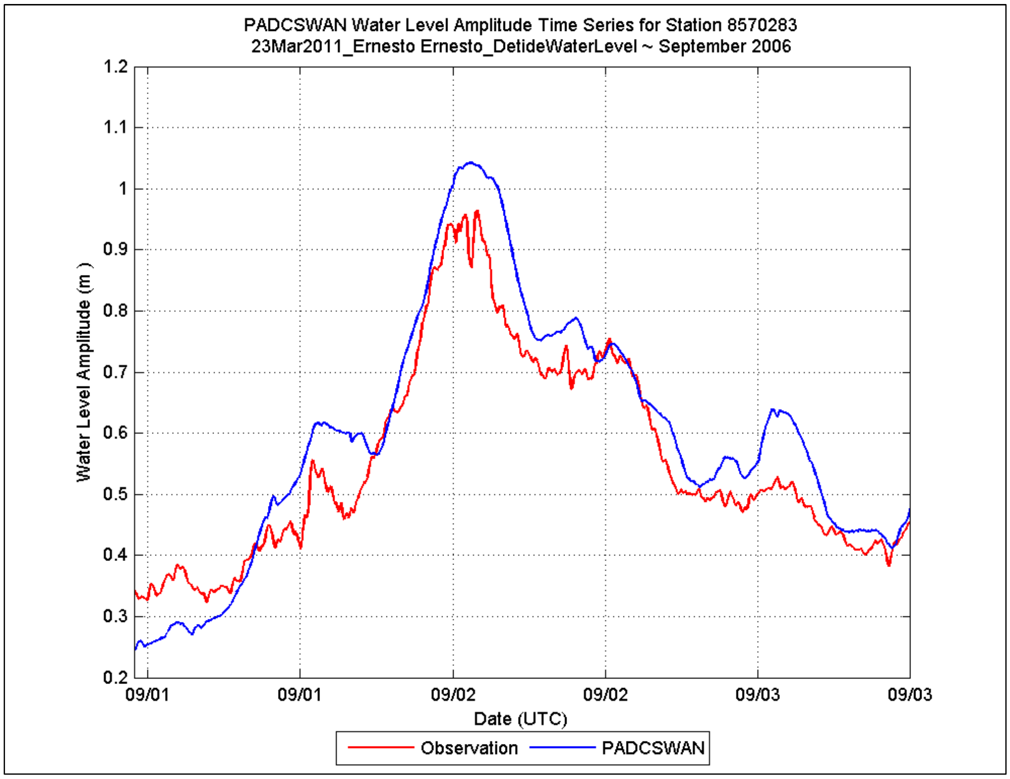

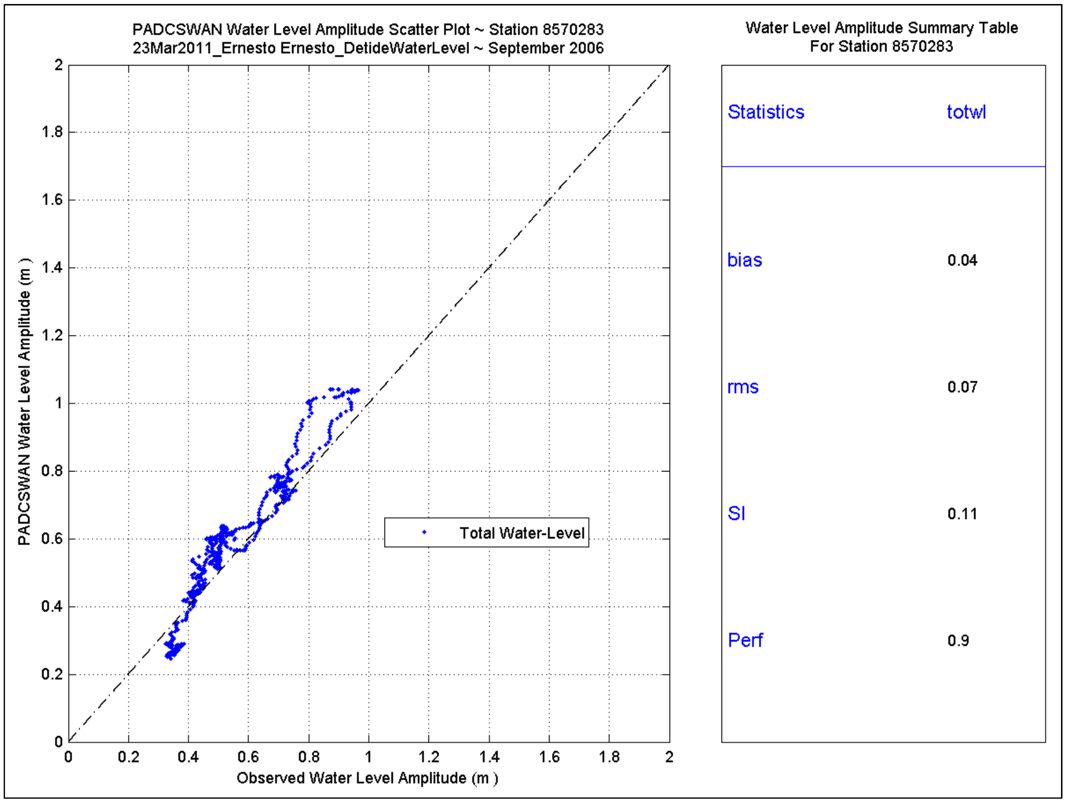

Water Level Amplitude Summary Table
For Station 8570283

Statistics	totwl
bias	0.04
rms	0.07
SI	0.11
Perf	0.9

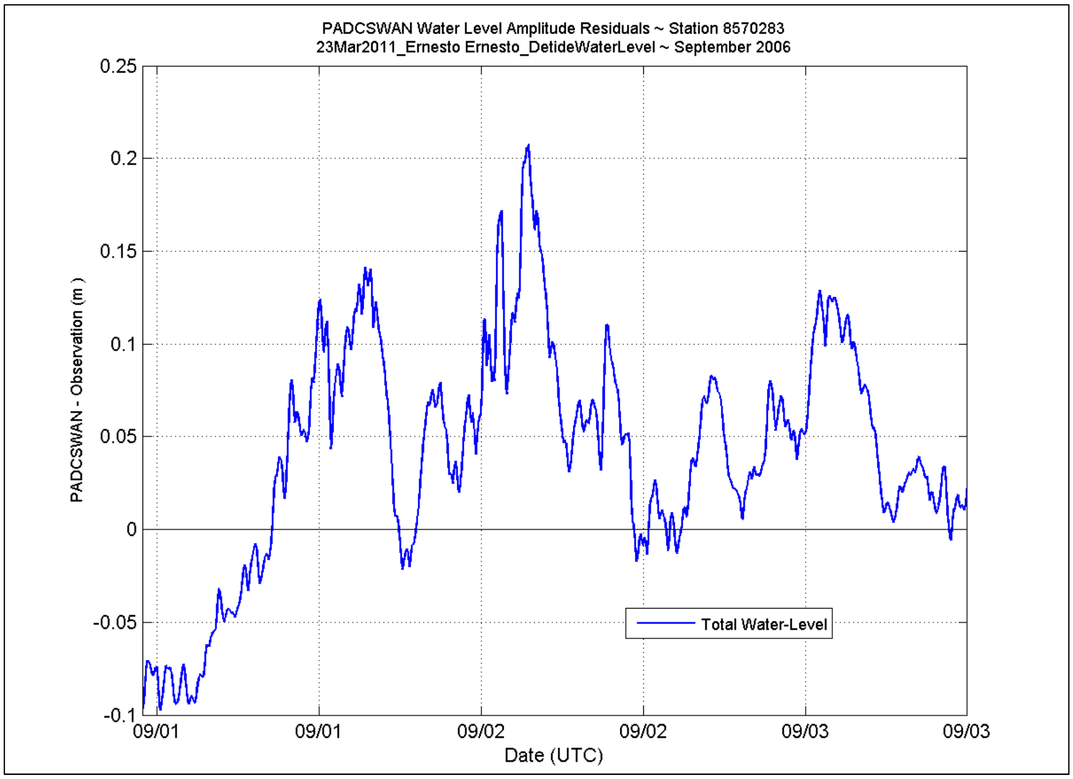
PADCSWAN Water Level Amplitude Residuals ~ Station 8570283
23Mar2011_Ernesto Ernesto_DetideWaterLevel ~ September 2006
PADCSWAN - Observation (m)
0.25
0.2
0.15
0.1
0.05
0
-0.05
-0.1
Total Water-Level
09/01
09/01
09/02
09/02
09/03
09/03
Date (UTC)

Station 8571892

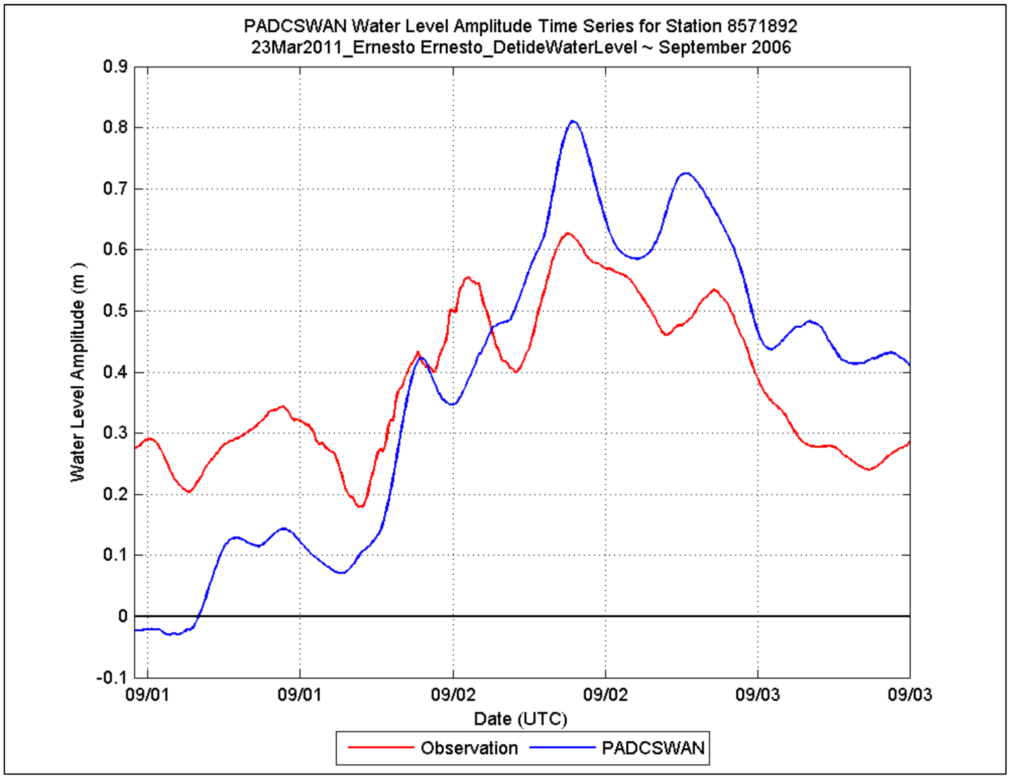

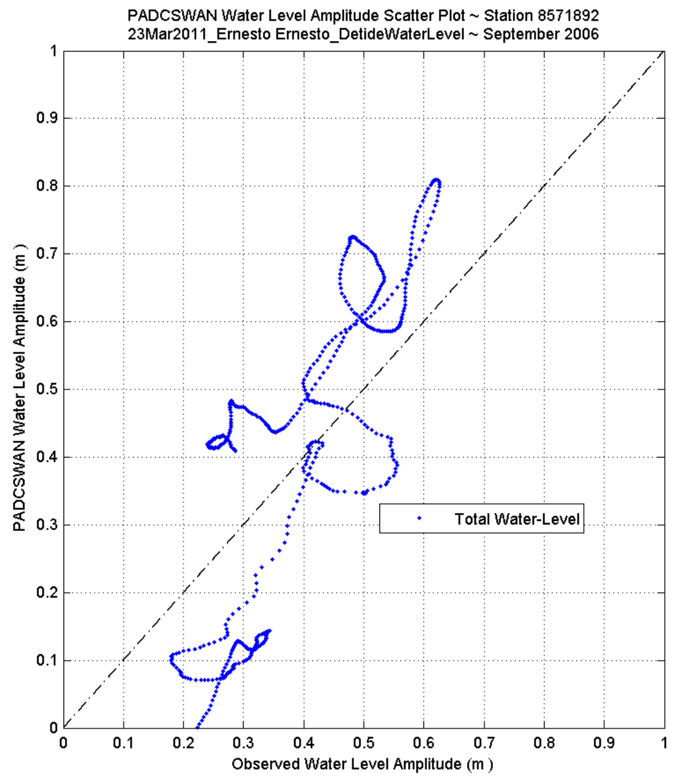

Water Level Amplitude Summary Table
For Station 8571892

Statistics	totwl
bias	0
rms	0.16
SI	0.43
Perf	0.79

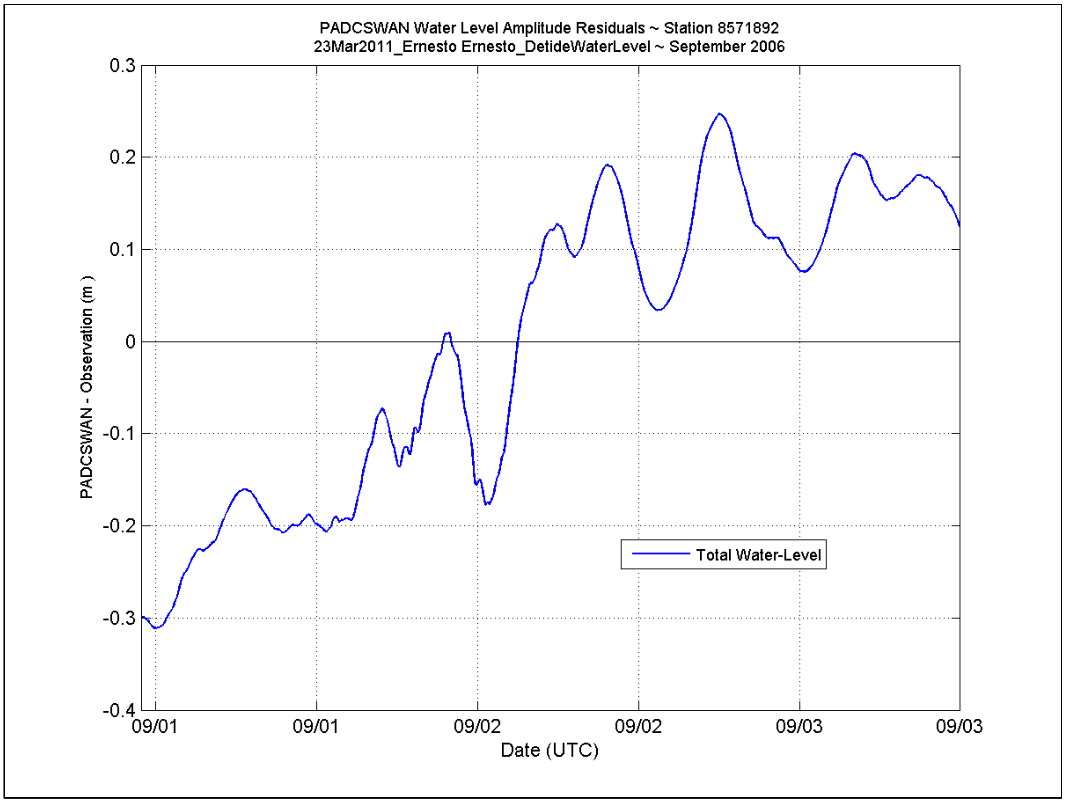
PADCSWAN Water Level Amplitude Residuals ~ Station 8571892
23Mar2011_Ernesto Ernesto_DetideWaterLevel ~ September 2006
PADCSWAN - Observation (m)
0.3
0.2
0.1
0
-0.1
-0.2
-0.3
-0.4
09/01
09/01
09/02
09/02
09/03
09/03
Date (UTC)
Total Water-Level

Station 8573364

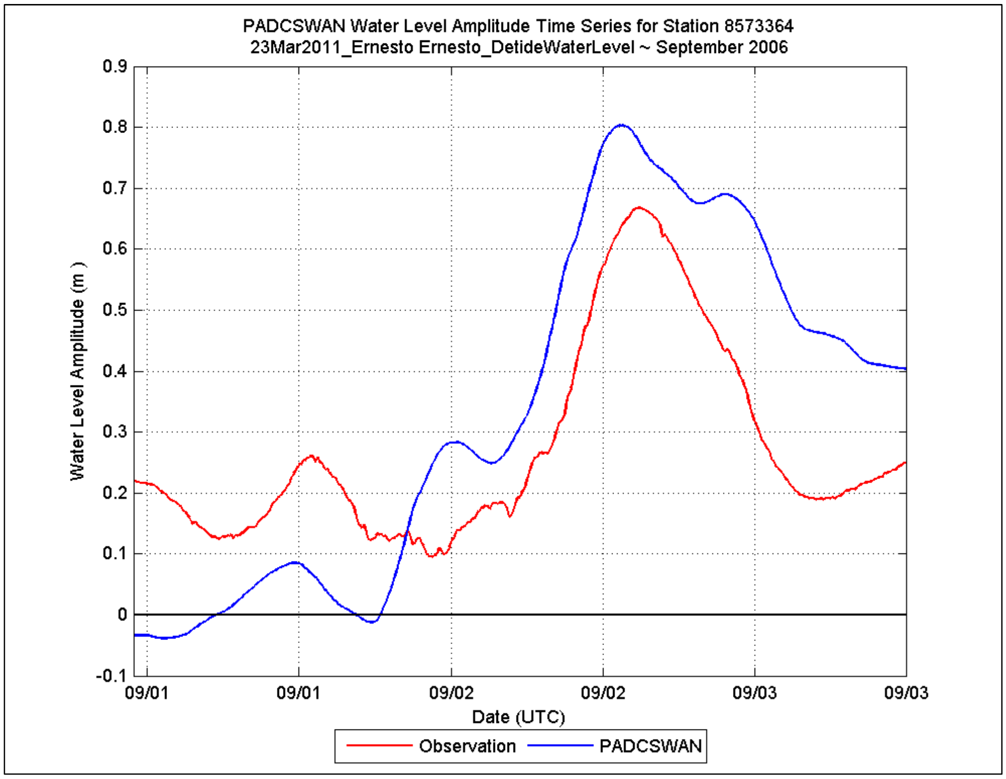

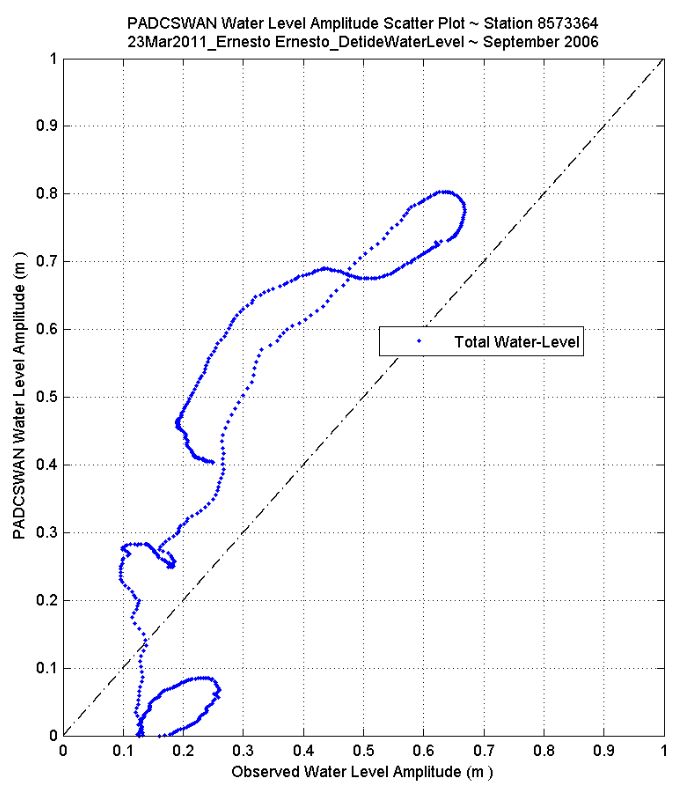

Water Level Amplitude Summary Table
For Station 8573364

Statistics	totwl
bias	0.06
rms	0.19
SI	0.65
Perf	0.6

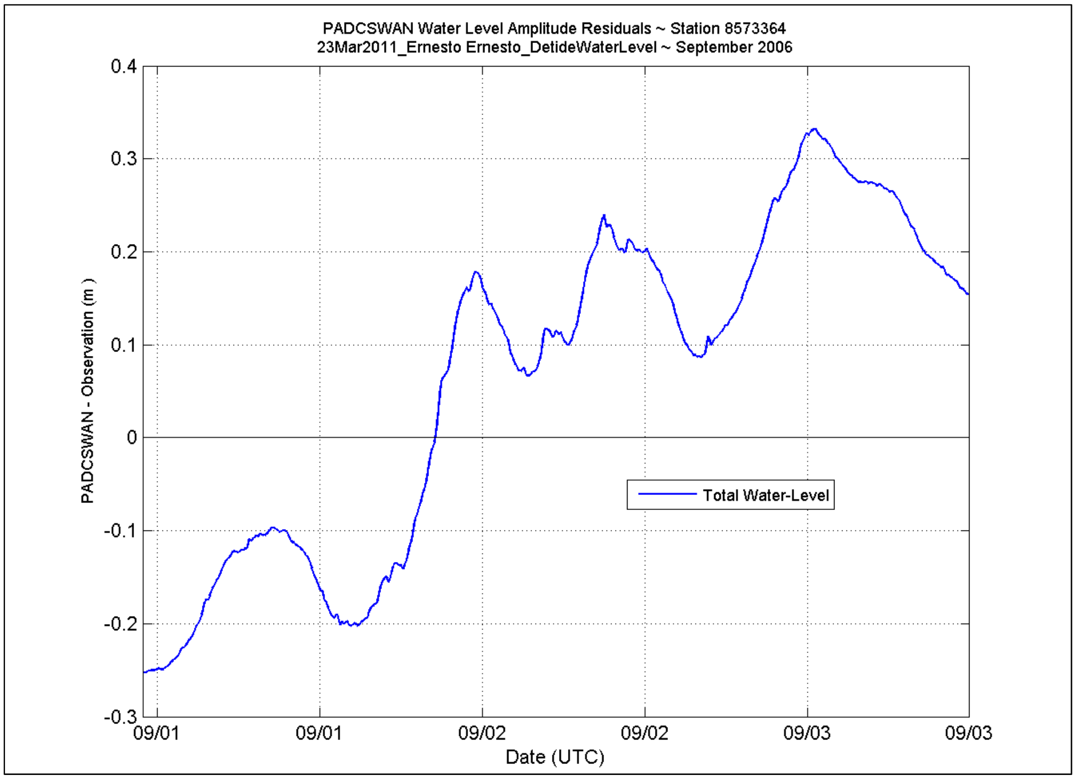
PADCSWAN Water Level Amplitude Residuals ~ Station 8573364
23Mar2011_Ernesto Ernesto_DetideWaterLevel ~ September 2006
PADCSWAN - Observation (m)
0.4
0.3
0.2
0.1
0
-0.1
-0.2
-0.3
09/01
09/01
09/02
09/02
09/03
09/03
Date (UTC)
Total Water-Level

Station 8574680

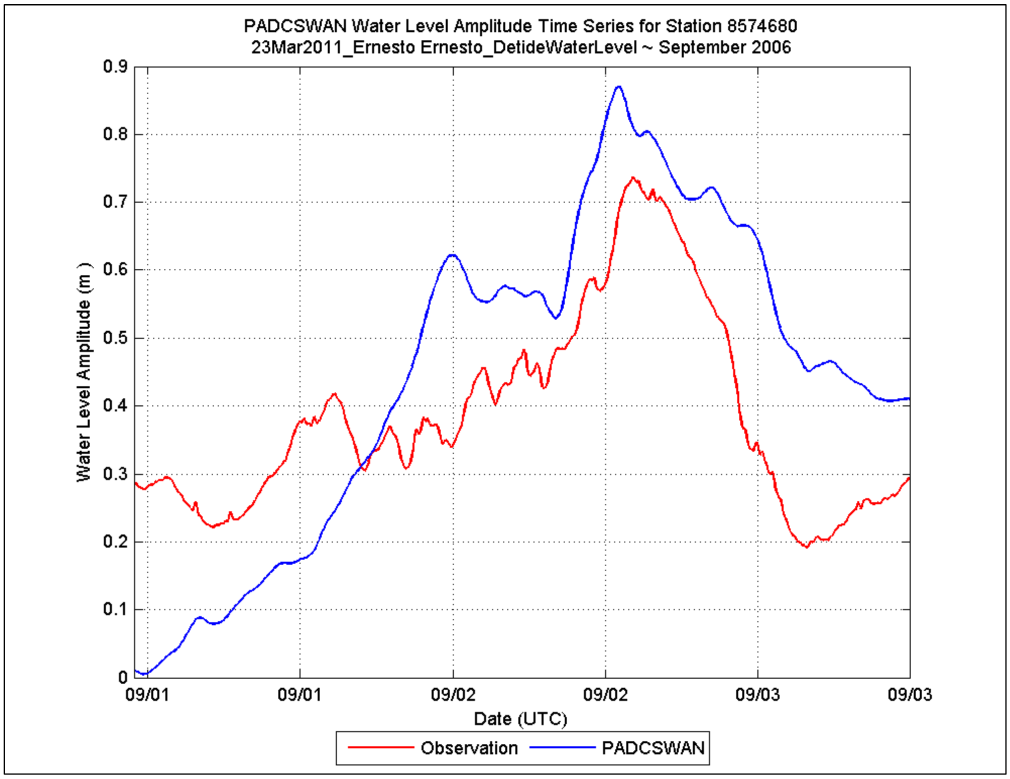

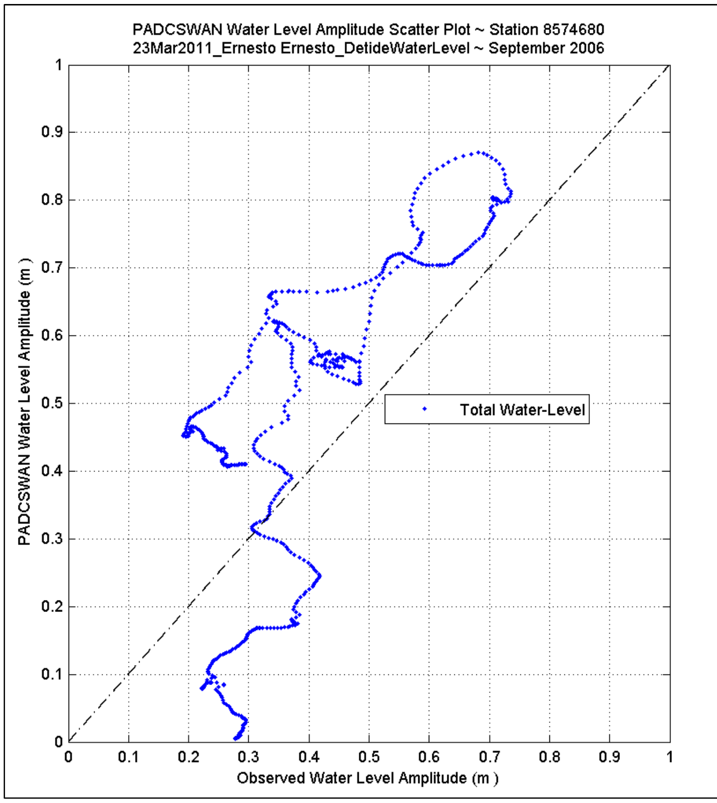

Water Level Amplitude Summary Table
For Station 8574680

Statistics	totwl
bias	0.06
rms	0.18
SI	0.43
Perf	0.71

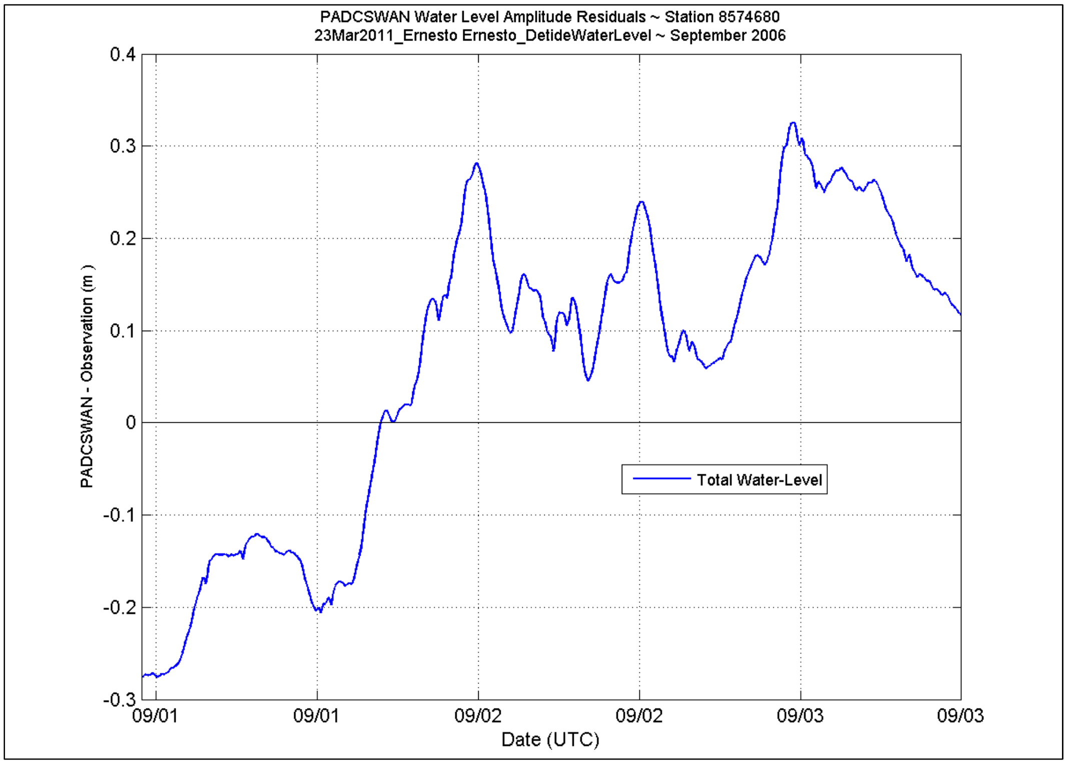
PADCSWAN Water Level Amplitude Residuals ~ Station 8574680
23Mar2011_Ernesto Ernesto_DetideWaterLevel ~ September 2006
PADCSWAN - Observation (m)
0.4
0.3
0.2
0.1
0
-0.1
-0.2
-0.3
09/01
09/01
09/02
09/02
09/03
09/03
Date (UTC)
Total Water-Level

Station 8575512

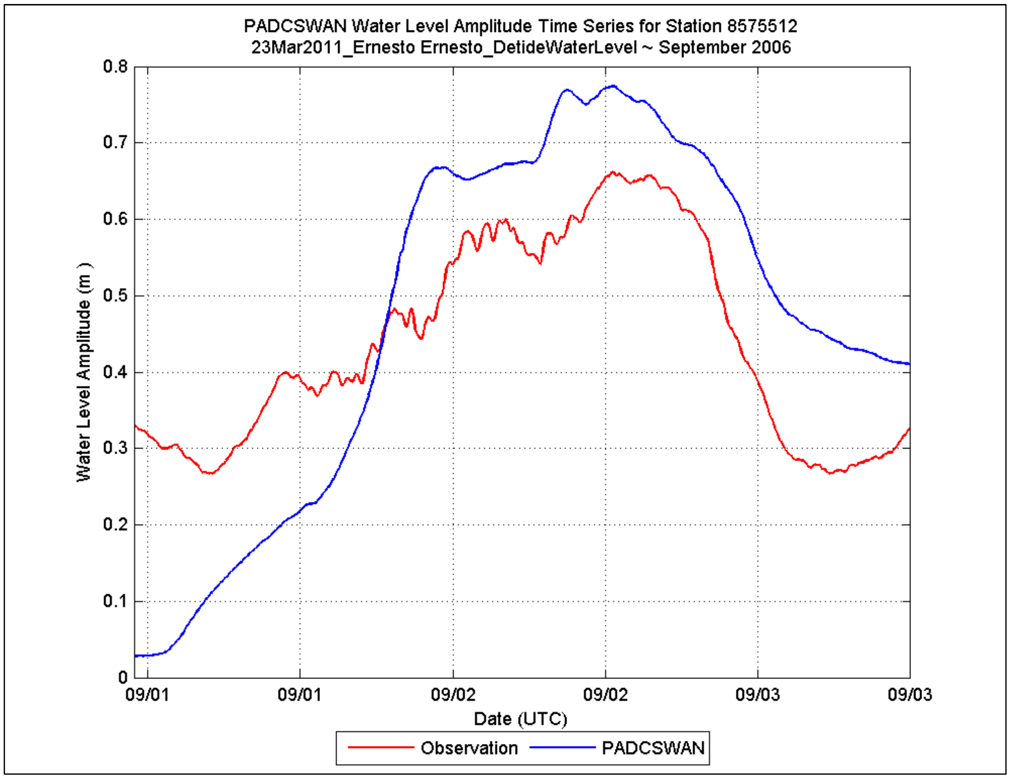

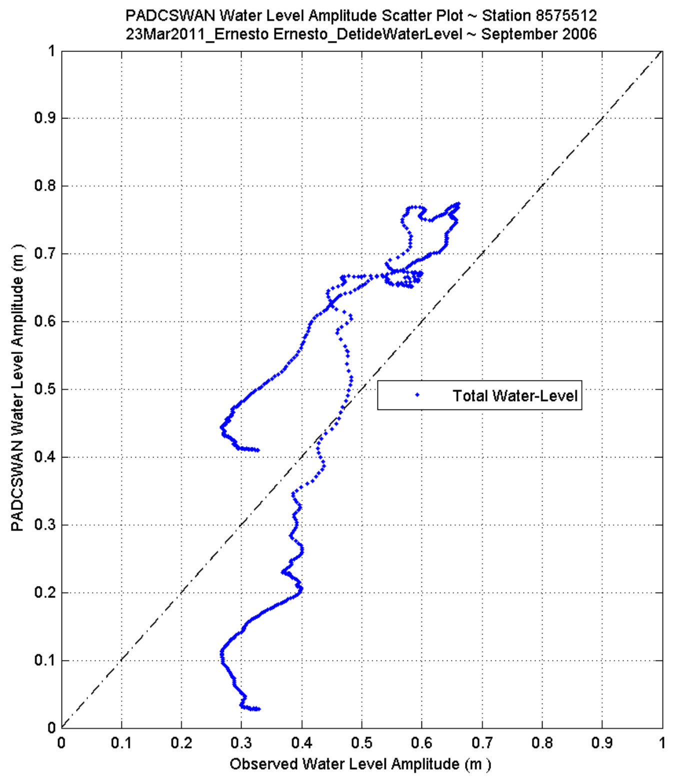

Water Level Amplitude Summary Table
For Station 8575512

Statistics	totwl
bias	0.03
rms	0.15
SI	0.34
Perf	0.8

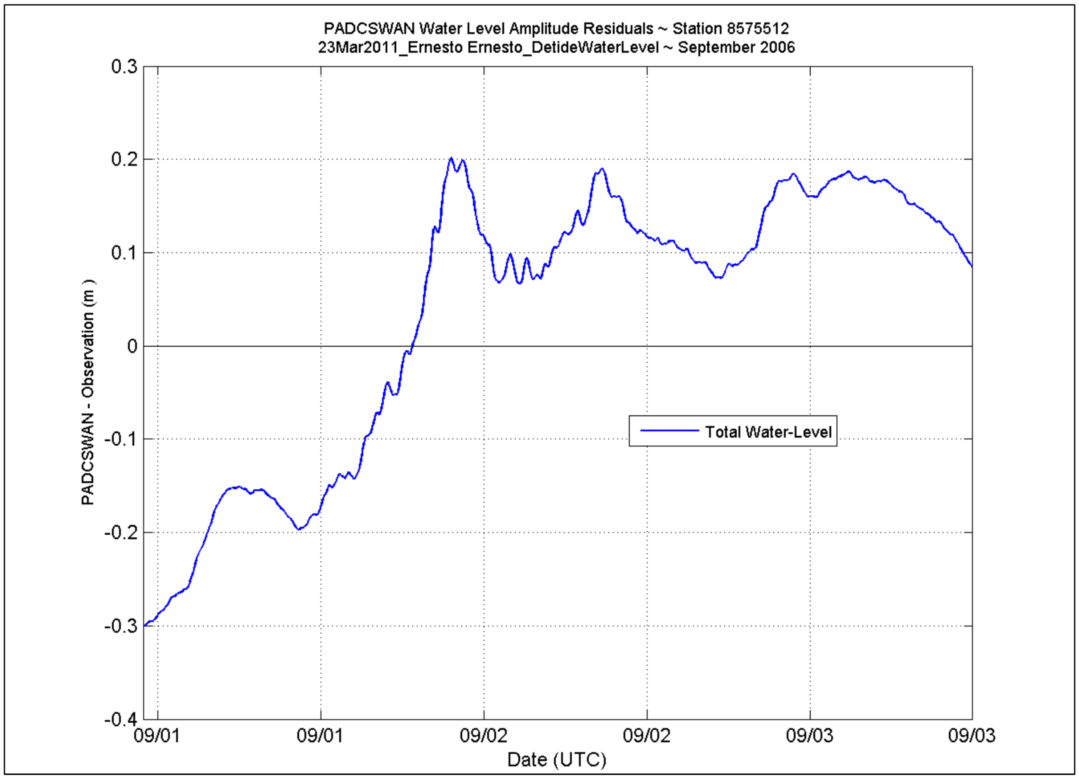
PADCSWAN Water Level Amplitude Residuals ~ Station 8575512
23Mar2011_Ernesto Ernesto_DetideWaterLevel ~ September 2006
PADCSWAN - Observation (m)
0.3
0.2
0.1
0
-0.1
-0.2
-0.3
-0.4
09/01
09/01
09/02
09/02
09/03
09/03
Date (UTC)
Total Water-Level

Station 8577330

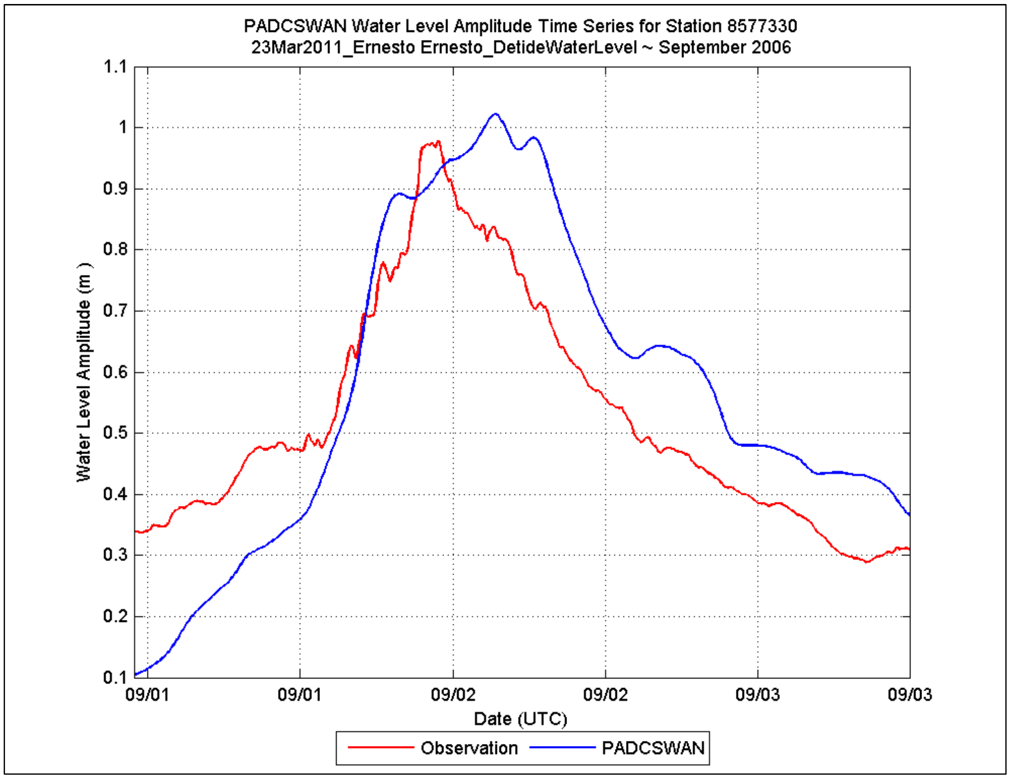

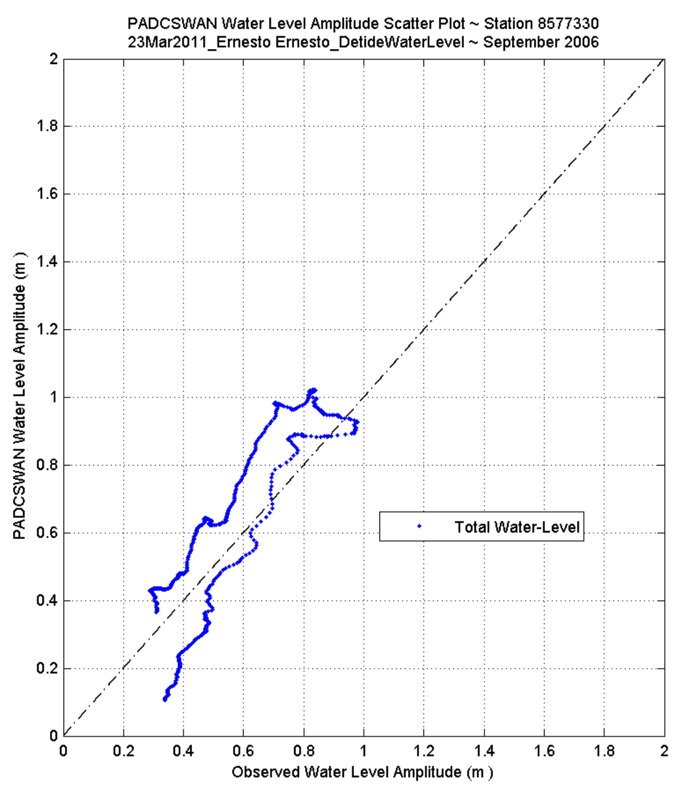

Water Level Amplitude Summary Table
For Station 8577330

Statistics	totwl
bias	0.04
rms	0.14
SI	0.26
Perf	0.83

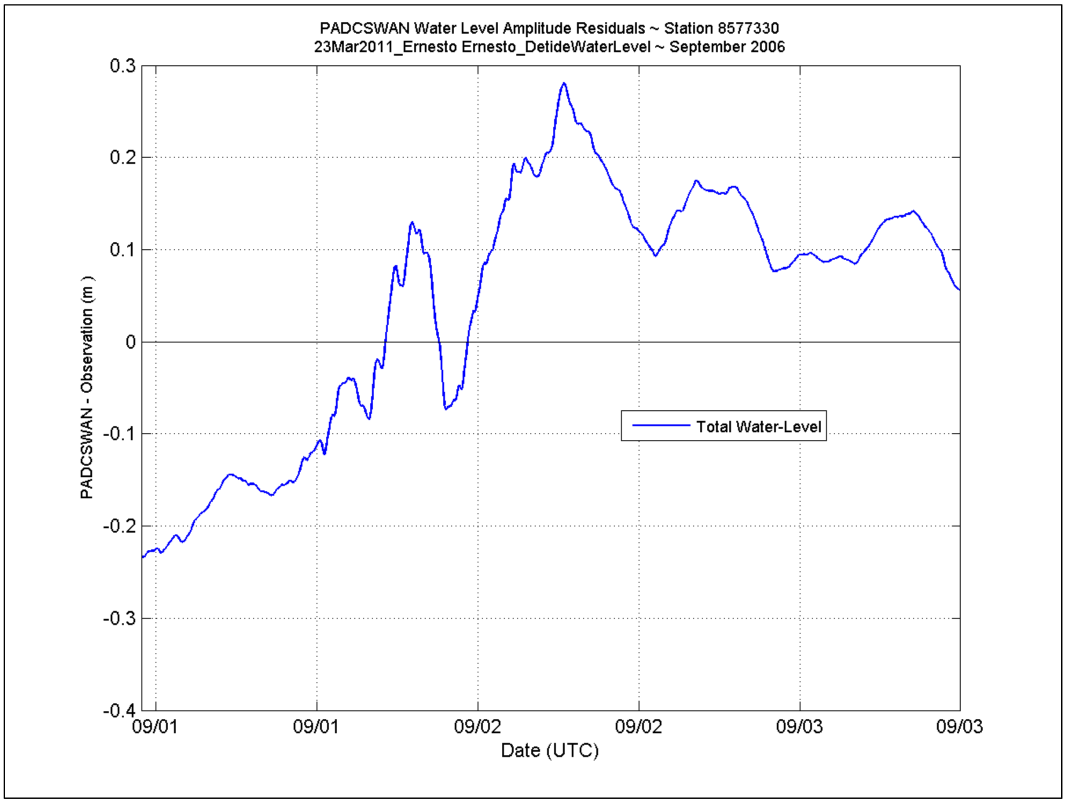
PADCSWAN Water Level Amplitude Residuals ~ Station 8577330
23Mar2011_Ernesto Ernesto_DetideWaterLevel ~ September 2006
PADCSWAN - Observation (m)
0.3
0.2
0.1
0
-0.1
-0.2
-0.3
-0.4
09/01
09/01
09/02
09/02
09/03
09/03
Date (UTC)
Total Water-Level

Station 8632200

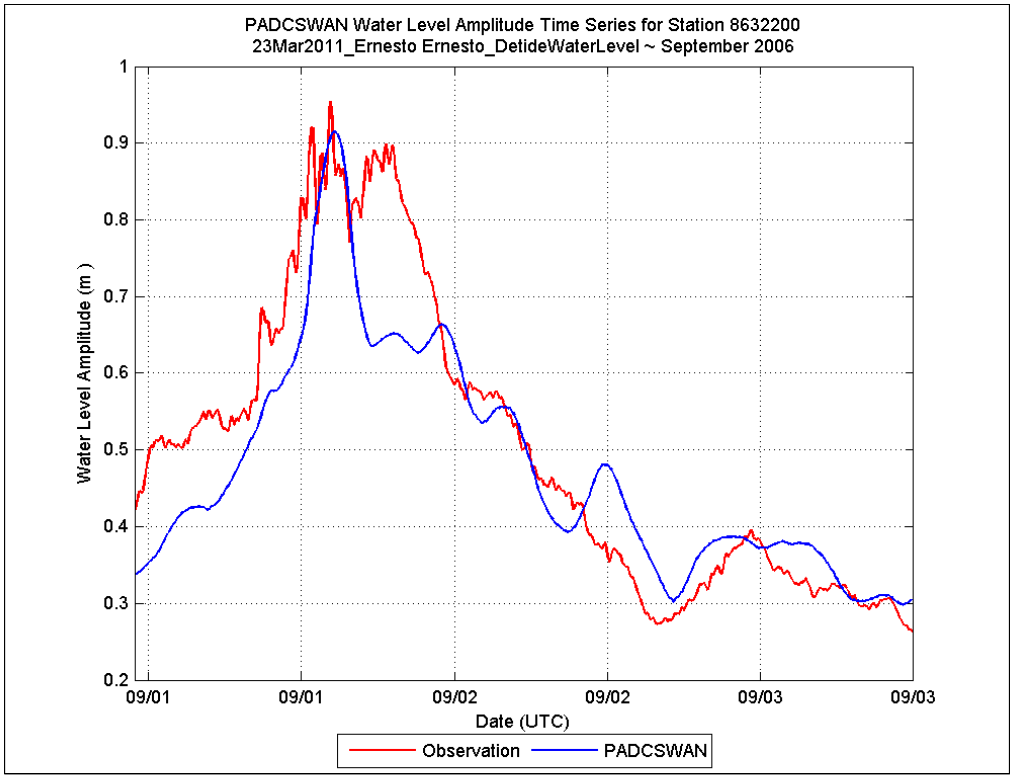
PADCSWAN Water Level Amplitude Time Series for Station 8632200
23Mar2011_Ernesto Ernesto_DetideWaterLevel ~ September 2006

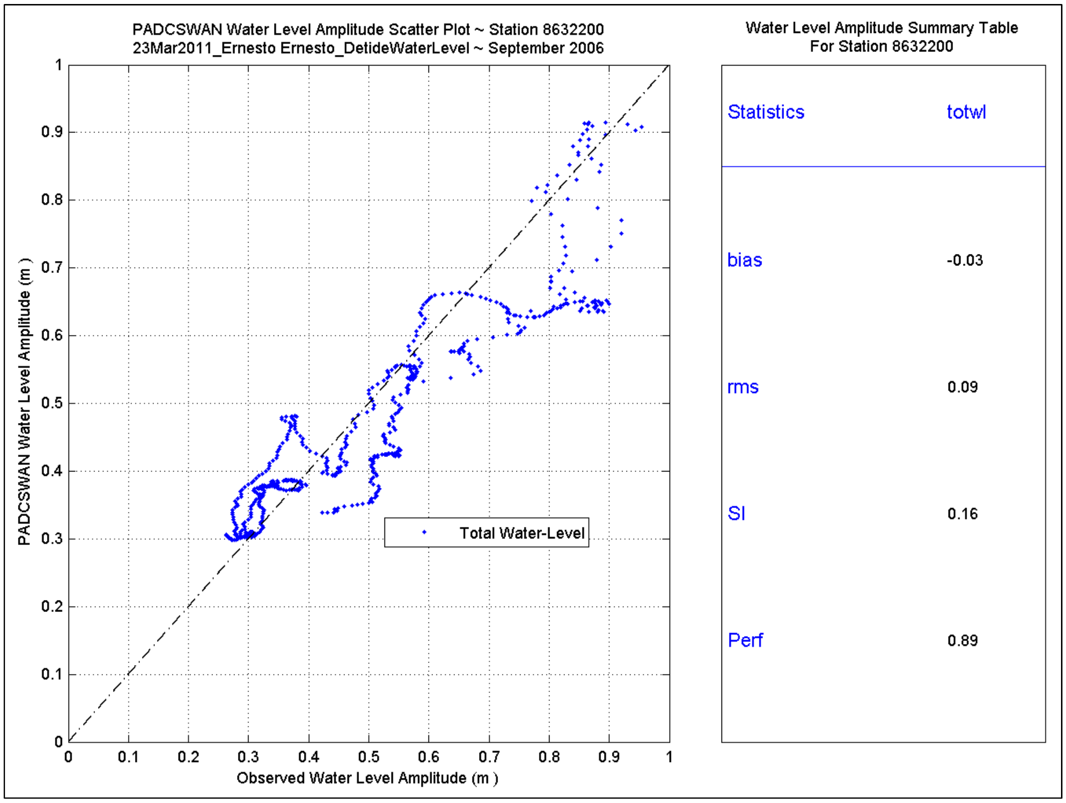
PADCSWAN Water Level Amplitude Scatter Plot ~ Station 8632200
23Mar2011_Ernesto Ernesto_DetideWaterLevel ~ September 2006

Water Level Amplitude Summary Table
For Station 8632200

Statistics	totwl
bias	-0.03
rms	0.09
SI	0.16
Perf	0.89

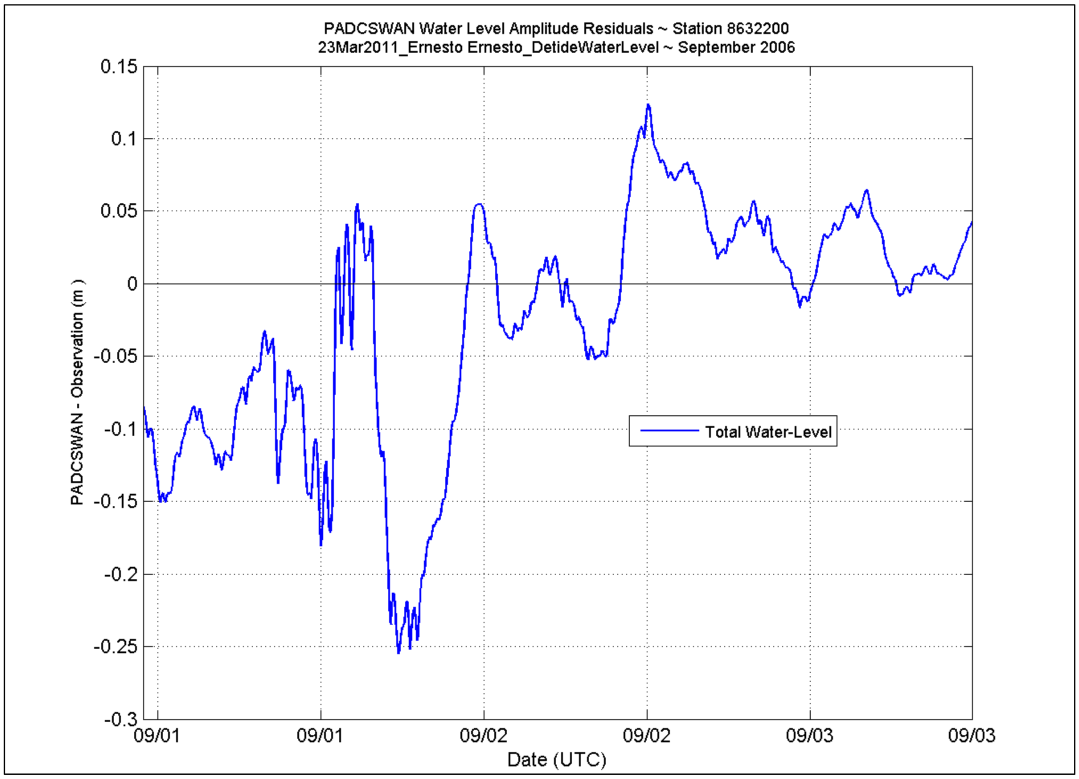
PADCSWAN Water Level Amplitude Residuals ~ Station 8632200
23Mar2011_Ernesto Ernesto_DetideWaterLevel ~ September 2006
PADCSWAN - Observation (m)
0.15
0.1
0.05
0
-0.05
-0.1
-0.15
-0.2
-0.25
-0.3
09/01
09/01
09/02
09/02
09/03
09/03
Date (UTC)
Total Water-Level

Station 8635750

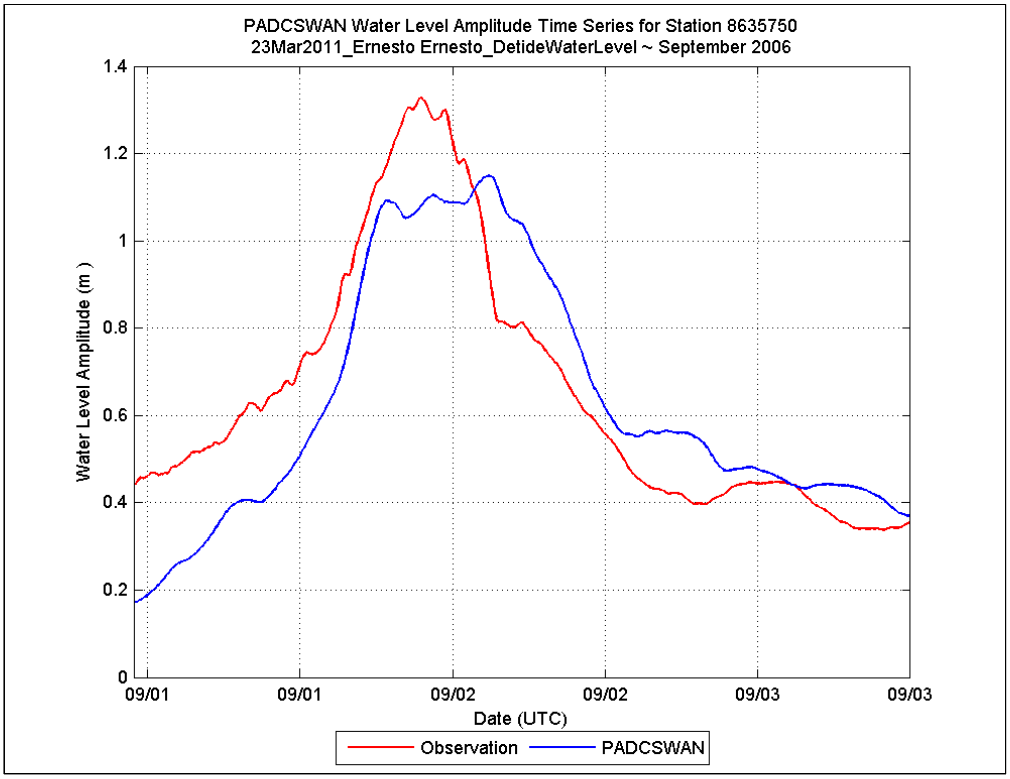

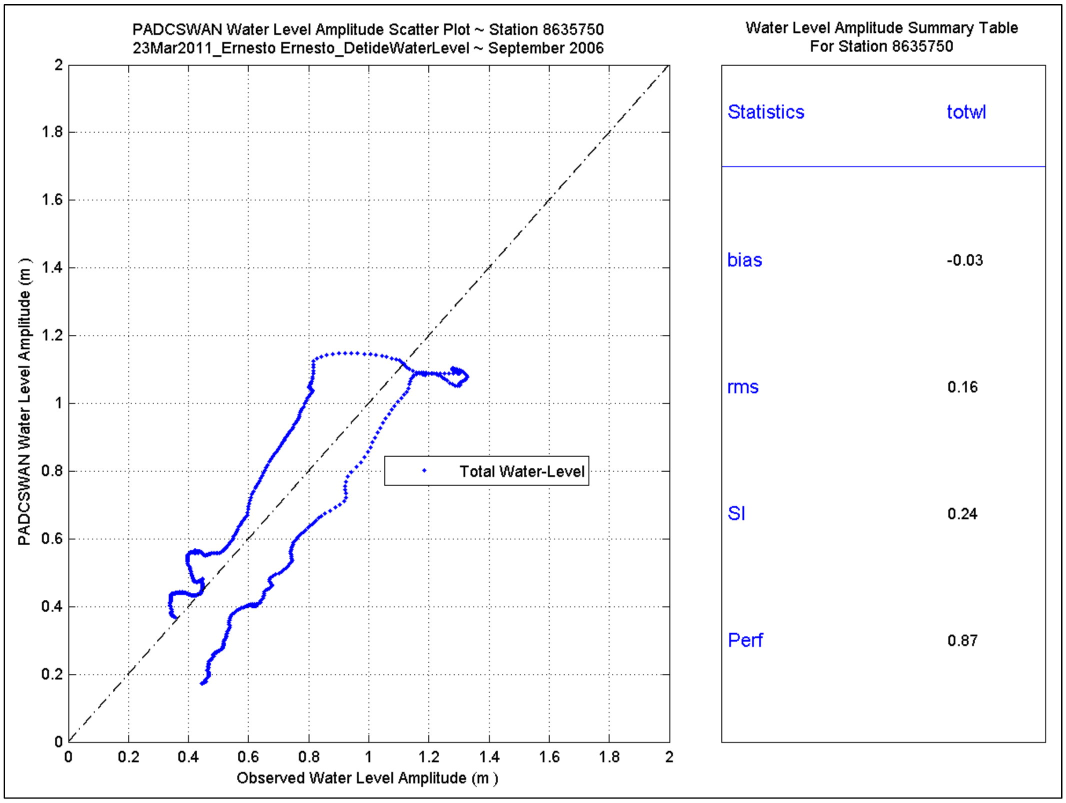

Water Level Amplitude Summary Table
For Station 8635750

Statistics	totwl
bias	-0.03
rms	0.16
SI	0.24
Perf	0.87

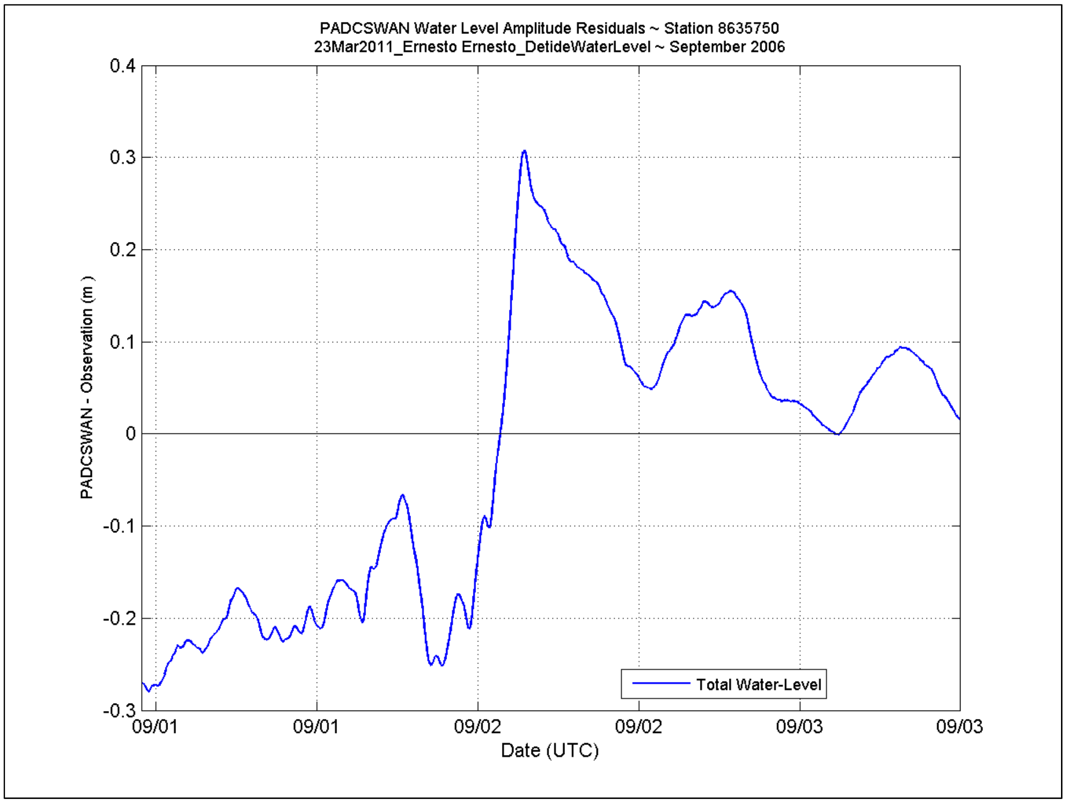
PADCSWAN Water Level Amplitude Residuals ~ Station 8635750
23Mar2011_Ernesto Ernesto_DetideWaterLevel ~ September 2006
PADCSWAN - Observation (m)
0.4
0.3
0.2
0.1
0
-0.1
-0.2
-0.3
09/01
09/01
09/02
09/02
09/03
09/03
Date (UTC)
Total Water-Level

Station 8637689

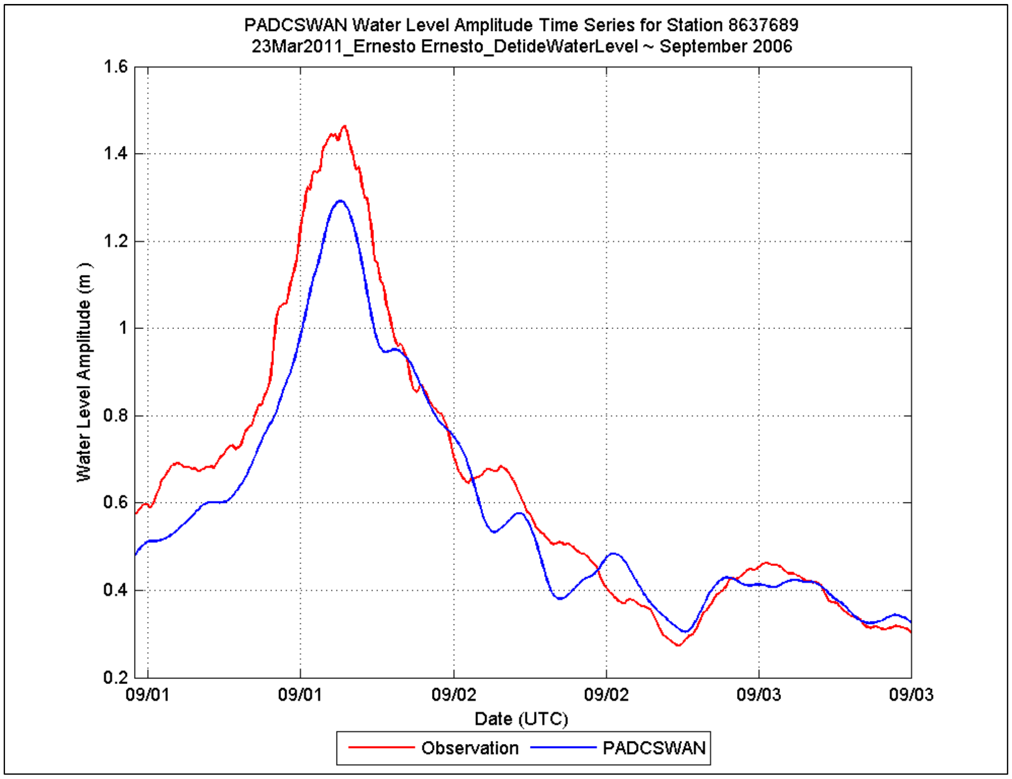

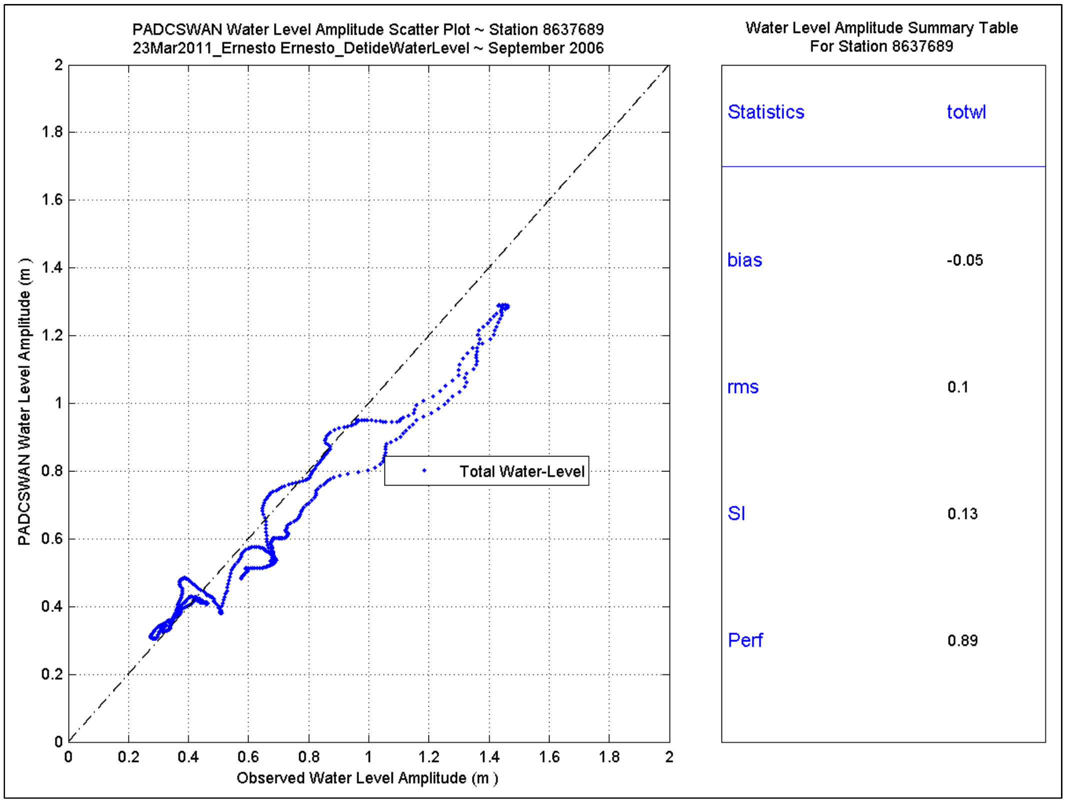

Water Level Amplitude Summary Table
For Station 8637689

Statistics	totwl
bias	-0.05
rms	0.1
SI	0.13
Perf	0.89

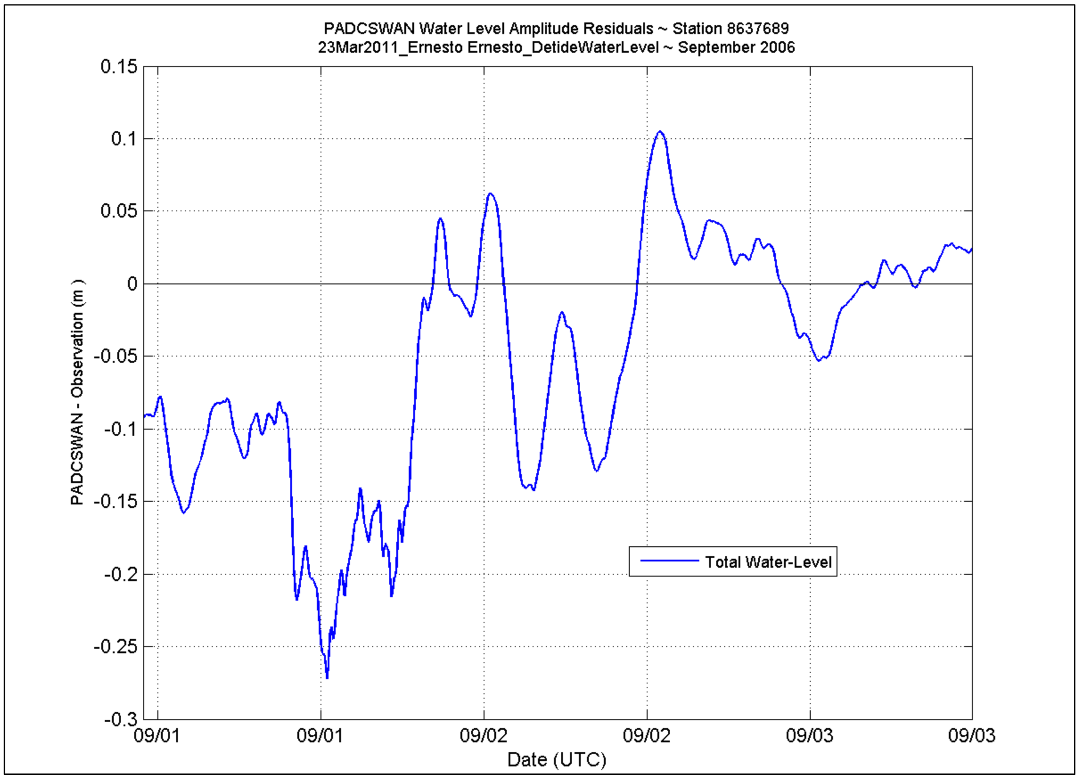
PADCSWAN Water Level Amplitude Residuals ~ Station 8637689
23Mar2011_Ernesto Ernesto_DetideWaterLevel ~ September 2006
PADCSWAN - Observation (m)
0.15
0.1
0.05
0
-0.05
-0.1
-0.15
-0.2
-0.25
-0.3
09/01
09/01
09/02
09/02
09/03
09/03
Date (UTC)
Total Water-Level

Station 8638610

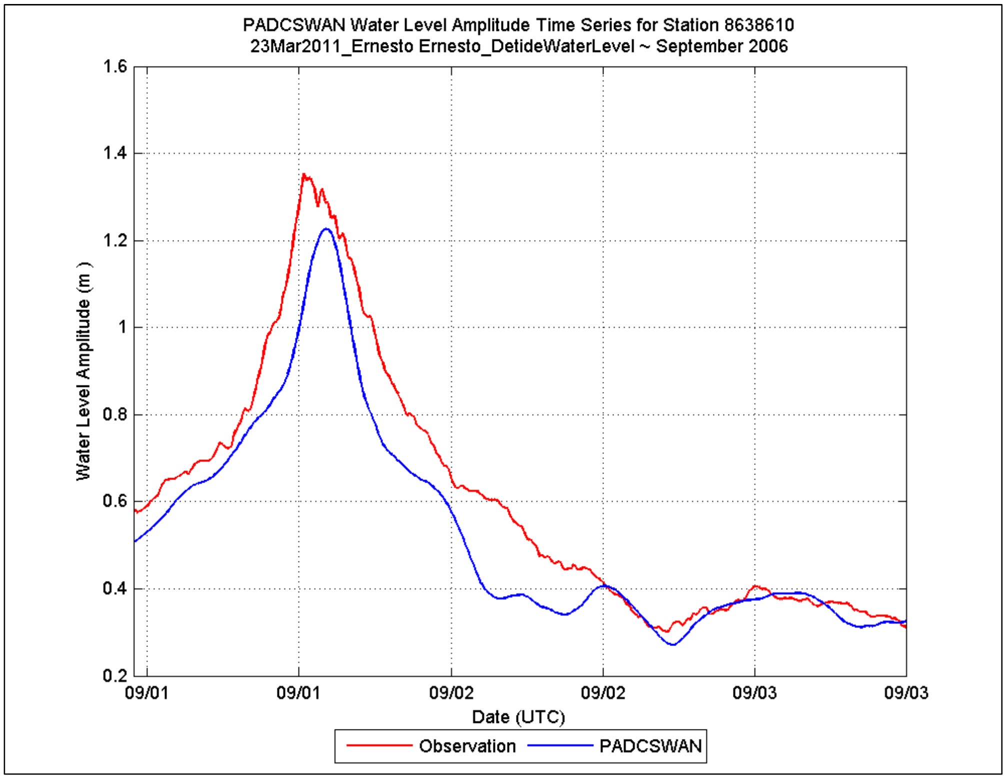

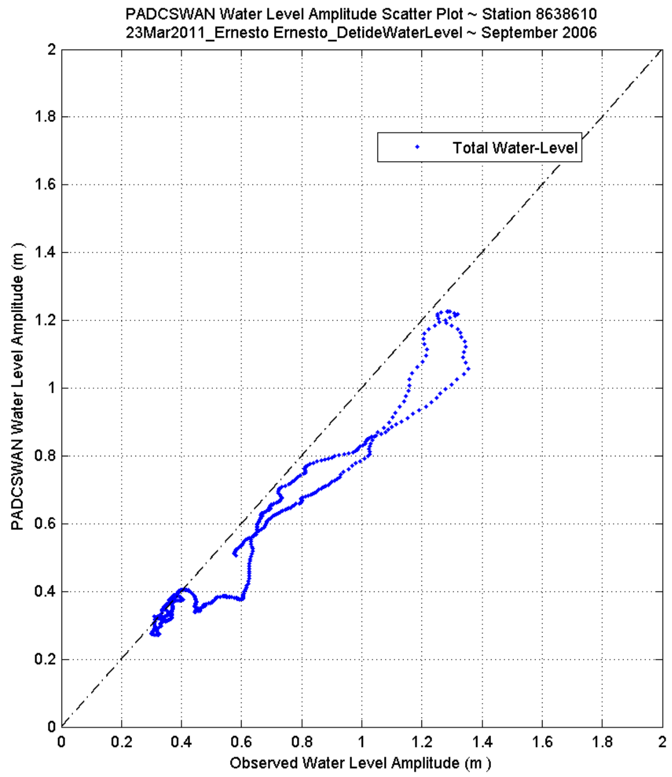

Water Level Amplitude Summary Table
For Station 8638610

Statistics	totwl
bias	-0.08
rms	0.11
SI	0.12
Perf	0.86

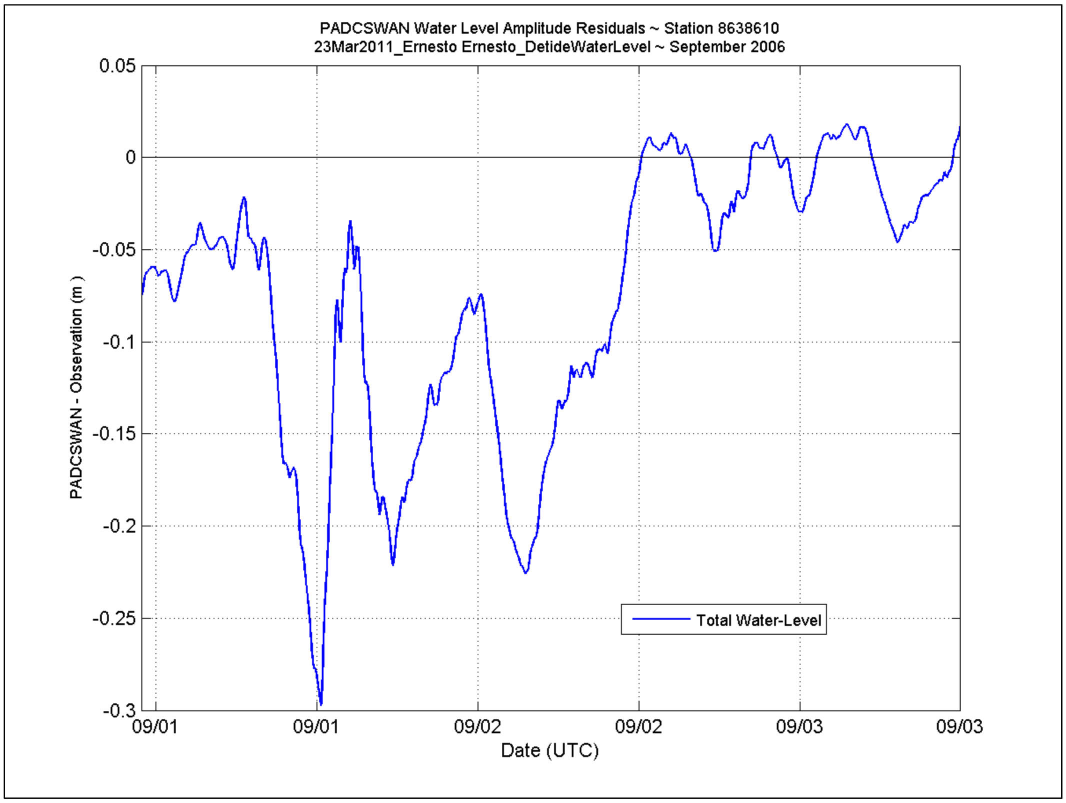
PADCSWAN Water Level Amplitude Residuals ~ Station 8638610
23Mar2011_Ernesto Ernesto_DetideWaterLevel ~ September 2006
PADCSWAN - Observation (m)
0.05
0
-0.05
-0.1
-0.15
-0.2
-0.25
-0.3
09/01
09/01
09/02
09/02
09/03
09/03
Date (UTC)
Total Water-Level

Station 8639348

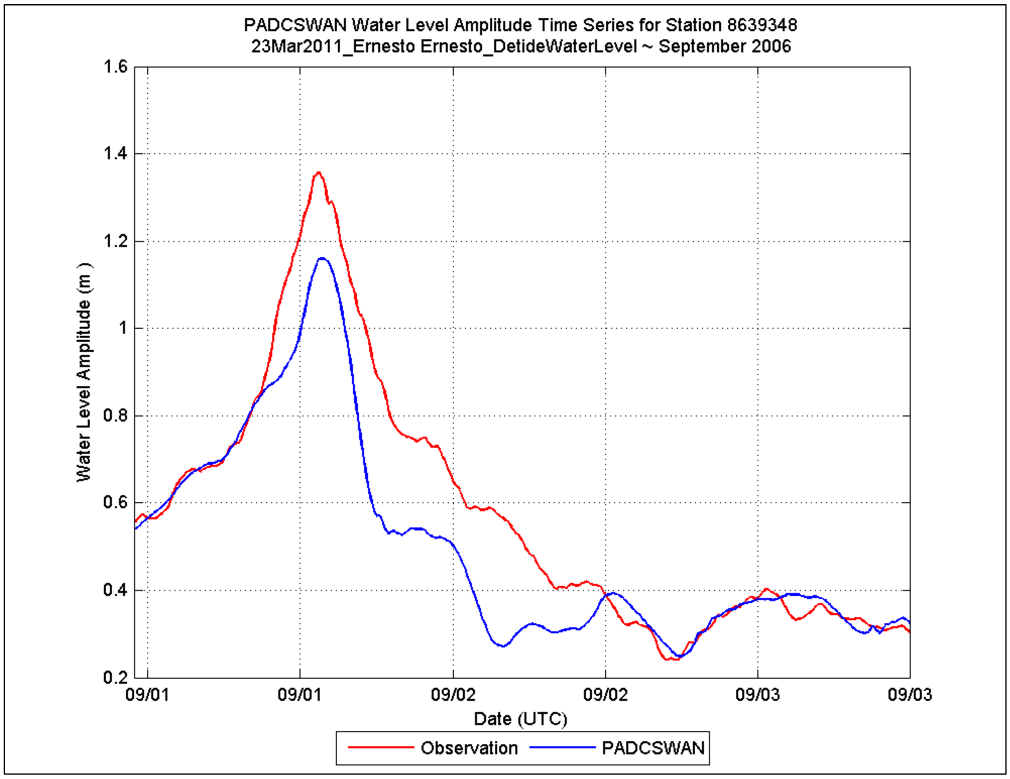

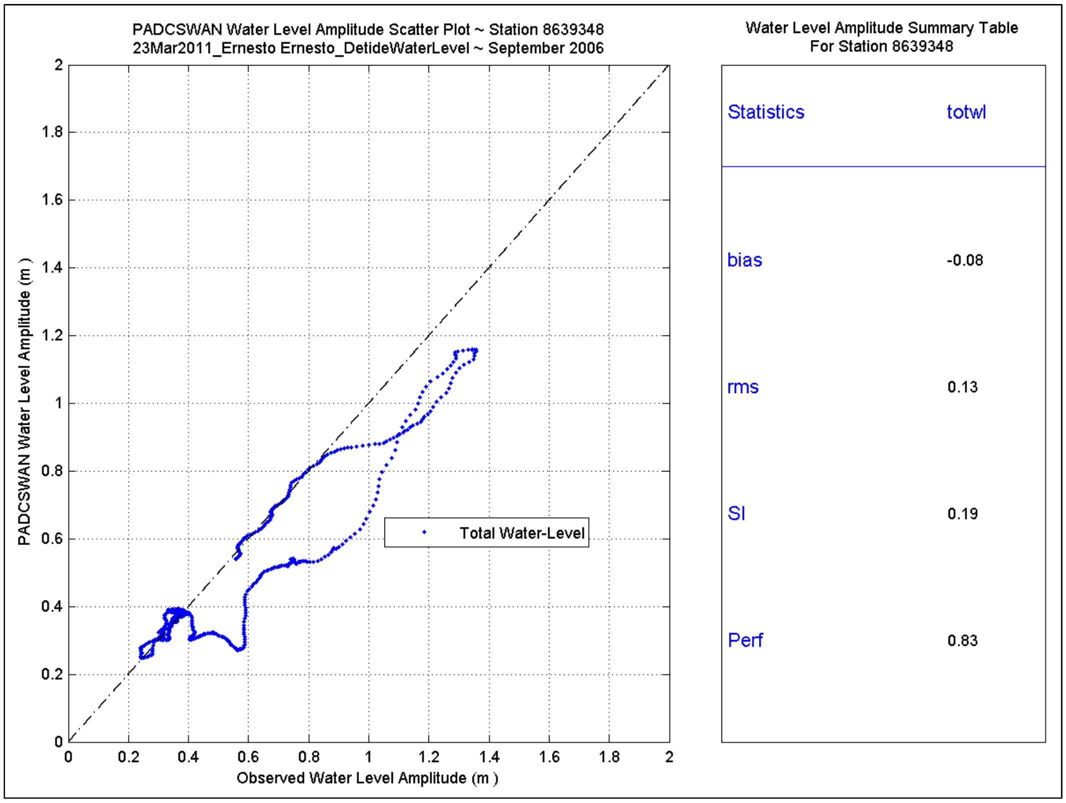

Water Level Amplitude Summary Table
For Station 8639348

Statistics	totwl
bias	-0.08
rms	0.13
SI	0.19
Perf	0.83

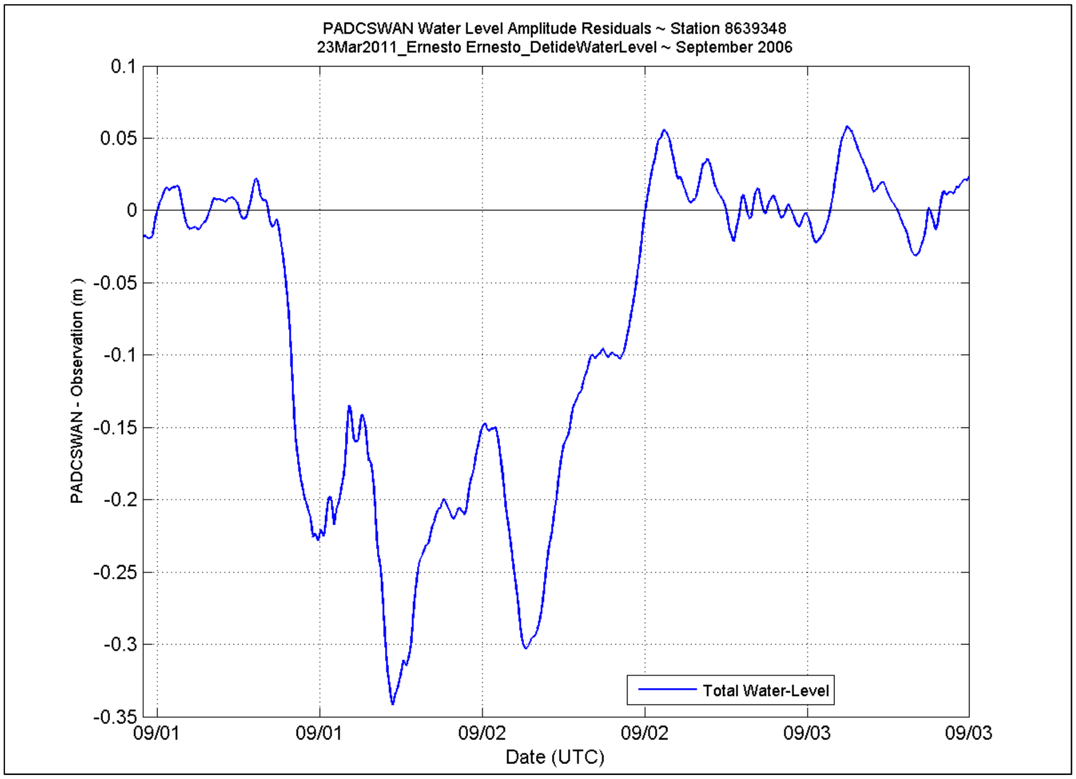
PADCSWAN Water Level Amplitude Residuals ~ Station 8639348
23Mar2011_Ernesto Ernesto_DetideWaterLevel ~ September 2006
PADCSWAN - Observation (m)
0.1
0.05
0
-0.05
-0.1
-0.15
-0.2
-0.25
-0.3
-0.35
09/01
09/01
09/02
09/02
09/03
09/03
Date (UTC)
Total Water-Level

Appendix C: Detided TidesSugeWaves Water Level Data, Extra-tropical Storm Ida

Data plots in this section refer to the PADCSWAN Detided TidesWindsWaves water level for Nor'easter Ida (Nor'Ida), November 2009.

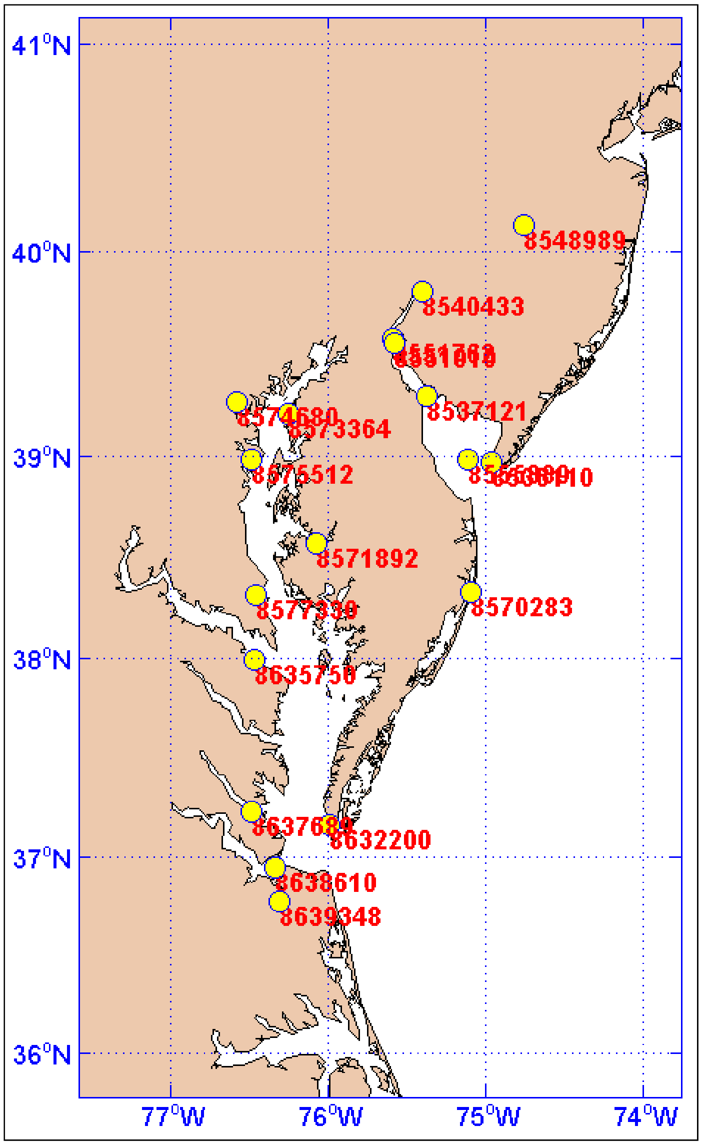
41°N
40°N
39°N
38°N
37°N
36°N
77°W
76°W
75°W
74°W
8548989
8540433
8537121
8574680
8573364
8575512
8571892
8570283
8577330
8635750
8637689
8632200
8638610
8639348

Figure C1. NOAA water level station locations for Detided TidesWindsWaves, Nor'Ida.

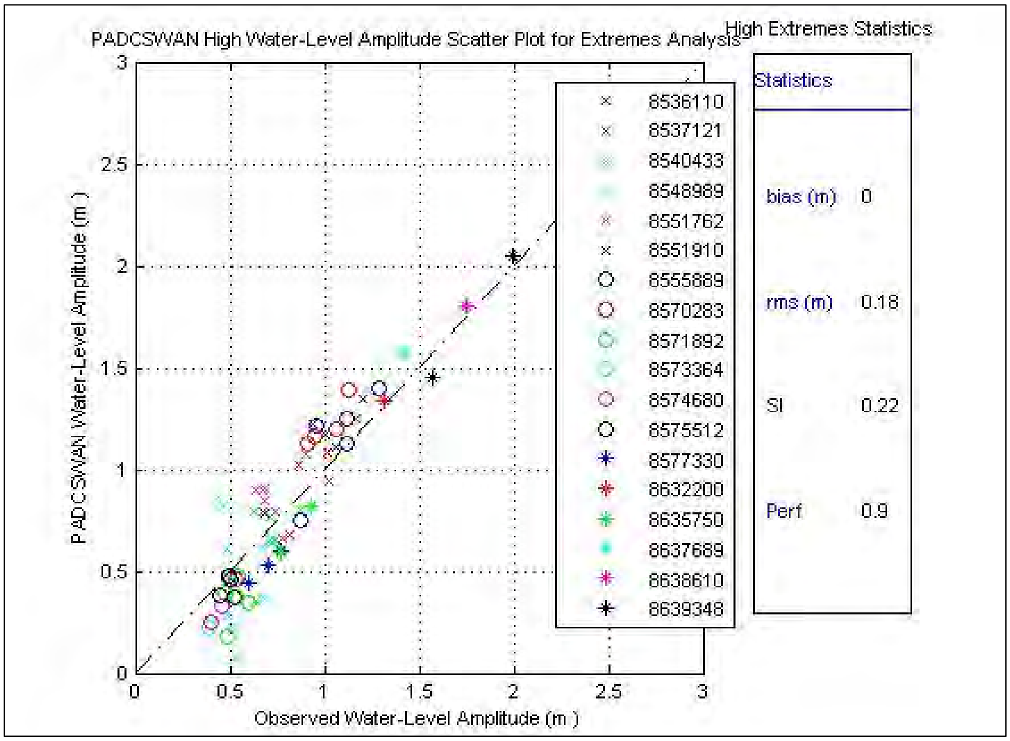

Figure C2. High-water level extremes analysis, Detided TidesWindsWaves, Nor'Ida.

Station 8536110

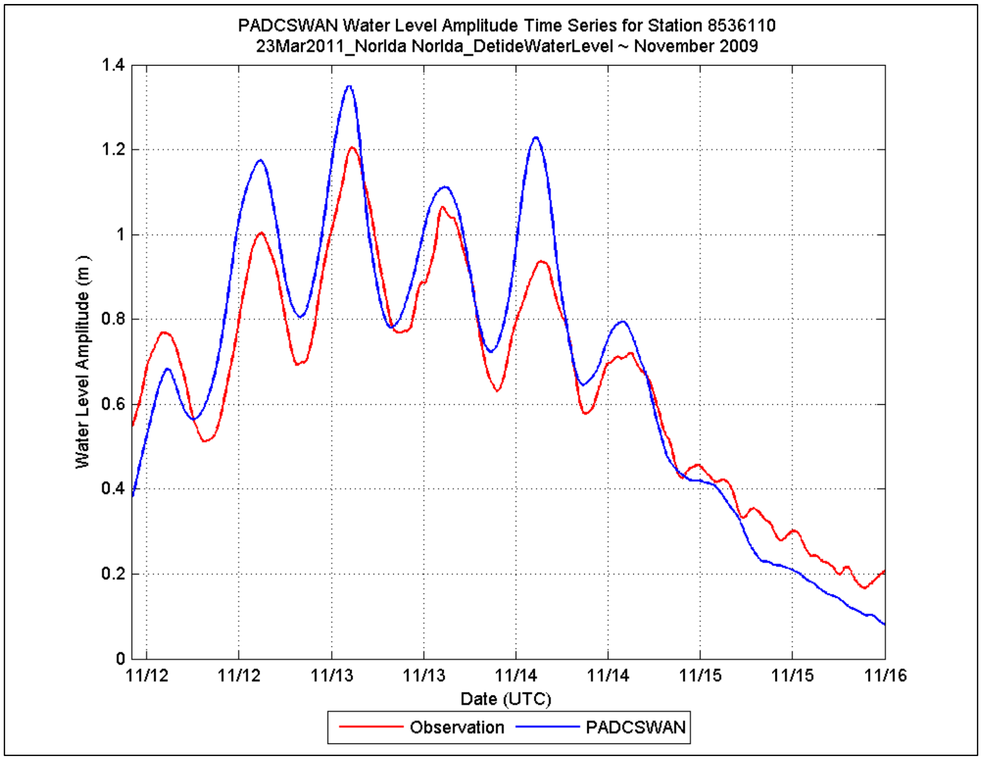

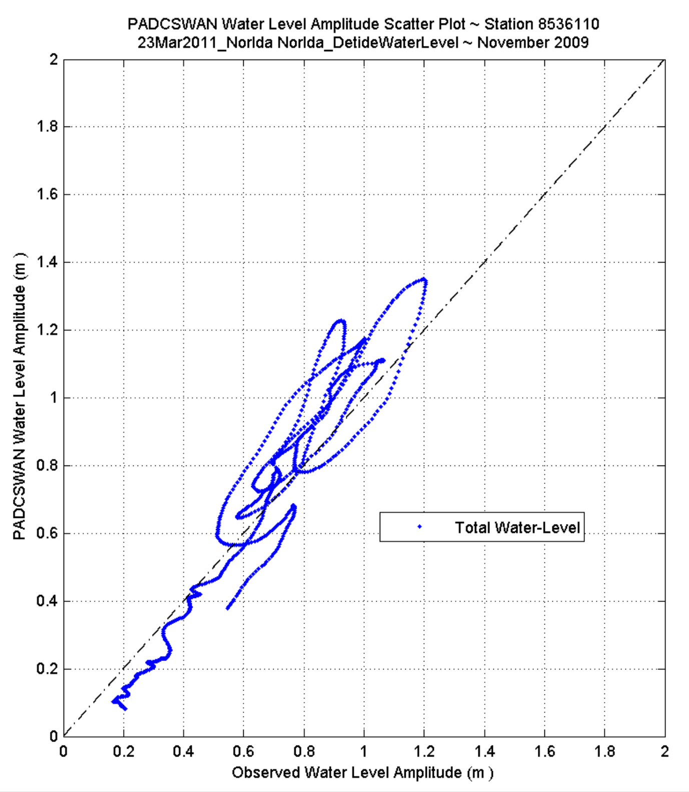

Water Level Amplitude Summary Table
For Station 8536110

Statistics	totwl
bias	0.03
rms	0.11
SI	0.16
Perf	0.9

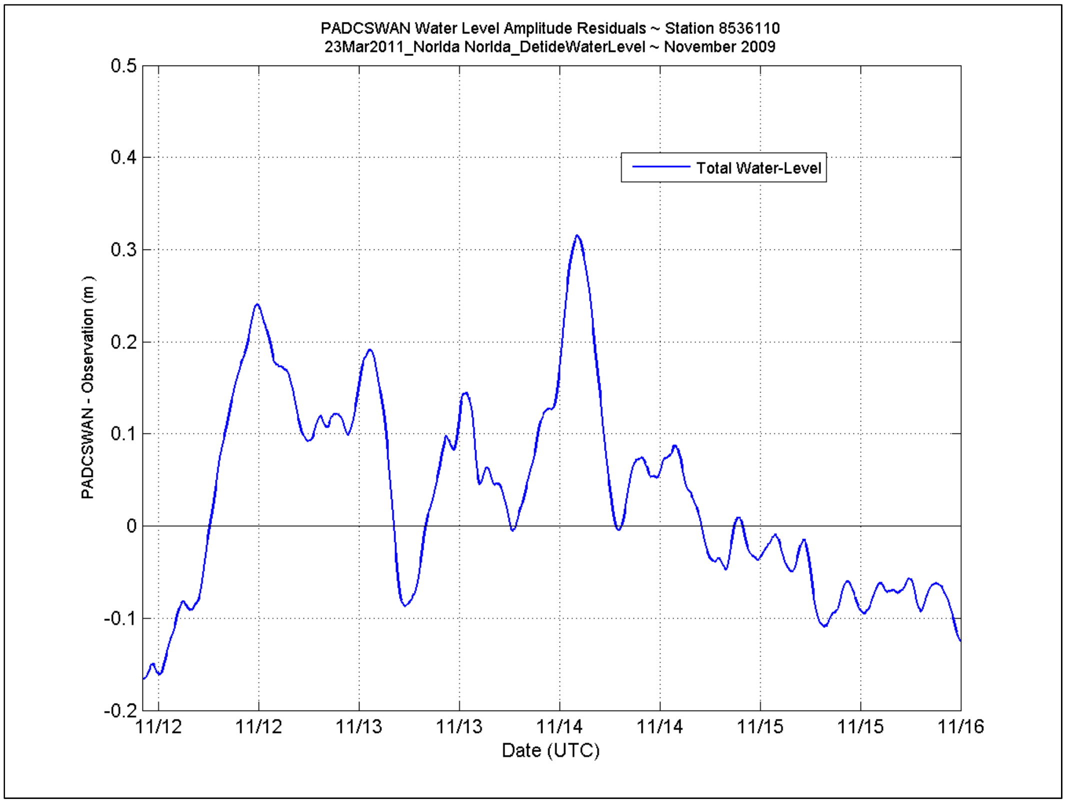
PADCSWAN Water Level Amplitude Residuals ~ Station 8536110
23Mar2011_Norlda Norlda_DetideWaterLevel ~ November 2009
Total Water-Level
PADCSWAN - Observation (m)
0.5
0.4
0.3
0.2
0.1
0
-0.1
-0.2
11/12
11/12
11/13
11/13
11/14
11/14
11/15
11/15
11/16
Date (UTC)

Station 8537121

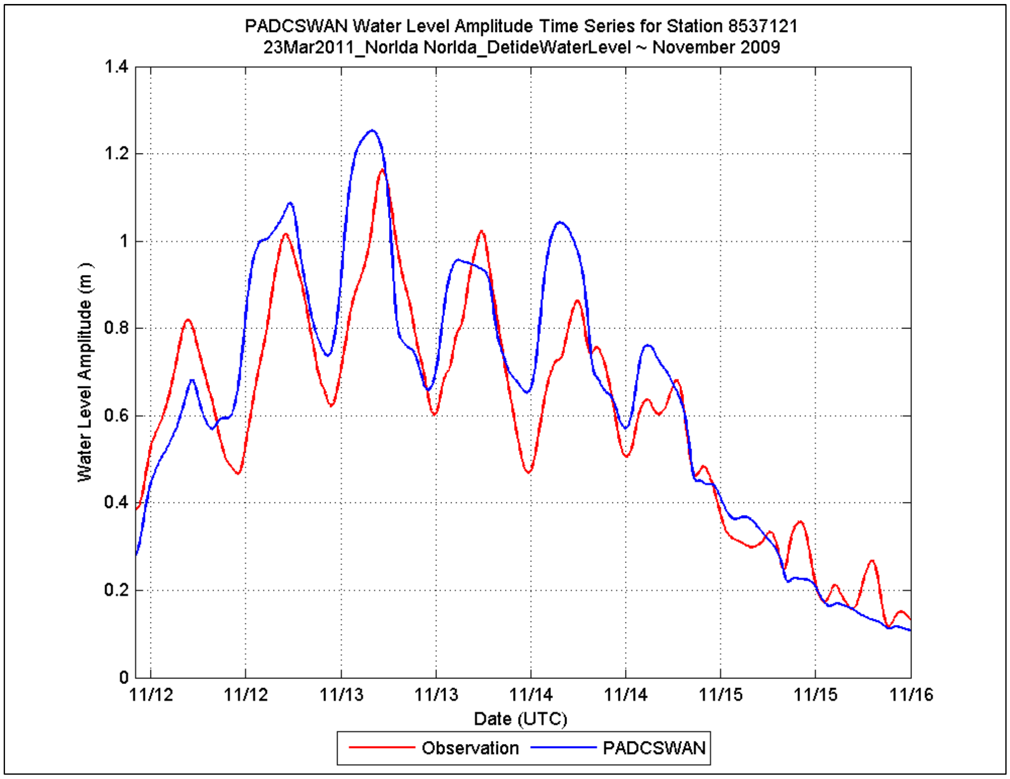

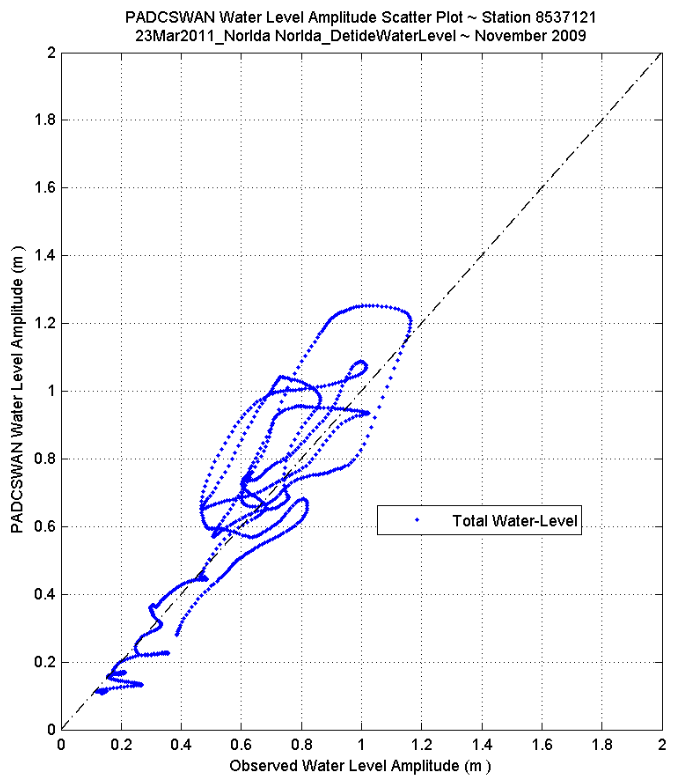

Water Level Amplitude Summary Table
For Station 8537121

Statistics	totwl
bias	0.04
rms	0.13
SI	0.21
Perf	0.87

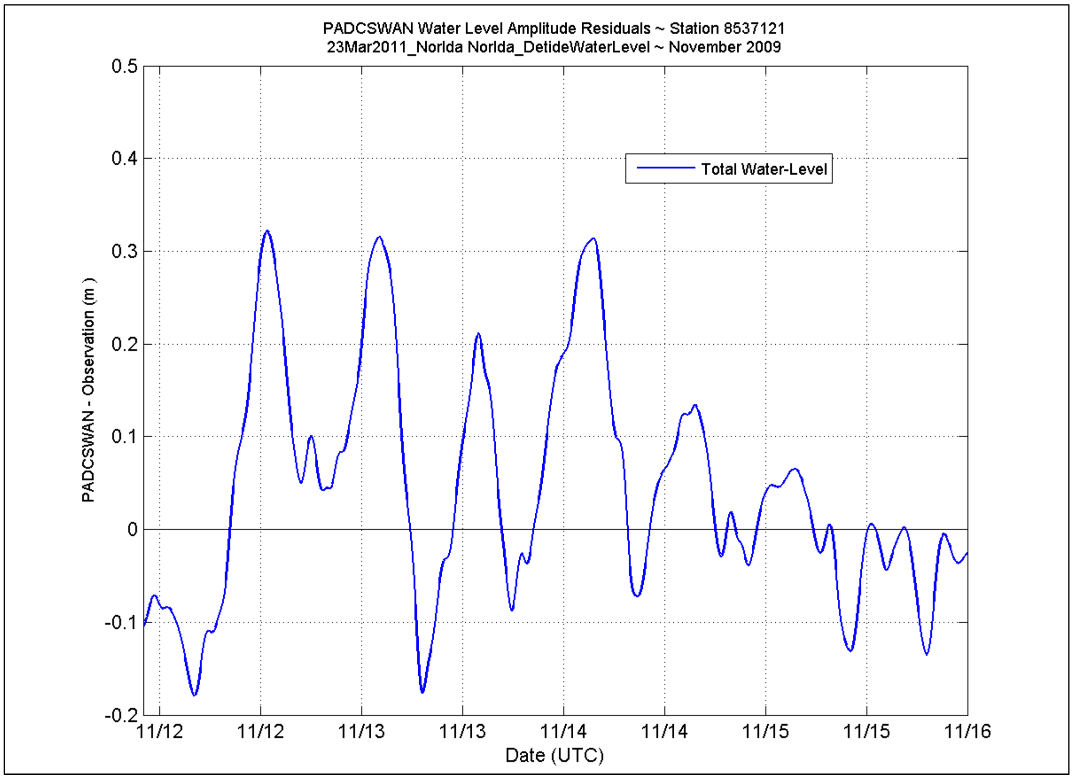
PADCSWAN Water Level Amplitude Residuals ~ Station 8537121
23Mar2011_Norlda Norlda_DetideWaterLevel ~ November 2009
Total Water-Level
PADCSWAN - Observation (m)
0.5
0.4
0.3
0.2
0.1
0
-0.1
-0.2
11/12
11/12
11/13
11/13
11/14
11/14
11/15
11/15
11/16
Date (UTC)

Station 8540433

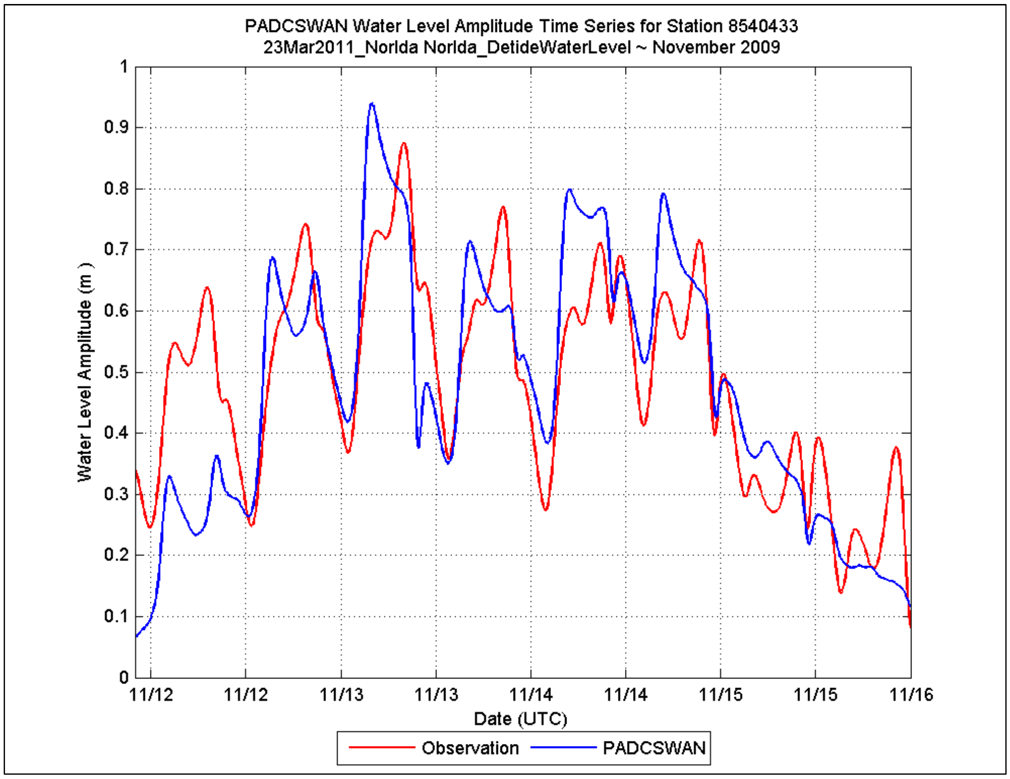

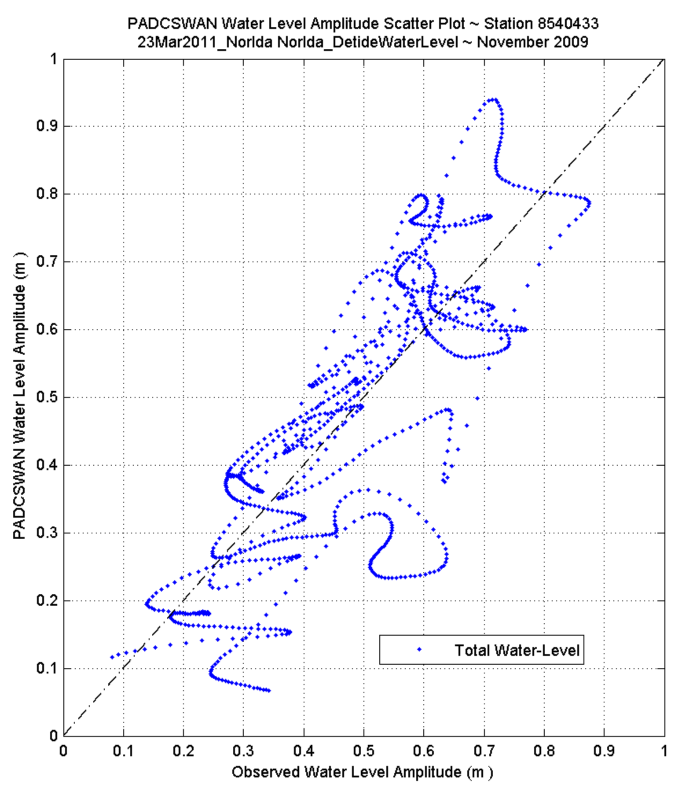

Water Level Amplitude Summary Table
For Station 8540433

Statistics	totwl
bias	-0.01
rms	0.12
SI	0.26
Perf	0.87

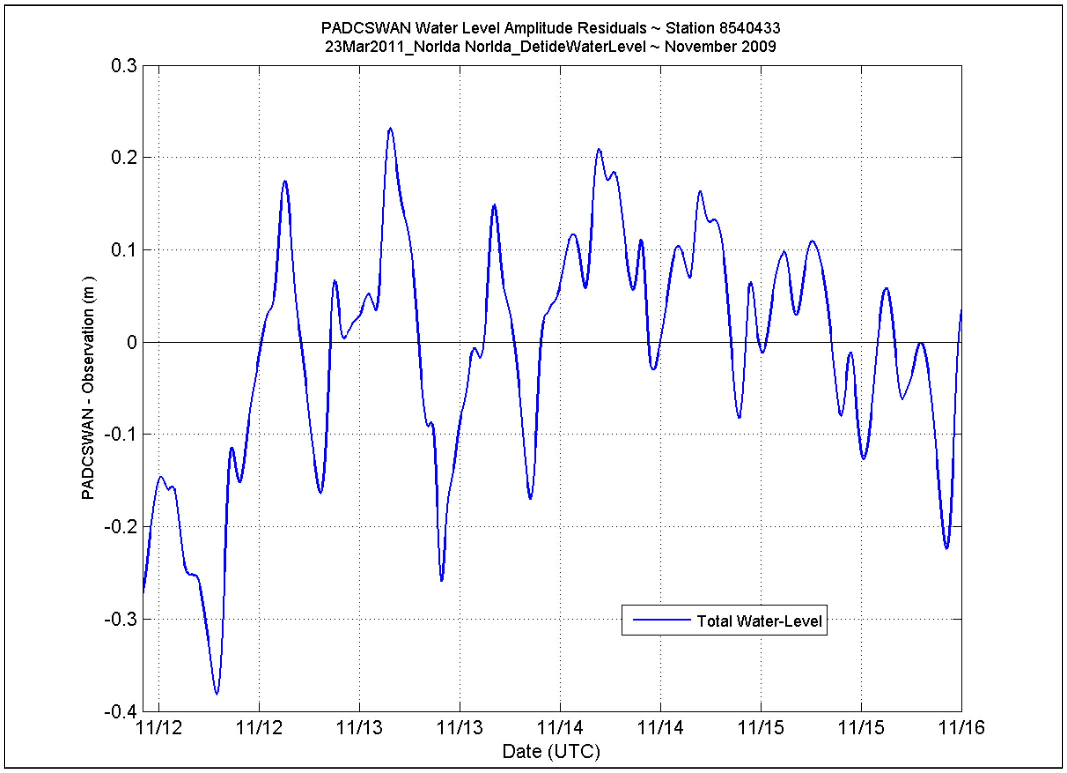
PADCSWAN Water Level Amplitude Residuals ~ Station 8540433
23Mar2011_Norlda Norlda_DetideWaterLevel ~ November 2009
PADCSWAN - Observation (m)
0.3
0.2
0.1
0
-0.1
-0.2
-0.3
-0.4
11/12
11/12
11/13
11/13
11/14
11/14
11/15
11/15
11/16
Date (UTC)
Total Water-Level

Station 8548989

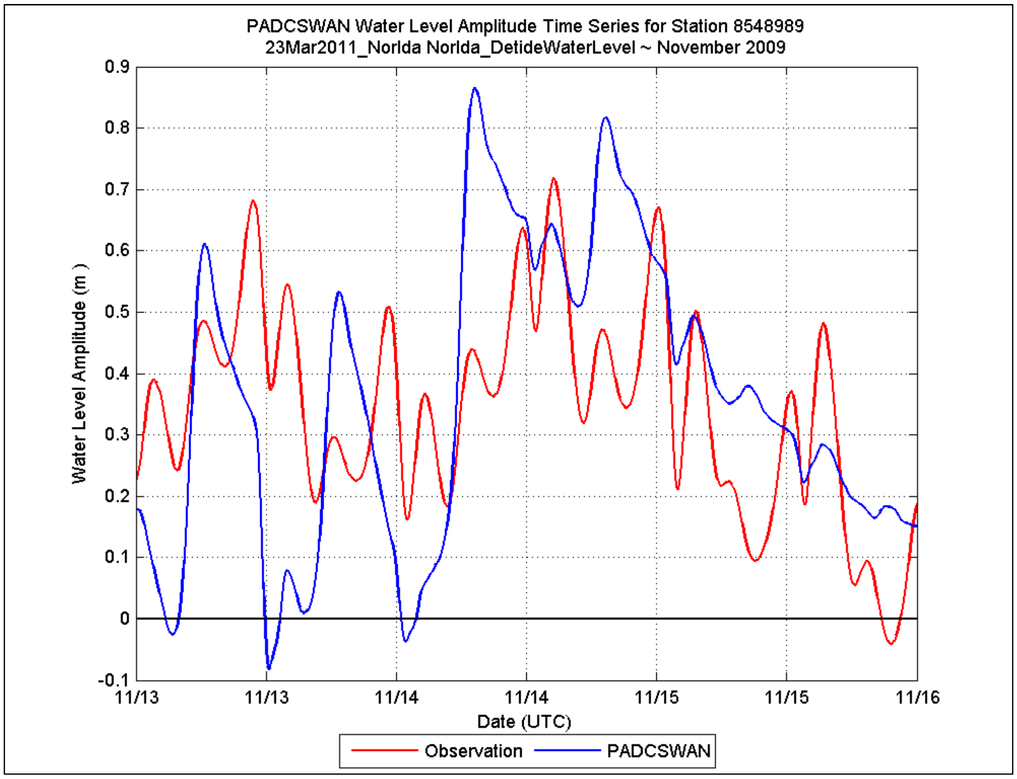

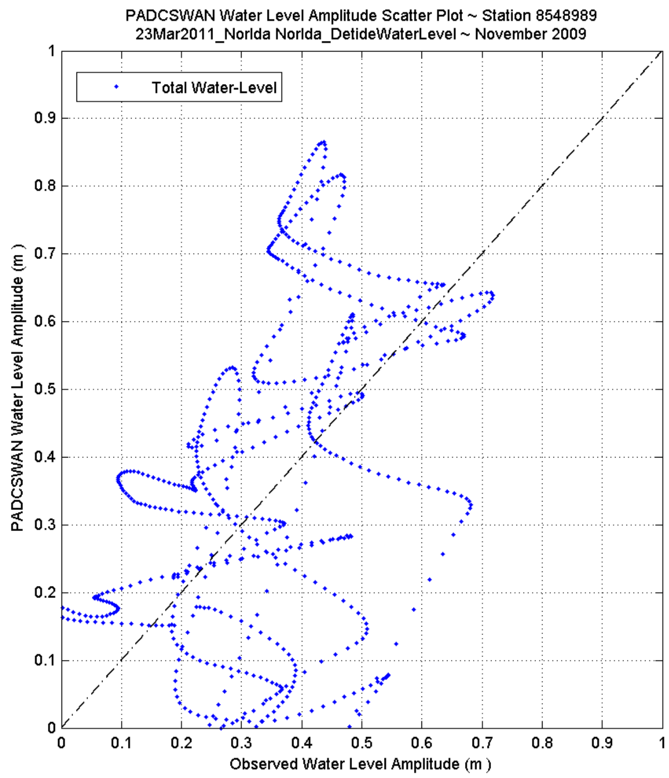

Water Level Amplitude Summary Table
For Station 8548989

Statistics	totwl
bias	0.01
rms	0.22
SI	0.65
Perf	0.69

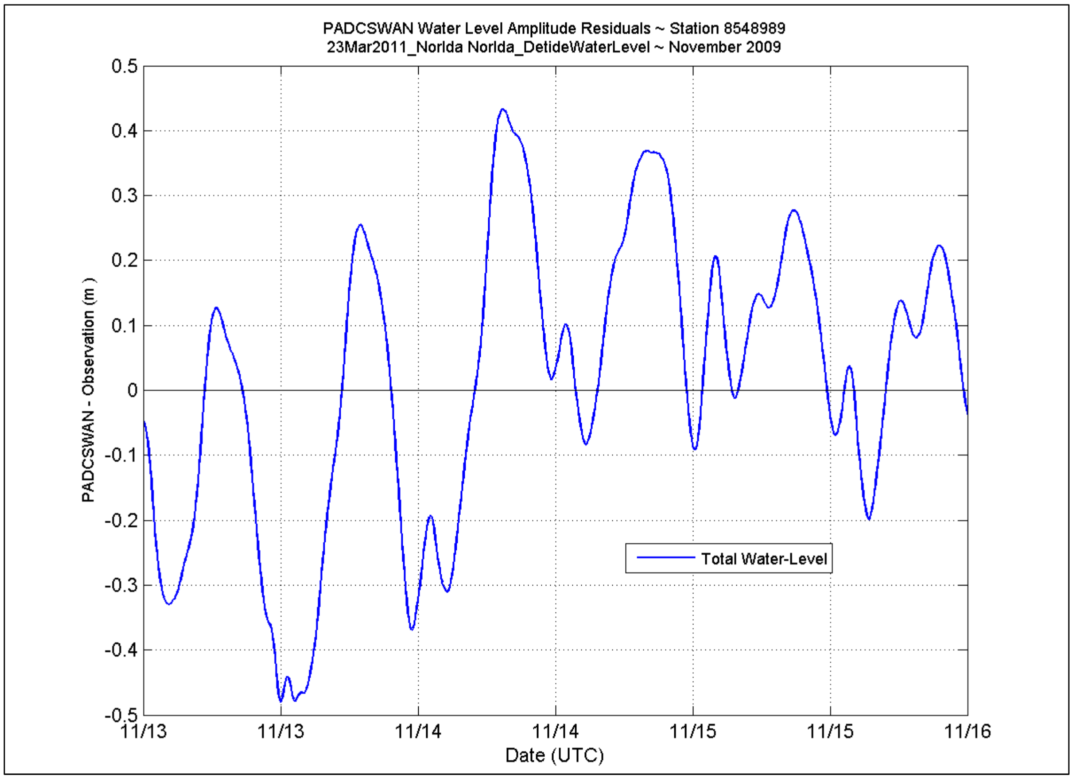
PADCSWAN Water Level Amplitude Residuals ~ Station 8548989
23Mar2011_Norlda Norlda_DetideWaterLevel ~ November 2009
PADCSWAN - Observation (m)
0.5
0.4
0.3
0.2
0.1
0
-0.1
-0.2
-0.3
-0.4
-0.5
11/13
11/13
11/14
11/14
11/15
11/15
11/16
Date (UTC)
Total Water-Level

Station 8551762

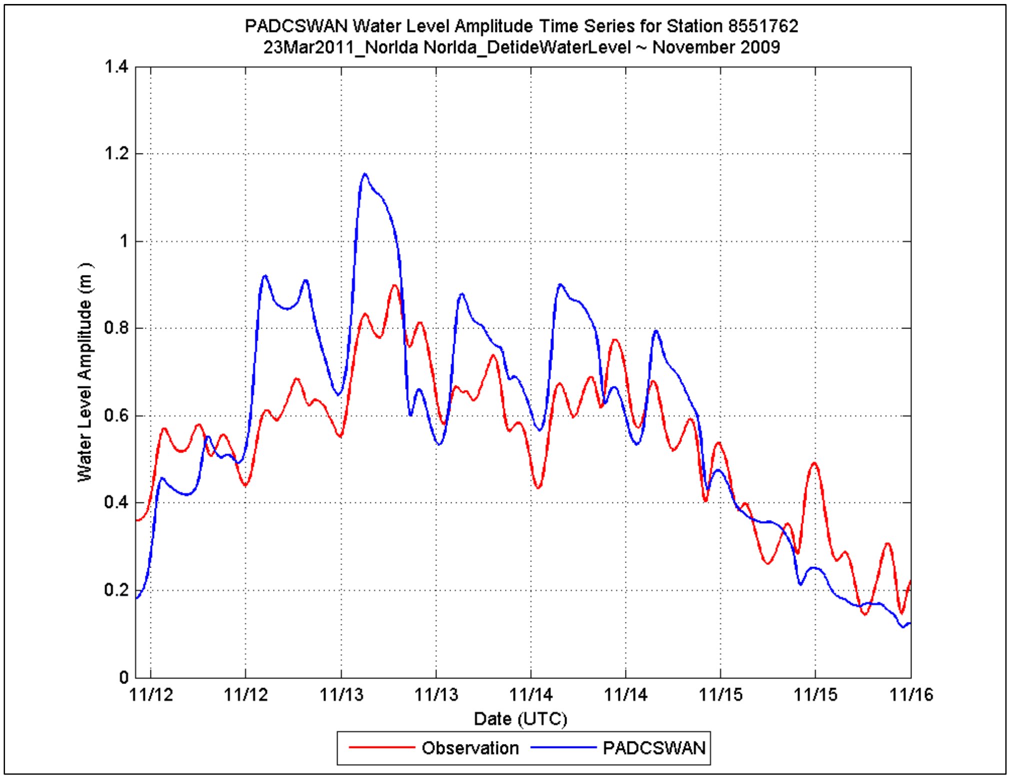

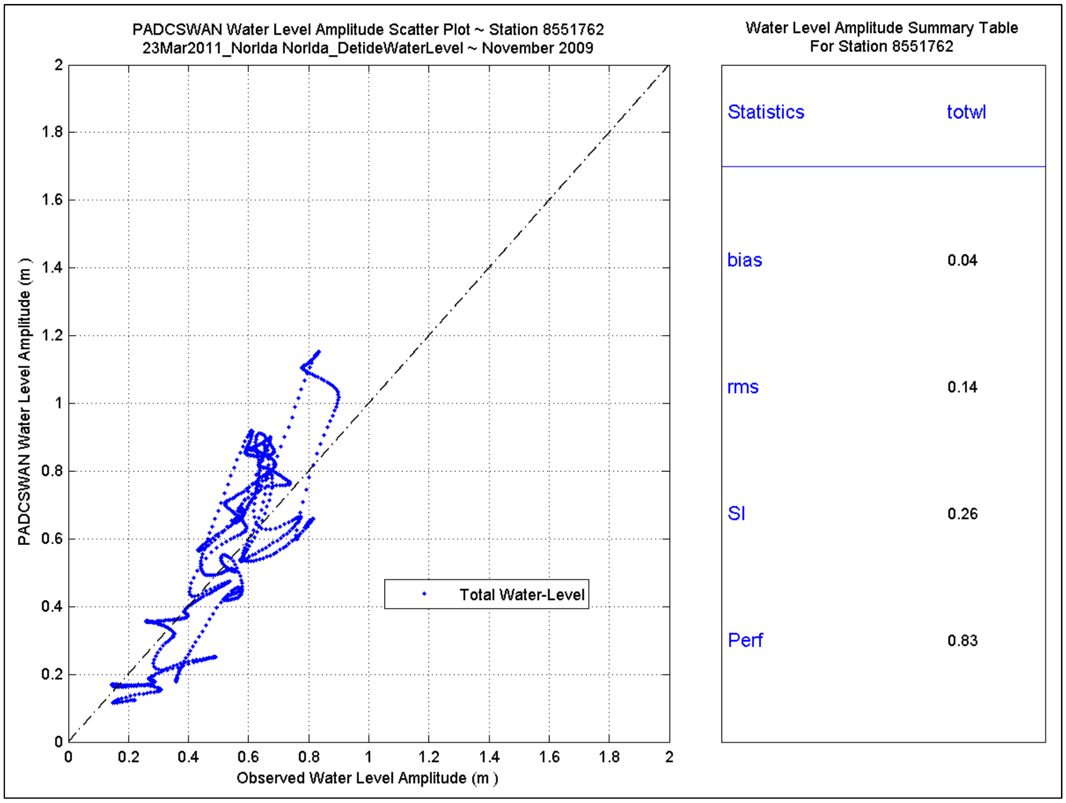

Water Level Amplitude Summary Table
For Station 8551762

Statistics	totwl
bias	0.04
rms	0.14
SI	0.26
Perf	0.83

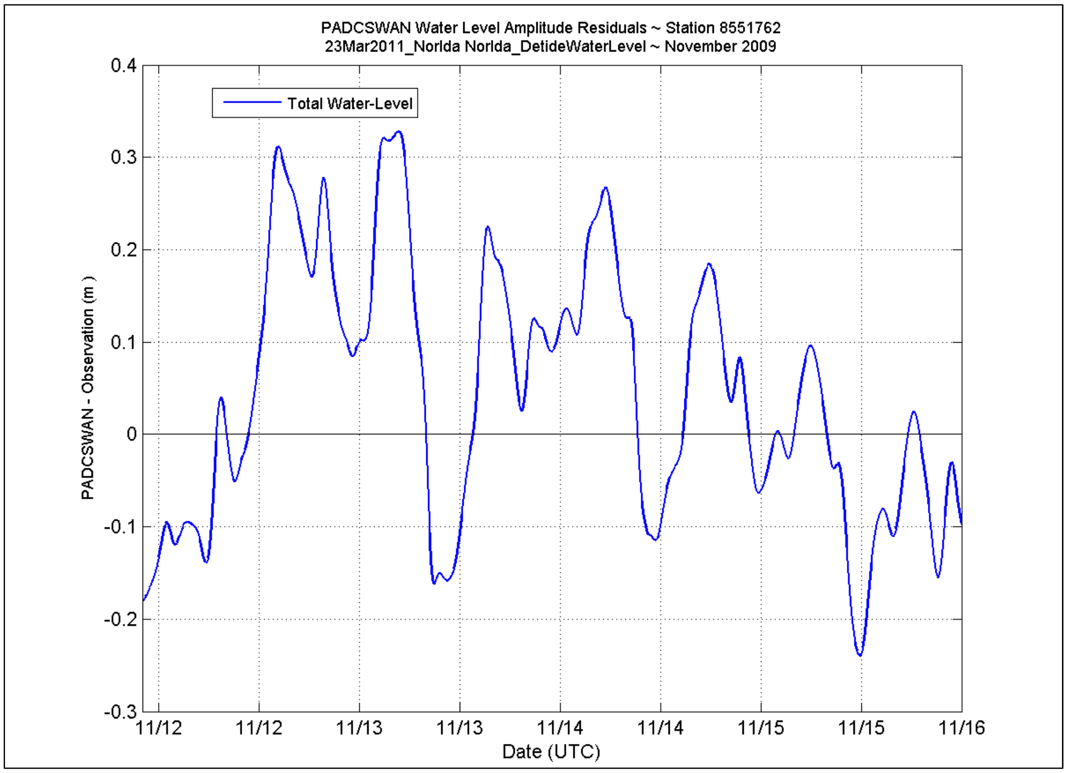
PADCSWAN Water Level Amplitude Residuals ~ Station 8551762
23Mar2011_Norlda Norlda_DetideWaterLevel ~ November 2009
Total Water-Level
PADCSWAN - Observation (m)
0.4
0.3
0.2
0.1
0
-0.1
-0.2
-0.3
11/12
11/12
11/13
11/13
11/14
11/14
11/15
11/15
11/16
Date (UTC)

Station 8551910

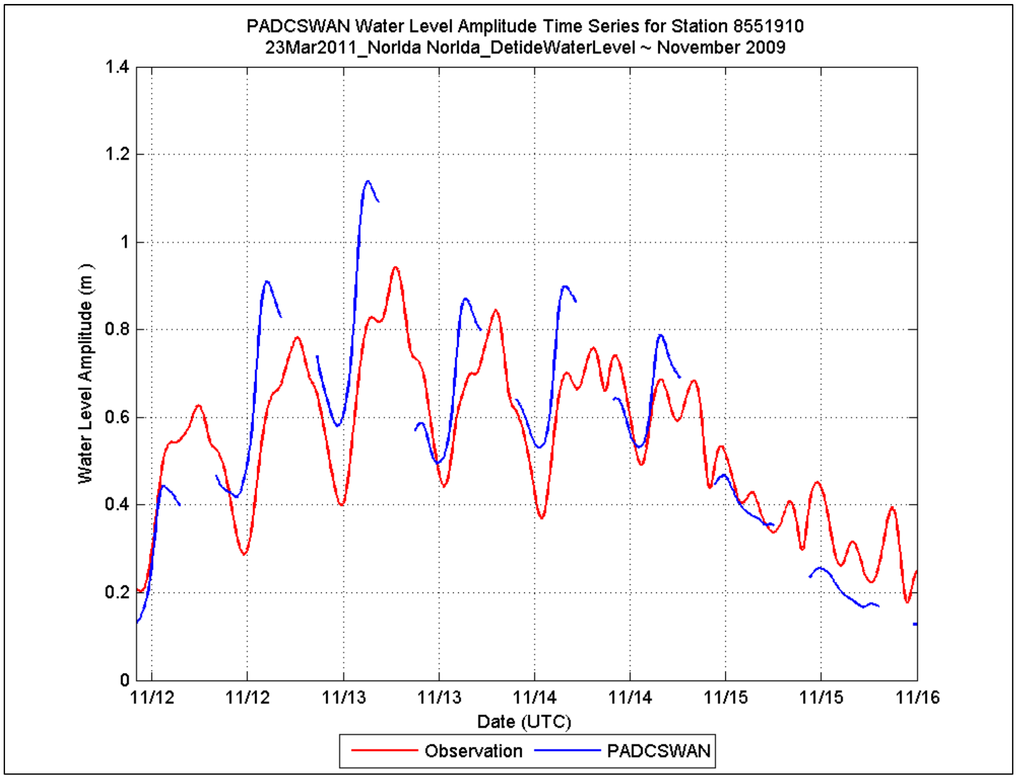

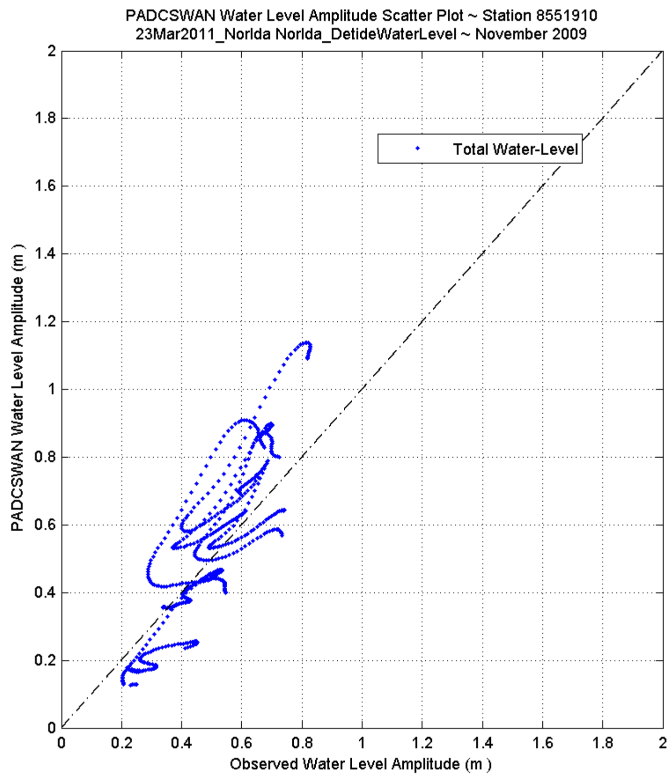

Water Level Amplitude Summary Table
For Station 8551910

Statistics	totwl
bias	0.05
rms	0.14
SI	0.26
Perf	0.82

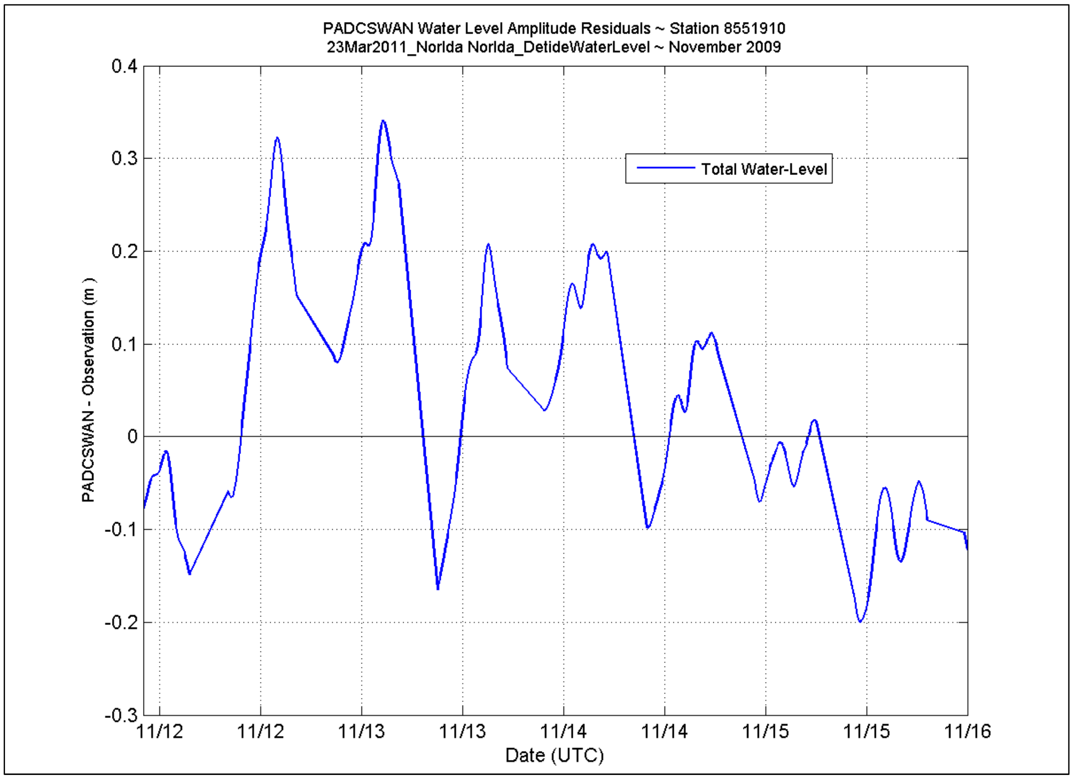
PADCSWAN Water Level Amplitude Residuals ~ Station 8551910
23Mar2011_Norlda Norlda_DetideWaterLevel ~ November 2009
Total Water-Level
PADCSWAN - Observation (m)
0.4
0.3
0.2
0.1
0
-0.1
-0.2
-0.3
11/12
11/12
11/13
11/13
11/14
11/14
11/15
11/15
11/16
Date (UTC)

Station 8555889

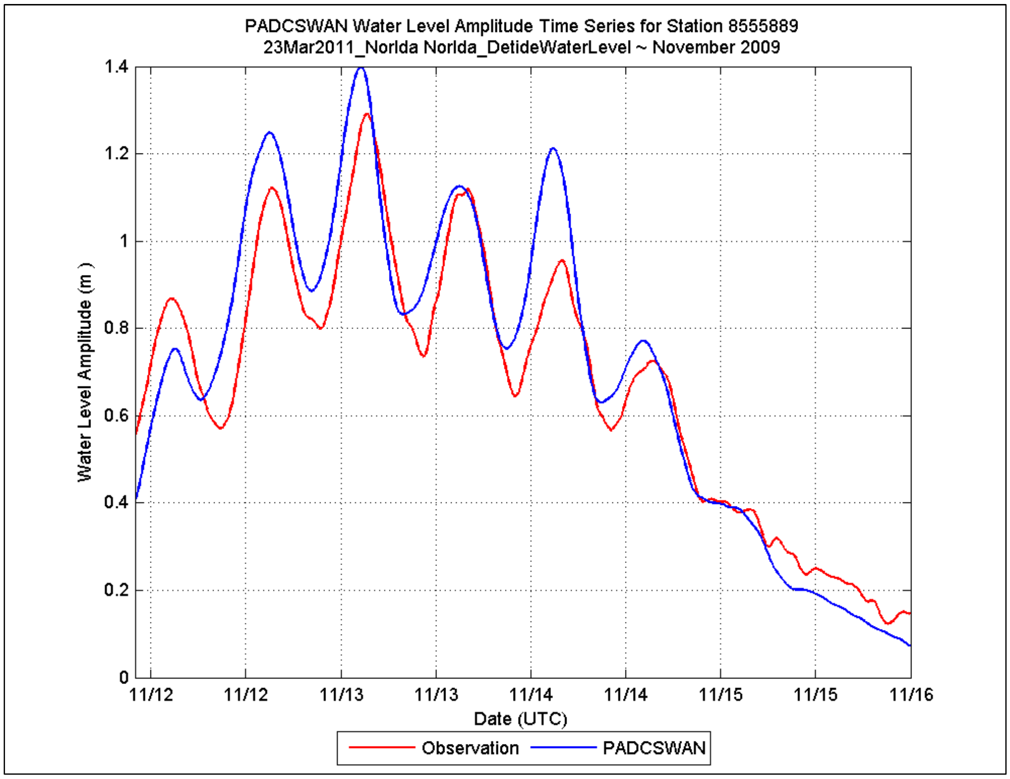

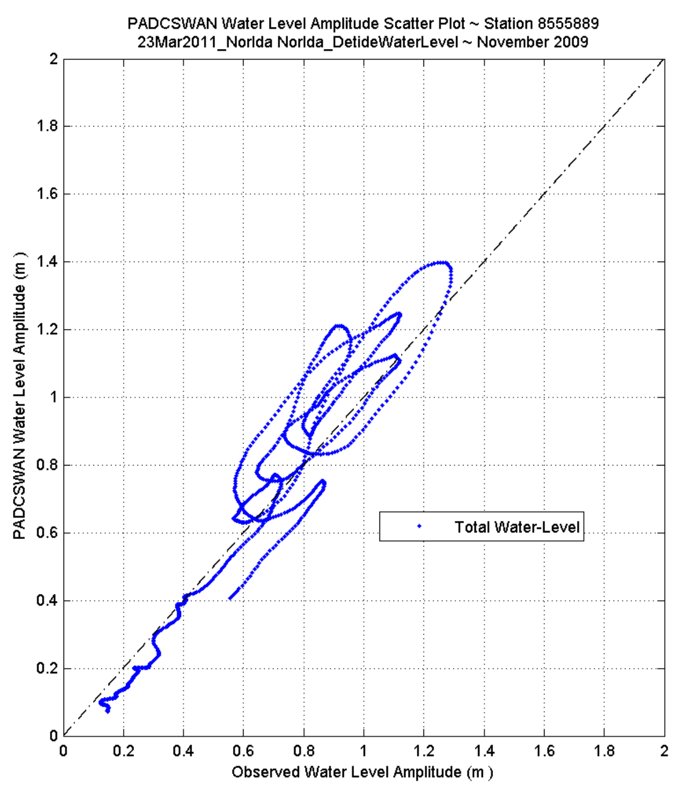

Water Level Amplitude Summary Table
For Station 8555889

Statistics	totwl
bias	0.03
rms	0.11
SI	0.16
Perf	0.9

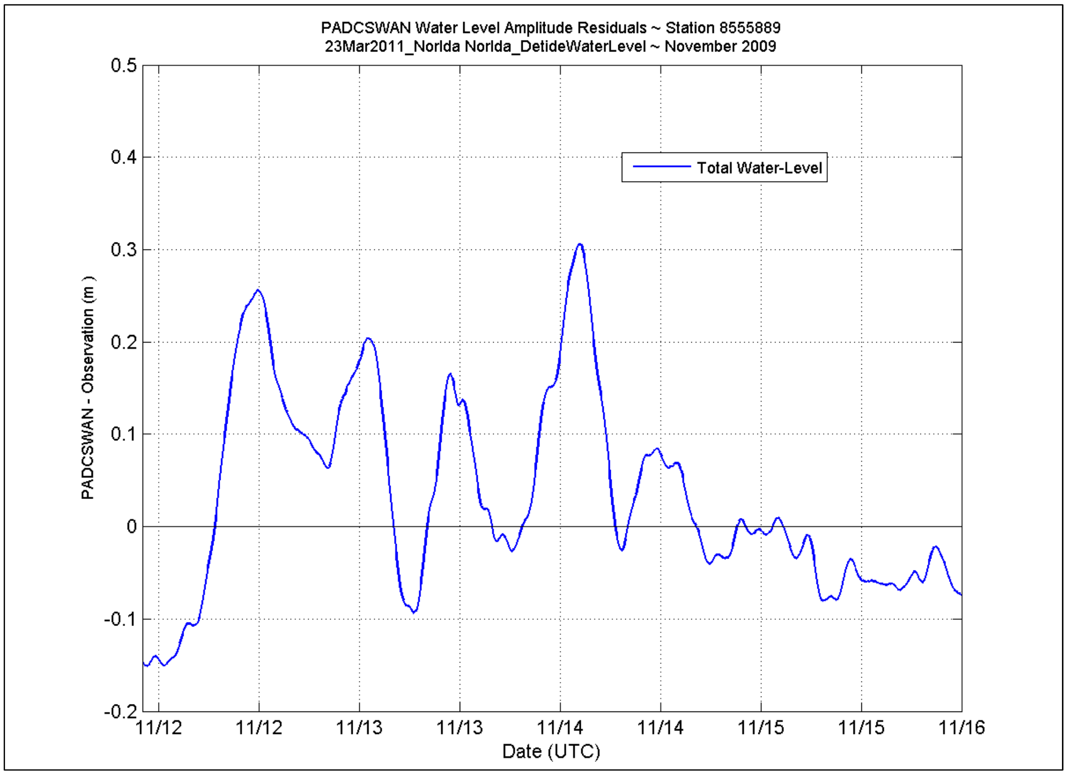
PADCSWAN Water Level Amplitude Residuals ~ Station 8555889
23Mar2011_Norlda Norlda_DetideWaterLevel ~ November 2009
Total Water-Level
PADCSWAN - Observation (m)
0.5
0.4
0.3
0.2
0.1
0
-0.1
-0.2
11/12
11/12
11/13
11/13
11/14
11/14
11/15
11/15
11/16
Date (UTC)

Station 8570283

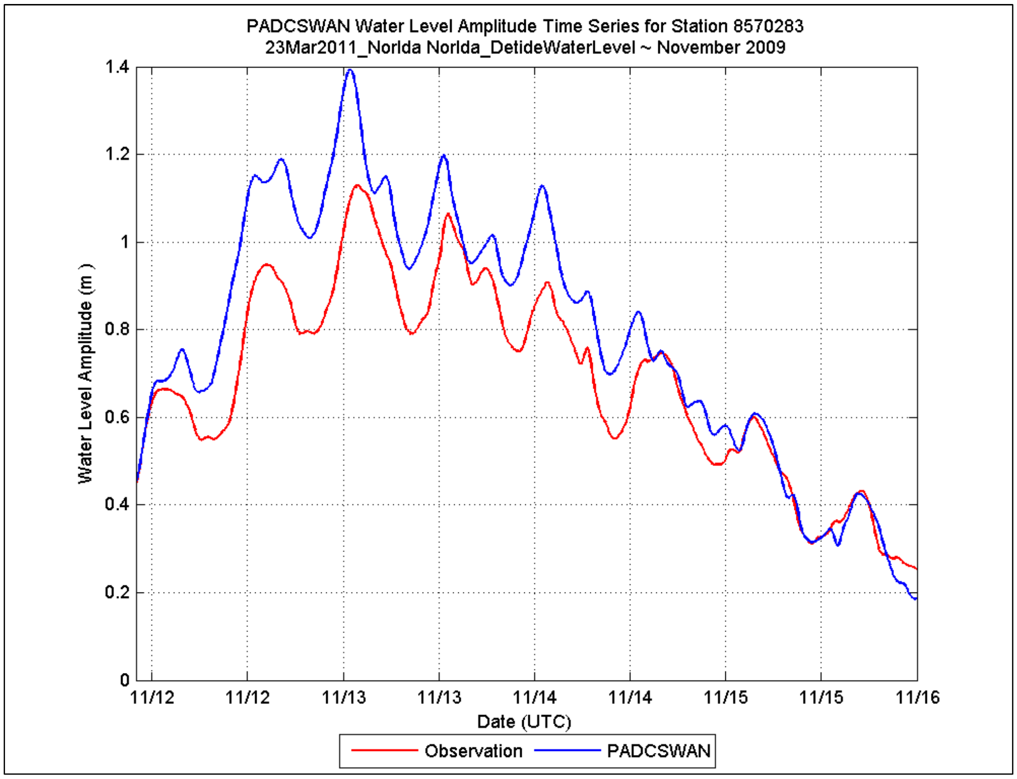

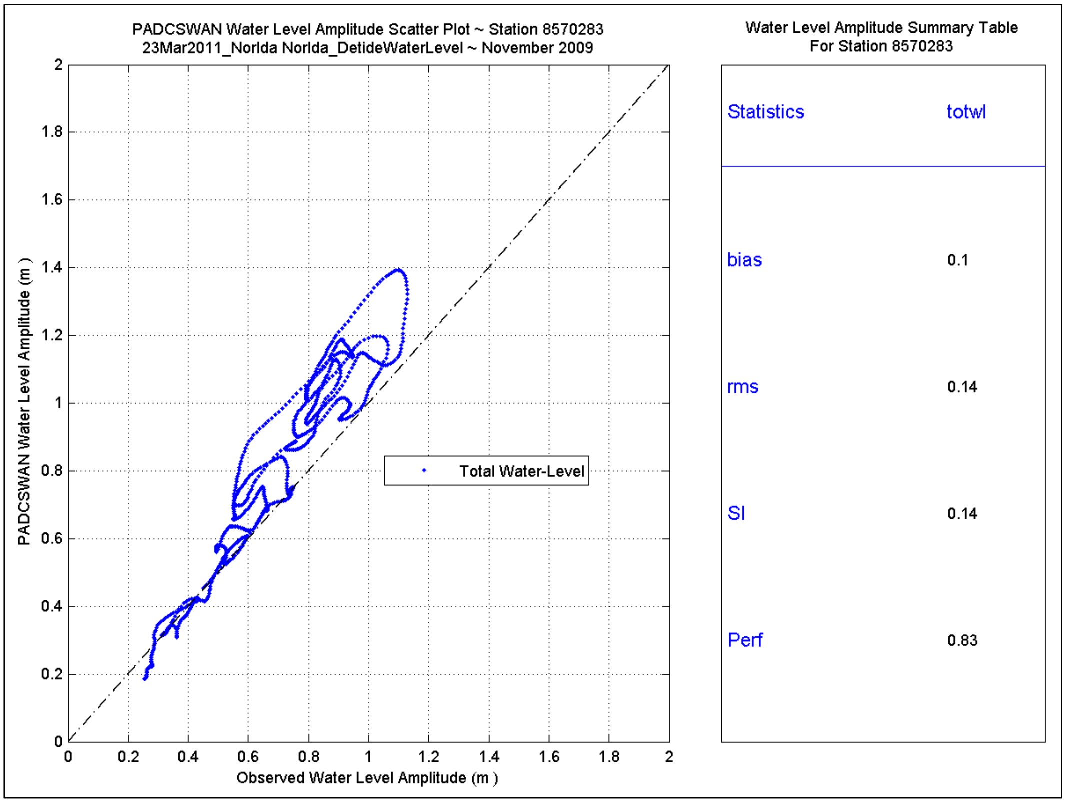

Water Level Amplitude Summary Table
For Station 8570283

Statistics	totwl
bias	0.1
rms	0.14
SI	0.14
Perf	0.83

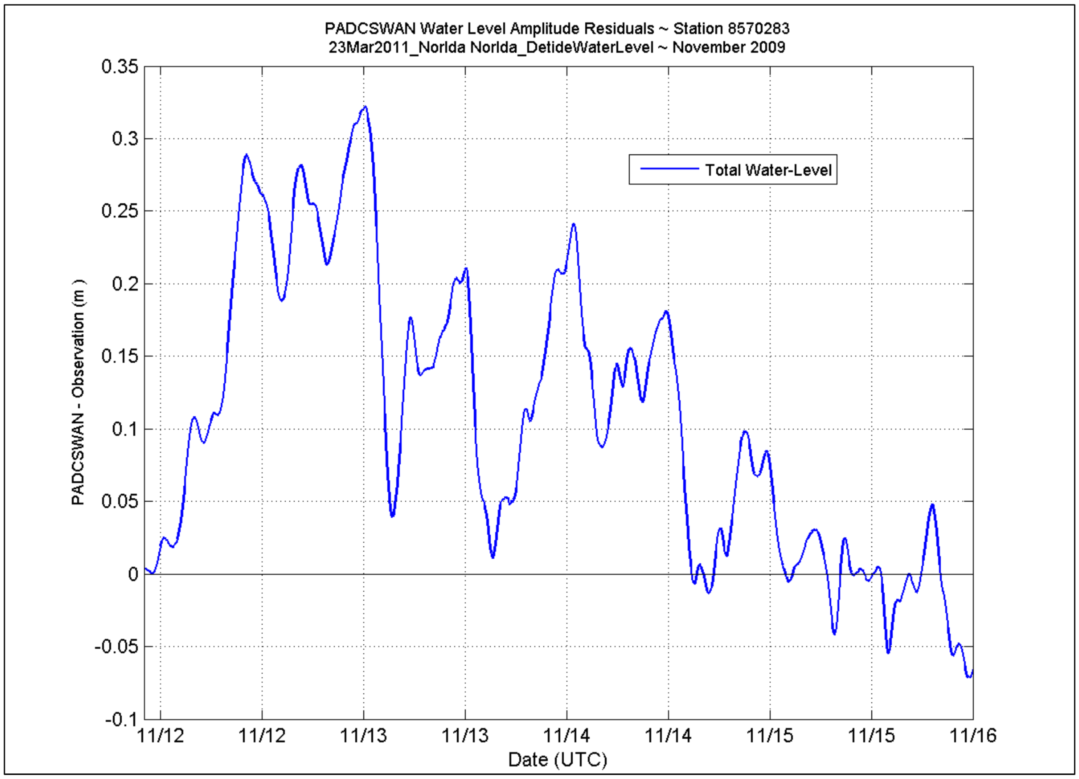
PADCSWAN Water Level Amplitude Residuals ~ Station 8570283
23Mar2011_Norlda Norlda_DetideWaterLevel ~ November 2009
PADCSWAN - Observation (m)
0.35
0.3
0.25
0.2
0.15
0.1
0.05
0
-0.05
-0.1
11/12
11/12
11/13
11/13
11/14
11/14
11/15
11/15
11/16
Date (UTC)
Total Water-Level

Station 8571892

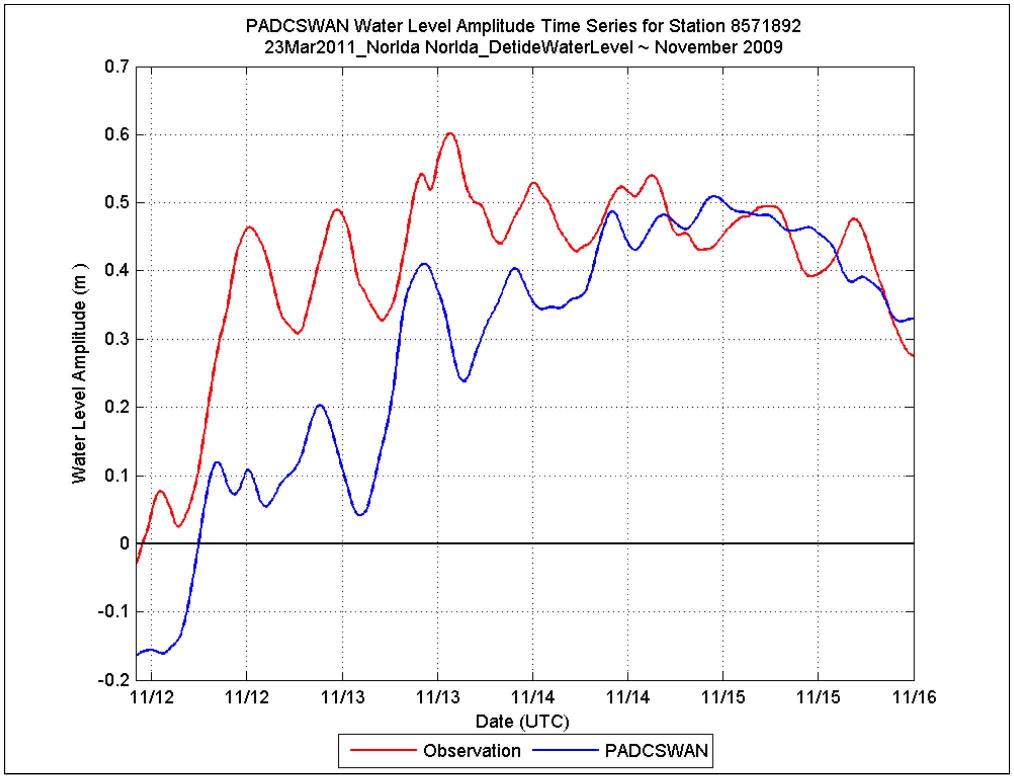

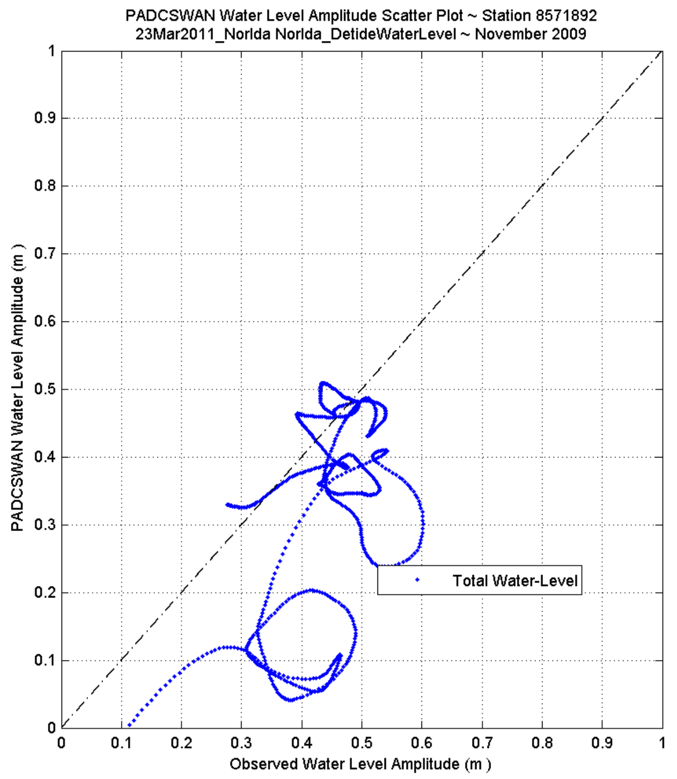

Water Level Amplitude Summary Table
For Station 8571892

Statistics	totwl
bias	-0.12
rms	0.17
SI	0.31
Perf	0.66

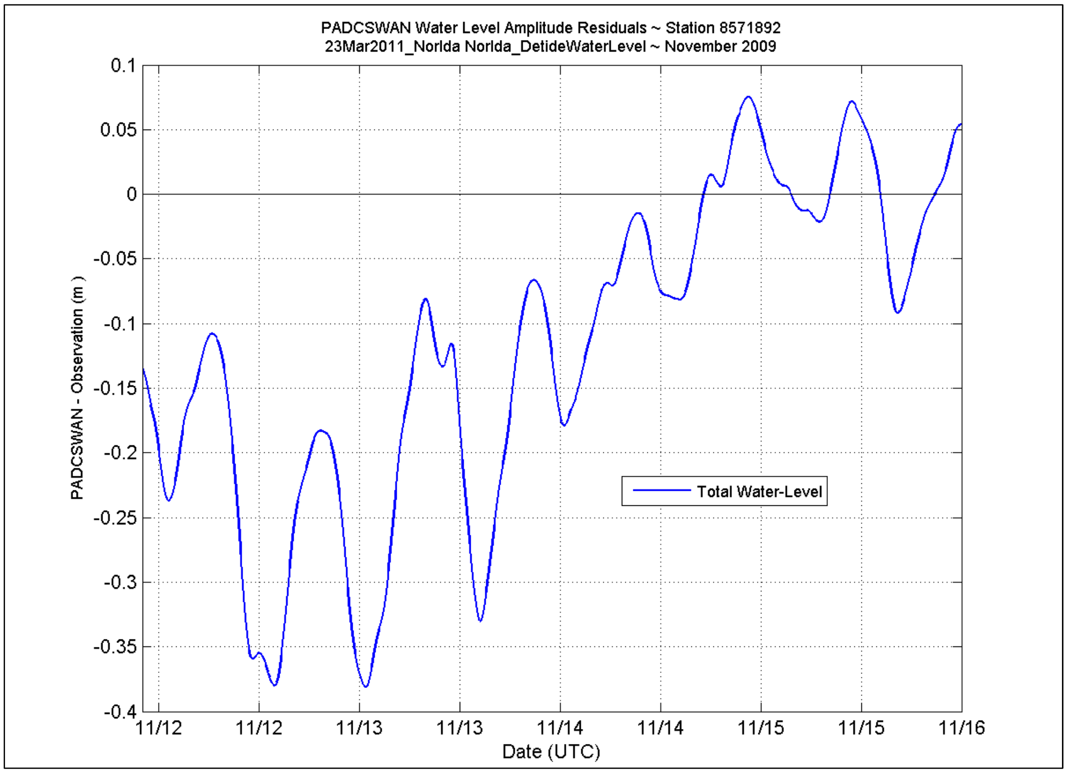
PADCSWAN Water Level Amplitude Residuals ~ Station 8571892
23Mar2011_Norlda Norlda_DetideWaterLevel ~ November 2009
PADCSWAN - Observation (m)
0.1
0.05
0
-0.05
-0.1
-0.15
-0.2
-0.25
-0.3
-0.35
-0.4
11/12
11/12
11/13
11/13
11/14
11/14
11/15
11/15
11/16
Date (UTC)
Total Water-Level

Station 8573364

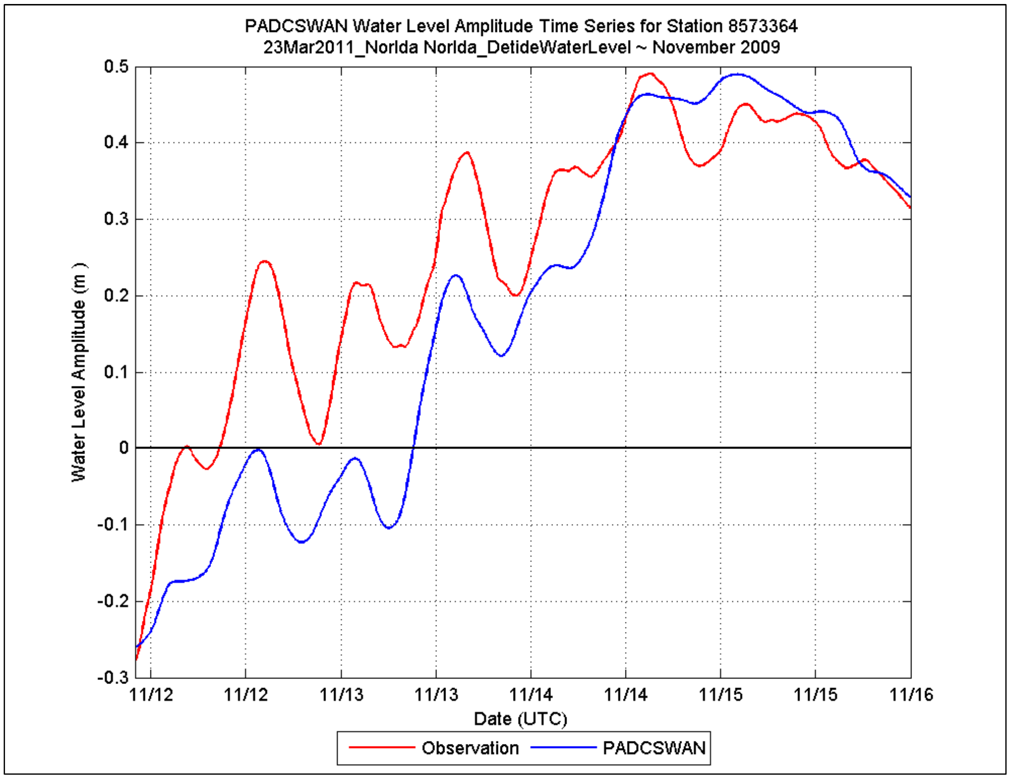

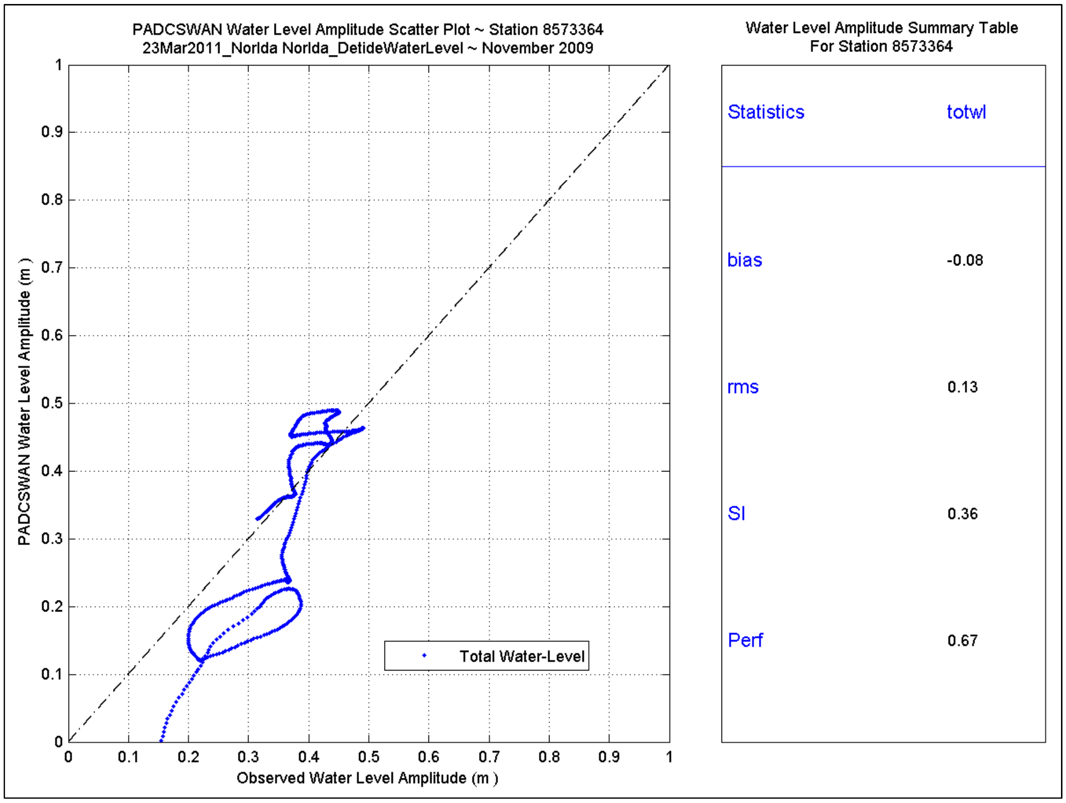

Water Level Amplitude Summary Table
For Station 8573364

Statistics	totwl
bias	-0.08
rms	0.13
SI	0.36
Perf	0.67

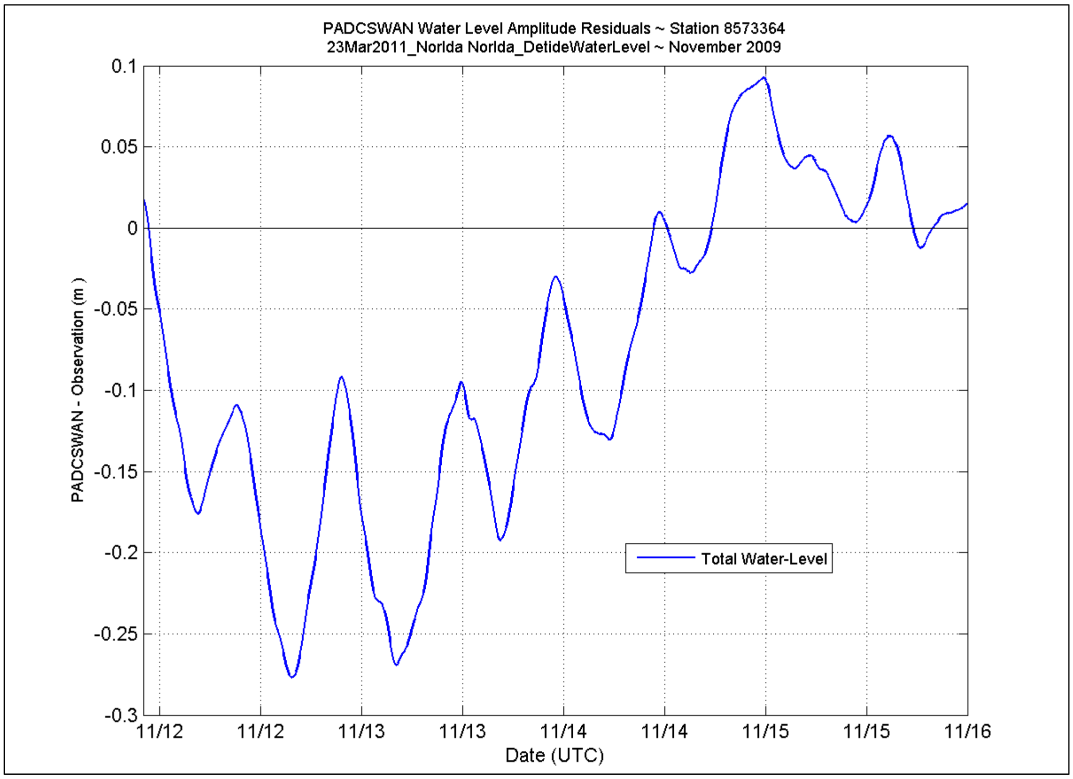
PADCSWAN Water Level Amplitude Residuals ~ Station 8573364
23Mar2011_Norlda Norlda_DetideWaterLevel ~ November 2009
PADCSWAN - Observation (m)
0.1
0.05
0
-0.05
-0.1
-0.15
-0.2
-0.25
-0.3
11/12
11/12
11/13
11/13
11/14
11/14
11/15
11/15
11/16
Date (UTC)
Total Water-Level

Station 8574680

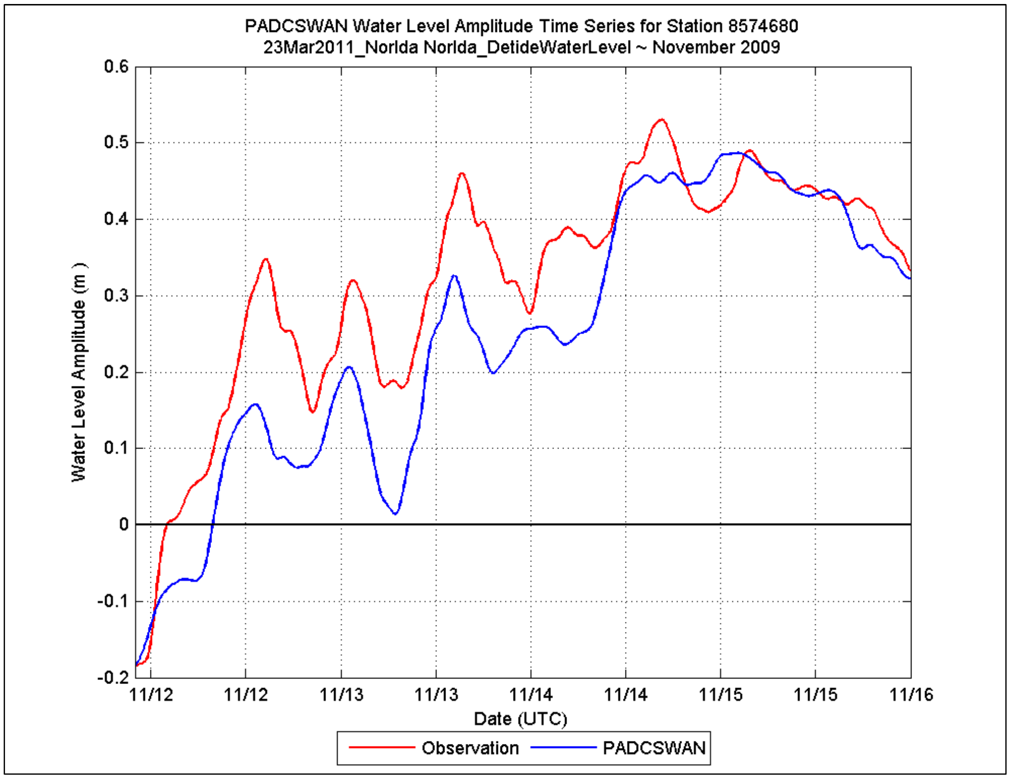

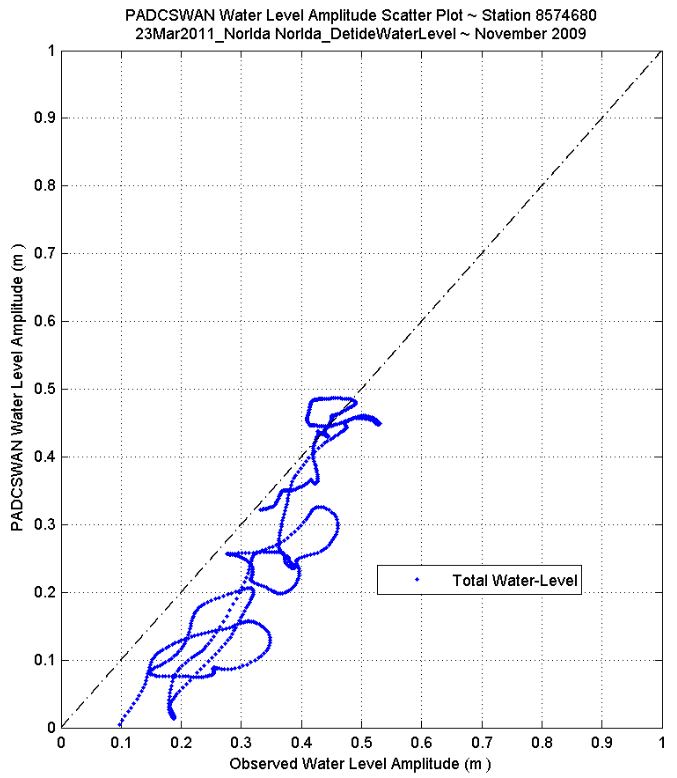

Water Level Amplitude Summary Table
For Station 8574680

Statistics	totwl
bias	-0.07
rms	0.1
SI	0.2
Perf	0.76

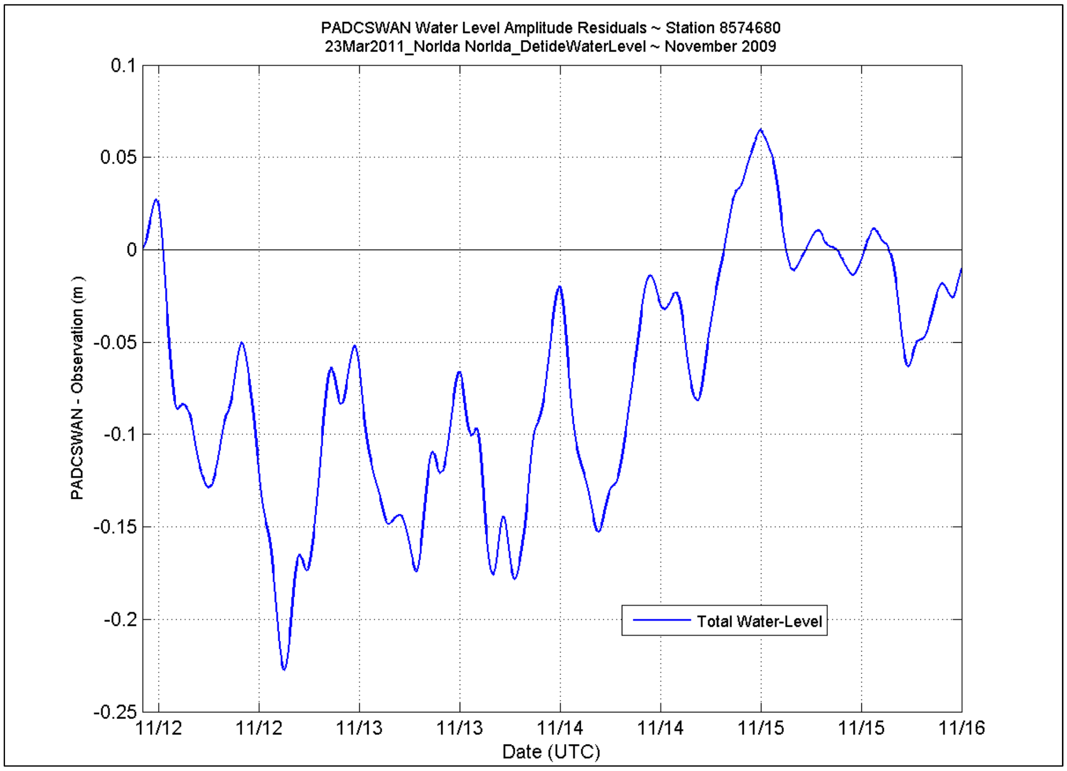
PADCSWAN Water Level Amplitude Residuals ~ Station 8574680
23Mar2011_Norlda Norlda_DetideWaterLevel ~ November 2009
PADCSWAN - Observation (m)
0.1
0.05
0
-0.05
-0.1
-0.15
-0.2
-0.25
11/12
11/12
11/13
11/13
11/14
11/14
11/15
11/15
11/16
Date (UTC)
Total Water-Level

Station 8575512

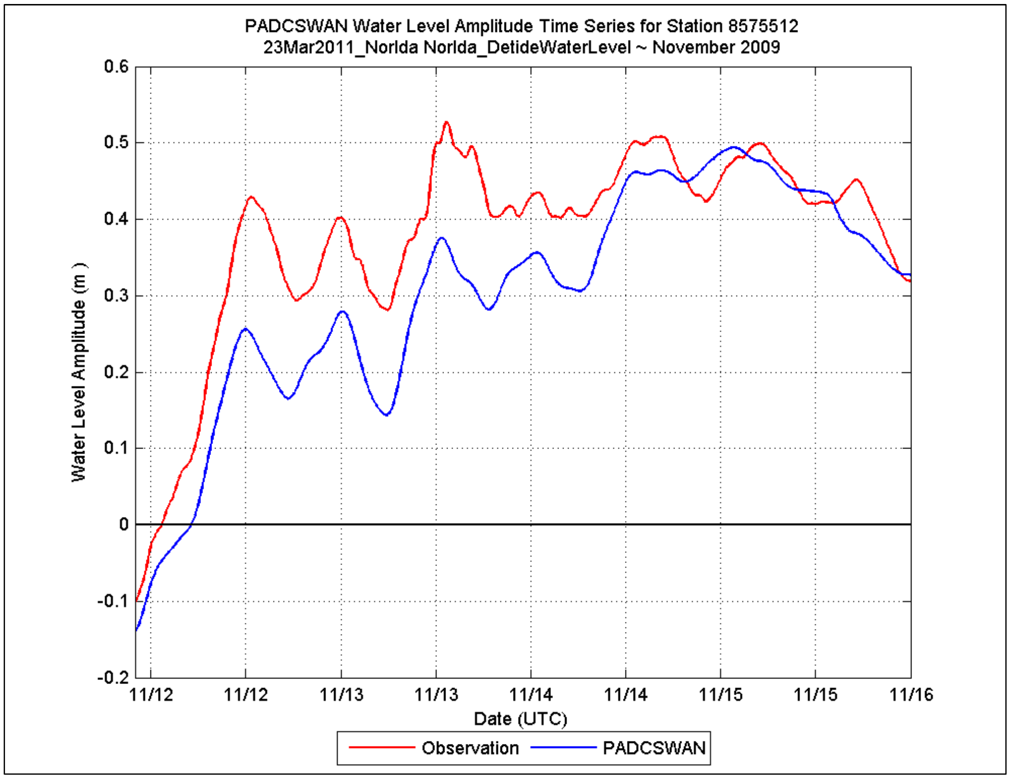

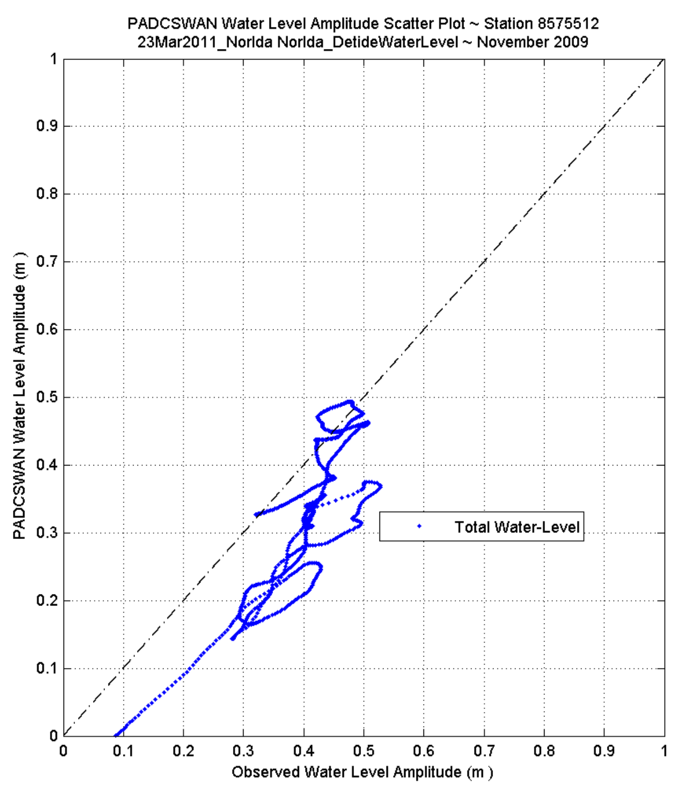

Water Level Amplitude Summary Table
For Station 8575512

Statistics	totwl
bias	-0.07
rms	0.09
SI	0.16
Perf	0.79

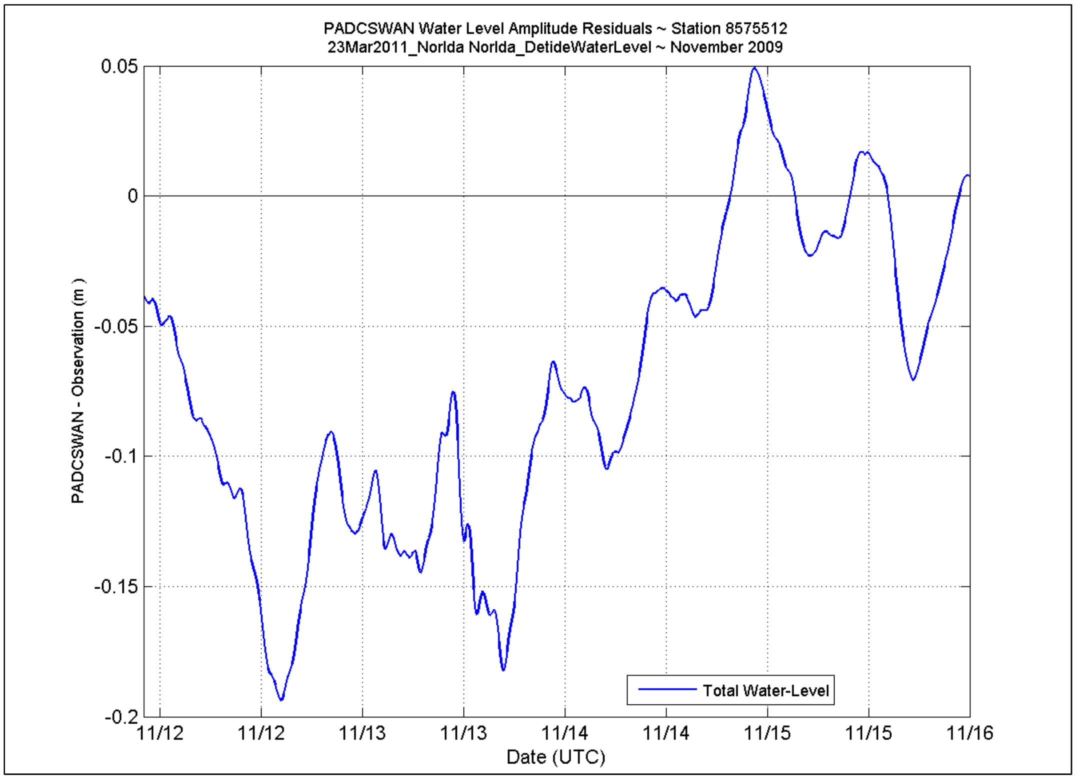
PADCSWAN Water Level Amplitude Residuals ~ Station 8575512
23Mar2011_Norlda Norlda_DetideWaterLevel ~ November 2009
PADCSWAN - Observation (m)
0.05
0
-0.05
-0.1
-0.15
-0.2
11/12
11/12
11/13
11/13
11/14
11/14
11/15
11/15
11/16
Date (UTC)
Total Water-Level

Station 8577330

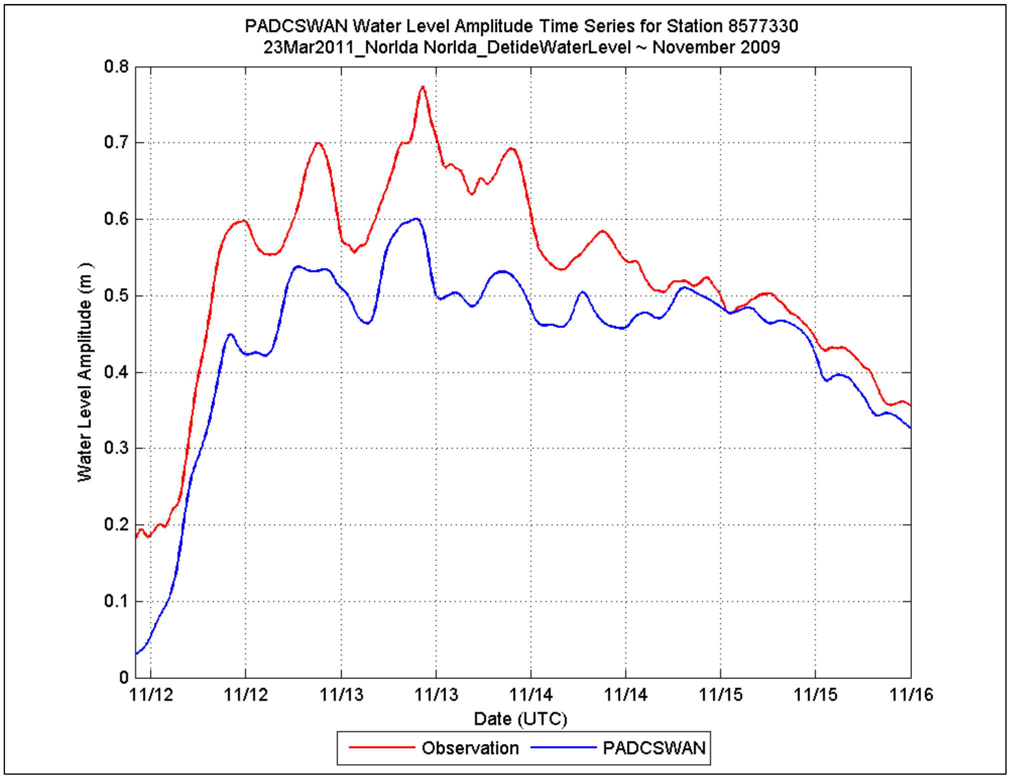

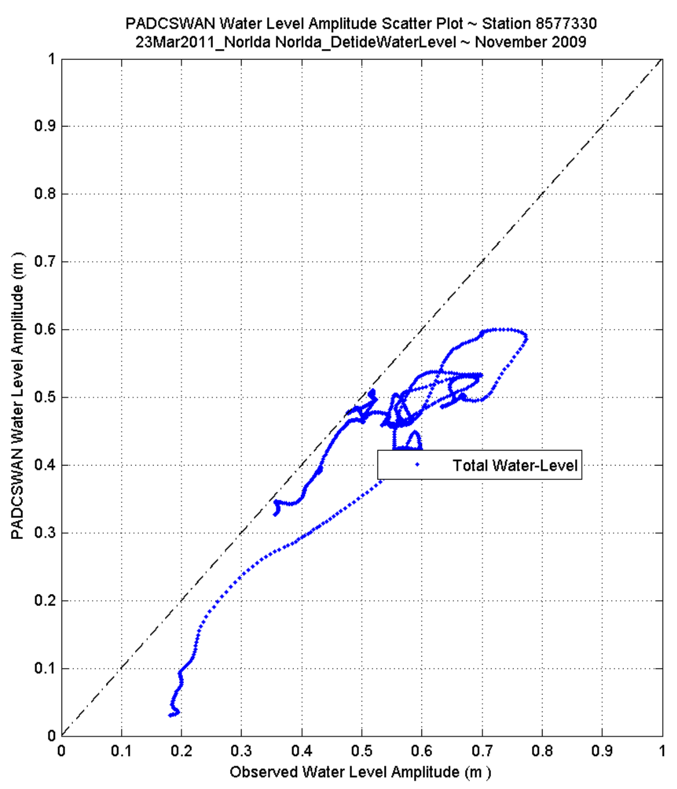

Water Level Amplitude Summary Table
For Station 8577330

Statistics	totwl
bias	-0.09
rms	0.1
SI	0.1
Perf	0.83

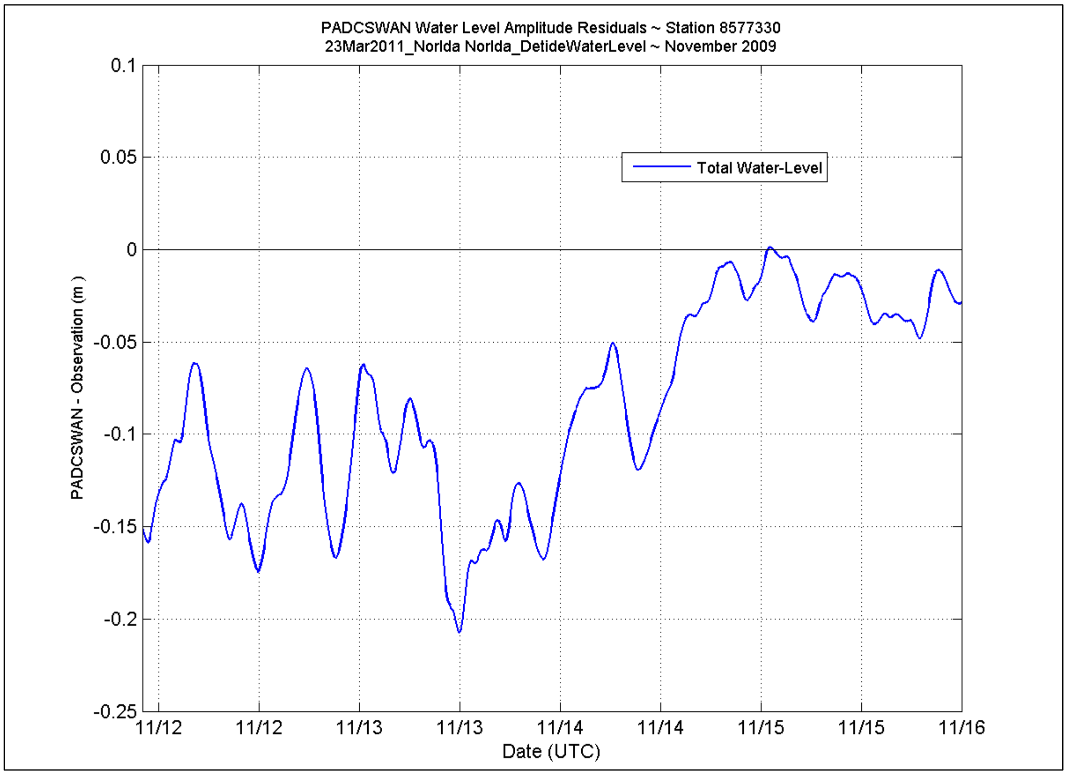
PADCSWAN Water Level Amplitude Residuals ~ Station 8577330
23Mar2011_Norlda Norlda_DetideWaterLevel ~ November 2009
Total Water-Level
PADCSWAN - Observation (m)
0.1
0.05
0
-0.05
-0.1
-0.15
-0.2
-0.25
11/12
11/12
11/13
11/13
11/14
11/14
11/15
11/15
11/16
Date (UTC)

Station 8635750

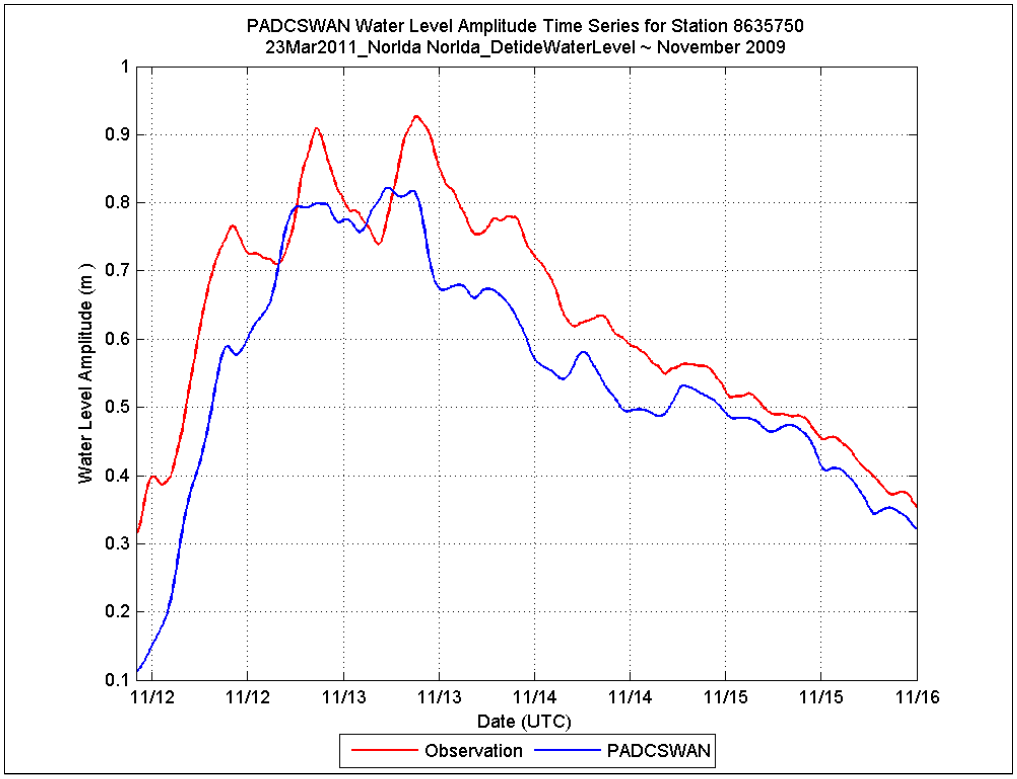

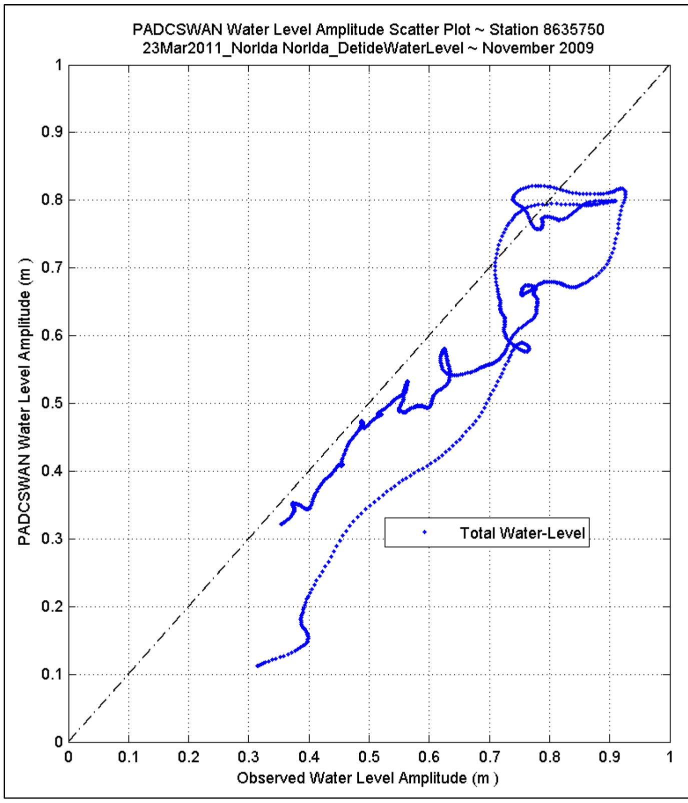

Water Level Amplitude Summary Table
For Station 8635750

Statistics	totwl
bias	-0.08
rms	0.1
SI	0.1
Perf	0.86

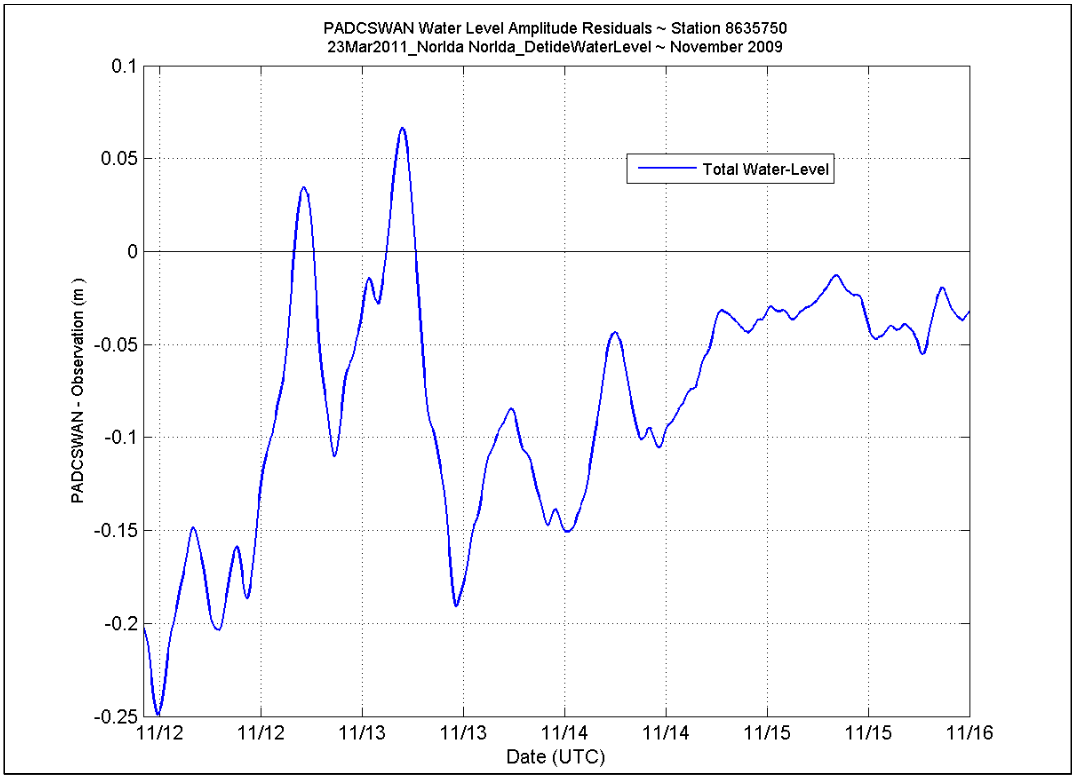
PADCSWAN Water Level Amplitude Residuals ~ Station 8635750
23Mar2011_Norlda Norlda_DetideWaterLevel ~ November 2009
Total Water-Level
PADCSWAN - Observation (m)
0.1
0.05
0
-0.05
-0.1
-0.15
-0.2
-0.25
11/12
11/12
11/13
11/13
11/14
11/14
11/15
11/15
11/16
Date (UTC)

Station 8632200

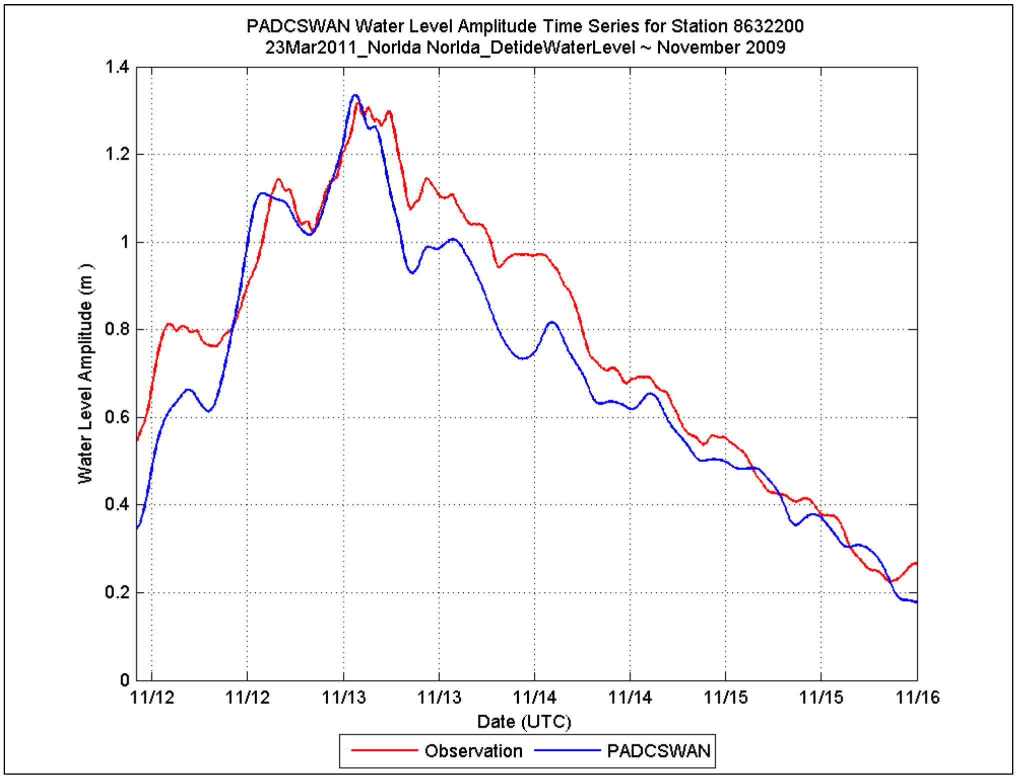

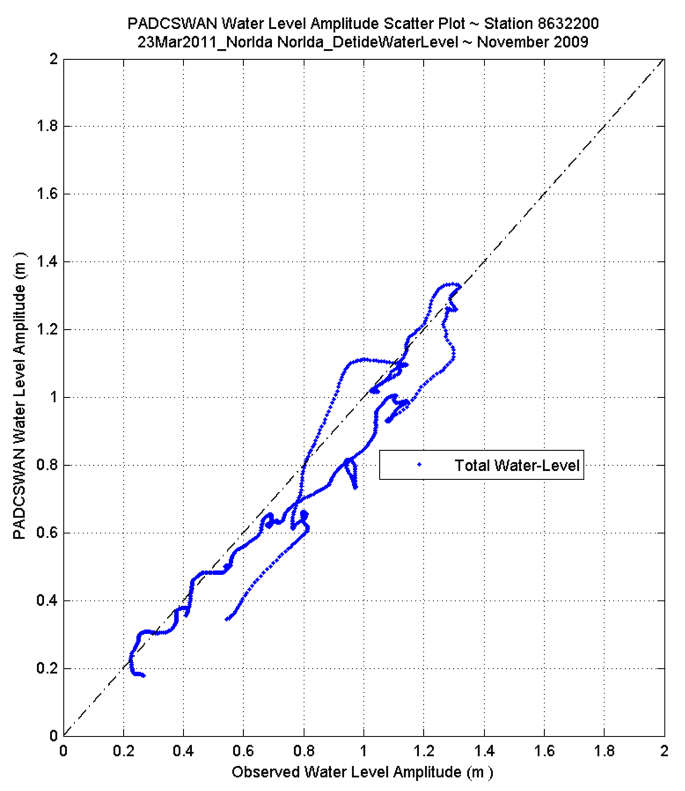

Water Level Amplitude Summary Table
For Station 8632200

Statistics	totwl
bias	-0.07
rms	0.1
SI	0.1
Perf	0.9

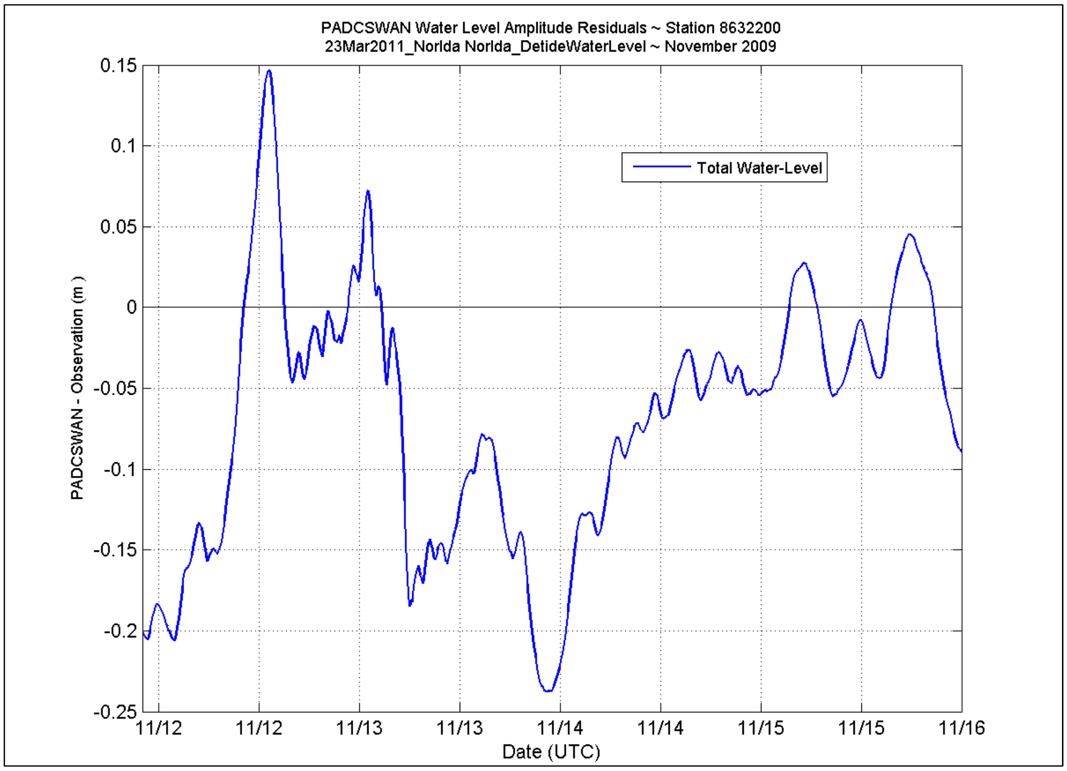

PADCSWAN Water Level Amplitude Residuals ~ Station 8632200
23Mar2011_Norlda Norlda_DetideWaterLevel ~ November 2009
PADCSWAN - Observation (m)
0.15
0.1
0.05
0
-0.05
-0.1
-0.15
-0.2
-0.25
11/12
11/12
11/13
11/13
11/14
11/14
11/15
11/15
11/16
Date (UTC)
Total Water-Level

Station 8637689

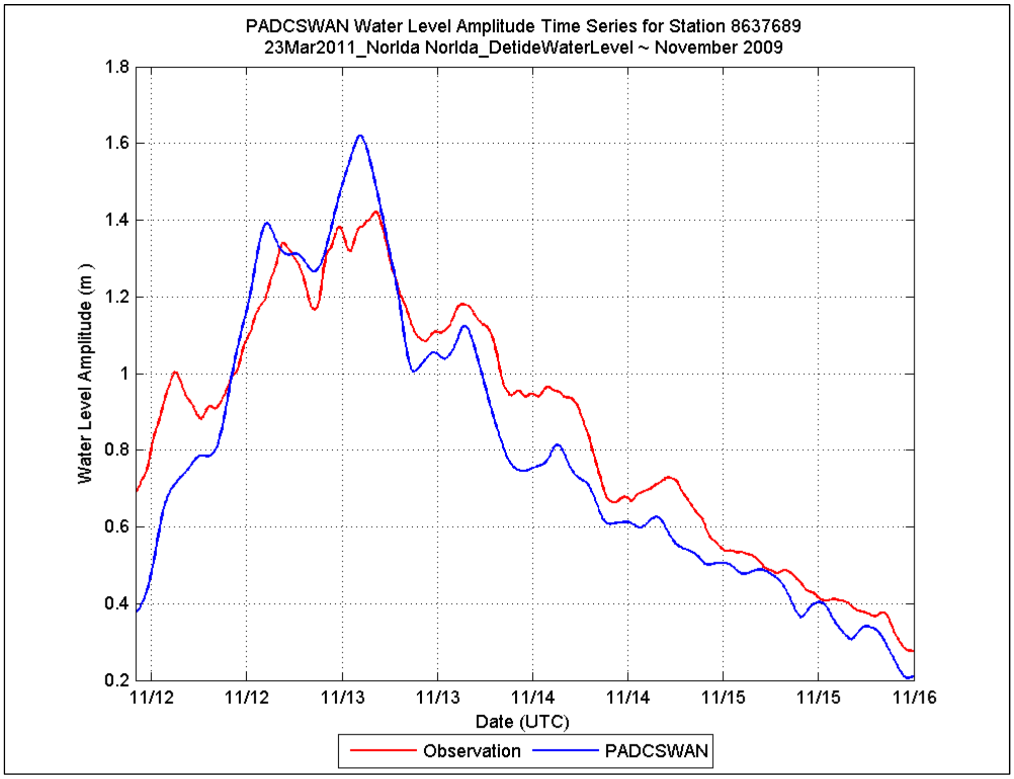

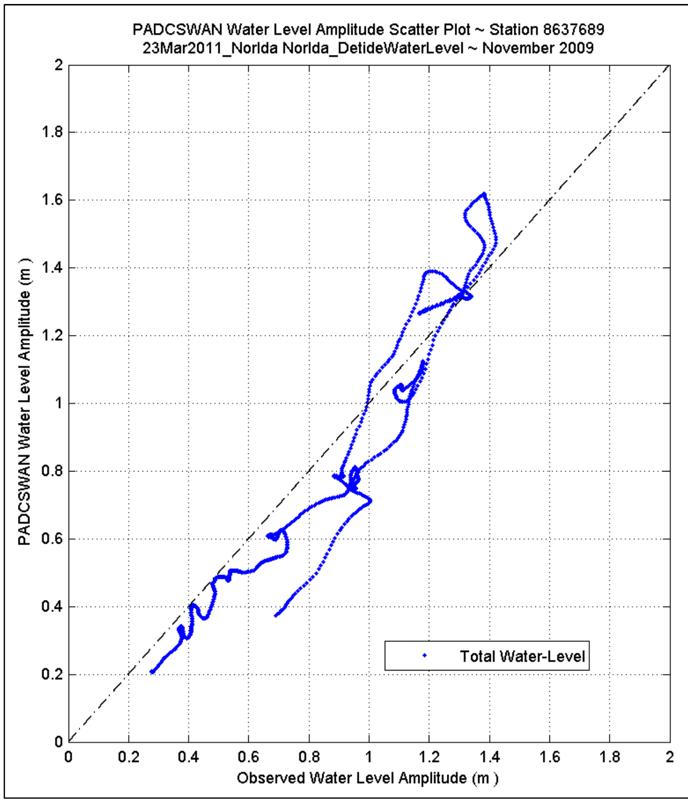

Water Level Amplitude Summary Table
For Station 8637689

Statistics	totwl
bias	-0.07
rms	0.13
SI	0.13
Perf	0.89

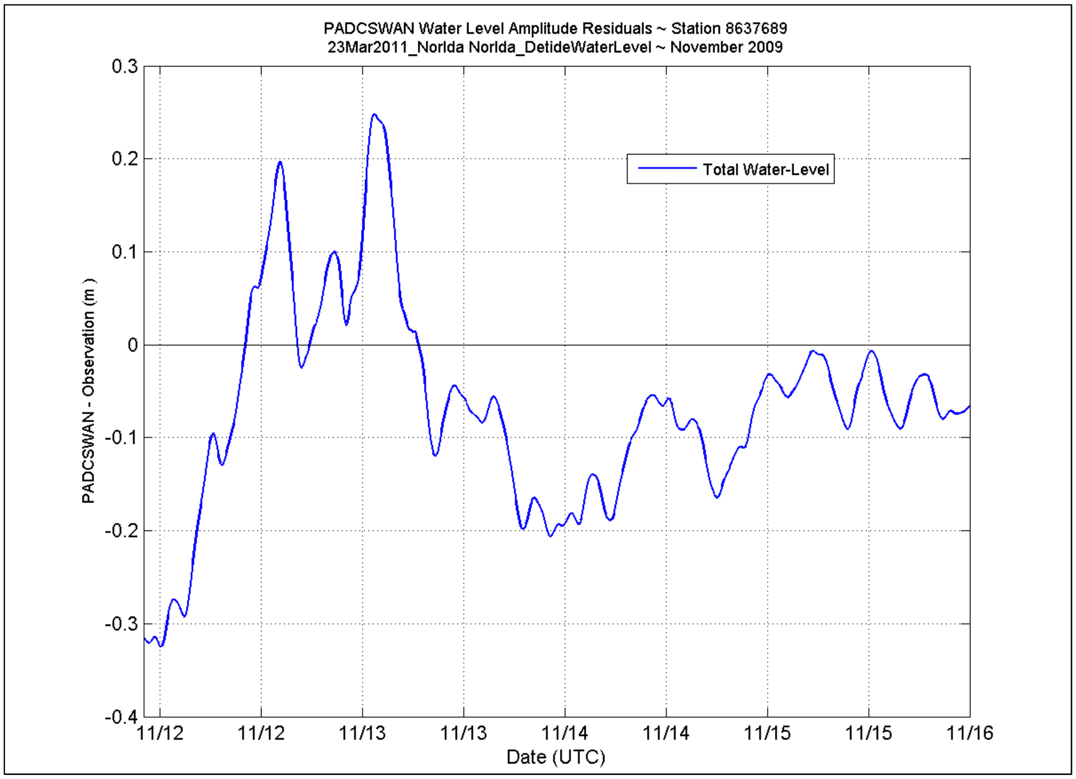
PADCSWAN Water Level Amplitude Residuals ~ Station 8637689
23Mar2011_Norlda Norlda_DetideWaterLevel ~ November 2009
Total Water-Level
PADCSWAN - Observation (m)
0.3
0.2
0.1
0
-0.1
-0.2
-0.3
-0.4
11/12
11/12
11/13
11/13
11/14
11/14
11/15
11/15
11/16
Date (UTC)

Station 8638610

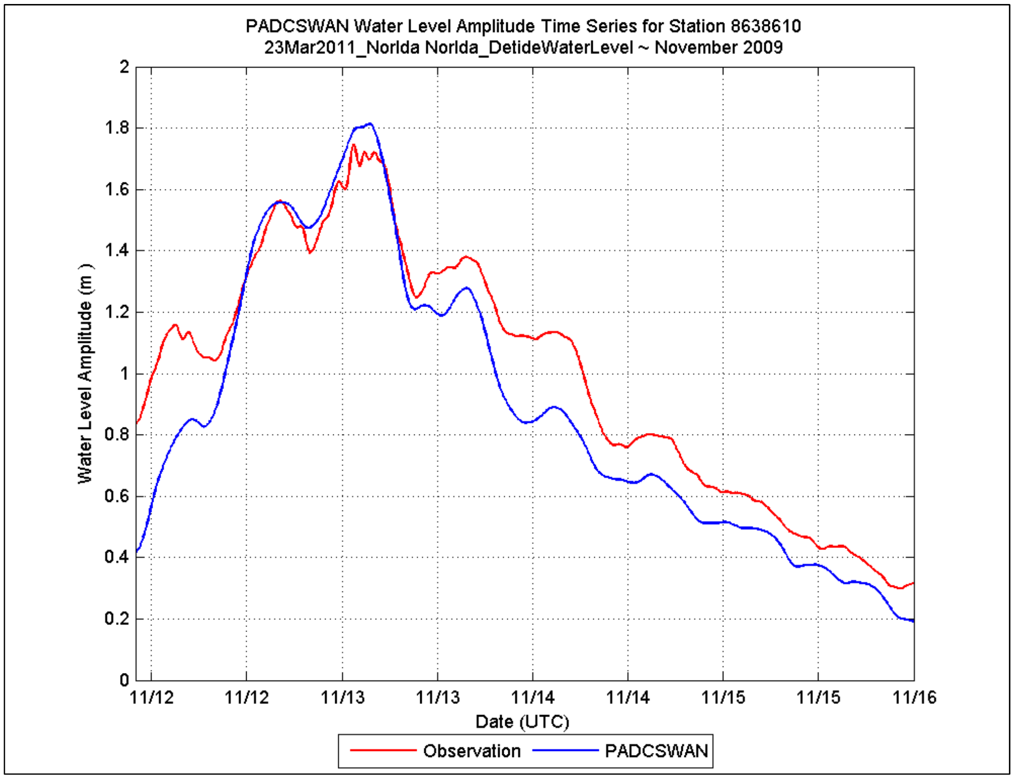

PADCSWAN Water Level Amplitude Time Series for Station 8638610
23Mar2011_Norlda Norlda_DetideWaterLevel ~ November 2009

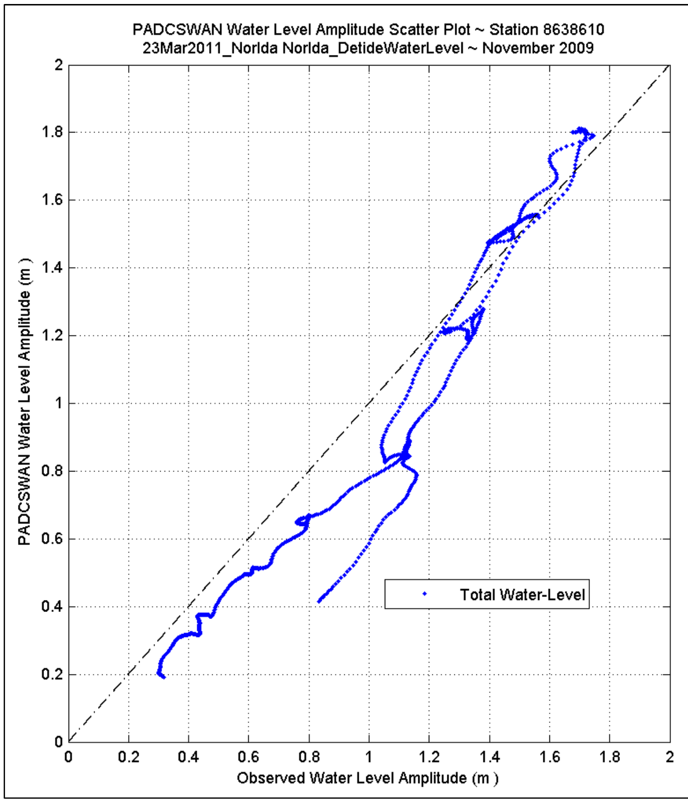

PADCSWAN Water Level Amplitude Scatter Plot ~ Station 8638610
23Mar2011_Norlda Norlda_DetideWaterLevel ~ November 2009

Water Level Amplitude Summary Table
For Station 8638610

Statistics	totwl
bias	-0.12
rms	0.17
SI	0.12
Perf	0.87

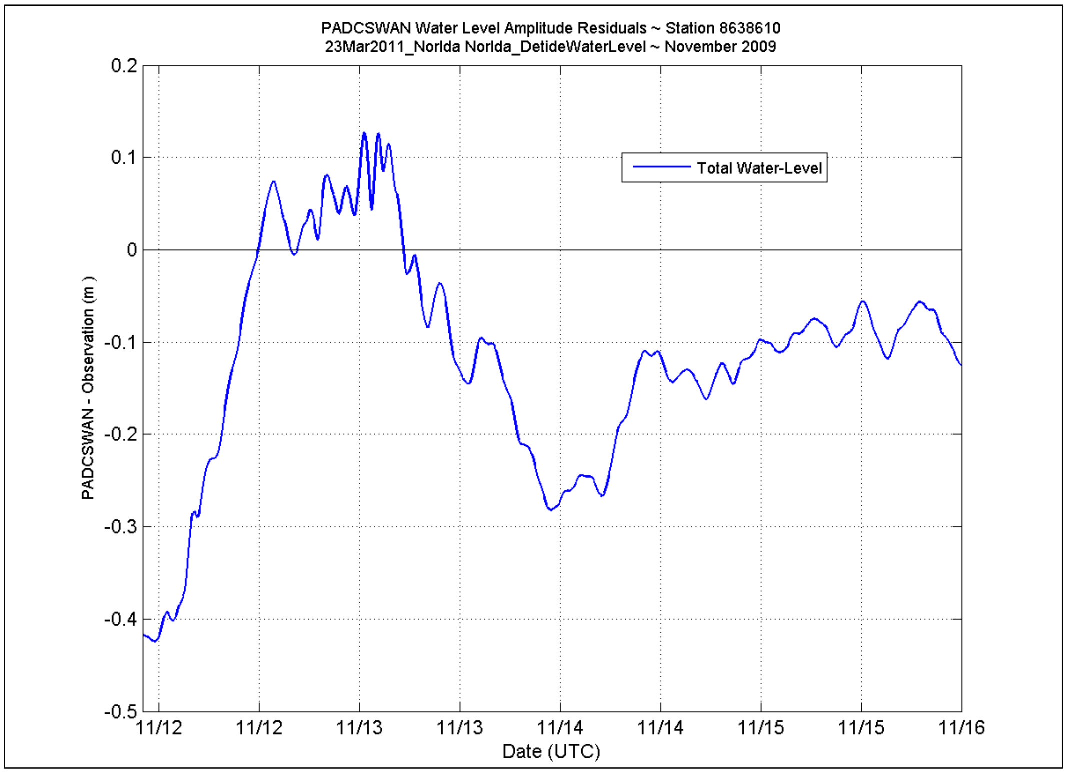
PADCSWAN Water Level Amplitude Residuals ~ Station 8638610
23Mar2011_Norlda Norlda_DetideWaterLevel ~ November 2009
Total Water-Level
PADCSWAN - Observation (m)
0.2
0.1
0
-0.1
-0.2
-0.3
-0.4
-0.5
11/12
11/12
11/13
11/13
11/14
11/14
11/15
11/15
11/16
Date (UTC)

Station 8639348

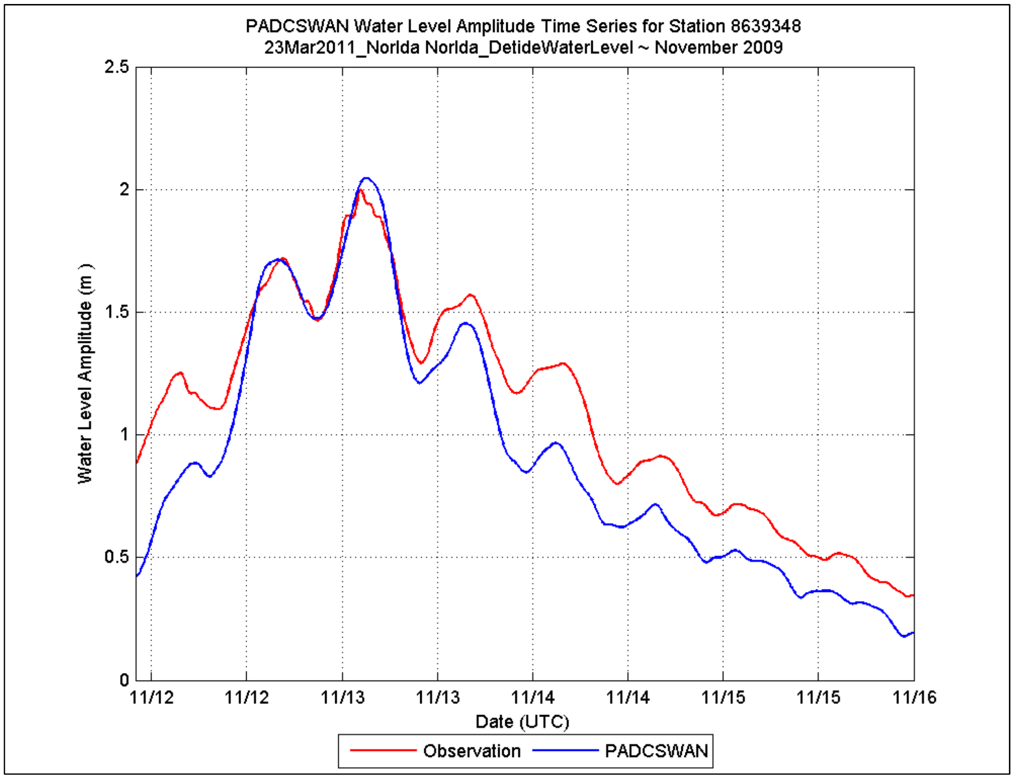

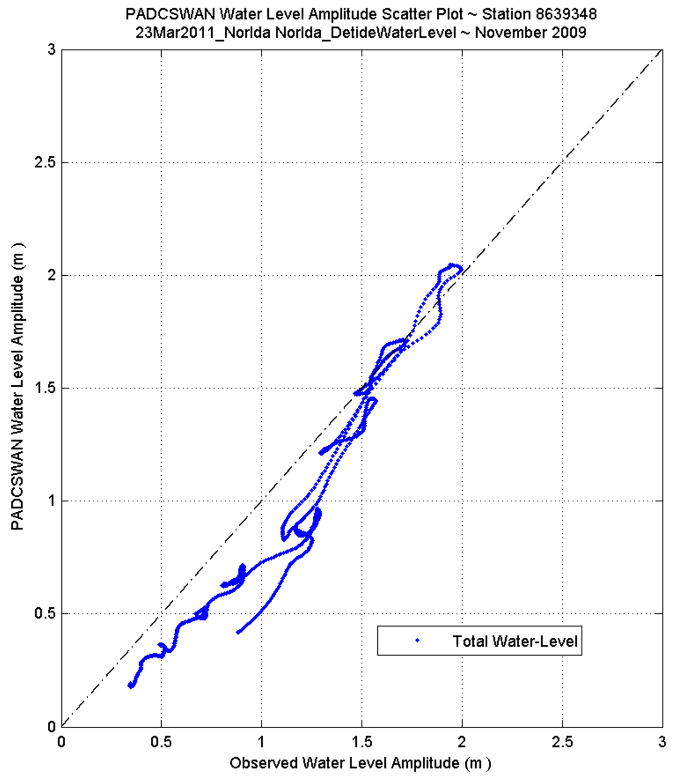

Water Level Amplitude Summary Table
For Station 8639348

Statistics	totwl
bias	-0.18
rms	0.22
SI	0.12
Perf	0.83

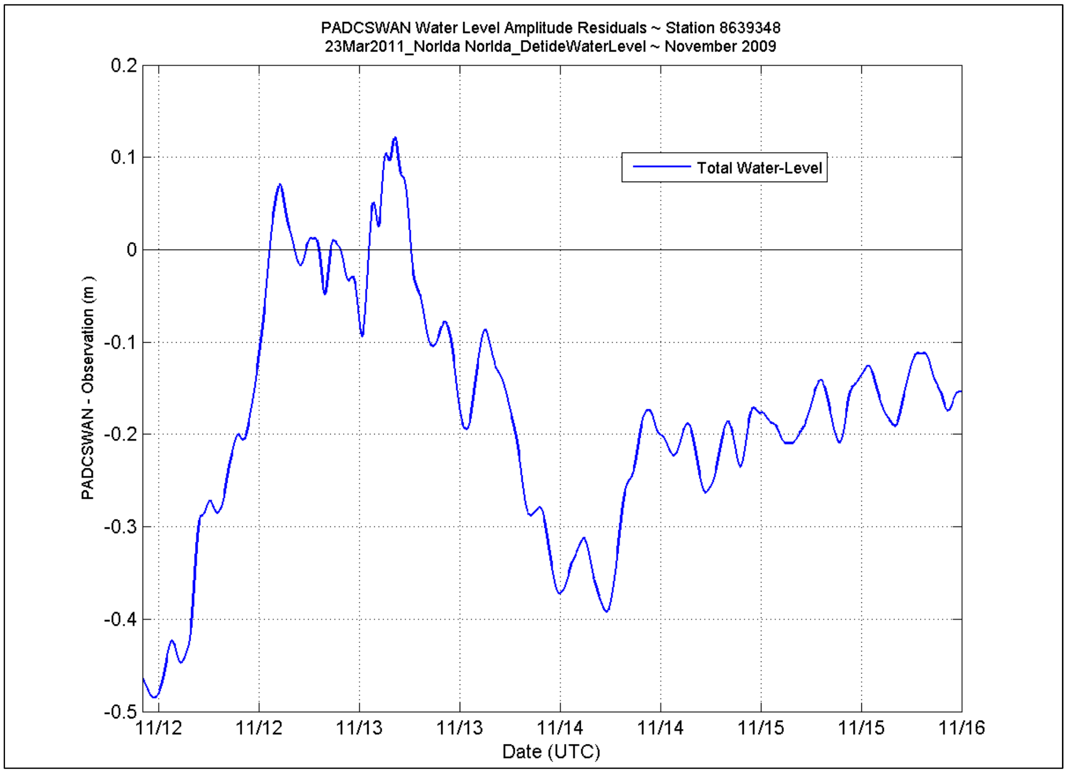
PADCSWAN Water Level Amplitude Residuals ~ Station 8639348
23Mar2011_Norlda Norlda_DetideWaterLevel ~ November 2009
PADCSWAN - Observation (m)
0.2
0.1
0
-0.1
-0.2
-0.3
-0.4
-0.5
Total Water-Level
11/12
11/12
11/13
11/13
11/14
11/14
11/15
11/15
11/16
Date (UTC)

Appendix D: USGS Real-Time Storm Surge Data, Extra-tropical Storm Ida

Data plots in this section refer to the PADCSWAN TidesWindsWaves water level analysis using USGS real-time storm surge data for Tropical Storm Nor'Ida, November 2009. Only data from resolved stations are presented in the section below.

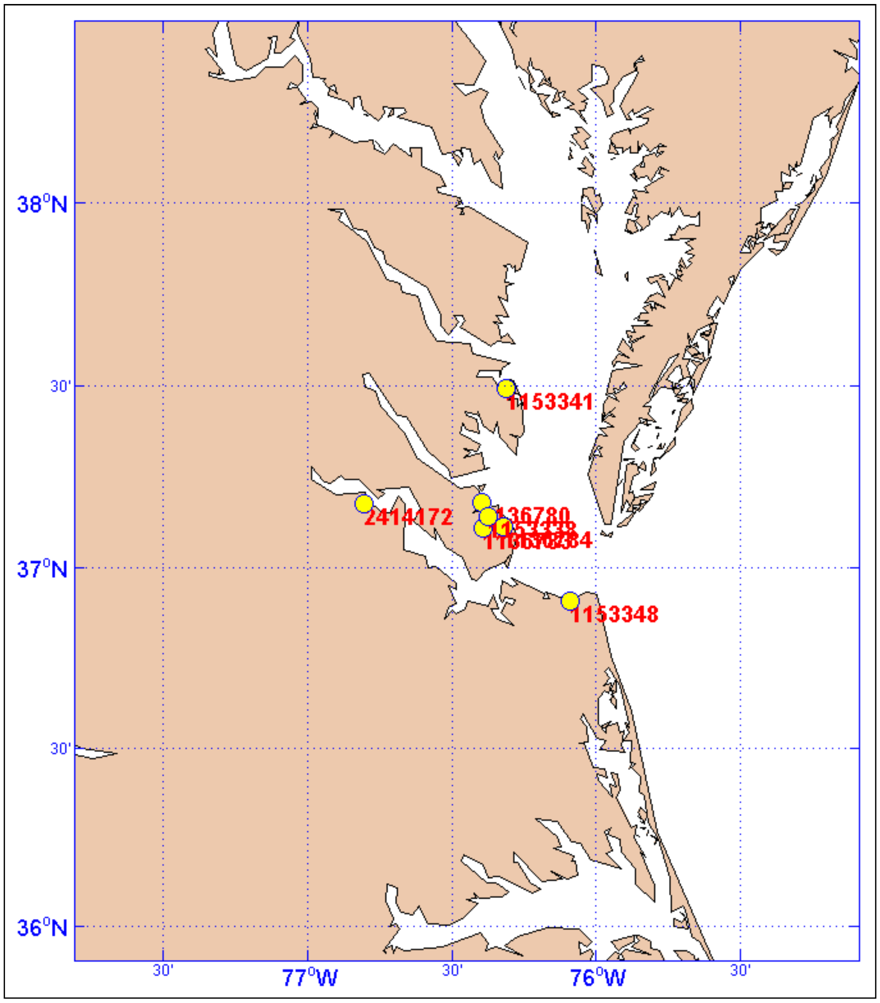
38°N
30'
37°N
30'
36°N
30'
77°W
30'
76°W
30'
1153341
2414172
136780
1153348

Figure D1. USGS real-time water level station locations for TidesWindsWaves, Nor'Ida.

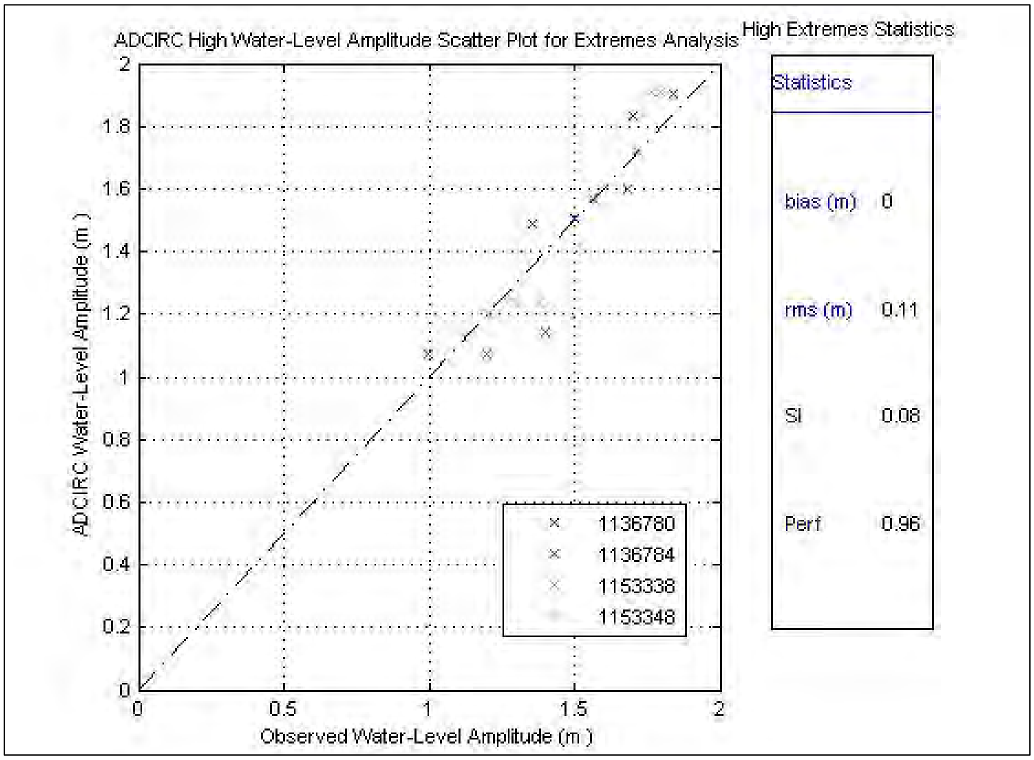

Figure D2. High-water level extremes analysis, TidesWindsWaves, Nor'Ida.

Station 1136780

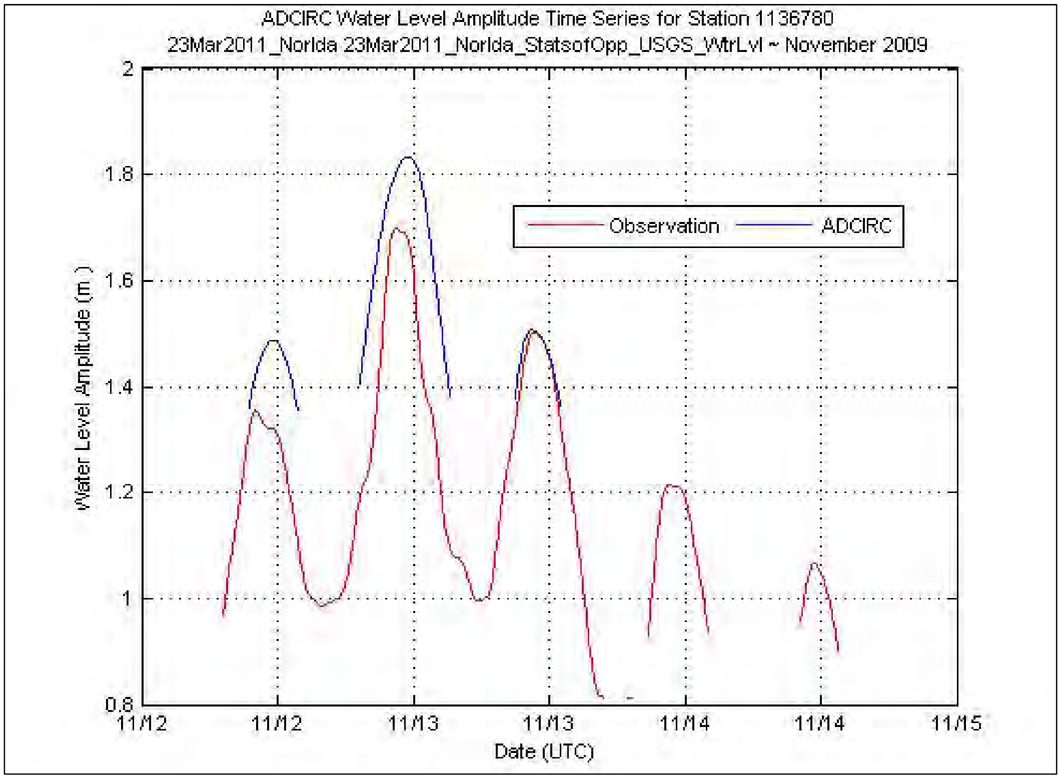

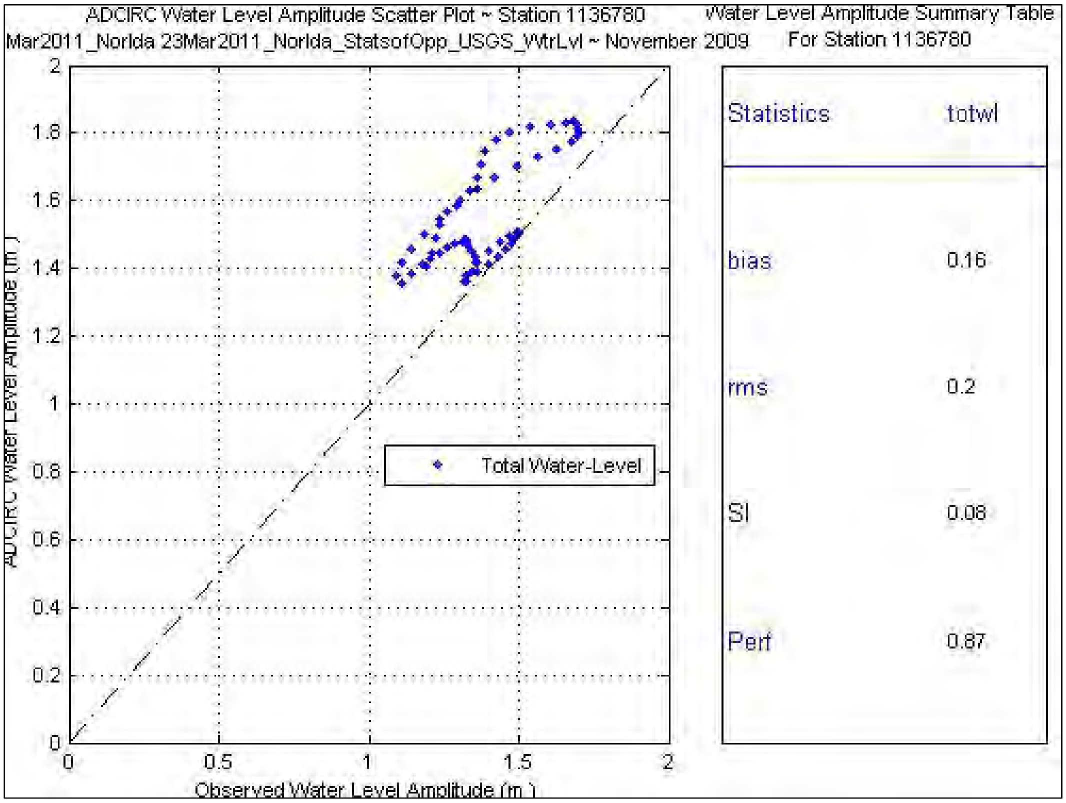

Water Level Amplitude Summary Table
For Station 1136780

Statistics	totwl
bias	0.16
rms	0.2
SI	0.08
Perf	0.87

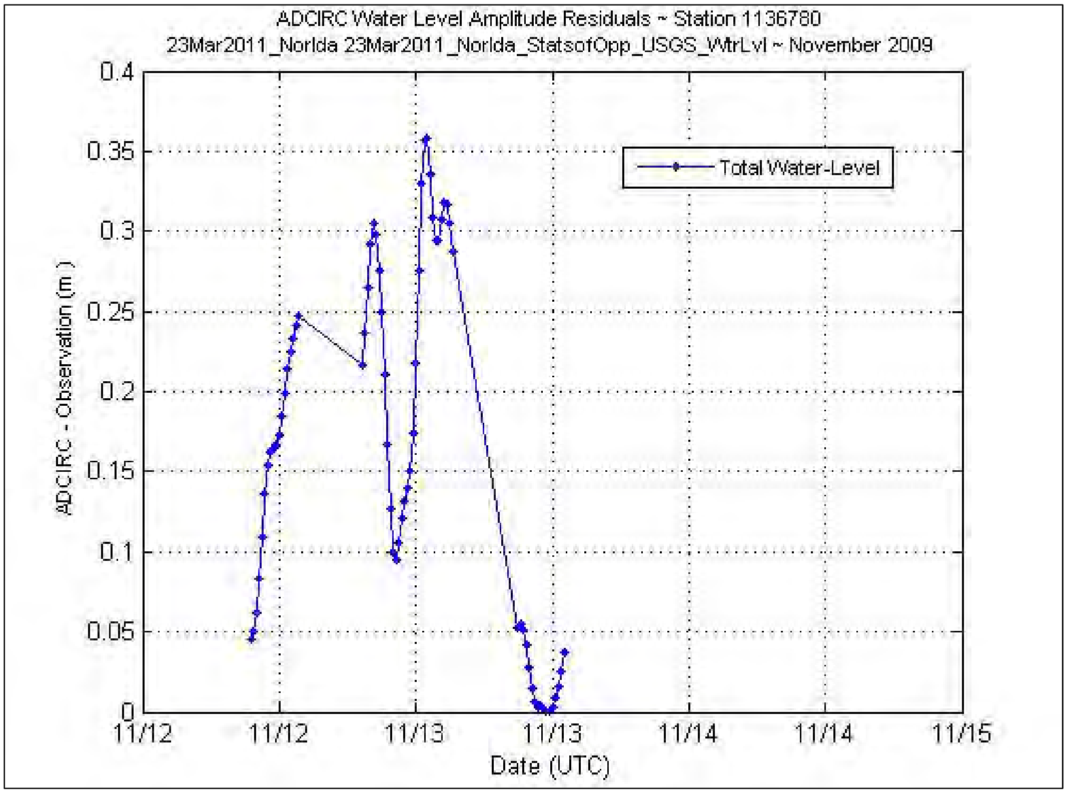
ADCIRC Water Level Amplitude Residuals ~ Station 1136780
23Mar2011_Norlda 23Mar2011_Norlda_StatsofOpp_USGS_WtrLvl ~ November 2009
ADCIRC - Observation (m)
0.4
0.35
0.3
0.25
0.2
0.15
0.1
0.05
0
11/12
11/12
11/13
11/13
11/14
11/14
11/15
Date (UTC)
Total Water-Level

Station 1136783

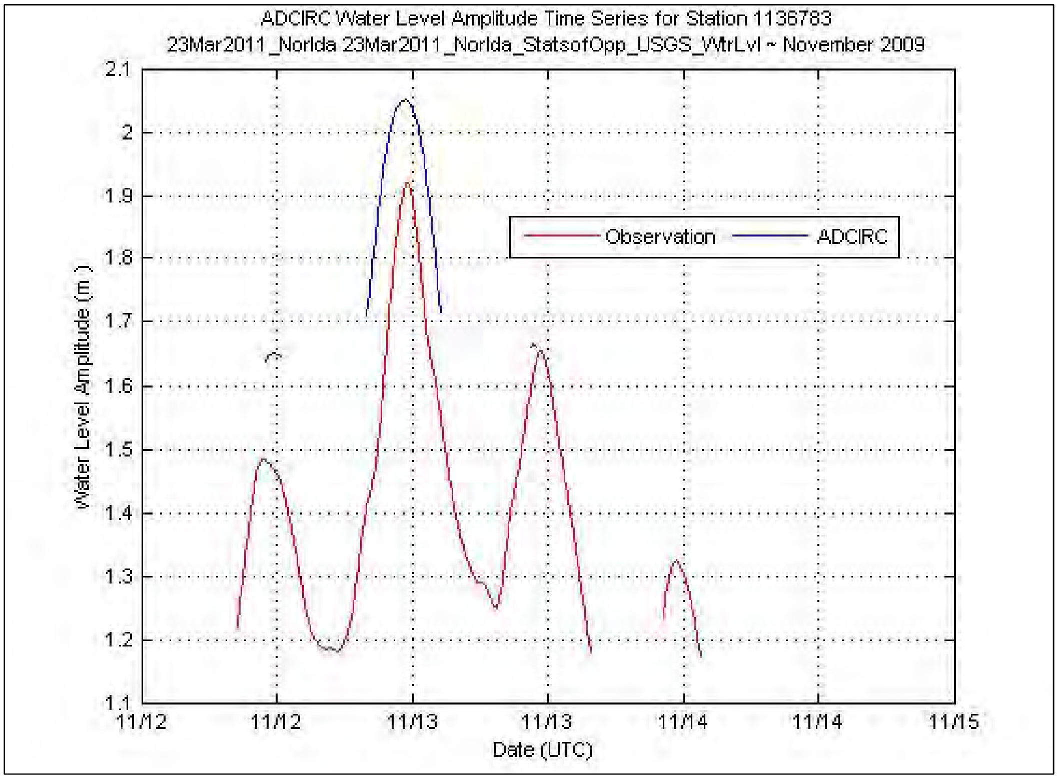

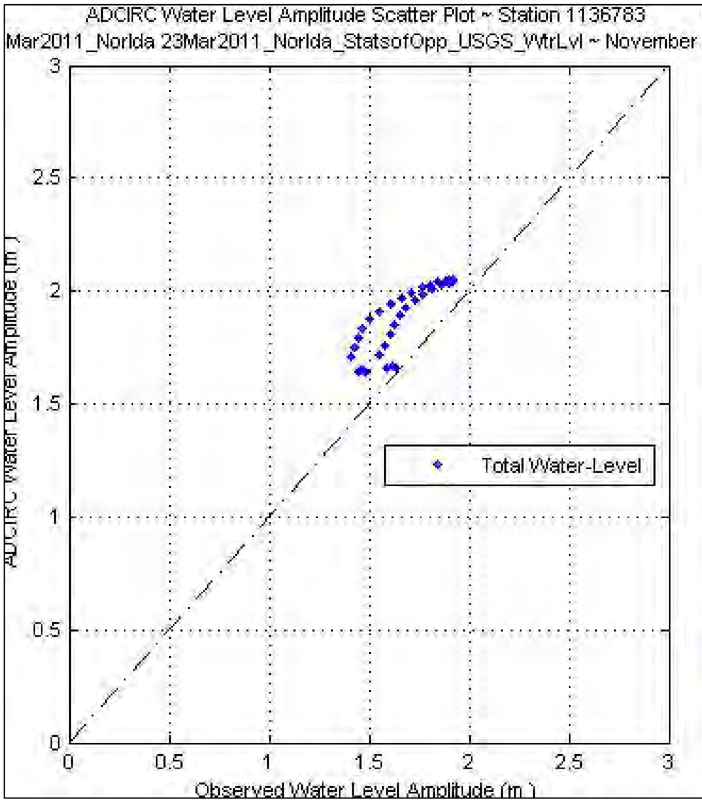

Water Level Amplitude Summary Table
For Station 1136783

Statistics	totwl
bias	0.21
rms	0.23
SI	0.05
Perf	0.87

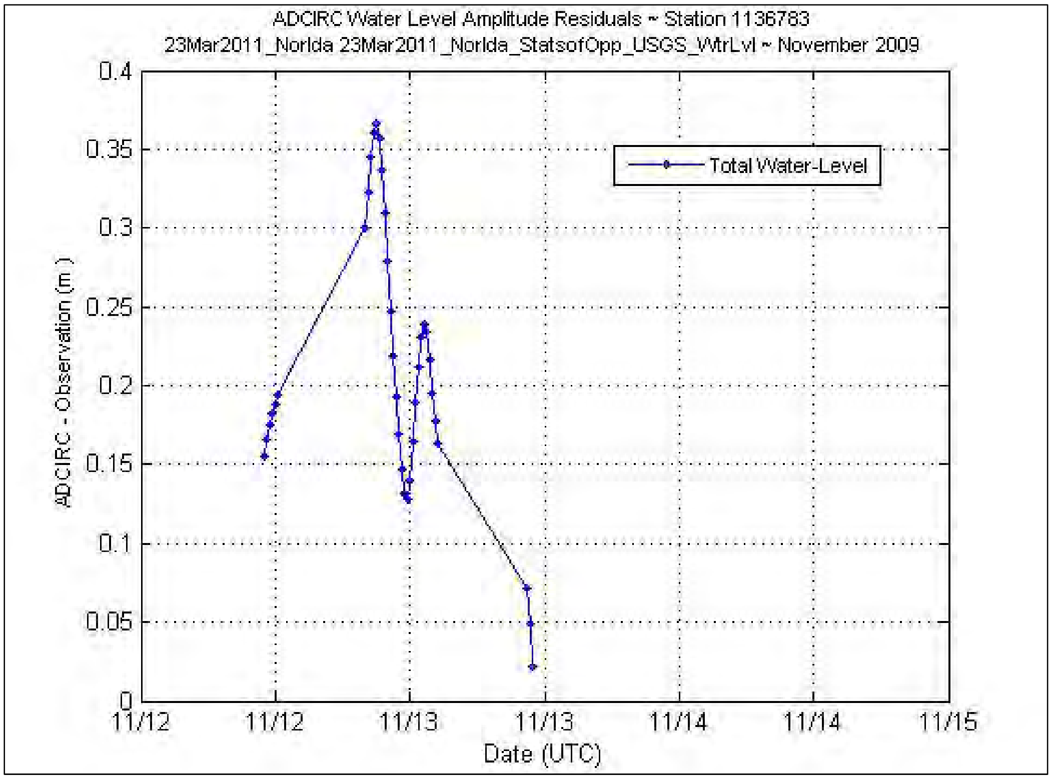
ADCIRC Water Level Amplitude Residuals ~ Station 1136783
23Mar2011_NorIda 23Mar2011_NorIda_StatsofOpp_USGS_WtrLvl ~ November 2009
Total Water-Level
ADCIRC - Observation (m)
0.4
0.35
0.3
0.25
0.2
0.15
0.1
0.05
0
11/12
11/12
11/13
11/13
11/14
11/14
11/15
Date (UTC)

Station 1136784

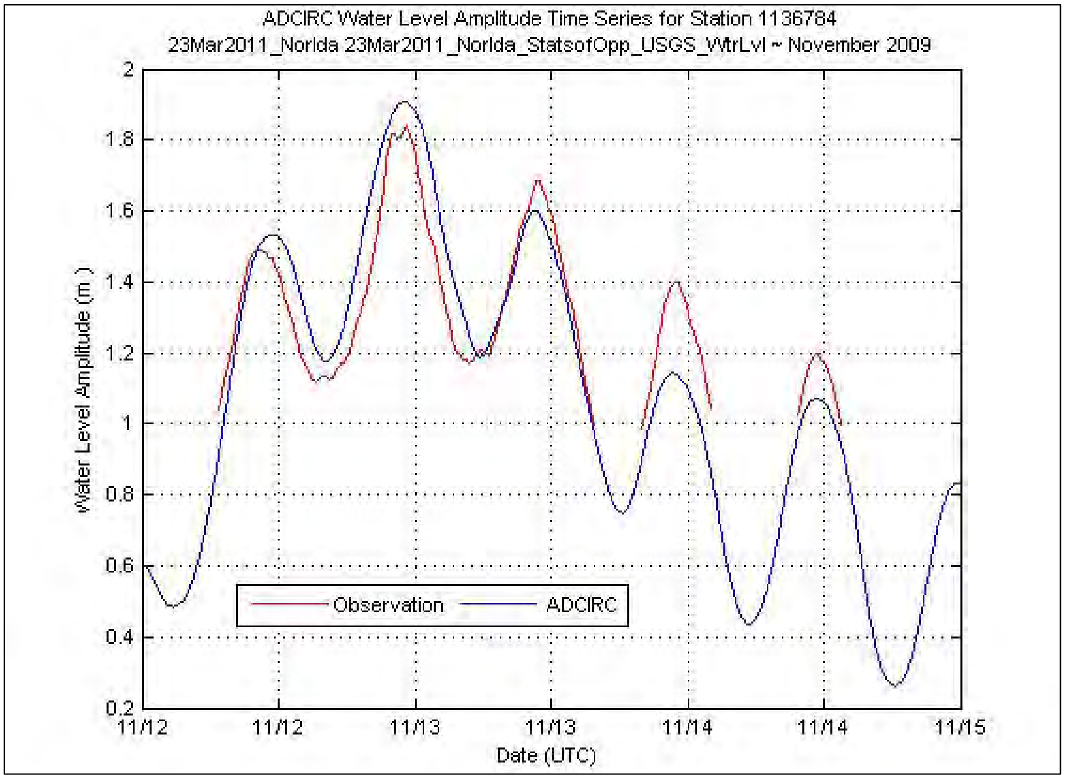

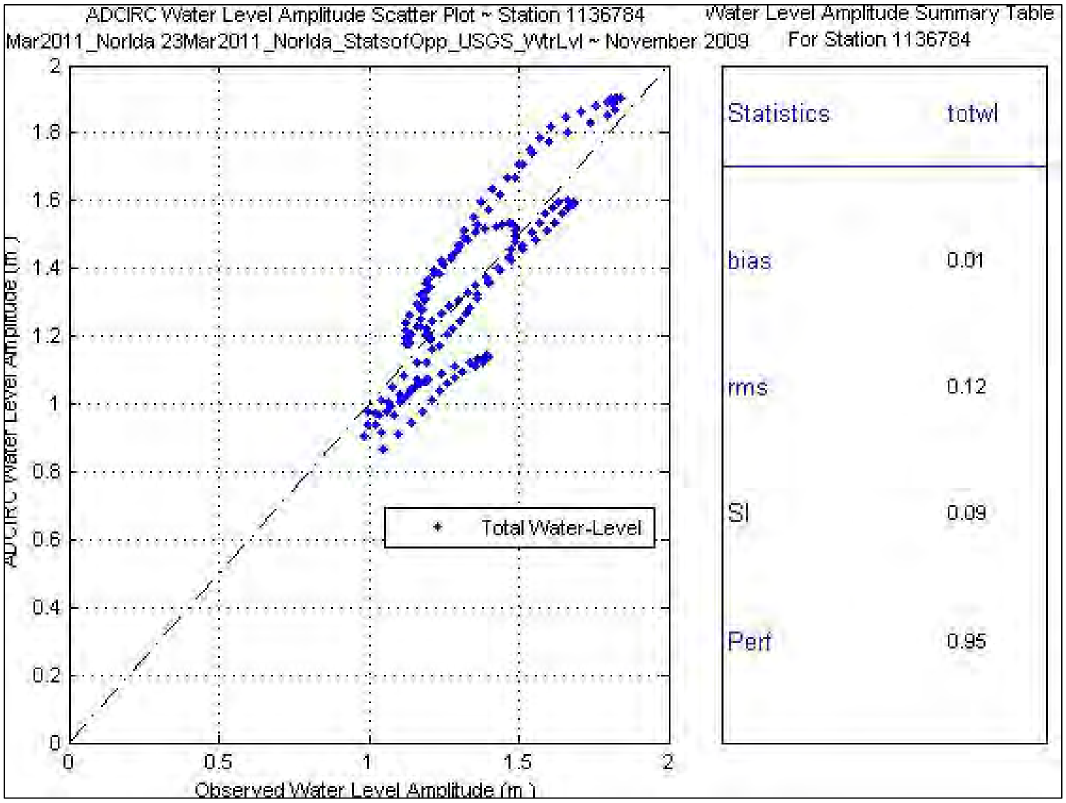

Water Level Amplitude Summary Table
For Station 1136784

Statistics	totwl
bias	0.01
rms	0.12
SI	0.09
Perf	0.95

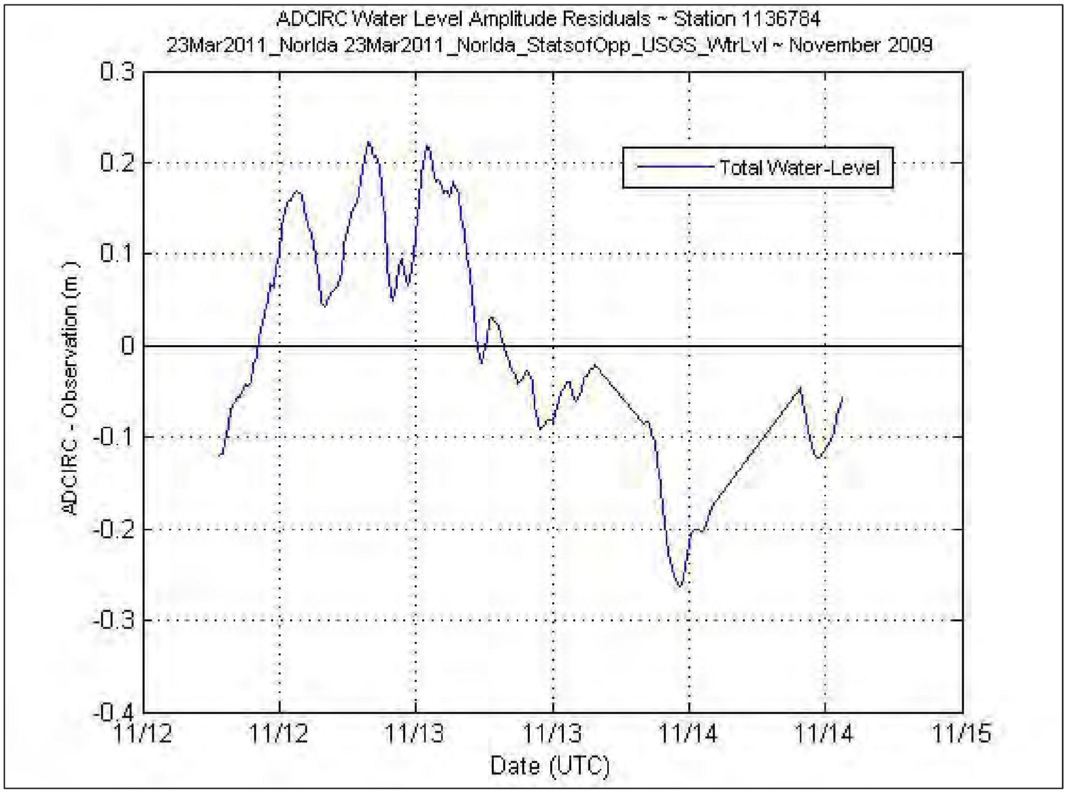
ADCIRC Water Level Amplitude Residuals ~ Station 1136784
23Mar2011_Norlda 23Mar2011_Norlda_StatsofOpp_USGS_WtrLvl ~ November 2009
Total Water-Level
ADCIRC - Observation (m)
0.3
0.2
0.1
0
-0.1
-0.2
-0.3
-0.4
11/12
11/12
11/13
11/13
11/14
11/14
11/15
Date (UTC)

Station 1153338

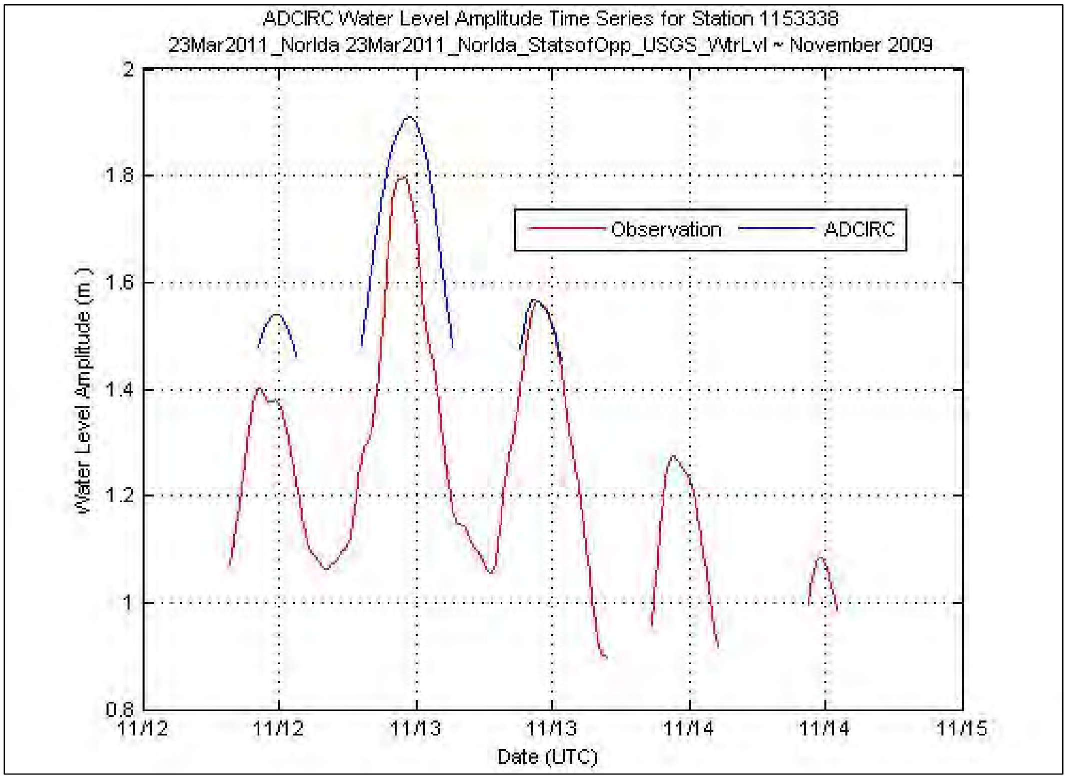

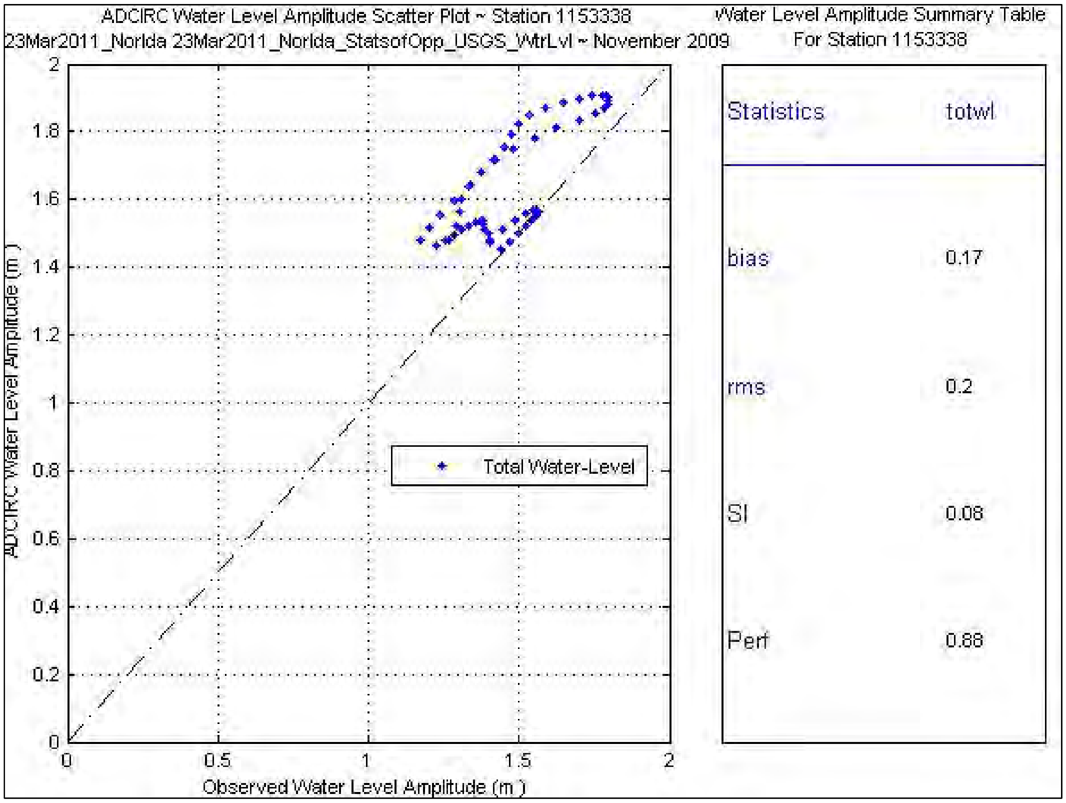

Water Level Amplitude Summary Table
For Station 1153338

Statistics	totwl
bias	0.17
rms	0.2
SI	0.08
Perf	0.88

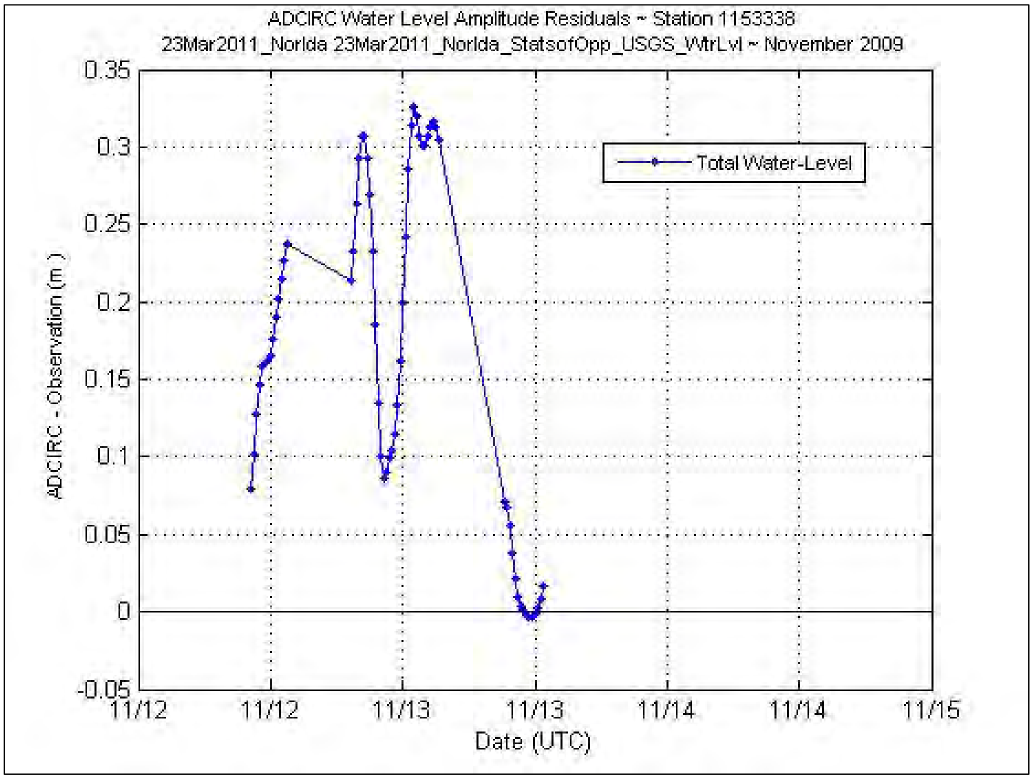
ADCIRC Water Level Amplitude Residuals ~ Station 1153338
23Mar2011_Norlda 23Mar2011_Norlda_StatsofOpp_USGS_WtrLvl ~ November 2009
ADCIRC - Observation (m)
0.35
0.3
0.25
0.2
0.15
0.1
0.05
0
-0.05
11/12
11/12
11/13
11/13
11/14
11/14
11/15
Date (UTC)
Total Water-Level

Station 1153348

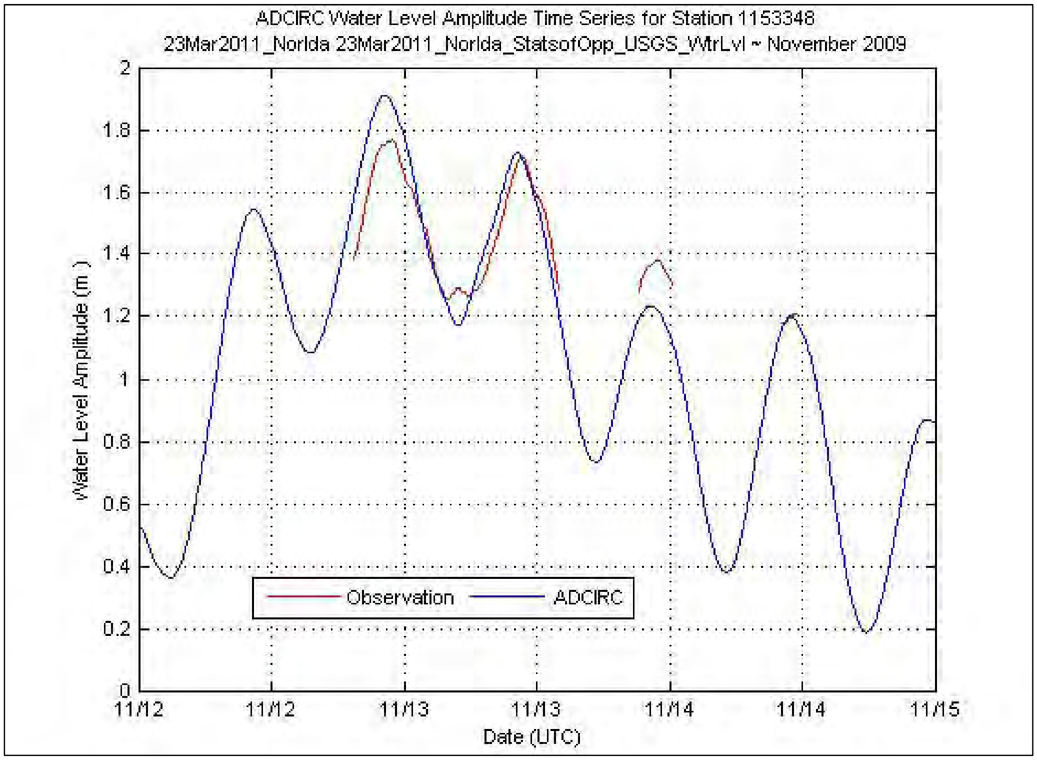

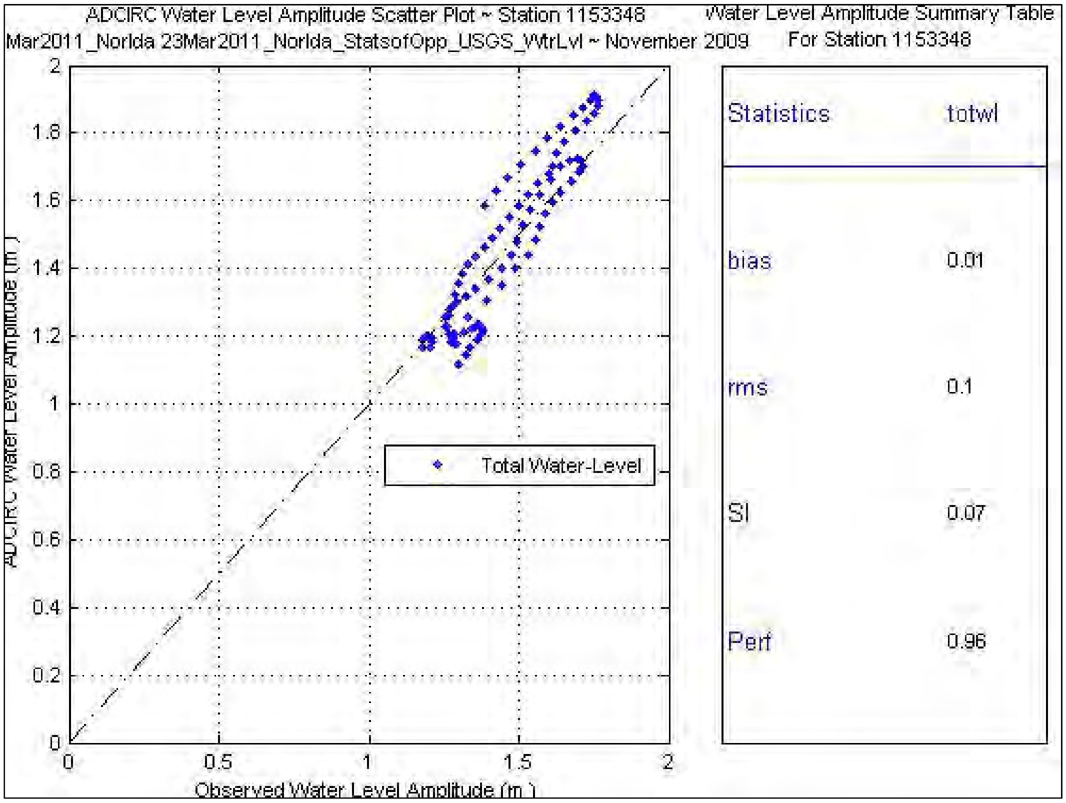

Water Level Amplitude Summary Table
For Station 1153348

Statistics	totwl
bias	0.01
rms	0.1
SI	0.07
Perf	0.96

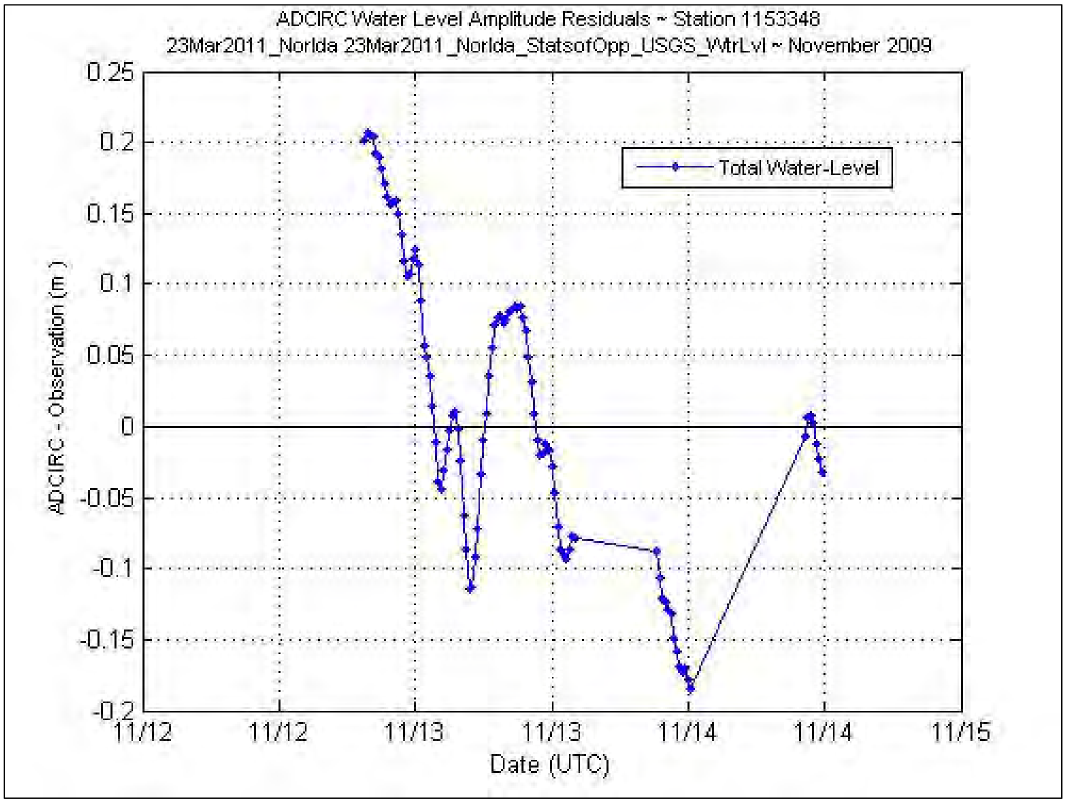
ADCIRC Water Level Amplitude Residuals ~ Station 1153348
23Mar2011_Norlda 23Mar2011_Norlda_StatsofOpp_USGS_WtrLvl ~ November 2009
Total Water-Level
ADCIRC - Observation (m)
0.25
0.2
0.15
0.1
0.05
0
-0.05
-0.1
-0.15
-0.2
11/12
11/12
11/13
11/13
11/14
11/14
11/15
Date (UTC)

Appendix E: TidesSugeWaves Water Level Data

For each storm, tided water level data were retrieved from the NOS Tides Online website in NAVD88. When NOAA data were not available in NAVD88, the datum translation information for each station, as published on NOS Tides Online, was used to translate the station data to NAVD88.

For Hurricanes Isabel and Ernesto, available 6.0-min water level observations from USGS tidal stream gauges were also collected for comparison to the PADCSWAN time series output. To obtain these data, each USGS district in Region III was contacted, and water level observations were requested for several days prior to, and after, each storm event. USGS data were provided in a variety of datums and time zones. Where necessary, the data were translated to NAVD88 using conversions provided by the USGS and then converted to UTC. These data are not available for Nor'Ida.

E-1 Hurricane Isabel, September 2003

Time series plots in this section refer to the PADCSWAN TidesWindsWaves water level analysis for Hurricane Isabel, September 2003.

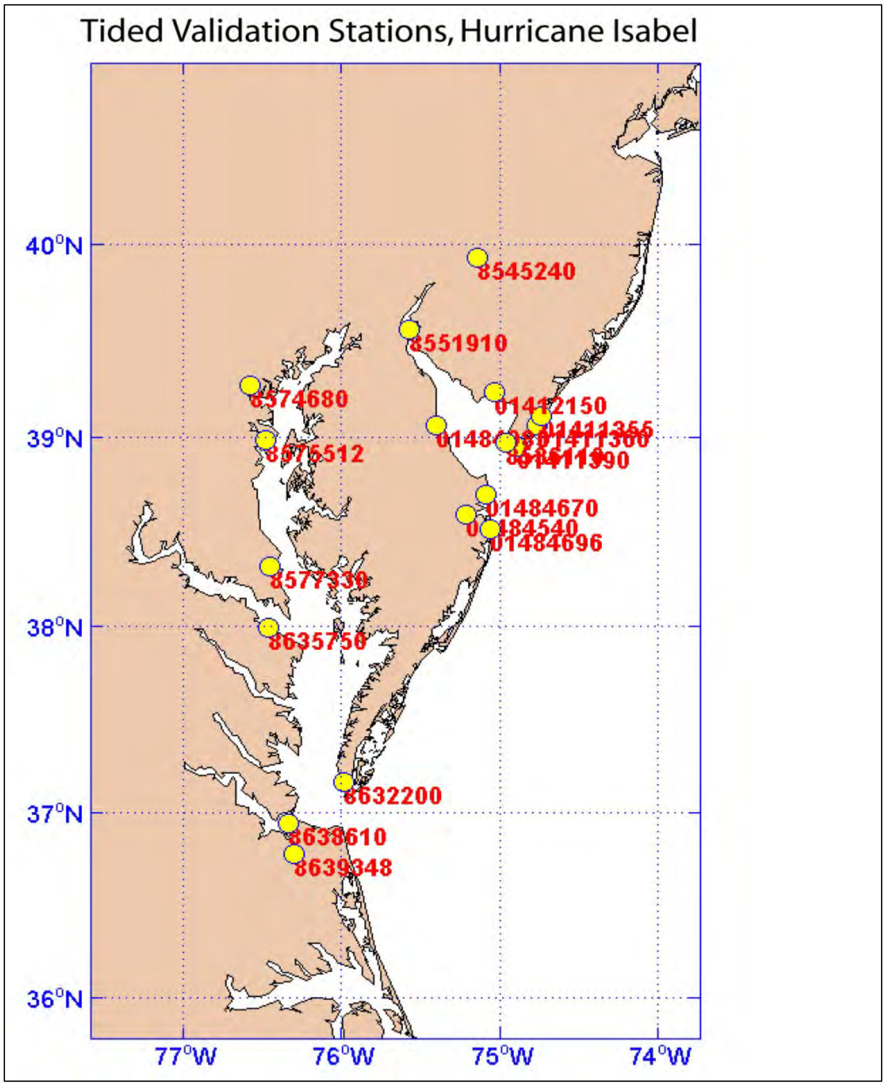
Tided Validation Stations, Hurricane Isabel
8545240
8551910
8574680
01412150
8575512
01411390
01484670
01484540
01484696
8577330
8635750
8632200
8638610
8639348
40°N
39°N
38°N
37°N
36°N
77°W
76°W
75°W
74°W

Figure E1. NOAA water level station locations for TidesWindsWaves, Isabel. Data plots for the analysis follow this location map.

Station 01411355

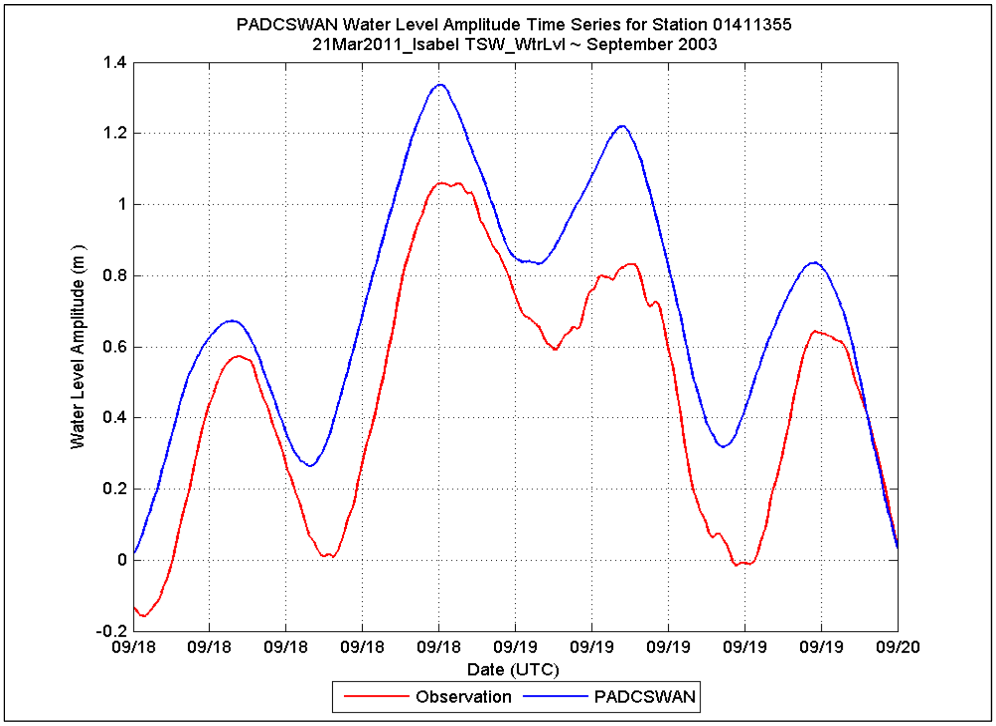

Station 01411360

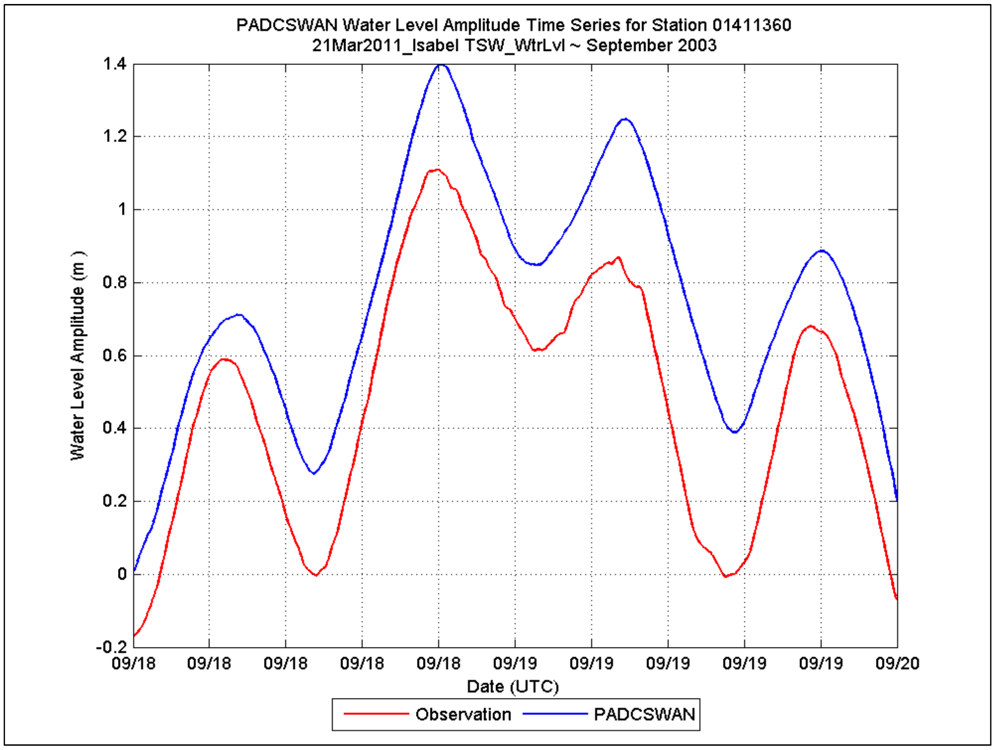

Station 01411390

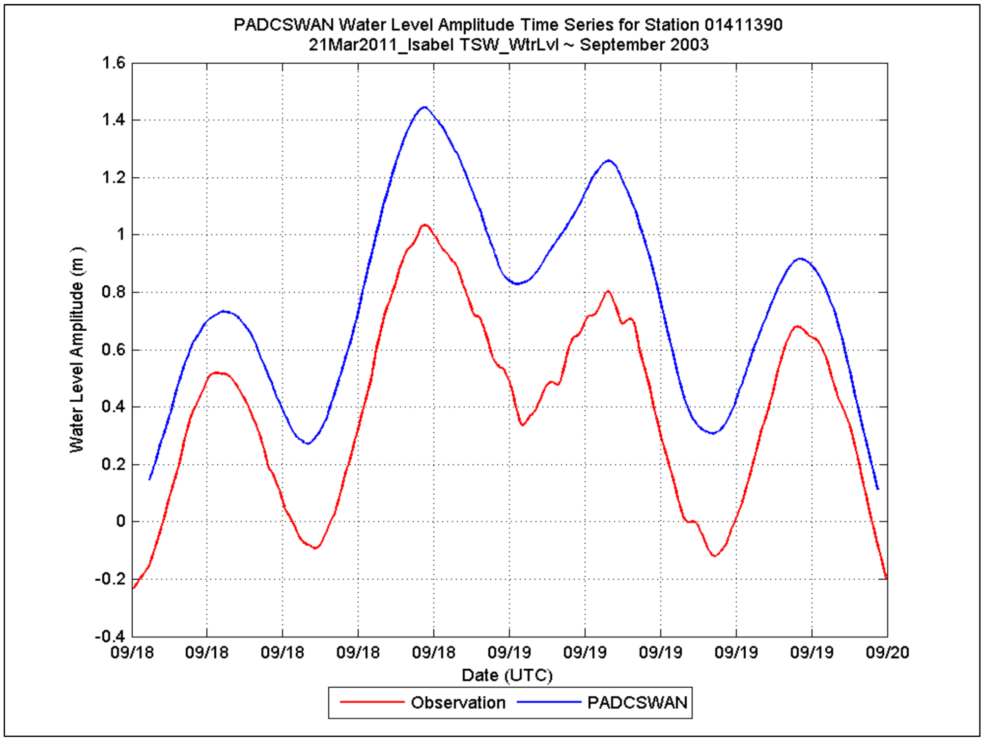

Station 01412150

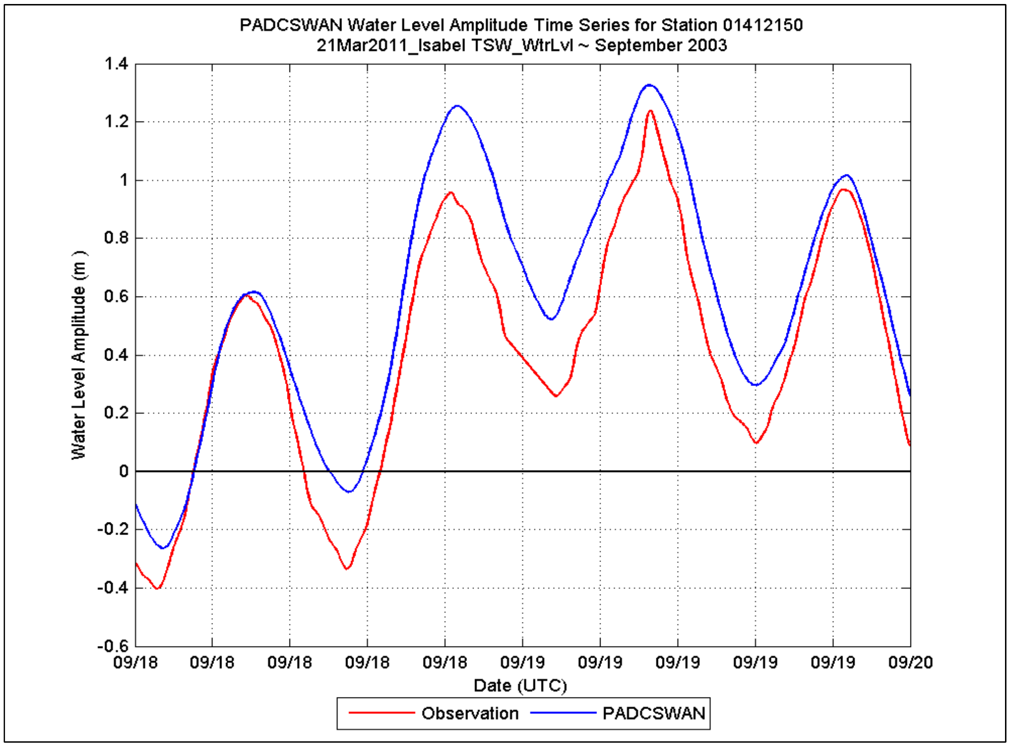

Station 01484085

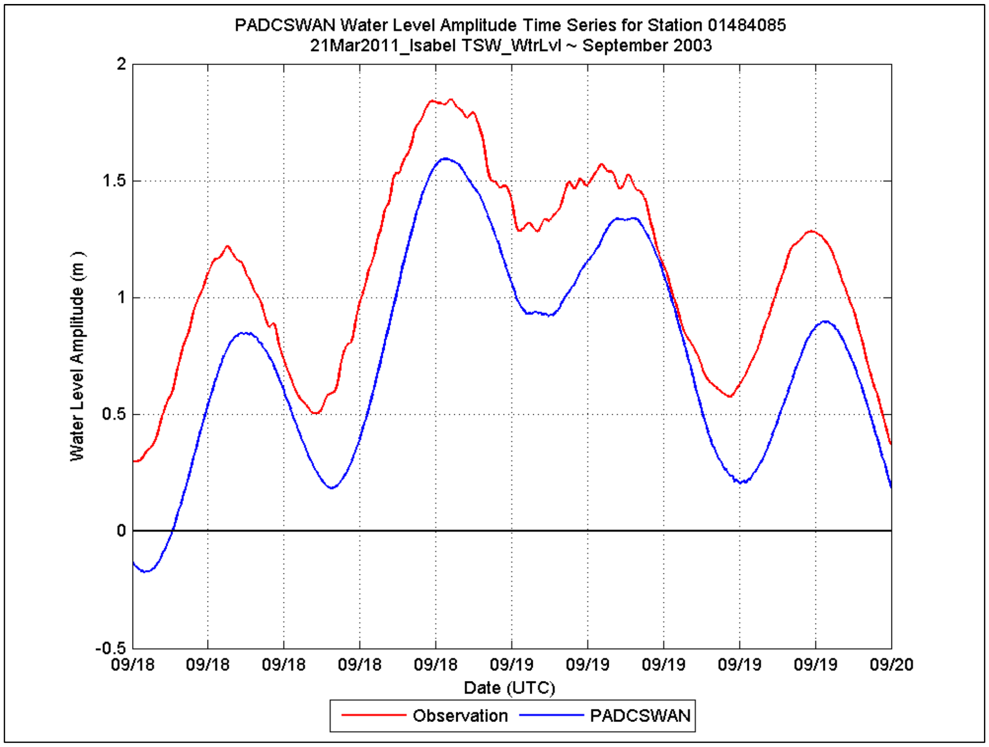

Station 01484540

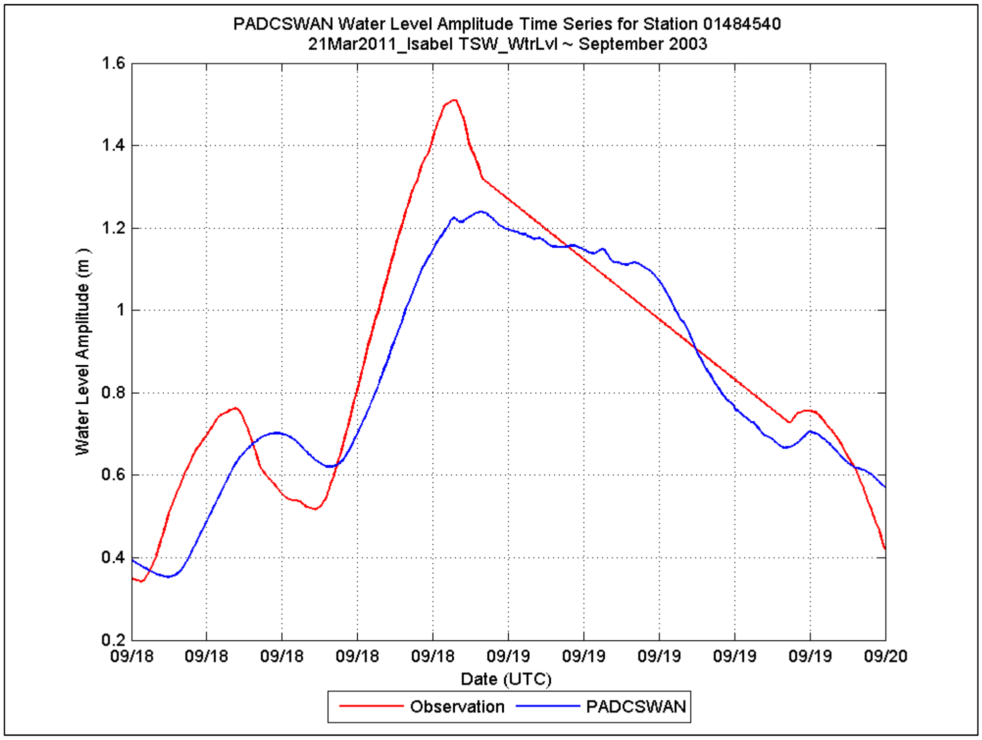

Station 01484670

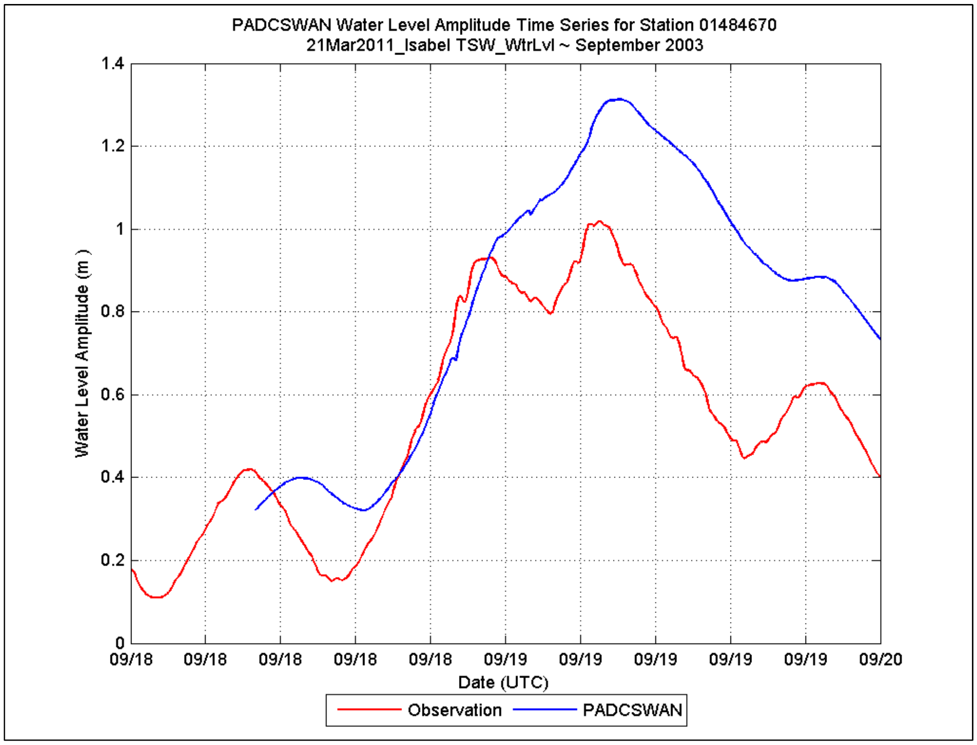

Station 01484696

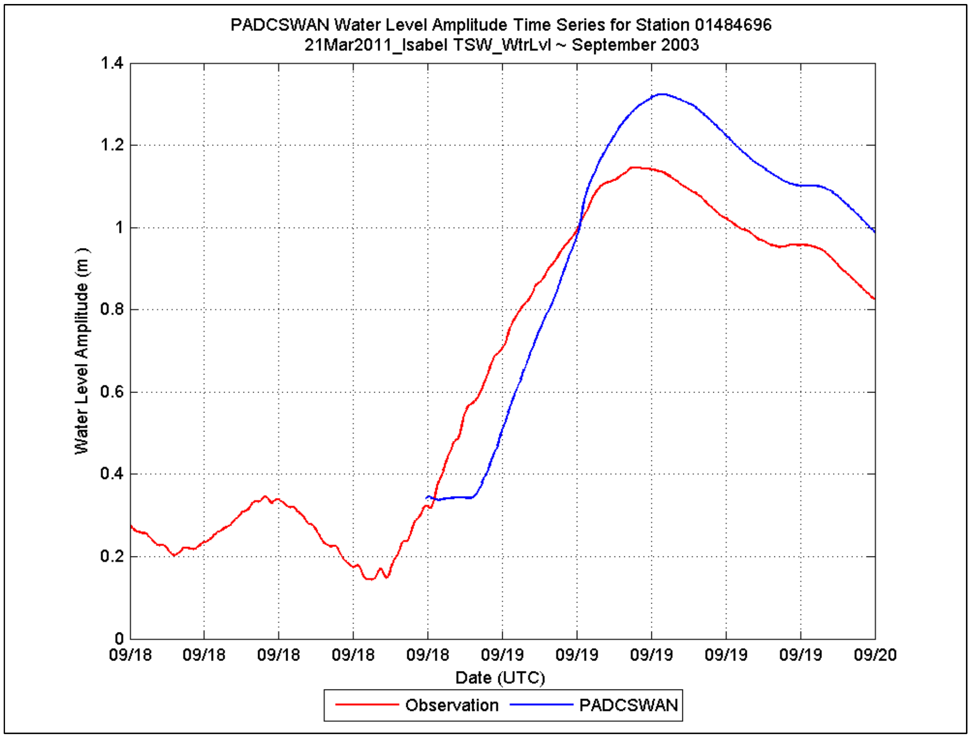

Station 8536110

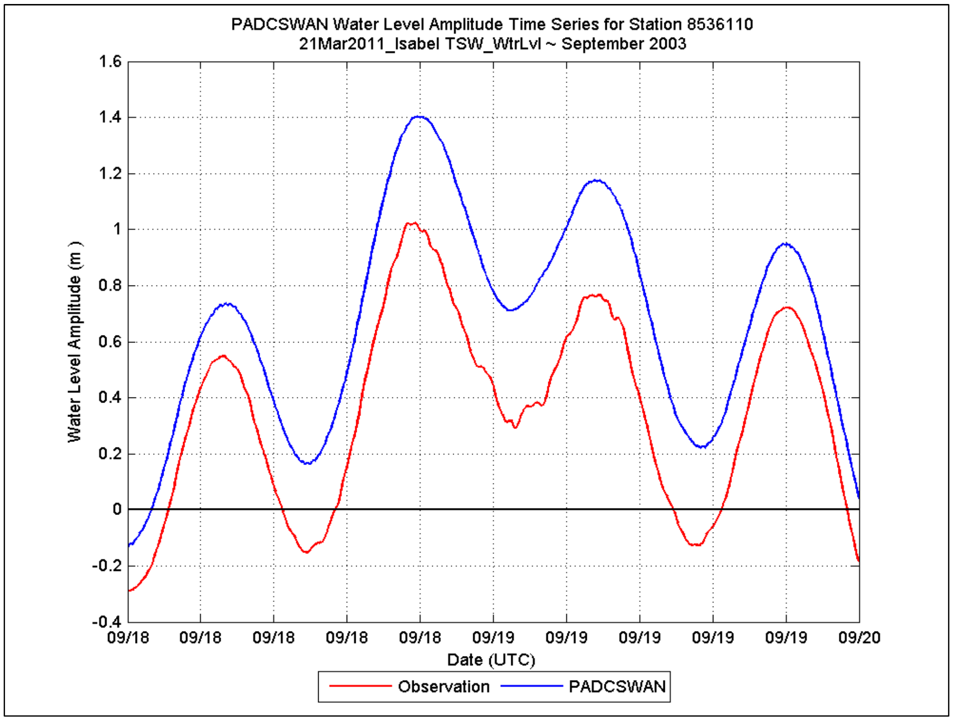

Station 8545240

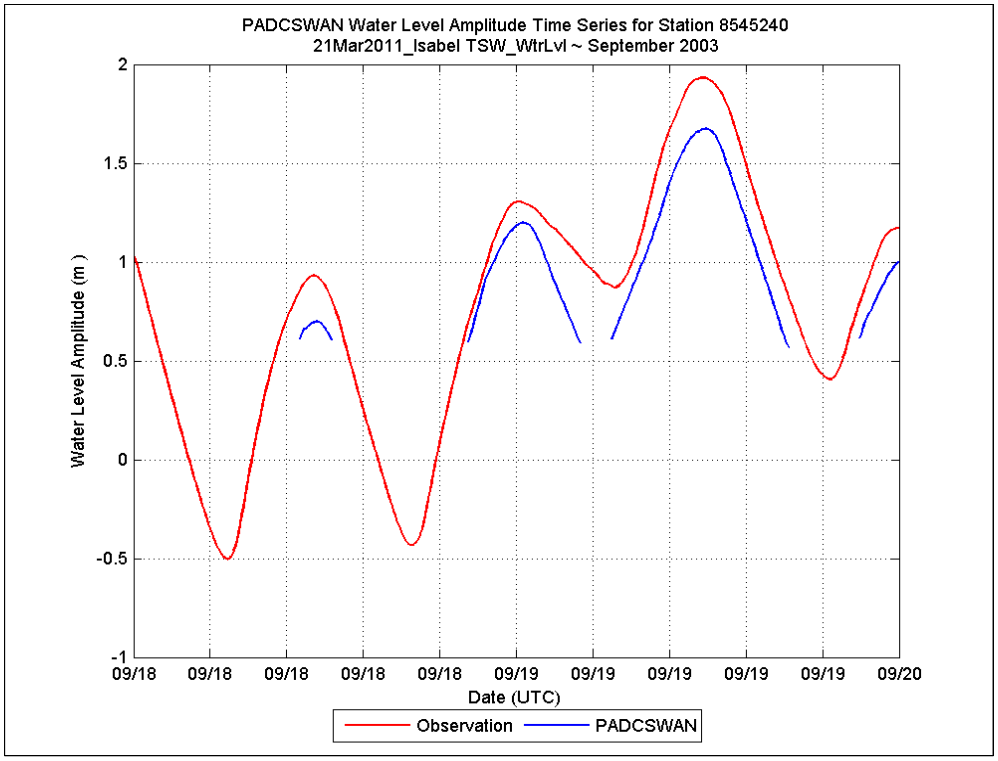

Station 8551910

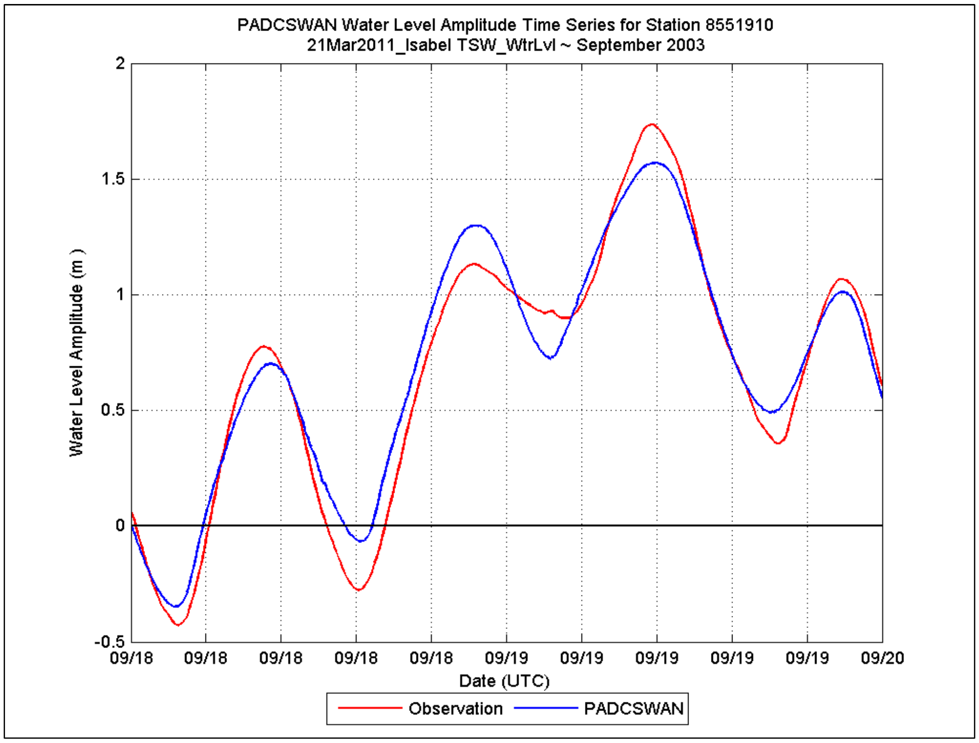

Station 8574680

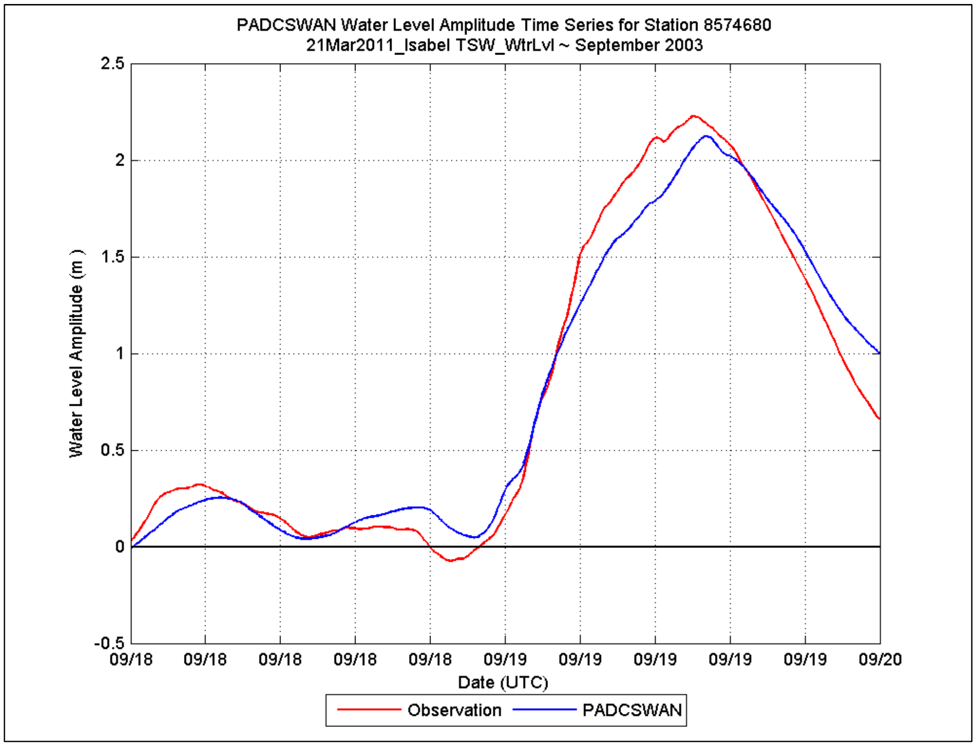

Station 8575512

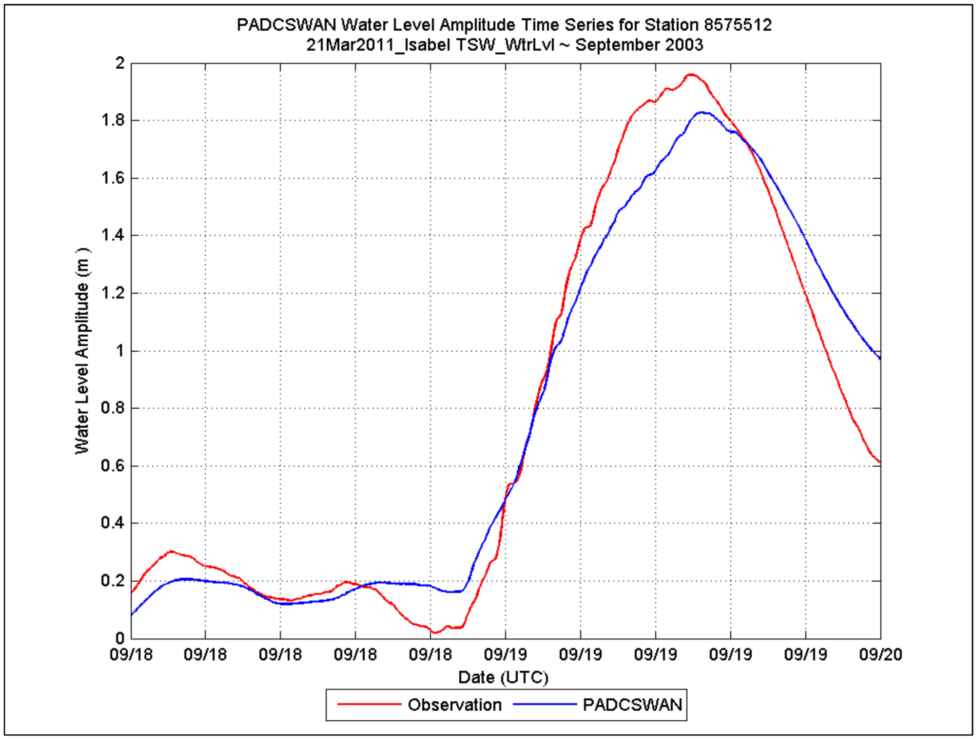

Station 8577330

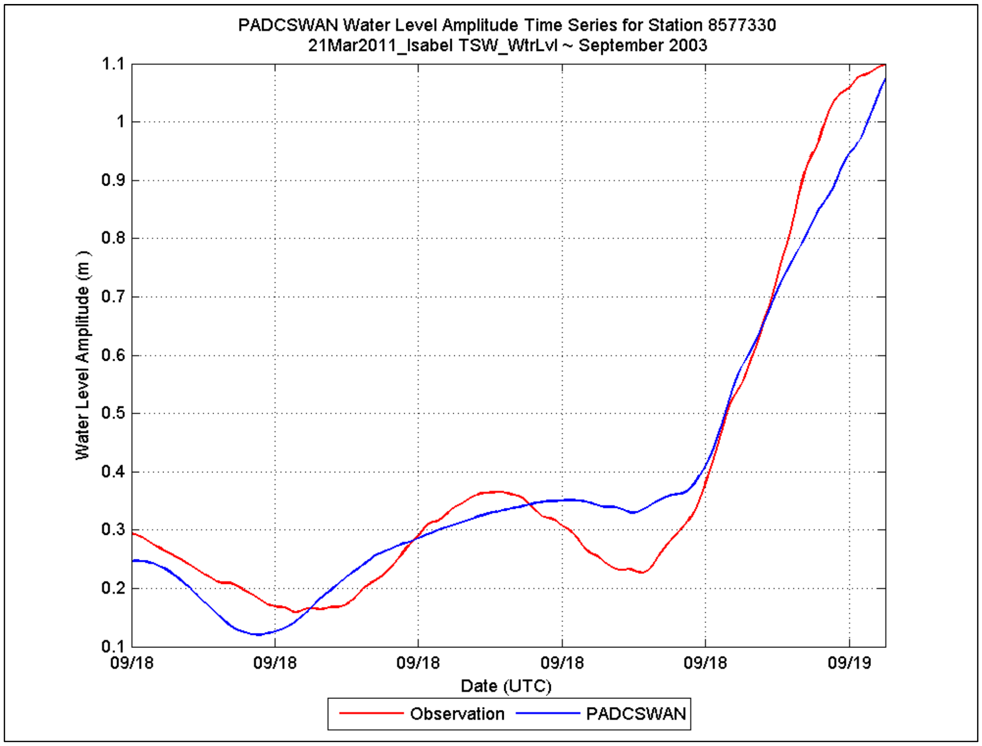

Station 8632200

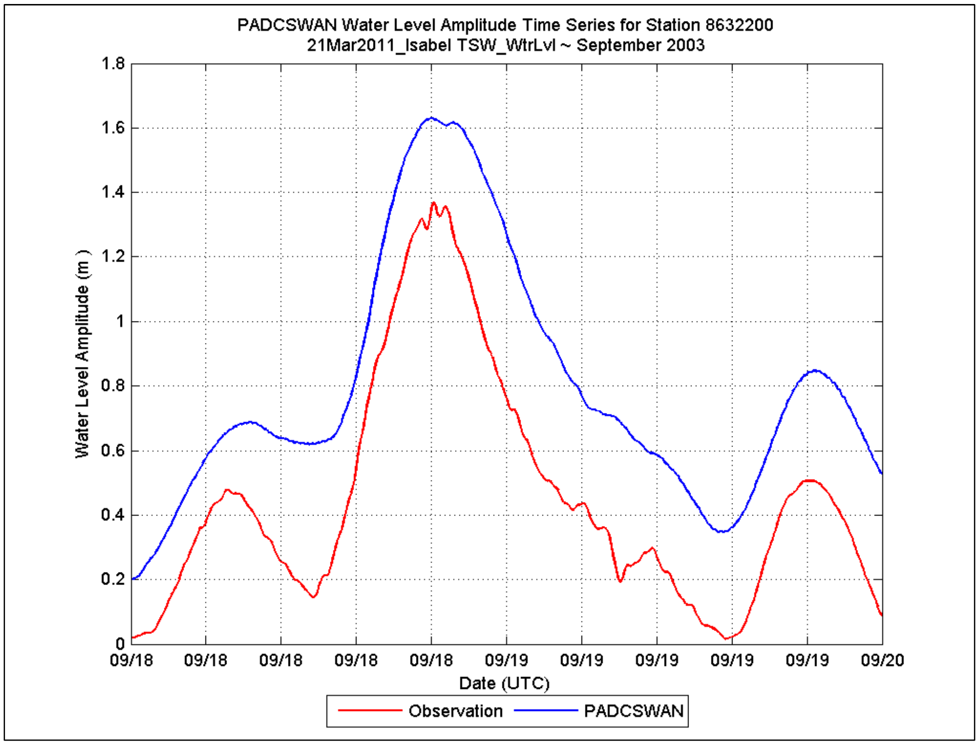

Station 8635750

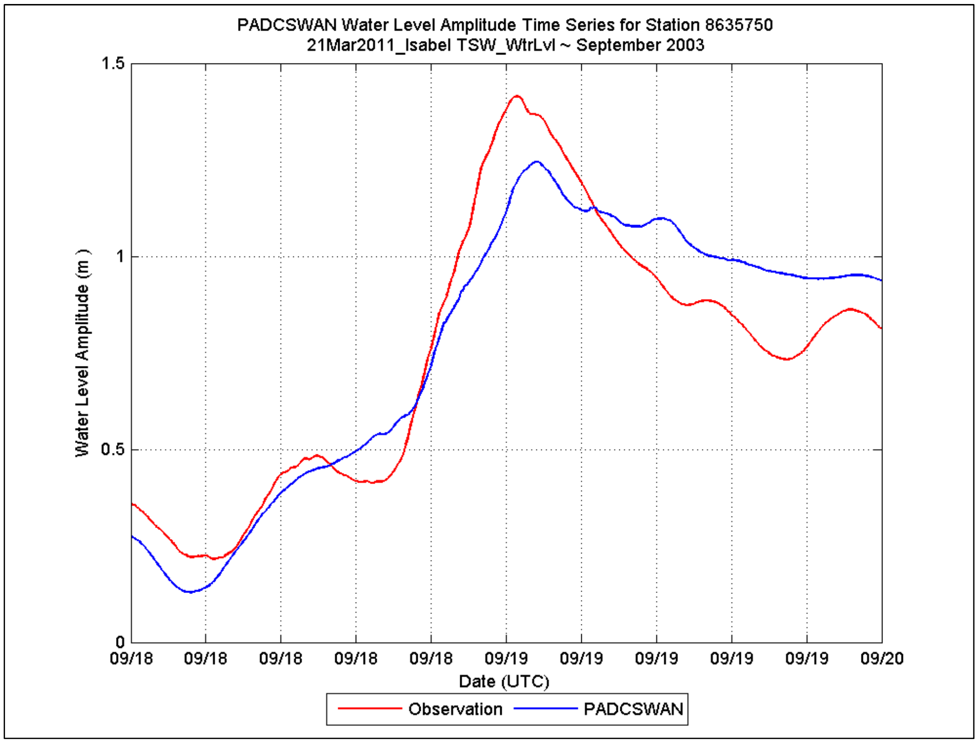

Station 8638610

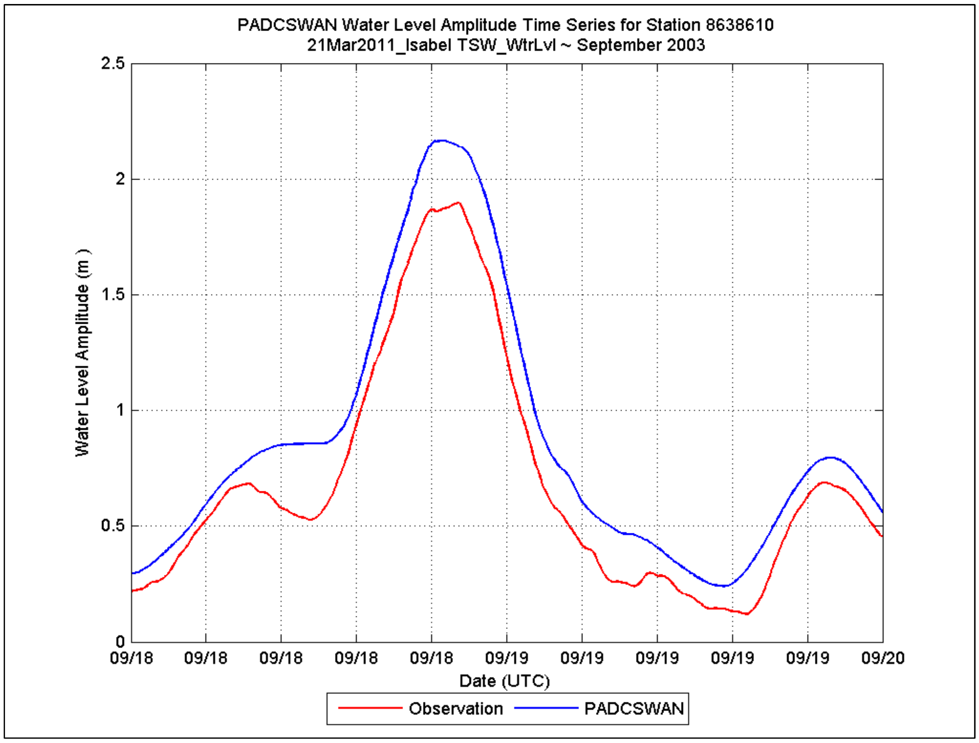

Station 8639348

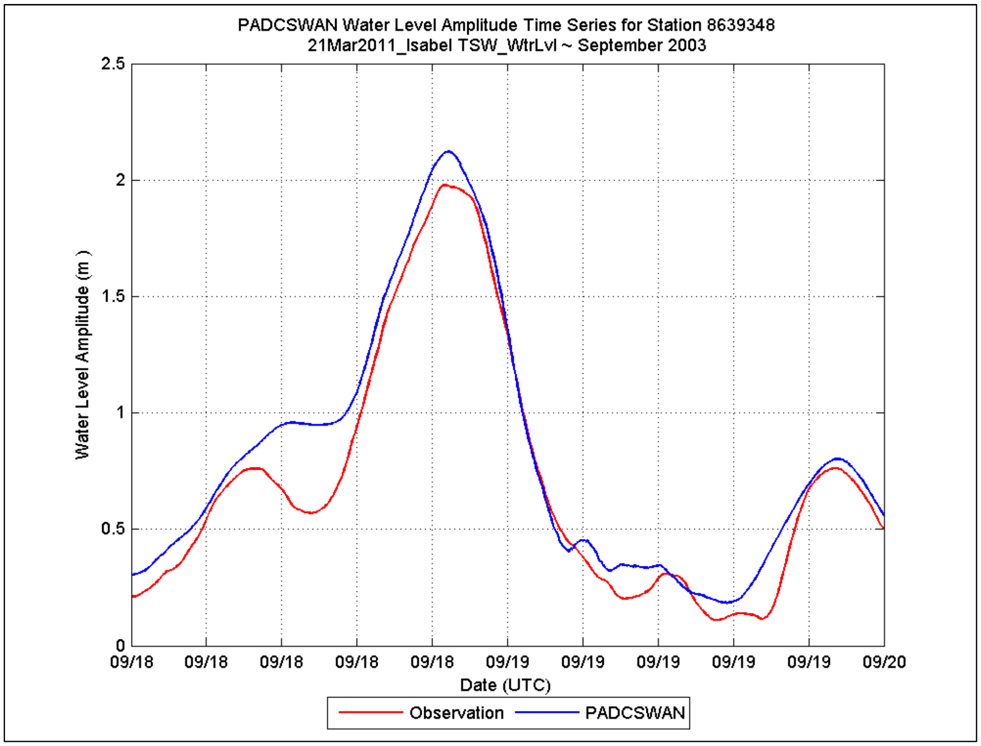

E-2 Hurricane Ernesto, August-September 2006

Data plots in this section refer to the PADCSWAN TidesWindsWaves water level analysis for Hurricane Ernesto, August-September 2006.

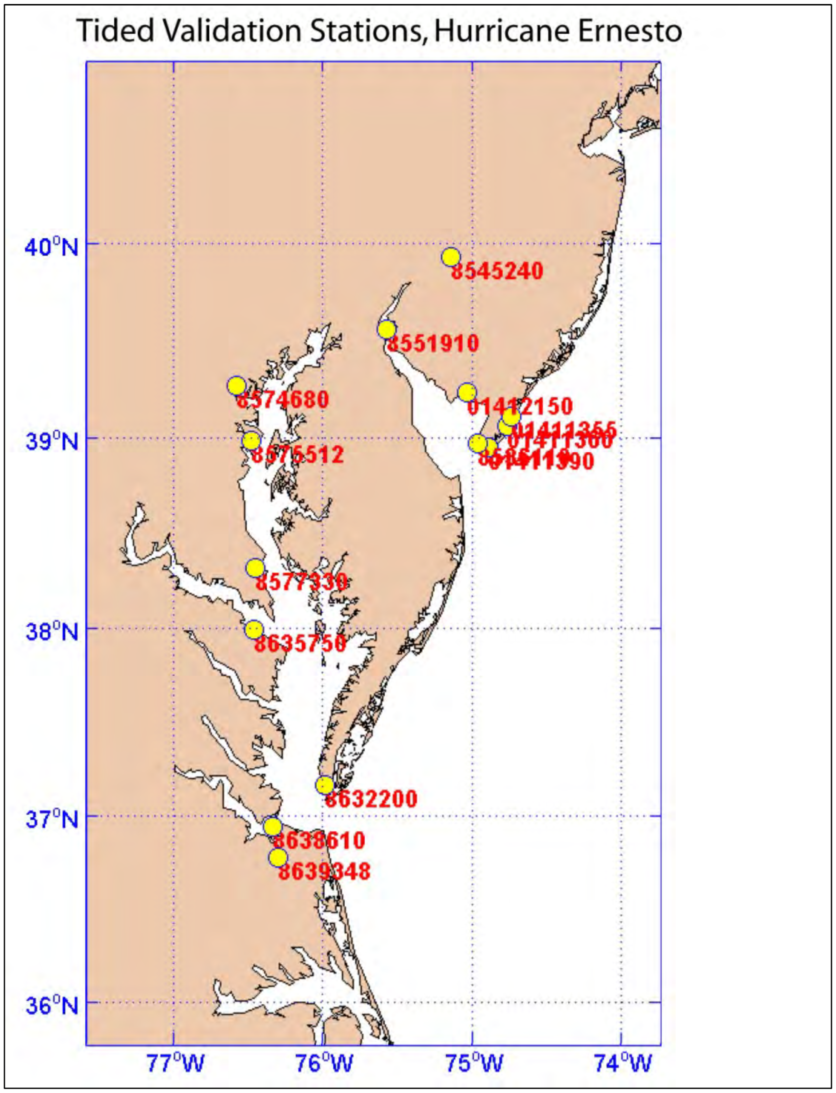
Tided Validation Stations, Hurricane Ernesto
40°N
39°N
38°N
37°N
36°N
77°W
76°W
75°W
74°W
8545240
8551910
8574680
8575512
01412150
01411356
01411300
01411390
8577330
8635750
8632200
8638610
8639348

Figure E2. NOAA water level station locations for TidesWindsWaves, Ernesto.Data plots for the analysis follow this location map.

Station 01411355

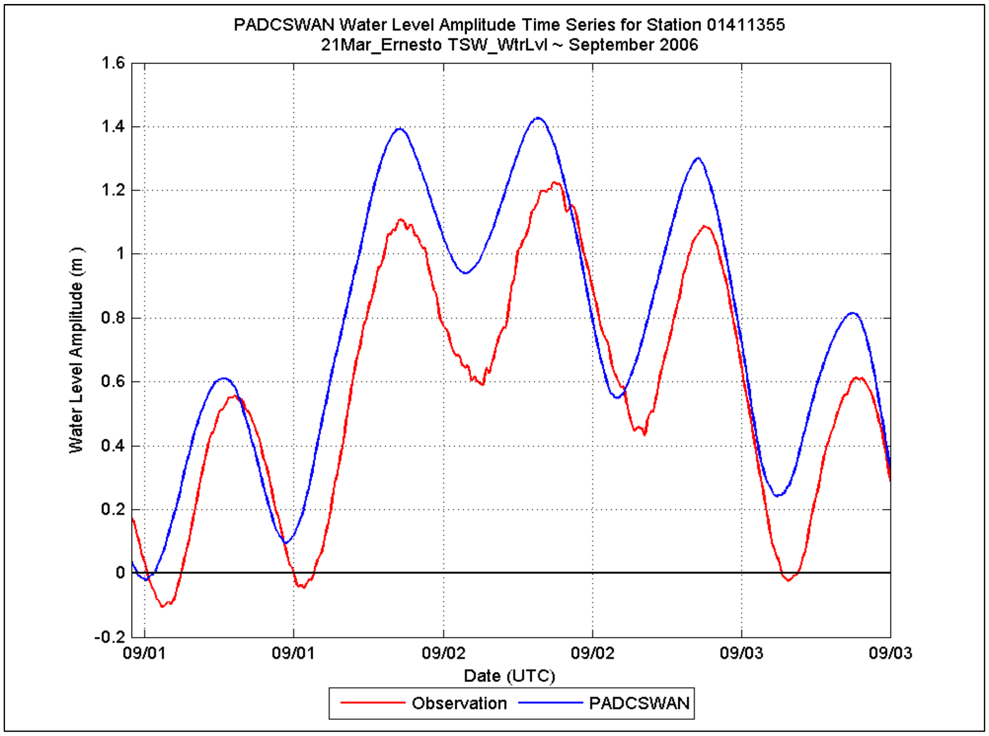

Station 01411360

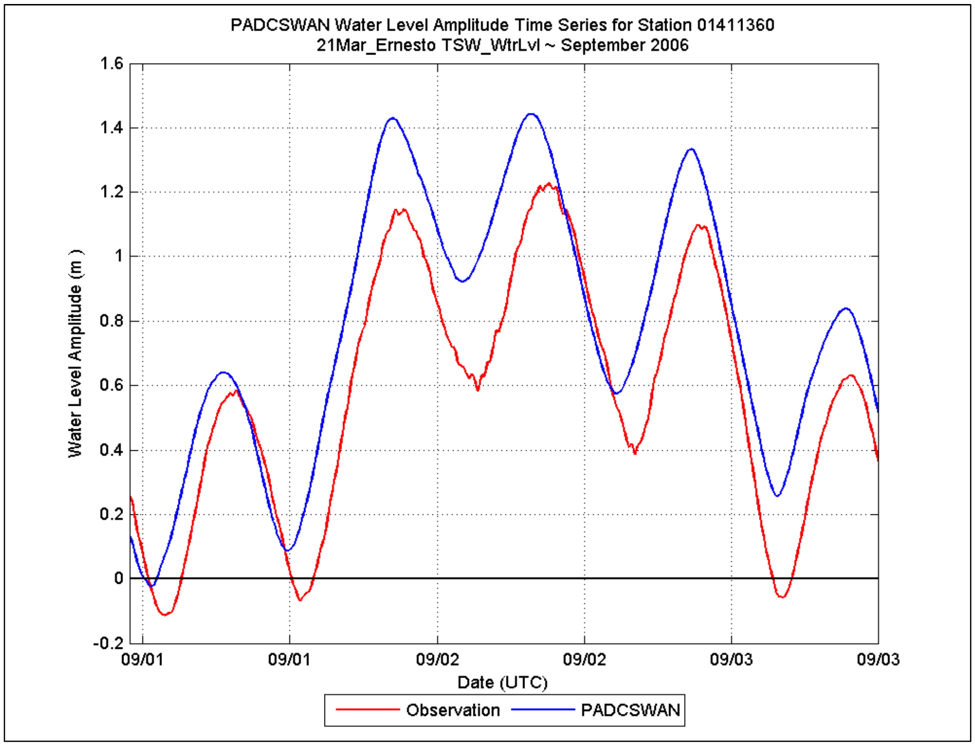

Station 01411390

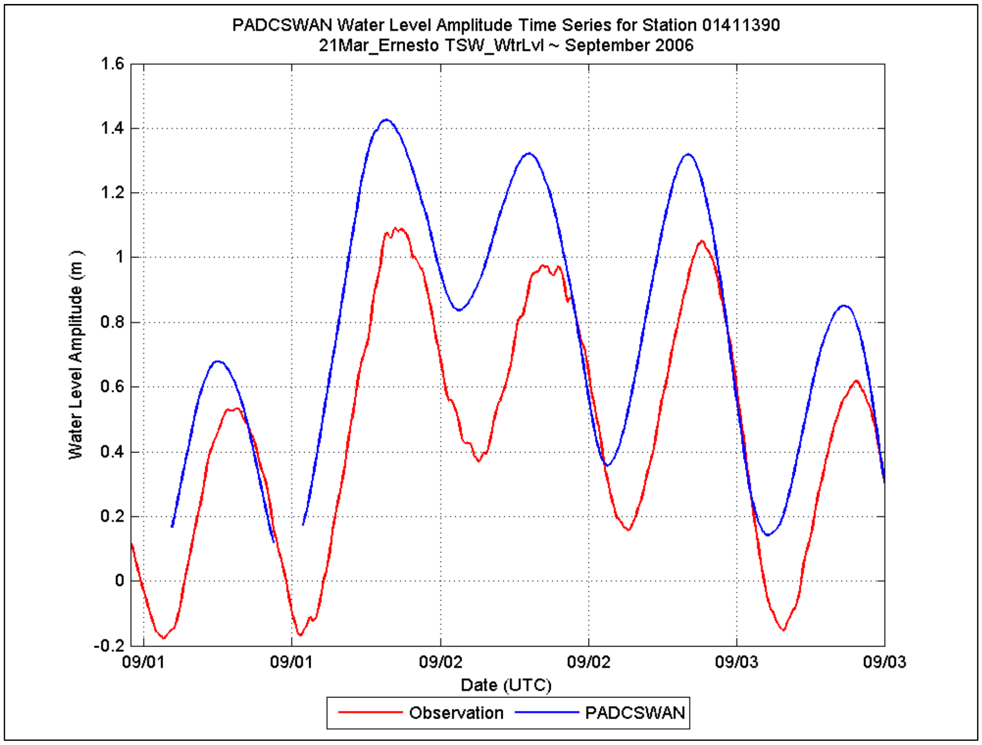

Station 01412150

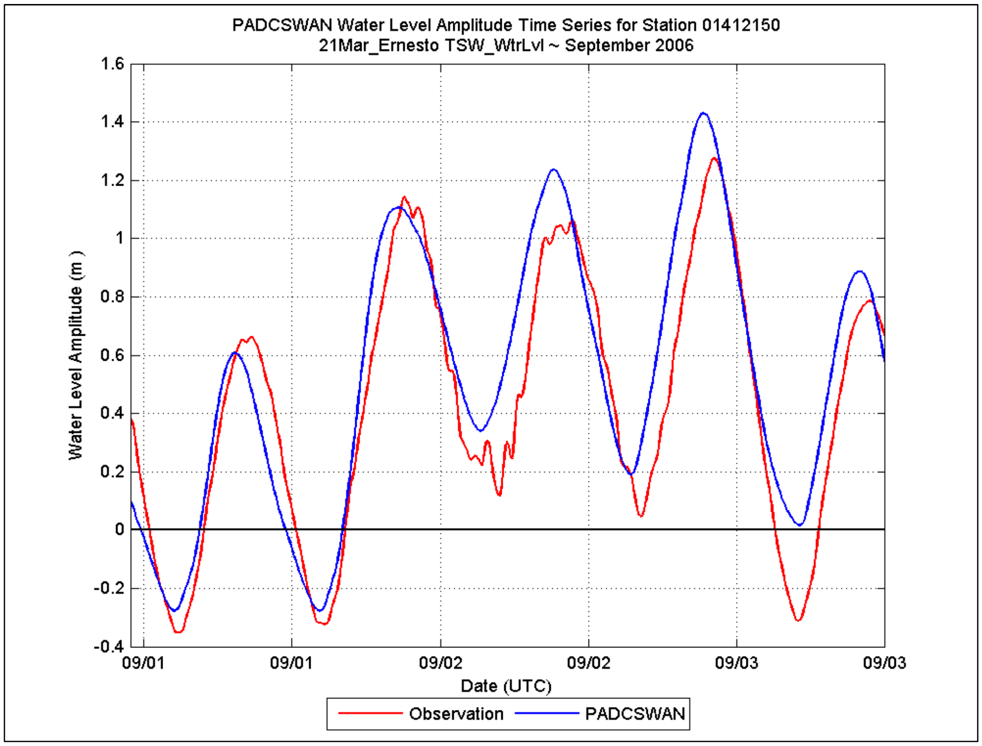

Station 8536110

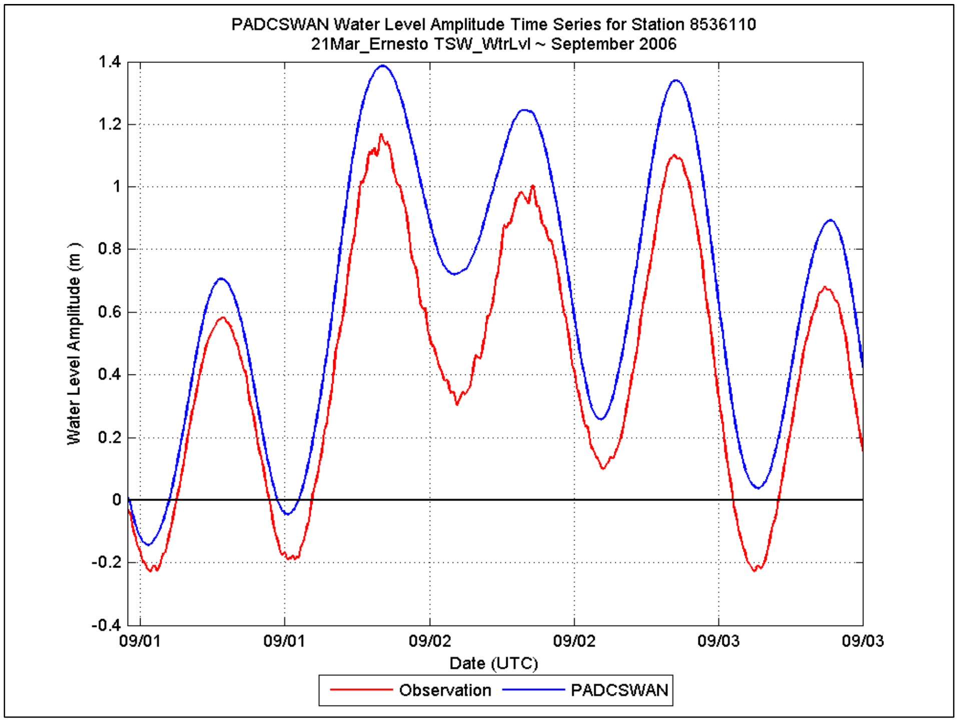

Station 8545240

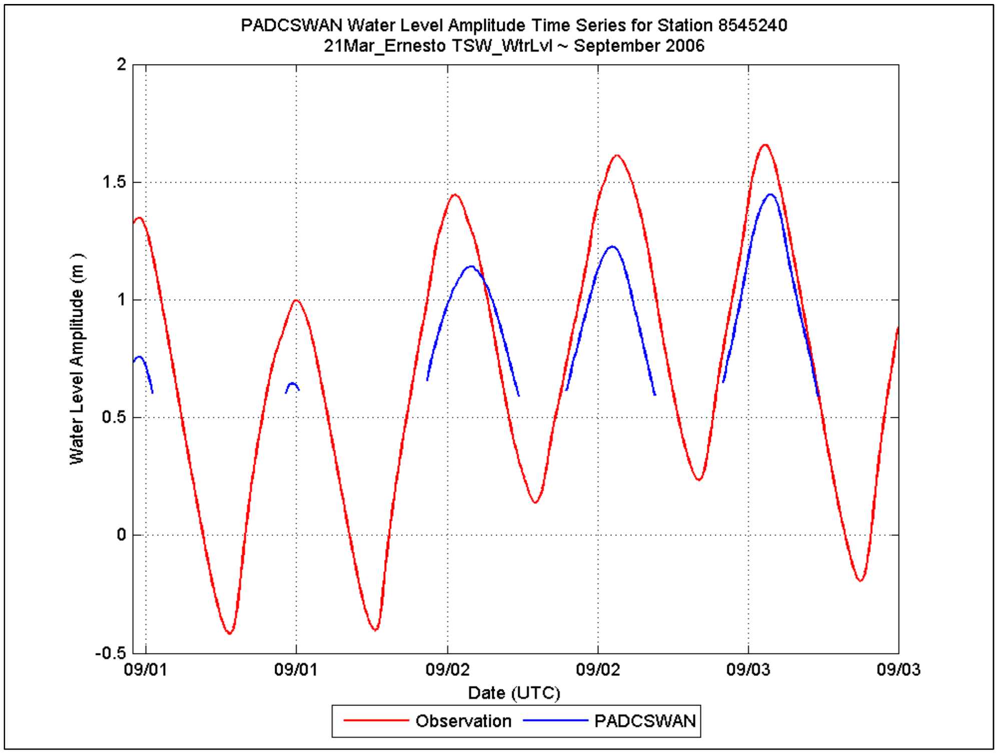

Station 8551910

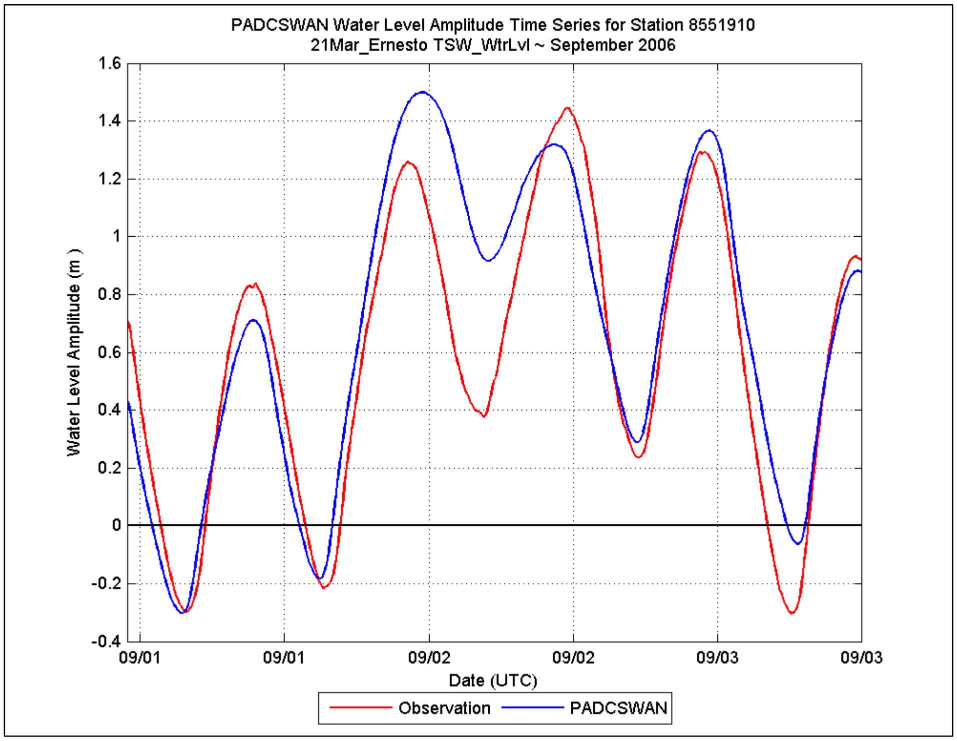

Station 8574680

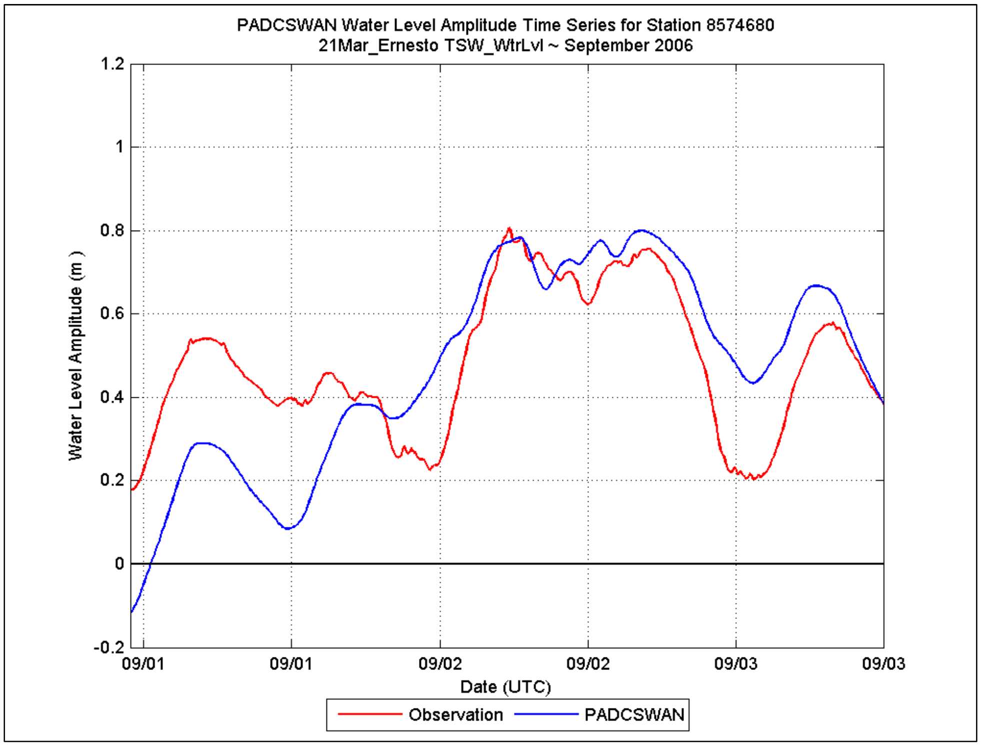

Station 8575512

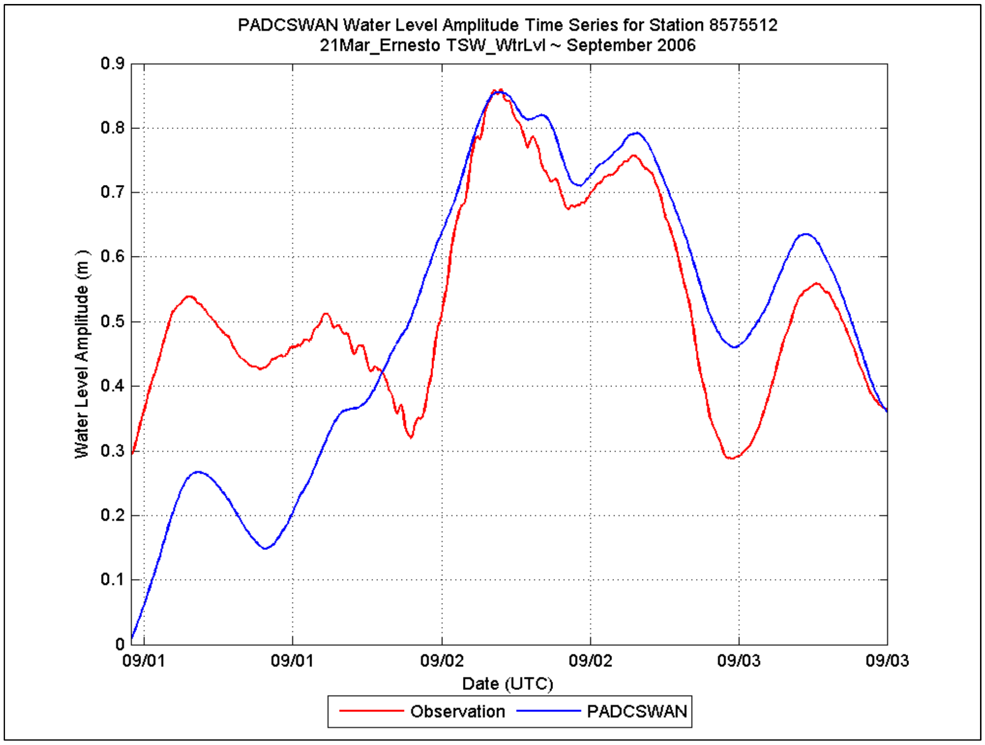

Station 8577330

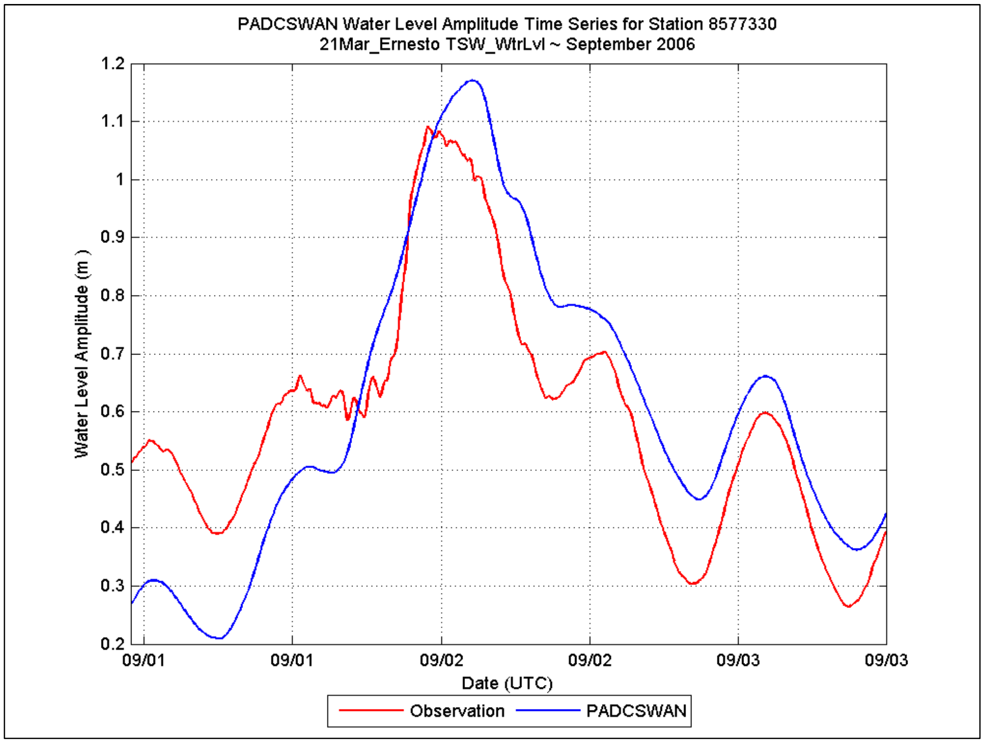

Station 8632200

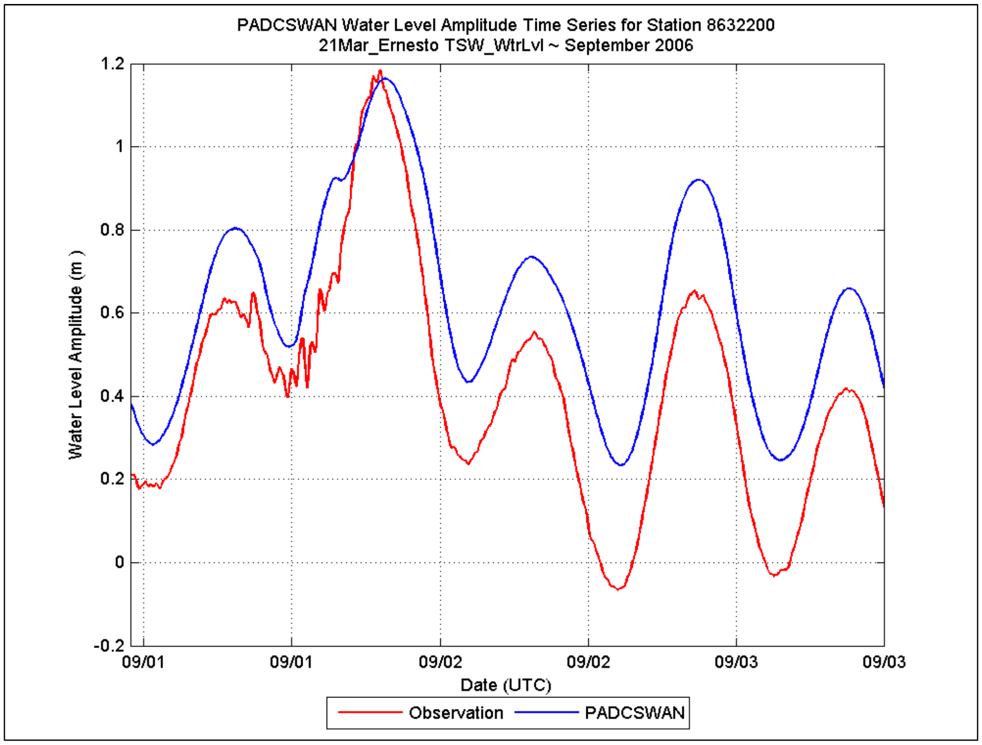

Station 8635750

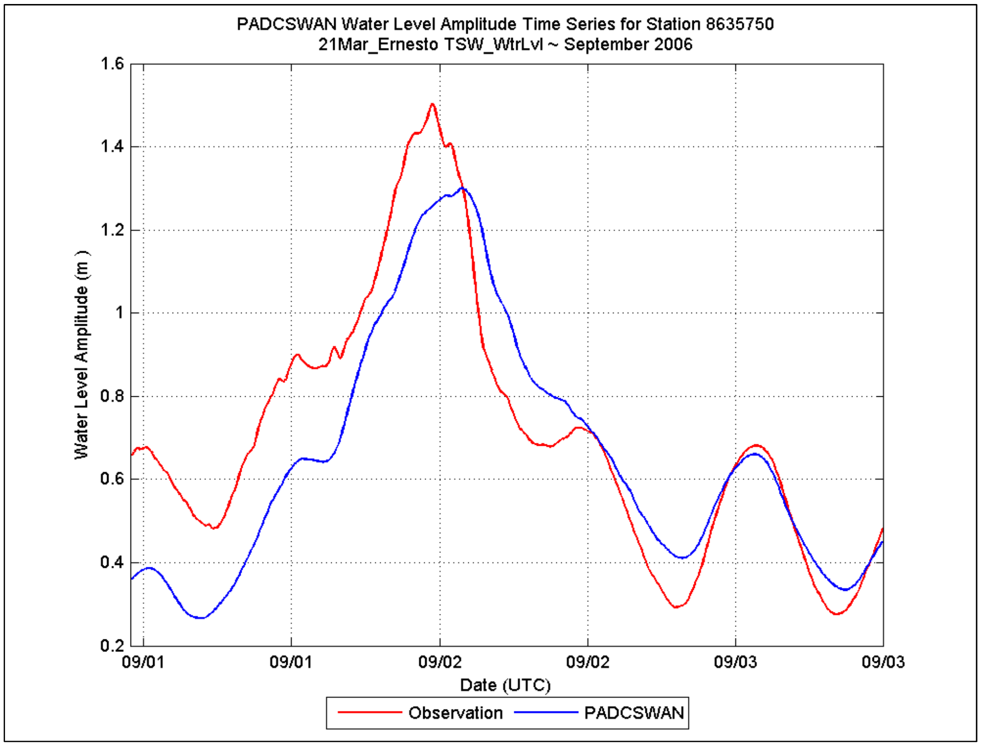

Station 8638610

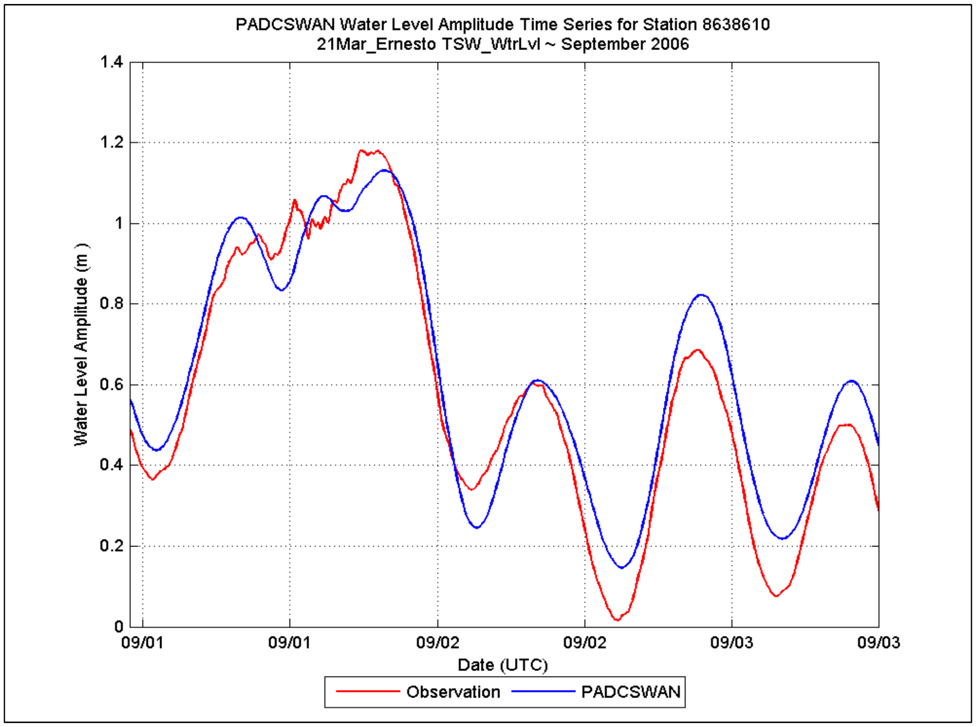

Station 8639348

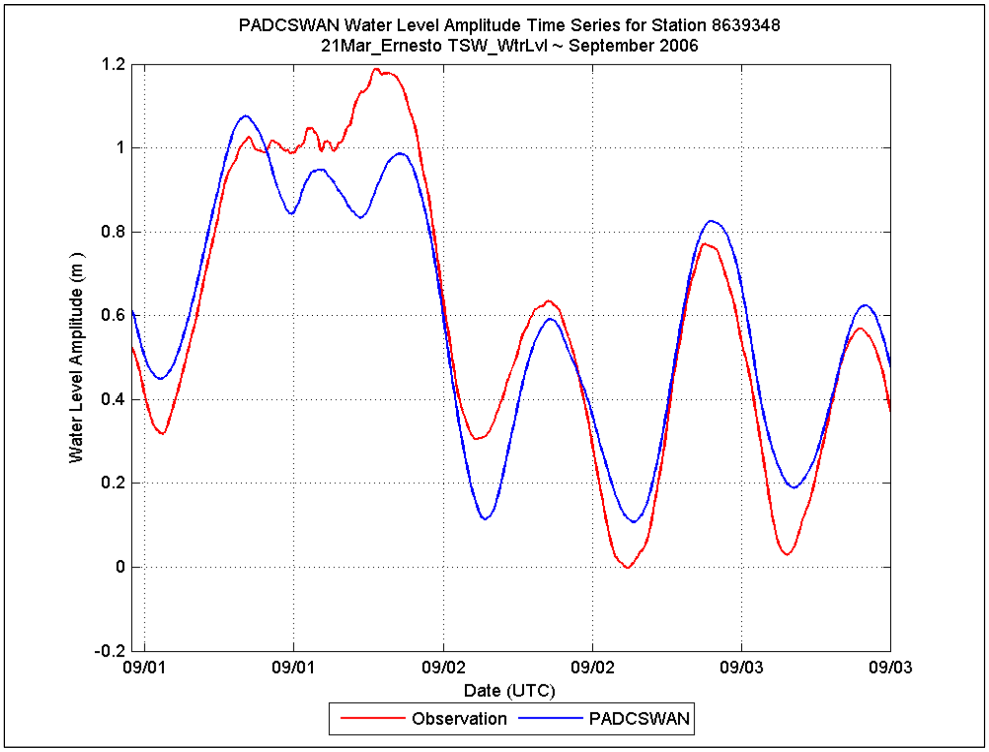

E-3 Nor’easter Ida (Nor’Ida), November 2009

Data plots in this section refer to the PADCSWAN TidesWindsWaves water level analysis for Nor’easter Ida (Nor’Ida), November 2009.

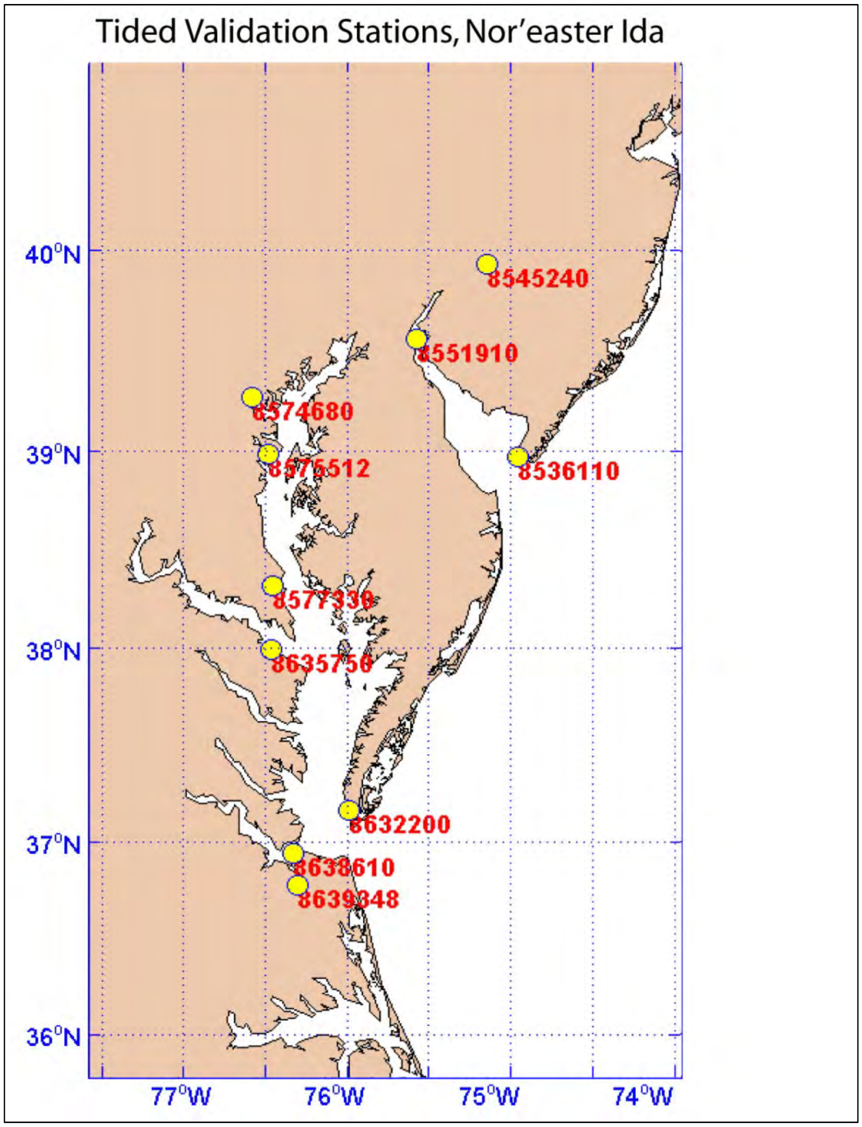
Tided Validation Stations, Nor’easter Ida
40°N
39°N
38°N
37°N
36°N
77°W
76°W
75°W
74°W
8545240
8551910
8574680
8575512
8536110
8577330
8635750
8632200
8638610
8639348

Figure E3. NOAA water level station locations for TidesWindsWaves, Nor’Ida. Data plots for the analysis follow the location map.

Station 8536110

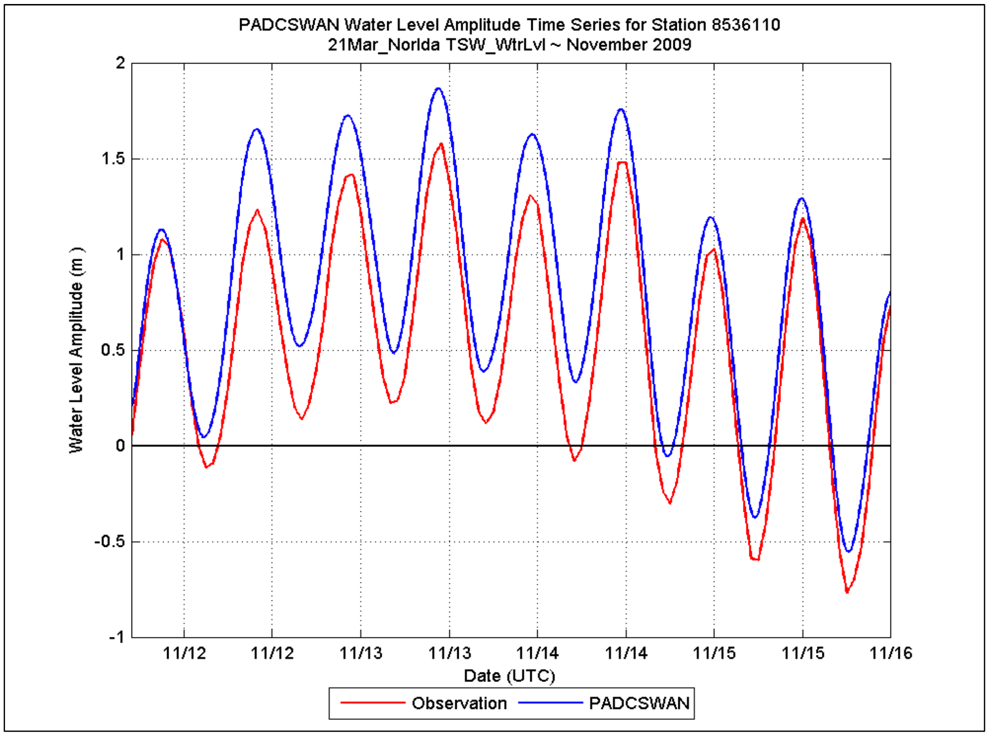

Station 8545240

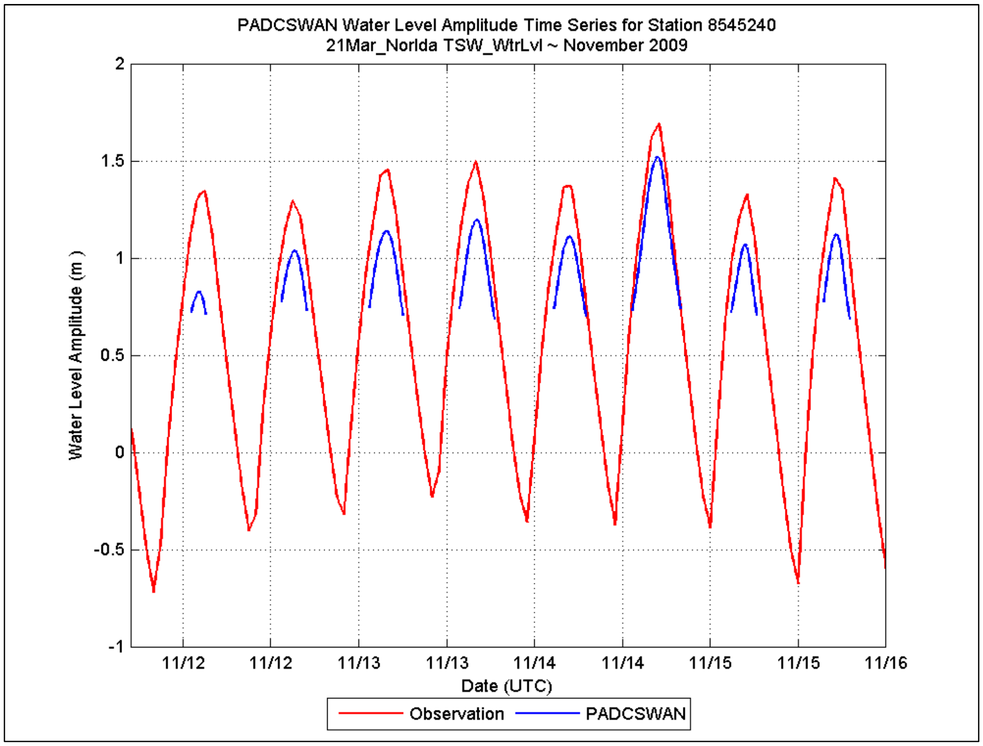

Station 8551910

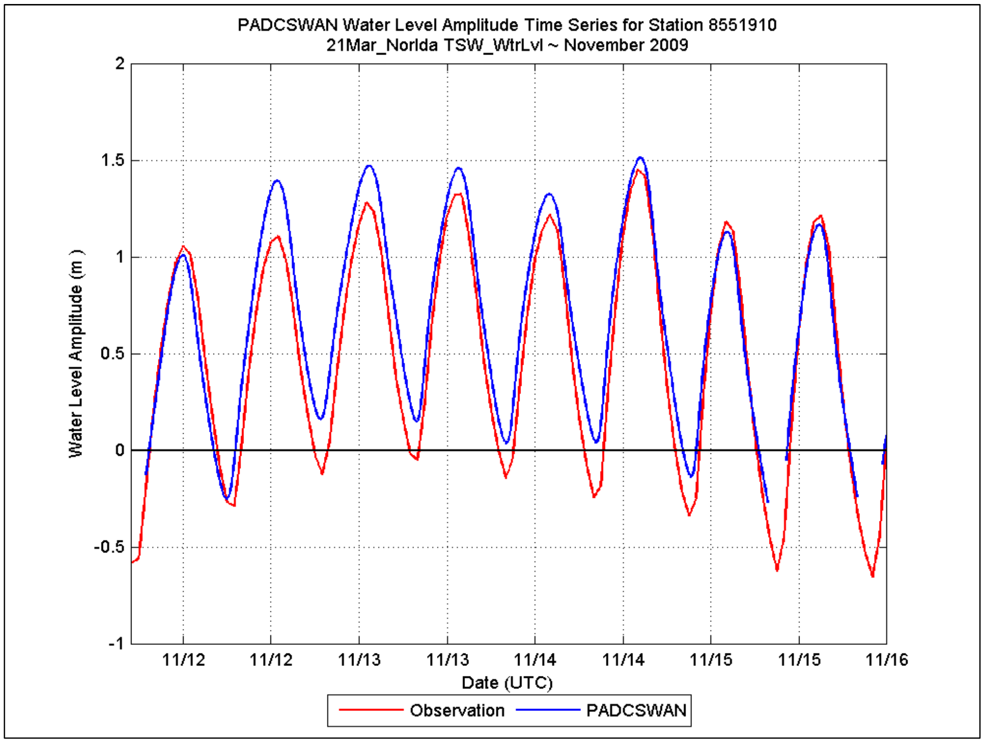

Station 8574680

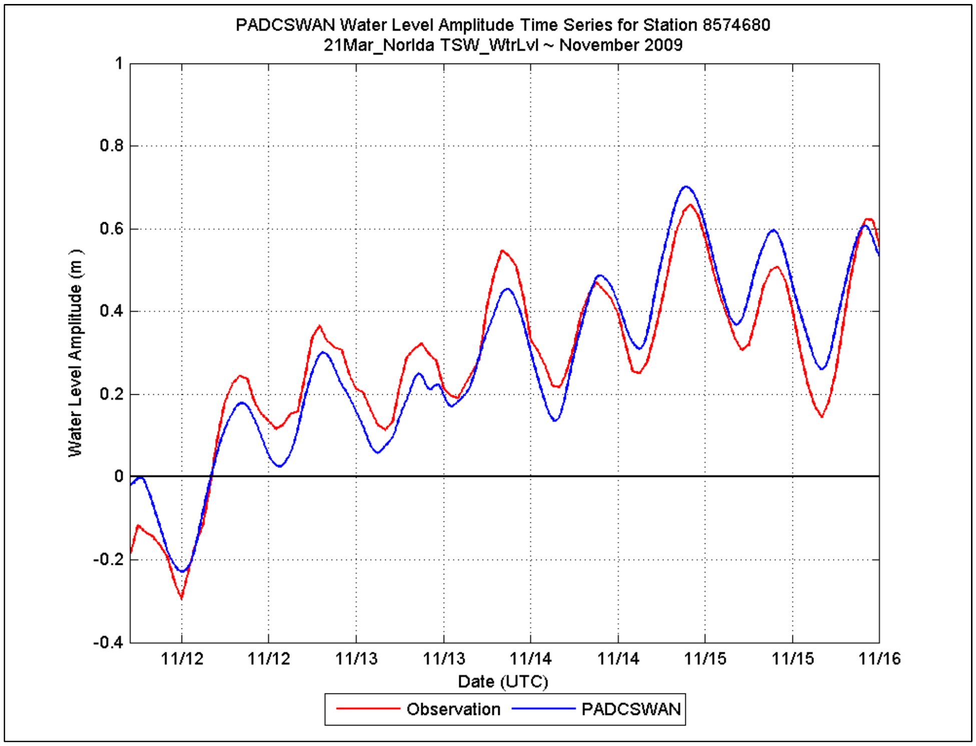

Station 8575512

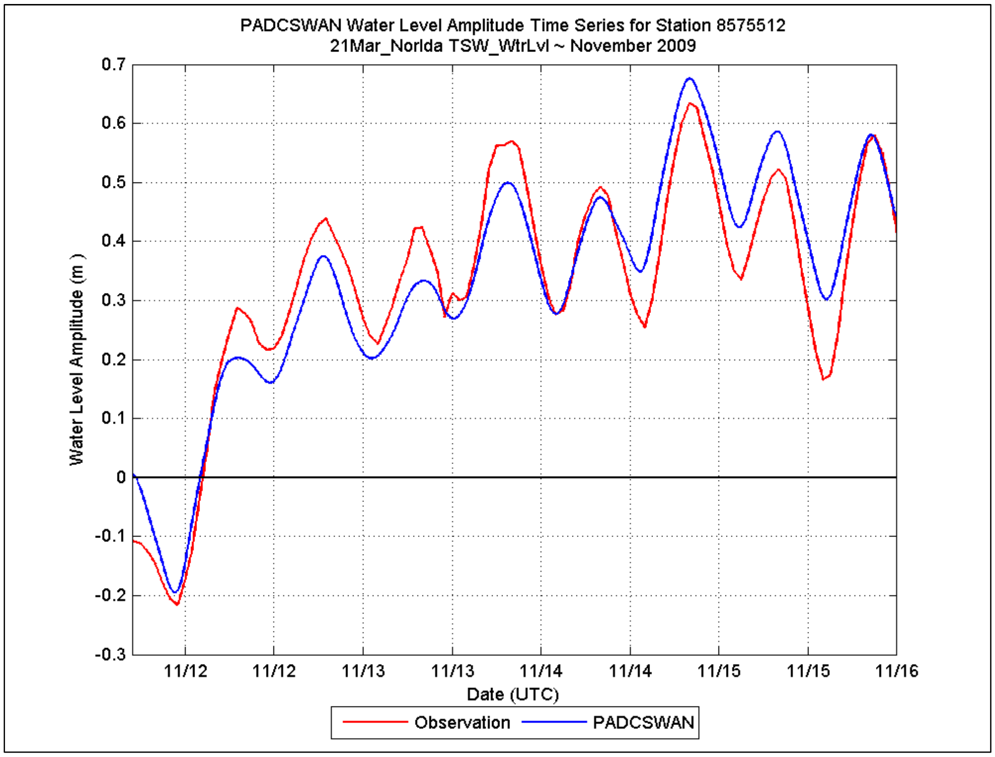

Station 8577330

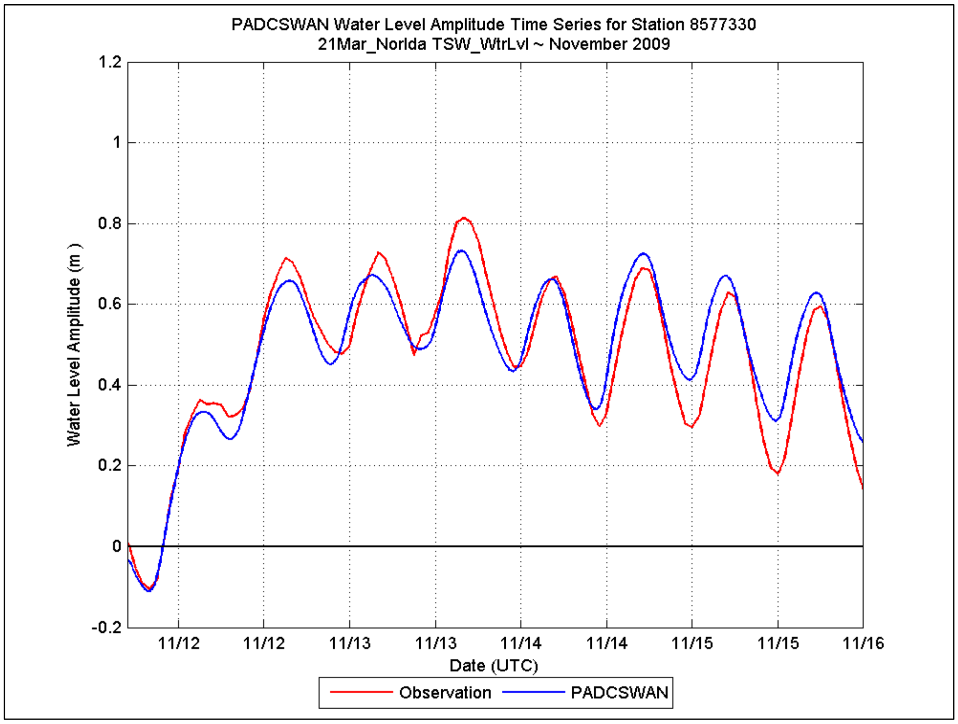

Station 8632200

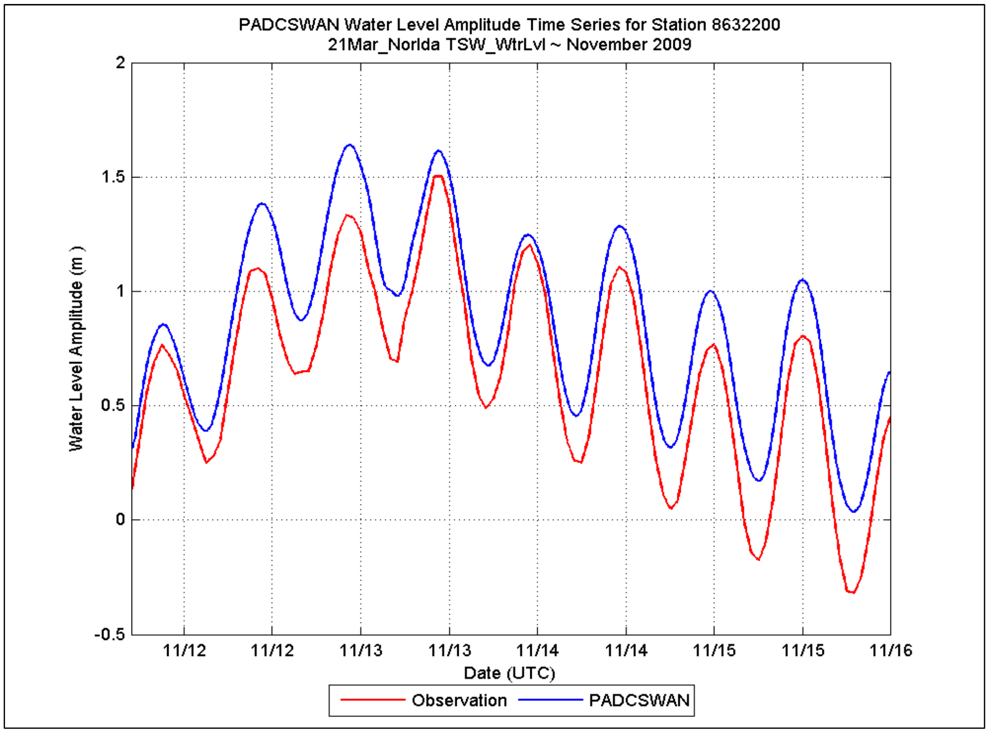

Station 8635750

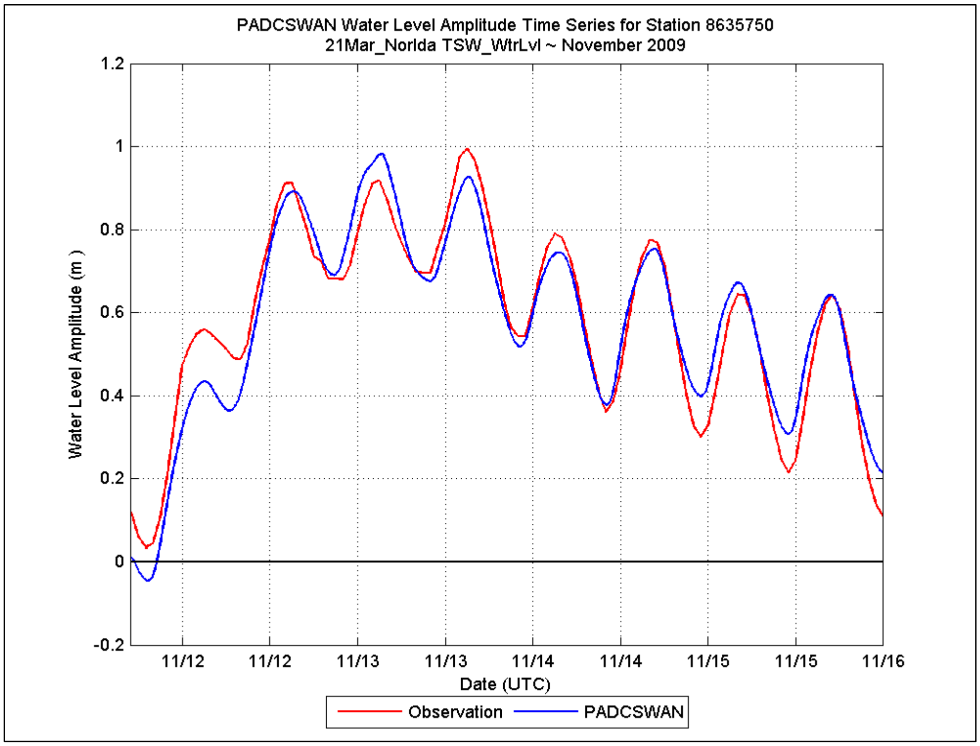

Station 8638610

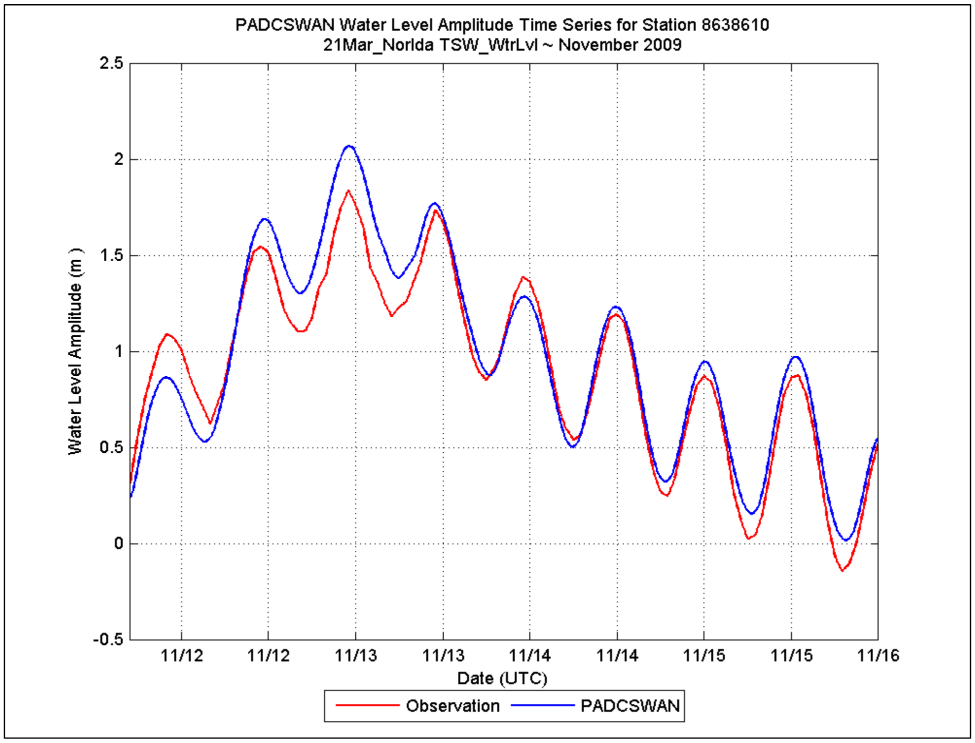

Station 8639348

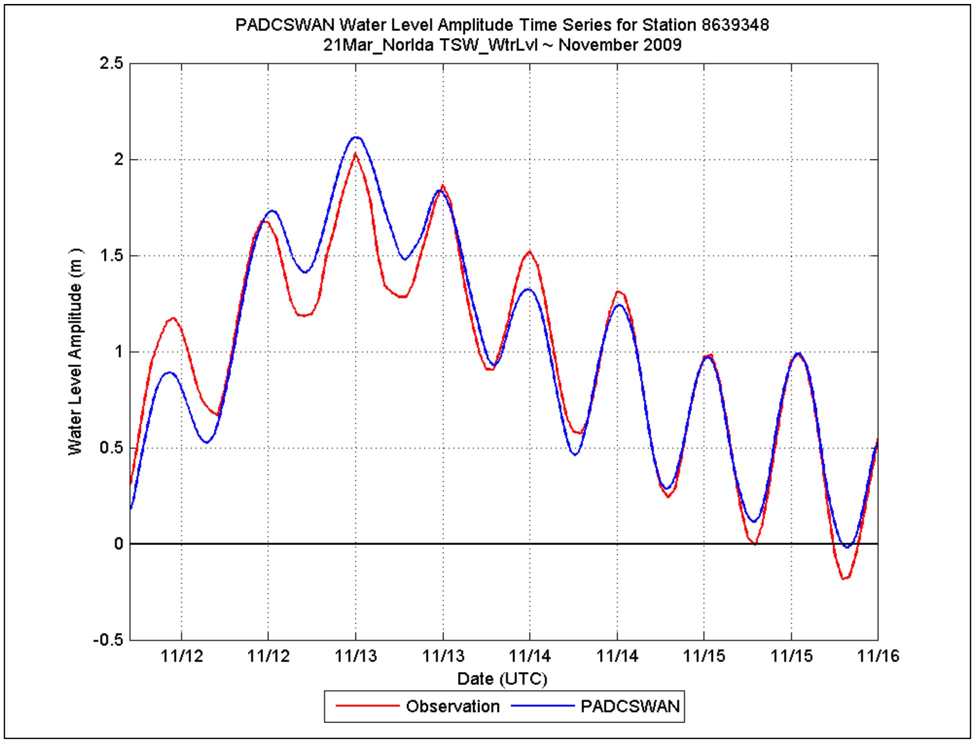

REPORT DOCUMENTATION PAGE

Form Approved
OMB No. 0704-0188

Public reporting burden for this collection of information is estimated to average 1 hour per response, including the time for reviewing instructions, searching existing data sources, gathering and maintaining the data needed, and completing and reviewing this collection of information. Send comments regarding this burden estimate or any other aspect of this collection of information, including suggestions for reducing this burden to Department of Defense, Washington Headquarters Services, Directorate for Information Operations and Reports (0704-0188), 1215 Jefferson Davis Highway, Suite 1204, Arlington, VA 22202-4302. Respondents should be aware that notwithstanding any other provision of law, no person shall be subject to any penalty for failing to comply with a collection of information if it does not display a currently valid OMB control number. **PLEASE DO NOT RETURN YOUR FORM TO THE ABOVE ADDRESS.**

1. REPORT DATE *(DD-MM-YYYY)*
July 2013

2. REPORT TYPE
Final TR

3. DATES COVERED *(From - To)*

4. TITLE AND SUBTITLE

Coastal Storm Surge Analysis: Modeling System Validation; Report 4: Intermediate Submission No. 2.0

5a. CONTRACT NUMBER

5b. GRANT NUMBER

5c. PROGRAM ELEMENT NUMBER

6. AUTHOR(S)

Jeffrey L. Hanson, Heidi M. Wadman, Brian Blandon, and Hugh Roberts

5d. PROJECT NUMBER

5e. TASK NUMBER

5f. WORK UNIT NUMBER
Work Unit J64C87

7. PERFORMING ORGANIZATION NAME(S) AND ADDRESS(ES)

Field Research Facility
US Army Engineer Research and Development Center
1261 Duck Road
Kitty Hawk, NC 27949

Renaissance Computing Institute
100 Europa Drive, Suite 540
Chapel Hill, NC 27517

ARCADIS
4999 Pearl East Circle, Suite 540
Boulder, CO 80301

8. PERFORMING ORGANIZATION REPORT NUMBER

ERDC/CHL TR-11-1

9. SPONSORING / MONITORING AGENCY NAME(S) AND ADDRESS(ES)
Federal Emergency Management Agency
615 Chestnut Street
One Independence Mall, Sixth Floor
Philadelphia, PA 19106-4404

10. SPONSOR/MONITOR'S ACRONYM(S)

12. DISTRIBUTION / AVAILABILITY STATEMENT
Approved for public release; distribution is unlimited.

13. SUPPLEMENTARY NOTES

14. ABSTRACT

The Federal Emergency Management Agency, Region III office, has initiated a study to update the coastal storm surge elevations within the states of Virginia, Maryland, and Delaware, and the District of Columbia including the Atlantic Ocean, Chesapeake Bay including its tributaries, and the Delaware Bay. This effort is one of the most extensive coastal storm surge analyses to date, encompassing coastal floodplains in three states and including the largest estuary in the world. The study will replace outdated coastal storm surge stillwater elevations for all Flood Insurance Studies in the study area, and serve as the basis for new coastal hazard analysis and ultimately updated Flood Insurance Rate Maps (FIRMs).

The end-to-end storm surge modeling system includes the Advanced Circulation Model for Oceanic, Coastal and Estuarine Waters (ADCIRC) for simulation of two-dimensional hydrodynamics. ADCIRC was dynamically coupled to the unstructured numerical wave model Simulating WAves Nearshore (unSWAN) to calculate the contribution of waves to total storm surge. The modeling system validation included a comprehensive tidal calibration followed by an assessment using carefully reconstructed wind and pressure fields from three major flood events for the Region III domain: Hurricane Isabel, Hurricane Ernesto, and Extratropical Storm Ida. Model skill was accessed by quantitative comparison of model output to wind, wave, water level, and high water mark observations.

Prior reports covered Submittal 1 requirements by providing details on the bathymetric/topographic digital environmental model (Report 1.1), description of the computational system (Report 1.2), and documenting the selection process for storms used in the study (Report 1.3). This report (2.0) completes the required Submittal 2 documentation by providing details of the modeling system calibration and performance.

15. SUBJECT TERMS
Chesapeake Bay
Chesapeake Bay
Delaware Bay
FEMA flood study
FEMA Region III
Historical storms
Hurricane risk
Storm surge modeling

16. SECURITY CLASSIFICATION OF:			**17. LIMITATION OF ABSTRACT**	**18. NUMBER OF PAGES**	**19a. NAME OF RESPONSIBLE PERSON: Ty V. Wamsley**
a. REPORT	**b. ABSTRACT**	**c. THIS PAGE**			**19b. TELEPHONE NUMBER *(include area code)***
Unclassified	Unclassified	Unclassified	Unclassified	260	(601) 634-2099